Methods in
Molecular Biology 2045

Springer Protocols

Kursad Turksen *Editor*

Stem Cells and Aging

Methods and Protocols

Second Edition

Humana Press

METHODS IN MOLECULAR BIOLOGY

For further volumes:
http://www.springer.com/series/7651

For over 35 years, biological scientists have come to rely on the research protocols and methodologies in the critically acclaimed *Methods in Molecular Biology* series. The series was the first to introduce the step-by-step protocols approach that has become the standard in all biomedical protocol publishing. Each protocol is provided in readily-reproducible step-by-step fashion, opening with an introductory overview, a list of the materials and reagents needed to complete the experiment, and followed by a detailed procedure that is supported with a helpful notes section offering tips and tricks of the trade as well as troubleshooting advice. These hallmark features were introduced by series editor Dr. John Walker and constitute the key ingredient in each and every volume of the *Methods in Molecular Biology* series. Tested and trusted, comprehensive and reliable, all protocols from the series are indexed in PubMed.

Stem Cells and Aging

Methods and Protocols

Second Edition

Edited by

Kursad Turksen

Ottawa, ON, Canada

Humana Press

Editor
Kursad Turksen
Ottawa, ON, Canada

ISSN 1064-3745 ISSN 1940-6029 (electronic)
Methods in Molecular Biology
ISBN 978-1-4939-9712-1 ISBN 978-1-4939-9713-8 (eBook)
https://doi.org/10.1007/978-1-4939-9713-8

Cover Illustration Caption: Artwork created by Kursad Turksen.

This Humana imprint is published by the registered company Springer Science+Business Media, LLC part of Springer Nature.
The registered company address is: 233 Spring Street, New York, NY 10013, U.S.A.

Preface

Our understanding of changes in stem cell populations during organismal aging is far from complete. Building upon the collection of protocols collected in the first edition on this topic, I have attempted to put together a new series of protocols that reflect current investigations in this very active area of research.

Once again, the protocols gathered here are faithful to the mission statement of the *Methods in Molecular Biology* series: They are well established and described in an easy to follow step-by-step fashion so as to be valuable for not only experts but also novices in the stem cell field. That goal is achieved because of the generosity of the contributors who have carefully described their protocols in this volume, and I am grateful for their efforts.

My thanks as well go to Dr. John Walker, the Editor in Chief of the *Methods in Molecular Biology* series, for giving me the opportunity to create this volume and for supporting me along the way.

I am also grateful to Patrick Marton, the Executive Editor of *Methods in Molecular Biology* and the Springer Protocols collection, for his continuous support from idea to completion of this volume.

I would like to thank David C. Casey, an Editor for *Methods in Molecular Biology*, for his outstanding editorial work during the production of this volume.

Finally, I would like to thank the production crew for putting together an outstanding volume.

Ottawa, ON, Canada ***Kursad Turksen***

Contents

Contributors

Noor Hayaty Abu Kasim • *Department of Restorative Dentistry, Faculty of Dentistry, University of Malaya, Kuala Lumpur, Malaysia; Regenerative Dentistry Research Group, Faculty of Dentistry, University of Malaya, Kuala Lumpur, Malaysia*

Hellen E. Ahrens • *Leibniz-Institute on Aging – Fritz-Lipmann-Institute, Jena, Germany*

Ceren Aksoy • *Research Coordination Department, Middle East Technical University, Ankara, Turkey*

Shuh-Wen Aung • *Department of Restorative Dentistry, Faculty of Dentistry, University of Malaya, Kuala Lumpur, Malaysia; Regenerative Dentistry Research Group, Faculty of Dentistry, University of Malaya, Kuala Lumpur, Malaysia*

Gilda A. Barabino • *Department of Biomedical Engineering, Grove School of Engineering, The City University of New York – The City College, New York, NY, USA*

Alexander G. Bassuk • *Department of Pediatrics, University of Iowa, Iowa City, IA, USA; Department of Neurology, University of Iowa, Iowa City, IA, USA*

Anthony T. Bejjani • *Department of Biology, American University of Beirut, Beirut, Lebanon*

Sangeeta Bhaskar • *Product Development Cell, National Institute of Immunology, New Delhi, India*

Cesar V. Borlongan • *Center of Excellence for Aging & Brain Repair, Morsani College of Medicine, University of South Florida, Tampa, FL, USA; Department of Neurosurgery and Brain Repair, Morsani College of Medicine, University of South Florida, Tampa, FL, USA*

Rasmus Jentoft Boutrup • *Section for Sport Science, Department of Public Health, Aarhus University, Aarhus, Denmark*

Huseyin Cagsin • *Department of Molecular Biology and Genetics, Faculty of Art and Sciences, Near East University, Nicosia, Cyprus*

Klemen Čamernik • *Faculty of Pharmacy, Department of Clinical Biochemistry, University of Ljubljana, Ljubljana, Slovenia*

Ya-Ju Chang • *Department of Ophthalmology, Columbia University, New York, NY, USA; Jonas Children's Vision Care, Bernard and Shirlee Brown Glaucoma Laboratory, Columbia University, New York, NY, USA*

Anastasia Cheng • *Research Institute of the McGill University Health Centre (MUHC), Montreal, QC, Canada*

Inés Colmegna • *Research Institute of the McGill University Health Centre (MUHC), Montreal, QC, Canada; Division of Rheumatology, Department of Medicine, McGill University, Montreal, QC, Canada*

Xuan Cui • *Department of Ophthalmology, Columbia University, New York, NY, USA; Jonas Children's Vision Care, Bernard and Shirlee Brown Glaucoma Laboratory, Columbia University, New York, NY, USA*

Marek Dobke • *Division of Plastic Surgery, University of California, San Diego, CA, USA*

Christina K. Ferrone • *Department of Pathology and Molecular Medicine, Queen's University, Kingston, ON, Canada*

Meenakshi Gaur • *Aelan Cell Technologies, San Francisco, CA, USA*

Renate Gehwolf • *Institute of Tendon and Bone Regeneration, Paracelsus Medical University – Spinal Cord Injury and Tissue Regeneration Center Salzburg, Salzburg, Austria; Austrian Cluster for Tissue Regeneration, Vienna, Austria*

Noël Ghanem • *Department of Biology, American University of Beirut, Beirut, Lebanon*

M. Grant Liska • *Department of Neurosurgery and Brain Repair, Center of Excellence for Aging and Brain Repair, University of South Florida, Morsani College of Medicine, Tampa, FL, USA*

Karl John Habashy • *Department of Biology, American University of Beirut, Beirut, Lebanon*

Nour N. Halaby • *Department of Biology, American University of Beirut, Beirut, Lebanon*

Yohei Hayashi • *Cell Resource Center for Biomedical Research, Institute of Development, Aging and Cancer (IDAC), Tohoku University, Sendai, Miyagi, Japan; Graduate School of Life Sciences, Tohoku University, Sendai, Miyagi, Japan; The Japan Agency for Medical Research and Development-Core Research for Evolutional Science and Technology (AMED-CREST), Tokyo, Japan*

Henriette Henze • *Leibniz-Institute on Aging – Fritz-Lipmann-Institute, Jena, Germany*

Sören S. Hüttner • *Leibniz-Institute on Aging – Fritz-Lipmann-Institute, Jena, Germany*

Carine Jaafar • *Department of Biology, American University of Beirut, Beirut, Lebanon*

Marie Juliane Jung • *Leibniz-Institute on Aging – Fritz-Lipmann-Institute, Jena, Germany*

Yuji Kaneko • *Department of Neurosurgery and Brain Repair, Center of Excellence for Aging and Brain Repair, University of South Florida, Morsani College of Medicine, Tampa, FL, USA*

Jea-Young Lee • *Department of Neurosurgery and Brain Repair, Center of Excellence for Aging and Brain Repair, University of South Florida, Morsani College of Medicine, Tampa, FL, USA*

Christine Lehner • *Institute of Tendon and Bone Regeneration, Paracelsus Medical University – Spinal Cord Injury and Tissue Regeneration Center Salzburg, Salzburg, Austria; Austrian Cluster for Tissue Regeneration, Vienna, Austria*

Roger Lin • *Department of Neurosurgery and Brain Repair, Center of Excellence for Aging and Brain Repair, University of South Florida, Morsani College of Medicine, Tampa, FL, USA*

Yuhui Lin • *The Waterhouse, NaoRococo, Singapore, Singapore*

Trenton Lippert • *Department of Neurosurgery and Brain Repair, Center of Excellence for Aging and Brain Repair, University of South Florida, Morsani College of Medicine, Tampa, FL, USA*

Victoria V. Lunyak • *Aelan Cell Technologies, San Francisco, CA, USA*

Vinit B. Mahajan • *Palo Alto Veterans Administration, Palo Alto, CA, USA; Omics Lab, Department of Ophthalmology, Byers Eye Institute, Stanford University, Palo Alto, CA, USA*

Janja Marc • *Faculty of Pharmacy, Department of Clinical Biochemistry, University of Ljubljana, Ljubljana, Slovenia*

Yasuhisa Matsui • *Cell Resource Center for Biomedical Research, Institute of Development, Aging and Cancer (IDAC), Tohoku University, Sendai, Miyagi, Japan; Graduate School of Life Sciences, Tohoku University, Sendai, Miyagi, Japan; The Japan Agency for Medical Research and Development-Core Research for Evolutional Science and Technology (AMED-CREST), Tokyo, Japan; Center for Regulatory Epigenome and Diseases, Tohoku University School of Medicine, Sendai, Miyagi, Japan*

MERDIYE MAVIS • *Department of Molecular Biology and Genetics, Faculty of Art and Sciences, Near East University, Nicosia, Cyprus*
YI-LIANG MIAO • *Institute of Stem Cell and Regenerative Biology, College of Animal Science and Veterinary Medicine, Huazhong Agricultural University, Wuhan, Hubei, China*
VICTORIA MOISEEVA • *Cell Biology Group, Department of Experimental and Health Sciences, Pompeu Fabra University (UPF), CIBER on Neurodegenerative Diseases (CIBERNED), Barcelona, Spain*
PURA MUÑOZ-CÁNOVES • *Cell Biology Group, Department of Experimental and Health Sciences, Pompeu Fabra University (UPF), CIBER on Neurodegenerative Diseases (CIBERNED), Barcelona, Spain; Spanish National Center on Cardiovascular Research (CNIC), Madrid, Spain; Institució Catalana de Recerca i Estudis Avançats (ICREA), Barcelona, Spain*
STÉPHANIE NADEAU • *CRCHUM et Institut du cancer de Montréal, Montreal, QC, Canada*
RENUKA R. NAIR • *Sree Chitra Tirunal Institute for Medical Sciences and Technology, Thiruvananthapuram, India*
HUNG NGUYEN • *Department of Neurosurgery and Brain Repair, Center of Excellence for Aging and Brain Repair, University of South Florida, Morsani College of Medicine, Tampa, FL, USA*
COURTNEY R. OGANDO • *Department of Biomedical Engineering, Grove School of Engineering, The City University of New York – The City College, New York, NY, USA*
SAAD OMAIS • *Department of Biology, American University of Beirut, Beirut, Lebanon*
RAJARSHI PAL • *Eyestem Research, Centre for Cellular and Molecular Platforms (CCAMP), Bangalore, India*
EUSEBIO PERDIGUERO • *Cell Biology Group, Department of Experimental and Health Sciences, Pompeu Fabra University (UPF), CIBER on Neurodegenerative Diseases (CIBERNED), Barcelona, Spain*
THAMIL SELVEE RAMASAMY • *Stem Cell Biological Laboratory, Department of Molecular Medicine, Faculty of Medicine, University of Malaya, Kuala Lumpur, Malaysia*
REENA J. RATHOD • *Eyestem Research, Centre for Cellular and Molecular Platforms (CCAMP), Bangalore, India*
MICHAEL J. RAUH • *Department of Pathology and Molecular Medicine, Queen's University, Kingston, ON, Canada*
FRANCIS RODIER • *CRCHUM et Institut du cancer de Montréal, Montreal, QC, Canada; Département de Radiologie, Radio-Oncologie et Médicine Nucléaire, Université de Montréal, Montreal, QC, Canada*
ALESSANDRA SACCO • *Development, Aging and Regeneration Program, Sanford Burnham Prebys Medical Discovery Institute, La Jolla, CA, USA*
SHERIN SAHEERA • *Sree Chitra Tirunal Institute for Medical Sciences and Technology, Thiruvananthapuram, India; Department of Biomedical Engineering, The University of Alabama, Birmingham, Birmingham, AL, USA*
MANUEL SCHMIDT • *Leibniz-Institute on Aging – Fritz-Lipmann-Institute, Jena, Germany*
SVENJA C. SCHÜLER • *Leibniz-Institute on Aging – Fritz-Lipmann-Institute, Jena, Germany*
NEDIME SERAKINCI • *Department of Medical Genetics, Faculty of Medicine, Near East University, Nicosia, Cyprus; Department of Molecular Biology and Genetics, Faculty of Art and Sciences, Near East University, Nicosia, Cyprus*
FERIDE SEVERCAN • *Department of Biophysics, Altınbaş University School of Medicine, İstanbul, Turkey; Department of Biological Sciences, Middle East Technical University, Ankara, Turkey*

Bindu Singh • *Product Development Cell, National Institute of Immunology, New Delhi, India*
Brooke Snetsinger • *Department of Pathology and Molecular Medicine, Queen's University, Kingston, ON, Canada*
Gabriel Spitzer • *Institute of Tendon and Bone Regeneration, Paracelsus Medical University – Spinal Cord Injury and Tissue Regeneration Center Salzburg, Salzburg, Austria; Austrian Cluster for Tissue Regeneration, Vienna, Austria*
Michael J. Stec • *Development, Aging and Regeneration Program, Sanford Burnham Prebys Medical Discovery Institute, La Jolla, CA, USA*
Harshini Surendran • *Eyestem Research, Centre for Cellular and Molecular Platforms (CCAMP), Bangalore, India*
Herbert Tempfer • *Institute of Tendon and Bone Regeneration, Paracelsus Medical University – Spinal Cord Injury and Tissue Regeneration Center Salzburg, Salzburg, Austria; Austrian Cluster for Tissue Regeneration, Vienna, Austria*
Matthew T. Tierney • *Robin Chemers Neustein Laboratory of Mammalian Cell Biology and Development, Howard Hughes Medical Institute, The Rockefeller University, New York, NY, USA*
Andreas Traweger • *Institute of Tendon and Bone Regeneration, Paracelsus Medical University – Spinal Cord Injury and Tissue Regeneration Center Salzburg, Salzburg, Austria; Austrian Cluster for Tissue Regeneration, Vienna, Austria*
Yi-Ting Tsai • *Department of Ophthalmology, Columbia University, New York, NY, USA; Institute of Human Nutrition, College of Physicians and Surgeons, Columbia University, New York, NY, USA*
Stephen H. Tsang • *Department of Ophthalmology, Columbia University, New York, NY, USA; Jonas Children's Vision Care, Bernard and Shirlee Brown Glaucoma Laboratory, Columbia University, New York, NY, USA; Institute of Human Nutrition, College of Physicians and Surgeons, Columbia University, New York, NY, USA; Department of Pathology and Cell Biology, Columbia University, New York, NY, USA*
Julia von Maltzahn • *Leibniz-Institute on Aging – Fritz-Lipmann-Institute, Jena, Germany*
Andrea Wagner • *Institute of Tendon and Bone Regeneration, Paracelsus Medical University – Spinal Cord Injury and Tissue Regeneration Center Salzburg, Salzburg, Austria; Austrian Cluster for Tissue Regeneration, Vienna, Austria*
Nadja Weissenbacher • *Institute of Tendon and Bone Regeneration, Paracelsus Medical University – Spinal Cord Injury and Tissue Regeneration Center Salzburg, Salzburg, Austria; Austrian Cluster for Tissue Regeneration, Vienna, Austria*
Dan-Ya Wu • *Institute of Stem Cell and Regenerative Biology, College of Animal Science and Veterinary Medicine, Huazhong Agricultural University, Wuhan, Hubei, China*
Christine L. Xu • *Department of Ophthalmology, Columbia University, New York, NY, USA; Jonas Children's Vision Care, Bernard and Shirlee Brown Glaucoma Laboratory, Columbia University, New York, NY, USA*
Yueh-Hsun Kevin Yang • *Department of Biomedical Engineering, Grove School of Engineering, The City University of New York – The City College, New York, NY, USA*
Xia Zhang • *Institute of Stem Cell and Regenerative Biology, College of Animal Science and Veterinary Medicine, Huazhong Agricultural University, Wuhan, Hubei, China*
Janja Zupan • *Faculty of Pharmacy, Department of Clinical Biochemistry, University of Ljubljana, Ljubljana, Slovenia*

Methods in Molecular Biology (2019) 2045: 1–11
DOI 10.1007/7651_2018_139

Published online: 30 May 2018

Assessing Muscle Stem Cell Clonal Complexity During Aging

Matthew T. Tierney, Michael J. Stec, and Alessandra Sacco

Abstract

Changes in muscle stem cell (MuSC) function during aging have been assessed using various in vivo and ex vivo systems. However, changes in clonal complexity within the aged MuSC pool are relatively understudied. Although the dissection of stem cell heterogeneity has greatly benefited from several technological advancements, including single cell sequencing, these methods preclude longitudinal measures of individual stem cell behavior. Instead, multicolor labeling systems enable lineage tracing with single cell resolution. Here, we describe a method of inducibly labeling MuSCs with the *Brainbow-2.1* multicolor lineage tracing reporter in vivo to track individual MuSC fate and assess clonal complexity in the overall MuSC pool throughout the mouse lifespan.

Keywords Aging, Brainbow, Clonal complexity, Multicolor lineage tracing, Satellite cell, Skeletal muscle

1 Introduction

Skeletal muscle tissue is comprised of long, multinucleated myofibers which are formed by the fusion of muscle stem cell (MuSC) precursors during development. In adult muscle tissue, MuSCs are maintained in a quiescent state beneath the basal lamina of the myofiber. Upon activation, MuSCs are able to self-renew and differentiate to contribute to myonuclear accretion and myofiber formation. Thus, MuSCs play important roles in regulating skeletal muscle development, regeneration, and homeostatic maintenance [1–3].

During aging, a decline in MuSC function and number leads to an impairment in muscle regenerative capacity [4]. However, while several studies have examined MuSC behavior at single cell resolution [5] or uncovered relevant subpopulations with functional distinctions [5–8], work directly examining how MuSC clonal complexity is regulated at the population level with age is lacking. Given that MuSCs are functionally heterogeneous [9], understanding how the diversity of the MuSC pool is affected throughout the lifespan will provide us with a greater depth of knowledge on how the MuSC population is regulated during aging. In this chapter, we describe a method that can be used to accurately assess MuSC fate

in mice by using in vivo multicolor lineage tracing [10]. Using the *Brainbow-2.1* genetic labeling strategy [11, 12], assessing longitudinal changes in MuSC clonal complexity can provide valuable information on the dynamics of the MuSC pool during aging.

2 Materials

2.1 Mice

Pax7-CreER™ mice [13] bred with $R26R^{Brainbow2.1}$ [11] mice are used to generate *Pax7-CreER*™/$R26R^{Brainbow2.1}$ mice. Mice heterozygous for both *Pax7-CreER*™ and $R26R^{Brainbow2.1}$ alleles are used for experiments.

2.2 Tissue Collection and Cryosectioning

1. Tamoxifen (catalog number T5648) suspended in corn oil at 20 mg/mL
2. 1 mL syringe with 21 G needle
3. Paraformaldehyde: 0.5% in PBS
4. Sucrose: 20% (w/v) in PBS
5. Biopsy cryomolds, 10 × 10 × 15 mm
6. O.C.T. compound
7. 2-Methylbutane
8. Microscope slides, Superfrost Plus, 25 × 75 × 1.0 mm
9. Research cryostat, CM3050 S (Leica)

2.3 Immunostaining

1. Hydrophobic PAP pen
2. Slide staining humidity box, black cover
3. Blocking buffer: PBS containing 20% normal goat serum, 0.1% Triton X-100
4. Antibodies
   (a) Rabbit anti-laminin 0.5 mg/mL (catalog number L9393) (Sigma)
   (b) Alexa Fluor 647 anti-rabbit secondary antibody (catalog number A-21245) (Thermo Fisher Scientific)
5. Fluoromount-G mounting medium
6. Microscope cover glass, 24 × 50 mm

2.4 Image Acquisition and Analysis

1. Confocal laser-scanning microscope, equipped with *458, 488, 514, 561, and 633 nm lasers*, Plan-Apochromat 20–40× objectives, and imaging software (Zeiss)
2. ImageJ software (National Institutes of Health)
3. Microsoft Excel 2016 (Microsoft Corporation)

3 Methods

3.1 Tissue Preparation and Immunostaining

1. Prior to harvesting skeletal muscles, induce *Brainbow-2.1* multicolor reporter expression in MuSCs by administering tamoxifen. Inject 100 mg/kg body weight of tamoxifen daily, for 5 consecutive days; via intraperitoneal injection using a 1-mL syringe with 21 G needle (*see* **Note 1**).
2. At the desired time point after tamoxifen-induced recombination, anesthetize the mouse and sacrifice according to the Institutional Animal Care and Use Committee (IACUC) guidelines.
3. Place the mouse on a surgical bench and clean the hind limbs with 70% ethanol. To harvest the tibialis anterior muscle, remove the skin covering the hind limbs and use a razor blade to sever the distal tendon. Carefully pull this tendon towards the knee, sliding a razor blade along the length of the tibia to cleanly separate the muscle, and remove by severing the proximal tendon (*see* **Note 2**).
4. Fix the tibialis anterior by placing the muscle in an Eppendorf tube filled with 0.5% paraformaldehyde for 4 h at 4 °C, then transferring the muscle to a 20% w/v sucrose solution overnight at 4 °C.
5. Place the fixed muscle in a biopsy cryomold filled with O.C.T. compound, positioned longitudinally to allow for cross sections to be cut. Place the bottom of the cryomold on top of liquid nitrogen-chilled 2-methylbutane until it is completely frozen over and then submerge for 1 min. Remove the cryomold and place on dry ice. Frozen samples can be stored at −80 °C until ready to be cryosectioned.
6. Set the cryostat chamber temperature to −20 °C, and allow the cryomold to reach temperature by placing it in the cryostat for several minutes before sectioning. Cut serial 10 μm sections of the cryomold on to serial slides (*see* **Note 3**). Make sure that the core ~80% of the muscle is sectioned in order to be able to choose the center of the muscle for analysis. Label and store unused slides at −20 °C until ready for immunostaining.
7. Remove slides from storage at −20 °C and let come to room temperature. Encircle muscle sections with a hydrophobic PAP pen and place slides in a humid incubation box, where all subsequent steps should be performed.
8. Block and permeabilize sections in blocking buffer for 1 h at room temperature (*see* **Note 4**).
9. Incubate sections with rabbit anti-laminin (1:200 dilution) diluted in blocking buffer for 2 h (or overnight) at room temperature.

10. Aspirate the primary antibody and perform three PBS washes for 5 min each. Incubate the sections with Alexa Fluor 647 anti-rabbit secondary antibody (1:400 dilution) at room temperature for 1 h.
11. Aspirate the secondary antibody and perform three PBS washes for 5 min each. Mount slides with Fluoromount-G mounting medium and microscope cover glass. Store the stained slides at 4 °C until ready to be imaged.

3.2 Image Acquisition

1. All images for fluorescent protein quantification should be acquired using a confocal laser-scanning microscope system and imaging software capable of "stitching" 2D mosaics of the muscle being analyzed (*see* **Note 5**).
2. Determine the desired field of view and z-resolution within the skeletal muscle for imaging. For complete spatial analyses, image acquisition of the entire muscle is desirable, and in the case of point analyses (i.e., single GFP^+ nuclei analysis), required (*see* **Note 6**).
3. Each fluorescent protein channel is acquired sequentially, to avoid spectral bleed through and ensure the accurate separation of the different fluorescent proteins. The excitation wavelengths and emission filter settings for each are listed below (*see* **Note 7**) (Fig. 1):
   (a) Cerulean (CFP): excitation 458 nm; emission filter 460–490 nm
   (b) Green (GFP): excitation 488 nm; emission filter 490–530 nm
   (c) Yellow (YFP): excitation 514 nm; emission filter 520–560 nm

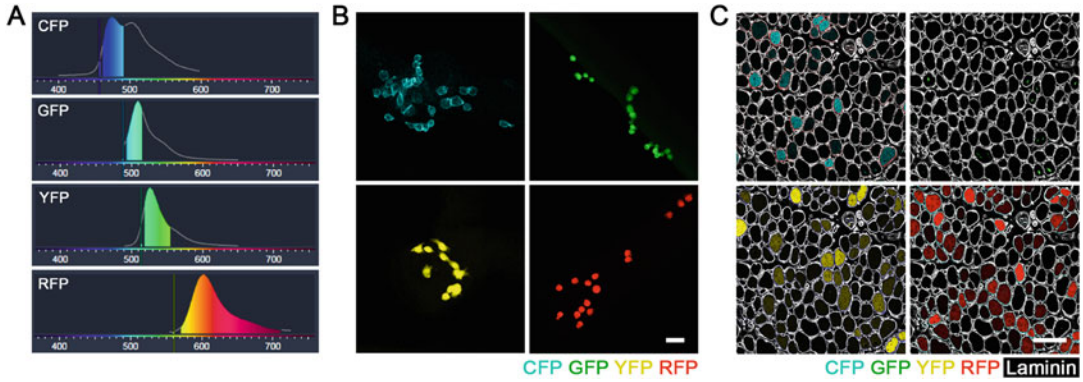

Fig. 1 Brainbow 2.1 image acquisition. (**a**) Emission spectra for each fluorescent protein. (**b**, **c**) Representative images of each fluorescent protein in myofiber-associated muscle stem cells (MuSCs) (in **b**) grown for 72 h in culture and MuSC-derived myofibers (in **c**) 7 days following acute barium chloride injury (scale bar = 20 and 50 μm, respectively)

(d) Red (RFP): excitation 561 nm; emission filter 570–620 nm

(e) Laminin/Alexa Fluor 647: excitation 633 nm; emission filter 640–750 nm

4. Once acquired, collect and save all images as layered .tiff files for analysis. Individual spectral signatures may be difficult to extract, depending on the imaging hardware being used. In particular, optimal separation of the GFP and YFP channels may not be possible as their spectra are highly overlapping (Fig. 1). In this case, various spectral unmixing strategies can be employed. The researcher may also take advantage of the nuclear and cytoplasmic localization of GFP and YFP, respectively, to allow for their distinction from one another (*see* **Note 8**).

3.3 Fluorescent Protein Quantification

1. Prepare separate images containing each individual fluorescent protein channel (CFP, GFP, YFP, and RFP) and the laminin immunostain as individual .tiff files. Adjust the brightness and contrast of the laminin image only, as needed to improve the detection of individual myofibers.
2. Run the myofiber cross sectional area (CSA) measurement macro by selecting *Plugin/Macro/Run* from the main ImageJ menu and then choose the file "Macro_seg_5_modif.ijm.txt" [14]. When prompted, choose the laminin image to be analyzed (*see* **Note 9**).
3. After the macro is finished running, manually inspect the CSA outlines in the pseudo-colored image outlining individual myofibers and add/delete outlines as appropriate (*see* **Note 10**) (Fig. 2).
4. When all myofibers are outlined, go to the regions of interest (ROI) manager and select *More/Save* to save the outlines.
5. Open the fluorescent protein images in ImageJ. Adjust image size if necessary, to be consistent with laminin image size for overlaying myofiber CSA outlines, and save as .tiff files.
6. For each fluorescent protein image separately, select *Edit/Selection/Add to Manager* (or alternatively, press the "t" key). In the ROI manager, select *More/Open*, and open the corresponding laminin outlines (from **step 4**) for that image. Select the box *Show All* in the ROI manager to see the outlines overlayed on the fluorescent protein image.
7. To measure the fluorescence intensity for each individual fiber, select *Analyze/Set Measurements* from the main menu, and select the box *Mean Gray Value* (*see* **Note 11**).

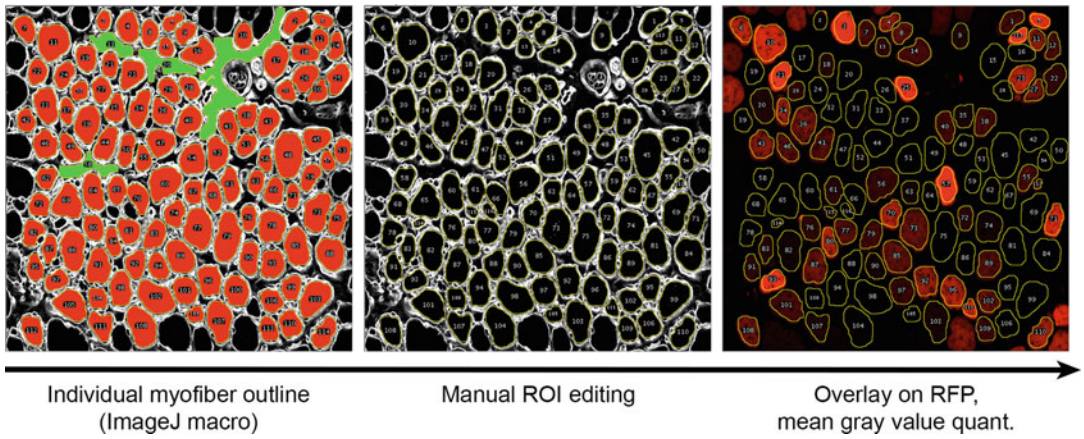

Fig. 2 Fluorescent protein quantification by myofiber masking. Workflow of myofiber masking using the ImageJ macro (masks with high confidence in red, masks with low confidence in yellow/green), manual refinement of the selected regions of interest (ROI), and the overlay of those ROIs on the corresponding image of a fluorescent protein for quantification

8. In the ROI Manager, click *Measure* and a window with the mean gray value for each fiber will appear. Select and copy all data into an Excel file.
9. Repeat this process for all of the fluorescent protein images, creating columns in the Excel spreadsheet for the mean gray value of the CFP, YFP, and RFP fluorescent proteins for each myofiber. Myofibers containing GFP^+ nuclei must be manually counted and assigned to the correct myofiber due to the nuclear localization of GFP in this system.
10. Once the data is compiled in Excel, a threshold is set for the mean gray value of each of the fluorescent proteins. When setting mean gray value thresholds for each color channel, it is useful to have a negative control sample to determine thresholds and prevent "false positive" determinations. To do this, prepare, immunostain, and image muscle sections from a wild-type mouse in parallel to *Pax7-CreER*™/*R26R*$^{Brainbow2.1}$ samples. Quantify the mean gray value of the myofibers in the wild-type sample for each of the fluorescent protein channels and use the highest mean gray value recorded for each of the channels for threshold determination.
11. If the mean gray value for a myofiber exceeds the mean gray value threshold, it is considered to be positive for that fluorescent protein. The number of fluorescent proteins that an individual myofiber is positive for is summed, and this data is used as a measure of the spatial distribution of labeled MuSC contribution to individual myofibers throughout the skeletal muscle examined.

3.4 Spatial Distribution Analysis

1. Prepare separate images containing either merged GFP and laminin fluorescent protein channels or the GFP channel only as individual .tiff files and upload to ImageJ.
2. To perform "cluster" analyses, groups of GFP^+ labeled myofibers are manually scored throughout the muscle, recording the number of adjacent myofibers containing GFP^+ MuSC-derived nuclei in each cluster. Determine the total area of the muscle being analyzed. Calculated distributions of myofiber cluster density and the number of GFP^+ myofibers within each cluster provide measures of clonal clustering in each experimental setting assessed (*see* **Note 12**).
3. To perform spatial "point" analyses, convert the GFP only image to an assortment of individual point measures by changing to an 8-bit grayscale image (select *Image/Type/8-bit* from the main menu), reversing the image (select *Edit/Invert)*, and making all signal binary (select *Process/Binary/Make Binary*).
4. To determine the position of each GFP^+ nuclei within the muscle, select *Analyze/Set Measurements* and check *Centroid*. Then, select *Analyze/Analyze Particles*, choose a range of particle sizes (*see* **Note 13**), toggle *Show Outlines*, check *Display Results*, and click *OK*. A table containing *x* and *y* coordinates will appear, along with the generation of a new image displaying the outline of each particle measured. Manually inspect the image to be sure that particle assignment is accurate (Fig. 3).
5. To determine Euclidean total distance "*d*" between GFP^+ nuclei, enter the following formula into Excel:

$$d = \sqrt{(x_2 - x_1)^2 + (y_2 - y_1)^2}$$

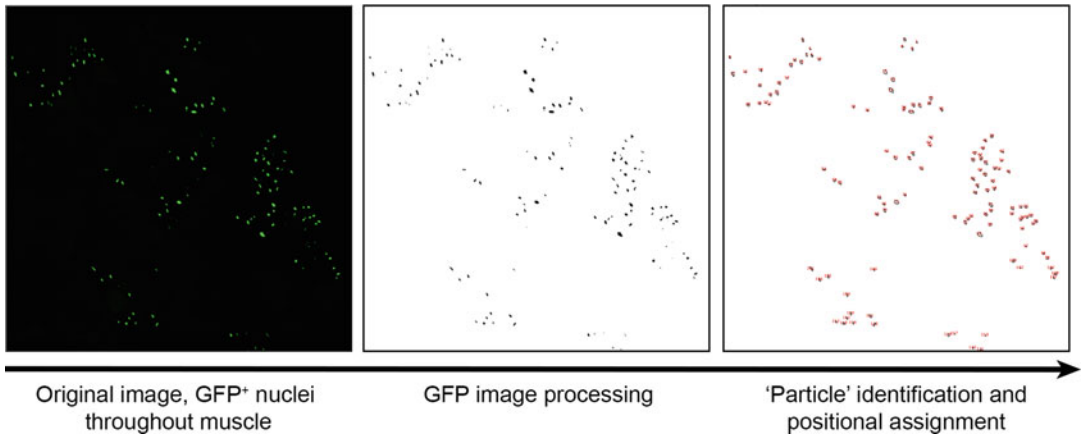

Fig. 3 Spatial distribution analysis using point measures. Workflow of image processing to convert GFP^+ MuSC-derived myonuclei to binary "particle" measures, their automated detection, and assignment of positional *x* and *y* coordinates for spatial measures

Convert this distance in pixels to the desired unit of length and bin accordingly to achieve a distribution of Euclidean distances within your sample.

6. To determine the nearest neighbor distance for each GFP$^+$ nuclei, select *Plugins/Nnd* from the main menu (*see* **Note 14**). A table containing the nearest neighbor distance will appear in pixels.
7. To calculate a nearest neighbor index (*see* **Note 15**), input the nearest neighbor distance "d," nuclei number "n," and nuclei density "ρ" into the following formula in Excel [15]:

$$\text{Index} = \frac{\sum d/n}{1/\left(2 \cdot \sqrt{\rho}\right)}$$

Cumulative nearest neighbor distributions can be plotted and compared to a Poisson, or random, distribution using the following formula [16]:

$$f(x) = 1 - e^{\left(\rho \cdot \pi \cdot d^2\right)}$$

4 Notes

1. Daily administration of 100 mg/kg body weight tamoxifen at postnatal day 24–28 in this model, in our hands, results in ~50% MuSC labeling frequency. This dosing regimen can and should be adjusted in accordance with the specific time frame being studied (development, adulthood, aging, etc.) and desired recombination efficiency, depending on the nature of the experiment.
2. Other muscles of the hind limb may be harvested for analysis, in accordance with the researcher's interests. To harvest the gastrocnemius and soleus muscles, sever the Achilles tendon and carefully pull up the limb until separated from the anterior compartment. Use a razor blade to remove these muscles from the hamstring and each other.
3. Several slides containing serial sections may be prepared to examine the expression patterns and spatial distributions of several proteins, in addition to laminin.
4. During the immunostaining process, make sure that the tissue sections do not completely dry during any of the steps, as this will increase background fluorescence.
5. For imaging all fluorescent proteins, we used an LSM170 laser-scanning confocal microscope with a 20×/0.8 Plan-Apochromat objective. For spatial analysis, laminin and GFP

composite images were stitched together and prepared in ZEN 2011 imaging software (Zeiss) using the Tiles module.

6. The acquisition of a complete 2D mosaic of the whole muscle can be limited to only GFP and laminin if desired, as only these are required for point analyses of GFP^+ nuclei. When imaging all fluorescent proteins for quantification in individual myofibers, individual images may be taken at representative points within the muscle, to limit image acquisition time to a reasonable length.
7. Main beam splitter (MBS) filters were used, matching the laser lines used for each fluorescent protein.
8. Mathematical subtraction of nonspecific GFP signal from YFP fluorescence can be achieved in ImageJ. Convert both images to 8-bit grayscale, select *Process/Image Calculator*, toggle the correct image names and *Subtract*, check *Create New Window*, and click *OK*. This is particularly useful when imaging regenerated skeletal muscle, as the central position of nuclei within each myofiber allows for their clear identification, distinction, and subtraction.
9. This macro requires that images to be analyzed be stored in the same folder as the macro file itself; prepare this folder prior to analysis in ImageJ.
10. While the majority of myofibers should be accurately recognized and colored in red, other myofibers may not be recognized, several myofibers may be interpreted as a single myofiber, or interstitial regions may be falsely identified as myofibers. Myofibers may be added after outlining by clicking *Add(t)* in the ROI manager, while non-myofibers may be eliminated by highlighting those regions and clicking *Delete* in the ROI manager.
11. Other measurements, including area and Feret's diameter, are available and can be selected for output as desired for correlation with fluorescent protein quantification.
12. The total number of GFP^+ myofibers per unit area should remain constant when comparing samples, as over a large enough area this acts as an indicator of recombination efficiency under most circumstances.
13. In particular, a minimum particle size should be specified to exclude nonspecific background "noise" of artifacts that are significantly smaller than nuclei.
14. Prior to beginning nearest neighbor analysis, download and install the ImageJ plugin found here: https://icme.hpc.msstate.edu/mediawiki/index.php/Nearest_Neighbor_Distances_Calculation_with_ImageJ.

15. The nearest neighbor index is expressed as a ratio of the observed and expected distances, given a random distribution. Using this metric, the spatial distribution of GFP^+ nuclei can be determined to be clustered (<1.0), random (=1.0), or regularly dispersed (1.1–2.5).

Acknowledgements

This work was supported by NIH grant R01 AR064873 (to A.S.), NIH grant F31 AR065923 (to M.T.T.), and NIH grant F32 AR070630 (to M.J.S.). We thank Leslie Boyd, Buddy Charbono, and the Cell Imaging and Animal Core Facilities at SBPMDI for technical support.

References

1. Yin H, Price F, Rudnicki MA (2013) Satellite cells and the muscle stem cell niche. Physiol Rev 93(1):23–67. https://doi.org/10.1152/physrev.00043.2011
2. Keefe AC, Lawson JA, Flygare SD, Fox ZD, Colasanto MP, Mathew SJ, Yandell M, Kardon G (2015) Muscle stem cells contribute to myofibres in sedentary adult mice. Nat Commun 6:7087. https://doi.org/10.1038/ncomms8087
3. Pawlikowski B, Pulliam C, Betta ND, Kardon G, Olwin BB (2015) Pervasive satellite cell contribution to uninjured adult muscle fibers. Skelet Muscle 5:42. https://doi.org/10.1186/s13395-015-0067-1
4. Sacco A, Puri PL (2015) Regulation of muscle satellite cell function in tissue homeostasis and aging. Cell Stem Cell 16(6):585–587. https://doi.org/10.1016/j.stem.2015.05.007
5. Sacco A, Doyonnas R, Kraft P, Vitorovic S, Blau HM (2008) Self-renewal and expansion of single transplanted muscle stem cells. Nature 456(7221):502–506. https://doi.org/10.1038/nature07384
6. Kuang S, Kuroda K, Le Grand F, Rudnicki MA (2007) Asymmetric self-renewal and commitment of satellite stem cells in muscle. Cell 129(5):999–1010. https://doi.org/10.1016/j.cell.2007.03.044
7. Rocheteau P, Gayraud-Morel B, Siegl-Cachedenier I, Blasco MA, Tajbakhsh S (2012) A subpopulation of adult skeletal muscle stem cells retains all template DNA strands after cell division. Cell 148(1–2):112–125. https://doi.org/10.1016/j.cell.2011.11.049
8. Collins CA, Olsen I, Zammit PS, Heslop L, Petrie A, Partridge TA, Morgan JE (2005) Stem cell function, self-renewal, and behavioral heterogeneity of cells from the adult muscle satellite cell niche. Cell 122(2):289–301. https://doi.org/10.1016/j.cell.2005.05.010
9. Tierney MT, Sacco A (2016) Satellite cell heterogeneity in skeletal muscle homeostasis. Trends Cell Biol 26(6):434–444. https://doi.org/10.1016/j.tcb.2016.02.004
10. Tierney MT, Stec MJ, Rulands S, Simons BD, Sacco A (2018) Muscle stem cells exhibit distinct clonal dynamics in response to tissue repair and homeostatic aging. Cell Stem Cell 22(1):119–127.e113. https://doi.org/10.1016/j.stem.2017.11.009. S1934-5909(17)30461-7 [pii]
11. Snippert HJ, van der Flier LG, Sato T, van Es JH, van den Born M, Kroon-Veenboer C, Barker N, Klein AM, van Rheenen J, Simons BD, Clevers H (2010) Intestinal crypt homeostasis results from neutral competition between symmetrically dividing Lgr5 stem cells. Cell 143(1):134–144. https://doi.org/10.1016/j.cell.2010.09.016
12. Livet J, Weissman TA, Kang H, Draft RW, Lu J, Bennis RA, Sanes JR, Lichtman JW (2007) Transgenic strategies for combinatorial expression of fluorescent proteins in the nervous system. Nature 450(7166):56–62. https://doi.org/10.1038/nature06293. nature06293 [pii]
13. Nishijo K, Hosoyama T, Bjornson CR, Schaffer BS, Prajapati SI, Bahadur AN, Hansen MS, Blandford MC, McCleish AT, Rubin BP,

Epstein JA, Rando TA, Capecchi MR, Keller C (2009) Biomarker system for studying muscle, stem cells, and cancer in vivo. FASEB J 23 (8):2681–2690. https://doi.org/10.1096/fj.08-128116

14. Noirez P, Torres S, Cebrian J, Agbulut O, Peltzer J, Butler-Browne G, Daegelen D, Martelly I, Keller A, Ferry A (2006) TGF-beta1 favors the development of fast type identity during soleus muscle regeneration. J Muscle Res Cell Motil 27(1):1–8. https://doi.org/10.1007/s10974-005-9014-9
15. Clark PJ, Evans FC (1954) Distance to nearest neighbor as a measure of spatial relationships in populations. Ecology 35(4):445–453. https://doi.org/10.2307/1931034
16. Diggle P (1983) Statistical analysis of spatial point patterns. Mathematics in biology. Academic Press, London, New York

Methods in Molecular Biology (2019) 2045: 13–23
DOI 10.1007/7651_2019_210

Published online: 16 February 2019

Simultaneous Isolation of Stem and Niche Cells of Skeletal Muscle: Applicability for Aging Studies

Eusebio Perdiguero, Victoria Moiseeva, and Pura Muñoz-Cánoves

Abstract

The maintenance of adult stem cells in their normal quiescent state depends on intrinsic factors and extrinsic signals originating from their microenvironment (also known as the stem cell niche). In skeletal muscle, its stem cells (satellite cells) lose their regenerative potential with aging, and this has been attributed, at least in part, to both age-associated changes in the satellite cells as in the niche cells, which include resident fibro-adipogenic progenitors (FAPs), macrophages, and endothelial cells, among others. To understand the regenerative decline of skeletal muscle with aging, there is a need for methods to specifically isolate stem and niche cells from resting muscle. Here we describe a fluorescence-activated cell sorting (FACS) protocol to simultaneously isolate discrete populations of satellite cells and niche cells from skeletal muscle of aging mice.

Keywords Stem cell, Satellite cell, Niche cells, Skeletal muscle, Quiescence, Aging, Flow cytometry, Enzymatic dissociation, FACS

1 Introduction

Aging of skeletal muscle alters the composition of the niche and has deleterious consequences on the functionality of its stem cells and hence on the tissue's regenerative capacity [1–3]. This age-associated decline in regenerative capacity is maximal at geriatric age [4, 5]. For the characterization of the cellular interactions of muscle stem cell with the non-muscle niche-resident cell types, it will be mandatory to isolate these discrete cell populations in a specific way and, if possible, simultaneously, to decrease experimental variability and minimize animal use and costs (particularly in aging studies), as well as users' effort. Surely, isolation of the stem cell niche components of muscle in young and aged mice will help understand regulatory interactions that can help to envision ways to improve aged muscle regeneration.

Satellite cells reside in a quiescent state beneath the basal lamina of myofibers until they are activated by damage or growth signals initiating a process of proliferation/differentiation or self-renewal

Eusebio Perdiguero and Pura Muñoz-Cánoves contributed equally to this work.

to repair adult skeletal muscle and or replenish the stem cell pool [6–9]. Most mammalian satellite cells can be identified by expression of the paired-box transcription factor Pax7, which only labels satellite cells in skeletal muscle. Many other proteins are known to mark satellite cells, including Integrin-α7, M-Cadherin, Caveolin-1, CD56/NCAM, CD29/Integrin-β1, and Syndecan 3 and 4 (reviewed in [6, 10, 11]). However, these markers are also expressed by other interstitial cells within the muscle tissue, so combinations of different markers are used to isolate satellite cells to purity.

Other cellular populations present in the adult skeletal muscle contribute and modulate muscle regeneration, including endothelial cells, pericytes/mesoangioblasts, Pw1+ cells (known as PICs), mesenchymal progenitors normally referred as fibro-adipogenic progenitors (FAPs), and different types of hematopoietic cells which infiltrate the damaged muscle, including neutrophils, circulating blood monocytes that differentiate into inflammatory macrophages and different types of lymphoid cells (eosinophils, Tregs, and CD8+ T cells) [12, 13]. Interplay between all these cell types has been demonstrated to be essential for myogenesis [14–17].

Using well-known markers for different cellular populations, we have set up a procedure to isolate by fluorescence-activated cell sorting (FACS) satellite cells, FAPs, macrophages, and endothelial cells from resting and regeneration skeletal muscle of mice. This procedure can be used both in young/adult as in aging mice.

2 Materials

2.1 Isolation of Satellite Cells, Macrophages, FAPs, and Endothelial Cells by FACS

1. Surgical tools (small scissors, scalpels, fine tip forceps, hemostatic forceps) are cleaned and sterilized by autoclaving.
2. Razor blades.
3. DMEM (Dulbecco's Modified Eagle Medium) high glucose, supplemented with 1% penicillin/streptomycin (P/S) and 10% Fetal Bovine Serum (FBS).
4. Red blood cell lysis buffer (BD Pharm Lyse, 555899).
5. FACS Buffer: Phosphate Buffered Saline (PBS) 1×, 5% Goat Serum.
6. Digestion mix: Liberase (Roche/Sigma-Aldrich, ref. 05401127001; final 0.02%), Dispase II (Sigma-Aldrich, D4693; final 0.05%), 4 μL stock 1 M $CaCl_2$ (final 0.4 mM), 50 μL stock 1 M $MgCl_2$ (final 5 mM) in 10 mL DMEM1% P/S (four limb muscles of one mouse require 10 mL of digestion mix).
7. Antibodies: PE/Cy7 anti-mouse/human Ly-6A/E (Sca-1) (Biolegend, 108114), APC/Cy7 anti-mouse F4/80

(Biolegend, 123118), α7-integrin R-Phycoerythrin (AbLab, 53-0010-05), APC anti-mouse CD31 (PECAM-1) (eBioscience 17-0311-82), BV711 Rat anti-mouse CD45 (BD Pharmingen, 563709).

8. DAPI, stock solution 1 mg/mL, final concentration 1 μg/mL.
9. 50 mL conical tubes (sterile).
10. A shacking water bath.
11. 100 μm, 70 μm, and 40 μm cell strainer filters.
12. Centrifuge with a cooling system for 15–50 mL conical tubes.
13. Centrifuge with a cooling system for 1.5 mL tubes.
14. Hemocytometer.
15. Flow cytometry analyzer (e.g., FACSAria II—BD Biosciences)
16. Flow cytometry analysis software: FACSDiva software (BD Biosciences, available for Windows) or FlowJo software (available for Windows and Mac http://www.flowjo.com/download-flowjo/).

2.2 Confirmation of the Identity of the Distinct FACS-Isolated Cell Populations by RT-qPCR

1. Total RNA isolation kit [e.g., RNeasy Micro kit (Qiagen, 74004)].
2. cDNA synthesis kit [e.g., SuperScript III Reverse Transcriptase (Invitrogen 1674043)].
3. Quantitative PCR apparatus [e.g., LightCycler 480 System using Light Cycler 480 SYBR Green I Master reaction mix (Roche Diagnostic Corporation)].
4. Specific primers for each selected mRNA (Sigma).

3 Methods

3.1 Isolation of Satellite Cells, Macrophages, FAPs, and Endothelial Cells by FACS

1. Euthanize mice according to institute regulations. The following steps should be performed in a tissue culture hood to in order to limit contamination (*see* **Notes 1–4**).
2. Skeletal muscles are dissected with small scissors from fore and hind limbs and collected in cold DMEM 1% P/S into 50 mL conical tubes (*see* **Note 5**).
3. Decant all the muscles collected in a petri dish, and remove DMEM 1% P/S completely.
4. Mince muscles with scissors.
5. Mince muscles further with razor blades.
6. Collect minced muscles into a 50 mL conical tube, and add cold DMEM 1% P/S. Leave muscle sediment, and remove

DMEM 1% P/S, discarding floating fat pieces. Repeat this step to further clean the sample from non-muscle pieces (*see* **Note 5**).

7. Remove DMEM 1% P/S as much as possible, and split the minced muscle into two 50 mL conical tubes.
8. Add 5 mL of the prepared digestion mix (Liberase/Dispase) to each tube (*see* **Notes 6–8**).
9. Incubate 1 h at 37 °C in a shaking water bath (*see* **Note 9**).
10. Centrifuge the samples at 50 × *g* for 10 min at 4 °C.
11. Collect the supernatant and discard the pellet (optional: the pellet can be washed and the supernatant collected and pooled with the previous one).
12. Filter the supernatant with 100 μm and then 70 μm cell strainer filters.
13. Centrifuge at 670 × *g* for 15 min at 4 °C; repeat twice. The supernatant is discarded at each round, and the pellet is resuspended gently in cold DMEM 1% P/S.
14. After the 2nd centrifugation, discard supernatant, and resuspend the pellet in 2 mL of red blood cells lysis buffer 1×. Incubate for 10 min in ice protected from light. Do not agitate.
15. Resuspend in 50 mL cold DMEM 1% P/S. At this step pool the two pellets of the same mouse, and filter through a 40 μM cells strainer filter.
16. Centrifuge at 670 × *g* for 15 min at 4 °C.
17. Discard the supernatant, and resuspend the pellet in 1 mL of cold DMEM 1% P/S.
18. Count the number of cells for each sample (*see* **Note 10**).
19. Centrifuge at 670 × *g* for 15 min at 4 °C, and resuspend the pellet at 1×10^4 cells/μL (1×10^6 cells in 100 μL) in FACS Buffer.
20. Incubate the cells with antibodies for 30 min in ice, protected from light. All antibodies are diluted at ratio 1:200 (*see* **Note 11**).
21. Centrifuge at 670 × *g* for 15 min at 4 °C.
22. Discard the supernatant, and resuspend the cell bulk in 1 mL of FACS Buffer for sample sorting.
23. Add DAPI (final concentration 1 μg/mL) 5 min prior FACS to detect and exclude dead cells. Filter the sample through a test tube with cell strainer cap to eliminate cell aggregation. The sample is now ready to be analyzed by FACS.

Table 1
Positive and negative selection of cell surface markers used to discriminate each cell population of interest

Cell population	Positive selection	Negative selection
Satellite cells	α7-integrin$^+$	CD45, F4/80, CD31$^-$
Macrophages	CD45$^+$, F4/80$^+$	–
FAPs	Sca1$^+$	CD45, F4/80, CD31, α7-integrin$^-$
Endothelial cells	CD31$^+$, α7-integrin$^+$	CD45, F4/80$^-$

24. We typically use the FACSAria II instrument for sorting, and we analyze the data using the FACSDiva or FlowJo software.
25. Analyze unstained control, single-stained, and fluorescence minus one (FMO) controls to set up the gating scheme for all cellular populations (*see* **Note 12**).
26. Analyze the samples. Cell granularity (side scatter, SSC), cell size (forward scatter, FSC), and DAPI staining are used to gate the events corresponding to live cells. Antibody combinations are then used to define all populations (*see* Table 1 and Fig. 1 for a representative example) (*see* **Note 13**).

3.2 Ex Vivo Confirmation of the Identity of the Distinct FACS-Isolated Cell Populations by RT-qPCR

Specific mRNAs expressed by each population allow demonstration of a successful isolation protocol (*see* Fig. 2).

1. After FACS (Sect. 3.1), cells may be collected Eppendorf tubes with 500 μL of FACS Buffer at 4 °C.
2. Centrifuge Eppendorf tubes at 14,000 × *g* for 5 min.
3. Remove supernatant (*see* **Note 14**).
4. Perform total RNA extraction of each cell population using RNeasy Micro kit following manufacturer's protocol.
5. Complementary DNA (cDNA) is synthesized from total RNA using SuperScript III Reverse Transcriptase according to manufacturer's protocol.
6. Real-time PCR reactions are performed on a LightCycler 480 System using Light Cycler 480 SYBR Green I Master reaction mix and specific primers.
7. Thermocycling conditions: initial step of 10 min at 95 °C, then 50 cycles of 15 s denaturation at 94 °C, 10 s annealing at 60 °C, and 15 s extension at 72 °C.
8. Reactions must be run in triplicate, and automatically detected threshold cycle (Ct) values are compared between samples.

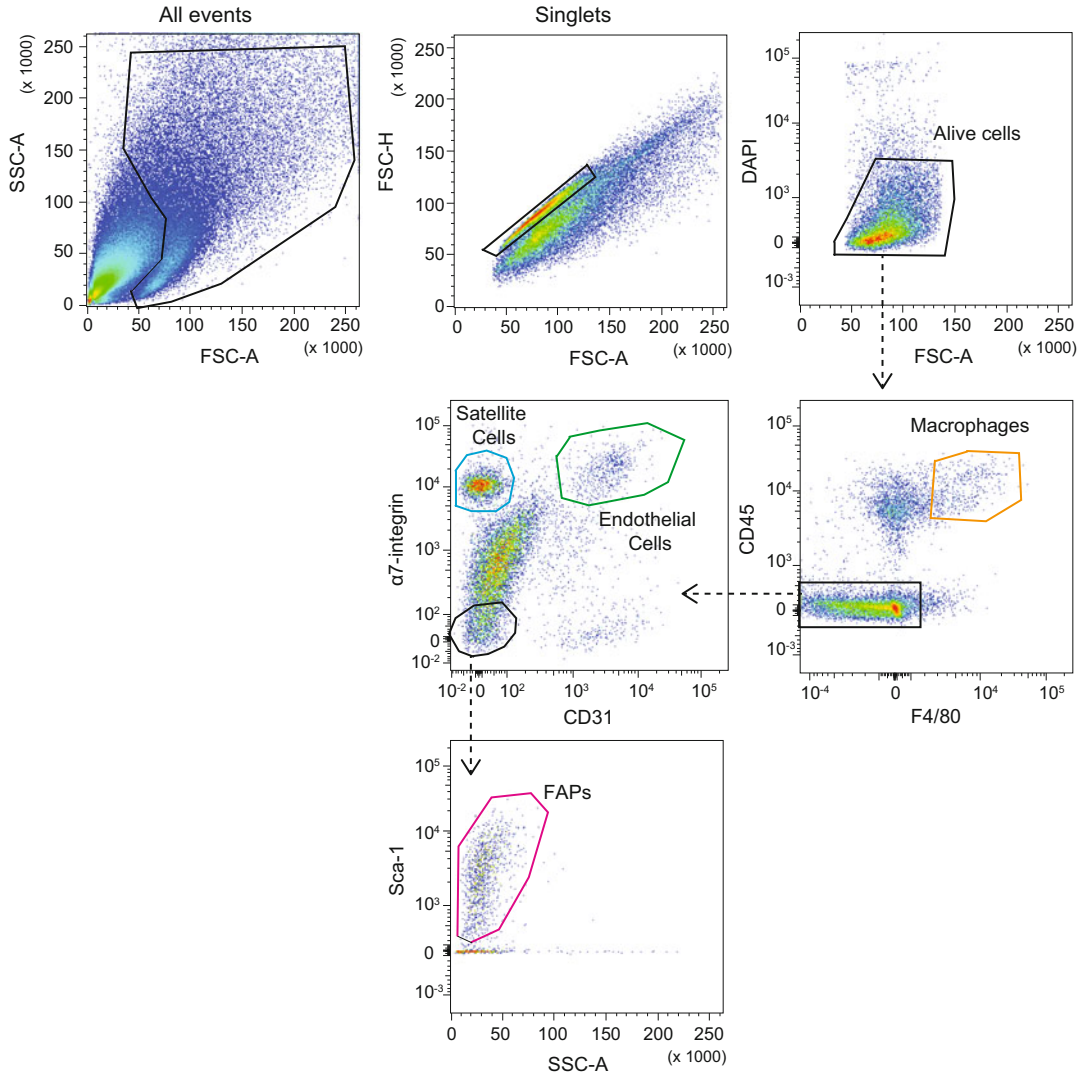

Fig. 1 Representative example of the FACS strategy and gating scheme to isolate satellite cells, macrophages, FAPs, and endothelial cells from resting muscles of wild-type mice. All singlet events are selected using forward (FSC) and side scatter (SSC) detectors. Subsequently, alive cells are chosen by DAPI. From there, macrophages are identified as $CD45^+$ $F4/80^+$ double-positive cells. Satellite cells are gated from CD45, $F4/80^-$ population as α7-integrin$^+$ meanwhile endothelial cells as α7-integrin$^+$ and $CD31^+$. Finally, FAPs are sorted by $Sca1^+$ staining from α7-integrin$^-$ $CD31^-$ cell population. Arrows show the sequence of gating used

9. Transcripts of the ribosomal protein L7 or GAPDH housekeeping genes can be used as endogenous control, with each unknown sample normalized to L7 or GAPDH content.
10. Primers used to confirm each cell populations of interest (*see* Table 2).

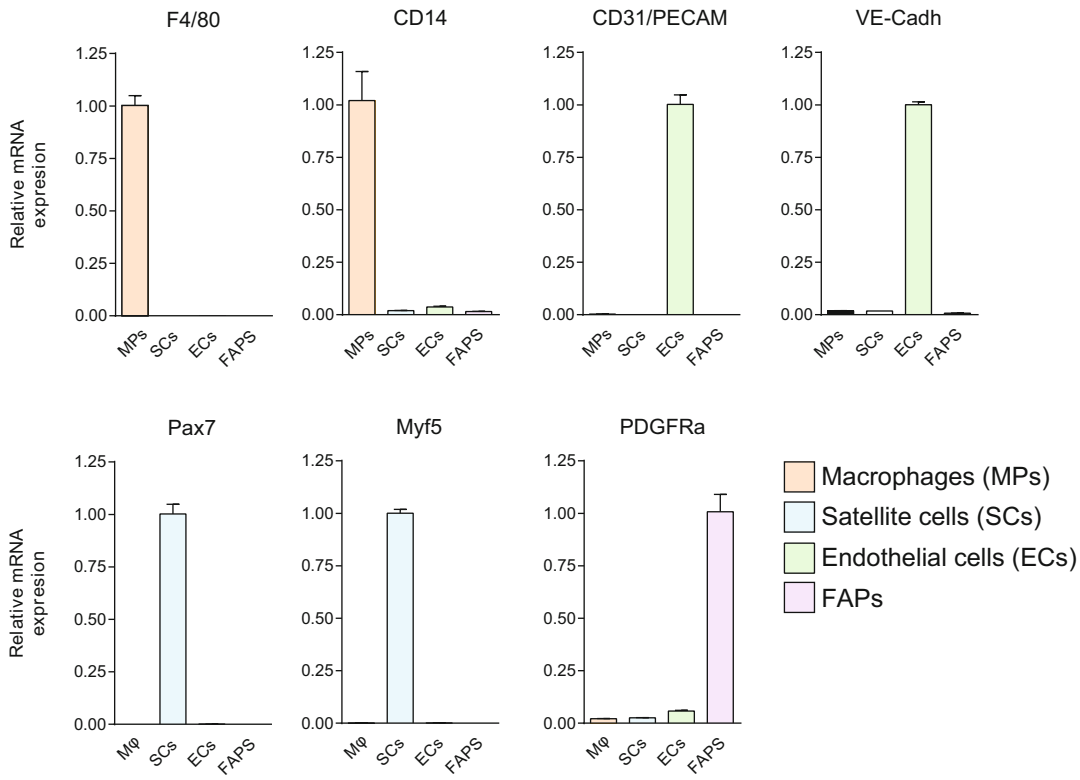

Fig. 2 Representative example ex vivo confirmation of the identity of the distinct FACS-isolated cell populations by RT-qPCR. Comparative qPCR analysis with indicated genes in isolated cellular populations. Specific genes for macrophages are F4/89 and CD14, for endothelial cells are CD31 (also known as PECAM) and VE-Cadherin, for satellite cells are Pax7 and Myf5, and for FAPS PDGFRα. Means ± SEM of at least three experiments

4 Notes

1. Anesthetize mice using approved protocols in your institution. Spray skin of the mouse with 70% ethanol. Cut and remove the skin, and expose the forelimb and hind limb muscles.
2. Classification of mice according to age: Young (2–3 months old), adult (6–8 months old), old (18–24 months old), geriatric (older than 28 months of age) [4].
3. For aging studies, as mouse mortality starts to increase around 18 months of age, increasing the number of mice cohorts to study old and geriatric age is highly recommended.
4. As sarcopenia and fibrosis increase with age [18], the amount of tissue obtained from old and geriatric mice is lower in comparison to young mice. In consequence, samples from old

Table 2
Primers used for RT-qPCR to confirm identity of each cell population sorted with proposed FACS panel

	Forward	Reverse
F4/80	CCCCAGTGTCCTTACAGAGTG	GTGCCCAGAGTGGATGTCT
CD14	AAAGAAACTGAAGCCTTTC	AGCAACAAGCCAAGCACAC
TLR4	GCCACCAGTTACAGATCGTC	AGAGAAACTTCCTGGGGAAA
Pax7	GTGTCTCCAAGATTCTGTGCCG	CAATCTTTTTCTCCACATCCGG
Myf5	CTGTCTGGTCCCGAAAGAAC	AAGCAATCCAAGCTGGACAC
CD31/PECAM	GTACGAGGTGAAGGTGCAT	AATGTGCAGCTGGTCCCC
VE-Cadh	AAATGAATCGCTGCCCCACT	TGTTAGCATCGACCCCGAAG
Tie1	CAGGCACAGCAGGTTGTAGA	GTGCCACCATTTTGACACTG
PDGFRα	TGGCATGATGGTCGATTCTA	CGCTGAGGTGGTAGAAGGAG
CD36	ATGGGCTGTGATCGGAACTG	GTCTTCCCAATAAGCATGTCTCC

and geriatric animals provide lower cell yield. For aging studies, increasing the number of mice (i.e., using pools) to sort cells at old and geriatric age is recommended.

5. To avoid cross-contamination from cell types from other close-by tissues, fine dissection technique should be master to exclude adipose tissue (white fat), nerves, and tendons. Remaining debris after the digestion, which includes tendons, obstruct cell strainers during sample filtration steps.
6. Collagenase D can be employed instead of Liberase in the digestion mix. However, the use of Collagenase D requires a multistep protocol, while Liberase allows faster, one-step procedure. Thus, we propose digestion with Liberase for skeletal muscle tissue.
7. Trypsin has been shown to affect the integrity of cell surface proteins on mammalian cells [19]. The endothelial cell receptor CD31 is particularly susceptible to proteolytic cleavage [20]. Therefore, tissue digestion with trypsin usage is not recommended for this FACS protocol.
8. A maximum of 1 g of tissue should be digested per tube; otherwise the digestion will provide lower cell yield.
9. Digestion time can be prolonged to increase its efficiency, especially, in the case of muscle tissue obtained from old and geriatric animals. However, sustained digestion may increase cell mortality, so we suggest do not exceed 2 h of digestion.

10. Count cells manually using and hemocytometer (i.e., Neubauer chamber) or any of the available automatic cell counter systems.
11. It is feasible to include additional positive satellite cell surface markers to this panel in order to increase the purity of the sorted satellite cell population. The antibody can be conjugated to FITC fluorochrome to avoid interference with the rest of cell surface markers used in this protocol. For this purpose, CD34, CXCR4, VCAM, and SM/C2.6 cell surface markers can be used [21–25].
12. Several controls are required to establish the correct gating of cell populations in the FACS machine:
    (a) Negative control: an unstained cell sample should be analyzed to determine the voltage of the lasers and autofluorescence of the sample.
    (b) Single stained controls: individual staining with each antibody conjugated to its fluorescent dye. This control is needed for compensation, a technique used to remove false signal resulting from spectral overlap between two fluorochromes. For example, the Sca1-PE/Cy7 and F4/80-APC/Cy7 antibodies used in this protocol have high spectral overlap; therefore, the compensation should be done properly to avoid non-specific cell sorting.
    (c) FMO (Fluorescence Minus One) controls: staining with all antibodies except one should be done for each color used in the panel. This type of staining is needed to discriminate properly the cell populations.
13. Using four-way purity precision mode, we can separate satellite cells, macrophages, FAPs, and endothelial cells simultaneously.
14. Cell pellet or extracted RNA can be stored at −80 °C until RNA isolation or cDNA synthesis, respectively.

Acknowledgments

Work in the authors' laboratory has been supported by the Spanish Ministry of Science, Innovation and Universities, Spain (grant SAF2015-67369-R; and SAF 2015-70270-REDT, a María de Maeztu Unit of Excellence award to UPF [MDM-2014-0370], and a Severo Ochoa Center of Excellence award to the CNIC [SEV-2015-0505]), the UPF-CNIC collaboration agreement, ERC-2016-AdG-741966, La Caixa-HEALTH, AFM, MDA, and H2020-UPGRADE. V.M is recipient of a FPI predoctoral fellowship.

References

1. Sousa-Victor P, Garcia-Prat L, Serrano AL, Perdiguero E, Munoz-Canoves P (2015) Muscle stem cell aging: regulation and rejuvenation. Trends Endocrinol Metab 26 (6):287–296. https://doi.org/10.1016/j.tem.2015.03.006
2. Mashinchian O, Pisconti A, Le Moal E, Bentzinger CF (2018) The muscle stem cell niche in health and disease. Curr Top Dev Biol 126:23–65. https://doi.org/10.1016/bs.ctdb.2017.08.003
3. Almada AE, Wagers AJ (2016) Molecular circuitry of stem cell fate in skeletal muscle regeneration, ageing and disease. Nat Rev Mol Cell Biol. https://doi.org/10.1038/nrm.2016.7
4. Sousa-Victor P, Gutarra S, Garcia-Prat L, Rodriguez-Ubreva J, Ortet L, Ruiz-Bonilla V, Jardi M, Ballestar E, Gonzalez S, Serrano AL, Perdiguero E, Munoz-Canoves P (2014) Geriatric muscle stem cells switch reversible quiescence into senescence. Nature 506 (7488):316–321. https://doi.org/10.1038/nature13013
5. Garcia-Prat L, Martinez-Vicente M, Perdiguero E, Ortet L, Rodriguez-Ubreva J, Rebollo E, Ruiz-Bonilla V, Gutarra S, Ballestar E, Serrano AL, Sandri M, Munoz-Canoves P (2016) Autophagy maintains stemness by preventing senescence. Nature 529 (7584):37–42. https://doi.org/10.1038/nature16187
6. Yin H, Price F, Rudnicki MA (2013) Satellite cells and the muscle stem cell niche. Physiol Rev 93(1):23–67. https://doi.org/10.1152/physrev.00043.2011
7. Relaix F, Zammit PS (2012) Satellite cells are essential for skeletal muscle regeneration: the cell on the edge returns centre stage. Development 139(16):2845–2856. https://doi.org/10.1242/dev.069088
8. Gros J, Manceau M, Thome V, Marcelle C (2005) A common somitic origin for embryonic muscle progenitors and satellite cells. Nature 435(7044):954–958. https://doi.org/10.1038/nature03572
9. Cornelison D, Perdiguero E (2017) Muscle stem cells: a model system for adult stem cell biology. Methods Mol Biol 1556:3–19. https://doi.org/10.1007/978-1-4939-6771-1_1
10. Boldrin L, Muntoni F, Morgan JE (2010) Are human and mouse satellite cells really the same? J Histochem Cytochem 58(11):941–955. https://doi.org/10.1369/jhc.2010.956201
11. Tedesco FS, Dellavalle A, Diaz-Manera J, Messina G, Cossu G (2010) Repairing skeletal muscle: regenerative potential of skeletal muscle stem cells. J Clin Invest 120(1):11–19. https://doi.org/10.1172/JCI40373
12. Tedesco FS, Moyle LA, Perdiguero E (2017) Muscle interstitial cells: a brief field guide to non-satellite cell populations in skeletal muscle. Methods Mol Biol 1556:129–147. https://doi.org/10.1007/978-1-4939-6771-1_7
13. Tidball JG (2017) Regulation of muscle growth and regeneration by the immune system. Nat Rev Immunol 17(3):165–178. https://doi.org/10.1038/nri.2016.150
14. Latroche C, Weiss-Gayet M, Muller L, Gitiaux C, Leblanc P, Liot S, Ben-Larbi S, Abou-Khalil R, Verger N, Bardot P, Magnan M, Chretien F, Mounier R, Germain S, Chazaud B (2017) Coupling between myogenesis and angiogenesis during skeletal muscle regeneration is stimulated by restorative macrophages. Stem Cell Reports 9 (6):2018–2033. https://doi.org/10.1016/j.stemcr.2017.10.027
15. Lemos DR, Babaeijandaghi F, Low M, Chang CK, Lee ST, Fiore D, Zhang RH, Natarajan A, Nedospasov SA, Rossi FM (2015) Nilotinib reduces muscle fibrosis in chronic muscle injury by promoting TNF-mediated apoptosis of fibro/adipogenic progenitors. Nat Med 21 (7):786–794. https://doi.org/10.1038/nm.3869
16. Kuswanto W, Burzyn D, Panduro M, Wang KK, Jang YC, Wagers AJ, Benoist C, Mathis D (2016) Poor repair of skeletal muscle in aging mice reflects a defect in local, interleukin-33-dependent accumulation of regulatory T cells. Immunity 44(2):355–367. https://doi.org/10.1016/j.immuni.2016.01.009
17. Panduro M, Benoist C, Mathis D (2018) Treg cells limit IFN-gamma production to control macrophage accrual and phenotype during skeletal muscle regeneration. Proceedings of the National Academy of Sciences of the United States of America 115(11): E2585–E2593. https://doi.org/10.1073/pnas.1800618115
18. Brack AS, Conboy MJ, Roy S, Lee M, Kuo CJ, Keller C, Rando TA (2007) Increased Wnt signaling during aging alters muscle stem cell fate and increases fibrosis. Science 317 (5839):807–810. https://doi.org/10.1126/science.1144090

19. Huang HL, Hsing HW, Lai TC, Chen YW, Lee TR, Chan HT, Lyu PC, Wu CL, Lu YC, Lin ST, Lin CW, Lai CH, Chang HT, Chou HC, Chan HL (2010) Trypsin-induced proteome alteration during cell subculture in mammalian cells. J Biomed Sci 17:36. https://doi.org/10.1186/1423-0127-17-36
20. Gayraud-Morel B, Pala F, Sakai H, Tajbakhsh S (2017) Isolation of muscle stem cells from mouse skeletal muscle. Methods Mol Biol 1556:23–39. https://doi.org/10.1007/978-1-4939-6771-1_2
21. Montarras D, Morgan J, Collins C, Relaix F, Zaffran S, Cumano A, Partridge T, Buckingham M (2005) Direct isolation of satellite cells for skeletal muscle regeneration. Science 309 (5743):2064–2067. https://doi.org/10.1126/science.1114758
22. Chakkalakal JV, Jones KM, Basson MA, Brack AS (2012) The aged niche disrupts muscle stem cell quiescence. Nature 490 (7420):355–360. https://doi.org/10.1038/nature11438
23. Cheung TH, Quach NL, Charville GW, Liu L, Park L, Edalati A, Yoo B, Hoang P, Rando TA (2012) Maintenance of muscle stem-cell quiescence by microRNA-489. Nature 482 (7386):524–528. https://doi.org/10.1038/nature10834
24. Fukada S, Higuchi S, Segawa M, Koda K, Yamamoto Y, Tsujikawa K, Kohama Y, Uezumi A, Imamura M, Miyagoe-Suzuki Y, Takeda S, Yamamoto H (2004) Purification and cell-surface marker characterization of quiescent satellite cells from murine skeletal muscle by a novel monoclonal antibody. Exp Cell Res 296(2):245–255. https://doi.org/10.1016/j.yexcr.2004.02.018
25. Sherwood RI, Christensen JL, Conboy IM, Conboy MJ, Rando TA, Weissman IL, Wagers AJ (2004) Isolation of adult mouse myogenic progenitors: functional heterogeneity of cells within and engrafting skeletal muscle. Cell 119(4):543–554. https://doi.org/10.1016/j.cell.2004.10.021

Methods in Molecular Biology (2019) 2045: 25–36
DOI 10.1007/7651_2019_209

Published online: 06 March 2019

Isolation and Culture of Individual Myofibers and Their Adjacent Muscle Stem Cells from Aged and Adult Skeletal Muscle

Sören S. Hüttner, Hellen E. Ahrens, Manuel Schmidt, Henriette Henze, Marie Juliane Jung, Svenja C. Schüler, and Julia von Maltzahn

Abstract

The isolation and culture of single floating myofibers with their adjacent muscle stem cells allow the analysis and comparison of muscle stem cells from aged and young mice. This method has the advantage that muscle stem cells are cultured on the myofiber, thereby culturing them in conditions as close to their endogenous niche as possible. Here we describe the isolation, culture, transfection with siRNA, and subsequent immunostaining for muscle stem cells on their adjacent myofibers from aged and young mice.

Keywords Muscle stem cell, Myofiber, Aging, Self-renewal, Differentiation, Collagenase, Transfection, Satellite cell

1 Introduction

Regeneration of skeletal muscle in the adult is carried out by muscle stem cells (MuSCs), also called satellite cells [1, 2]. MuSCs in the adult are located between the basal lamina and the sarcolemma of a myofiber and are characterized by the expression of the transcription factor Pax7 [3]. Under normal resting conditions, MuSCs are quiescent and also express Sprouty1 [4]. Following injury of the muscle or due to other stimuli, they get activated [5]. After activation MuSCs differentiate into myoblasts is accompanied by the expression of MyoD, which then further differentiate into myotubes and mature into myofibers, the contractile units of skeletal muscle [5, 6].

The dysfunction of MuSCs during aging is a major contributor to the decreased regenerative capacity of aged skeletal muscle. Multiple signaling pathways are upregulated in aged muscle stem cells such as JAK/STAT or p38 signaling [7–9]. Furthermore aged or geriatric MuSCs are characterized by entering a pre-senescence state and aberrant expression of Hoxa9 following activation [10, 11].

Since muscle stem cells lose their stem cell properties and differentiate into myoblasts when cultured directly on cell culture plates, the functionality of muscle stem cells can only be investigated in vivo or in vitro by using the single floating myofiber culture system, where MuSCs are cultured on their adjacent myofiber. MuSCs on myofibers can then be analyzed for the expression of different myogenic markers such as Pax7 and MyoD to determine their state of differentiation. Quiescent as well as self-renewing MuSCs are characterized by the expression of Pax7, while proliferating MuSCs express Pax7 and MyoD, and early differentiating cells like myoblasts are only positive for MyoD. After 42 h of culture on their adjacent myofibers MuSCs have divided once, divisions are oriented either apical-basal or planar [6]. Multicellular clusters are formed after 72 h of culture consisting of self-renewing MuSCs, proliferating MuSCs, and further differentiated cells; each cluster is formed by a single MuSC [3, 6, 12]. The composition of a cluster can be analyzed for the number or percentages of Pax7 only, Pax7/MyoD double, and MyoD only positive cells to investigate the ability to self-renew, to proliferate, and to differentiate. During aging the numbers of MuSCs are decreased [8, 11]. Furthermore, MuSCs from aged mice have a reduced ability to activate and proliferate [8, 10, 11].

Investigation of the influence of signaling pathways or specific proteins on the functionality of MuSCs on their adjacent myofibers can be performed by using chemical inhibitors of signaling pathways, siRNAs, incubation with the respective signaling molecules, or overexpression using viral transduction [13–15] (*see* **Note 1**).

2 Materials

All materials for the isolation and culture of single myofibers need to be as sterile as possible. Therefore, we recommend performing dissection of the mouse and isolation of single myofibers under a semi-sterile dissection hood.

1. Tissue culture plates:

   Coat all tissue culture plates (per mouse: 3–4 wells of a 12-well plate for the isolation and 4–8 wells of a 24-well plate for culturing) with sterile HS (horse serum) for approximately 5 min. Remove the HS and let the plates dry for 5 min.

2. Myofiber culture medium:

   20% FBS (fetal bovine serum), 1% chicken embryo extract in DMEM (Dulbecco's modified Eagle's medium; 4.5 g/l glucose, 580 mg/l L-glutamine with 110 mg/ml sodium pyruvate), filter through 0.22 μm filter before use. 30 min before starting the isolation, add the medium to the prepared

tissue culture plates (24 well), and incubate them in a 37 °C incubator with 5% CO_2 to equilibrate the medium.

3. Myofiber isolation medium:
   20% FBS (fetal bovine serum) in DMEM (Dulbecco's modified Eagle's medium; 4.5 g/l glucose, 580 mg/l L-glutamine with 110 mg/ml sodium pyruvate), filter through 0.22 μm filter before use. 30 min before starting the isolation, add the medium to the prepared tissue culture plates (12 well), and incubate them in a 37 °C incubator with 5% CO_2 to equilibrate the medium.
4. Collagenase digestion solution:
   0.2% collagenase type I (Sigma #C0130) in DMEM (Dulbecco's modified Eagle's medium; 4.5 g/l glucose, 580 mg/l L-glutamine with 110 mg/ml sodium pyruvate), filter through 0.22 μm filter before use. For two EDL (extensor digitorum longus) muscles 2.5 ml of collagenase digestion solution are sufficient, transferred to a sterile 15 ml reaction tube. Preheat the solution 10 min before starting the isolation in a 37 °C circulating water bath (*see* **Note 2**).
5. Dissection tools:
   Fine forceps (Dumont 7, curved or straight)
   Vannas spring scissors (cutting edge: 5 mm, tip diameter: 0.35 mm)
   Hardened fine curved scissors (cutting edge: 24 mm)
   Fine forceps (Dumont 7b)
6. Stereo binocular microscope (0.8–5× magnification)
7. Pipettes for dissociation of the muscles:
   Prepare two kinds of sterile Pasteur pipettes: one large bore pipette for dissociation of the muscle and one small bore pipette for transfer of myofibers. Use a diamond pen to cut the glass Pasteur pipette to generate an opening of about 0.3 cm, and heat polish to smoothen the pipette's edges. Also heat polish the small bore pipette. Flame to sterilize. Coat each pipette with HS before use.
8. Permeabilization buffer:
   0.1% Triton X-100, 0.1 M Glycine in PBS (pH 7.4)
9. Blocking solution for immunofluorescence:
   5% HS in PBS (pH 7.4)
10. PFA:
    2% PFA in PBS (pH 7.4)
11. Antibodies for immunostaining:
    Pax7 (PAX7, Developmental hybridoma bank, mouse IgG1; use undiluted)
    MyoD (clone 5F11, Merck-Millipore, rat; dilution 1:100)

Alexa Fluor 546 goat anti-mouse IgG1 (Invitrogen; dilution 1:1000)
Alexa Fluor 488 goat anti-rat IgG (Invitrogen; dilution 1:1000)

12. DAPI staining solution:
    10 μg/ml DAPI (4′,6-diamidino-2-phenylindole) in PBS (pH 7.4)

3 Methods

3.1 Dissection and Digestion of the EDL Muscle

1. Sacrifice the mouse according to animal welfare regulations (*see* **Note 3**).
2. Transfer the sacrificed mouse to a dissection bench (semi-sterile). Spray the whole mouse and dissection tools with 70% ethanol.
3. Remove the skin from the hind limb. Use forceps to lift up the skin at the ankle, and cut the skin with curved scissors up to the region over the knee, thereby exposing the underlying muscles (*see* **Note 4**; Fig. 1a). Make sure that no hairs are stuck to the exposed muscles, since they are the highest risk of contamination.
4. Remove the fascia surrounding the muscles by ripping them with fine forceps (Dumont 7). Pinch the fascia at the ankle at the side of the tibia bone with the forceps (close the forceps! Otherwise they will bend), and move the forceps toward the knee (Fig. 1b, c). The fascia will rip, and the tendon of the EDL (extensor digitorum longus) at the knee will be visible (Fig. 1d).
5. Use curved fine forceps (Dumont 7) to expose the distal tendon of the TA (tibialis anterior) muscle (Fig. 1e; this is the tendon lying on top of the tendons at the ankle). Lift up the tendon with the forceps, and use another set of fine forceps to detach the TA muscle from the underlying EDL (extensor digitorum longus) muscle. Therefore, move the closed forceps up to the knee (approximately up to 0.2 cm below the knee) without injuring the EDL muscle.
6. Lift the tendon of the TA muscle with the fine forceps, and cut the tendon with fine spring scissors (Fig. 1f). Pull the TA muscle up to the proximal end (Fig. 1g); cut it at the knee or rip it off (Fig. 1h). The EDL will be fully exposed now (Fig. 1i).
7. Grab the now fully exposed tendon of the EDL at the distal end (Fig. 1j; *see* **Note 5**), cut the tendon with fine spring scissors (Fig. 1k), and pull the EDL muscle carefully toward the knee (Fig. 1l). Do not touch the EDL muscle and do not stretch the muscle! Only handle the muscle at the tendon (*see* **Note 6**).

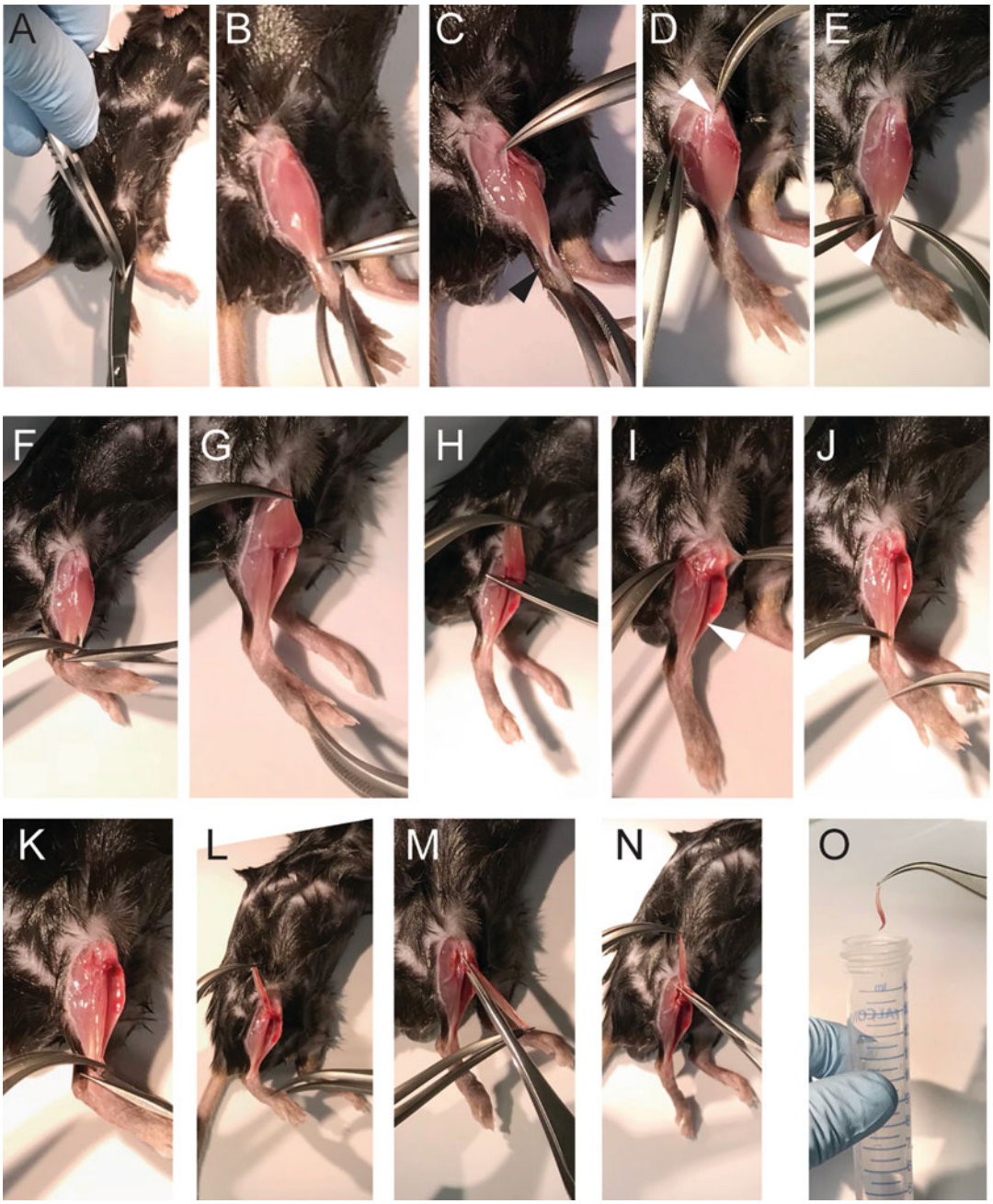

Fig. 1 Isolation of murine EDL muscle. (**a**) Hind limb of an adult mouse, (**b**) exposure of the TA muscle with its tendon, (**c**) removing of the fascia. (**d**) The proximal tendon of the EDL is now visible, marked by an arrowhead. (**e**–**h**) Removing of the TA muscle, (**i**) hind limb after removal of the TA muscle, the EDL muscle is now exposed, marked by an arrowhead. (**j**–**o**) Dissection and transfer of the EDL muscle to the collagenase digestion solution

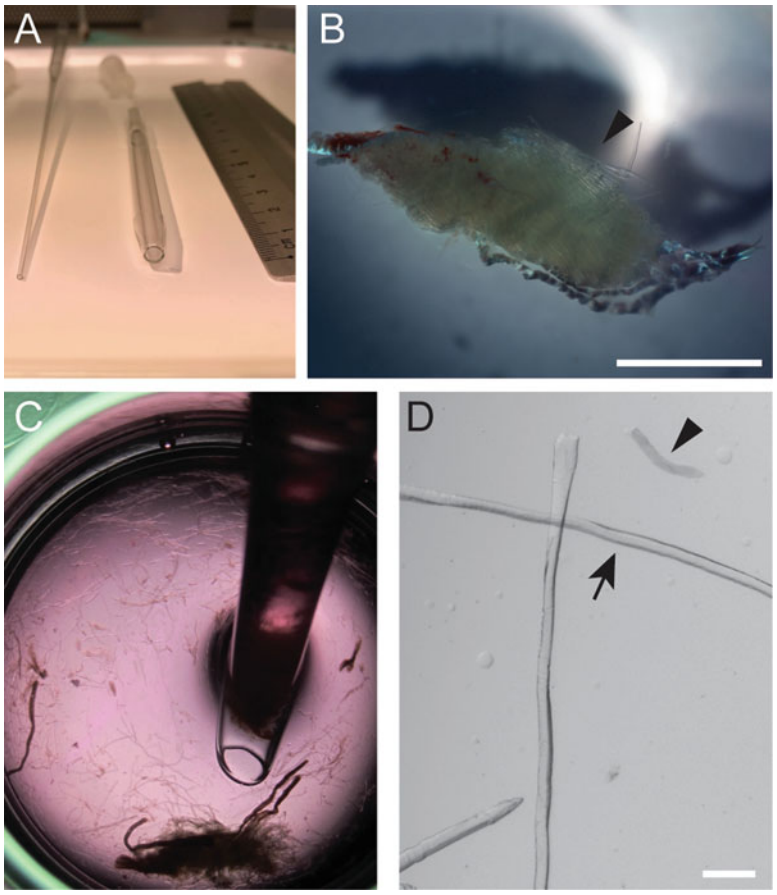

Fig. 2 Dissociation of the EDL muscle. (**a**) Small and large bore Pasteur pipettes for dissociation of the EDL muscle, (**b**) EDL muscle after 1 h digestion in collagenase digestion solution, (**c**) dissociation of the EDL muscle in a 12-well plate, (**d**) bright field image of isolated myofibers, the arrow marks a long intact alive myofiber, the arrowhead marks a short hyper contracted myofiber. Scale bar: 200 μm

8. At the knee there are two tendons visible (Fig. 1m). The tendon of the EDL is the one closer to the knee (see also Fig. 1d). Carefully pull the EDL toward the outside of the knee, and then cut the proximal tendon (Fig. 1n). Transfer the EDL gently to the preheated reaction tube containing the collagenase digestion solution (Fig. 1o).
9. Repeat the procedure with the other leg.
10. Transfer the reaction tube with the two EDL muscles from one mouse into the 37 °C circulating water bath. Incubate until the myofibers are visible (Fig. 2b). The time of digestion is depending on collagenase activity, age of the mouse, and the amount of fibrosis. General digestion times are adult mouse

(2–6 months of age), 1 h, and aged mouse (18 months and older), 1.5–2 h, depending on the amount of fibrotic tissue.

3.2 Dissociation of Single Myofibers

1. Transfer the digested EDL muscles into a well of a 12-well plate filled with 2.5 ml myofiber isolation medium (equilibrated in the incubator for about 30 min before use) using the large bore Pasteur pipette (Fig. 2a).
2. The next steps are done using a stereo binocular microscope with a 0.8–5-fold magnification under a dissection bench (semi-sterile) (*see* **Note 7**).
3. Dissociate the muscles until single myofibers come off using the large bore Pasteur pipette (Fig. 2c; *see* **Notes 8** and **9**).
4. When about 50 myofibers have come off the muscle, transfer non-contracted single myofibers (shiny bright myofibers; Fig. 2d) into a new well of a 12-well plate filled with equilibrated 2.5 ml myofiber isolation medium. Transfer the myofibers with the small bore Pasteur pipette (Fig. 2a) releasing them gently into the myofiber isolation medium (*see* **Notes 10–12**).
5. Repeat **Steps 3** and **4** until you have enough myofibers for your experiment (*see* **Note 12**).

3.3 Culture of Single Myofibers and siRNA Transfection of MuSCs on Single Myofibers

1. Transfer about 50 non-contracted single myofibers into a well of a 24-well plate filled with 500 μl of myofiber culture medium.
2. Culture the single myofibers in a 37 °C incubator with 5% CO_2.
3. Transfection of MuSCs is done after 4 h of culture using Lipofectamine RNAiMAX: the final concentration of the siRNA equals 5 pmol. Add the reaction mix (25 μl OptiMEM with the respective amount of siRNA in one reaction tube mixed with 25 μl OptiMEM and 1.5 μl of Lipofectamine RNAiMAX, and then add the mixture to the 500 μl of myofiber culture medium). It is not necessary to change the myofiber culture medium. For longer culture periods (over 48 h), a second transfection after 24 h of culture might be considered.

3.4 Immunostaining of MuSCs on Single Myofibers

1. Perform the immunostaining using a stereo binocular microscope with a 0.8–5-fold magnification.
2. Fix the single myofibers with their adjacent MuSCs using 2% PFA for 5 min at room temperature. Therefore, remove the myofiber culture medium with a small bore pipette (HS coated) leaving a little bit of myofiber medium (about 150 μl) in the well to allow the myofibers to float in the medium. Then carefully add 500 μl of PFA (2%). Perform all further steps in a 24 well coated with HS (*see* **Notes 13** and **14**).

3. Wash the myofibers three times with PBS (500 μl per washing step, 5 min incubation time per washing step). Leave a little bit of solution in the 24 well to avoid sticking of the myofibers to the culture dish. Do this for all further steps unless stated otherwise.
4. Permeabilize the myofibers with permeabilization buffer (500 μl) for 10 min at room temperature.
5. Block unspecific binding of antibodies by incubation with blocking solution (500 μl–1 ml) for 1 h at room temperature.
6. Dilute the MyoD antibody (clone 5F11, rat, 1:100, Merck-Millipore) in Pax7 antibody (PAX7 from Developmental hybridoma bank, mouse IgG1, undiluted), use 250 μl per well of a 24-well plate, and incubate overnight at 4° C.
7. Wash three times with PBS at room temperature (5 min per washing step).
8. Incubate with secondary antibodies (250 μl per well, incubation for 1 h at room temperature in the dark, therefore use tin foil to wrap the culture plate). Dilute Alexa Fluor 546 goat anti-mouse IgG1 specific antibody and Alexa Fluor 488 goat anti-rat antibody in blocking solution (1:1000). Every following step should be done under light reduced conditions.
9. Wash twice with PBS at room temperature (5 min per washing step).
10. Perform DAPI staining (500 μl per well, final concentration: 10 μg/ml) for 5 min at room temperature.
11. Wash twice with PBS at room temperature (5 min per washing step).
12. During the final washing steps, label the glass microscope slides on which the myofibers will be mounted. A PAP pen can be used to draw a hydrophobic circle around the edges of the glass slides, thereby avoiding spilling of myofiber containing liquid over the edges of the slide.
13. After the final washing step, transfer the stained myofibers to the glass microscope slide in the smallest volume possible. Make sure the single myofibers are spread out on the glass microscope slide, so you can count the MuSCs on each myofiber separately.
14. Remove the liquid with a 200 μl pipette. Make sure that the myofibers are not dragged over the slide; rather leave a little bit of liquid on the slide.
15. Add two to three drops of mounting medium, and apply a cover slip, thereby avoiding the generation of air bubbles (*see* **Note 15**).

16. Let the slides dry at room temperature for at least 20–60 min before analyzing them at the microscope. Make sure that the cover slip is not moving on the slide when counting the cells using a fluorescence microscope. If necessary let the mounting medium harden over night at 4 °C (*see* **Notes 16–18**).

4 Notes

1. Also fix some myofibers with their adjacent MuSCs directly after isolation. This gives you a reference for the number of MuSCs per myofiber before culture.
2. Always prepare the collagenase digestion solution on the day of myofiber isolation.
3. Also perform cervical dislocation. This results in bleeding at the neck and less bleeding after cutting the TA muscle.
4. Make sure that the dissection is done as sterile as possible; otherwise the risk of contamination is quite high. We recommend using two sets of forceps and scissors, one for cutting the fur and one for cutting the muscles. That minimizes the risk of contamination.
5. Make sure that you handle the EDL muscles only at the tendons; otherwise the muscle will contract and the myofibers will die.
6. If the EDL muscle is ripping when pulling it toward the knee, you have grabbed the distal tendon at the location after it branches. Use your free hand to grab the part of the tendon you missed at the foot. Loosen it and grab both tendon parts with one forceps and continue the dissection.
7. Using a heated plate for keeping the myofibers warm when dissociating them increases the overall survival of myofibers, especially for myofibers isolated from aged mice.
8. If the opening of the large bore pipette is too wide, the myofibers will not come apart. Try with a smaller one.
9. If more than 30% of your isolated myofibers are hyper contracted, the force applied is too high. Either try dissociating with less force or use a large bore pipette with a bigger opening.
10. An additional washing step in a 12-well plate filled with myofiber isolation medium (2.5 ml) decreases sticking together of myofibers.
11. Isolation of myofibers from two EDL muscles should give enough myofibers for analyzing 5–6 conditions (with 50 myofibers per condition each).

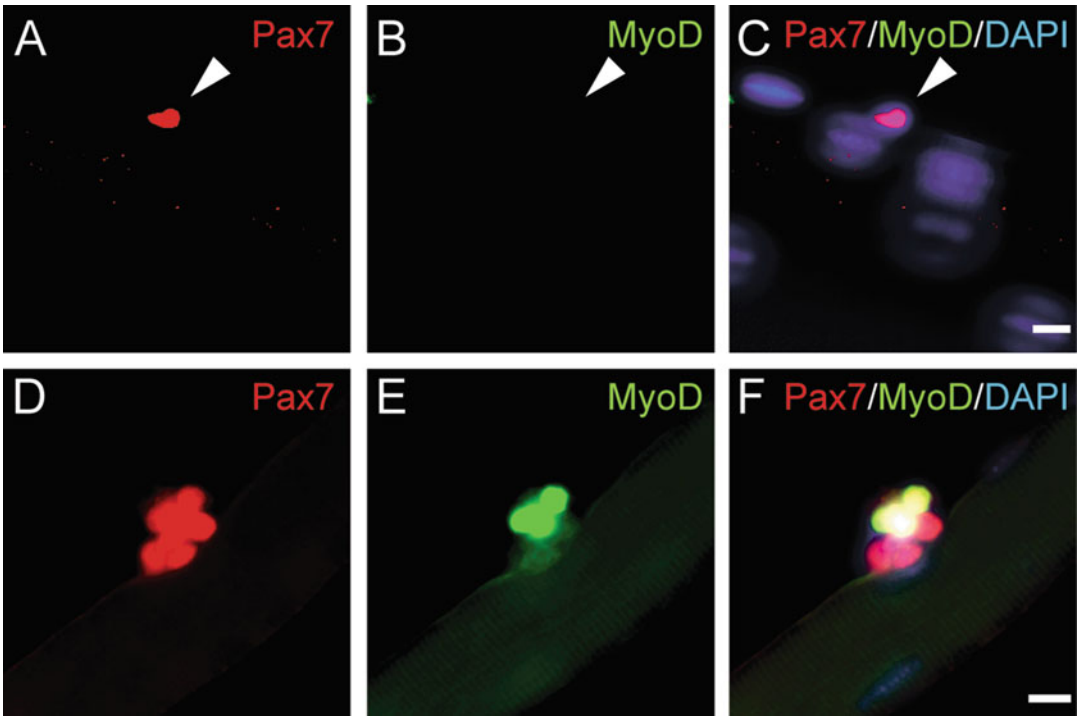

Fig. 3 Immunostaining of isolated myofibers with their adjacent MuSCs. Representative immunostaining of a MuSC on its adjacent myofiber fixed directly after isolation or a cluster of MuSCs after 72 h of culture. Staining with antibodies directed to Pax7 (**a**, **d**), MyoD (**b**, **e**), and DAPI (**c**, **f**). The arrowhead in **a**–**c** denotes the MuSC. Scale bar: 10 μm

12. Make sure that you start dissociating the myofibers only when you see the first myofibers coming off the digested muscle. Otherwise incubate longer.
13. MuSCs on their adjacent myofibers can be cultivated up to 96 h under floating conditions. The transfer of isolated myofibers into the 24 well containing the myofiber culture medium is regarded as 0 h.
14. Myofibers isolated from aged mice have a higher tendency to attach to each other during culture than myofibers isolated from young animals. To dissociate them you can add the PBS for washing after the fixation with a little bit more force than normally. Make sure that you do not wash the clusters of MuSCs off the myofiber.
15. Check that the staining was successful before mounting all myofibers. Therefore take out a few myofibers, mount them, and check at the microscope for successful staining (Fig. 3). It is not necessary to wait for the mounting medium to harden for this test.

16. If there are only very few clusters per myofiber formed (less than five for young animals and less than two or three for old animals), this can have multiple reasons: the clusters might have been washed off or might have been ripped off during mounting of the myofibers. It is also possible that the myofiber culture medium is not containing adequate amounts of growth factors. Try a new batch of chicken embryo extract or FBS.
17. Dead myofibers can be easily identified under the light microscope since they are hyper contracted and very short (Fig. 2d).
18. Adding antibiotics to the myofiber isolation and culture medium will affect the MuSCs. Therefore, it is not advisable.

Acknowledgments

This work was supported by a grant from the DFG to J.v.M (MA-3975/2-1). We would like to thank Christine Poser and Christina Picker for excellent technical assistance.

References

1. Lepper C, Partridge TA, Fan CM (2011) An absolute requirement for Pax7-positive satellite cells in acute injury-induced skeletal muscle regeneration. Development 138 (17):3639–3646. https://doi.org/10.1242/dev.067595
2. Murphy MM, Lawson JA, Mathew SJ, Hutcheson DA, Kardon G (2011) Satellite cells, connective tissue fibroblasts and their interactions are crucial for muscle regeneration. Development 138(17):3625–3637. https://doi.org/10.1242/dev.064162
3. Bentzinger CF, von Maltzahn J, Rudnicki MA (2010) Extrinsic regulation of satellite cell specification. Stem Cell Res Ther 1(3):27. https://doi.org/10.1186/scrt27
4. Shea KL, Xiang W, LaPorta VS, Licht JD, Keller C, Basson MA, Brack AS (2010) Sprouty1 regulates reversible quiescence of a self-renewing adult muscle stem cell pool during regeneration. Cell Stem Cell 6(2):117–129. https://doi.org/10.1016/j.stem.2009.12.015
5. von Maltzahn J, Bentzinger CF, Rudnicki MA (2013) Characteristics of satellite cells and multipotent adult stem cells in the skeletal muscle. Stem cells and cancer stem cells. Springer, 12:63–73
6. Bentzinger CF, Wang YX, Rudnicki MA (2012) Building muscle: molecular regulation of myogenesis. Cold Spring Harb Perspect Biol 4(2). https://doi.org/10.1101/cshperspect.a008342
7. Bernet JD, Doles JD, Hall JK, Kelly Tanaka K, Carter TA, Olwin BB (2014) p38 MAPK signaling underlies a cell-autonomous loss of stem cell self-renewal in skeletal muscle of aged mice. Nat Med 20(3):265–271. https://doi.org/10.1038/nm.3465
8. Price FD, von Maltzahn J, Bentzinger CF, Dumont NA, Yin H, Chang NC, Wilson DH, Frenette J, Rudnicki MA (2014) Inhibition of JAK-STAT signaling stimulates adult satellite cell function. Nat Med 20(10):1174–1181. https://doi.org/10.1038/nm.3655
9. Tierney MT, Aydogdu T, Sala D, Malecova B, Gatto S, Puri PL, Latella L, Sacco A (2014) STAT3 signaling controls satellite cell expansion and skeletal muscle repair. Nat Med 20 (10):1182–1186. https://doi.org/10.1038/nm.3656
10. Schworer S, Becker F, Feller C, Baig AH, Kober U, Henze H, Kraus JM, Xin B, Lechel A, Lipka DB, Varghese CS, Schmidt M, Rohs R, Aebersold R, Medina KL, Kestler HA, Neri F, von Maltzahn J, Tumpel S, Rudolph KL (2016) Epigenetic stress responses induce muscle stem-cell ageing by Hoxa9 developmental signals. Nature 540 (7633):428–432. https://doi.org/10.1038/nature20603

11. Sousa-Victor P, Gutarra S, Garcia-Prat L, Rodriguez-Ubreva J, Ortet L, Ruiz-Bonilla V, Jardi M, Ballestar E, Gonzalez S, Serrano AL, Perdiguero E, Munoz-Canoves P (2014) Geriatric muscle stem cells switch reversible quiescence into senescence. Nature 506 (7488):316–321. https://doi.org/10.1038/nature13013
12. von Maltzahn J, Chang NC, Bentzinger CF, Rudnicki MA (2012) Wnt signaling in myogenesis. Trends Cell Biol 22(11):602–609. https://doi.org/10.1016/j.tcb.2012.07.008
13. Pasut A, Jones AE, Rudnicki MA (2013) Isolation and culture of individual myofibers and their satellite cells from adult skeletal muscle. J Vis Exp (73):e50074. https://doi.org/10.3791/50074
14. Bentzinger CF, Wang YX, von Maltzahn J, Soleimani VD, Yin H, Rudnicki MA (2013) Fibronectin regulates Wnt7a signaling and satellite cell expansion. Cell Stem Cell 12 (1):75–87. https://doi.org/10.1016/j.stem.2012.09.015
15. von Maltzahn J, Zinoviev R, Chang NC, Bentzinger CF, Rudnicki MA (2013) A truncated Wnt7a retains full biological activity in skeletal muscle. Nat Commun 4:2869. https://doi.org/10.1038/ncomms3869

Methods in Molecular Biology (2019) 2045: 37–92
DOI 10.1007/7651_2018_174

Published online: 06 March 2019

Methods and Strategies for Procurement, Isolation, Characterization, and Assessment of Senescence of Human Mesenchymal Stem Cells from Adipose Tissue

Meenakshi Gaur, Marek Dobke, and Victoria V. Lunyak

Abstract

Human adipose-derived mesenchymal stem (stromal) cells (hADSC) represent an attractive source of the cells for numerous therapeutic applications in regenerative medicine. These cells are also an efficient model to study biological pathways of stem cell action, tissue injury and disease. Like any other primary somatic cells in culture, industrial-scale expansion of mesenchymal stromal cells (MSC) leads to the replicative exhaustion/senescence as defined by the "Hayflick limit." The senescence is not only greatly effecting in vivo potency of the stem cell cultures but also might be the cause and the source of clinical inconsistency arising from infused cell preparations. In this light, the characterization of hADSC replicative and stressor-induced senescence phenotypes is of great interest.

This chapter summarizes some of the essential protocols and assays used at our laboratories and clinic for the human fat procurement, isolation, culture, differentiation, and characterization of mesenchymal stem cells from adipose tissue and the stromal vascular fraction. Additionally, we provide manuals for characterization of hADSC senescence in a culture based on stem cells immunophenotype, proliferation rate, migration potential, and numerous other well-accepted markers of cellular senescence. Such methodological framework will be immensely helpful to design standards and surrogate measures for hADSC-based therapeutic applications.

Keywords Adipose tissue, Differentiation, Fat procurement, Mesenchymal stem cells, Proliferation, Senescence, Senescence messaging secretome (SMS), Stromal vascular fraction

1 Introduction

Tissue and organ behavior is strongly influenced by a heterogeneous subset of adult mesenchymal stem/stromal cells (MSC) that reside and can be isolated from almost every type of connective tissues in the adult organism as well as neonatal tissues including placenta, umbilical cord (UC), and amnion [1–3]. Their developmental origin is still a subject of debate. However, it is widely accepted that embryonic MSC can be traced to neuroepithelium and neural crest [3, 4], while adult MSC are commonly considered to be derived from mural cells (also termed pericytes) residing in the subendothelial, perivascular niche [5, 6]. The initial enthusiasm for using these cells in regenerative medicine was prompted by a demonstration

that MSC can be easily expanded and have a capacity for differentiation into cells of multiple mesenchymal lineages both ex vivo and in vivo [7, 8]. Recent studies, however, have redirected the attention of the scientists to yet another remarkable ability of these cells. Much like endothelium and stromal cell, MSC can interact and regulate cells of both the innate and adaptive immune system, triggering several essential effector functions in the normal tissue and the pathological settings [2, 3, 9]. Remarkably, after in vivo administration and/or in response to endogenous or exogenous damage, MSC can migrate to injured tissue and promote establishment of anti-inflammatory, antiproliferative, and antiapoptotic environment, thus fostering both tissue remodeling and survival (Fig. 1A) [10–14]. The current paradigm is that MSC accomplish many of these therapeutically relevant functions via a paracrine mechanism. A broad spectrum of secretory factors produced by MSC such as cytokines, chemotactic, ECM remodeling, and growth factors has been reported (as reviewed in [6, 15, 16] and demonstrated in [11, 17, 18]). Based on these remarkable properties, a subtype of MSC human adipose-derived stem (stromal) cells or hADSC have been tested in a significant number of clinical trials [15]. hADSC coordinate regenerative and reparative responses, directly through their differentiation into cells of mesenchymal origin via presentation of surface signals and activation of major signalling pathways (shown in Fig. 1A). Importantly, the experimental evidence further points to the ability of these cells to modulate tissue and organ microenvironments via paracrine secretion of cytokines and growth factors and due to direct or indirect effects on hematopoietic stem/progenitor cells development and functional differentiation (reviewed in [6] and [15]).

Residing in the perivascular niche, hADSC demonstrated self-renewal and tri-lineage differentiation potential ex vivo as illustrated in a series of studies and summarized in Fig. 2A. However, throughout life one can envision that similar to other adult stem cells, changes in the quantity and quality of MSC might influence tissue homeostasis and metabolism, slow down regeneration rate, and promote tissue deterioration. The robust adult stem cell exhaustion is thought to occur due to the process called cellular senescence. Cellular senescence is not a single unique and unambiguous cell state: it can be inflicted by various endogenous and exogenous stressors, under the influence of which the cells engage a distinct, but coordinated network of effector pathways ultimately leading to cell cycle arrest [6]. These effector pathways converge to exhibit substantial differences in the manifestation of the senescence phenotypes on cell-autonomous and paracrine levels (reviewed in detail in [6]). Such senescence-related deficiencies have also been shown to compromise MSC-mediated immunological responses and their capacity to differentiation (Fig. 2B) [19, 20]. What emerges from the aggregate studies is an unanticipated degree of complexity and

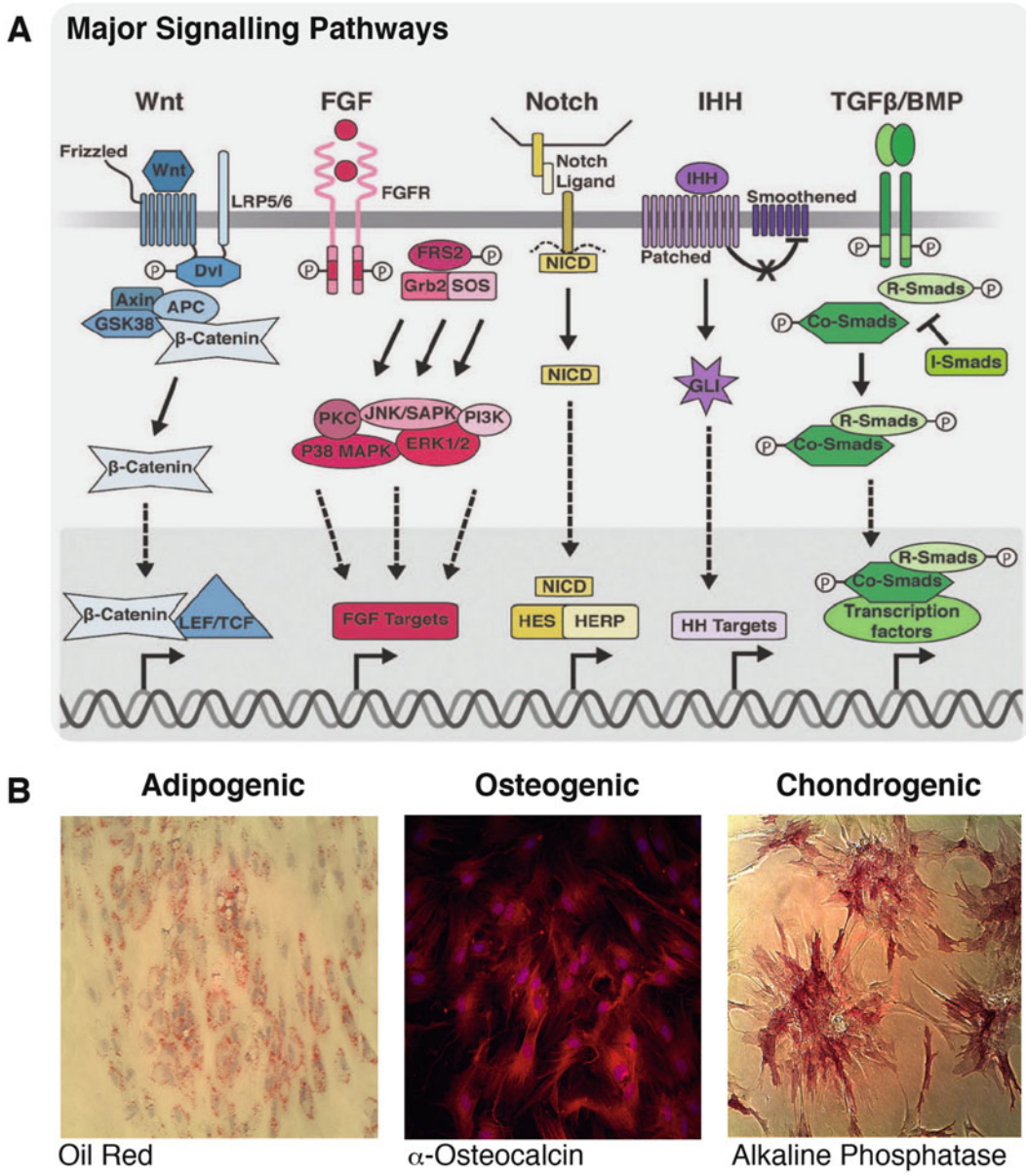

Fig. 1 Pathways involved in maintaining ADSC signalling and multipotency. (**A**) Cartoon outlining major signalling pathways controlling hADSC lineage commitment and differentiation. (**B**) Representative examples of hADSC differentiation potential. Oil red staining of lipid droplets upon adipogenic differentiation; immunostaining with osteocalcin antibodies for detection of osteogenic differentiation, and alkaline phosphatase (AP) staining depicting chondrogenic differentiation

connectivity by which distinct cellular signalling pathways controlling senescence impact on many processes associated with tissue and organs homeostasis and contribute to disease initiation and progression [6].

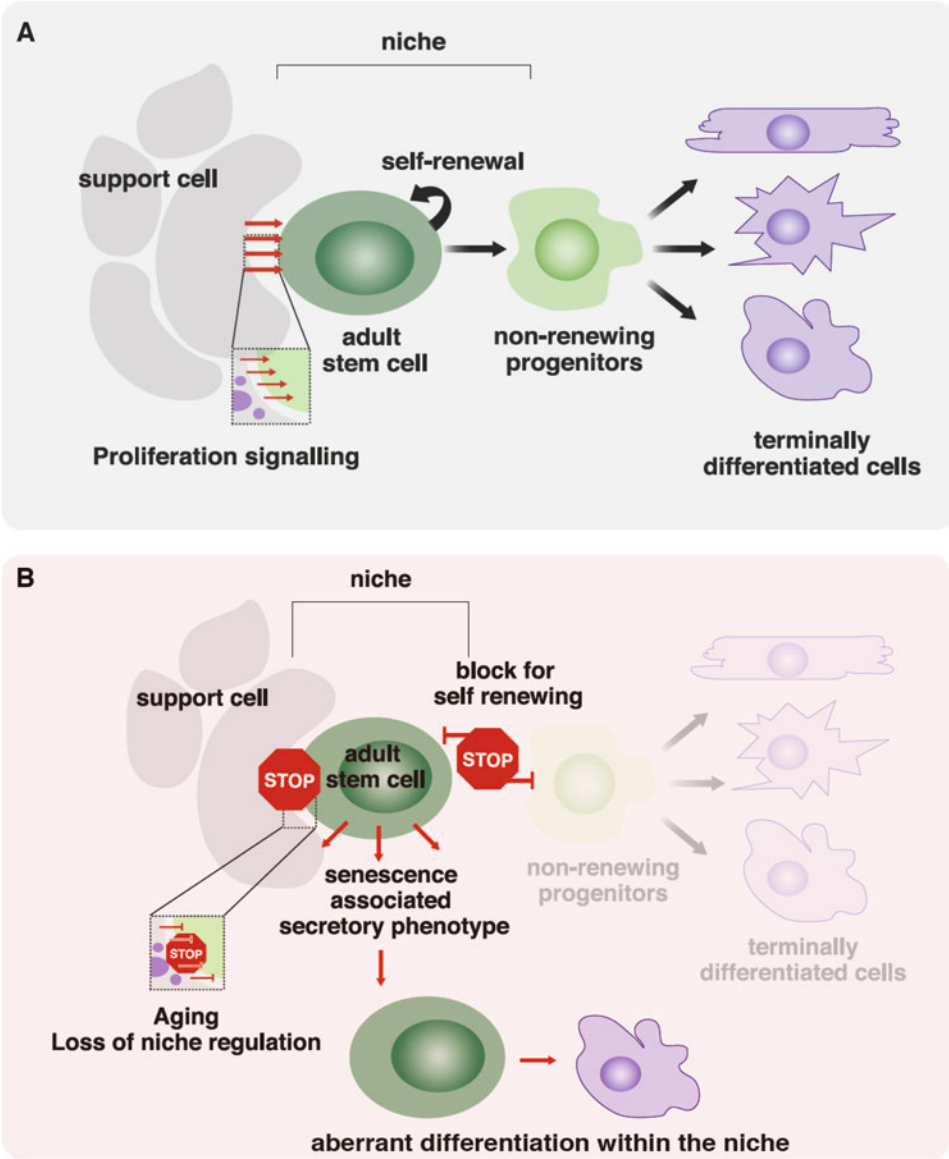

Fig. 2 Diagramed illustration of an ADSC niche cross-talk in maintenance of stemness and differentiation. Cartoon illustration of autocrine–paracrine signalling within niche in normal maintenance of MSC (**A**) and upon senescence (**B**). The signalling molecules emanating from the niche work to create a microenvironment that is required throughout life and is necessary for the maintenance of the proper stem cell content (stem cells number and multipotency) (**A**). These pathways are susceptible to organismal aging and drive cell senescence (**B**). While metabolically active, the senescent cells are characterized by inhibition of self-renewal and loss of differentiation capacity. The senescent cells signalling further reinforce the aging of the stem cell niche

Importantly, similar to other types of the MSC, senescence of hADSC by replicative exhaustion or genotoxic stress during ex vivo culturing (expansion) imposes cell-autonomous and non-cell-autonomous restrictions. These limitations encompass signalling,

metabolic, and cytoskeletal changes, which ultimately result in the diminished ability of hADSC to cope with DNA damage and other stressors as well as their therapeutic potential ([16, 21, 22] and reviewed in [6] and [15]). Reportedly, these changes result in the loss of tissue repair capacity due to drastically decreased self-renewal capacity of hADSC (pool preservation impact) and increased secretion of pro-inflammatory and matrix-degrading proteins and peptides (microenvironment modulation) that have local and/or systemic implications for overall tissue homeostasis and context-dependent restrains on success of therapeutic regenerative outcomes (Fig. 2B) [3, 6, 16, 21, 23–25].

The success of the hADSC transplantation therapy may depend on a variety of factors, which importantly might depend on the ability of these cells to undergo replicative, stress-induced, and oncogene-induced cellular senescence in local microenvironment or upon expansion of these cells ex vivo. Senescence messaging secretome (SMS), a broad spectrum of signalling molecules secreted by senescent hADSC, might not only affect the homing of the transplanted cells to specific organs and their interaction with vascular endothelium to provide for transmigration, but also, ultimately, to communicate with the immune system to control tissue and organ homeostasis.

Much of the necessary understanding and characterization of multilineage potential of MSC comes from regenerative or tissue-engineering studies of expanded MSC from bone marrow aspirate [26–28]. Notably, most studies do not account for how variability in procurement protocols, enrichment techniques, plating density, or media type or supplementation influence cellular senescence of ex vivo expanded material, which in its turn can significantly impair engraftment, remodeling capacity, hematopoietic interactions, and drug resistance of transplanted material. In this chapter, we provide the straightforward, step-by-step protocols for procurement of human fat tissue as well as the methods for isolation, expansion, and characterization of human adipose-derived stem cells from subcutaneous fat depots. The methods we are providing here do not rely exclusively on cell surface markers but instead provide a comprehensive assessment of hADSC proliferation, a rate of population doubling as well as a wide-ranging spectrum of cellular senescence markers that allow to fully characterizing the quality of the hADSC material for research and clinical applications. We also offer the detailed protocols for assessment of stem cell migratory and secretory properties in culture conditions. These techniques could be useful for the development of better ex vivo culture protocols and direct evaluation of hADSC cultures after cryopreservation and as a semiquantitative analysis of patient-to-patient variations in disease models.

2 Materials

2.1 Patient Preparation for Fat Procurement

1. Clinical principles
2. Consultation
3. Laboratory tests
4. Informed consent
5. Patient readiness for fat procurement procedure
6. Donor site selection
7. Other procedural and surgical variables

2.2 Subcutaneous Adipose Tissue Procurement

2.2.1 Reagents

1. 1% Lidocaine with 1:100,000 epinephrine injectable and 0.5% lidocaine with 1:200,000 epinephrine (Hospira, Inc., Lake Forest, IL, USA)
2. 250 mL or 1000 mL Sterile injectable saline 0.9% (Baxter International, Deerfield, IL, USA)
3. 1000 mL Ringer Lactate injectable (Baxter International, Deerfield, IL, USA)
4. Injectable sodium bicarbonate 5% (25 g/500 mL) (Baxter International, Deerfield, IL, USA)
5. Covidien 4 × 4″ sterile gauze packages (Vitality Medical, Salt Lake City, UT, USA)
6. Betadine solution (10% povidone-iodine topical solution) (Purdue Products, Stanford, CT, USA)

2.2.2 Equipment and Supplies

1. Aspiration cannulas
2. 15 or 16G Sharp injection one 1¼″ long needles (Becton Dickinson & Co., Franklin Lakes, NJ, USA)
3. 3, 5, and 10 mL Luer-Lok syringes (Becton Dickinson & Co., Franklin Lakes, NJ, USA)
4. Multihole Coleman Aspiration Cannulas straight and curved, 15 and 23 cm long (Mentor Worldwide, LLC, Santa Barbara, CA, USA)
5. 10 mL Luer-Lok syringes (Becton Dickinson & Co., Franklin Lakes, NJ, USA)
6. Tulip GEMS Carraway Harvester with spiral 3 port design, commonly used cannula for small and large volume fat procurements (Tulip Medical Products, Sand Diego, CA, USA)
7. Tumescent Infiltration Cannulas (alternatives)
8. Coleman Infiltration Straight Cannulas Style I 7 and 15 cm long (Mentor Worldwide, LLC, Santa Barbara, CA, USA)
9. Tulip Tumescent Infiltrator SuperLuer-Lok 2.1 mm × 20 cm (Tulip Medical Products, San Diego, CA, USA)

10. Vacuum source (alternatives)
11. 3 mL Syringe with 15–16G needle (Becton Dickinson and Co., Franklin Lakes, NJ, USA). Useful for very small amounts of fat procurement
12. 10 mL Luer-Lok syringe with Snap-Lok fitted into the plunge of the syringe: when the plunger is pulled out, the lock snaps open on the barrel lip, holding effortlessly the syringe under vacuum (Tulip Medical Products, San Diego, CA, USA)
13. For large volume fat aspirations, multiple technologies and systems are on the market including popular systems and aspirators designed for liposuction. LipiVage D System employs closed, sterile circuit, gentle on fat cells (employs low negative pressure), fat is ready in minutes after aspiration and draining fluids from the specimen for subsequent use (clinical or research), single hole harvesting Luer-Lok 3 mm, 19 cm cannula is available from the manufacturer as well as tubing (no cannula/tubing/vacuum source compatibility problems) (Genesis Biosystems, Lewisville, TX, USA) [29]
14. Hypodermic needles for injection of local anesthetics: 25 or 27G, 1¼″ long (Becton Dickinson and Co., Franklin Lakes, NJ, USA)
15. No. 11 disposable surgical blade (Robbins Instruments, Chatham, NJ, USA)
16. 5/0 Nylon suture with P3 needle (Ethicon, Johnson & Johnson, Somerville, NJ, USA)
17. Steri-Stripes (e.g., large ones like 25 mm × 125 mm for compression and reduction of swelling) (3 M Health Care, St. Paul, MN, USA)
18. Mepilex 3 × 3″ (or other sizes as per Molnlycke Catalogue) self-adherent, flexible dressing for cannula insertion site (Molnlycke Health Care, Norcross, GA, USA)
19. Autoclavable syringe rack (Mentor Worldwide, LLC, Santa Barbara, CA, USA)
20. MediLite [capable of spinning six 10 mL syringes simultaneously with rpm up to 3100 (Mentor Worldwide, LLC, Santa Barbara, CA, USA)]
21. Single-Use Large Volume Lipoaspirate Decanting Canister 1000 mL (Tulip Medical Products, San Diego, CA, USA)
22. Tulip Anaerobic Transfer and Fat Emulsifier Set, Luer-Lok to Luer-Lok (component of the Tulip Nanofat System) (Tulip Medical Products, San Diego, CA, USA)
23. Tulip Fat Emulsifier Set (standardizes the texture of lipoaspirate) (Tulip Medical Products, San Diego, CA, USA)

24. SoftFil Fat injection blunt microcannula 25 or 27G suitable also for nanofat injection (Soft Medical Aesthetics, Paris, France)

2.3 Stromal Vascular Fraction

2.3.1 Reagents

1. DMEM/F12 complete medium: Add 450 mL Dulbecco's modified Eagle medium/nutrient mixture F-12 (Thermo Fisher Scientific, Waltham, MA, USA), 50 mL fetal bovine serum (FBS) (HyClone, Logan, UT), 5 mL of penicillin–streptomycin (10,000 U/mL penicillin and 10,000 μg/mL streptomycin), and 5 mL of L-glutamine (200 mM) (all from Thermo Fisher Scientific, Waltham, MA, USA) (*see* **Note 2**)
2. Phosphate-buffered saline (PBS) (Thermo Fisher Scientific, Waltham, MA, USA)
3. Celase™ (Cytori Therapeutics, San Diego, CA) (*see* **Note 3**)
4. Red blood cell lysis buffer or ACK lysis buffer: Contains 150 mM NH_4Cl, 10 mM $KHCO_3$, 0.1 mM EDTA (pH 7.3). 8.26 g NH_4Cl (0.15 M), 1 g $KHCO_3$ (10 mM), and 37.2 mg Na_2EDTA (0.1 mM) in 800 mL MilliQ water. Adjust pH to 7.3 using 1 N HCl and add MilliQ water to make the final volume to 1 L. Filter-sterilize through a 0.2-μm filter unit. The buffer is stable for up to 6 months at room temperature (*see* **Note 4**)
5. Hank's buffered salt solution (HBSS) (Thermo Fisher Scientific, Waltham, MA, USA)
6. TrypLE™ (Thermo Fisher Scientific, Waltham, MA, USA)
7. Acridine orange (AO) and propidium iodide (PI): AO/PI reagent (Logos Biosystems, South Korea)
8. 70% Ethanol in a spray bottle

2.3.2 Equipment and Supplies

1. T175 cell-culture flasks (Thermo Fisher Scientific, Waltham, MA, USA)
2. Centrifuge tubes 15 and 50 mL (Thermo Fisher Scientific, Waltham, MA, USA)
3. Serological pipettes 5, 10, and 25 mL (Thermo Fisher Scientific, Waltham, MA, USA)
4. Disposable 2 mL aspirating pipettes (Thermo Fisher Scientific, Waltham, MA, USA)
5. 0.22 μm Pore size Nalgene membrane filtration unit (Thermo Fisher Scientific, Waltham, MA, USA)
6. Centrifuge with swing bucket rotor with maximum rpm limit 4200 (Eppendorf, Hamburg, Germany)
7. Weighing balance
8. 37 °C Bead bath (Thermo Fisher Scientific, Waltham, MA, USA)

9. Humidified 37 °C incubator at 5% CO_2 and 20% O_2 levels
10. Luna Stem automated cell counter (Logos Biosystems, South Korea)
11. Luna Stem cell counting slides (Logos Biosystems, South Korea)
12. Microscope with camera (Leica Microsystems, Buffalo Grove, IL, USA)

2.4 ADSC Surface Marker Analysis by Flow Cytometry

2.4.1 Reagents

All reagents and antibodies were purchased from Thermo Fisher Scientific, Waltham, MA, USA, unless marked otherwise.

1. CD11b
2. CD14
3. CD19
4. CD29
5. CD31
6. CD34
7. CD44
8. CD45
9. CD73
10. CD80
11. CD86
12. CD90-PE
13. CD105-PE
14. CD106
15. CD166
16. 4′,6-Diamidino-2-phenylindole (DAPI) (Millipore Sigma, St. Louis, MO, USA)
17. PE mouse IgG2b, kappa Isotype Control (for CD45 and CD44)
18. PE anti-mouse IgG2a, kappa Isotype Control (for CD31)
19. PE/Cy7 Rat IgG2a, kappa Isotype Control (for CD90 and CD105)
20. FC block (TruStain fcX anti-mouse CD16/32)
21. FACS buffer: PBS containing 2% FBS (HyClone), 1 mM EDTA (Millipore Sigma, St. Louis, MO, USA), and 0.1% sodium azide (Millipore Sigma, St. Louis, MO, USA)
22. Phosphate-buffered saline (PBS) (Thermo Fisher Scientific, Waltham, MA, USA)
23. TrypLE™ (Thermo Fisher Scientific, Waltham, MA, USA)
24. Acridine orange (AO) and propidium iodide (PI): AO/PI reagent (Logos Biosystems, South Korea)

2.4.2 Equipment and Supplies

1. 1.5 mL Microfuge tubes (Thermo Fisher Scientific, Waltham, MA, USA)
2. 37 °C Bead bath (Thermo Fisher Scientific, Waltham, MA, USA)
3. Humidified 37 °C incubator at 5% CO_2 and 20% O_2 levels
4. Luna Stem automated cell counter (Logos Biosystems, South Korea)
5. Luna Stem cell counting slides (Logos Biosystems, South Korea)
6. Tabletop microfuge (Thermo Fisher Scientific, Waltham, MA, USA)
7. Guava easyCyte Mini System (Guava Technologies, Millipore Sigma, USA)
8. FlowJo software (FlowJo, LLC, Ashland, OR, USA) or flow cytometry data analysis software

2.5 Establishing the hADSC Lines

2.5.1 Reagents

1. DMEM/F12 complete medium: Add 450 mL Dulbecco's modified Eagle medium/nutrient mixture F-12 (Thermo Fisher Scientific, Waltham, MA, USA), 50 mL fetal bovine serum (FBS) (HyClone, Logan, UT), 5 mL of penicillin–streptomycin (10,000 U/mL penicillin and 10,000 μg/mL streptomycin), and 5 mL of L-glutamine (200 mM) (all from Thermo Fisher Scientific, Waltham, MA, USA) (*see* **Note 2**)
2. Phosphate-buffered saline (PBS) (Thermo Fisher Scientific, Waltham, MA, USA)
3. TrypLE™ (Thermo Fisher Scientific, Waltham, MA, USA)
4. Acridine orange (AO) and propidium iodide (PI), AO/PI reagent (Logos Biosystems, South Korea)
5. Synth-a-Freeze™ CTS Cryopreservation medium ((Thermo Fisher Scientific, Waltham, MA, USA)

2.5.2 Equipment and Supplies

1. Threaded cryovials (Thermo Fisher Scientific, Waltham, MA, USA)
2. Freezing containers (Thermo Fisher Scientific, Waltham, MA, USA)
3. Humidified 37 °C incubator at 5% CO_2 and 20% O_2 levels
4. Microscope (Leica Microsystems, Buffalo Grove, IL, USA)
5. Luna Stem automated cell counter (Logos Biosystems, South Korea)
6. Luna Stem cell counting slides (Logos Biosystems, South Korea)
7. −80 °C Freezer (Thermo Fisher Scientific, Waltham, MA, USA)

8. Liquid nitrogen storage boxes (Thermo Fisher Scientific, Waltham, MA, USA)
9. Liquid nitrogen storage tank (Thermo Fisher Scientific, Waltham, MA, USA)
10. Brother P-touch compact label maker, PTD400
11. NitroTAG cryogenic barcode labels (GA International LabTAG, Champlain, NY, USA)

2.6 Thawing the Cryopreserved hADSC

2.6.1 Reagents

1. DMEM/F12 complete medium: Add 450 mL Dulbecco's modified Eagle medium/nutrient mixture F-12 (Thermo Fisher Scientific, Waltham, MA, USA), 50 mL fetal bovine serum (FBS) (HyClone, Logan, UT), 5 mL of penicillin–streptomycin (10,000 U/mL penicillin and 10,000 μg/mL streptomycin), and 5 mL of L-glutamine (200 mM) (all from Thermo Fisher Scientific, Waltham, MA, USA) (*see* **Note 2**)
2. 70% Ethanol in a spray bottle
3. Acridine orange (AO) and propidium iodide (PI): AO/PI reagent (Logos Biosystems, South Korea)

2.6.2 Equipment and Supplies (all from Thermo Fisher Scientific, Waltham, MA, USA)

1. 1 mL or 2 mL pipettes
2. 15 mL centrifuge tubes
3. 37 °C Bead bath (Thermo Fisher Scientific, Waltham, MA, USA)
4. Centrifuge with swing bucket rotor with maximum rpm limit 4200 (Eppendorf, Hamburg, Germany)
5. T175 Tissue culture flasks
6. Humidified 37 °C incubator at 5% CO_2 and 20% O_2 levels
7. Luna Stem automated cell counter (Logos Biosystems, South Korea)
8. Luna Stem cell counting slides (Logos Biosystems, South Korea)

2.7 Measuring hADSC Proliferation

2.7.1 Reagents

1. DMEM/F12 complete medium: Add 450 mL Dulbecco's modified Eagle medium/nutrient mixture F-12 (Thermo Fisher Scientific, Waltham, MA, USA), 50 mL fetal bovine serum (FBS) (HyClone, Logan, UT), 5 mL of penicillin–streptomycin (10,000 U/mL penicillin and 10,000 μg/mL streptomycin), and 5 mL of L-glutamine (200 mM) (all from Thermo Fisher Scientific, Waltham, MA, USA) (*see* **Note 2**)
2. 1 μCi ^{3}[H]-thymidine (Perkin-Elmer, Boston, MA, USA)
3. Scintillation fluid (Perkin-Elmer, Boston, MA, USA)
4. Phosphate-buffered saline (PBS) (Thermo Fisher Scientific, Waltham, MA, USA)

5. TrypLE™ (Thermo Fisher Scientific, Waltham, MA, USA)
6. Acridine orange (AO) and propidium iodide (PI), AO/PI reagent (Logos Biosystems, South Korea)
7. Blocking solution: 4% normal donkey serum (NDS) (Abcam, Cambridge, MA, USA) in PBS
8. BrdU (Bu20a) mouse mAb primary antibody (Cell Signalling Technology, Danvers, MA, USA)
9. Donkey anti-mouse Alexa Fluor 594 secondary antibody (Thermo Fisher Scientific, Waltham, MA, USA)
10. DAPI (Millipore Sigma, St. Louis, MO, St. Louis, MO, USA)
11. 1.5 M HCl
12. 70% Ethanol
13. ProLong™ Gold antifade mountant (Thermo Fisher Scientific, Waltham, MA, USA)

2.7.2 Equipment and Supplies

1. NanoDrop (ND-1000; NanoDrop Technologies Inc.)
2. Glass fiber filters
3. Liquid scintillation counter (LS 6500; Beckman Instruments)
4. Tissue culture treated Nunc Lab-Tek 4-chamber slides (Thermo Fisher Scientific, Waltham, MA, USA)
5. Coverslips 24 × 60 mm (Thermo Fisher Scientific, Waltham, MA, USA)
6. Luna Stem automated cell counter (Logos Biosystems, South Korea)
7. Luna Stem cell counting slides (Logos Biosystems, South Korea)
8. Rocking platform shaker
9. Zeiss AxioImager M1 fluorescence microscope (Carl Zeiss Microscopy GmbH, Jena, Germany)

2.8 Identification of Senescent hADSC

2.8.1 Reagents

1. DMEM/F12 complete medium: Add 450 mL Dulbecco's modified Eagle medium/nutrient mixture F-12 (Thermo Fisher Scientific, Waltham, MA, USA), 50 mL fetal bovine serum (FBS) (HyClone, Logan, UT), 5 mL of penicillin–streptomycin (10,000 U/mL penicillin and 10,000 μg/mL streptomycin), and 5 mL of L-glutamine (200 mM) (all from Thermo Fisher Scientific, Waltham, MA, USA) (*see* **Note 2**)
2. Phosphate-buffered saline (PBS) (Thermo Fisher Scientific, Waltham, MA, USA)
3. TrypLE™ (Thermo Fisher Scientific, Waltham, MA, USA)

4. Senescence Detection Kit (BioVision Inc., Milpitas, CA, USA)
5. 70% Glycerol in MilliQ water for mounting
6. 53BP1 antibody (Millipore Sigma, St. Louis, MO, USA)
7. $p21^{WAF1/CIP}$ rabbit mAb Alexa Fluor 647 conjugate antibody (Cell Signalling Technology, Danvers, MA, USA)
8. γH2AX antibody (Millipore Sigma, St. Louis, MO, USA)
9. DAPI stock solution: Prepare DAPI (Millipore Sigma, St. Louis, MO, St. Louis, MO, USA) stock solution at 0.5 mg/mL concentration in MilliQ water and store it in small aliquots of 250 μL at −20 °C in the dark for several months
10. Donkey anti-mouse Alexa Fluor 594 secondary antibody (for γH2AX and BrdU) (Thermo Fisher Scientific, Waltham, MA, USA)
11. Donkey anti-rabbit Alexa Fluor 594 (for 53BP1) (Thermo Fisher Scientific, Waltham, MA, USA)
12. 4% Formaldehyde in PBS (Thermo Fisher Scientific, Waltham, MA, USA)
13. 0.5% Triton X-100: 5 μL Triton X-100 in 995 mL PBS
14. Blocking solution: 4% normal donkey serum (NDS) (Abcam, Cambridge, MA, USA) in PBS
15. ProLong™ Gold antifade mountant (Thermo Fisher Scientific, Waltham, MA, USA)
16. Acridine orange (AO) and propidium iodide (PI), AO/PI reagent (Logos Biosystems, South Korea)

2.8.2 Equipment and Supplies

1. Tissue culture treated Nunc Lab-Tek 4-chamber slides (Thermo Fisher Scientific, Waltham, MA, USA)
2. Coverslips 24 × 60 mm (Thermo Fisher Scientific, Waltham, MA, USA)
3. Luna Stem automated cell counter (Logos Biosystems, South Korea)
4. Luna Stem cell counting slides (Logos Biosystems, South Korea)
5. Rocking platform shaker
6. Zeiss AxioImager M1 fluorescence microscope (Carl Zeiss Microscopy GmbH, Jena, Germany)

2.9 hADSC Differentiation

2.9.1 Reagents

1. Human mesenchymal stem cell functional identification kit (R&D Systems Inc., Minneapolis, MN, USA). This kit contains the following supplements:
   (a) Adipogenic Supplement (containing 0.5 mL of a 100× concentrated solution containing hydrocortisone, isobutylmethylxanthine, and indomethacin in 95% ethanol; Adipogenic Supplement provided in the kit is enough to supplement 50 mL of medium). Store tightly sealed at 2–8 °C for up to 6 months
   (b) Osteogenic Supplement (2.5 mL of a 20× concentrated solution containing dexamethasone, ascorbate-phosphate, and β-glycerolphosphate. Osteogenic Supplement provided in the kit is enough to supplement 50 mL of medium). Aliquot and store in a −20 °C freezer for up to 6 months. Avoid repeated freeze–thaw cycles
   (c) Chondrogenic Supplement (0.5 mL of a 100× concentrated solution containing dexamethasone, ascorbate-phosphate, proline, pyruvate, and recombinant TGF-β3 enough to supplement 50 mL of medium). Aliquot and store in a −20 °C freezer for up to 6 months. Avoid repeated freeze–thaw cycles
   (d) ITS Supplement (0.5 mL of a 100× concentrated solution containing insulin, transferrin, selenious acid, bovine serum albumin, and linoleic acid; ITS supplement provided in the kit is enough to supplement 50 mL of medium)
2. α-MEM Basal Media (90 mL of α-MEM, 10% FBS (HyClone, Logan, UT), 100 U/mL penicillin, 100 μg/mL streptomycin, and 2 mM L-glutamine (all from Thermo Fisher Scientific, Waltham, MA, USA))
3. DMEM/F12 Basal Media: Add 49 mL Dulbecco's modified Eagle medium/nutrient mixture F-12 (Thermo Fisher Scientific, Waltham, MA, USA), 500 μL ITS supplement from the differentiation kit (R&D Systems Inc., Minneapolis, MN, USA), 500 μL of penicillin–streptomycin (10,000 U/mL penicillin and 10,000 μg/mL streptomycin), and 500 μL of L-glutamine (200 mM) (all from Thermo Fisher Scientific, Waltham, MA, USA)
4. TrypLE™ (Thermo Fisher Scientific, Waltham, MA, USA)
5. PBS (Thermo Fisher Scientific, Waltham, MA, USA)
6. Ascorbic acid (50 μM) (Millipore Sigma, St. Louis, MO, USA)
7. Dexamethasone (100 nM) (Millipore Sigma, St. Louis, MO, USA)

8. Transforming growth factor-β (TGF-β) (10 ng/mL) (Millipore Sigma, St. Louis, MO, USA)
9. 4% Paraformaldehyde in PBS (Millipore Sigma, St. Louis, MO, USA)
10. 1% BSA in PBS
11. Triton X-100 (Millipore Sigma, St. Louis, MO, USA)
12. Acridine orange (AO) and propidium iodide (PI), AO/PI reagent (Logos Biosystems, South Korea)

2.9.2 Equipment and Supplies

1. 24-Well culture plates (Thermo Fisher Scientific, Waltham, MA, USA)
2. 12 mm Coverslips (Thermo Fisher Scientific, Waltham, MA, USA)
3. 15 mL Centrifuge tubes (Thermo Fisher Scientific, Waltham, MA, USA)
4. Liquid barrier marker pen (Thermo Fisher Scientific, Waltham, MA, USA)
5. Pipettes and pipette tips (Thermo Fisher Scientific, Waltham, MA, USA)
6. 0.22 μm Pore size Nalgene membrane filtration unit (Thermo Fisher Scientific, Waltham, MA, USA)
7. Serological pipettes (Thermo Fisher Scientific, Waltham, MA, USA)
8. Fine pointed curved forceps (Thermo Fisher Scientific, Waltham, MA, USA)
9. Humidified 37 °C incubator at 5% CO_2 and 20% O_2 levels
10. Centrifuge with swing bucket rotor with maximum rpm limit 4200 (Eppendorf, Hamburg, Germany)
11. Luna Stem automated cell counter (Logos Biosystems, South Korea)
12. Luna Stem cell counting slides (Logos Biosystems, South Korea)
13. Inverted microscope (Leica MC170HD Digital Camera, Germany)
14. 2–8 °C Refrigerator
15. 37 °C Bead bath (Thermo Fisher Scientific, Waltham, MA, USA)
16. Zeiss AxioImager M1 fluorescence microscope (Carl Zeiss Microscopy GmbH, Jena, Germany)

2.10 Ex Vivo hADSC Migration and Invasion Assays

2.10.1 Reagents

1. Serum-free α-MEM (500 mL minimum essential medium (MEM), 5 mL penicillin–streptomycin (10,000 U/mL penicillin and 10,000 μg/mL streptomycin), and 5 mL of L-glutamine (200 mM) (all from Thermo Fisher Scientific, Waltham, MA, USA). Filter using 0.22 μm pore size Nalgene membrane filtration unit (Thermo Fisher Scientific, Waltham, MA, USA), and store at 4 °C
2. Cytokines IL-2, IL-6, IL-8, HMGB1, and TNF-α (all from PeproTech Inc., Rocky Hill, NJ, USA)
3. 4% Paraformaldehyde (Millipore Sigma, St. Louis, MO, USA)
4. 5% Toluidine blue (Millipore Sigma, St. Louis, MO, USA)

2.10.2 Equipment and Supplies

1. Transwell filters were from Corning Incorporated (Acton, MA, USA)
2. 24-Well transwell plates with 8 μm pore size filters (Corning, Tewksbury, MA, USA)
3. Bright-field microscope (NikonTE300, DXM1200 Digital Camera, Japan)

2.11 Detection of ADSC Secretory Proteins

2.11.1 Reagents

1. DMEM/F12 complete medium: Add 450 mL Dulbecco's modified Eagle medium/nutrient mixture F-12 (Thermo Fisher Scientific, Waltham, MA, USA), 50 mL fetal bovine serum (FBS) (HyClone, Logan, UT), 5 mL of penicillin–streptomycin (10,000 U/mL penicillin and 10,000 μg/mL streptomycin), and 5 mL of L-glutamine (200 mM) (all from Thermo Fisher Scientific, Waltham, MA, USA) (*see* **Note 2**)
2. StemPro MSC SFM xeno-free medium complete: Add 500 mL StemPro MSC SFM xeno-free medium, 5 mL of StemPro MSC SFM xeno-free supplement, and 5 mL Glutamax-1 CTS (all from Thermo Fisher Scientific, Waltham, MA, USA) and store at 4 °C. The medium is stable for 2 weeks
3. PBS (Thermo Fisher Scientific, Waltham, MA, USA)
4. Qubit Protein assay kit (Thermo Fisher Scientific, Waltham, MA, USA)
5. Human cytokine antibody array C2000 kit (RayBiotech Inc., Norcross, GA). It contains the following reagents:
   (a) Antibody arrays
   (b) 8-Well incubation tray with lid
   (c) Blocking buffer
   (d) Biotinylated antibody cocktail
   (e) 1000× HRP-streptavidin concentrate: Prepare a 1× working solution of HRP-streptavidin by adding 10 μL of the 1000× HRP-streptavidin concentrate into 15 mL

centrifuge tube containing 9990 μL of blocking buffer to get 10 mL final volume

(f) 20× Wash buffer I: Dilute 10 mL of 20× Wash buffer I with MilliQ water to get 200 mL of 1× wash buffer I

(g) 20× Wash buffer II: Dilute 10 mL of 20× Wash buffer II with MilliQ water to get 200 mL of 1× wash buffer II

(h) 2× Cell Lysis buffer concentrate

(i) Detection buffer C

(j) Detection buffer D

2.11.2 Equipment and Supplies

1. Custom-made 2-chamber slides containing ECM-like 3D scaffolds
2. Aspirating pipettes (Thermo Fisher Scientific, Waltham, MA, USA)
3. 15 and 50 mL Centrifuge tubes (Thermo Fisher Scientific, Waltham, MA, USA)
4. Centrifuge with swing bucket rotor with maximum rpm limit 4200 (Eppendorf, Hamburg, Germany)
5. Qubit 2.0 Fluorometer (Thermo Fisher Scientific, Waltham, MA, USA)
6. Omega Lum C imaging system (Gel Company, San Francisco, CA)
7. LI-COR Image Studio Lite Software (LI-COR Biotechnology, Lincoln, NE)

2.12 Mycoplasma Testing in hADSC Cultures

2.12.1 Reagents

1. MycoAlert™ Mycoplasma Detection kit (Lonza, Bend, OR, USA)
2. MycoAlert™ Assay Control Set (Lonza, Bend, OR, USA)

2.12.2 Equipment and Supplies

1. 15 mL Centrifuge tubes (Thermo Fisher Scientific, Waltham, MA, USA)
2. Centrifuge with swing bucket rotor with maximum rpm limit 4200 (Eppendorf, Hamburg, Germany)
3. 96-Well white solid flat bottom plate for luminometer (Thermo Fisher Scientific, Waltham, MA, USA)
4. Microlumat-Plus luminometer (Berthold Technologies, Tennessee)

3 Methods

3.1 Patient Preparation for Fat Procurement

3.1.1 Clinical Principles

Patient preparation for fat procurement is very similar to preparations for lipoaspirate procedures for other indications such as fat harvest for immediate transfer or liposuction for body contouring. It is a surgical procedure necessitating the same work-up and safety steps as other lipoaspiration procedures.

3.1.2 Consultation

Patient consultation allows patient evaluation for physical health and anatomic characteristics. In fat procurement cases, typically smaller than for body contouring liposuction amounts of fatty tissue are harvested. However, the potential for contour alteration always exists and the assessment of patient body image and psychological readiness for such change is necessary. A thorough medical history and physical examination is part of the consultation. Specifically, absolute and relative contraindications for surgical procedure (and anesthesia) have to be identified. Some preexisting conditions, for example, mitral valve prolapse or the presence of joint implants, may require peri-procedure administration of antibiotics. Since "tissue" injury during lipoaspiration may lead to bleeding, anticoagulative medications may have to be stopped until coagulation parameters normalize. In younger females, pregnancy test prior to any procedure is a policy in many institutions.

3.1.3 Laboratory Tests

Preoperative battery of screening tests for lipoaspiration under general anesthesia: blood hemoglobin, hematocrit, bleeding time, sodium and potassium (if the patient takes diuretics), glucose, and pregnancy test (if applicable). If general anesthesia is planned: electrocardiogram is indicated for individuals older than 45 years.

3.1.4 Informed Consent

Informed consent should include information regarding the principles of fat procurement, and objectives of the treatment (if any) or cells storage for research or future clinical application. It is important to emphasize that in patients with poor skin elasticity skin surface may change after fat procurement (and subcutaneous tissue volume depletion). Common procedure sequelae and complications such as swelling, bruising and some pain, numbness, scarring, and skin retraction have to be listed and patient has to be educated about the steps to prevent or minimize the risk of their occurrence. Risks associated with more extensive procedures include hematoma, pulmonary embolism, contours deformity as well as risks related to general anesthesia (if applicable). The consent form has to be signed.

3.1.5 Patient Readiness for Fat Procurement Procedure

Patient logistical preparations include copious shower prior to the arrival to the medical facility, light meal the night before (or no solid meals at least 8 h before the procedure if done under sedation or general anesthesia unless instructed otherwise). In fact, many clinicians implemented Protocols for Fat Procurement, which include also preparatory steps for a patient (listed above). Such protocols are helpful as they reduce the risk of conflicting information or misinformation and are complementary with the quality of informed consent process.

3.1.6 Donor Site Selection

There is no ideal fat donor site. Although there are some morphological and biochemical differences between adipose tissue in different body location, there is no evidence that there is better isolated stromal vascular fraction (SVF) cells survival, function, or volume retention linked with a specific donor site [30, 31]. Therefore, choosing of a procurement site should be based on ease and safety of access as well as the patient preference. Considering frequent need for the second harvest (e.g., for repeated transfer), it is practical to take advantage of bilaterality of donor sites. For example, fat procurement from the abdominal wall may utilize left mid-abdominal field (which may flatten due to the subcutaneous fat depletion) and symmetry can be restored a few months later by lipoaspiration of the right side.

3.1.7 Other Procedural and Surgical Variables

If a clinician procuring fatty tissue does for others, some technical issues have to be agreed on. Other than the fat harvest site, the vacuum source (and the parameters of negative pressure exerted on tissue), type of tissue tumescence prior to aspiration, and type of cannulas should be known to tissue recipients. The scientists have to be particularly sensitive to the fact that fat procuring surgeons may use the extraction technology that may not be optimal for cells viability. For example, ultrasonic-assisted liposuction may alter cell membranes and disrupt cells. However, some investigations indicated that ultrasound-assisted fat harvest technology delivers cell populations with equally viable and similar differentiation capabilities as simple suction-assisted liposuction [32]. Fat specimen processing steps, which are performed by the surgeon before fat is delivered to the lab, are equally important [33]. There has to be consensus among all members of the clinical and scientific team if fat aspirate should be centrifuged immediately after harvest (if yes low rpm is favored), and similar parties understanding regarding sterile specimen filtration and purification systems (closed circuit systems are preferred) have to be in place.

3.2 Subcutaneous Adipose Tissue Procurement

3.2.1 Clinical Principles

Subcutaneous fat procurement procedure arrangements depend on clinical or scientific needs and the volume of fat required. For smaller amounts of fat, local anesthesia or regional nerve blocks suffice. For larger or multiple sites harvest, general anesthesia should be employed. Following the harvest, subsequent steps of specimen processing may include decanting, and washing to concentrate and purify fat cells. Additionally, enzymatic dissociation may also be employed to be followed by product filtration and/or centrifugation, and ultimately cell enrichment by plating into culture site (taking advantage of cell plastic adherence) may be chosen [34].

3.2.2 Position of the Patient

Patient's position should be comfortable and ensuring safety. The movement of the cannula should be parallel or away from deeper fascial plane. The access has to be ergonomic for the physician.

3.2.3 Local Anesthesia

In local anesthesia cases, typically the infiltration solution consists of 0.5% lidocaine with 1:200,000 epinephrine or 1% lidocaine solution with 1:100,000 epinephrine buffered with sodium bicarbonate to reduce pain on injection (also *see* Table 1). Local anesthetic (e.g., 1% lidocaine with 1:100,000 epinephrine injectable using a labeled syringe, for safety and to avoid wrong administration) percutaneously into subcutaneous fat (Fig. 3A). The anesthetized field should be marked. Approximately 10 min later, when local anesthesia and vasoconstriction are in effect fat aspiration can be commenced.

Table 1
Typical content of tumescent solution

Ingredient	Quantity	Final concentration or pH
Normal saline (0.9%)	1 L	–
Lidocaine 2% (select one)[a]	50 mL 37.5 mL 25 mL	0.1% 0.075% 0.05%
Epinephrine (1:1000)	1 mL	0.1%
Sodium bicarbonate (8.45%)	12.5 mL	pH 7.4
Triamcinolone acetonide (optional)	10 mg	–

In the tumescent technique of fat aspiration, a relatively large volume of diluted solution for local anesthesia is injected into the fat beneath the skin, causing the targeted area to be numb (e.g., by lidocaine), vasoconstriction (due to epinephrine addition), and tissue Table swelling (which temporarily reduces blood perfusion) reduce bleeding and the amount of blood in procured fat. Empirically, it is known that bicarbonates reduce pain due to lidocaine and epinephrine injection

[a]The different values for lidocaine dosage are alternatives; only one of these quantities should be infused in any given bag of saline

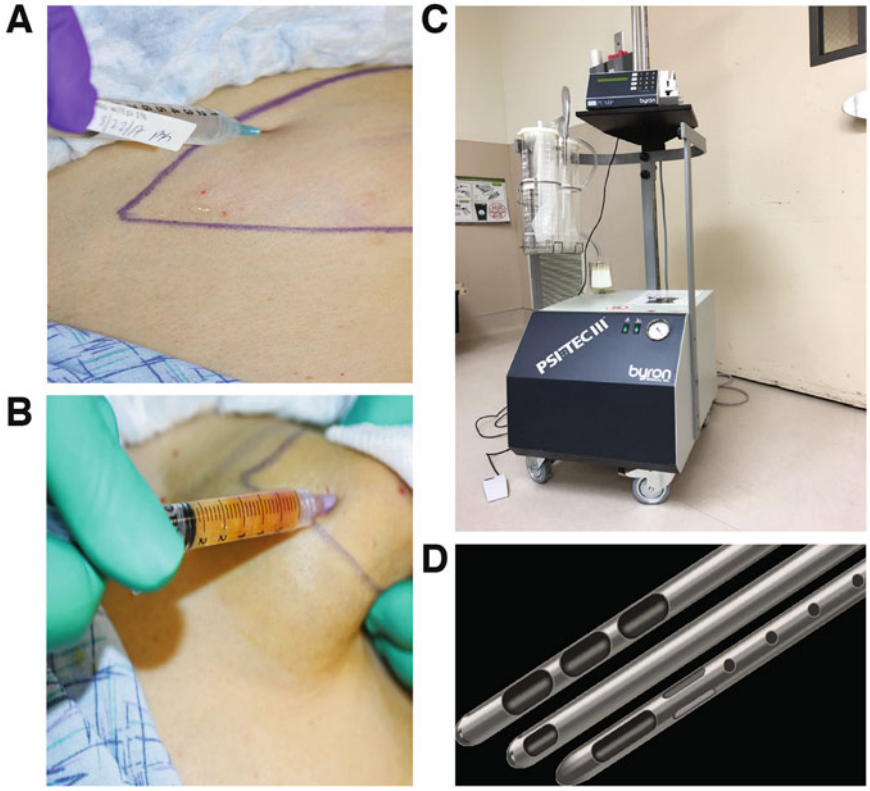

Fig. 3 Fat procurement. (**A**) Area targeted for fat procurement should be marked and it surface decontaminated. Percutaneous infiltration with 1% lidocaine with 1:100,000 epinephrine-induced local anesthesia and vasoconstriction. For larger volume operations, power infiltration of the targeted area with tumescent solution can be used. It induces not only the local anesthesia, vasoconstriction but also tissue swelling, enhancing the process of subsequent liposuction (Table 1). (**B**) Luer-Lok 3 cc syringe armed with 16G sharp needle allows quick aspiration of subcutaneous fat. (**C**) Byron PSI-TEC III is an example of modern large, useful for operating rooms, aspiration platform with high volume tunable vacuum technology. Peristaltic tumescent solution infiltration pump is on the top shelf of the system. (**D**) The various fat aspiration cannula tip aspiration designs are available in different length, diameter, and handle sizes to accommodate a broad range of fat procurement sites and to reduce surgeon's fatigue

3.2.4 Tumescence

1. For enhancement of local anesthesia, and reduction of blood admixture in the specimen and loss in general and the latter in general anesthesia cases, tissue tumescence is employed. Frequently, tumescence solution contains 0.1% lidocaine with 1:400,000 to 1:800,000 epinephrine in normal saline or Ringer's lactate solution.
2. Surgical blades No. 11 (for stab incisions), Luer-Lok 10 mL syringes or infusion system with a pump to be connected to a bag with tumescent solution, attached to blunt infiltration cannula (e.g., Mentor Worldwide, LLC, Santa Barbara, CA, USA).

3. The tumescent fluid (using an adipose tissue infiltration blunt cannula on a 5–10-cc syringe) can be infiltrated into the fat plane through approximately 2 mm stab skin incision using No. 11 blade.
4. Advance back and forth the cannula in multiple directions, breaking down fibrous tissue between fat mini-pockets. Tumescent solution (with lesser concentration of lidocaine than solution used for straight local anesthesia) should be left undisturbed for 30–40 min prior to progressing to the next operative step. In general, the volume of tumescent solution should be equal to or less than the amount of fat to be procured (Fig. 3A).

3.2.5 Drug Records Log

Maintain records of administered drugs namely local anesthesia and tumescence drugs. Total lidocaine dosage should not exceed 35 mg/kg of body weight and 5–10 μg/kg of epinephrine [35, 36].

3.2.6 Office-Based, Small Fat Amounts Procurement, Steps

1. Cleanse the selected site skin with astringent cleanser and using sterile gauze coat the surface with Betadine solution (10% povidone-iodine topical solution) (Fig. 3B).
2. After prepping, drape the harvest area with sterile towels.
3. Check if local anesthesia/tumescence and vasoconstriction are in effect by pin-prick with 25 or 27G needle.
4. A 4 Coleman multi-hole cannula attached to a 3-cc, 5–cc, or 10-cc Luer-Lok syringe is introduced into the deep subcutaneous fat plane through previously made stab incision and with the plunger of the syringe pulled back to create negative pressure, moving cannula back and forth lipoaspiration is performed (*see* **Note 1**).
5. Cross-tunneling through the tissue including passing cannulas at right angle through the donor site fat "bulge" allows fat procurement and minimizing the risk of creating grooving.
6. Alternatively, sharp, large bore needles (15 or 16G) attached to 3 cc Luer-Lok syringes can be used for both skin penetration and aspiration (Fig. 3B). Within a few minutes, several 3 cc fat aliquots can be obtained.

3.2.7 Macro-, Micro-, and Nanofat

Macrofat is procured through classic aspiration using systems designed for operating rooms equipped with a set of cannulas (Fig. 3C, D). Microfat is harvested with multiport small cannula 2 mm or less, and Nanofat is obtained from Microfat by emulsification and filtration of the aspirate. Nanofat Transfer System, with proprietary filtering system, eliminates larger specimen particles (Tulip Medical Products, San Diego, CA, USA). Nanofat does

not contain large adipocytes; it is rich in cells from the stromal vascular fraction with significant presence of the CD34+ subfraction. Nanofat appears to be superior in lipofilling as well as for research purposes [37].

Selection of Cannulas

The use of larger cannulas (e.g., 5 mm in diameter as opposed to 3 mm) results in lesser damage adipocytes. It appears that the decrease in shear stress force during tissue aspiration is important for cells survival; the larger fat globules obtained may carry a protected inner core of adipocytes for cultures or transfer [38]. Multiple types of cannulas used are shown in Fig. 3D.

Technical Recommendations

In low negative pressure fat aspiration systems (like AquaVage or LipiVage), 18 in Hg is the recommended maximum vacuum during fat procurement for transfers (Fig. 4A–E). Many systems allow setting up the level of negative pressure exerted (Fig. 3C). AquaVage System allows for procedurally simple and quick washing of the harvested fat. The harvesting cannula is placed in the washing solution (e.g., Ringer's lactate) with the aspirator in the "on" position and the solution will wash through the fat specimen and exit the filter to the waste canister leaving the fat within the filter ready for laboratory proceedings or immediate injection (Fig. 4B–D). After fat is washed with Ringer Lactate in the canister, all tumescent fluid should be evacuated by opening Y-assembly clamp. To further air-dry the fat (if chosen), remove evacuation tubing and the aspirator on prior transfer for further uses (culture, and transfer). Fatty aspirate can be also purified by simple sedimentation (Fig. 4E). During all fat procurement procedures, constant evaluation of skin surface contour is conducted checking for uniform thinning of subcutaneous fat and avoidance of indentations. Even if relative small amounts of fatty tissue are procured, it is worthy to remember that abrupt ending of fat removal may create a step deformity. To avoid such a problem, fat aspiration should be tapered off at the periphery of the field.

Alternative to AquaVage/LipiVage, fat aspirate processing system utilized by the authors is the Revolve™ System (Life Cell/Allergan, Bridgewater, NJ, USA) (Fig. 5). Revolve™ system is a single-use, sterile, intended for harvesting, filtering, and collecting lipoaspirate for research or transferring as a part of clinical operation device (Fig. 5A). This closed system allows control of such variables as type of wash and straining through its 200 μm filter mesh. Port for Luer-Lok type syringe-assisted extraction of practically dry mass of adipose specimen (Fig. 5B).

Upon completion of fat procurement, small wounds can be closed using 5/0 nylon suture. Alternatively, skin wound edges can be approximated and covered with Steri-Stripes.

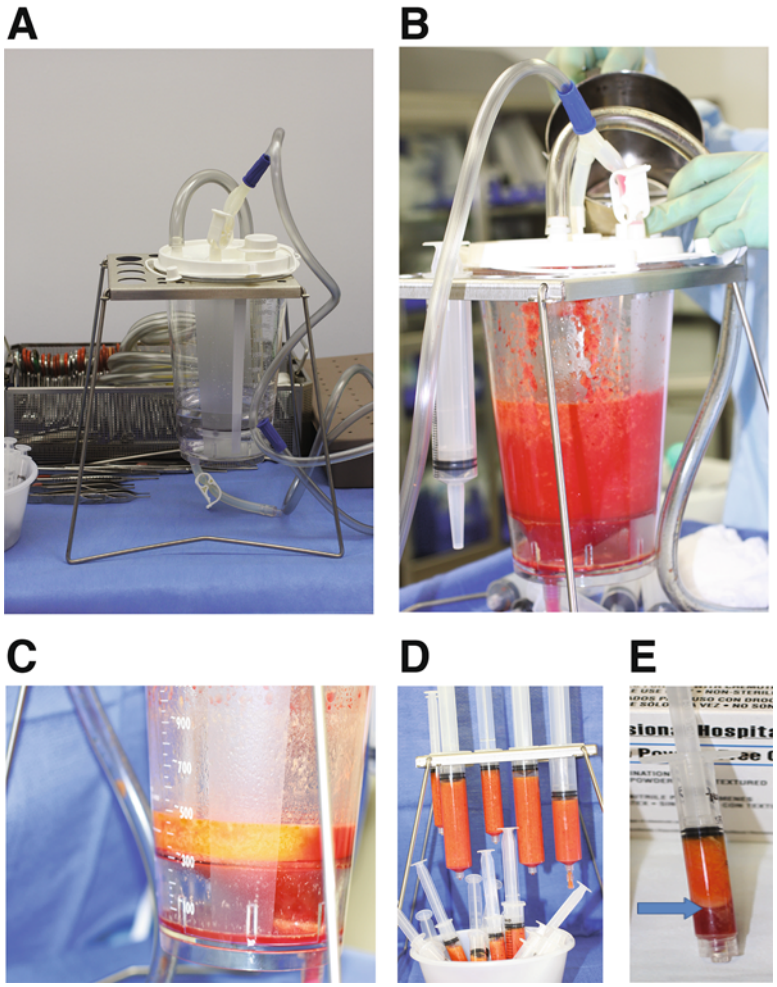

Fig. 4 AquaVage fat harvesting and collection system. (**A**) AquaVage is a sterile, single-use, closed system for fat harvesting and collection. The container, which is placed on the stand on the operating table, can be connected inline with any aspiration system (*see* also Fig. 3 (panel **C**)). (**B**) The container has a built-in filter that allows to separate fat from fluids and small impurities. After fat aspiration, irrigation fluid (e.g., Ringer's lactate) can be aspirated facilitating the purification of the fat aspirate. (**C**) After "wash out fluid" is evacuated, practically a dry, fat mass remains (note the difference in fat appearance in **B** and **C** panels). (**D**) Purified fat (in syringes) may be used for laboratory proceedings or immediate transfer procedures. (**E**) Fat specimen allowed to purify by simple sedimentation of fluid phase. The arrow marks the pellet known to contain high concentration of thrombocytes, pericytes, stem cells (stromal vascular fraction pellet)

3.3 Stromal Vascular Fraction (SVF)

The original, pioneering work on the isolation of adipose-derived stem cells (ADSC) from liposuction waste typically involves 8–10 h of continuous intense effort making it a labor-intensive endeavor and increasing the risk of culture contaminations due to excessive

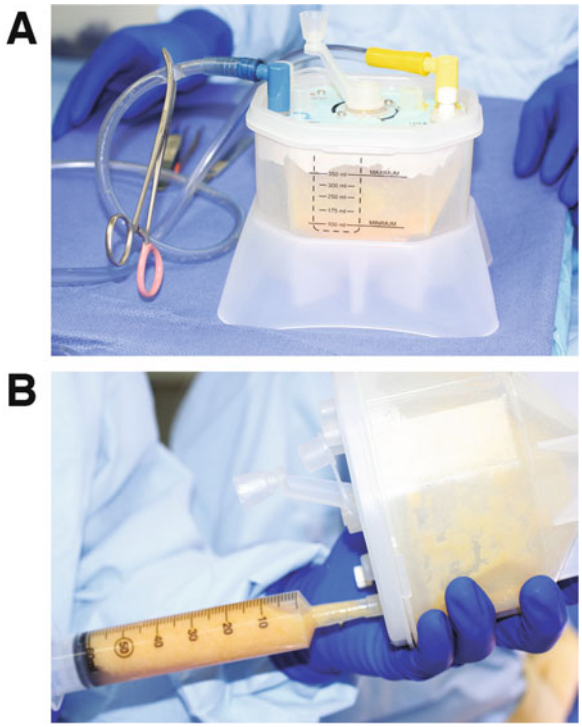

Fig. 5 Revolve™ fat grafting system. *Revolve System* (LifeCell/Acelity, San Antonio, TX) is a single-use, sterile (see the canister on the operating room table), disposable device intended for processing of fat tissue harvested by liposuction. (**A**) Outer canister filled with fat with inner filter basket (200 μm pores) that allows fat to be separated from blood and the tumescent fluid (or washout solution) by manual, slow, "centrifugation." (**B**) After fat filtration, the "dry" fat mass can be transferred to syringes for immediate surgical transfer or for laboratory processing

handling [34, 35]. This technique was enhanced and simplified in recent years with the development of technological and chemical framework that allows for the rapid and effective isolation and expansion of the patient-derived mesenchymal stem cells. The reduction in the acquisition time and developing standards for the quality controls during ADSC isolation and passaging in culture is indispensible for advancing regenerative medicine therapeutics.

There are several methods that can be found in the literature for carrying out an isolation of ADSC from the lipoaspirates. ADSC used in this research were isolated from healthy adult female donors aged between 32 and 45 years old, undergoing routine liposuction procedures. The samples were shipped as 20–30 mL frozen lipoaspirate aliquots (as described in Subheading 3.2 above) in 50 mL centrifuge tubes to the lab as per protocols for shipment of biological samples, and processed within 24 h of procurement of

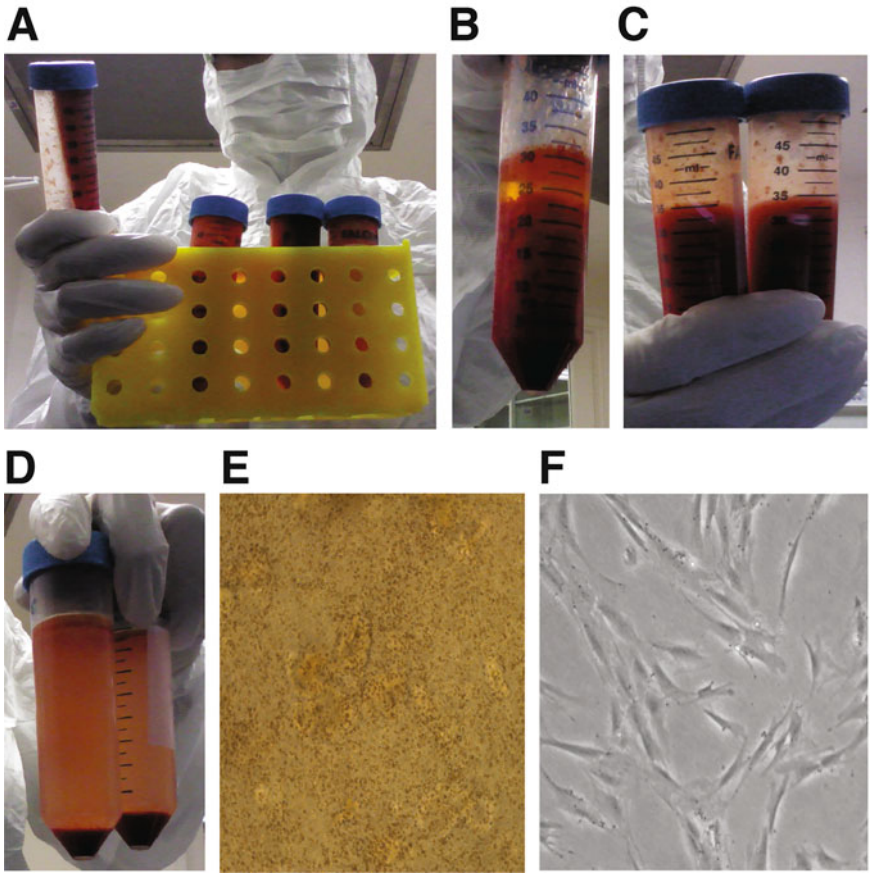

Fig. 6 Isolation of stromal vascular fraction (SVF) from patient's lipoaspirate. The lipoaspirates were procured from healthy adult female donors aged between 32 and 45 years in the clinic using AquaVage system and shipped as 20–30 mL lipoaspirate aliquots in 50 mL centrifuge tubes on ice. hADSC were isolated within 24 h post-procurement of lipoaspirate (**A**–**D**). (**A**) Frozen lipoaspirate (fat) post-shipping on ice from the clinical facility. (**B**) Following centrifugation, three distinct layers were obtained namely oil layer on top, aqueous layer, and cell pellet. (**C**) Processed ADSC-pellet post-removal of fat (oil) layer contained red blood cells which were subsequently removed by red blood cell (RBC) lysis leaving the SVF cell pellet shown in (**D**). The isolated SVF fraction 24 h post-plating yielded about 10–15% adherent hADSC in the flask (**E**) that reached about 50–80% confluence after 7–10 days in the culture (**F**)

tissue (Fig. 6A). Human ADSC isolation protocol was approved by the Local Ethics Committee at the fat procurement clinical site.

1. Warm up the DMEM/F12 complete medium (*see* **Note 2**) by placing in a 37 °C bead bath before adding to the cells in culture. Perform the cell handling steps under sterile conditions inside a biosafety cabinet, and always follow the proper personal protective equipment (PPE) guidelines set by Occupational Safety and Health Administration (OSHA) for handling human tissue.

2. Spray the two 50 mL centrifuge tubes containing the 35 mL lipoaspirate each with 70% ethanol and wipe it dry. Weigh the lipoaspirate sample.
3. Transfer 30 mL of lipoaspirate into a new 50-mL tube and add 0.75 mL of Celase™ for up to 50 mL lipoaspirate (*see* **Note 3**). Place the tube in the 37 °C beads bath for 30 min and extend the incubation in increments of 5 min if necessary, until there are no noticeable clumps left in the tube.
4. In the biosafety hood, mix the lipoaspirate sample gently. Inactivate Celase™ by diluting it to 100-fold with 10% FBS-containing media for 30 min. Centrifuge at 400 × *g* for 5 min. This centrifugation step will result in separation into 3 distinct layers (Fig. 6B). Discard the top two layers of the supernatant and save the pellet. Repeat the wash steps until there is no fat layer on the top (Fig. 6C).
5. Resuspend the pellet in 5 mL of PBS and add 5 mL of red cell lysis buffer (1:1 ratio) (*see* **Note 4**) and pipette up and down gently to lyse the erythrocytes present in the pellet until the sample turns light pink (Fig. 6D). Add 25 mL of PBS to the sample and centrifuge at 400 × *g* for 10 min at room temperature. Discard the supernatant leaving the SVF pellet (*see* **Note 5**).
6. Resuspend the SVF pellet with 10 mL DMEM/F12 complete medium. Count the cells by taking 18 μL of sample and 2 μL of AO/PI reagent (*see* **Note 6**). Total cells obtained from 60 mL SVF yields about 0.8×10^7 to 1×10^7 cells. Plate cells in 40 mL DMEM/F12 complete medium in one T175 flask. Place the flask in the humidified incubator at 37 °C, 5% CO_2, and 20% O_2 levels.
7. Aspirate the floating cells (refer to Fig. 6E) and the medium after 48 h and add 35 mL complete DMEM/F12 medium.
8. When the cells reach 80% confluence in approximately 5–7 days (Fig. 6F), aspirate the culture medium from the flask and wash the cells with 10 mL PBS. Remove PBS and add 10 mL TrypLE™. Swirl the flask to cover all the cells with TrypLE™ and incubate at 37 °C for 5 min or until the cells detach.
9. Check by observing the cells under the microscope.
10. Add 15 mL of DMEM/F12 complete medium to inactivate TrypLE™, collect the cells, and centrifuge at 200 × *g* for 5 min. Add 10 mL PBS to the cell pellet and resuspend the cells gently but thoroughly.
11. Perform the cell count by taking 18 μL of cell suspension and mixing it with 2 μL of AO/PI as described in **step 6** above.

12. Plate 250,000 cells in a T175 flask in 35 mL of complete DMEM/F12 medium and transfer to a humidified incubator at 37 °C maintained at 5% CO_2 and 20% O_2.
13. Calculate the cumulative population doublings (PD) by summing the population doublings (PD = log ($N/N0$) × 3.33, where $N0$ is the number of cells plated in the flask and N is the number of cells harvested at this passage) across multiple passages as a function of the number of days it was grown in culture as described earlier [20] and shown in Fig. 7A.

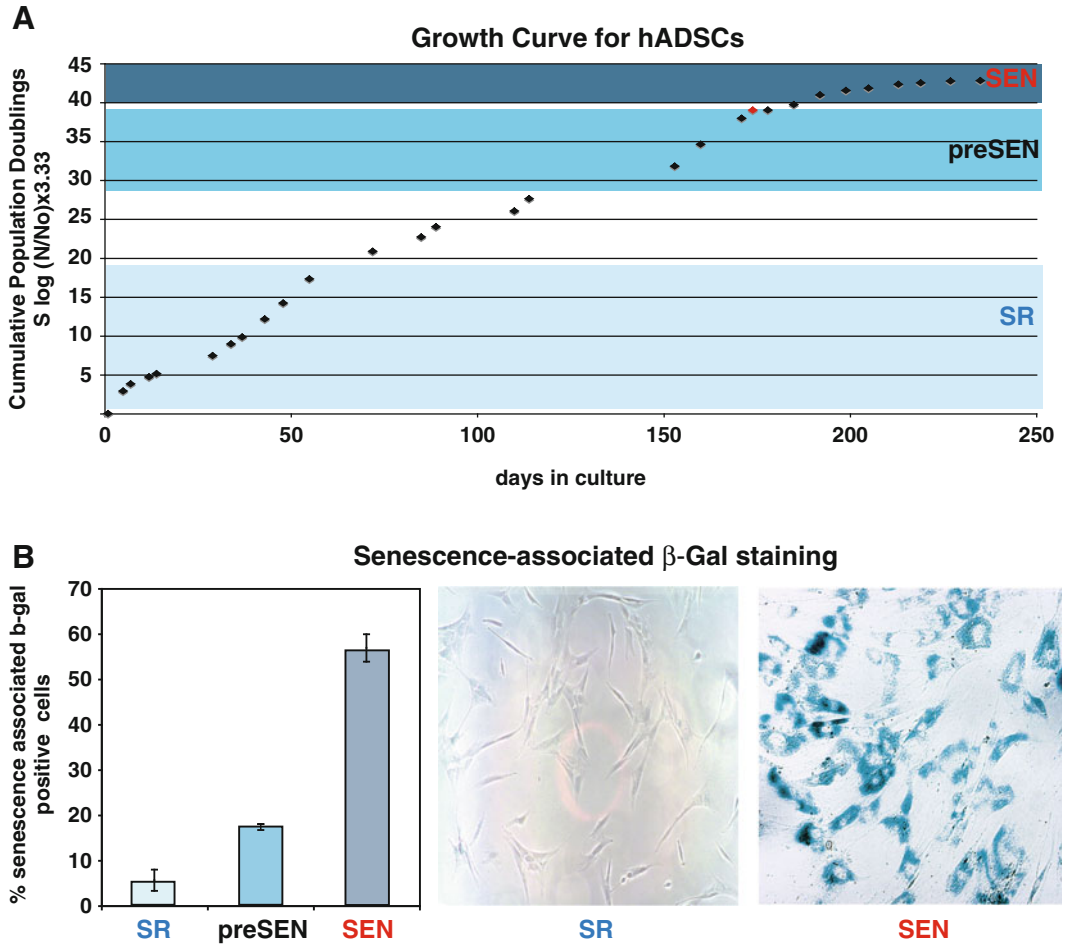

Fig. 7 Proliferative and senescent properties of hADSC. (**A**) Growth curve of the hADSC is represented as cumulative population doubling over day in culture. Three distinct states are shown: SR—self-renewing (population doubling <17); preSEN—presenescent (population doubling 29–38); SEN—senescent (population doubling >39). Replication capacity of hADSC declines with ex vivo aging. (**B**) Colorimetric detection of senescence-associated β-galactosidase (SA-β-Gal) activity in self-renewing (SR), presenescent (preSEN), and senescent (SEN) hADSC. Examples of hADSC's morphological changes (10× magnification) shown in inserts. Bar graphs correspond to percentage of SA-β-Gal positive cells with progressive ex vivo hADSC expansion, based on three independent experiments. Error bars are standard deviations from the mean

3.4 ADSC Surface Marker Analysis by Flow Cytometry

The isolated hADSC can be characterized by the presence (CD13, CD29, CD44, CD73 CD90, CD105, and CD166) and absence (CD11b, CD14, CD31, CD34, CD45, and CD106) of the surface markers for MSC in accordance with the minimum definition criteria set by the International Society for Cellular Therapy [39].

1. For surface markers analysis using flow cytometry, collect the hADSC from an 80% confluent T175 flask by TrypLE™ dissociation and perform cell counts as described earlier in Subheading 3.3, **steps 8** through **11**.
2. Count and cells resuspend in FACS buffer at a final concentration of 5×10^6 cells/mL. Add 5 μg of TruStain fcX for 5×10^6 cells (recommended concentration from the manufacturer is 1 μg of TruStain fcX for 1×10^6 cells) and incubate on ice for 10 min. No need to wash the cells.
3. Label one 1.5-mL microfuge tube for each antibody and its isotype control.
4. Mix the cells gently and add 5×10^5 cells (100 μL) in each microfuge tube. Add each antibody or its isotype control at recommended concentration from the supplier in the labeled microfuge tubes and incubate for 30 min on ice in dark with fluorochrome-labeled antibodies (*see* **Note 7**).
5. Wash with 1 mL FACS buffer/tube for 5 min on ice in dark followed by centrifugation at $400 \times g$ at room temperature.
6. Repeat wash step two times and resuspend the cell pellet gently in 500 μL FACS buffer.
7. Carefully transfer the resuspended cells to pre-labeled FACS tubes and analyze in a Guava EasyCyte Mini System.
8. Data analysis was done using FlowJo software and representative FACS as shown in Fig. 8A, B.

3.5 Establishing the ADSC Lines

1. Expand the freshly isolated ADSC from SVF by maintaining the cells in DMEM/F12 complete medium, changing medium every 72–96 h.
2. Passage the cells at 70–80% confluence using TrypLE™ select as described in Subheading 3.3, **steps 8** through **11**.
3. After performing the counts, plate 2×10^5 cells/T175 flask in fresh DMEM/F12 complete medium, replacing fresh medium every 72–96 h for cell expansion (*see* **Note 8**).
4. For long-term storage, trypsinize the cells, wash, and count as described in Subheading 3.3, **steps 8** through **11**.
5. Centrifuge the cells at $200 \times g$ for 5 min and save the cell pellet.
6. Resuspend cells at 1×10^6/mL density in Synth-a-Freeze™ cryopreservation medium and aliquot 1×10^6 cells (1 mL) in each cryovial pre-labeled with a liquid nitrogen safe label

A

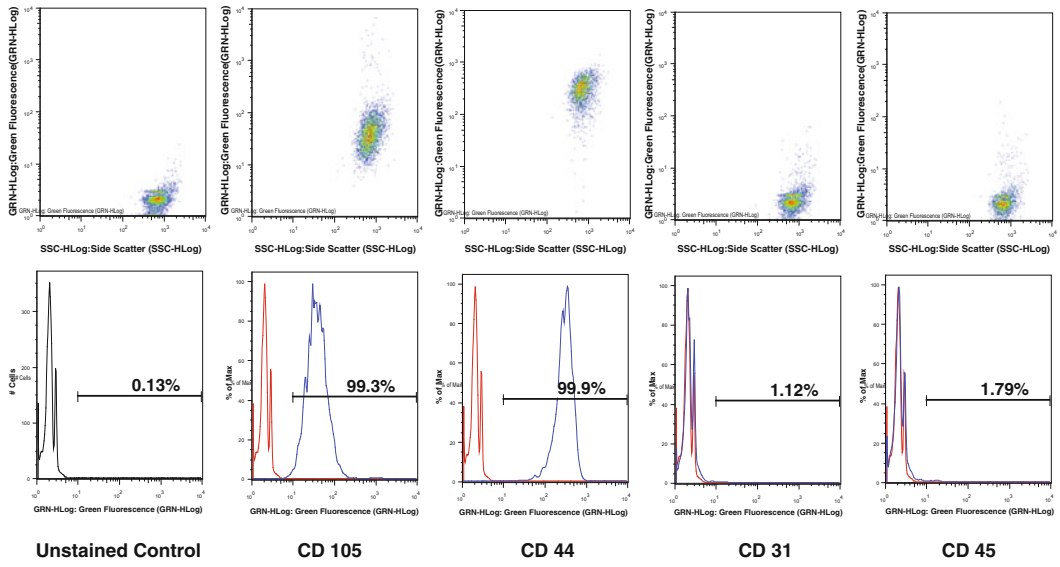

B

Chromosome	Gene	Expression	
		SR	SEN
Negative Markers			
16	CD 11b	-	-
5	CD 14	-	-
17	CD 31	-	-
1	CD 34	-	-
1	CD 45	-	-
1	CD 106	-	-
4	ABC G2	-	-
3	CD 10	+	+
2	CD 49d	+	+
Stromal Markers			
15	CD 13	++	++
10	CD 29	++	++
11	CD 44	++	++
6	CD 73	++	++
11	CD 90	++	++
9	CD 105	+	++
3	CD 166	++	++

Fig. 8 Immunophenotype of hADSC. (**A**) Representative FACS analysis of hADSC. SR (PD8) hADSC were stained with FITC (CD 31, CD44, and CD 45) or Alexa Fluor-488 (CD105)-conjugated antibodies against cell surface markers and subjected to flow cytometry analysis. The cell populations are shown as fluorescence to side scatter graphs (top), and the histograms (bottom) of stained cells (blue line) compared to unstained cells (red line); with the percentage of positive cells indicated. (**B**) The table summarizes immunostability of hADSC in self-renewing (SR) and senescent (SEN) states, which were assessed by expression of MSC-positive and MSC-negative CD markers

containing barcode to identify the cell line number, PD, and freezing date.

7. Store the vials at −80 °C in cryo-containers for 24–48 h and transfer the vials to liquid nitrogen storage boxes. Place the liquid nitrogen storage boxes in the liquid nitrogen storage tank for subsequent use.
8. Always maintain a record for the cell lines stored in the liquid nitrogen tank and record all the vials removed or added to the liquid nitrogen storage boxes in a logbook.

3.6 Thawing of Cryopreserved hADSC

The quality of stem cells after long-term cryogenic storage is an important question in the era of personalized cell banking and cell therapy. Recently, the potency of mesenchymal stromal cells (MSC) was tested after 23–25 years of bone marrow cryopreservation [40]. The data evaluating the long-term preservation of human bone marrow cells as a source of the MSC have shown that cultivation after thawing cells has showed no reduction in MSC essential surface marker molecules and cultured MSC demonstrated differentiation capacity in vitro into osteoblasts and adipocytes. Here, we describe our protocol for thawing hADSC from long-term cryopreservation in the lab and cells obtained from commercial banks.

1. Do not thaw the cryopreserved cells until the recommended pre-warmed medium and plasticware and/or glassware are on hand.
2. Remove the vial of hADSC from liquid nitrogen tank and incubate in a 37 °C bead bath. Closely monitor until the cells are completely thawed. Maximum cell viability is dependent on the rapid and complete thawing of frozen cells.
3. As soon as the cells are completely thawed, disinfect the outside of the vial with 70% ethanol. Make sure to not disturb the writing on the tube. We recommend barcoding labels instead of using marker writings. Proceed immediately to the next step.
4. In a laminar flow hood, use a 1- or 2-mL pipette to transfer the cells to a sterile 15-mL centrifuge tube. Be careful not to introduce any bubbles during the transfer process.
5. Using a 10-mL pipette, slowly add dropwise 9 mL of pre-warmed DMEM/F12 complete media (*see* Subheading 2.5.1, **item 1** for media composition) or a suitable alternative medium of choice to the 15 mL centrifuge tube containing the cells (*see* **Note 9**).
6. Gently mix the cell suspension by slowly pipetting up and down twice. Be careful to not introduce any air bubbles. IMPORTANT: Do not vortex the cells.
7. Centrifuge the tube at 300 × *g* for 2–3 min to pellet the cells.

8. Decant as much of the supernatant as possible. **Steps** from **3** to **8** are necessary to remove the residual cryopreservative (DMSO).
9. Resuspend the cells in a total volume of 10 mL of DMEM/F12 complete media or a suitable alternative of choice, pre-warmed to 37 °C and count the cells by taking 18 μL of sample and 2 μL of AO/PI reagent on a Luna Stem counter.
10. Plate the cell suspension into two T175 tissue culture flasks at a cell density of 3–5 × 10^5 cells/T175 flask in 35 mL of fresh DMEM/F12 complete medium.
11. Maintain the cells at 37 °C in a humidified 37 °C incubator with 5% CO_2 and 20% O_2.
12. Next day, exchange the medium with fresh DMEM/F12 complete media (pre-warmed to 37 °C).
13. Replace with fresh medium every 3–4 days thereafter.
14. When the cells are approximately 80% confluent, they can be dissociated with TrypLE™ and passaged further or frozen for later use.

3.7 Measuring hADSC Proliferation

Control of cell proliferation is an important property of the healthy hADSC cultures. Direct measurement generally involves the incorporation of a labeled nucleoside into genomic DNA. DNA synthesis is also relatively specific for cell division because "unscheduled" DNA synthesis is quantitatively minor [41]. Measurement of new DNA synthesis is therefore essentially synonymous with measurement of cell proliferation. Biochemistry of DNA synthesis and the routes of the label entry are schematically shown in Fig. 9. Here, we describe two methods for measuring DNA replication and, hence, cell proliferation that is applicable in the cell cultures, namely the tritiated thymidine ([^{3}H]-dT) and BrdU methods [16, 21, 22]. We have validated this technique in vivo by comparing measured cell proliferation rates to values estimated by independent techniques. It is important to note that [^{3}H]-dT is a potent antimetabolite that has been used to kill dividing cells [42]; the toxicity of introducing radioisotopes into DNA is avoided here by using stable isotopes. The toxicities of nucleoside analogues per se (e.g., BrdU) are avoided by labeling with a physiologic substrate as shown in [41]. Experimental evidence also suggests that many thymidine-labeled stem cells die after being transplanted (as done for studies on stem cell transplantation research where many labeled stem cells die after being transplanted into the mice brain. The released chemical was taken up by the neighboring cells (dividing and nondividing), which may be mistaken as transplanted cells [43, 44].

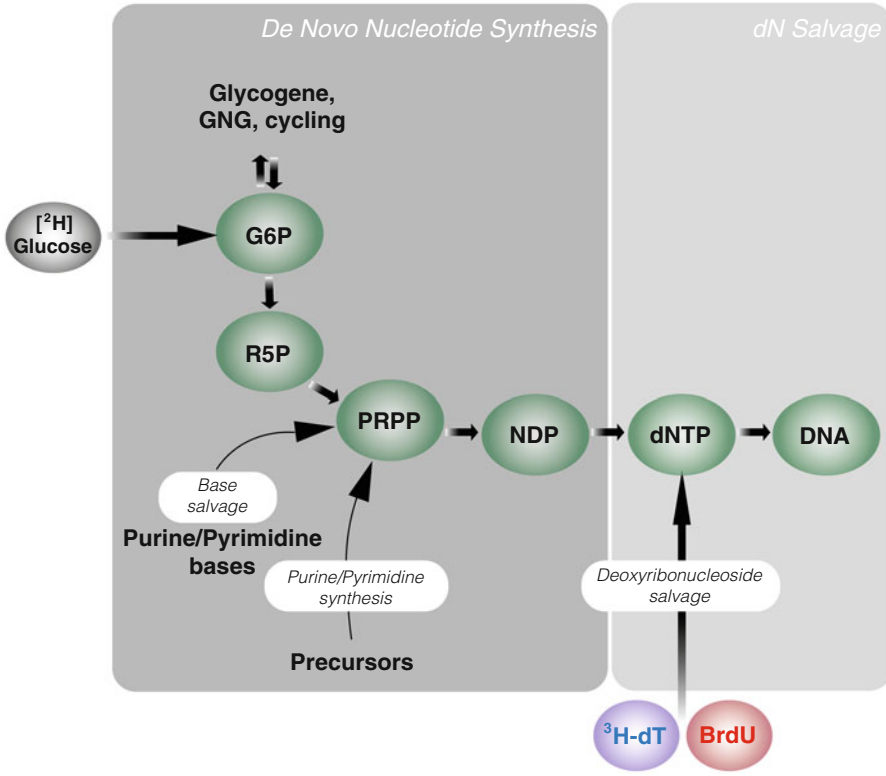

Fig. 9 Biochemistry of DNA synthesis and routes of label entry. Not all intermediates are shown. *G6P* Glc 6-phosphate, *R5P* ribose 5-phosphate, *PRPP* phosphoribosepyrophosphate, *[^{3}H]-dT* tritiated thymidine

3.7.1 Establishment of Proliferation Index ([^{3}H]-Thymidine Uptake into Cellular DNA)

Radioactive tagging of newly synthesized DNA with 3H-labeled thymidine ([^{3}H]-dT) is the most frequently applied technique. The thymidine incorporation assay, the most common assay, utilizes a strategy wherein a radioactive nucleoside, 3H-thymidine, is incorporated into new strands of chromosomal DNA during mitotic cell division. A scintillation beta-counter is used to measure the radioactivity in DNA recovered from the cells in order to determine the extent of cell division that has occurred in response to a test agent. The tritiated thymidine ([^{3}H]-dT) labeling index has been used for estimation of the proportion of S-phase cells in asynchronous cell populations as described elsewhere [45, 46]. However in later years, it has been demonstrated that incorporated tritiated thymidine ([^{3}H]-dT) might suppress cell proliferation by induction of DNA strand breaks and induction of chromosomal aberrations [47]. These effects are a function of specific activity, concentration, or exposure time [47].

1. 10,000 cells were treated by adding 1 μCi ^{3}[H]-thymidine (Perkin-Elmer, Boston, MA, USA) to DMEM/F12 complete medium for 24 h.

2. Use unlabeled control cell culture to estimate the background level.
3. Harvest labeled cells in the area designated for radioactive materials area and isolate DNA according to standard DNA isolation procedure (*see* **Note 10**). Air-dry the chromosomal DNA and dissolve the DNA pellet in water. DNA can be quantified with NanoDrop (ND-1000; NanoDrop Technologies Inc.).
4. Spot labeled DNA onto glass fiber filters with filtered–distilled water using a pipetman.
5. [^{3}H]-thymidine uptake into cellular DNA was measured with liquid scintillation counter (LS 6500; Beckman Instruments).
6. Perform all the experiments in triplicates.
7. Intake per 1 μg of DNA is calculated and plotted. Exemplified results are shown in Fig. 10A.

3.7.2 BrdU Immunofluorescent Staining

Gratzner in 1982 [48] developed a monoclonal antibody to immunofluorescence, or avidin–biotin complexes [49–52]. Monoclonal antibody (MAb) techniques for detection of BrdU have the advantages of simplicity and speed over standard autoradiography. The standard non-synchronized proliferating cultures of ADSC contain approximately 20% of BrdU positive cells [16, 21, 23]. We use this method to demonstrate that senescent hADSC self-renew poorly, and as a result show diminished levels of bromodeoxyuridine

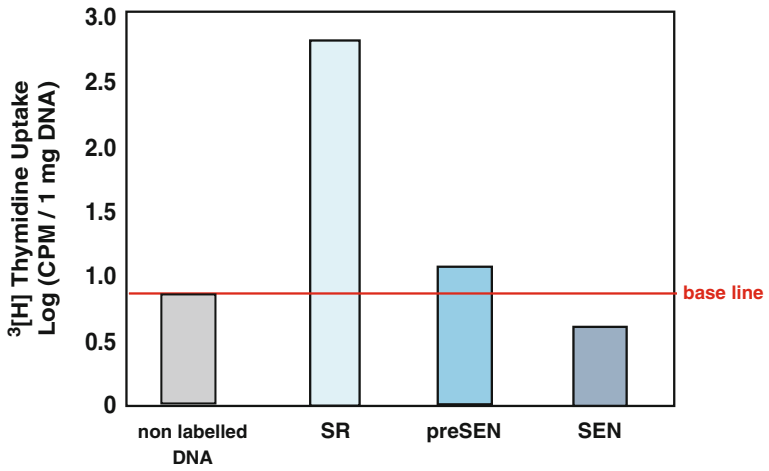

Fig. 10A ^{3}[H]-thymidine uptake to measure proliferation of hADSC cultures. Replication capacity of hADSC declines with ex vivo aging. Proliferation in self-renewing (SR), presenescent (preSEN), and senescent cells (SEN) hADSC was measured by 3[H]-thymidine uptake. Results are presented as the amount of ^{3}[H]-thymidine (cpm) incorporated during DNA synthesis per 1 μg of isolated DNA. DNA from cells not exposed to ^{3}[H]-thymidine was used as a background radiation control

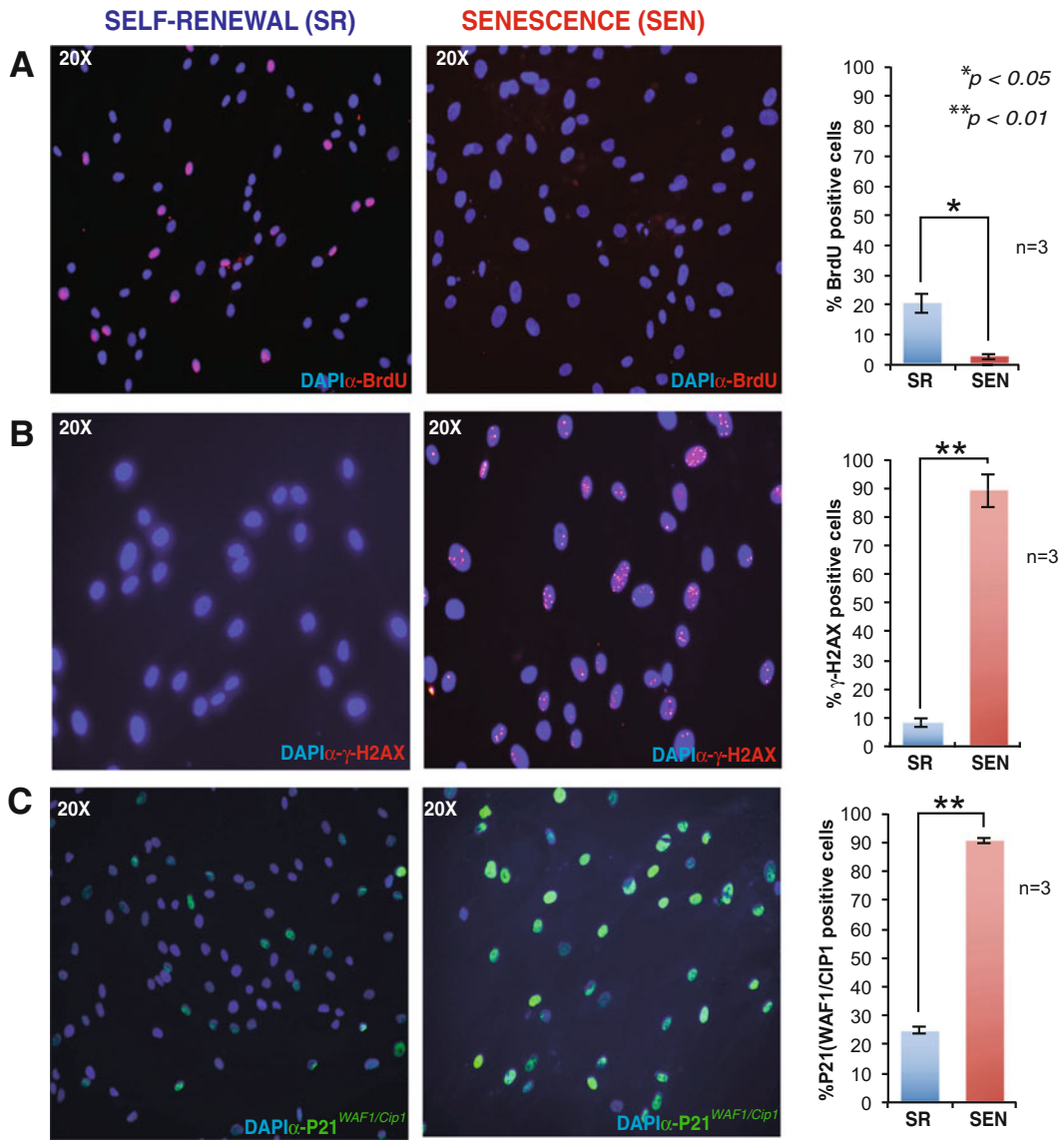

Fig. 10B Ex vivo senescence of hADSC is associated with formation of persistent DNA damage foci and $P21^{WAF1/Cip1}$ upregulation. Immunohistochemical detection of 5′-bromo-2′deoxyuridine (BrdU) incorporation, $P21^{WAF1/Cip1}$, and γH2AX in senescent (SEN) and self-renewing (SR) populations of hADSC. Examples (20× magnification) are shown in inserts. DNA was detected with DAPI. Quantification of senescent phenotype in hADSC: bar graphs correspond to a percentage of BrdU, γH2AX, and $P21^{WAF1/Cip1}$ positive cells in DAPI-stained total cell population, based on three independent experiments ($n = 3$). Total amount of the cells counted in three experiments: BrdU staining—(SR) $n_1 = 61$, $n_2 = 62$, $n_3 = 76$ (SEN) $n_1 = 56$, $n_2 = 133$, $n_3 = 88$; $P21^{WAF1/Cip1}$ staining—(SR: $n_1 = 193$, $n_2 = 143$, $n_3 = 179$) (SEN: $n_1 = 180$, $n_2 = 156$, $n_3 = 173$); γH2AX immunostaining—(SR $n_1 = 207$, $n_2 = 208$, $n_3 = 152$) (SEN $n_1 = 142$, $n_2 = 215$, $n_3 = 142$). Bars are the standard deviations from the mean

(BrdU) incorporation into DNA and can be identified and quantitated following immunofluorescence staining of incorporated BrdU [16, 21, 23]. We follow the protocol down below:

1. Harvest hADSC cultured in DMEM/F12 complete medium from a T175 at 80% confluence by trypsinizing the cells and perform cell counts as described in Subheading 3.3, **steps 8–11**.
2. Plate 20,000 hADSC in the 4-chamber glass slides in 500 μL DMEM/F12 complete medium and culture overnight in a humidified 37 °C cell-culture incubator with 5% CO_2 and 20% O_2.
3. Prepare BrdU at 0.03 mg/mL in DMEM/F12 complete medium. Aspirate the media from the chamber slide and add 500 μL BrdU-containing medium in each well and incubate for 1 h at room temperature.
4. Aspirate media and fix the cells with cold 70% ethanol. Incubate for 5 min. Aspirate ethanol and wash the cells three times with PBS.
5. Add 1.5 M HCl and incubate for 30 min at RT.
6. Aspirate HCl and wash the cells three times with PBS.
7. Block with blocking buffer (5% normal donkey serum) for 1 h at RT on a rocker.
8. Dilute the antibody 1:1000 in blocking buffer. Incubate with primary antibody overnight at 4 °C.
9. Wash the cells three times with PBS at room temperature.
10. Incubate with secondary antibody Donkey anti-mouse Alexa 594 diluted 1:500 in blocking buffer.
11. Wash the cells two times each for 5 min with PBS at room temperature.
12. Wash two times with distilled water for 5 min each.
13. For nuclear staining, incubate the cells with DAPI staining solution (1:1000 dilution of DAPI stock with PBS) for 10–15 min at room temperature (*see* **Note 11**).
14. Wash two times with distilled water for 5 min each at room temperature.
15. Mount the slide in ProLong™ Gold anti-fade aqueous mounting medium.
16. Epifluorescence images were acquired on a Zeiss AxioImager M1 fluorescence microscope.
17. Count the percentage of BrdU positive cells as percentage of DAPI-stained nuclei in three representative fields. No less than about 200 cells should be counted in each experiment. Exemplified results are shown in Fig. 10B (panel A). The standard deviations of the mean were calculated and plotted as bars.

3.8 Identification of Senescent hADSC

It had been discovered by Hayflick [53] that primary cells in culture can undergo a limited number of cell division cycles (about 40–60) before they lose their ability to proliferate resulting in the persistent cell cycle arrested cellular stage in which cells remain viable (see for review in [6]). This process, known as cellular senescence, is characterized by altered gene expression and secretion of numerous cytokines, growth factors, and modulators of extracellular matrix. Besides replicative exhaustion, cellular senescence of cultured stem cells is also caused by other factors such as prolonged stress caused by drug-induced DNA damage, irradiation, hypoxia, or reactive oxygen species (ROS) and by the presence of inflammatory and certain growth factors [6, 22]. Therefore, for performing downstream cell-based assays, as well as for applying the hADSC in clinical applications, the status of senescent cells in the cultures has to be considered in order to maximize effectiveness of the treatment and develop therapeutic standards [54]. Senescent cells are quantitated by assessing the expression of senescence markers such as: senescence-associated β-galactosidase activity, markers of persistent DNA damage γH2AX and p53 binding protein-1 (53BP1), marker of cell cycle arrest $p21^{WAF1/CIP}$, and by the absence of detectable cellular proliferation activity measured by BrdU or [^{3}H]-dT incorporation described in Subheadings 3.7.1 and 3.7.2 [16, 21, 55].

3.8.1 Senescence-Associated SA-β-Galactosidase Assay

The expression of pH-dependent senescence-associated β-galactosidase activity (SA-β Gal) is markedly different for proliferating vs. senescent cells and has been used as an indicator for identification of senescent cells [56]. The assay for monitoring the expression of pH-dependent senescence-associated β-galactosidase activity (SA-β Gal) is routinely performed in our culturing facility by using Senescence Detection Kit (BioVision) following manufacturer's protocol and as previously published in [16, 21–23].

1. Harvest hADSC cultured in DMEM/F12 complete medium from a T175 at 80% confluence by trypsinizing the cells and perform cell counts as described in Subheading 3.3, **steps 8** through **11**.
2. Plate 20,000 hADSC in the 4-chamber glass slides in 500 μL of DMEM/F12 complete medium and culture overnight in a humidified 37 °C cell-culture incubator with 5% CO_2 and 20% O_2.
3. Next day, remove the medium and wash the cells with PBS warmed up to 37 °C in advance of experiment.
4. Fix the hADSC using fixative solution provided in the kit, for 15 min at room temperature.

5. Wash the cells twice with PBS. Aspirate PBS and add 0.5 mL of staining solution mix containing X-Gal and staining supplement supplied in the kit.
6. Incubate at 37 °C overnight in the incubator or until the intense color develops.
7. Repeat the wash steps twice with PBS, mount with 70% glycerol (*see* **Note 12**) and capture the images using a microscope (Nikon, TE300, DXM1200 Digital Camera, Japan).
8. A representative example of data analysis is shown in Fig. 7B.

3.8.2 Immunofluorescence Staining for Senescence Markers γH2AX and p53 Binding Protein-1 (53BP1)

Senescent hADSC manifest a dramatic downregulation of the genes encoding cell cycle progression and can be identified by their large size and activation of DNA damage response (DDR) pathways. As hADSC approach senescence, both mediators of DDR, phosphorylated form of histone variant H2AX (γH2AX), and p53 binding protein-1 (53BP1) exhibit characteristic persistent DNA damage foci. The number of these foci increases from very rare in self-renewing hADSC to almost 90% in hADSC approaching senescence and can be monitored by staining for these markers namely 53BP1 and γH2AX as previously described in [16, 21–23].

1. Harvest hADSC cultured in DMEM/F12 complete medium from a T175 at 80% confluence by trypsinizing the cells and perform cell counts as described in Subheading 3.3, **steps 8** through **11**.
2. Plate 20,000 hADSC in 4-chamber glass slides in 500 μL DMEM/F12 complete medium and culture overnight in a humidified 37 °C cell-culture incubator with 5% CO_2 and 20%.
3. Next day, remove the medium and wash the cells with PBS. Fix the cultured hADSC with 4% paraformaldehyde for 15 min at room temperature (*see* **Note 13**).
4. Wash the cells three times with PBS. Aspirate PBS and permeabilize the cells using 0.5% Triton X-100 for 20 min.
5. Wash the cells three times with PBS.
6. Add the blocking solution (5% normal donkey serum in PBS) and incubate the slides at RT for 1 h.
7. Perform all the incubation steps with antibody and washes on a rocking platform shaker.
8. Remove the blocking solution and add the primary antibody diluted (1:20) (please *see* **Note 14** for instructions) in blocking solution and incubate at RT for 1 h.
9. Wash the cells three times with PBS. Aspirate PBS and incubate with secondary antibody at 1:500 dilution (*see* **Note 15**) in blocking buffer for 1 h at RT.
10. Wash the cells two times each for 5 min with PBS.

11. Wash two times with distilled water for 5 min each.
12. Perform nuclear staining, incubate the cells with DAPI staining solution (1:1000-fold dilution of DAPI stock with PBS) for 10–15 min at room temperature (*see* **Note 11**).
13. Wash the cells twice for 5 min with distilled water.
14. Mount the slide in ProLong Gold anti-fade aqueous mounting medium. Epifluorescence images were acquired on a Zeiss AxioImager M1 fluorescence microscope under 20× magnification.
15. Perform cell count for calculating the percentage of positively stained 53BP1 and $P21^{WAF1/CIP}$ and plot as percentage of DAPI-stained nuclei in three fields.
16. A representative example of data analysis is shown in Fig. 10B (panel B).

Examples (20× magnification) are shown in inserts of Fig. 10B. Quantification of senescent phenotype in hADSC: bar graphs correspond to a percentage of 53BP1 and γH2AX positive cells in DAPI-stained total cell population, based on three independent experiments ($n = 3$). During senescence, the percentage of the 53BP1 and γH2AX increases to approximately 90% of the total cell population as shown in [16, 21–23]. About 200 cells were counted in each experiment. The standard deviations of the mean were calculated and plotted as bars.

3.8.3 $p21^{WAF1/CIP}$ Immunofluorescent Staining

1. Harvest hADSC cultured in DMEM/F12 complete medium from a T175 at 80% confluence by trypsinizing the cells and perform cell counts as described in Subheading 3.3, **steps 8** through **11**.
2. Plate 20,000 hADSC in the 4-chamber glass slides in 500 μL DMEM/F12 complete medium and culture overnight in a humidified 37 °C incubator with 5% CO_2 and 20%.
3. Aspirate media and fix the cells with 0.5 mL of 4% paraformaldehyde for 30 min (*see* **Note 13**) at room temperature.
4. Perform three washes with PBS for 10 min each.
5. Permeabilize the cells with 0.5% Triton X-100 in PBS for 15 min at room temperature.
6. Wash the cells three times with PBS for 10 min.
7. Block the cells in 5% normal donkey serum for 1 h at room temperature.
8. Incubate with $p21^{WAF1/CIP}$ primary antibody overnight at 4 °C at 1:1000 dilution (*see* **Note 14**) in NDS blocking solution.
9. Next day, wash the cells two times with PBS for 5 min each.
10. Wash twice with distilled water for 5 min each.

11. For nuclear staining, incubate the cells with DAPI staining solution (1:1000 dilution of DAPI stock with PBS) for 10–15 min at room temperature (*see* **Note 11**).
12. Wash the cells twice with PBS.
13. Mount the slide in ProLong™ Gold anti-fade aqueous mounting medium (Invitrogen). Epifluorescence images were acquired on a Zeiss AxioImager M1 fluorescence microscope with Spotfire 3.2.4 software (Diagnostics Instruments).
14. Example image (20× magnification) is shown in Fig. 10B (panel C).
15. Quantification of senescent phenotype in hADSC: bar graphs correspond to a percentage of $P21^{WAF1/Cip1}$ positive cells in DAPI-stained total cell population, based on three independent experiments ($n = 3$).

No less than 200 cells should be counted in each experiment. The standard deviations of the mean were calculated and plotted as bars.

3.9 hADSC Differentiation

Usage of hADSC in regenerative medicine was prompted by a demonstration that these cells after ex vivo expansion have a capacity for differentiation into cells of multiple mesenchymal lineages both ex vivo and in vivo [57, 58]. Major signalling pathways that drive such differentiation are schematically shown in Fig. 1 (panel A). Here, we list the differentiation protocols routinely used in our lab. Representative examples are shown in Fig. 1 (panel B).

3.9.1 Adipogenic Differentiation

We used Human Mesenchymal Stem Cell functional identification kit (R&D systems) containing adipogenic, osteogenic, chondrogenic, and ITS supplement for differentiation of hADSC to adipocytes and followed manufacturer's recommended protocols.

1. Trypsinize the hADSC at PD 5–15 from an 80% confluent T175, and count the cells (*see* **Note 16**).
2. Plate 2×10^4 cells/cm^2 into each well of a 24-well plate in α-MEM basal medium and incubate in a 37 °C and 5% CO_2 incubator until 100% confluent after 24–48 h. Do not induce differentiation until the cells are 100% confluent.
3. Prepare the adipogenic differentiation medium by adding 50 μL of pre-warmed adipogenic supplement to 5 mL of α-MEM basal medium.
4. To induce adipogenic differentiation, replace the medium with 0.5 mL adipogenic differentiation medium and continue cell culture in a 37 °C and 5% CO_2 incubator.

5. Change the medium with 0.5 mL fresh pre-warmed adipogenic differentiation medium every 3–4 days and continue the culture for 21 days.
6. The lipid vacuoles will start to appear at day 7 in differentiation wells.
7. On day 21, remove the adipogenic medium and wash the cells three times with 1 mL PBS.
8. Fix the hADSC with 4% PFA at RT for 15 min (*see* **Note 13**).
9. Wash the cells with 60% isopropanol followed by staining with 0.6% Oil Red O solution (*see* **Note 17**) for 45 min at RT.
10. Remove Oil Red O solution, wash with 60% isopropanol followed by a wash with distilled water.
11. Capture the images using a microscope (Nikon, TE300, DXM1200 Digital Camera, Japan).
12. Representative example is shown in Fig. 1 (panel B).

3.9.2 Osteogenic Differentiation

1. Trypsinize the hADSC at PD 5–15 from an 80% confluent T175, and count the cells (refer to Subheading 3.3, **steps 8** through **11**).
2. Plate 4×10^3 cells/cm^2 into each well of a 24-well plate in α-MEM basal medium and incubate in a humidified 37 °C incubator at 5% CO_2 and 20% O_2 levels, until 50–70% confluent after 24–48 h. Do not let the cells grow more than 70% confluent prior to starting osteogenic differentiation.
3. Prepare the osteogenesis differentiation medium by adding 250 μL of osteogenic supplement to 5 mL of in α-MEM basal medium.
4. To induce differentiation, replace the medium with 0.5 mL osteogenic differentiation medium and place the cells in a humidified 37 °C incubator at 5% CO_2 and 20% O_2 levels.
5. Refresh the medium (0.5 mL/well) every 3–4 days and culture the cells for 21 days.
6. After 21 days, wash the cells twice with 1 mL of PBS, and fix the cells with 0.5 mL of 4% PFA in PBS for 20 min at room temperature. (Please *see* **Note 13**.)
7. Wash the cells three times with 0.5 mL of 1% BSA in PBS for 5 min.
8. Permeabilize and block the cells with 0.5 mL of 0.3% Triton X-100, 1% BSA, and 10% normal donkey serum in PBS at room temperature for 45 min.
9. Dilute the reconstituted anti-Osteocalcin antibody in PBS containing 0.3% Triton X-100, 1% BSA, and 10% normal donkey serum to a final concentration of 10 μg/mL. Add 300 μL/well

of anti-Osteocalcin antibody working solution and place it at 4 °C overnight (*see* **Note 14**).

10. Wash the cells three times with 0.5 mL of 1% BSA in PBS for 5 min.
11. Add 300 μL/well secondary antibody diluted at 1:200 in 1% BSA in PBS, and incubate the cells for 1 h at room temperature (*see* **Note 14**).
12. Wash the cells three times with 0.5 mL of 1% BSA in PBS for 5 min.
13. Stain with DAPI as described in Subheading 3.7.2, **step 13** (*see* **Note 11**).
14. Carefully remove the coverslips with forceps and mount cell side down onto a drop of mounting medium on a glass slide and capture the images using a microscope (Nikon TE300, DXM1200 Digital Camera, Japan).
15. Representative example is shown in Fig. 1 (panel B).

3.9.3 Chondrogenic Differentiation

1. Trypsinize the hADSC at PD 5–15 from an 80% confluent T175, and count the cells as described in Subheading 3.3, **steps 8** through **11**.
2. Add 2.5×10^5 hADSC, resuspended in complete DMEM/F12 medium into one 15-mL centrifuge tube and centrifuge at $200 \times g$ for 5 min at room temperature.
3. Aspirate the supernatant and wash the cells by resuspending the cells gently in PBS, followed by centrifugation at $200 \times g$ for 5 min at room temperature.
4. To induce chondrogenic differentiation, aspirate the PBS and add 1.5 mL of chondrogenic differentiation medium.
5. Centrifuge the tube at $200 \times g$ for 5 min at room temperature so that the cell pellet is obtained at the bottom. Loosen the cap of the tube and replace it in a humidified 37 °C incubator at 5% CO_2 and 20% O_2 levels.
6. Refresh the chondrogenic differentiation medium every 3–4 days and culture the cells for 21 days.
7. After 21 days, centrifuge the 15 mL tube containing differentiated hADSC at $200 \times g$ for 5 min at room temperature.
8. Aspirate the medium and wash the cells twice with 1 mL PBS by centrifugation at $200 \times g$ for 5 min at room temperature. Resuspend the cells in 500 μL of PBS.
9. On a glass slide, draw a circle using the barrier marking pen and transfer 100 μL of gently mixed cell pellet to glass slide inside the marked area. Air-dry the cell pellet.

10. Fix the cells with 10% formaldehyde at RT for 15 min (*see* **Note 13**).
11. Wash three times with distilled water.
12. Stain the differentiated chondrogenic cells by analyzing alkaline phosphatase activity using BCIP/NBT (5-Bromo-4-chloro-3-indolyl phosphate/Nitro blue tetrazolium) as a substrate.
13. Dissolve one BCIP/NBT tablet (SigmaFast™ BCIP-NBT; Sigma Aldrich) in 10 mL distilled water to make the substrate solution. Store in the dark and use within 2 h.
14. Wash the fixed differentiated chondrocytes cells once with PBS containing 0.05% Tween 20.
15. Carefully aspirate the washing buffer and add 0.5 mL BCIP/NBT substrate solution to each well. Incubate at room temperature in the dark for 5–10 min. Monitor staining progress every 2–3 min, until reaction is complete as evidenced by stained cells.
16. Gently aspirate the substrate solution and wash the cells with PBS containing 0.05% Tween 20.
17. Analyze the cells and record the images using a microscope (Nikon, TE300, DXM1200 Digital Camera, Japan).
18. Representative example of alkaline phosphate staining is shown in Fig. 1 (panel B).

3.10 Ex Vivo hADSC Migration Assay and Invasion Assays

One of the important characteristics of MSC and hADSC in particular is their ability to migrate to sites of damaged tissue [6, 23]. Previous reports have demonstrated that pro-inflammatory cytokines were able to increase the migration of human MSC as well as to induce the production of chemokines and chemotactic factors that permit MSC to suppress immune reactions [6, 59–61].

It has been suggested that replicative senescence can modify the migratory properties of hADSC and may possibly influence hADSC response to the inflammatory environment as well as their immunomodulation output upon transplantation [23]. We observed that senescent hADSC showed significantly higher basal migration capacity than their counterparts that are in the linear range of their proliferative capacity [23]. We recommend measuring the response of hADSC cultures to different cytokine chemoattractants. The factors IL-2, IL-6, IL-8 as well as TNF-α and HMGB1 have been previously reported as potent chemoattractants inducing migration of different stem cell types [62, 63]. Our data indicate that hADSC at late passages have an increased ability to migrate in comparison to early passages, indicating that replicative senescence increases the migratory properties of hADSC in response to the tested chemoattractants. Interestingly, upon senescence of hADSC,

interleukin-2 (IL-2) became the most potent chemotaxis stimulant whereas the TNF-α is less potent among the tested chemoattractants in these experiments (as published in [23]). It is therefore important to measure migratory capacity of the cells lines in the culture and evaluate the impact of replicative senescence on migratory capacity. We are using transwell filters from Corning Incorporated (Acton, MA, USA) for our migration assays. The migration assays are performed as described in [63] using 8 μL thick transwell chambers.

1. All the cytokines (IL-2, IL-6, IL-8, HMGβ1, and TNF-α) are obtained from PeproTech Inc. (Rocky Hill, NJ, USA).
2. For the transwell migration assay, resuspend 1.0×10^4 cells in 80 μL of serum-free α-MEM and seed the cells in the upper chamber of 24-well transwell plates containing 8 μm pore size filters (Corning, Costar, USA).
3. In the lower chamber, add 600 μL of DMEM or medium containing either single cytokine or its combination (IL-2, IL-6, IL-8, TNF-α, and HMGβ1) (please *see* **Note 18**).
4. We use the following concentrations of cytokines: 50 ng/mL IL-2, IL-6, IL-8, and HMGβ1; 30 ng/mL TNF-α as described in [63].
5. Incubate the cultures of hADSC at 37 °C in the cell culturing incubator for 16 h.
6. Remove the cells retained in the upper chamber with a sterile swab.
7. Fix the cells that had migrated through the filter with 4% paraformaldehyde for 20 min at room temperature and stained overnight with 5% toluidine blue (*see* **Note 13**).
8. Count the cells at the lower side, in five different randomly selected 10× fields using a bright-field microscope (NikonTE300, DXM1200 Digital Camera, Japan).
9. These representative examples of the experiments with hADSC from two female donors aged 32 and 45, either self-renewing (SR) or senescent (SEN) populations, are shown in [23].
10. Each donor was sampled more than three times. The median values and range of values should be plotted. Statistical difference was evaluated by *t*-test with *P*-value (*p*) should be depicted.
11. The graphic should represent the mean of ten independent experiments ($n = 10$) as published in [23].

3.11 Detection of hADSC Secretory Proteins

The primary trophic property of hADSC as any other MSC is secretion of mitogenic growth factors such as transforming growth factor-alpha (TGF-α), TGF-β, hepatocyte growth factor (HGF), epithelial growth factor (EGF), basic fibroblast growth factor

(FGF-2), vascular endothelial growth factor (VEGF), and insulin-like growth factor-1 (IGF-1). All of these factors, when present in the systemic milieu, have shown to increase fibroblasts along with epithelial and endothelial cell division or differentiation [6, 64–68].

This secretome provides for MSC-triggered cellular communication circuitry, which is necessary for tissue or organ remodeling and regeneration. Interestingly, the secretion of a wide array of growth factors and anti-inflammatory proteins by MSC could also be modulated in response to inflammatory molecules, such as interlukin-1 (IL-1), IL-2, IL-12, tumor necrosis factor-alpha (TNF-α), and interferon-gamma (INF-γ), and also can be affected in autocrine and paracrine manner by the senescent cells present in the cultures (see for review [6, 67]). Senescence messaging system or SMS can provide complex signalling guidance to many inflammatory cells, including T-cells, natural killer cell, B-cells, monocytes, macrophages, and dendritic cells as described in [3, 6, 66, 69, 70].

Here, we describe the method for measuring secretory phenotype on hADSC both in their proliferative and senescence states as previously published by our laboratory [6, 16].

1. hADSC at PD 5–12 maintained in culture in DMEM/F12 complete medium were used. We either used a two-dimensional (2D) culture or maintained hADSC culture on sterile custom-made ECM-like scaffolds to imitate 3D cellular distribution. For this protocol, we used the 2-chamber slides following the manufacturer's recommendations.
2. If 3D culturing is favored for the experiment, rinse the 2-chamber scaffold-containing slides with 1.5 mL PBS twice and preincubate with 1.5 mL PBS for 15 min at 37 °C.
3. Trypsinize the hADSC at PD 5–12 maintained in culture in DMEM/F12 complete medium and prepare the single cell suspension as described earlier in Subheading 3.3, **steps 8** through **11**.
4. Centrifuge the cells at 200 × *g* for 5 min at room temperature in 15 mL centrifuge tube.
5. Aspirate the medium and wash the cells with 10 mL PBS twice by centrifugation at 200 × *g* for 5 min at room temperature.
6. Resuspend the cells in 5 mL of StemPro MSC SFM xeno-free complete medium (refer to Subheading 2.12.1.2). Adjust the cell counts to 5000 cells/mL in StemPro MSC SFM xeno-free complete medium. Add 2 mL per chamber to obtain 10,000 cells in each chamber (2500/cm^2) in the xeno-free complete medium.
7. Set up two medium-only chambers containing no hADSC but 2 mL of StemPro MSC SFM xeno-free complete medium as

negative controls for estimation of baseline levels in the medium.

8. After 24 h in culture, aspirate the medium and add 2.8 mL of the fresh StemPro MSC SFM xeno-free complete medium to all the chamber slides containing hADSC as well as to the negative control chambers (containing no cells). This medium will be collected as conditioned medium.
9. Collect the conditioned medium at 48 h or desired experimental time points post-medium change. For medium-only control, collect the medium from wells with no cells at the same time intervals as the experimental samples.
10. Estimate total protein in the supernatant using Qubit 2.0 Fluorometer (Thermo Fisher Scientific).
    (a) Label three thin-walled clear 0.5-mL PCR tubes for each standard and one tube per sample.
    (b) Prepare the Qubit working solution by diluting the Qubit reagent (from the kit) 1:200 in Qubit buffer. Prepare just enough Qubit working solution each time for the standards and the total number of samples to be analyzed.
    (c) Add 10 μL of standards (from the kit) and 190 μL of Qubit working solution to the pre-labeled PCR tubes for standards.
    (d) Add 1 μL or 2 μL of conditioned medium samples collected from all the chambers containing hADSC as well as negative control chambers in pre-labeled PCR tubes and add Qubit working solution to bring the final volume to 200 μL.
    (e) Incubate the PCR tubes at room temperature for 15 min.
    (f) Place the tubes into Qubit 2.0 fluorometer and record the readings.
    (g) Using the dilution calculator feature on Qubit 2.0 fluorometer, enter the dilution used for the samples and determine the total protein concentration in the samples.
11. Analyze the hADSC-conditioned medium from the chambers containing hADSC and no cell control medium using Human cytokine antibody array C2000 (RayBiotech Inc., Norcross, GA) that detects 174 human secretory proteins. We follow the manufacturer's instructions for performing the assays. All the steps for sample application, washes, and antibody incubations were performed on a rocking platform shaker.
12. Remove the kit from storage and allow the components to equilibrate to room temperature.
13. Carefully remove the Antibody Arrays labeled C6, C7, or C8 from the plastic packaging and place each membrane (printed

side up) into a well of the Incubation Tray provided in the kit. Place one membrane per well.

14. Add 2 mL of blocking buffer into each well and incubate for 30 min at room temperature.
15. For sample application, aspirate the blocking buffer from each well with a pipette and add 700 μL of conditioned medium samples as well as negative control samples (medium-only samples) and incubate the tray at room temperature on a rocking platform shaker for 2 h.
16. Aspirate samples from each well with a pipette and perform the washes.
17. Add 2 mL of 1× Wash Buffer I into each well and incubate for 5 min at room temperature and aspirate. Repeat this two more times for a total of three washes using fresh buffer and aspirating out the buffer completely each time.
18. Add 2 mL of 1× Wash Buffer II into each well and incubate for 5 min at room temperature and aspirate. Repeat this two more times for a total of three washes using fresh buffer and aspirating out the buffer completely each time.
19. Pipette 1 mL of the prepared Biotinylated Antibody Cocktail into each well and incubate overnight at 4 °C on a rocking platform shaker.
20. Aspirate Biotinylated Antibody Cocktail from each well and wash the membranes as described above in **steps 17** and **18**.
21. Add 2 mL of 1× HRP-Streptavidin (diluted freshly just before use) into each well and incubate for 2 h at room temperature. Aspirate HRP-Streptavidin from each well and repeat the wash steps as described earlier in **steps 17** and **18**.
22. Transfer the membranes, printed side up, onto a sheet of blotting paper lying on a flat surface and remove any excess wash buffer by blotting the membrane edges with another piece of blotting paper.
23. Transfer and place the membranes, printed side up, onto a plastic sheet (provided) lying on a flat surface. Do not allow membranes to dry out during detection.
24. Prepare the detection buffer by adding equal volumes (1:1) of Detection Buffer C and Detection Buffer D in a 15-mL centrifuge tube and mix well (500 μL/membrane).
25. Carefully pipette 500 μL of the detection buffer mixture onto each membrane and incubate for 2 min at room temperature (DO NOT ROCK OR SHAKE).
26. Immediately visualize the signals and capture the digital images for densitometry data collection using Omega Lum C imaging system (Gel Company, San Francisco, CA).

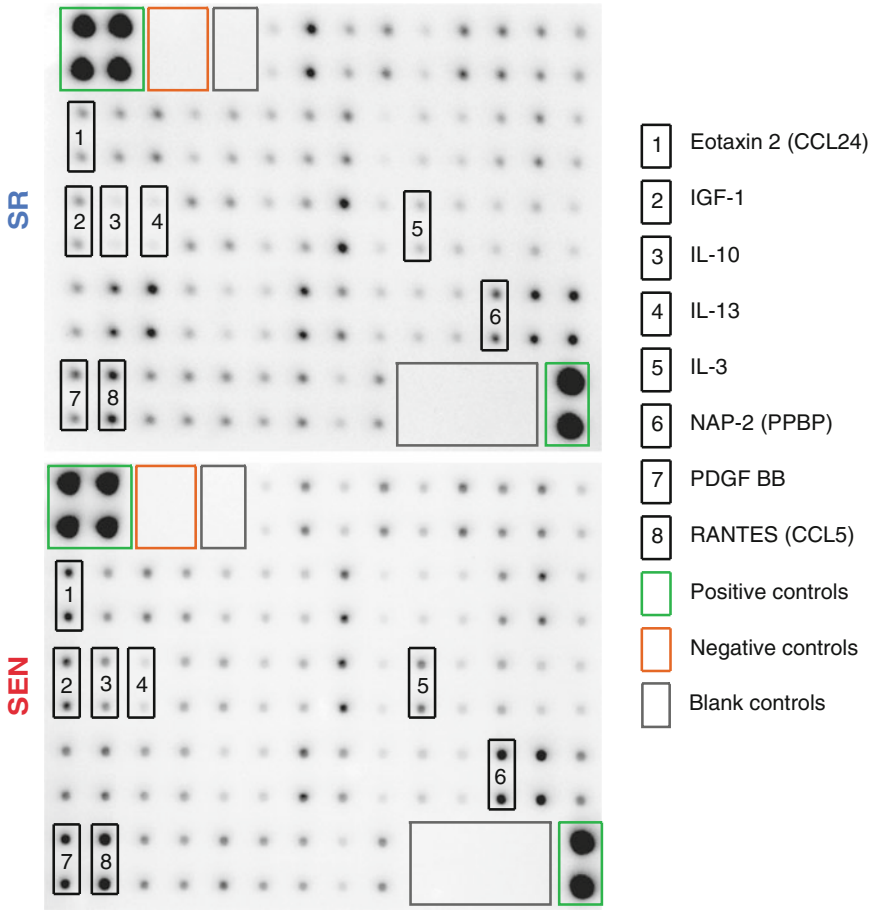

Fig. 11 Secretory phenotype of hADSC culture. A representative example of cytokine array membrane is shown. Self-renewing (SR) (*top*) and bleomycin-induced senescent (SEN) hADSC (*bottom*) were cultured on scaffold for collection of conditioned medium at 48 h for microarray analysis. The conditioned medium from self-renewing (SR) or bleomycin-induced senescent (SEN) hADSC collected at 48 h was subjected to human cytokine array. Example spots showing upregulated proteins for SEN hADSC are indicated by black boxes numbered from 1 to 8 and the corresponding names of the proteins are indicated on the right. Spot signal densitometry data extraction was performed for each cytokine (2 replicates; black boxes), positive controls (6 replicates; green boxes), negative controls (4 replicates; orange boxes), and blank controls (10 replicates; gray boxes) using LI-COR Image Studio Lite Software

27. Representative examples of array membranes are shown in Fig. 11.
28. The array membranes can be stored for long-term storage by placing them gently between two plastic sheets taped together stored at −20 °C in a sealed Ziploc bag for future reference.
29. Spot signal densitometry data and raw data extraction was performed for all the samples of conditioned medium and the negative controls from densitometry image analysis using LI-COR Image Studio Lite Software (LI-COR Biotechnology, Lincoln, NE) as described in [16].

3.12 Mycoplasma Testing in hADSC Cultures

hADSC cultures should be routinely screened for any contaminations to maintain the quality of cells. Mycoplasma contamination is one of the common one yet is difficult to detect early enough in cultures. Mycoplasma contamination leads to slowdown of the proliferation rate of cells by depletion of nutrients from the culture medium and, therefore, may induce changes in gene expression. The MycoAlert™ assay detects mycoplasma contamination by lysis of mycoplasma resulting in release of mycoplasmal enzymes that react with the MycoAlert™ substrate catalyzing the conversion of ADP to ATP. The measurement of the level of ATP prior to addition of the MycoAlert™ substrate and after the addition generates a ratio that is indicative of the presence of mycoplasma. This increase in ATP level is measured in a luminometer. The assay is conducted at room temperature (18–22 °C), the optimal temperature for luciferase activity.

1. Warm up all reagents to room temperature prior to use.
2. Reconstitute the provided MycoAlert™ reagent and MycoAlert™ substrate in MycoAlert™ assay buffer and leave at room temperature for 15 min.
3. Centrifuge 2 mL of ADSC culture supernatant in a centrifuge tube at 1500 rpm (200 × *g*) for 5 min to eliminate the floating cells, if any.
4. Carefully transfer 100 μL of supernatant, without disturbing the pellet into one pre-labeled well of a 96-well luminometer plate. For controls, take 100 μL each of fresh medium, negative (MycoAlert™ buffer) and the positive control.
5. Program the luminometer to take a 1 s integrated reading.
6. Add 100 μL of MycoAlert™ reagent to each sample and wait 5 min.
7. Place the 96-well plate in the luminometer and record the numbers (Reading A).
8. To each sample and control wells, add 100 μL of MycoAlert™ and incubate at room temperature for 10 min.
9. Replace the plate in luminometer and record the numbers (Reading B).
10. To calculate the ratio, divide Reading B by Reading A (Ratio = Reading B/Reading A).
11. The ratio obtained can be interpreted as follows. A ratio of less than 0.9 indicates the absence of any mycoplasma while a ratio greater than 1.2 indicates mycoplasma contamination in the culture. The ratio between 0.9 and 1.2 is considered unclear/borderline contamination and the test should be repeated for the culture after 24 h to confirm the results.
12. An example of assays performed on multiple hADSC lines is shown in Table 2.

Table 2
Mycoplasma screening for hADSC cultures

hADSC lines	Reading 1A	Reading 2A	Average A	Reading 1B	Reading 2B	Average B	Ratio B/A	Result
F38-cell line	47	48	47.5	22	21	21.5	0.453	Negative
F45-cell line 1	50	46	48	19	21	20	0.417	Negative
F45-cell line 2	48	47	47.5	15	16	15.5	0.326	Negative
F49-cell line	52	45	48.5	20	21	20.5	0.423	Negative
Negative control	93	91	92	12	11	11.5	0.125	Negative
Positive control	5	3	4	4	4	4	1.000	Positive

An example of mycoplasma screening assay is presented. The hADSC lines from four female donors aged 32–49 were tested for mycoplasma contamination along with the negative and positive assay controls as labeled in the leftmost column. A ratio of (Reading B/Reading A) less than 0.9 indicates the absence of any mycoplasma while a ratio greater than 1.2 indicates mycoplasma contamination in the culture

4 Conclusions

In recent years, researchers have been looking for new and safer methods for MSC isolation and expansion from adipose tissue. Autologous stem cell therapies are successfully used in numerous clinical applications demonstrating that hADSC as well as bone marrow-derived MSC are a promising source of cell-based therapies for the treatment of multiple diseases ranging from traumatic calvarial bone disease and acute steroid-refractory graft-versus-host disease to the treatments of cardiovascular diseases and healing chronic wounds. At the same time, adipose tissues preparation, techniques to expand and maintain cell culture ex vivo, the degree of purity needed for a clinical application, methods for monitoring and ensuring the quality of the ADSC, and techniques to evaluate cells, and degree of cellular senescence in culture before implantation should also be identified and standardized. Such standardized methods will reduce the risk of contamination and increase the reproducibility of ADSC-based therapeutic end points. We believe that the set of techniques and protocols provided in this chapter will be useful for establishing the standardized and Good Manufacturers Practice (GMP)-conformed culture, isolation, and expansion protocols for the clinical application of hADSC.

5 Notes

1. 10 mL Luer-Lok syringe with Snap-Lok fitted into the plunge of the syringe helps to perform the procedure effortlessly. Insert the Snap-Lok when the plunger is pulled out, then push the plunger down, insert the cannula into the tissue, pull out the plunger, the lock snaps open on the barrel lip and will hold the syringe under vacuum (Tulip Medical Products, San Diego, CA, USA).
2. Prepare DMEM/F12 complete medium by adding 10%FBS, 100 U/mL penicillin, 100 μg/mL streptomycin, and 2 mM L-glutamine. Filter using 0.22 μm pore size Nalgene membrane filtration unit (Thermo Fisher Scientific, Waltham, MA, USA), and store at 4 °C until use. Complete DMEM/F12 medium is stable for up to 3 weeks at 4 °C.
3. Celase™ is a mixture of highly purified collagenase and neutral protease enzymes. The lyophilized Celase™ enzyme is stable when stored unopened at −25 to −15 °C through the expiration date printed on the label. To reconstitute Celase™, remove the cap and wipe the rubber stopper with alcohol wipe. Using a sterile needle, add 5 mL of sterile PBS by piercing through the rubber stopper of the vial. Mix well by inverting the vial several times and use within 4 h after reconstituting. Avoid repeated freezing and thawing.
4. Red blood lysis buffer (ACK lysis buffer) is also commercially available in smaller volumes from multiple vendors.
5. If there is still a lot of fat/oil on the walls of the tube, add 25 mL of PBS, and spin again at 400 × *g* and discard the supernatant. Repeat this step until all the sticky fat is removed.
6. Take 18 μL of the SVF suspension and add 2 μL of AO/PI reagent. Mix gently and load 10 μL into the chamber port in the Luna Stem counting slide. Press the image button for the image overlay to check live and dead cells. Count and record the number of cells and the picture for each sample. We typically get approximately 0.8×10^7 to 1×10^7 cells from 60 mL lipoaspirate (after removal of oil layer) at this step.
7. For FACS staining of surface markers, you could start with 0.5–5 μg/mL antibody concentrations if you are not sure about the correct working concentration for any antibody.
8. Expand the earliest passage of freshly isolated hADSC primary hADSC by plating $2.5–3.5 \times 10^5$ cells in a T175 flask. For expansion of newly generated hADSC lines, use lower PD (PD 4-15) as the hADSC cultures at higher PD result in lower differentiation efficiency during adipogenesis, osteogenesis, and chondrogenesis due to increase in senescent cells.

9. When thawing the frozen MSC, do not add the entire volume of media all at once to the cells. This may result in decreased cell viability due to osmotic shock.
10. We recommend performing several 70% ethanol washes for the chromosomal DNA pellet to efficiently remove unincorporated [^{3}H]-dT. Avoid use of vacuum drying equipment to prevent radioactive contamination of the lab equipment.
11. For preparing the working DAPI staining solution, dilute the DAPI stock 1:1000-fold with PBS to get 0.5 μg/mL final concentration. DAPI can be used at a wide working concentration range of 0.5–5 μg/mL depending on the experiment.
12. 70% Glycerol preparation: Prepare 70% glycerol in MilliQ water, autoclave and store at room temperature.
13. Refer to manufacture's MSDS for safe handling of 4% paraformaldehyde and OSHA mandated protective equipment (e.g., safety goggles, gloves, and gown). The aldehydic waste is collected in the appropriately labeled liquid hazardous waste container.
14. Usage of antibody from different vendor or different batch of the same vendor will require optimization in amount of antibody added to the slide. We recommend performing a serial dilution experiment to optimize the antibody concentration. Please follow the antibody manufacturer product description sheet for the recommendation of dilution series.
15. Optimize the antibody concentration for each new batch of antibody. Please follow antibody manufacturer product description sheet for the recommendation of dilution series.
16. hADSC cultures at higher PD (20 and higher as shown in Fig. 1 (panel B)) result in lower differentiation efficiency during adipogenesis, osteogenesis, and chondrogenesis due to increased level of senescent cells as described in Subheading 3.8.
17. Oil Red O staining solution: Add 0.5 g oil red O powder in 100% isopropanol. Mix thoroughly for 5 min. Prepare a 0.6% Oil Red O staining solution by mixing 6:4 parts MilliQ water. Filter using 0.22 μm pore size Nalgene membrane filtration unit (Thermo Fisher Scientific, Waltham, MA, USA).
18. All stock solutions are prepared according to manufacturer instructions. We recommend to aliquot stock solution since freezing and thawing the cytokines can decrease their ability to interact with receptors.

References

1. Hass R, Kasper C, Bohm S, Jacobs R (2011) Different populations and sources of human mesenchymal stem cells (MSC): a comparison of adult and neonatal tissue-derived MSC. Cell Commun Signal 9:12. https://doi.org/10.1186/1478-811X-9-12
2. Singer NG, Caplan AI (2011) Mesenchymal stem cells: mechanisms of inflammation. Annu Rev Pathol 6:457–478. https://doi.org/10.1146/annurev-pathol-011110-130230
3. Uccelli A, Moretta L, Pistoia V (2008) Mesenchymal stem cells in health and disease. Nat Rev Immunol 8(9):726–736. https://doi.org/10.1038/nri2395
4. Takashima Y, Era T, Nakao K, Kondo S, Kasuga M, Smith AG, Nishikawa S (2007) Neuroepithelial cells supply an initial transient wave of MSC differentiation. Cell 129(7):1377–1388. https://doi.org/10.1016/j.cell.2007.04.028
5. Jiang Y, Berry DC, Tang W, Graff JM (2014) Independent stem cell lineages regulate adipose organogenesis and adipose homeostasis. Cell Rep 9(3):1007–1022. https://doi.org/10.1016/j.celrep.2014.09.049
6. Lunyak VV, Amaro-Ortiz A, Gaur M (2017) Mesenchymal stem cells secretory responses: senescence messaging secretome and immunomodulation perspective. Front Genet 8:220. https://doi.org/10.3389/fgene.2017.00220
7. Lindner U, Kramer J, Rohwedel J, Schlenke P (2010) Mesenchymal stem or stromal cells: toward a better understanding of their biology? Transfus Med Hemother 37(2):75–83. https://doi.org/10.1159/000290897
8. Ullah I, Subbarao RB, Rho GJ (2015) Human mesenchymal stem cells—current trends and future prospective. Biosci Rep 35(2). https://doi.org/10.1042/BSR20150025
9. Ben-Ami E, Miller A, Berrih-Aknin S (2014) T cells from autoimmune patients display reduced sensitivity to immunoregulation by mesenchymal stem cells: role of IL-2. Autoimmun Rev 13(2):187–196. https://doi.org/10.1016/j.autrev.2013.09.007
10. Aso K, Tsuruhara A, Takagaki K, Oki K, Ota M, Nose Y, Tanemura H, Urushihata N, Sasanuma J, Sano M, Hirano A, Aso R, McGhee JR, Fujihashi K (2016) Adipose-derived mesenchymal stem cells restore impaired mucosal immune responses in aged mice. PLoS One 11(2):e0148185. https://doi.org/10.1371/journal.pone.0148185
11. Attar-Schneider O, Zismanov V, Drucker L, Gottfried M (2016) Secretome of human bone marrow mesenchymal stem cells: an emerging player in lung cancer progression and mechanisms of translation initiation. Tumour Biol 37(4):4755–4765. https://doi.org/10.1007/s13277-015-4304-3
12. Bartholomew A, Sturgeon C, Siatskas M, Ferrer K, McIntosh K, Patil S, Hardy W, Devine S, Ucker D, Deans R, Moseley A, Hoffman R (2002) Mesenchymal stem cells suppress lymphocyte proliferation in vitro and prolong skin graft survival in vivo. Exp Hematol 30(1):42–48
13. Chen Y, Xiang LX, Shao JZ, Pan RL, Wang YX, Dong XJ, Zhang GR (2010) Recruitment of endogenous bone marrow mesenchymal stem cells towards injured liver. J Cell Mol Med 14(6B):1494–1508. https://doi.org/10.1111/j.1582-4934.2009.00912.x
14. Di Nicola M, Carlo-Stella C, Magni M, Milanesi M, Longoni PD, Matteucci P, Grisanti S, Gianni AM (2002) Human bone marrow stromal cells suppress T-lymphocyte proliferation induced by cellular or nonspecific mitogenic stimuli. Blood 99(10):3838–3843
15. Gaur M, Dobke M, Lunyak VV (2017) Mesenchymal stem cells from adipose tissue in clinical applications for dermatological indications and skin aging. Int J Mol Sci 18(1). https://doi.org/10.3390/ijms18010208
16. Gaur M, Wang L, Amaro-Ortiz A, Dobke MI, King Jordan I, Lunyak VV (2017) Acute genotoxic stress-induced senescence in human mesenchymal cells drives a unique composition of senescence messaging secretome (SMS). J Stem Cell Res Ther 7(8):396. https://doi.org/10.4172/2157-7633.1000396
17. Eggenhofer E, Luk F, Dahlke MH, Hoogduijn MJ (2014) The life and fate of mesenchymal stem cells. Front Immunol 5:148. https://doi.org/10.3389/fimmu.2014.00148
18. Ponte AL, Marais E, Gallay N, Langonne A, Delorme B, Herault O, Charbord P, Domenech J (2007) The in vitro migration capacity of human bone marrow mesenchymal stem cells: comparison of chemokine and growth factor chemotactic activities. Stem Cells 25(7):1737–1745. https://doi.org/10.1634/stemcells.2007-0054
19. Liu R, Chang W, Wei H, Zhang K (2016) Comparison of the biological characteristics of mesenchymal stem cells derived from bone marrow and skin. Stem Cells Int 2016:3658798. https://doi.org/10.1155/2016/3658798

20. Signer RA, Morrison SJ (2013) Mechanisms that regulate stem cell aging and life span. Cell Stem Cell 12(2):152–165. https://doi.org/10.1016/j.stem.2013.01.001
21. Lopez MF, Niu P, Wang L, Vogelsang M, Gaur M, Krastins B, Zhao Y, Smagul A, Nussupbekova A, Akanov AA, Jordan IK, Lunyak VV (2017) Opposing activities of oncogenic MIR17HG and tumor suppressive MIR100HG clusters and their gene targets regulate replicative senescence in human adult stem cells. NPJ Aging Mech Dis 3:7. https://doi.org/10.1038/s41514-017-0006-y
22. Wang J, Geesman GJ, Hostikka SL, Atallah M, Blackwell B, Lee E, Cook PJ, Pasaniuc B, Shariat G, Halperin E, Dobke M, Rosenfeld MG, Jordan IK, Lunyak VV (2011) Inhibition of activated pericentromeric SINE/Alu repeat transcription in senescent human adult stem cells reinstates self-renewal. Cell Cycle 10(17):3016–3030. https://doi.org/10.4161/cc.10.17.17543
23. Niu P, Smagul A, Wang L, Sadvakas A, Sha Y, Perez LM, Nussupbekova A, Amirbekov A, Akanov AA, Galvez BG, Jordan IK, Lunyak VV (2015) Transcriptional profiling of interleukin-2-primed human adipose derived mesenchymal stem cells revealed dramatic changes in stem cells response imposed by replicative senescence. Oncotarget 6(20):17938–17957. https://doi.org/10.18632/oncotarget.4852
24. Perin EC, Sanz-Ruiz R, Sanchez PL, Lasso J, Perez-Cano R, Alonso-Farto JC, Perez-David-E, Fernandez-Santos ME, Serruys PW, Duckers HJ, Kastrup J, Chamuleau S, Zheng Y, Silva GV, Willerson JT, Fernandez-Aviles F (2014) Adipose-derived regenerative cells in patients with ischemic cardiomyopathy: the PRECISE trial. Am Heart J 168(1):88–95.e82. https://doi.org/10.1016/j.ahj.2014.03.022
25. Rumman M, Dhawan J, Kassem M (2015) Concise review: quiescence in adult stem cells: biological significance and relevance to tissue regeneration. Stem Cells 33(10):2903–2912. https://doi.org/10.1002/stem.2056
26. Holton J, Imam MA, Snow M (2016) Bone marrow aspirate in the treatment of chondral injuries. Front Surg 3:33. https://doi.org/10.3389/fsurg.2016.00033
27. Kern S, Eichler H, Stoeve J, Kluter H, Bieback K (2006) Comparative analysis of mesenchymal stem cells from bone marrow, umbilical cord blood, or adipose tissue. Stem Cells 24(5):1294–1301. https://doi.org/10.1634/stemcells.2005-0342
28. Tuan RS, Boland G, Tuli R (2003) Adult mesenchymal stem cells and cell-based tissue engineering. Arthritis Res Ther 5(1):32–45
29. Cheriyan T, Kao HK, Qiao X, Guo L (2014) Low harvest pressure enhances autologous fat graft viability. Plast Reconstr Surg 133(6):1365–1368. https://doi.org/10.1097/PRS.0000000000000185
30. Li K, Gao J, Zhang Z, Li J, Cha P, Liao Y, Wang G, Lu F (2013) Selection of donor site for fat grafting and cell isolation. Aesthetic Plast Surg 37(1):153–158. https://doi.org/10.1007/s00266-012-9991-1
31. Shim YH, Zhang RH (2017) Literature review to optimize the autologous fat transplantation procedure and recent technologies to improve graft viability and overall outcome: a systematic and retrospective analytic approach. Aesthetic Plast Surg 41(4):815–831. https://doi.org/10.1007/s00266-017-0793-3
32. Duscher D, Atashroo D, Maan ZN, Luan A, Brett EA, Barrera J, Khong SM, Zielins ER, Whittam AJ, Hu MS, Walmsley GG, Pollhammer MS, Schmidt M, Schilling AF, Machens HG, Huemer GM, Wan DC, Longaker MT, Gurtner GC (2016) Ultrasound-assisted liposuction does not compromise the regenerative potential of adipose-derived stem cells. Stem Cells Transl Med 5(2):248–257. https://doi.org/10.5966/sctm.2015-0064
33. Canizares O Jr, Thomson JE, Allen RJ Jr, Davidson EH, Tutela JP, Saadeh PB, Warren SM, Hazen A (2017) The effect of processing technique on fat graft survival. Plast Reconstr Surg 140(5):933–943. https://doi.org/10.1097/PRS.0000000000003812
34. Kapur SK, Dos-Anjos Vilaboa S, Llull R, Katz AJ (2015) Adipose tissue and stem/progenitor cells: discovery and development. Clin Plast Surg 42(2):155–167. https://doi.org/10.1016/j.cps.2014.12.010
35. Klein JA (1990) Tumescent technique for regional anesthesia permits lidocaine doses of 35 mg/kg for liposuction. J Dermatol Surg Oncol 16(3):248–263
36. Gupta N, Gupta V (2014) Life-threatening complication following infiltration with adrenaline. Indian J Anaesth 58(2):225–227. https://doi.org/10.4103/0019-5049.130850
37. Tonnard P, Verpaele A, Peeters G, Hamdi M, Cornelissen M, Declercq H (2013) Nanofat grafting: basic research and clinical applications. Plast Reconstr Surg 132(4):1017–1026. https://doi.org/10.1097/PRS.0b013e31829fe1b0
38. Tambasco D, Arena V, Finocchi V, Grussu F, Cervelli D (2014) The impact of liposuction cannula size on adipocyte viability. Ann Plast Surg 73(2):249–251. https://doi.org/10.1097/SAP.0b013e31828a0ac1

39. Dominici M, Le Blanc K, Mueller I, Slaper-Cortenbach I, Marini F, Krause D, Deans R, Keating A, Prockop D, Horwitz E (2006) Minimal criteria for defining multipotent mesenchymal stromal cells. The International Society for Cellular Therapy position statement. Cytotherapy 8(4):315–317. https://doi.org/10.1080/14653240600855905
40. Shen JL, Huang YZ, Xu SX, Zheng PH, Yin WJ, Cen J, Gong LZ (2012) Effectiveness of human mesenchymal stem cells derived from bone marrow cryopreserved for 23-25 years. Cryobiology 64(3):167–175. https://doi.org/10.1016/j.cryobiol.2012.01.004
41. Macallan DC, Fullerton CA, Neese RA, Haddock K, Park SS, Hellerstein MK (1998) Measurement of cell proliferation by labeling of DNA with stable isotope-labeled glucose: studies in vitro, in animals, and in humans. Proc Natl Acad Sci U S A 95(2):708–713
42. Asher E, Payne CM, Bernstein C (1995) Evaluation of cell death in EBV-transformed lymphocytes using agarose gel electrophoresis, light microscopy and electron microscopy. II. Induction of non-classic apoptosis ("para-apoptosis") by tritiated thymidine. Leuk Lymphoma 19(1–2):107–119. https://doi.org/10.3109/10428199509059664
43. Burns TC, Ortiz-Gonzalez XR, Gutierrez-Perez M, Keene CD, Sharda R, Demorest ZL, Jiang Y, Nelson-Holte M, Soriano M, Nakagawa Y, Luquin MR, Garcia-Verdugo JM, Prosper F, Low WC, Verfaillie CM (2006) Thymidine analogs are transferred from prelabeled donor to host cells in the central nervous system after transplantation: a word of caution. Stem Cells 24(4):1121–1127. https://doi.org/10.1634/stemcells.2005-0463
44. Kuan CY, Schloemer AJ, Lu A, Burns KA, Weng WL, Williams MT, Strauss KI, Vorhees CV, Flavell RA, Davis RJ, Sharp FR, Rakic P (2004) Hypoxia-ischemia induces DNA synthesis without cell proliferation in dying neurons in adult rodent brain. J Neurosci 24(47):10763–10772. https://doi.org/10.1523/JNEUROSCI.3883-04.2004
45. Lin P, Allison DC (1993) Measurement of DNA content and of tritiated thymidine and bromodeoxyuridine incorporation by the same cells. J Histochem Cytochem 41(9):1435–1439. https://doi.org/10.1177/41.9.8354883
46. Steel GG (1977) Growth kinetics of tumours. Cell population kinetics in relation to the growth and treatment of cancer. Q Rev Biol 54(1)
47. Pollack A, Bagwell CB, Irvin GL 3rd (1979) Radiation from tritiated thymidine perturbs the cell cycle progression of stimulated lymphocytes. Science 203(4384):1025–1027
48. Gratzner HG (1982) Monoclonal antibody to 5-bromo- and 5-iododeoxyuridine: a new reagent for detection of DNA replication. Science 218(4571):474–475
49. Madhavan H (2007) Simple laboratory methods to measure cell proliferation using DNA synthesis property. J Stem Cells Regen Med 3(1):12–14
50. Gunduz N (1985) The use of FITC-conjugated monoclonal antibodies for determination of S-phase cells with fluorescence microscopy. Cytometry 6(6):597–601. https://doi.org/10.1002/cyto.990060615
51. Wilson GD, McNally NJ, Dunphy E, Karcher H, Pfragner R (1985) The labelling index of human and mouse tumours assessed by bromodeoxyuridine staining in vitro and in vivo and flow cytometry. Cytometry 6(6):641–647. https://doi.org/10.1002/cyto.990060621
52. Sasaki K, Ogino T, Takahashi M (1986) Immunological determination of labeling index on human tumor tissue sections using monoclonal anti-BrdUrd antibody. Stain Technol 61(3):155–161
53. Hayflick L, Moorhead PS (1961) The serial cultivation of human diploid cell strains. Exp Cell Res 25:585–621
54. Varghese J, Griffin M, Mosahebi A, Butler P (2017) Systematic review of patient factors affecting adipose stem cell viability and function: implications for regenerative therapy. Stem Cell Res Ther 8(1):45. https://doi.org/10.1186/s13287-017-0483-8
55. Noren Hooten N, Evans MK (2017) Techniques to Induce and quantify cellular senescence. J Vis Exp (123). doi:https://doi.org/10.3791/55533
56. Lee BY, Han JA, Im JS, Morrone A, Johung K, Goodwin EC, Kleijer WJ, DiMaio D, Hwang ES (2006) Senescence-associated beta-galactosidase is lysosomal beta-galactosidase. Aging Cell 5(2):187–195. https://doi.org/10.1111/j.1474-9726.2006.00199.x
57. Seo MJ, Suh SY, Bae YC, Jung JS (2005) Differentiation of human adipose stromal cells into hepatic lineage in vitro and in vivo. Biochem Biophys Res Commun 328(1):258–264. https://doi.org/10.1016/j.bbrc.2004.12.158
58. Schaffler A, Buchler C (2007) Concise review: adipose tissue-derived stromal cells--basic and clinical implications for novel cell-based

therapies. Stem Cells 25(4):818–827. https://doi.org/10.1634/stemcells.2006-0589

59. Ren G, Zhang L, Zhao X, Xu G, Zhang Y, Roberts AI, Zhao RC, Shi Y (2008) Mesenchymal stem cell-mediated immunosuppression occurs via concerted action of chemokines and nitric oxide. Cell Stem Cell 2 (2):141–150. https://doi.org/10.1016/j.stem.2007.11.014
60. Aggarwal S, Pittenger MF (2005) Human mesenchymal stem cells modulate allogeneic immune cell responses. Blood 105 (4):1815–1822. https://doi.org/10.1182/blood-2004-04-1559
61. Glennie S, Soeiro I, Dyson PJ, Lam EW, Dazzi F (2005) Bone marrow mesenchymal stem cells induce division arrest anergy of activated T cells. Blood 105(7):2821–2827. https://doi.org/10.1182/blood-2004-09-3696
62. Galvez BG, San Martin N, Rodriguez C (2009) TNF-alpha is required for the attraction of mesenchymal precursors to white adipose tissue in Ob/ob mice. PLoS One 4(2):e4444. https://doi.org/10.1371/journal.pone.0004444
63. Perez LM, Bernal A, San Martin N, Galvez BG (2013) Obese-derived ASCs show impaired migration and angiogenesis properties. Arch Physiol Biochem 119(5):195–201. https://doi.org/10.3109/13813455.2013.784339
64. Bai L, Lennon DP, Caplan AI, DeChant A, Hecker J, Kranso J, Zaremba A, Miller RH (2012) Hepatocyte growth factor mediates mesenchymal stem cell-induced recovery in multiple sclerosis models. Nat Neurosci 15 (6):862–870. https://doi.org/10.1038/nn.3109
65. Chen PM, Liu KJ, Hsu PJ, Wei CF, Bai CH, Ho LJ, Sytwu HK, Yen BL (2014) Induction of immunomodulatory monocytes by human mesenchymal stem cell-derived hepatocyte growth factor through ERK1/2. J Leukoc Biol 96(2):295–303. https://doi.org/10.1189/jlb.3A0513-242R
66. Ichim TE, Alexandrescu DT, Solano F, Lara F, Campion Rde N, Paris E, Woods EJ, Murphy MP, Dasanu CA, Patel AN, Marleau AM, Leal A, Riordan NH (2010) Mesenchymal stem cells as anti-inflammatories: implications for treatment of Duchenne muscular dystrophy. Cell Immunol 260(2):75–82. https://doi.org/10.1016/j.cellimm.2009.10.006
67. Murphy MB, Moncivais K, Caplan AI (2013) Mesenchymal stem cells: environmentally responsive therapeutics for regenerative medicine. Exp Mol Med 45:e54. https://doi.org/10.1038/emm.2013.94
68. O'Cearbhaill ED, Punchard MA, Murphy M, Barry FP, McHugh PE, Barron V (2008) Response of mesenchymal stem cells to the biomechanical environment of the endothelium on a flexible tubular silicone substrate. Biomaterials 29(11):1610–1619. https://doi.org/10.1016/j.biomaterials.2007.11.042
69. Ben-Ami E, Berrih-Aknin S, Miller A (2011) Mesenchymal stem cells as an immunomodulatory therapeutic strategy for autoimmune diseases. Autoimmun Rev 10(7):410–415. https://doi.org/10.1016/j.autrev.2011.01.005
70. Yi T, Song SU (2012) Immunomodulatory properties of mesenchymal stem cells and their therapeutic applications. Arch Pharm Res 35(2):213–221. https://doi.org/10.1007/s12272-012-0202-z

Methods in Molecular Biology (2019) 2045: 93–105
DOI 10.1007/7651_2019_217

Published online: 25 April 2019

Quantifying Senescence-Associated Phenotypes in Primary Multipotent Mesenchymal Stromal Cell Cultures

Stéphanie Nadeau, Anastasia Cheng, Inés Colmegna, and Francis Rodier

Abstract

Cellular senescence is a tumor suppressor mechanism that removes potentially neoplastic cells from the proliferative pool. Senescent cells naturally accumulate with advancing age; however, excessive/aberrant accumulation of senescent cells can disrupt normal tissue function. Multipotent mesenchymal stromal cells (MSCs), which are actively evaluated as cell-based therapy, can undergo replicative senescence or stress-induced premature senescence. The molecular characterization of MSCs senescence can be useful not only for understanding the clinical correlations between MSCs biology and human age or age-related diseases but also for identifying competent MSCs for therapeutic applications. Because MSCs are involved in regulating the hematopoietic stem cell niche, and MSCs dysfunction has been implicated in age-related diseases, the identification and selective removal of senescent MSC may represent a potential therapeutic target. Cellular senescence is generally defined by senescence-associated (SA) permanent proliferation arrest (SAPA) accompanied by persistent DNA damage response (DDR) signaling emanating from persistent DNA lesions including damaged telomeres. Alongside SA cell cycle arrest and DDR signaling, a plethora of phenotypic hallmarks help define the overall senescent phenotype including a potent SA secretory phenotype (SASP) with many microenvironmental functions. Due to the complexity of the senescence phenotype, no single hallmark is alone capable of identifying senescent MSCs. This protocol highlights strategies to validate MSCs senescence through the measurements of several key SA hallmarks including lysosomal SA Beta-galactosidase activity (SA-βgal), cell cycle arrest, persistent DDR signaling, and the inflammatory SASP.

Keywords Senescence, Stem cells, Immunofluorescence, Senescence-associated beta-galactosidase, Sandwich enzyme-linked immunosorbent assay, Senescence-associated secretory phenotype, DNA damage foci, Mesenchymal stromal stem cell, Multipotent mesenchymal stromal cell

1 Introduction

Mesenchymal stromal cells (MSCs) are multipotent progenitor cells that in vitro can differentiate into multiple cell types including osteoblasts, chondrocytes, and adipocytes [1]. MSCs exist in every tissue including the bone marrow, adipose tissue, umbilical cord, placenta, skeletal muscle, and dental pulp [2, 3]. In the bone marrow, MSCs are an important component of the hematopoietic stem cell (HSC) niche. We have previously shown that aged or senescent MSCs can influence HSC quiescence [4, 5]. MSCs have high proliferative potential and are easily isolated for ex vivo culture, providing accessible material for research and cell therapy [6, 7].

MSCs possess unique properties that justify their use as cell-based therapies [6–9]. Most importantly, following tissue injury MSCs can release factors that through paracrine mechanisms affect resident endothelial cells, fibroblasts, and tissue resident stem cells to promote tissue repair. This is mediated through enhancing angiogenesis and limiting damaging inflammatory responses [10, 11]. However, the therapeutic efficacy of MSCs has not been demonstrated uniformly in clinical trials due to the lack of standardization of cell products. Factors such as MSCs' passage number, cell culture conditions, and donor age/disease status can influence the biology and overall therapeutic function of these cells. Similarly, MSCs aging and senescence negatively affect their ability to regulate the hematopoietic stem cell niche and are implicated in age-associated immune diseases [12, 13]. Therefore, the selective removal of senescent MSCs may represent a potential target to enhance the function of MSCs products [4–6]. In this context, the molecular evaluation of MSCs aging-senescence ex vivo could be a useful tool to understand or assess the functional status of these cells.

In 1961, the phenomena of cellular aging or replicative senescence were described in human fibroblasts [14]. Replicative senescence is characterized by a limited proliferative capacity in culture that results from telomere shortening occurring at each cell division in normal cells [14, 15]. Since then, other inducers of senescence have been reported including cellular stress (reactive oxygen species (ROS), culture stress, irradiation (IR), chemotherapy), activated oncogenes (RAS, MEK/MAPK), and chromatin alterations (HDAC inhibitors) [16–21]. Choosing senescence as a cell fate decision depends heavily on the type of stress and on the cell type. For example, in response to DNA damage, stromal cells like MSCs and fibroblasts will almost exclusively favor senescence, while thymocytes will favor apoptosis [22, 23]. In vivo senescent cells accumulate during aging and in diseases of premature aging [24–28]. The contribution of resident senescent cells to multiple age-associated pathologies and to cancer therapy-induced organ dysfunctions is established using multiple genetic mouse models [28–37]. Resident senescent cells proposed to directly promote tissue dysfunction include preadipocytes and adipocytes, both of whom are closely related to MSCs and other stromal cells like fibroblasts [37–39].

Cellular senescence is a complex phenotype. Thus, determining the senescent state of a cell requires the evaluation of multiple senescence-associated (SA) biomarkers. The most typical is a stable proliferation arrest (SAPA) associated with persistent DNA damage response (DDR) signaling. The latter emanates from persistent DNA lesions including damaged telomeres [15, 40, 41]. Additional phenotypic hallmarks that define the senescent phenotype include metabolic changes, endoplasmic reticulum stress, mitochondria

dysregulation, and chromatin/epigenetic remodelling [42]. In this context, a variety of SA biomarkers have been used to characterize MSCs senescence including morphological changes (increased size and granularity); irreversible state of cell cycle arrest (SAPA); SA apoptosis resistance (SAAR); increased lysosomal activity leading to SA Beta-galactosidase activity (SA-βgal); the presence of a pro-inflammatory SA secretory phenotype (SASP); increased levels of the tumor suppressors P16, P21, or P53; DNA damage response activation (DNA-SCARS); the formation of senescence-associated heterochromatic foci (SAHF); epigenetic modifications; and altered microRNA expression profiles [43–49]. In this protocol, we specifically highlight procedures that we have used to detect SA-βgal activity, to validate SAPA using DNA synthesis EdU labeling, to visualize DDR activation via DNA-SCARS formation as detected using 53bp1/γH2AX/PML nuclear foci, and to assess SASP activation via IL-6/IL-8 secretion measurements [5, 13, 41, 50, 51].

2 Materials

2.1 Cell Culture

1. Non-senescent MSCs culture should be performed at low passage (P) to limit the presence of naturally occurring replicative senescent cells (usually P2–P6 or population doublings (PD) ≤12). Culture MSCs under standard conditions, i.e., 37 °C, 5% CO_2, complete cell culture medium (Low Glucose Dulbecco's modified Eagle's medium [DMEM] (WISENT Inc. cat. no. 319-010-CL) supplemented with 10% fetal bovine serum (FBS) (Gibco Invitrogen cat. no. 12662) and 1% penicillin–streptomycin (Sigma cat. no. P4333)).
2. Negative and positive senescence (SEN) controls. Negative-SEN control for all SA biomarkers below should be an actively growing reference population (i.e., MSCs P2–P6). Positive-SEN control for all SA biomarkers below should be derived from the same MSCs P2–P6 population exposed to irradiation (MSC-SEN-IR; 10 Gray X-ray in a single dose) and allowed to recover for 10 days or grown to replicative senescence (the last passage of the culture when the cells have completely stopped proliferation; MSC-SEN-REP) [5, 41]. MSCs irradiation: Seed cell in a six-well plate (6–8 × 10^4 cells/well) in complete DMEM, allow to recover for 2 days, and treat cells with 10 Gray (Gy) of gamma irradiation [5]. Senescence markers will appear 8–10 days postirradiation. Senescent cells can be reseeded between days 3 and 5 postirradiation for use in the protocols below (*see* **Note 1**).

2.2 General Buffer and Staining Product

1. Wash buffer: Phosphate-buffered saline (PBS) (137 mM NaCl, 2.7 mM KCl, 10 mM Na_2HPO_4, 1.8 mM KH_2PO_4, pH 7.4) (WISENT Inc. cat. no. 311-425 CL).
2. Fixing solution, formalin 10% (4% formaldehyde) (Sigma-Aldrich, Saint-Louis, MO, USA).
3. Nucleus staining: DNA dye Hoechst 33342 solution (dilution 1/5000) (Sigma-Aldrich cat. no. 23491-52-3).

2.3 Senescence-Associated β-Galactosidase

1. SA-βgal staining solution: 40 mM citric acid ($C_6H_8O_7 \cdot H_2O$)/ sodium phosphate (dibasic) (NaH_2PO_4), 5 mM potassium hexacyano-ferrate (II) trihydrate solution (K4[Fe(CN) 6]·$3H_2O$), 5 mM potassium hexacyano-ferrate (III) (K3[Fe (CN)6]), 150 mM sodium chloride (NaCl), 2 mM magnesium chloride ($MgCl_2 \cdot 6H_2O$), and 1 mg/mL X-gal in distilled water. For preparation details and complete protocol: [52].

2.4 Immunofluorescence: Cell Cycle Arrest by EdU Labeling

1. EdU molecular probe (5-ethynyl-2′-deoxyuridine) stock 10 mM in DMSO (Invitrogen cat. no. A10187).
2. EdU (5-ethynyl-2′-deoxyuridine) staining solution: 100 mM Tris–HCl pH8.5, 1 mM copper(II) sulfate ($CuSO_4$), 100 mM ascorbic acid ($C_6H_8O_6$), 50 μM Alexa Fluor Hapten dye 488 nm or 647 nm (Life Technologies cat. no. A-10277, A-10266) in distilled water.

2.5 Immunofluorescence: DNA Damage Foci and DNA-SCARS by 53bp1, γH2AX and PML Labeling

1. Four-well chamber slide w/Cover Lab-Tek II RS Glass slide sterile (Nalge Nunc International cat. no. 154526), coverslips (Select coverslip based on the optics of the microscope used to image DNA damage foci), and mounting Media: Vectashield (Vector Laboratories cat. no. H-1000).
2. Permeabilizing solution: 0.5% Triton X-100 in PBS. Triton X-100 (Sigma-Aldrich cat. no. 93443). Blocking solution: 1% BSA in PBS with 4% Normal Donkey Serum (Jackson ImmunoResearch cat. no. 001-000-162, Sigma-Aldrich cat. no. D966). BSA IgG-Free Protease-Free (Jackson Immunoresearch cat. no. 001-000-161).
3. Antibody dilution buffer: 1% BSA with 4% donkey serum in PBS (blocking solution).
4. DNA damage antibodies: PML (Santa Cruz Biotechnology, Inc. cat. no. sc-9862) (dilution 1/500), γH2AX (Upstate Biotechnology, Inc. cat. no. 05636) (dilution 1/2000), 53BP1 (Novus Biologicals cat. no. NB 100-304) (dilution 1/2000).
5. Secondary antibody: Alexa-Fluor donkey anti-goat/anti-mouse/anti-rabbit 488 nm/568 nm/647 nm (dilution 1/800) (Life Technologies cat. no. A-11055, A-10037, A-31573).

2.6 ELISA: Senescence-Associated Secretory Phenotype (SASP) Represented by IL-6 and IL-8 Cytokine

1. Cytokine detection kit ELISA (IL-6, IL-8). Human IL-6 kit (BD OptEIA cat. no. 555220) and Human IL-8 kit (BD OptEIA cat. no. 555244).

3 Methods

3.1 Senescence-Associated β-Galactosidase: By Chromogenic Assay

Senescent cells display lysosomal beta-galactosidase hyper-activation that is detectable at pH 6.0 and distinct from the normal baseline beta-galactosidase enzymatic activity detectable at pH 4.0 [52]. This SA-βgal activity can be preferentially detected using appropriate acidic conditions and its substrate X-gal, which becomes an insoluble blue compound trapped in the cell when cleaved by the enzyme [52, 53].

1. Seed 2–4 × 10^4 cells (aim for 60–75% cell confluence) in a six-well plate, and culture for 2–3 days or more if necessary to reach the target confluence level (80–85%). Be careful that the cells are not overly confluent because high cell density influences the SA-βgal staining.
2. Wash cells twice using room temperature PBS.
3. Fix cells with fixing solution (1–2 mL/well) for 5 min at room temperature. Note that over-fixation can limit the effectiveness of the staining reaction. The staining reaction below works better on freshly fixed cells.
4. Wash cells twice with PBS.
5. Add freshly prepared SA-βgal staining solution (1–2 mL per well), and incubate 16–24 h at 37 °C without CO_2 (in a bacterial incubator with humidity). As reaction speed can vary between individual primary cultures and with local culture conditions, determine the exact staining incubation duration by observing the development of a blue color in the positive control cells. Very few blue cells should be observed in the negative control after staining, whereas 75–100% of the positive senescence control (e.g., MSC-SEN-IR or MSC-SEN-REP) should have diffuse blue staining in almost all of the cell's cytoplasm [5].
6. Wash cells briefly twice with PBS and keep in PBS.
7. Quantify the number of blue SA-βgal-positive cells under a brightfield microscope with phase contrast. DNA staining with Hoechst (355 nm fluorescence microscopy) allows all the cell nuclei to be visualized and therefore facilitate with cell

counting. For this nuclear counterstain, add 1 mL of Hoechst (1/5000) in PBS for 5–10 min at room temperature in wash #2 above, and briefly wash twice with PBS.

3.2 Immunofluorescence: Cell Cycle Arrest by EdU Labeling

When cells enter senescence, they exhibit a stable G0/G1 cell cycle arrest through the actions of tumor suppressor proteins like p16, p21, p53, and Rb [54, 55]. Single-cell DNA synthesis analysis allows precise quantitative evaluation of proliferative and non-proliferative cells within a population. 5-ethynyl-2′-deoxyuridine (EdU) is a thymidine analogue that is effectively incorporated into cellular DNA during cell cycle S-phase and has been used to validate proliferation arrest during senescence [5, 50]. The subsequent in vitro reaction of incorporated EdU with a fluorescent azide in a copper-catalyzed [3 +2] cycloaddition reveals the single-cell proliferative status in fixed cells and can be quantified accurately using fluorescence.

1. Seed 2–4 × 10^4 cells in a six-well plate (60–75% confluence), and culture for 2–3 days to let the cell recover (*see* **Note 2**). Be careful that the cells are not overly confluent at the beginning of the EdU pulse because high cell density influences the EdU staining via contact inhibition cell proliferation arrest [56]. Note that a positive control for quiescence (cell cycle arrest) can be added using either contact inhibition in one well or serum starvation (0.02% FBS) for 48 h preceding the EdU pulse described below in **Step 3** (for this control the EdU pulse must be done in 0.02% FBS media to prevent cells from reentering the cell cycle).
2. Aspirate culture media, add 1–2 mL of complete medium (10% FBS, 1% Pen-Strep) containing 1 μM EdU, and keep in the incubator for 24–72 h depending on the desired length of EdU pulse labeling (the longest 72 h pulse is the most stringent to evaluate cell senescence as it will capture all the cells that have attempted proliferation over a 3-day period).
3. Wash cells with PBS once.
4. Fix cells with Fixing solution (1–2 mL/well) for 10 min at room temperature.
5. Wash cells twice with PBS.
6. Add 1 mL/well of freshly prepared EdU staining solution, and incubate the plate for 30 min at room temperature, protected from light.
7. Wash twice with 1 mL of 0.5% Triton X-100 in PBS and once with PBS alone.
8. Add 1 mL of Hoechst (1/5000) in PBS to label nuclei for 60 min at room temperature, protected from light.
9. Wash cells twice with PBS and keep in PBS.

10. Observe cells under an inverted fluorescent microscope. Determine the percent of labeled nuclei by counting the number of total (Hoechst stained) and labeled nuclei (EdU) in several randomly chosen fields (generally ≥100–150 total nuclei). Cells must be analyzed immediately, or alternatively, digital microscopic pictures can be acquired immediately, and data analyzed later using appropriate image analysis software. For a 3-day EdU pulse, a senescence control MSC-SEN-IR or MSC-SEN-REP EdU should yield 0–10% positive nuclei, and proliferating MSC P2–P6 should yield 80–100% positive nuclei.

3.3 Immunofluorescence: DNA Damage FOCI and DNA-SCARS by 53bp1, γH2AX, and PML Labeling

The presence of persistent DNA damage foci caused by telomere dysfunction or by the accumulation of DNA double-strand breaks (DSBs) is one of the defining characteristics of cellular senescence [15, 57, 58]. Immunofluorescence strategies that allow high resolution intranuclear DSB detection are based on the detection of DNA damage signaling and repair machinery components that are recruited or modified in situ on the chromatin surrounding the DSBs. These factors participate in the amplification of a micrometer-sized chromatin mark at the DSB site termed DNA damage foci [41, 59]. Given their size, these DNA damage foci can be visualized using antibodies that recognize the tumor suppressor p53-binding protein 1 (53BP1) known to re-localize on these marks or using antibodies that recognize the phosphorylated form of histone H2AX (γH2AX), a histone variant of the H2A protein family phosphorylated rapidly following DSB formation [60, 61]. While DNA damage foci are often transient in nature, persistent DSBs termed DNA segments with chromatin alterations reinforcing senescence (DNA-SCARS) are particularly important to define the senescent state [41]. DNA-SCARS allows the maintenance of key senescence phenotypes like SAPA and SASP and are characterized by the juxtaposition of promyelocytic leukemia protein (PML) nuclear bodies (PML-NBs) with DNA damage foci composed of either 53BP1 or γH2AX (or both) [41]. To differentiate transient DNA damage foci from DNA-SCARS, we suggest to look for the colocalization of γH2AX-53BP1 DNA damage foci (this dual colocalization validate DNA damage foci) with PML-NBs (this triple colocalization validate DNA-SCARS). In the absence of DSBs, 53BP1 has a diffuse nucleoplasmic staining inside the nucleus, but following a break, 53BP1 re-localize to DNA damage foci. Alternatively, γH2AX staining is absent before the induction of DNA damage, and de novo phosphorylation will make a γH2AX signal appear at sites of DSBs. PML is abundant in the nucleus, and PML-NBs can be readily detected as nuclear foci under all conditions, but some PML-NBs (not necessarily all) will colocalize to persistent DSBs [41]. Generally, senescent MSCs have between 0 and 5 persistent DNA damage foci per cell [5].

1. Seed 1×10^4 cells per well in a four-well chamber slide (60–75% confluence), and culture for 2–3 days.
2. Wash cells with PBS once.
3. Fix cells with Fixing solution (0.5 mL/well) for 10 min at room temperature.
4. Wash cells twice with PBS.
5. Permeabilize cells with 0.5% Triton in PBS (0.5 mL/well) for 30 min.
6. Wash twice in PBS (1 mL per well).
7. Block cells with blocking solution (0.5 mL/well) for 60 min at room temperature.
8. Incubate with primary antibodies diluted in blocking solution (0.25 mL/well), overnight at 4 °C.
9. Wash 3 times for 5 min each with PBS.
10. Incubate with secondary antibodies diluted in blocking solution (0.25 mL/well) 60 min at room temperature protected from light.
11. To label nuclei, add 0.25 mL of Hoechst (1/5000) in PBS, and incubate for 5–10 min at room temperature, protected from light.
12. Wash 3 times for 5 min each with PBS.
13. Drain the last wash, remove the plastic chambers, remove excess PBS, and mount using Vectashield and an appropriate coverslip for the optics of the microscope used in the next step.
14. Observe cells using a fluorescence microscope at 200–400× magnification. Determine the number of colocalized foci per nuclei in several randomly chosen fields (generally 100–150 total nuclei). To facilitate the analysis, use a software like AxioVision (Assay builder).
15. Between imaging sessions, keep slides flat and in the dark at −20 °C (can be stored for several years).

3.4 ELISA: Senescence-Associated Secretory Phenotype (SASP) Represented by IL-6 and IL-8 Cytokine

One of the most potent and potentially detrimental manifestations of cellular senescence is the presence of a microenvironmentally active pro-inflammatory SASP [62, 63]. The SASP has an autocrine effect on the senescent cell itself but more importantly conveys a plethora of effects on surrounding cells. The SASP is driven by the DDR and the NF-κB transcription factor. It is composed of a variety of SASP factors with specificities for each cell type/cultures built around a general pro-inflammatory core including interleukins, chemokines, growth factors, and secreted proteases [64, 65]. Among others, MSC-SASP has been reported to display increased levels of LEPTIN, TGFα, IL8, EOTAXIN, IFNγ, VCAM1, IFNβ, IL4, IL-6, ICAM-1, FGFβ, IL-10, and MCP1. The levels of those factors are usually tenfold

higher in senescent compared to normal cells [5, 13, 66]. Enzyme-linked immunosorbent assay (ELISA) is a specific and highly quantitative method to detect selected soluble factors of the SASP.

1. Seed 1–1.5 × 10^5 cells in a six-well plate (75–85% confluence goal), and culture for 1–2 days.
2. Aspirate culture media, wash twice with PBS, add 1 mL of serum free medium (DMEM low glucose, 1% Pen-Strep), and keep in the incubator for 24 h. Note that the total volume added needs to be recorded as it will be used to normalize the concentration of SASP-factors per volume (i.e., the final unit reported is cells/mL).
3. Collect the supernatants in sterile 1.5 mL plastic tubes and keep on ice (freeze at −80 °C if ELISA will be done later). Spin down cell debris for 5 min at 300 × *g*, and transfer the supernatant to another 1.5 mL tube; keep on ice. Alternatively, store at −80 °C until ready for **step 5**.
4. Following supernatant collection, wash cells with PBS prior to detaching cells with 0.25% trypsin-EDTA (WISENT Inc. cat. No. 325-045-EL) for 5 min at 37 °C (0.5 mL/well), and count the number of cells.
5. Proceed to IL-6 and IL-8 quantification using ELISA Human IL-6 kit (BD OptEIA cat. no. 555220) and Human IL-8 kit (BD OptEIA cat. no. 555244) according to the manufacturers protocol. Perform ELISA measurements in triplicates, and choose the best dilution to be in the linear range of the standard curve (we suggest starting with a dilution between 1/2 and 1/66). Average the triplicate measurements, and normalize the result using cell number and dilution factor (and media volume changes if a volume different from 1 mL was used) in order to report the final concentration with units of pg/mL cell.

4 Notes

1. As an alternative to radiation, MSC-SEN positive controls can be prepared using radiomimetic drugs such as bleomycin, neocarzinostatin, or zeocin [67, 68].
2. For EdU staining, the protocol above proposes cell culture in six-well plates (9.6 cm^2 area per well). Alternatively, glass chamber slides (0.70 cm^2 or 1.70 cm^2 (Sigma-Aldrich cat. no. 354108, 354104)) can be used for a better image and long-term preservation of the samples before imaging (several years at −20 °C, in the dark). Cell number should be adjusted according to surface area. Vectashield should be used for mounting (Vector Laboratories cat. no. H-1000) as described above for DNA damage foci immunofluorescence.

Acknowledgments

We thank Dr. Rodier and Dr. Colmegna's laboratory members for their valuable comments and discussions. This effort was supported by the Institut du cancer de Montréal (ICM to FR), the Israel Cancer Research Foundation (ICRF to FR), and the Canadian Institute for Health Research (CIHR MOP114962 to FR and MOP287233 to IC/FR). FR is a researcher at CRCHUM/ICM, which receives support from the Fonds de recherche du Québec – Santé (FRQS). FR is supported by a FRQS junior I–II career awards (22624, 33070). IC is a Chercheur Boursier Senior from FRQS. SN is supported by a FRQS PhD scholarship and a Canderel-ICM excellence award.

References

1. Jackson L, Jones DR, Scotting P, Sottile V (2007) Adult mesenchymal stem cells: differentiation potential and therapeutic applications. J Postgrad Med 53(2):121–127
2. Tirino V, Paino F, d'Aquino R, Desiderio V, De Rosa A, Papaccio G (2011) Methods for the identification, characterization and banking of human DPSCs: current strategies and perspectives. Stem Cell Rev 7(3):608–615. https://doi.org/10.1007/s12015-011-9235-9
3. Miura M, Gronthos S, Zhao M, Lu B, Fisher LW, Robey PG, Shi S (2003) SHED: stem cells from human exfoliated deciduous teeth. Proc Natl Acad Sci U S A 100(10):5807–5812. https://doi.org/10.1073/pnas.0937635100
4. Aqmasheh S, Shamsasanjan K, Akbarzadehlaleh P, Pashoutan Sarvar D, Timari H (2017) Effects of mesenchymal stem cell derivatives on hematopoiesis and hematopoietic stem cells. Adv Pharm Bull 7(2):165–177. https://doi.org/10.15171/apb.2017.021
5. O'Hagan-Wong K, Nadeau S, Carrier-Leclerc-A, Apablaza F, Hamdy R, Shum-Tim D, Rodier F, Colmegna I (2016) Increased IL-6 secretion by aged human mesenchymal stromal cells disrupts hematopoietic stem and progenitor cells' homeostasis. Oncotarget 7(12):13285–13296. https://doi.org/10.18632/oncotarget.7690
6. Galipeau J, Sensebe L (2018) Mesenchymal stromal cells: clinical challenges and therapeutic opportunities. Cell Stem Cell 22(6):824–833. https://doi.org/10.1016/j.stem.2018.05.004
7. Bobis S, Jarocha D, Majka M (2006) Mesenchymal stem cells: characteristics and clinical applications. Folia Histochem Cytobiol 44(4):215–230
8. Jacobs SA, Roobrouck VD, Verfaillie CM, Van Gool SW (2013) Immunological characteristics of human mesenchymal stem cells and multipotent adult progenitor cells. Immunol Cell Biol 91(1):32–39. https://doi.org/10.1038/icb.2012.64
9. Rohban R, Pieber TR (2017) Mesenchymal stem and progenitor cells in regeneration: tissue specificity and regenerative potential. Stem Cells Int 2017:5173732. https://doi.org/10.1155/2017/5173732
10. Pittenger MF, Martin BJ (2004) Mesenchymal stem cells and their potential as cardiac therapeutics. Circ Res 95(1):9–20. https://doi.org/10.1161/01.RES.0000135902.99383.6f
11. Ma S, Xie N, Li W, Yuan B, Shi Y, Wang Y (2014) Immunobiology of mesenchymal stem cells. Cell Death Differ 21(2):216–225. https://doi.org/10.1038/cdd.2013.158
12. Kizilay Mancini O, Lora M, Cuillerier A, Shum-Tim D, Hamdy R, Burelle Y, Servant MJ, Stochaj U, Colmegna I (2018) Mitochondrial oxidative stress reduces the immunopotency of mesenchymal stromal cells in adults with coronary artery disease. Circ Res 122(2):255–266. https://doi.org/10.1161/CIRCRESAHA.117.311400
13. Kizilay Mancini O, Lora M, Shum-Tim D, Nadeau S, Rodier F, Colmegna I (2017) A proinflammatory secretome mediates the impaired immunopotency of human mesenchymal stromal cells in elderly patients with atherosclerosis. Stem Cells Transl Med 6(4):1132–1140. https://doi.org/10.1002/sctm.16-0221

14. Hayflick L, Moorhead PS (1961) The serial cultivation of human diploid cell strains. Exp Cell Res 25:585–621
15. d'Adda di Fagagna F, Reaper PM, Clay-Farrace L, Fiegler H, Carr P, Von Zglinicki T, Saretzki G, Carter NP, Jackson SP (2003) A DNA damage checkpoint response in telomere-initiated senescence. Nature 426 (6963):194–198. https://doi.org/10.1038/nature02118
16. de Magalhaes JP, Passos JF (2018) Stress, cell senescence and organismal ageing. Mech Ageing Dev 170:2–9. https://doi.org/10.1016/j.mad.2017.07.001
17. Chandeck C, Mooi WJ (2010) Oncogene-induced cellular senescence. Adv Anat Pathol 17(1):42–48. https://doi.org/10.1097/PAP.0b013e3181c66f4e
18. Rodier F, Campisi J (2011) Four faces of cellular senescence. J Cell Biol 192(4):547–556. https://doi.org/10.1083/jcb.201009094
19. van Deursen JM (2014) The role of senescent cells in ageing. Nature 509(7501):439–446. https://doi.org/10.1038/nature13193
20. Luo Y, Zou P, Zou J, Wang J, Zhou D, Liu L (2011) Autophagy regulates ROS-induced cellular senescence via p21 in a p38 MAPKalpha dependent manner. Exp Gerontol 46 (11):860–867. https://doi.org/10.1016/j.exger.2011.07.005
21. Munro J, Barr NI, Ireland H, Morrison V, Parkinson EK (2004) Histone deacetylase inhibitors induce a senescence-like state in human cells by a p16-dependent mechanism that is independent of a mitotic clock. Exp Cell Res 295(2):525–538. https://doi.org/10.1016/j.yexcr.2004.01.017
22. Lowe SW, Schmitt EM, Smith SW, Osborne BA, Jacks T (1993) p53 is required for radiation-induced apoptosis in mouse thymocytes. Nature 362(6423):847–849. https://doi.org/10.1038/362847a0
23. Goldstein JC, Rodier F, Garbe JC, Stampfer MR, Campisi J (2005) Caspase-independent cytochrome c release is a sensitive measure of low-level apoptosis in cell culture models. Aging Cell 4(4):217–222. https://doi.org/10.1111/j.1474-9726.2005.00163.x
24. Ahmed AS, Sheng MH, Wasnik S, Baylink DJ, Lau KW (2017) Effect of aging on stem cells. World J Exp Med 7(1):1–10. https://doi.org/10.5493/wjem.v7.i1.1
25. Childs BG, Gluscevic M, Baker DJ, Laberge RM, Marquess D, Dananberg J, van Deursen JM (2017) Senescent cells: an emerging target for diseases of ageing. Nat Rev Drug Discov 16 (10):718–735. https://doi.org/10.1038/nrd.2017.116
26. Gonzalez LC, Ghadaouia S, Martinez A, Rodier F (2016) Premature aging/senescence in cancer cells facing therapy: good or bad? Biogerontology 17(1):71–87. https://doi.org/10.1007/s10522-015-9593-9
27. Demaria M (2017) Senescent cells: new target for an old treatment? Mol Cell Oncol 4(3): e1299666. https://doi.org/10.1080/23723556.2017.1299666
28. Baker DJ, Wijshake T, Tchkonia T, LeBrasseur NK, Childs BG, van de Sluis B, Kirkland JL, van Deursen JM (2011) Clearance of p16Ink4a-positive senescent cells delays ageing-associated disorders. Nature 479 (7372):232–236. https://doi.org/10.1038/nature10600
29. Demaria M, Ohtani N, Youssef SA, Rodier F, Toussaint W, Mitchell JR, Laberge RM, Vijg J, Van Steeg H, Dolle ME, Hoeijmakers JH, de Bruin A, Hara E, Campisi J (2014) An essential role for senescent cells in optimal wound healing through secretion of PDGF-AA. Dev Cell 31(6):722–733. https://doi.org/10.1016/j.devcel.2014.11.012
30. Chang J, Wang Y, Shao L, Laberge RM, Demaria M, Campisi J, Janakiraman K, Sharpless NE, Ding S, Feng W, Luo Y, Wang X, Aykin-Burns N, Krager K, Ponnappan U, Hauer-Jensen M, Meng A, Zhou D (2016) Clearance of senescent cells by ABT263 rejuvenates aged hematopoietic stem cells in mice. Nat Med 22(1):78–83. https://doi.org/10.1038/nm.4010
31. Baker DJ, Childs BG, Durik M, Wijers ME, Sieben CJ, Zhong J, Saltness RA, Jeganathan KB, Verzosa GC, Pezeshki A, Khazaie K, Miller JD, van Deursen JM (2016) Naturally occurring p16(Ink4a)-positive cells shorten healthy lifespan. Nature 530(7589):184–189. https://doi.org/10.1038/nature16932
32. Childs BG, Baker DJ, Wijshake T, Conover CA, Campisi J, van Deursen JM (2016) Senescent intimal foam cells are deleterious at all stages of atherosclerosis. Science 354 (6311):472–477. https://doi.org/10.1126/science.aaf6659
33. Baar MP, Brandt RMC, Putavet DA, Klein JDD, Derks KWJ, Bourgeois BRM, Stryeck S, Rijksen Y, van Willigenburg H, Feijtel DA, van der Pluijm I, Essers J, van Cappellen WA, van IWF, Houtsmuller AB, Pothof J, de Bruin RWF, Madl T, Hoeijmakers JHJ, Campisi J, de Keizer PLJ (2017) Targeted apoptosis of senescent cells restores tissue homeostasis in response to chemotoxicity and aging. Cell

169(1):132–147.e116. https://doi.org/10.1016/j.cell.2017.02.031

34. Demaria M, O'Leary MN, Chang J, Shao L, Liu S, Alimirah F, Koenig K, Le C, Mitin N, Deal AM, Alston S, Academia EC, Kilmarx S, Valdovinos A, Wang B, de Bruin A, Kennedy BK, Melov S, Zhou D, Sharpless NE, Muss H, Campisi J (2017) Cellular senescence promotes adverse effects of chemotherapy and cancer relapse. Cancer Discov 7(2):165–176. https://doi.org/10.1158/2159-8290.CD-16-0241
35. Farr JN, Xu M, Weivoda MM, Monroe DG, Fraser DG, Onken JL, Negley BA, Sfeir JG, Ogrodnik MB, Hachfeld CM, LeBrasseur NK, Drake MT, Pignolo RJ, Pirtskhalava T, Tchkonia T, Oursler MJ, Kirkland JL, Khosla S (2017) Targeting cellular senescence prevents age-related bone loss in mice. Nat Med 23(9):1072–1079. https://doi.org/10.1038/nm.4385
36. Jeon OH, Kim C, Laberge RM, Demaria M, Rathod S, Vasserot AP, Chung JW, Kim DH, Poon Y, David N, Baker DJ, van Deursen JM, Campisi J, Elisseeff JH (2017) Local clearance of senescent cells attenuates the development of post-traumatic osteoarthritis and creates a pro-regenerative environment. Nat Med 23(6):775–781. https://doi.org/10.1038/nm.4324
37. Xu M, Pirtskhalava T, Farr JN, Weigand BM, Palmer AK, Weivoda MM, Inman CL, Ogrodnik MB, Hachfeld CM, Fraser DG, Onken JL, Johnson KO, Verzosa GC, Langhi LGP, Weigl M, Giorgadze N, LeBrasseur NK, Miller JD, Jurk D, Singh RJ, Allison DB, Ejima K, Hubbard GB, Ikeno Y, Cubro H, Garovic VD, Hou X, Weroha SJ, Robbins PD, Niedernhofer LJ, Khosla S, Tchkonia T, Kirkland JL (2018) Senolytics improve physical function and increase lifespan in old age. Nat Med 24(8):1246–1256. https://doi.org/10.1038/s41591-018-0092-9
38. Kirkland JL, Tchkonia T, Zhu Y, Niedernhofer LJ, Robbins PD (2017) The clinical potential of senolytic drugs. J Am Geriatr Soc 65(10):2297–2301. https://doi.org/10.1111/jgs.14969
39. Zhu Y, Tchkonia T, Pirtskhalava T, Gower AC, Ding H, Giorgadze N, Palmer AK, Ikeno Y, Hubbard GB, Lenburg M, O'Hara SP, LaRusso NF, Miller JD, Roos CM, Verzosa GC, LeBrasseur NK, Wren JD, Farr JN, Khosla S, Stout MB, McGowan SJ, Fuhrmann-Stroissnigg H, Gurkar AU, Zhao J, Colangelo D, Dorronsoro A, Ling YY, Barghouthy AS, Navarro DC, Sano T, Robbins PD, Niedernhofer LJ, Kirkland JL (2015) The Achilles' heel of senescent cells: from transcriptome to senolytic drugs. Aging Cell 14(4):644–658. https://doi.org/10.1111/acel.12344
40. Fumagalli M, Rossiello F, Clerici M, Barozzi S, Cittaro D, Kaplunov JM, Bucci G, Dobreva M, Matti V, Beausejour CM, Herbig U, Longhese MP, d'Adda di Fagagna F (2012) Telomeric DNA damage is irreparable and causes persistent DNA-damage-response activation. Nat Cell Biol 14(4):355–365. https://doi.org/10.1038/ncb2466
41. Rodier F, Munoz DP, Teachenor R, Chu V, Le O, Bhaumik D, Coppe JP, Campeau E, Beausejour CM, Kim SH, Davalos AR, Campisi J (2011) DNA-SCARS: distinct nuclear structures that sustain damage-induced senescence growth arrest and inflammatory cytokine secretion. J Cell Sci 124(Pt 1):68–81. https://doi.org/10.1242/jcs.071340
42. Hernandez-Segura A, Nehme J, Demaria M (2018) Hallmarks of cellular senescence. Trends Cell Biol 28(6):436–453. https://doi.org/10.1016/j.tcb.2018.02.001
43. Turinetto V, Vitale E, Giachino C (2016) Senescence in human mesenchymal stem cells: functional changes and implications in stem cell-based therapy. Int J Mol Sci 17(7). https://doi.org/10.3390/ijms17071164
44. Wagner W, Horn P, Castoldi M, Diehlmann A, Bork S, Saffrich R, Benes V, Blake J, Pfister S, Eckstein V, Ho AD (2008) Replicative senescence of mesenchymal stem cells: a continuous and organized process. PLoS One 3(5):e2213. https://doi.org/10.1371/journal.pone.0002213
45. Legzdina D, Romanauska A, Nikulshin S, Kozlovska T, Berzins U (2016) Characterization of senescence of culture-expanded human adipose-derived mesenchymal stem cells. Int J Stem Cells 9(1):124–136. https://doi.org/10.15283/ijsc.2016.9.1.124
46. Deryabin PI, Borodkina AV, Nikolsky NN, Burova EB (2015) Relationship between p53/p21/Rb and mapk signaling pathways in human endometrium-derived stem cells under oxidative stress. Tsitologiia 57(11):788–795
47. Medeiros Tavares Marques JC, Cornelio DA, Nogueira Silbiger V, Ducati Luchessi A, de Souza S, Batistuzzo de Medeiros SR (2017) Identification of new genes associated to senescent and tumorigenic phenotypes in mesenchymal stem cells. Sci Rep 7(1):17837. https://doi.org/10.1038/s41598-017-16224-5
48. Contrepois K, Coudereau C, Benayoun BA, Schuler N, Roux PF, Bischof O, Courbeyrette R, Carvalho C, Thuret JY, Ma Z, Derbois C, Nevers MC, Volland H, Redon CE, Bonner WM, Deleuze JF, Wiel C,

Bernard D, Snyder MP, Rube CE, Olaso R, Fenaille F, Mann C (2017) Histone variant H2A.J accumulates in senescent cells and promotes inflammatory gene expression. Nat Commun 8:14995. https://doi.org/10.1038/ncomms14995

49. Narita M, Nunez S, Heard E, Narita M, Lin AW, Hearn SA, Spector DL, Hannon GJ, Lowe SW (2003) Rb-mediated heterochromatin formation and silencing of E2F target genes during cellular senescence. Cell 113(6):703–716
50. Laberge RM, Adler D, DeMaria M, Mechtouf N, Teachenor R, Cardin GB, Desprez PY, Campisi J, Rodier F (2013) Mitochondrial DNA damage induces apoptosis in senescent cells. Cell Death Dis 4:e727. https://doi.org/10.1038/cddis.2013.199
51. Rodier F, Coppe JP, Patil CK, Hoeijmakers WA, Munoz DP, Raza SR, Freund A, Campeau E, Davalos AR, Campisi J (2009) Persistent DNA damage signalling triggers senescence-associated inflammatory cytokine secretion. Nat Cell Biol 11(8):973–979. https://doi.org/10.1038/ncb1909
52. Debacq-Chainiaux F, Erusalimsky JD, Campisi J, Toussaint O (2009) Protocols to detect senescence-associated beta-galactosidase (SA-betagal) activity, a biomarker of senescent cells in culture and in vivo. Nat Protoc 4(12):1798–1806. https://doi.org/10.1038/nprot.2009.191
53. Dimri GP, Lee X, Basile G, Acosta M, Scott G, Roskelley C, Medrano EE, Linskens M, Rubelj I, Pereira-Smith O et al (1995) A biomarker that identifies senescent human cells in culture and in aging skin in vivo. Proc Natl Acad Sci U S A 92(20):9363–9367
54. Barnum KJ, O'Connell MJ (2014) Cell cycle regulation by checkpoints. Methods Mol Biol 1170:29–40. https://doi.org/10.1007/978-1-4939-0888-2_2
55. Qian Y, Chen X (2013) Senescence regulation by the p53 protein family. Methods Mol Biol 965:37–61. https://doi.org/10.1007/978-1-62703-239-1_3
56. Pani G, Colavitti R, Bedogni B, Anzevino R, Borrello S, Galeotti T (2000) A redox signaling mechanism for density-dependent inhibition of cell growth. J Biol Chem 275(49):38891–38899. https://doi.org/10.1074/jbc.M007319200
57. McHugh D, Gil J (2018) Senescence and aging: causes, consequences, and therapeutic avenues. J Cell Biol 217(1):65–77. https://doi.org/10.1083/jcb.201708092
58. d'Adda di Fagagna F (2008) Living on a break: cellular senescence as a DNA-damage response. Nat Rev Cancer 8(7):512–522. https://doi.org/10.1038/nrc2440
59. Polo SE, Jackson SP (2011) Dynamics of DNA damage response proteins at DNA breaks: a focus on protein modifications. Genes Dev 25(5):409–433. https://doi.org/10.1101/gad.2021311
60. Kuo LJ, Yang LX (2008) Gamma-H2AX—a novel biomarker for DNA double-strand breaks. In Vivo 22(3):305–309
61. Rappold I, Iwabuchi K, Date T, Chen J (2001) Tumor suppressor p53 binding protein 1 (53BP1) is involved in DNA damage-signaling pathways. J Cell Biol 153(3):613–620
62. Malaquin N, Martinez A, Rodier F (2016) Keeping the senescence secretome under control: molecular reins on the senescence-associated secretory phenotype. Exp Gerontol 82:39–49. https://doi.org/10.1016/j.exger.2016.05.010
63. Coppe JP, Desprez PY, Krtolica A, Campisi J (2010) The senescence-associated secretory phenotype: the dark side of tumor suppression. Annu Rev Pathol 5:99–118. https://doi.org/10.1146/annurev-pathol-121808-102144
64. Malaquin N, Carrier-Leclerc A, Dessureault M, Rodier F (2015) DDR-mediated crosstalk between DNA-damaged cells and their microenvironment. Front Genet 6:94. https://doi.org/10.3389/fgene.2015.00094
65. Chien Y, Scuoppo C, Wang X, Fang X, Balgley B, Bolden JE, Premsrirut P, Luo W, Chicas A, Lee CS, Kogan SC, Lowe SW (2011) Control of the senescence-associated secretory phenotype by NF-kappaB promotes senescence and enhances chemosensitivity. Genes Dev 25(20):2125–2136. https://doi.org/10.1101/gad.17276711
66. Sepulveda JC, Tome M, Fernandez ME, Delgado M, Campisi J, Bernad A, Gonzalez MA (2014) Cell senescence abrogates the therapeutic potential of human mesenchymal stem cells in the lethal endotoxemia model. Stem Cells 32(7):1865–1877. https://doi.org/10.1002/stem.1654
67. Povirk LF (1996) DNA damage and mutagenesis by radiomimetic DNA-cleaving agents: bleomycin, neocarzinostatin and other enediynes. Mutat Res 355(1-2):71–89
68. Chankova SG, Dimova E, Dimitrova M, Bryant PE (2007) Induction of DNA double-strand breaks by zeocin in Chlamydomonas reinhardtii and the role of increased DNA double-strand breaks rejoining in the formation of an adaptive response. Radiat Environ Biophys 46(4):409–416. https://doi.org/10.1007/s00411-007-0123-2

Methods in Molecular Biology (2019) 2045: 107–117
DOI 10.1007/7651_2018_197

Published online: 28 November 2018

Adipogenic and Osteogenic Differentiation of In Vitro Aged Human Mesenchymal Stem Cells

Courtney R. Ogando, Gilda A. Barabino, and Yueh-Hsun Kevin Yang

Abstract

Multipotent mesenchymal stem cells (MSCs) are an attractive candidate for regeneration of damaged cells, tissues, and organs. Due to limited availabilities, MSC populations must be rapidly expanded to satisfy clinical needs. However, senescence attributed to extensive in vitro expansion compromises the regenerative and therapeutic potential of MSCs. In this chapter, we describe a step-by-step protocol that aims to induce adipogenic and osteogenic differentiation of in vitro aged human MSCs and highlight noteworthy issues that may arise during the process.

Keywords Adipogenesis, Differentiation, Expansion, Flow cytometry, Histology, Mesenchymal stem cell, Osteogenesis, Senescence

Abbreviations

APC	Allophycocyanin
BSA	Bovine serum albumin
ddH_2O	Ultrapure water
DMSO	Dimethyl sulfoxide
EDTA	Ethylenediaminetetraacetic acid
FBS	Fetal bovine serum
FGF-2	Basic fibroblast growth factor
FITC	Fluorescein isothiocyanate
HBSS	Hank's balanced salt solution
HEPES	4-(2-Hydroxylethyl)-1-piperazineethanesulfonic acid
hgDMEM	High glucose Dulbecco's modified Eagle's medium
lgDMEM	Low glucose Dulbecco's modified Eagle's medium
MSCs	Mesenchymal stem cells
PBS	Phosphate-buffered saline
Pen/Strep	Penicillin/streptomycin
PerCP-Cy5.5	Peridinin-chlorophyll protein complex-cyanine 5.5
RPE	R-phycoerythrin

1 Introduction

Mesenchymal stem cells (MSCs) were first identified by Friedenstein et al. in 1976 and were characterized as colony-forming cells that had a homogeneously fibroblastic appearance and could remain inactive for 2–4 days post-seeding before starting to replicate rapidly in vitro [1]. MSCs which can be extracted from a variety of sources such as adipose tissue, lung tissue, umbilical cord blood, and bone marrow are multipotent progenitor cells with the ability to differentiate into different cell lineages of mesodermal origin such as chondrocytes, adipocytes, osteoblasts, and more [2, 3]. Despite their rare number in the body [4], their strong potential for self-renewal in the undifferentiated form allows MSCs to produce abundant daughter cells with similar functionalities [5, 6]. When expanded in vitro, however, MSC populations can experience progressive senescence, which potentially deteriorates their stem cell phenotype and their proliferative and differentiation capabilities [7–9]. It has been reported that MSCs may be continuously passaged for up to a cell population doubling number of 30–40 before they stop propagating [10–12].

In this protocol, we systematically demonstrate how to differentiate in vitro aged human MSCs toward adipogenic and osteogenic lineages. MSCs tested herein have an overall cell population doubling number of around 25 [7]. MSC senescence during in vitro expansion is confirmed by progressive morphological changes over time (Fig. 1) and decreased expression of certain MSC surface antigens, such as CD146 (Fig. 2). When exposed to selected differentiation conditions, aged MSCs are able to develop into lipid-

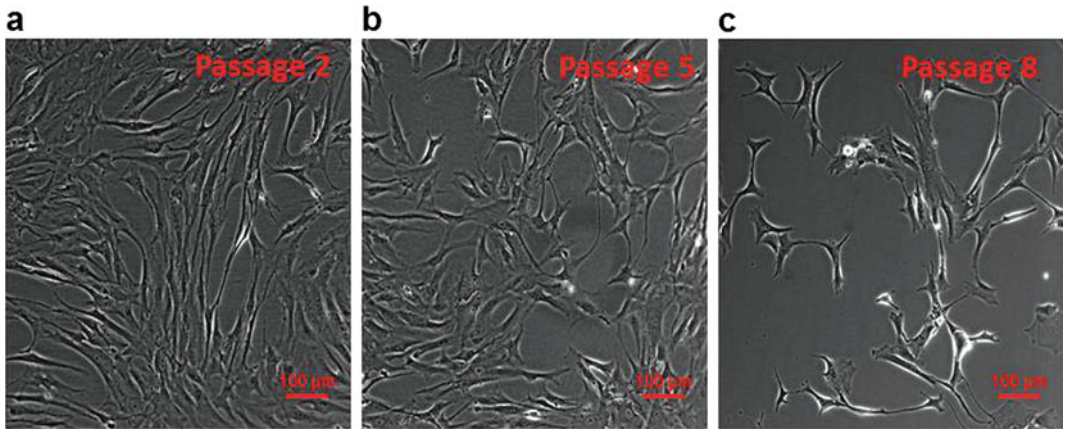

Fig. 1 Morphology of human MSCs at passages 2, 5, and 8. During in vitro expansion, MSCs at passages 2 (**a**) and 5 (**b**) were able to maintain the typical spindle shape, whereas those at passage 8 (**c**) displayed irregular and inhomogeneous morphology with an increased cell size. Phase-contrast images were taken on the seventh day of each passage. Scale bar: 100 μm

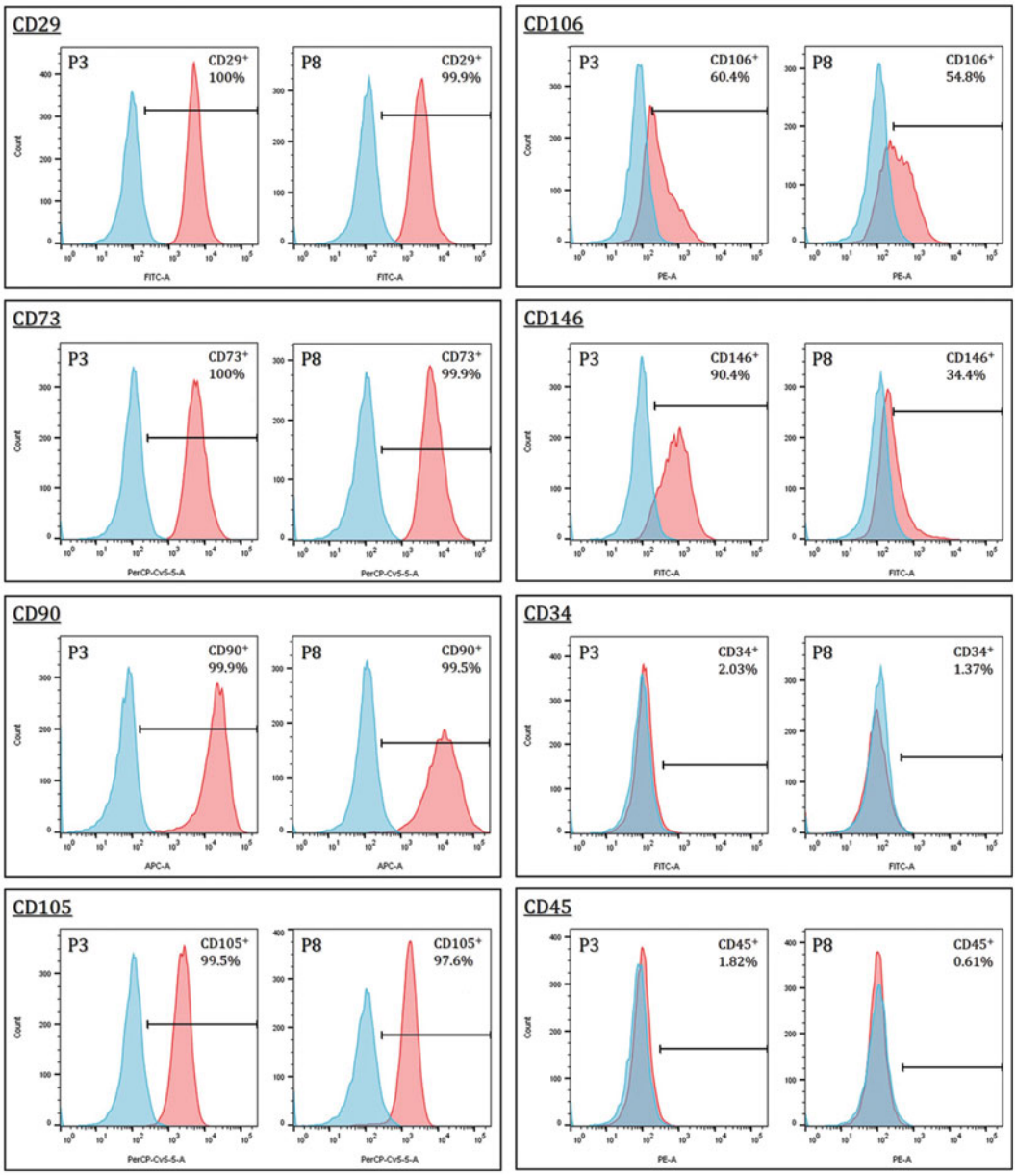

Fig. 2 Flow cytometry analysis on surface antigen expression of human MSCs at passages 3 and 8. MSCs were fluorescently labeled for evaluation of specific positive (CD29, CD73, CD90, CD105, CD106, CD146) and negative markers (CD34, CD45). While MSC senescence did not impact expression of most tested antigens, the level of CD146 decreased with increasing passage number. In addition, about 50–60% of MSC populations were positive for CD106 regardless of passage number. MSCs at either passage were negative for CD34 and CD45. Red and blue histograms represent marker molecules and negative isotype controls, respectively

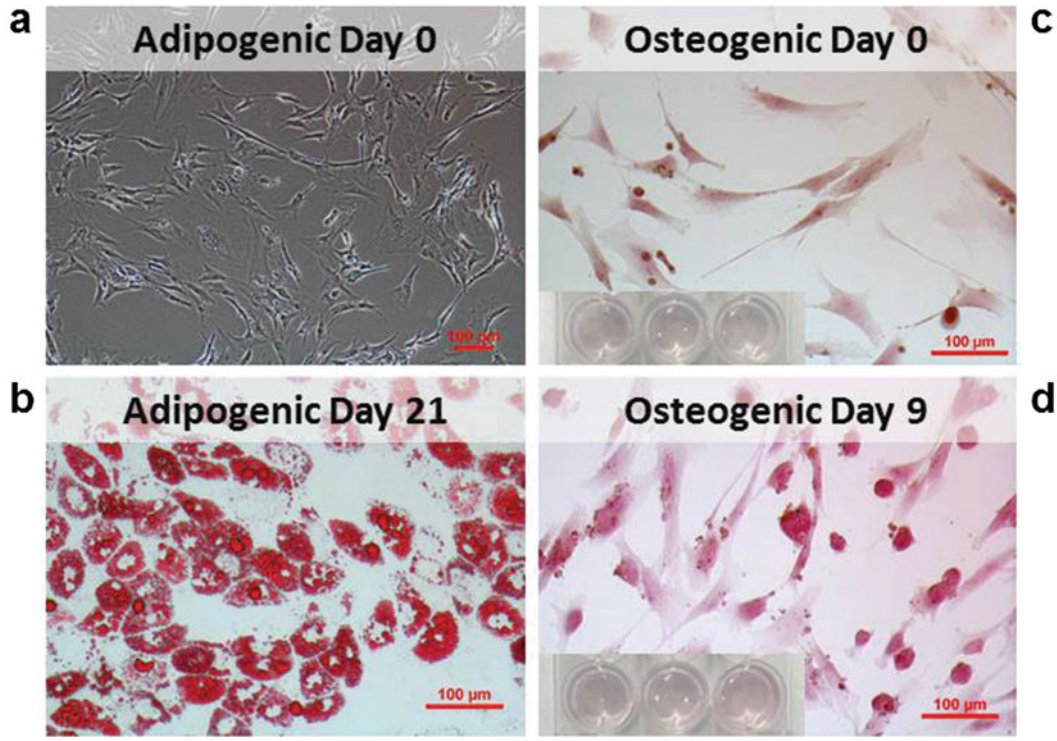

Fig. 3 Histology of in vitro aged human MSCs (passage 8) undergoing adipogenic or osteogenic differentiation. (**a**, **b**) Adipogenic samples were stained with Oil Red O, and lipid vacuoles are shown in a red color. MSCs at passage 8 synthesized abundant lipids after treated with adipogenic media for 21 days. (**c**, **d**) Osteogenic samples were stained with Alizarin Red, and calcium is shown in a red color. Since osteogenic cultures were only stable for up to 2 weeks (*see* **Note 19**), histology was performed on day 9, and calcium deposition by aged MSCs was limited. Scale bar: 100 μm

producing adipocytes (Fig. 3a, b),whereas osteogenesis is significantly compromised as evidenced by limited synthesis of calcium (Fig. 3c, d).

2 Materials

2.1 MSC Cultivation

1. Human MSCs extracted from bone marrow or other sources [2] (*see* **Note 1**).
2. Expansion media: lgDMEM (1 g/L D-glucose, 4 mM L-glutamine, 25 mM HEPES, 110 mg/L sodium pyruvate), 10% v/v FBS, 1% v/v Pen/Strep, 1 ng/mL FGF-2 (*see* **Note 2**). Stored at 4 °C.
3. Osteogenic media: hgDMEM (4.5 g/L D-glucose, 4 mM L-glutamine), 3.72 mg/mL sodium bicarbonate, 10% v/v FBS, 1% v/v Pen/Strep, 50 μg/mL ascorbic acid, 10 mM β-glycerophosphate. Stored at 4 °C.

4. Adipogenic media: hgDMEM (4.5 g/L D-glucose, 4 mM L-glutamine), 3.72 mg/mL sodium bicarbonate, 10% v/v FBS, 1% v/v Pen/Strep, 1 μM dexamethasone, 0.5 mM indomethacin, 60 μM 3-isobutyl-1-methylxanine, 10 μg/mL insulin (*see* **Note 3**). Stored at 4 °C.
5. Trypsin/EDTA mixture: 1× HBSS, 0.25% w/v trypsin, 1 mM EDTA. Stored at -20 °C.
6. Humidified incubator.
7. Light microscope.

2.2 Flow Cytometry

1. Mouse anti-human antibodies: anti-CD29 (FITC-conjugated), anti-CD34 (FITC-conjugated), anti-CD45 (RPE-conjugated), anti-CD73 (PerCP-Cy5.5-conjugated), anti-CD90 (APC-conjugated), anti-CD105 (PerCP-Cy5.5-conjugated), anti-CD106 (RPE-conjugated), ant-CD146 (FITC-conjugated), and corresponding mouse isotype controls.
2. Blocking buffer: 1× PBS, 1% w/v BSA. Store at 4 °C.
3. Antibody staining solutions: 1:10 antibody-to-1× PBS (*see* **Note 4**).
4. 5-mL polystyrene round-bottom tube with cell strainer cap.
5. Flow cytometer.

2.3 Histology

1. 10% formalin.
2. Alizarin Red staining solution: 2% w/v Alizarin Red S in ddH_2O. Adjust pH level to 4.1–4.3 using 1 M hydrochloric acid and 1 N sodium hydroxide. Filter the solution through a 0.22 μm filter. Stored at 4 °C in the dark.
3. Oil Red O staining solution: Three parts of 0.3% w/v Oil Red O in 99% isopropanol (stock solution) (*see* **Note 5**) with two parts of ddH_2O. Filter the working solution through a 0.22 μm filter (*see* **Note 6**).
4. 60% isopropanol.

3 Methods

All cell culture procedures are carried out in a laminar flow biological safety hood.

3.1 In Vitro Expansion of MSCs

1. Retrieve cryopreserved MSCs from liquid nitrogen storage (*see* **Note 7**). To defrost, incubate and constantly shake cryovial (s) containing frozen MSCs in a water bath set to 37 °C until only a small amount of the cell solution remains frozen. Hold the vial(s) in hand until the remaining ice has melted.

2. Transfer the defrosted cell solution into a 15 mL conical centrifuge tube and spin down at 400 × *g* for 10 min.
3. Aspirate the supernatant from the tube without disturbing the cell pellet and resuspend the cells in fresh expansion media.
4. Perform cell count using the trypan blue exclusion assay [13].
5. Seed MSCs onto tissue culture plastic at a desired density (*see* **Note 8**) and culture them in a humidified incubator (37 °C, 5% CO_2) for 10 days.
6. Exchange media 24 h after seeding (*see* **Note 9**) and every 3 days thereafter.
7. Observe and record cell morphology throughout the cultivation period using a phase-contrast microscope (*see* **Note 10**).
8. At harvest (day 10), gently rinse MSC monolayers three times with 1× PBS (*see* **Note 11**), followed by 3-min treatment with the trypsin/EDTA mixture at 37 °C to detach adherent cells (*see* **Note 12**).
9. Neutralize the trypsin/EDTA mixture with fresh expansion media at a 1:2, trypsin/EDTA-to-media ratio (*see* **Note 13**).
10. Use a 5 mL serological pipet to collect the solution containing detached cells and transfer them to a conical centrifuge tube (*see* **Note 14**).
11. Centrifuge the collected cells at 400 × *g* for 10 min.
12. Remove the supernatant and resuspend the cells in fresh expansion media.
13. Perform cell count.
14. Process the collected MSCs either for subculture up to passage 8 (repeat **steps 5–13**) (*see* **Note 15**) or for flow cytometry analysis.

3.2 Flow Cytometry

1. Rinse the collected MSCs at designated passages once with 1× PBS.
2. Divide the cell solution into small aliquots in 1.5-mL Eppendorf tubes based on the number of samples required for antibody treatment (*see* **Note 16**).
3. Centrifuge the cells at 300 × *g* for 5 min.
4. Aspirate PBS and incubate each sample with 100 μL of the blocking buffer for 30 min. Gently mix the cells every 15 min (*see* **Note 17**).
5. Centrifuge the cells at 300 × *g* for 5 min.
6. Aspirate the blocking buffer and treat each sample with 100 μL of a designated antibody staining solution (*see* **Note 18**).

7. Wrap the samples in aluminum foil and incubate them for 45 min in the dark. Gently mix the cells every 15 min.
8. Centrifuge the cells at 300 × *g* for 5 min.
9. Remove the antibody staining solutions and resuspend each sample in 1 mL of 1× PBS.
10. Transfer each sample to a 5 mL polystyrene round-bottom tube by filtering the cell solution through the cell strainer cap attached to the tube. Label each tube with the respective antibody and fluorescent dye.
11. Keep the samples in the dark before analyzing them using a flow cytometer.

3.3 Adipogenic and Osteogenic Differentiation

1. At the end of the eighth passage (following the steps described in Subheading 3.1), replace expansion media with either adipogenic or osteogenic media without detaching MSC monolayers from tissue culture plastics.
2. Culture the cells for an additional period of up to 21 days with adipogenic or osteogenic media and exchange media every 3 days.
3. Terminate the cultures at designated time points for histological evaluation (*see* **Note 19**).

3.4 Histology

The protocol below is applicable to cultures in a 12-well plate.

1. Aspirate adipogenic or osteogenic media and rinse the cells three times with 1× PBS.
2. Fix the cells in 1 mL of 10% formalin for 1 h at room temperature.
3. After fixation, remove the formalin solution and wash the cells twice with 2 mL of ddH_2O.
4. *For adipogenesis:*
   (a) Add 2 mL of 60% isopropanol to cover each cell monolayer and incubate the samples for 5 min.
   (b) After removing 60% isopropanol, add 2 mL of the Oil Red O staining solution to each well.
   (c) Slowly rotate the plate to ensure that the Oil Red O staining solution evenly covers the cell monolayers and incubate the samples for 5 min.
   (d) Aspirate the Oil Red O solution and rinse the cells multiple times with ddH_2O until the staining solution is completely removed.

For osteogenesis:

(a) Add 1 mL of the Alizarin Red S staining solution to each well and incubate the samples at room temperature in the dark for 45 min.

(b) Aspirate the Alizarin Red S solution and rinse the cells multiple times with ddH_2O until the staining solution is completely removed.

5. Keep the samples in 1× PBS until they are ready to be viewed under a microscope.

4 Notes

1. Bone marrow MSCs isolated from a 21-year-old Hispanic male donor was used in this demonstration.
2. Dissolve 100 μg of FGF-2 in 200 μL of sterile ddH_2O (stock concentration: 500 μg/mL); do not vortex. Mix 1 μL of the FGF-2 stock solution with 99 μL of sterile ddH_2O to prepare 5 μg/mL FGF-2 working solution. DO NOT add the FGF-2 working solution directly to bulk expansion media. Add 1 μL of the FGF-2 working solution per 5 mL of expansion media during each medium exchange.
3. DO NOT add insulin directly to bulk adipogenic media since it tends to degrade rapidly.
4. Each sample is only labelled with one of the fluorescently tagged antibodies. Therefore, one antibody staining solution must be individually prepared for each sample.
5. The Oil Red O stock solution is stable for 1 year and can be stored at room temperature.
6. The Oil Red O working solution is only stable for 2 h.
7. MSCs are cryopreserved in freezing media composed of 65% expansion media, 30% FBS, and 5% DMSO.
8. The initial seeding density for MSC expansion is preferably 1,400 viable cells per cm^2 or 2.5×10^5 viable cells per T-175 flask.
9. It is crucial to exchange expansion media 24 h after seeding to remove non-adherent and/or dead cells.
10. Morphological changes, such as non-spindle shape deformation and increase in cell size, are expected as MSC passage number increases (Fig. 1).

11. The volume of PBS used in the rinsing step should be the same as expansion media used for feeding. The purpose of rinsing MSC monolayers with 1× PBS is to remove any remaining expansion media and non-adherent cells.
12. If the cells have not detached from the culture surface after the initial 3-min incubation with the trypsin/EDTA mixture, gently tap the side of the culture vessel couple times to facilitate cell detachment. If strong affinity between MSCs and the culture surface has occurred (usually in early passages), incubate the cells with the trypsin/EDTA mixture at 37 °C for an additional period of up to 2 min and repeat the tapping step.
13. The required volume of the trypsin/EDTA mixture should be kept at a minimum but sufficient to cover the entire cell monolayer. In general, it is equal to one third of the total volume of fresh media used to feed the cells.
14. To maximize cell yield, collect some cell suspension solution in a 5 mL serological pipet and rinse the culture surface from top to bottom while tilting the culture vessel at 45° to flush detached cells toward one of the corners on the lower end. Repeat this step several times before transferring the cell suspension solution to a conical centrifuge tube.
15. MSCs at higher passages may not reach full confluency within the 10-day culture period given an initial cell seeding density of 1,400 cells per cm^2. In such cases, a longer culture period or a higher cell seeding density may be considered.
16. The preferred number of MSCs for flow cytometry analysis is at least 5×10^5 cells per sample.
17. Gentle mixing should be applied every 15 min during incubation to avoid sedimentation of cells. This action maximizes the exposure of every single cell to the added reagents and thus improves the efficiency of both blocking and antibody-labelling steps.
18. When incubating the cells with antibody staining solutions, be aware that fluorescent dye-conjugated antibodies are extremely light sensitive. Therefore, samples should be kept in the dark all the time from this point.
19. When undergoing osteogenic differentiation, MSCs at passage 8 start to peel off or detach from the plastic surface after 10–14 days in culture (Fig. 4). For optimal outcome, histological analysis of osteogenically differentiated samples should be performed between weeks 1 and 2.

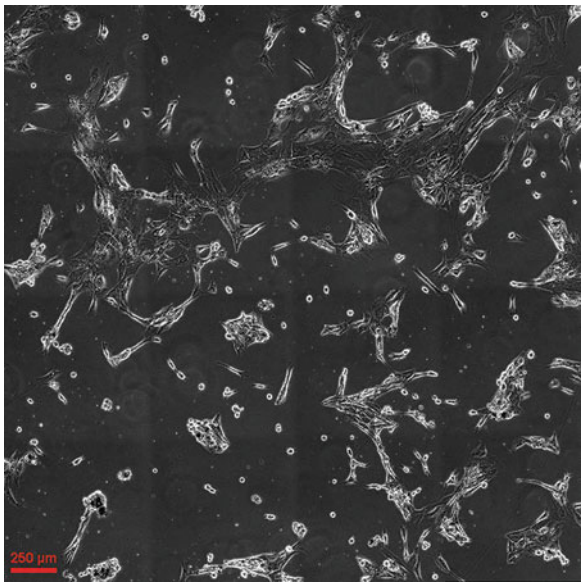

Fig. 4 Spontaneous detachment of in vitro aged human MSCs (passage 8) undergoing osteogenic differentiation. When cultivated with osteogenic media, MSCs at passage 8 began to shrink and spontaneously detached from the surface after 10–14 days in culture. The phase-contrast image was taken on the 14th day of osteogenic induction. Scale bar: 250 μm

Acknowledgments

This work was supported by the City College of New York Research Award (to GAB) and partially by the Professional Staff Congress – City University of New York Research Award (Grant number 61584-00 49 to YHKY).

References

1. Friedenstein AJ, Gorskaja J, Kulagina NN (1976) Fibroblast precursors in normal and irradiated mouse hematopoietic organs. Exp Hematol 4(5):267–274
2. Chamberlain G, Fox J, Ashton B et al (2007) Concise review: mesenchymal stem cells: their phenotype, differentiation capacity, immunological features, and potential for homing. Stem Cells 25(11):2739–2749
3. Yang Y-H, Lee AJ, Barabino GA (2012) Coculture-driven mesenchymal stem cell-differentiated articular chondrocyte-like cells support neocartilage development. Stem Cells Transl Med 1(11):843–854
4. Friedenstein AJ, Latzinik NW, Grosheva AG et al (1982) Marrow microenvironment transfer by heterotopic transplantation of freshly isolated and cultured cells in porous sponges. Exp Hematol 10(2):217–227
5. Prockop DJ (1997) Marrow stromal cells as stem cells for non-hematopoietic tissues. Science 276(5309):71–74
6. Pittenger MF, Mackay AM, Beck SC et al (1999) Multilineage potential of adult human mesenchymal stem cells. Science 284(5411):143–147
7. Yang Y-HK, Ogando CR, Wang See C et al (2018) Changes in phenotype and differentiation potential of human mesenchymal stem cells aging in vitro. Stem Cell Res Ther 9 (1):131
8. Digirolamo CM, Stokes D, Colter D et al (1999) Propagation and senescence of human

marrow stromal cells in culture: a simple colony-forming assay identifies samples with the greatest potential to propagate and differentiate. Br J Haematol 107(2):275–281

9. Colter DC, Class R, DiGirolamo CM et al (2000) Rapid expansion of recycling stem cells in cultures of plastic-adherent cells from human bone marrow. Proc Natl Acad Sci U S A 97(7):3213–3218
10. Baxter MA, Robert FW, Simon NJ et al (2008) Study of telomere length reveals rapid aging of human marrow stromal cells following in vitro expansion. Stem Cells 22(5):675–682
11. Bruder SP, Jaiswal N, Haynesworth SE (1997) Growth kinetics, self-renewal, and the osteogenic potential of purified human mesenchymal stem cells during extensive subcultivation and following cryopreservation. J Cell Biochem 64(2):278–294
12. Muraglia A, Cancedda R, Quarto R (2000) Clonal mesenchymal progenitors from human bone marrow differentiate in vitro according to a hierarchical model. J Cell Sci 113(7):1161–1166
13. Strober W (2001) Trypan blue exclusion test of cell viability. Curr Protoc Immunol 21(1): A.3B.1–A.3B.2

Methods in Molecular Biology (2019) 2045: 119–129
DOI 10.1007/7651_2018_201

Published online: 30 November 2018

Human Skeletal Muscle-Derived Mesenchymal Stem/Stromal Cell Isolation and Growth Kinetics Analysis

Klemen Čamernik, Janja Marc, and Janja Zupan

Abstract

The most studied sources of mesenchymal stem/stromal cells (MSCs) are bone marrow and adipose tissue. However skeletal muscle represents an interesting source of diverse subpopulations of MSCs, such as paired box 7 (Pax-7)-positive satellite cells, fibro-/adipogenic progenitors, PW1-positive interstitial cells and others. The specific properties of some of these muscle-derived cells have encouraged the development of cell therapies for muscle regeneration. However, the identity and multilineage potential of the diverse muscle-resident cells should first be evaluated in vitro, followed by in vivo clinical trials to predict their regenerative capacity. Here, we present protocols for the isolation of MSCs from skeletal muscle using enzymatic digestion and mechanical trituration. We also provide a method to determine their specific growth rate, a feature that is of particular interest when designing cell therapies.

Keywords Cell growth kinetics, Collagenase digestion, Isolation, Mesenchymal stem/stromal cells, Skeletal muscle

1 Introduction

Mesenchymal stem/stromal cells (MSCs) represent a heterogeneous population of stem cells that can undergo multilineage differentiation into bone, cartilage and adipose tissue [1]. They are present throughout adult life and have important roles in tissue repair; as such, they have great promise for regenerative medicine and tissue engineering. MSCs were first discovered in the bone marrow by Friedenstein and colleagues [2] and have since been found in many other adult tissues.

Depending on tissue type, different methods of MSC isolation can be used, ranging from simple filtration to enzymatic digestion and mechanical trituration. While bone marrow and adipose tissue remain the most studied sources of MSCs, and also the main sources used in current cell therapies, skeletal muscle represents an interesting source of diverse MSC subpopulations with different characteristics [3]. Paired box 7 (Pax-7)-positive satellite cells generally undergo myogenic differentiation and contribute to skeletal muscle regeneration [4], whereas fibro-/adipogenic progenitors generally form adipose and fibrous tissue and are thought to

contribute to myosteatosis [5]. Another interesting MSC subpopulation is PW1-positive interstitial cells (PICs), which can differentiate not only into osteoblasts, adipocytes and chondrocytes but also into both striated and smooth muscle cells [6].

One of the features sought after in cell therapies is the specific growth rate, which is a measure of the MSC proliferation capacity and an important parameter of the cell kinetics. A high specific growth rate is of interest when expanding cells in vitro for cell therapies, where millions of cells are required [7]. Cell kinetics analysis is also a useful tool for studying the effects of different media compositions, materials and growth factors on the proliferation rates of MSCs [8, 9].

In this chapter, we describe the protocols for isolating MSCs from skeletal muscle using the enzymatic digestion and mechanical trituration techniques, as well as describing a quick and relatively simple method for determining the specific growth rates of isolated muscle-derived MSCs. The protocols in this chapter have been optimised for isolation of MSCs from human *gluteus medius* muscle of patients with osteoarthritis who were undergoing total hip replacement (age range, 46–93 years). These protocols can also be used for other skeletal muscle sources, pathologies and species. However, the yield of viable cells, subpopulation composition and cell characteristics might vary depending on the source tissue. The enzymatic digestion time and growth medium composition might also have to be modified.

2 Materials

All materials must be autoclaved before use. All reagents must be filter-sterilised, unless otherwise specified. Diligently follow all waste disposal regulations when disposing of biological waste materials. The majority of the reagents used are biologically or chemically hazardous. Material safety and data sheets for all chemicals should be read before use, and the chemicals should be handled appropriately.

2.1 General Equipment

1. Laminar air flow (LAF) cabinet: Used to carry out all of the sterile procedures involving the primary cells. Good laboratory practice recommends the dedication of a single specific LAF cabinet to primary cells only. Simultaneous use of the LAF cabinet for working with other cells types, and in particular immortalised cell lines, is strongly ill-advised.
2. Cell culture incubator with hypoxic conditions: 37 °C; 5% CO_2 and 5% O_2; relative humidity, 85% to 95% [10].
3. Cell culture incubator with normoxic conditions: 37 °C; 5% CO_2; relative humidity, 85% to 95%.

4. Inverted microscope for monitoring cells, culturing, trypsinisation and counting.
5. Benchtop centrifuge suitable for 15-mL and 50-mL conical tubes.
6. Analytical balance (range, 0.01–120 g).
7. Water bath with shaker.
8. Vortex mixer.

2.2 Plastics and Glassware

1. Serological pipettes (5 mL, 10 mL).
2. Micropipettes (10 μL, 200 μL, 1,000 μL) with appropriate tips.
3. Scissors, tweezers.
4. Surgical scalpel.
5. Syringe filters (0.22 μm).
6. Cell strainer (70 μm).
7. T25 flasks (preferably with vented filter caps).
8. Twelve-well and 6-well plates.
9. Haemocytometer and cover slips.
10. Conical tubes (15 mL, 50 mL).
11. Polystyrene bijou containers (7 mL) or equivalent sample containers.
12. Tubes (0.5 mL).

2.3 Cell Isolation and Culture Reagents

1. Phosphate-buffered saline (PBS; 10×): Weigh out 80.0 g NaCl, 2.0 g KCl, 14.4 g Na_2HPO_4 and 2.4 g KH_2PO_4, and dissolve in 1.0 L distilled water. Measure the pH of the solution and adjust it to pH 7.4 using 1.0 M NaOH. Autoclave or filter-sterilise.
2. PBS (1×): In a laminar flow cabinet, dilute 20 mL 10× PBS in 180 mL distilled water. Mix well. Autoclave or filter-sterilise.
3. Growth medium: Low-glucose Dulbecco's modified Eagle's medium (LG-DMEM), with 20% foetal bovine serum, 10% horse serum, 2 mM L-glutamine (100× stock, 20 mM), 2% antibiotic/antimycotic (100× stock, 8.5 g/L sodium chloride, amphotericin B 0.025 g/L, 6.028 g/L penicillin G sodium salt, 10 g/L streptomycin sulphate). To prepare a 50 mL aliquot, add 1 mL 100× antibiotic/antimycotic stock solution, 0.5 mL 200 mM (100×) L-glutamine stock solution, 5 mL horse serum and 10 mL foetal bovine serum in a 50-mL conical tube. Make up to 50 mL with LG-DMEM (*see* **Note 1**).
4. Collagenase D (1%): Weigh out 10 mg collagenase D per tissue sample, and dissolve it in 1.0 mL of prewarmed growth medium. Filter-sterilise.

5. Ethanol for sterilisation (70%).
6. 0.25% trypsin/ethylenediaminetetraacetic acid (EDTA).
7. Trypan blue.

3 Methods

Before starting, assure the sterility of the LAF cabinet by wiping all of its inside surfaces with 70% ethanol (from a spray bottle), place the plastic and glassware needed inside the LAF cabinet, and close the LAF cabinet, and put the UV light on for at least 30 min. All procedures involving sample and cell handling and reagent preparation are performed inside the LAF cabinet, unless otherwise indicated. All items should be sprayed with 70% ethanol when they are placed inside the LAF cabinet. For the protection of both the investigator and the samples, protective gear should be worn at all times, including a laboratory coat, latex gloves, surgical mask and appropriate footwear, such as shoe covers. It is also highly recommended for a small piece of the sample or donor blood to be sent for testing for infectious agents, such as HIV, hepatitis viruses and cytomegalovirus. All precautions necessary to prevent cross-contamination should be taken.

3.1 Cell Isolation

1. Following surgical removal of the muscle biopsy in the operating theatre, store the tissue in cold growth medium (in an ice bath) until MSCs isolation (*see* **Note 2**).
2. The isolation of the MSCs should be performed as soon as possible. If the cells cannot be isolated from the tissue within a few hours after sampling, the sample can be stored at 4 °C, but should not be stored for longer than 24 h.
3. Prewarm the growth medium to 37 °C in a water bath. Transfer the medium to the LAF cabinet, maintaining it as sterile throughout the procedure (i.e. follow standard sterile procedures).
4. *Optional step*: To weigh the muscle tissue, prefill a sterile 7-mL bijou container with 4 mL PBS (1×), place this on an analytical balance, and set the balance 'tare' to zero. In the LAF cabinet, transfer the muscle biopsy to this 7-mL bijou container, and place it on the analytical balance again. Record the weight of the muscle tissue. In our experience, MSCs can be isolated from 100 to 900 mg of muscle tissue.
5. Thoroughly wash the muscle tissue in the bijou container two to three times with PBS (1×), to remove blood cells. After the final wash, the PBS solution containing the muscle should be as clear as shown in Fig. 1a.
6. Add 9 mL growth medium to a sterile 15-mL conical tube.

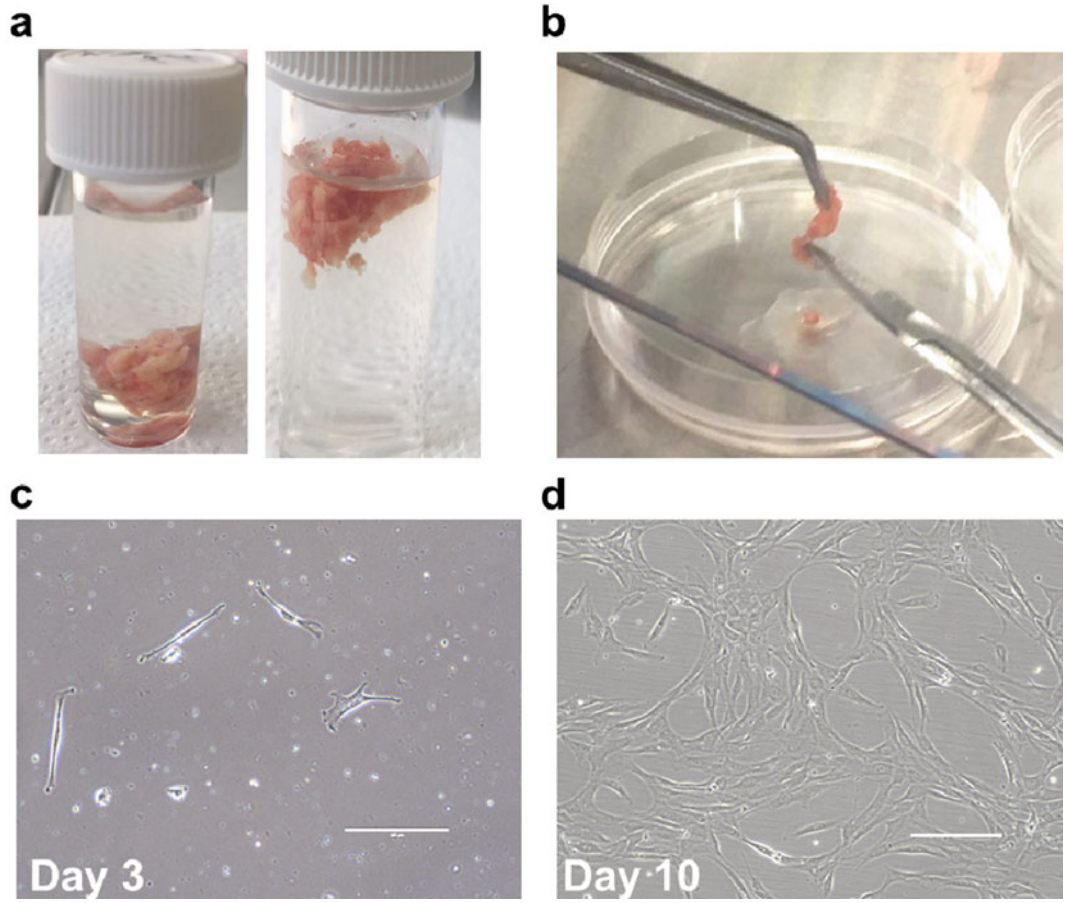

Fig. 1 Isolation of muscle-derived MSCs. (**a**) Two representative muscle samples during isolation of MSCs, after several washes in PBS. (**b**) The size of the muscle fragments suitable for collagenase digestion after cutting the muscle biopsy sample with scissors. (**c**) Plastic-adherent cells with fibroblast-like morphology can be seen as early as day 3. (**d**) After 10 days, cells start to form colonies. Scale bars: 200 μm. PBS, phosphate-buffered saline

7. Transfer the muscle to a petri dish with a small volume of PBS (1×), and remove any visible fat and connective tissue, if present. Cut the muscle into small fragments using scissors, as shown on Fig. 1b (*see* **Note 3**).
8. Using tweezers, transfer the muscle pieces to the 15-mL conical tube from **step 6**.
9. Prepare 1% collagenase D solution (*see* **Note 4**). Add 1 mL 1% collagenase D solution to the conical tube containing the muscle fragments in 9 mL growth media, to obtain a 0.1% collagenase D final concentration. Seal the tube cap with parafilm and vortex briefly.
10. Incubate the tube with the muscle in the collagenase solution for 60 min in a water bath at 37 °C under vigorous shaking.

Alternatively, if the water bath has no shaking option, you can vortex the tube every 15–20 min during this digestion.

11. At the end of the digestion, transfer the tube with the muscle tissue back to the LAF cabinet, and filter the supernatant through a 70-μm strainer placed over a new sterile 50-mL conical tube.
12. Resuspend the remaining muscle fragments in 10 mL fresh growth medium.
13. Vigorously triturate these remaining muscle fragments by passing them repetitively (20 times) through a 10-mL pipette until the tissue bits pass easily through the tip of the pipette. Allow the suspension to settle, and then filter the supernatant through the 70-μm strainer placed over the same 50-mL conical tube as in **step 9**.
14. Repeat the same step once more, which will result in approximately 30 mL of final cell suspension.
15. Spin down the cells in the suspension using low-speed centrifugation, at 300 × *g* for 5 min.
16. Aspirate the supernatant carefully, trying not to disturb the cell pellet. Gently resuspend the cell pellet in 1 mL fresh growth media (gentle tapping and swirling of the tube, you can also use micropipette).
17. Transfer the cell suspension to a sterile T25 culture flask or into several replicates in six-well plates, and culture the cells undisturbed in a cell culture incubator under hypoxic conditions for 3 days.
18. After 3 days, replace half of the medium with fresh medium, and examine the cells under a microscope. Single plastic-adherent cells of heterogeneous morphology can be spotted in the middle of cell debris, as shown on Fig. 1c (*see* **Note 5**).
19. After 10 days in culture, defined colonies can be observed, as shown on Fig. 1d.

3.2 Cell Growth Kinetics

1. When cultured cells reach 70% confluence, remove the container (i.e. flask, plates) from the incubator, and place it in a LAF cabinet.

3.2.1 Preparation of the Cells

2. Remove the growth medium (aspirate), and wash the cells with PBS (1×) (*see* **Note 6**).
3. Add 1 mL trypsin to the T25 flask and tip, and rotate the flask so that the trypsin is evenly distributed over the entire surface of the cell layer. If six-well plates are used, add 200 μL trypsin per well.
4. Incubate the cells in a cell culture incubator with normoxic conditions for 3 min. Check under the microscope whether the

cells have detached from the plastic surface, which can be seen by their rounded morphology (*see* **Note 7**). If they do not appear rounded, leave them in the trypsin for a few minutes longer, in the incubator.

5. When the cells have detached, add 9 mL fresh medium to the T25 flask, and wash the cells several times using the same serological pipette. Transfer all of the contents of the flask to a 15-mL conical tube.
6. Centrifuge the tube with the cell suspension at 300 × *g* for 5 min, to pellet the cells.
7. Carefully remove most of the supernatant, and then add 1 mL fresh medium. Gently resuspend the cell pellet using a pipette.
8. Transfer 100 μL of the cell suspension to a 0.5-mL tube. Add 100 μL trypan blue to this cell suspension, and mix it gently by pipetting it up and down.
9. Use 10 μL of this suspension to count the number of viable cells, as described in the next section.

3.2.2 Cell Counting

1. Clean the haemocytometer with 70% ethanol, and position the cover slip tightly over the two chambers located on the centre of the haemocytometer.
2. Position the haemocytometer on a flat, even surface.
3. Carefully add 10 μL of the trypan blue-stained cell suspension to each chamber of the haemocytometer, and allow the cell suspension to diffuse evenly throughout the chambers.
4. Place the haemocytometer with the cells under a phase contrast microscope, and set to 10× magnification.
5. Haemocytometer consists of a grid of nine main squares (with subdivisions), as shown on Fig. 2a. When counting the cells, count the cells in the four main corner squares (Fig. 2a, 1–4).
6. Find the grid, and focus the microscope so that both the grid and the cells are visible, as shown in Fig. 2b.
7. To standardise the counting, you should always count the cells that might lie on the grid lines on the left and top of a square (Fig. 2b, blue circles), and instead, ignore the cells that might lie on the grid lines on the right and bottom (Fig. 2b, red circles).
8. Following this procedure, count the number of unstained or bright (i.e. viable) cells in the four main corner squares (Fig. 2a, 1–4). Ideally, 100 to 150 cells should be counted to increase the counting accuracy (*see* **Note 8**). You can also decide to count the cells in centre square only (Fig. 2a, 5), if the number

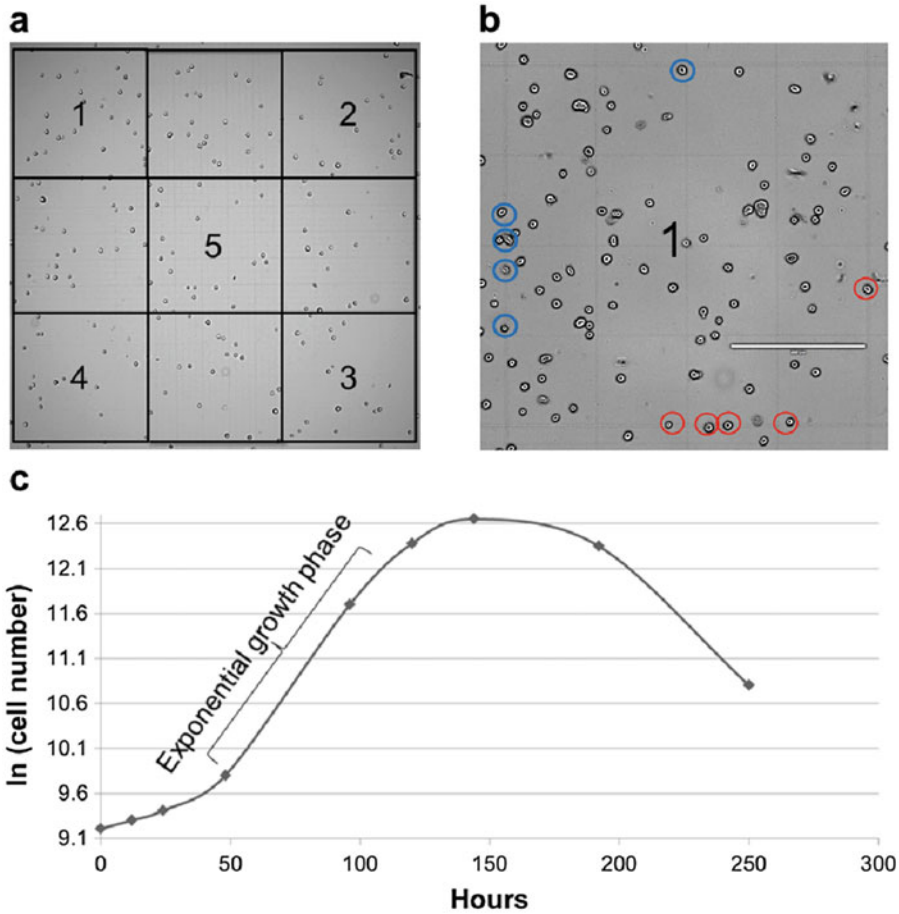

Fig. 2 Cell growth kinetics analysis. (**a**) The grid of the haemocytometer consists of nine main squares (with subdivisions), separated by triple lines. The five main corner squares where the cell counting takes place, depending on the number of the cells, are indicated as 1 to 5. (**b**) Corner square number 1 at higher magnification showing haematocytometer grid. The cells circled in blue should be counted, while the cells circled red should be ignored. Scale bar: 400 μm. (**c**) Cell growth curve, with the exponential phase as indicated

of cell in this area is sufficient. The number of viable cells in 1 mL of the cell suspension can then be calculated using the following equation:

$$\begin{aligned}&\text{Concentration (cells/mL suspension)}\\&\quad = (\text{number of live cells counted in all squares}\\&\qquad \times \text{dilution factor used} \times 10,000)/\\&\qquad (\text{number of squares counted}).\end{aligned}$$

3.2.3 Growth Curves

1. Seed 10,000 viable cells as four replicates (wells) of a 12-well plate, and incubate these in an incubator under normoxic conditions. Change the growth medium every 2 days to 3 days.
2. To create a growth curve, the cells should be counted after 48, 96, 168 and 216 h. At each time point, trypsinise the cells in one replicate, and count them, as described above. Count the cells in each well at least four times (*see* **Note 9**).
3. Express the total number of cells at each time point as the natural logarithm (ln), and plot a graph of ln (cell number) as a function of time, as shown on Fig. 2c.
4. Calculate the specific growth rate from the exponential phase of the cell growth, as shown on Fig. 2c, using the following formula:

$$\mu = (lnN_{t2} - lnN_{t1})/(t_2 - t_1),$$

where μ is the specific growth rate, t is time and $N_{t1/t2}$ are the numbers of cells at times $t1$ and $t2$, respectively.

5. Cell doubling times (DT) can be calculated using the following formula:

$$\mathrm{DT} = \ln 2/\mu.$$

4 Notes

1. Ready-made commercial media are also available for isolation of MSCs from different sources. The advantage of these commercially available media is the consistency of their composition, whereas 'homemade' growth medium compositions can vary when using sera from different batches and manufacturers. The 'homemade' medium compositions can also vary between laboratories and can influence the cell culture composition, in terms of subpopulations of cells. These differences can also influence MSC characteristics, such as growth rate.
2. To standardise the sampling procedure, the tissue samples should always be taken from the same anatomical location. Care should be taken to avoid necrotic or damaged tissue that can occur as a consequence of the surgical procedure, as this can affect the properties of the resident cells.
3. Trituration is a process used to reduce the sizes of the muscle fragments and to mechanically release the cells into the medium. It is therefore important to cut the tissue into fragments, but not to mince it. If the fragments are too small, it makes the trituration step less effective.

4. The collagenase D solution should be prepared fresh immediately before use. For long-term storage of a collagenase D working solution, it is advisable to follow the instructions on the reagent data sheet.
5. The cells isolated using this collagenase digestion method represent a heterogeneous population of different muscle-resident stem cells. For specific subpopulation enrichment, differential plating methods can be used or fluorescence-activated or magnetic sorting methods based on cell-surface antigens.
6. It is important to wash the cells thoroughly with PBS prior to trypsinisation, as the growth medium contains high levels of serum, which contains trypsin inhibitors.
7. Trypsin is a protease that cleaves cell proteins. Prolonged exposure to trypsin can kill cells or damage the cell-surface antigens. This can make surface antigen-based identification of cell populations difficult [11]. It is therefore important to limit the exposure time to trypsin to a minimum. One good rule of thumb is to let the cells obtain a round morphology and wait until about 30% of the cells are detached and floating around in the medium. This usually happens within 1 to 2 min of incubation, but can take longer depending on the cell type and cell source. You can speed up the detachment process by gently taping on the bottom and sides of the culture flask/plate. This will help to detach most of the cells. Cells that are still detaching will detach during the washing process. You can also detach the cells using a cell scraper. Trypsin substitutes that are less harmful to cells are also commercially available.
8. A minimum of 100 cells should be counted to ensure reliable counting. If the number of cells is too low, you can centrifuge the cells again and resuspend them in a smaller volume of medium. Do not forget to take this into account when applying the dilution factor. Conversely if the cell number is so high that you can no longer distinguish between two individual cells, dilute the cell suspension, and again apply the dilution factor when calculating the cell number.
9. When counting cells during specific growth rate analysis, we are interested in the total cell number at a certain time. Trypan blue staining to exclude dead cells is therefore not necessary, unless the cells are to be used for subsequent experiments, where cell viability is an important factor.

Acknowledgements

This work was supported by the Slovenian Research Agency, J3-7245 Research Project and P3-0298 Research Programme and by the ARTE Project EU Interreg Italia Slovenia 2014-2020.

References

1. Horwitz EM, Le BK, Dominici M et al (2005) Clarification of the nomenclature for MSCs: the International Society for Cellular Therapy position statement. Cytotherapy 7:393–395
2. Friedenstein AJ, Gorskaja JF, Kulagina NN (1976) Fibroblast precursors in normal and irradiated mouse hematopoietic organs. Exp Hematol 4:267–274
3. Čamernik K, Barlič A, Drobnič M et al (2018) Mesenchymal stem cells in the musculoskeletal system: from animal models to human tissue regeneration? Stem Cell Rev 14(3):346–369. https://doi.org/10.1007/s12015-018-9800-6
4. Relaix F, Zammit PS (2012) Satellite cells are essential for skeletal muscle regeneration: the cell on the edge returns centre stage. Development 139:2845–2856. https://doi.org/10.1242/dev.069088
5. Hamrick MW, McGee-Lawrence ME, Frechette DM (2016) Fatty infiltration of skeletal muscle: mechanisms and comparisons with bone marrow adiposity. Front Endocrinol (Lausanne) 7:1–7. https://doi.org/10.3389/fendo.2016.00069
6. Cottle BJ, Lewis FC, Shone V et al (2017) Skeletal muscle-derived interstitial progenitor cells (PICs) display stem cell properties, being clonogenic, self-renewing, and multi-potent *in vitro* and *in vivo*. Stem Cell Res Ther 8 (1):158. https://doi.org/10.1186/s13287-017-0612-4
7. Mizukami A, Swiech K (2018) Mesenchymal stromal cells: from discovery to manufacturing and commercialization. Stem Cells Int 2018:4083921. https://doi.org/10.1155/2018/4083921
8. Heathman TRJ, Rafiq QA, Chan AKC et al (2016) Characterization of human mesenchymal stem cells from multiple donors and the implications for large-scale bioprocess development. Biochem Eng J 108:14–23. https://doi.org/10.1016/j.bej.2015.06.018
9. Qi W, Yuan W, Yan J et al (2014) Growth and accelerated differentiation of mesenchymal stem cells on graphene oxide/poly-l-lysine composite films. J Mater Chem B 2:5461–5467. https://doi.org/10.1039/C4TB00856A
10. Tsai C-C, Yew T-L, Yang D-C et al (2012) Benefits of hypoxic culture on bone marrow multipotent stromal cells. Am J Blood Res 2:148–159
11. Autengruber A, Gereke M, Hansen G et al (2012) Impact of enzymatic tissue disintegration on the level of surface molecule expression and immune cell function. Eur J Microbiol Immunol 2:112–120. https://doi.org/10.1556/EuJMI.2.2012.2.3

Methods in Molecular Biology (2019) 2045: 131–144
DOI 10.1007/7651_2018_200

Published online: 30 November 2018

Complete Assessment of Multilineage Differentiation Potential of Human Skeletal Muscle-Derived Mesenchymal Stem/Stromal Cells

Klemen Čamernik and Janja Zupan

Abstract

The minimal criteria for mesenchymal stem/stromal cell (MSC) identification set by the International Society for Cellular Therapy include plastic adherence, presence and absence of a set of surface antigens and in vitro multilineage differentiation. This differentiation is assessed through stimulation of MSCs with defined combination and concentration of growth factors towards specific lineages and histological confirmation of the presence of differentiated cells. Here we provide protocols for multilineage differentiation, namely, osteogenesis, adipogenesis, chondrogenesis and myogenesis. We also provide their respective histological analyses.

Keywords Differentiation, Histology, Mesenchymal stem/stromal cells (MSCs), Myogenesis, Skeletal muscle

1 Introduction

The human body has a remarkable ability to regenerate and heal damaged tissues. This ability is attributed to a special population of multipotent progenitor cells, known as mesenchymal stem/stromal cells (MSCs) [1, 2]. MSCs were originally described for the bone marrow [3], since then progenitor cells with similar characteristics have been discovered in most connective tissues of the body [4, 5]. Although MSCs have been under investigations for decades, their identification is still difficult, and their roles are still not clear, especially in aging and chronic diseases.

In 2006, the International Society for Cellular Therapy published a set of guidelines for the identification of MSCs [6]. These minimal criteria include plastic adherence, presence and absence of a set of surface antigens and in vitro differentiation into osteoblasts, chondrocytes and adipocytes [6]. This ability of MSCs to differentiate is not only of interest for their identification but also has great value in tissue engineering and regenerative medicine. In recent years, it has been discovered that there are many subpopulations of MSCs in the adult organism, each of which has different

multilineage differentiation abilities [7]. If the multilineage potential of these cells can be defined, we can then find the most appropriate MSC population to be used in specific cell therapies or tissue engineering.

Here, we describe protocols for the complete assessment of multilineage differentiation of MSCs, namely, osteogenesis, chondrogenesis, adipogenesis and myogenesis. The protocols presented here are optimised for use on skeletal muscle-derived MSCs. Despite this, and excluding myogenic differentiation, all of the protocols defined here can be used for MSCs isolated from any tissue. However, the numbers of cells seeded, growth medium composition and concentrations of growth factors will need to be adjusted for specific tissue sources. In particular, the myogenic differentiation medium might require addition of other factors, such as 5-azacytidine [8, 9].

2 Materials

All of the reagents must be filter-sterilised unless otherwise specified. All waste disposal regulations should be diligently followed when disposing of biological waste materials. The majority of the reagents used are hazardous. The material safety and data sheets for all of the chemicals should be consulted before their use, and the chemicals should be handled appropriately.

2.1 General Equipment for Cells and Histological Assessment

1. Laminar air flow (LAF) cabinet to carry out all of the sterile procedures involving primary cells. Good laboratory practice indicates that a single LAF cabinet should be dedicated to primary cells only. Simultaneous use of the laminar flow cabinet for working with other cell types is strongly ill-advised and in particular with immortalised cell lines.
2. Cell culture incubator with normoxic conditions: 37 °C; 5% CO_2; relative humidity, 85 to 95%.
3. Inverted phase contrast or bright-field microscope for monitoring cell cultures, trypsinisation and counting, and for evaluation of the results of differentiation.
4. Inverted fluorescent microscope for evaluation of the results of myogenesis.
5. Benchtop swing-out bucket centrifuge for 15-mL conical tubes.
6. Benchtop centrifuge for 1.5-mL tubes.
7. Analytical balance for weighing powdered reagents.
8. Water bath.
9. Serological glass pipettes (5 mL, 10 mL).

10. Micropipettes (10 μL, 200 μL, 1,000 μL) and pasteur pipettes (5 mL).
11. Filter paper.
12. Syringe filters (0.2 μm) and syringes (10 mL).
13. Twenty-four-well plates, 25 cm^2 (T25) or 75 cm^2 (T75) flasks suitable for tissue culture.
14. Conical tubes (15 mL, 50 mL).
15. Haemocytometer with cover slips.
16. pH meter.
17. 0.25% trypsin/ethylenediaminetetraacetic acid (EDTA).
18. Phosphate-buffered saline (PBS; 10×): Weigh out 80.0 g NaCl, 2.0 g KCl, 14.4 g Na_2HPO_4 and 2.4 g KH_2PO_4, and dissolve them together in 1.0 L distilled water. Measure the pH of the solution, and adjust to pH 7.4 using 1.0 M NaOH. Autoclave or filter-sterilise.
19. PBS (1×): In a laminar flow cabinet, dilute 20 mL PBS (10×) with 180 mL distilled water. Mix well. Autoclave or filter-sterilise.
20. Growth medium: Low-glucose Dulbecco's modified Eagle's medium (LG-DMEM), 20% foetal bovine serum, 10% horse serum, 2 mM L-glutamine, 2% antibiotic/antimycotic (100× stock; 8.5 g/L sodium chloride, amphotericin B 0.025 g/L, 6.028 g/L penicillin G sodium salt, 10 g/L streptomycin sulphate). Add 1 mL 100× antibiotic/antimycotic stock solution, 0.5 mL 200 mM (100×) L-glutamine stock solution, 5 mL horse serum and 10 mL foetal bovine serum to a 50 mL conical tube. Make up to 50 mL with LG-DMEM (*see* **Note 1**).
21. Neutral buffered formalin (NBF; 10%).
22. Distilled water.
23. Spectrophotometer plate reader.
24. Cryostat.
25. Peel away cryo-embedding moulds, microscope slides for cryo-sections and coverslips.
26. Fume hood and laboratory oven.
27. Vortex mixer.

2.2 Osteogenic Differentiation

Osteogenic differentiation medium: Growth medium, 5 mM ß-glycerophosphate (*see* **Note 2**), 50 μg/mL ascorbic acid-2-phosphate, 100 nM dexamethasone. To prepare 5 mL osteogenic medium, add 250 μL 100 mM ß-glycerophosphate, 50 μL 5 mg/mL ascorbic acid-2-phosphate and 50 μL 10 μM dexamethasone. Make up to 5 mL with complete growth medium. All of the stock

solutions should be prepared as several replicates and kept frozen for single use only, to avoid freeze-thaw cycles.

2.3 Adipogenic Differentiation

Adipogenic differentiation medium: Growth medium, 0.5 μM dexamethasone, 50 μM isobutylmethylxanthine, 10 μM indomethacin, 10 μg/mL human recombinant insulin. To prepare 5 mL adipogenic medium, add 250 μL 10 μM dexamethasone, 5 μL 50 mM isobutylmethylxanthine, 5 μL 10 mg/mL insulin and 5 μL 10 mM indomethacin. Make up to 5 mL with complete growth medium. All of the stock solutions should be prepared as several replicates and kept frozen for single use only, to avoid freeze-thaw cycles.

2.4 Chondrogenic Differentiation

Chondrogenic differentiation medium: serum-free high-glucose DMEM (HG-DMEM) supplemented with 1% antibiotic/antimycotic (100× stock; 8.5 g/L sodium chloride, amphotericin B 0.025 g/L, 6.028 g/L penicillin G sodium salt, 10 g/L streptomycin sulphate) and 2 mM L-glutamine, 0.1 μM dexamethasone, 50 μg/mL ascorbic acid-2-phosphate, 1% insulin-transferrin-selenium (ITS+; 1.0 mg/mL bovine insulin, 0.55 mg/mL human transferrin, 0.5 μg/mL sodium selenite, 50 mg/mL bovine serum albumin, 470 μg/mL linoleic acid), 10 ng/mL transforming growth factor ß1 (TGFβ1). To prepare 5 mL chondrogenic medium, add 50 μL 10 μM dexamethasone, 50 μL 5 mg/mL ascorbic acid-2-phosphate, 50 μL ITS+ (100×), 5 μL 10 ng/μL TGFβ1 and 50 μL antibiotic/antimycotic stock solution (100×) and 50 μL 200 mM (100×) L-glutamine stock solution. Make up to 5 mL with HG-DMEM. All of the stock solutions should be prepared as several replicates for single use only, to avoid freeze-thaw cycles.

2.5 Myogenic Differentiation

1. Myogenic differentiation medium: HG-DMEM supplemented with 1% antibiotic/antimycotic and 2 mM L-glutamine, 2% horse serum, 100 nM hydrocortisone, 1% ITS+. To prepare 5 mL of myogenic medium, add 100 μL horse serum, 50 μL 10 mM hydrocortisone stock solution, 50 μL ITS+ (100×) and 50 μL antibiotic/antimycotic stock solution (100×) and 50 μL 200 mM (100×) L-glutamine stock solution. Make up to 5 mL with HG-DMEM.
2. Gelatine (0.1%): Weigh 100 mg of gelatine powder and dissolve it in 100 mL of distilled water. Sterilise by autoclaving and store at 4 °C.

2.6 Alizarin Red S Staining for Osteogenesis

1. Alizarin Red S (2%): Weigh out 2.0 g Alizarin Red S powder, and add 100 mL distilled water (*see* **Note 3**). Filter the solution through plain laboratory filter paper. Adjust the pH to 4.1 to 4.3 using 1.0 M NaOH.

2. Acetic acid (10%): Add 5 mL glacial acetic acid (i.e. undiluted) to a 50-mL conical tube, and make this up to 50 mL with distilled water.

2.7 Oil Red O Staining for Adipogenesis

1. Oil Red O stock solution: Weigh out 0.5 g Oil Red O powder, and dissolve it in 100 mL 100% isopropanol. The working solution is prepared by mixing the Oil Red O stock solution with distilled water at a ratio of 3:2. To prepare 5 mL of working solution, add 3 mL Oil Red O stock solution to 2 mL distilled water. Allow this to stand for 10 min. Filter the solution through a syringe filter (*see* **Note 4**).
2. Isopropanol (60%, 100%).
3. Crystal violet (1%): Weigh out 0.1 g crystal violet, and dissolve it in 10 mL distilled water.

2.8 Toluidine Blue Staining for Chondrogenesis

Toluidine blue: Weigh out 0.1 g toluidine blue powder, and dissolve it in 20 mL distilled water. Adjust pH to 1.0 to 1.5 using 0.5% HCl (prepare by adding 68 μL concentrated [37%] HCl to 5 mL distilled water).

2.9 Desmin Immunofluorescence Staining for Myogenesis

1. Blocking buffer/antibody dilution buffer: Weigh out 0.5 g bovine serum albumin, and dissolve it in 50 mL PBS (1×). Add 150 μL 0.3% Triton X-100.
2. Primary antihuman desmin antibody.
3. Secondary fluorochrome-conjugated antibody.
4. Mounting reagent with 4′,6-diamidino-2-phenylindole (DAPI).

3 Methods

Both fresh and cryopreserved cells can be used. It is best to use cells of lower passage number (p1–p5), as there is evidence that differentiation abilities change with in vitro aging [10]. All procedures carried out with cell cultures are performed in a LAF cabinet, up to the point of fixing the cell cultures, which is done in a fume hood. All of the subsequent histological analyses can be done at the laboratory bench at room temperature, unless otherwise specified.

3.1 Preparation of the Cells

1. To ensure adequate numbers of cells for the differentiation experiments, grow the cells in T25 or T75 flasks in a cell incubator under normoxic conditions (*see* **Note 5**).
2. Allow the cell culture to grow to 70% confluence.
3. Remove the growth medium from the T25 flask, and wash the cells with PBS (1×) (*see* **Note 6**).

4. Add 1 mL trypsin and tip, and rotate the flask so that the trypsin is evenly distributed over the entire surface of the cell monolayer.
5. Incubate the cells until all of them show a rounded morphology and the majority of them are detached and floating in the medium (*see* **Note 7**).
6. Add 9 mL fresh medium to the flask, and wash the cells by pipetting the medium up and down three or four times. Then transfer all of the contents of the flask to a 15-mL tube.
7. Centrifuge the cells at 300 × *g* for 5 min (to pellet them).
8. Carefully remove all of the supernatant (aspirate), and add 1 mL fresh medium. Gently resuspend the cell pellet (gentle tapping and swirling, you can also use micropipette).
9. Take 10 μL of the cell suspension, and mix it with the same volume of trypan blue.
10. Using the trypan blue-stained suspension, count the number of viable cells under an inverted phase contrast or bright-field microscope.

3.2 Osteogenesis and Alizarin Red S Staining

1. Seed the cells at a density of 10,000 to 20,000 cells/cm^2 in 24-well plates as at least two replicates (*see* **Note 8**). Grow the cells until they reach 80% to 90% confluence, which will usually take 1 to 3 days.
2. When the cells are at 80% to 90% confluent, add the osteogenic medium. The cells in the control wells should receive growth medium without osteogenic supplements.
3. Change the osteogenic medium every 2 to 3 days, for 21 days (*see* **Note 9**).
4. After 21 days, stain the cells with Alizarin Red S, to assess the degree of mineralisation (*see* **Note 10**).
5. Transfer the 24-well plate to a laminar flow cabinet, and remove the cell medium from all of the wells.
6. Wash the wells with PBS (1×), three times.
7. Add 300 μL 10% NBF to each well, and incubate the plate for 20 min.
8. Remove the 10% NBF and wash the cells three times with distilled water.
9. Add 200 μL 2% Alizarin Red S solution to each well, and incubate for 30 min.
10. Remove the Alizarin Red S from the wells, and wash each well three times with distilled water (*see* **Note 11**).

11. Dry the wells by tilting the 24-well plate at an angled while removing the remaining solution at the edges with a pipette. Be careful not to disturb the cell layer.
12. Image the wells under the microscope. Areas where mineralisation has taken place are stained red, as shown on Fig. 1a. Untreated control wells should remain unstained, as shown on Fig. 1b.
13. Add 200 μL 10% acetic acid to each well, and incubate for 30 min.
14. Scrape the detached monolayer, and transfer the contents of each well together with the cells into a separate 1.5-mL tube.
15. Briefly vortex these tubes and incubate for 10 min at 85 °C. To prevent evaporation, the tubes can be sealed with parafilm, or 200 μL mineral oil can be added on top of the liquid in each tube.

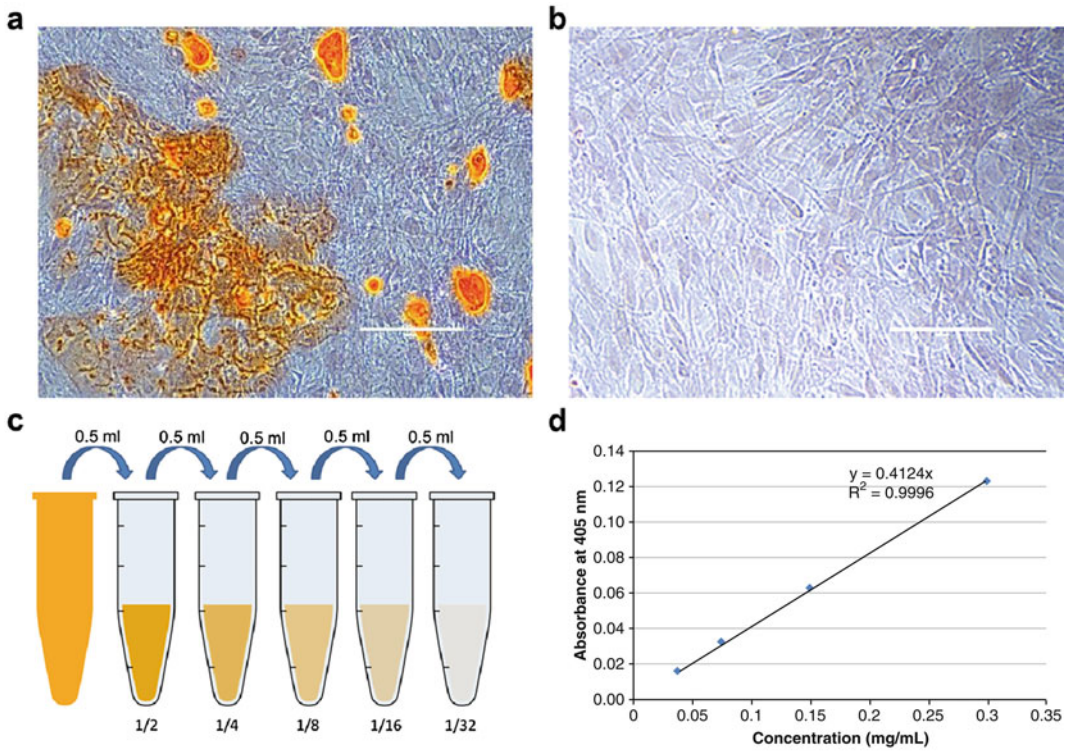

Fig. 1 Osteogenesis and Alizarin Red S staining. (**a**, **b**) Alizarin Red staining to evaluate osteogenic differentiation. Areas of mineralisation are stained red (**a**). An untreated sample that received growth medium without osteogenic supplements shows no visible mineralisation (**b**). Scale bars: 200 μm. (**c**) Preparation of serial dilutions of Alizarin Red S for the standard curve. (**d**) Standard curve for absorbance at 405 nm versus concentrations of serial dilutions, to perform linear regression and calculate the concentrations in the unknown samples

16. Transfer the tubes immediately to an ice bath, and incubate for 5 min.
17. Transfer 50 μL of the solution to a 96-well plate.
18. To create an Alizarin Red S standard curve, prepare six 1.5-mL tubes. Add 990 μL 10% acetic acid to the first tube and 500 μL to all of the other tubes.
19. Add 10 μL Alizarin Red S to the first tube, and vortex thoroughly.
20. Create serial dilutions by taking 500 μL from the first tube and adding it to the next tube, and vortex thoroughly. Repeat for all of the tubes along the series, as shown on Fig. 1c.
21. Transfer 50 μL of the solution from each tube to a 96-well plate (with the samples from **step 17**) in duplicates, and measure the absorbance at 405 nm using spectrophotometer plate reader.
22. Absorbance versus Alizarin Red S concentrations can be plotted as shown on Fig. 1d. Using linear regression analysis, the concentration of Alizarin Red S can be calculated from the absorbance of each sample.

3.3 Adipogenesis and Oil Red O Staining

1. Seed cells at a density of 10,000 to 20,000 cells/cm^2 in a 24-well plate, in at least two replicates, and let the cells reach 70% confluence.
2. Upon reaching confluence, wait for 3 to 5 more days, and then add the adipogenic medium to the treated wells. The control wells should receive growth media without adipogenic supplements.
3. Change the adipogenic medium every 2 to 3 days, for 21 days.
4. You should be able to identify adipocytes under the microscope as soon as day 7.
5. After 21 days, remove the medium from both the control and treated wells, and wash the wells three times with PBS (1×).
6. Add 300 μL 10% NBF to each well, and incubate for 20 min.
7. Remove the 10% NBF, and wash the wells with 60% isopropanol for 1 min.
8. Remove the isopropanol, and add 200 μL Oil Red O working solution. Incubate the 24-well plate for 30 min, protected from light.
9. Remove the Oil Red O from all of the wells, and wash the wells with 60% isopropanol for 1 min.
10. Wash the cells three times with distilled water.
11. *Optional step:* Prepare 1% crystal violet stock solution by dissolving 0.1 g crystal violet powder in 10 mL distilled water. Prepare 0.2% crystal violet solution by adding 2 mL 1% crystal

violet solution to 8 mL distilled water. Add 200 μL 0.2% crystal violet to the control and treated wells, and incubate for 1–2 min. Remove the crystal violet solution, and wash the wells three times with distilled water.

12. Let the plates dry and examine the cells under the microscope. The lipid droplets in the adipocytes should be stained bright red, as shown on Fig. 2a, b, and if the crystal violet staining is included as well, the cells should be violet, as shown in Fig. 2b.

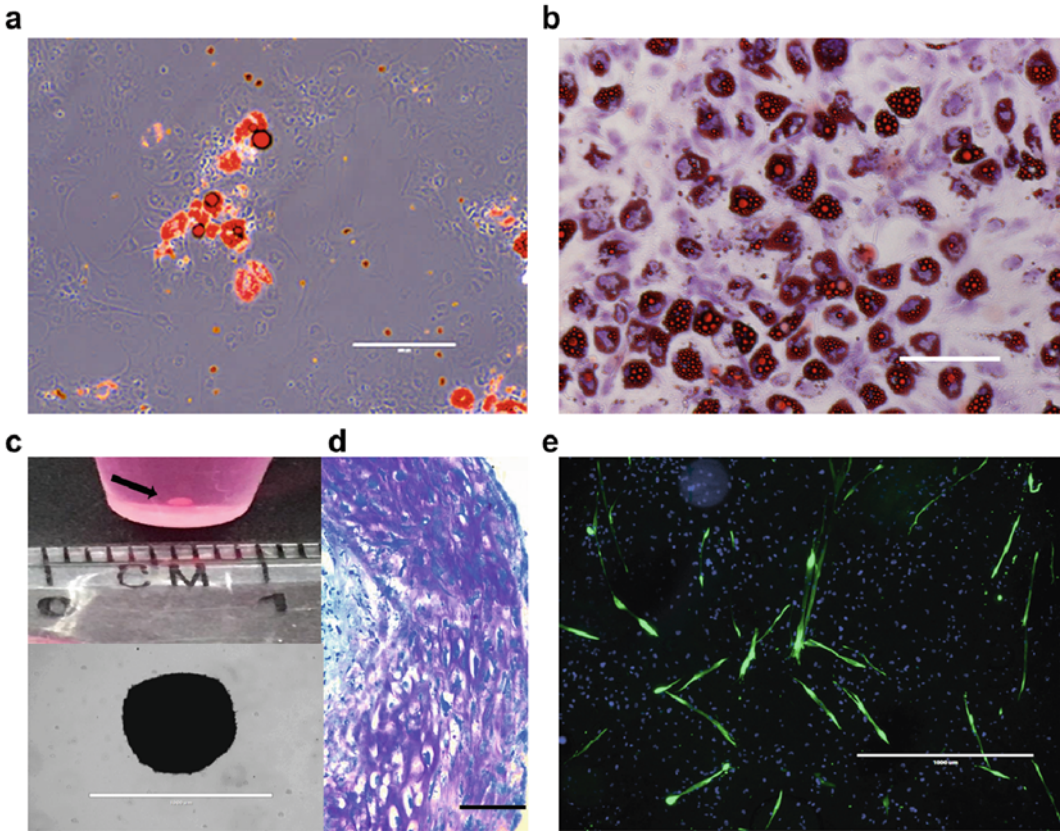

Fig. 2 Assessment of adipogenic, chondrogenic and myogenic differentiation. (**a**, **b**) Oil Red O staining of adipogenic differentiation under phase contrast microscopy, where lipid droplets formed by the adipocytes are stained red (**a**), and bright-field microscopy where the cells are stained violet following optional staining with crystal violet (**b**). (**c**) Chondrogenic pellets formed at the bottom of the conical tubes following the chondrogenic treatment (*top*). Chondrogenic pellet under a bright-field microscope at 4× magnification (*bottom*). (**d**) Toluidine blue staining of cryosections of a chondrogenic pellet. Purple metacromasia is clearly visible, which indicates the cartilage proteoglycan. (**e**) Immunofluorescent assessment of myogenic differentiation. Green, fluorescently labelled desmin-positive multinucleated cells; blue, DAPI-stained nuclei of the cells. Scale bars: 1 cm (**c** *top*), 200 μm (**a, b, d**), 1,000 μm (**c** *bottom*, **e**). DAPI, 4′,6-diamidino-2-phenylindole

3.4 Chondrogenesis and Toluidine Blue Staining of the Pellet Cryosections

1. Add a suspension of 150,000 cells into 1 mL chondrogenic medium without TGF-ß1 in two 15-mL conical tubes (one as control, one as treated).
2. Centrifuge both tubes at 380 × *g* for 10 min in a swinging bucket centrifuge (*see* **Note 12**).
3. Carefully transfer the tubes from the centrifuge to the incubator without disturbing the cell pellet.
4. Unscrew the caps of the tubes slightly, and incubate the cells under normoxic conditions for 24 h.
5. After 24 h, add TGF-ß1 to the treated wells to a final concentration of 10 ng/μL.
6. Change the medium every 2 to 3 days, for 21 days. Be careful not to aspirate the pellet that is formed (Fig. 2c).
7. Remove the medium from the tubes being careful not to aspirate the pellet. Wash the pellet three times with PBS (1×).
8. Add 300 μL 10% NBF to each tube, and incubate for 20 min.
9. Remove the 10% NBF, and wash the cells three times with PBS (1×).
10. Add 1 mL 15% sucrose to each tube and incubate for 1 h.
11. Replace the 15% sucrose with 30% sucrose solution, and incubate overnight at 4 °C.
12. Carefully take the cell pellet from the sucrose solution, and place it into cryo moulds prefilled with tissue freezing medium.
13. Snap freeze the cell pellet in liquid nitrogen. Frozen samples can be stored at −80 °C until cryosectioning.
14. Cut 8-μm-thick cryosections, and place them on the microscopic slides suitable for cryosections (*see* **Note 13**).
15. Fix the slides with cryosections for 10 min in 10% NBF.
16. Wash the slides with distilled water for 10 min.
17. Using a pasteur pipette, cover the sections with toluidine blue solution for 30 s.
18. Wash the slides in distilled water.
19. Dry the slides at 50 °C for at least 15 min.
20. Wash the slides twice in xylene.
21. Mount the stained sections with mounting medium and coverslip, and examine the cells under a bright-field microscope. If the chondrogenic differentiation is successful, purple metachromasia will be observed, as shown in Fig. 2d.

3.5 Myogenic Differentiation and Desmin Immunofluorescence Staining

1. In the LAF cabinet, add 200 μL sterile 0.1% gelatine solution to each well of the required 24-well plates. Distribute the solution evenly over the bottom of the wells, and leave at room temperature for 2 to 3 h.
2. Remove the remaining gelatine solution using a pipette.
3. Seed 20,000 cells per well in the gelatine pre-coated 24-well plates in at least two replicates.
4. After 24 h, replace the growth medium with myogenic differentiation medium for the treated wells. The control wells should receive growth media without the myogenic supplements.
5. Replace the medium every day for the first 3 days and then every 2 to 3 days until day 21.
6. Multinucleated cells should be visible as soon as day 7 following the induction of myogenic differentiation.
7. After 21 days, stain the cells using an anti-desmin antibody, to reveal the desmin-positive cells.
8. Remove the medium, and wash the cells three times with PBS (1×).
9. Add 300 μL 10% NBF to each well, and incubate for 20 min.
10. Remove the 10% NBF, and wash the wells three times with PBS (1×) for 5 min each.
11. Add 300 μL blocking buffer to each well for 60 min.
12. While blocking, prepare the primary antibody by diluting it as suggested by the manufacturer, in antibody dilution buffer. The optimal concentration of the primary antibody should be determined in advance.
13. Remove the blocking solution, and apply 100 μL of the diluted primary antibody to each well. Cover the wells with parafilm to prevent evaporation.
14. Incubate overnight at 4 °C.
15. The next day, rinse the wells three times in PBS (1×) for 5 min each.
16. Add 100 μL fluorochrome-conjugated secondary antibody diluted in antibody dilution buffer, and leave for 3 h at room temperature, protected from light.
17. Rinse the wells three times with PBS (1×) for 5 min each.
18. Add one drop of mounting reagent with DAPI to each well, and place a circular cover slip over the cells (*see* **Note 14**).
19. Examine the cells under a fluorescence microscope using an appropriate filter and channel for the fluorochrome-conjugated to the secondary antibody. Desmin-positive multinucleated cells of up to 1 mm long will be visible, as shown in Fig. 2e.

4 Notes

1. Ready-made commercial media are also available for cell growth, as well as for differentiation of MSCs from different sources. The advantage of commercially available media is consistency in their composition, whereas 'homemade' growth medium composition can vary, in particular when using sera from different batches and manufacturers.
2. ß-Glycerophosphate >5 mM can be toxic to cells; moreover, it can cause non-osteogenic dystrophic mineralisation and hence false-positive results [11].
3. Use distilled water when working with Alizarin Red S. Tap water contains calcium, which binds to Alizarin Red S and can cause its precipitation.
4. If Oil Red O does not dissolve, you can place the solution in a 37 °C water bath for 15 to 20 min and mix frequently. When filtering the stock solution through a syringe filter, small undissolved particles can sometimes block the filter. Do not use force to push the liquid through the filter, as the pressure might cause the filter to rupture. The stock solution is stable for 1 month; however, the working solution is only stable for 1 h, and so it must be prepared fresh every time. Keep both the stock and working solution protected from light.
5. Some laboratories use hypoxic conditions to expand the cells, i.e. 5% O_2 and 5% CO_2. This is not recommended if subsequent differentiation experiments are to be performed, as hypoxia has been shown to influence the ability of MSCs to undergo differentiation. Hypoxia preconditioned cells should be kept in normoxic conditions until confluence [12].
6. The cells must be thoroughly washed, as the growth medium contains high levels of serum, which is a trypsin inhibitor.
7. Prolonged exposure to trypsin can kill cells or damage cell surface antigens [13]. It is therefore important to limit the exposure time of trypsin to a minimum. Normally, about 30% of the cells will detach within 1 to 2 min of incubation with trypsin. Gentle taping on the bottom and sides of the culture flask will help to detach most of the cells.
8. Seeded cells need to be evenly distributed throughout the well. This can be achieved by moving the plate up and down and left and right and 'drawing' an infinity symbol on the work surface. If the cells are unevenly distributed, they can form clumps. During osteogenesis these structures easily detach and can pull away the entire monolayer.
9. Be gentle when changing the medium. In the final days of osteogenesis (after about day 15), the cells can start to detach.

This can be exacerbated by medium changes. To minimise monolayer detachment, only half of the osteogenic medium in a well can be changed each time. One option is also to add double the amount of osteogenic medium when cell detachment is observed and leave the cells undisturbed until day 21.

10. During osteogenic differentiation, mineralisation occurs. Alizarin Red S is an anionic dye that binds to calcium released during mineralisation, and it will stain areas of mineralisation red.
11. For Alizarin Red S extraction and quantification, it is very important for the dye to be completely removed from the walls of the wells, as it can have a large effect on the absorbance readings.
12. A swinging bucket centrifuge must be used for this method for the cells to settle evenly at the bottom of the tube. Alternatively, if such a centrifuge is not available, the micromass method or hanging drop method can be used for chondrogenic differentiation [14, 15].
13. Microscope slides suitable cryosections have a permanent positive charge that enables the cryosections to adhere better to slides; hence tissue loss during consecutive staining is reduced.
14. For the best results, incubate the wells overnight at room temperature and protected from light. For long-term storage, store the plates at 4 °C, protected from light.

Acknowledgements

This work was supported by the Slovenian Research Agency, J3-7245 Research Project and P3-0298 Research Programme.

References

1. Kalinina NI, Sysoeva VY, Rubina KA et al (2011) Mesenchymal stem cells in tissue growth and repair. Acta Nat 3:30–37
2. Qi K, Li N, Zhang Z et al (2018) Tissue regeneration: the crosstalk between mesenchymal stem cells and immune response. Cell Immunol 326:86–93. https://doi.org/10.1016/j.cellimm.2017.11.010
3. Friedenstein AJ, Gorskaja JF, Kulagina NN (1976) Fibroblast precursors in normal and irradiated mouse hematopoietic organs. Exp Hematol 4:267–274
4. Beane OS, Fonseca VC, Cooper LL et al (2014) Impact of aging on the regenerative properties of bone-marrow-, muscle-, and adipose-derived mesenchymal stem/ stromal cells. PLoS One 9:1–22. https://doi.org/10.1371/journal.pone.0115963
5. Wagner W, Wein F, Seckinger A et al (2005) Comparative characteristics of mesenchymal stem cells from human bone marrow, adipose tissue, and umbilical cord blood. Exp Hematol 33:1402–1416
6. Dominici M, Le BK, Mueller I et al (2006) Minimal criteria for defining multipotent mesenchymal stromal cells. The International Society for Cellular Therapy position statement. Cytotherapy 8:315–317
7. Čamernik K, Barlič A, Drobnič M et al (2018) Mesenchymal stem cells in the musculoskeletal

system: from animal models to human tissue regeneration. Stem Cell Rev 14(3):346–369. https://doi.org/10.1007/s12015-018-9800-6

8. Burlacu A, Rosca AM, Maniu H et al (2008) Promoting effect of 5-azacytidine on the myogenic differentiation of bone marrow stromal cells. Eur J Cell Biol 87:173–184. https://doi.org/10.1016/j.ejcb.2007.09.003
9. Wakitani S, Saito T, Caplan A (1995) Myogenic cells derived from rat bone marrow mesenchymal stem cells exposed to 5-azacytidine. Muscle Nerve 18:1417–1426
10. Yang Y-HK, Ogando CR, Wang See C et al (2018) Changes in phenotype and differentiation potential of human mesenchymal stem cells aging *in vitro*. Stem Cell Res Ther 9:131. https://doi.org/10.1186/s13287-018-0876-3
11. Langenbach F, Handschel JR (2013) Effects of dexamethasone, ascorbic acid and ß-glycerophosphate on the osteogenic differentiation of stem cells *in vitro*. Stem Cell Res Ther 4:117. https://doi.org/10.1186/scrt328
12. Xu N, Liu H, Qu F et al (2013) Hypoxia inhibits the differentiation of mesenchymal stem cells into osteoblasts by activation of Notch signaling. Exp Mol Pathol 94:33–39. https://doi.org/10.1016/j.yexmp.2012.08.003
13. Autengruber A, Gereke M, Hansen G et al (2012) Impact of enzymatic tissue disintegration on the level of surface molecule expression and immune cell function. Eur J Microbiol Immunol 2:112–120. https://doi.org/10.1556/EuJMI.2.2012.2.3
14. Zuliani CC, Bombini MF, de AKC et al (2018) Micromass cultures are effective for differentiation of human amniotic fluid stem cells into chondrocytes. Clinics (Sao Paulo) 73:e268. https://doi.org/10.6061/clinics/2018/e268
15. Ruedel A, Hofmeister S, Bosserhoff A-K (2013) Development of a model system to analyze chondrogenic differentiation of mesenchymal stem cells. Int J Clin Exp Pathol 6:3042–3048

Methods in Molecular Biology (2019) 2045: 145–154
DOI 10.1007/7651_2018_199

Published online: 30 November 2018

Human Synovium-Derived Mesenchymal Stem Cells: Ex Vivo Analysis

Janja Zupan

Abstract

Synovium-derived mesenchymal stem/stromal cells (MSCs) have been shown to have superior features in comparison with MSCs from other tissue sources. As they are far less recognised compared to bone marrow- or adipose tissue-derived MSCs, I provide here a detailed procedure on how to isolate MSCs from human synovium. This includes determination of the proportions of viable cells in ex vivo isolated fractions before the seeding of the cells and a description of how to carry out colony-forming fibroblast assays to quantify the clonogenicity of these cells.

Keywords Colony-forming unit fibroblast assay, Human, Isolation, Mesenchymal stem/stromal cells, Synovium

1 Introduction

The synovium is a small membrane that wraps around our synovial joints, and it has been identified as a source of mesenchymal stem/stromal cells (MSCs) with promising features for joint regeneration [1–3]. Following joint injury, synovial hyperplasia occurs as a result of the activation of MSCs that can repair cartilage and even form rudimentary joint-like structures de novo [4]. In comparison with more well-recognised sources of MSCs, such as bone marrow and adipose tissue, those from the synovium have been attributed with superior features, including in particular chondrogenesis and cartilage repair [3]. As the most common joint disorder, osteoarthritis, is poorly treated non-surgically, cell therapies that include synovial MSCs might represent an alternative to joint replacement surgery [5, 6].

MSCs are plastic adherent and clonogenic, so they can attach to plastic surfaces and form colonies, while haematopoietic and other more short-lived cells can be removed from cultures during medium changes. The required minimal criteria for MSCs set by the International Society for Cell Therapy is an immunophenotype defined as >95% of all of the culture-expanded cells positive for CD73, CD90, and CD105; <2% of all of the cells negative for

CD45, CD14, CD19, CD34, and HLA-DR surface molecules; and trilineage differentiation (in vitro ability to undergo adipogenesis, osteogenesis, and chondrogenesis) [7]. Recently, these cells have been recognised as far more heterogeneous and complex, which suggests that no ubiquitous population of 'MSCs' with identical differentiation capacities exists [8].

The synovium consists of two layers: the intima inner layer, which is composed of one or two sheets of macrophages or fibroblast-like synoviocytes, and the subintima outer layer, which is composed of two to three layers of synoviocytes lying over loose connective tissue that is rich in fibroblasts, which secrete collagen and other extracellular matrix proteins [9]. Due to the complexity of this tissue, other cells are isolated that either do not attach to plastic or have a limited life span and do not fulfil the minimal criteria for MSCs. Most conveniently, human synovium can be harvested as waste material during joint arthroplasty [10]. MSCs can also be isolated from synovium of donors post mortem [11]. As the synovium is a soft tissue, it is easy to harvest and handle, with no accessories such as curettes or hammers needed to break down the tissue when isolating the MSCs [11]. Although MSCs are relatively easy to work with, there is large heterogeneity in the laboratory setting for their isolation and cultivation, such as for the growth medium used (in particular, the serum component), the tissue digestion (e.g. time, type of collagenase), the culture expansion conditions (e.g. hypoxia), and others [12].

Here I provide a detailed procedure of how to isolate MSCs from human synovium. This includes determination of the proportions of viable cells in ex vivo isolated fractions before seeding the cells. I also describe how to carry out the colony-forming fibroblast assay (CFU-F) with the cells, to quantify their clonogenicity.

2 Materials

All reagents prepared should be filter-sterilised, and all accessories used should be sterile (*see* **Note 1**). Store all reagents at 4 °C unless otherwise specified. Use 70% ethanol for between-sample sterilisation of gloves and all surgical accessories. Prepare all solutions using ultrapure water. Diligently follow all waste disposal regulations when disposing of biological waste materials.

2.1 Tissue Digestion and Cell Isolation

1. A laminar flow cabinet is used to carry out all of the sterile procedures involving the primary cells. Good laboratory practice recommends the dedication of a single specific laminar flow cabinet to primary cells only. Simultaneous use of the laminar flow cabinet for working with other cells types, and in particular immortalised cell lines, is strongly ill-advised.

2. Cell culture incubator with hypoxic conditions: 37 °C; 5% CO_2 and 5% O_2; relative humidity, 85% to 95%.
3. Cell growth medium: high-glucose (4.5 g/L glucose) Dulbecco's modified Eagle's medium (DMEM), with 10% foetal bovine serum, 2 mM L-glutamine (100× stock: 200 mM), and 2% antibiotic/antimycotic (100× stock: 8.5 g/L sodium chloride, 0.025 g/L amphotericin B, 6.028 g/L penicillin G sodium salt, 10 g/L streptomycin sulphate) (*see* **Note 2**).
4. Phosphate-buffered saline (PBS), sterile.
5. Collagenase D: from *Clostridium histolyticum*, non-sterile powder. You will need 10 mg per 100 mg synovium.
6. Cell strainer (pore size, 70 μm), sterile, individually wrapped.
7. Syringe filter (pore size, 0.2 μm) and syringe (5 mL).
8. Scalpel, scissors, tweezers, petri dish, bijou sterile container (7 mL).
9. Conical tubes (15 mL, 50 mL).
10. Serological pipettes (5 mL, 10 mL).
11. Micropipettes (10 μL, 200 μL, 1,000 μL), with appropriate tips.

2.2 Viability of Ex Vivo Isolated Cells

1. Cell staining buffer: 2 mM ethylenediaminetetraacetic acid (EDTA) in PBS with 0.5% foetal bovine serum. Dissolve 0.0584 g EDTA (molecular weight, 292.24) in 100 mL PBS, and add 500 μL foetal bovine serum, and filter-sterilise.
2. Erythrocyte lysing solution (1×): add 1 mL lysing solution (10×) to 9 mL ultrapure water.
3. Viability dye: prepare working solution by diluting 1:10 in PBS. Keep protected from light.
4. FACS tubes: round-bottomed polystyrene tubes (5 mL), 96-well plates, tubes (1.5 mL).
5. Flow cytometer.

2.3 Colony-Forming Fibroblast Assay

1. Growth medium: high-glucose (4.5 g/L glucose) DMEM, with 10% foetal bovine serum, 2 mM L-glutamine (100× stock: 200 mM), and 2% antibiotic/antimycotic (100× stock: 8.5 g/L sodium chloride, 0.025 g/L amphotericin B, 6.028 g/L penicillin G sodium salt, 10 g/L streptomycin sulphate) (*see* **Note 2**).
2. Six-well plates.
3. Neutral buffered formalin (NBF, 10%), diluted in PBS to 4% NBF.
4. Crystal violet stock solution (1% w/v): dissolve 0.1 g methyl violet powder in 10 mL distilled water. For 0.1% (v/v) crystal violet working solution, add 1 mL 1% (w/v) crystal violet stock

solution to 10 mL ultrapure water, and filter (pore size, 0.2 μm).

5. 0.25% trypsin/EDTA.

3 Methods

Following synovium sampling (in the operating theatre), the tissue should be placed in growth medium (Fig. 1a) and stored at 4 °C until transfer to the laboratory for primary cell culturing. Carry out all of the procedures in the laminar flow cabinet, unless otherwise specified.

3.1 Tissue Digestion and Cell Isolation

1. Prefill 7-mL bijou sterile containers with sterile PBS, seal them tightly, and place them on a microbalance. Set the tare to zero.
2. Take the bijou container to the laminar flow cabinet. Remove the synovial tissue from the growth medium, and place it into the bijou container with PBS (Fig. 1b).
3. Place on the microbalance and record the net weight of the tissue.
4. Take the bijou container with the synovial tissue back to the laminar flow cabinet. Dissect the synovial tissue in the bijou container using scissors, to create smaller fragments. Wash the tissue in PBS three times to remove haematopoietic cells.
5. Transfer the tissue fragments using tweezers to a 15-mL conical tube prefilled with 9 mL growth medium.
6. Immediately before use, dissolve 10 mg/mL collagenase D in growth medium. For one sample, you will need 10 mg collagenase D. Filter-sterilise (*see* **Note 3**).
7. Add 1 mL 10 mg/mL collagenase solution to the 15-mL tube with the synovium for 1 mg/mL final collagenase concentration (total volume now 10 mL).
8. Incubate in a shaking water bath at 37 °C at high speed (120 rotations) for 1 h.
9. Vortex three times for 10 s.
10. Wait until the tissue settles down, and then transfer the supernatant to a new 50-mL conical tube.
11. Add 10 mL fresh growth medium to the digested synovium, vortex again for three times for 10 s, and add the supernatant to the same 50-mL tube.
12. Repeat step 11 once more (giving approximately 30 mL total cell suspension).
13. Pass the cell suspension through a 70 μm cell strainer placed over a new 50-mL tube.

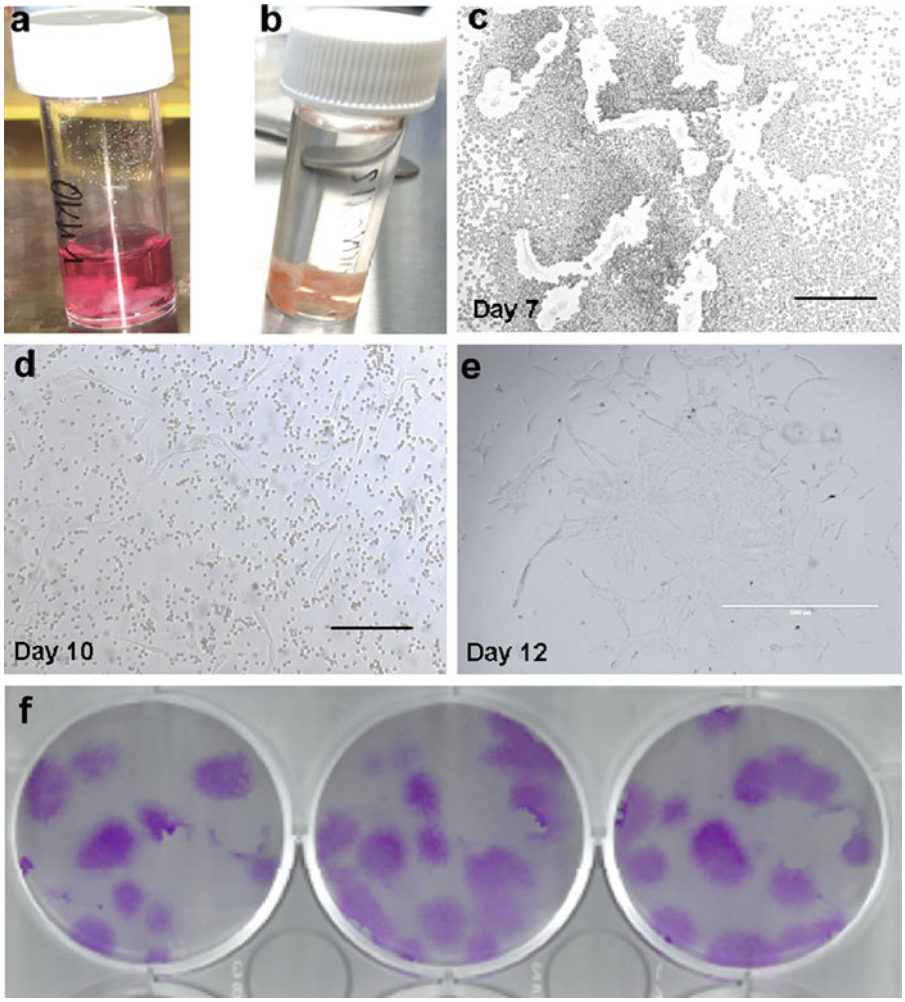

Fig. 1 Plastic adherence of freshly isolated cells from human synovium. (**a**, **b**) Representative images of synovial tissue biopsy used for MSC isolation in growth medium (**a**) and PBS (**b**). (**c**, **d**) Synovium-derived MSCs show plastic adherence after 3–7 days (**c**), while haematopoietic cells do not attach to the surface of the wells and are washed away during the medium changes (**d**). (**e**) Colonies can be observed after 10–14 days. (**f**) Six-well plates (three replicates) showing crystal violet-stained colonies used in the colony-forming fibroblast assay. Scale bars: 200 μm (**c, d**), 1,000 μm (**e**). PBS, phosphate-buffered saline

14. Centrifuge the cells at 300 × *g* for 5 min, remove the supernatant, and resuspend the cell pellet in 1 mL fresh growth medium. The cells can now be used for seeding or ex vivo analysis (*see* **Note 4**).

3.2 Viability of Ex Vivo Isolated Cells (Fig. 2)

All of the below-described procedures can be carried out under non-sterile conditions on the laboratory bench at room temperature, if not specified otherwise.

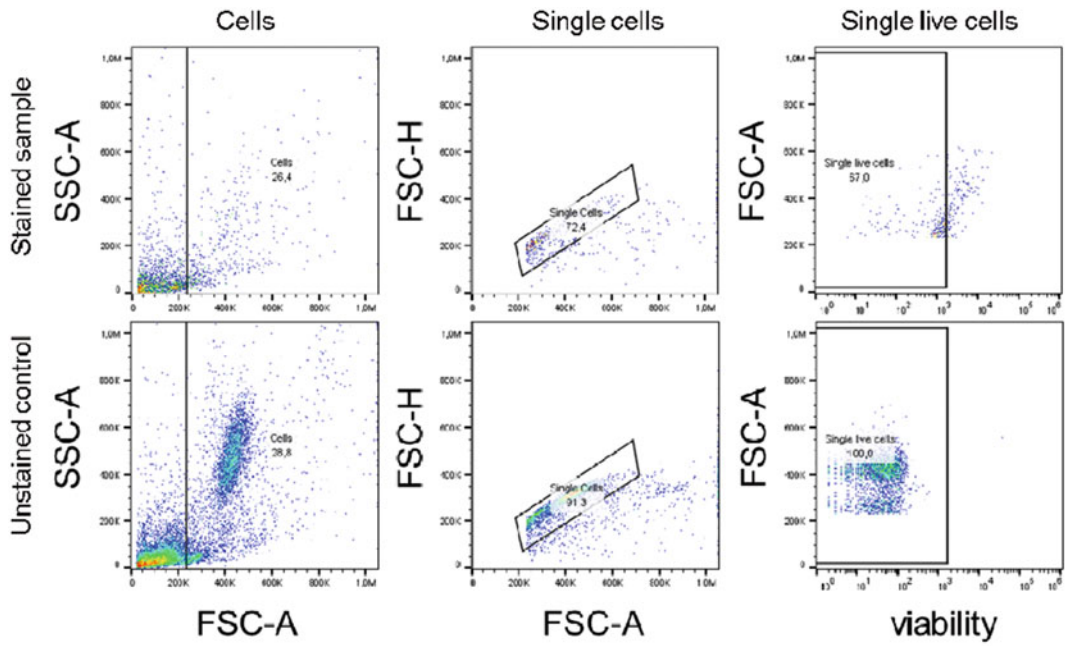

Fig. 2 Viability of ex vivo cells. Quantification of an aliquot of freshly isolated cells through flow cytometry, to determine the proportion of viable cells. Dot plots are shown for FSC-A versus SSC-A for cells, FSC-A versus FSC-H for single cells, and viability dye channel versus FSC-A to select viable cells. The cells were stained with the viability dye (upper row) or were unstained cells, to set up the gate (lower row). *FSC* forward scatter, *SSC* side scatter, *A* area, *H* height

1. Transfer 100 μL of 1 mL freshly isolated cell suspension to 1 mL cell staining buffer in a 1.5-mL tube. Centrifuge for 3 min at 300 × *g*. Remove the supernatant carefully, so as not to disturb the cell pellet.
2. Add 1 mL erythrocyte lysing solution (1×) to the cell pellet (*see* **Note 5**).
3. Vortex the 1.5-mL tube for 5 s and incubate for 10 min, protected from light.
4. Centrifuge 300 × *g* for 5 min.
5. Aspirate the supernatant completely.
6. Resuspend in 100 μL cell staining buffer, and transfer 50 μL aliquots to the wells of 96-well plates (*see* **Note 6**).
7. Cover the 96-well plates with parafilm, and centrifuge at 300 × *g* for 5 min.
8. Remove the supernatant. These can be done easily by flipping over the 96-well plates.
9. Add 100 μL viability dye per well, cover with parafilm, and leave for 30 min in dark and on ice (*see* **Note 7**).

10. Wash the cells by adding 100 μL PBS and centrifuging the 96-well plates at 300 × *g* for 5 min. Remove the supernatant by flipping over the 96-well plates.
11. Resuspend the cell pellets by adding 150 μL PBS to each well of the 96-well plates. Transfer the cell suspensions to FACS tubes prefilled with 400 μL PBS.
12. Analyse the cells using a flow cytometer. Create four dot plots: forward scatter area (FSC-A) versus side scatter area (SSC-A), FSC height (FSC-H) versus FSC-A, to select single cells and exclude doublets, and viability versus FSC-A dye, to select live cells. Set up the voltages for all of the dot plots based on an unstained sample. Record all of the stained samples, as well as the unstained control, under the same voltage conditions. At least 100,000 single live cells should be recorded.

3.3 Colony-Forming Fibroblast Activity Assay

1. Use two six-well plates to seed nine replicates. One six-well plate (with triplicates) will be used for histology, and six replicates will be used for trypsinisation and counting of the attached cells (*see* **Note 8**). Add 2 mL growth medium per well.
2. Add 100 μL aliquots of 1 mL freshly isolated cells per well.
3. Incubate at 37 °C with 5% CO_2 (*see* **Note 8**).
4. You should be able to see the attached cells as early as day 4 (Fig. 1c, d). Gently change half of the medium.
5. It takes 10–14 days for the colonies to grow and form (Fig. 1e). Inspect the colonies thoroughly every day after day 10, as they might overgrow (*see* **Note 9**).
6. Removed the medium and wash the wells with PBS.
7. Fix the cells using 5% NBF for 10 min.
8. You can now work on the bench. Remove the NBF and wash the wells with ultrapure water.
9. Add methyl violet working solution, at 500 μL per well, and leave for 15 min.
10. Remove the methyl violet and wash the wells with distilled water.
11. Leave the six-well plates to dry at room temperature, and then scan the plates. This can be done simply using a scanner and placing a white sheet on top of each six-well plate (Fig. 1f).
12. Count the number of colonies in all of the replicate wells, and calculate the number of colonies per well.
13. The cells in the remaining six replicates are meant for trypsinisation and further culture expansion. Remove the medium and wash all of the wells with PBS. Add 100 μL trypsin, and incubate the plates in an incubator (37 °C, 5% CO_2) for 5 min. Check under a microscope after 3 min to see if the

cells have detached. If not, a gentle shake of the six-well plates might help. Once the cells have fully detached, add 1 mL fresh medium to each well, and collect all of the replicates in one 15-mL conical tube. Centrifuge the cells at 300 × *g* for 3 min, remove the supernatant, and cell resuspend the pellet in 1 mL fresh medium. Count the cells using a haemocytometer, and calculate the number of counted cells per replicate trypsinised (six wells).

14. The CFU-F activity is calculated as the proportion (percentage) of the colonies counted per well divided by the number of cells counted per well (*see* **Note 10**).

4 Notes

1. Make sure in advance that you have all of the necessary materials, stocks, and equipment sterilised (e.g. scissors, scalpel handles). If you are isolating large numbers of samples simultaneously, make sure you have enough media prepared in advance.
2. To ensure consistency in the isolating and culturing of the MSCs, foetal bovine serum should be batch tested. Here, commercially available media for MSCs can be superior. However, MSCs can be isolated and successfully cultured in laboratory-prepared DMEM.
3. Wear a mask when weighing out the collagenase. Always include a dead volume for approximately one sample when preparing the collagenase solution. The losses are due to the filter-sterilising of the collagenase solution. To avoid running out of collagenase powder, try to keep a good record of the collagenase powder used. The best solution is to include a list where each user records the amount used and the remaining amount available for use.
4. It is imperative to take all measures necessary to prevent contamination of your samples at all stages, i.e. from surgical removal to laboratory isolation and cultivation. Until the primary cultures are established, we tend to use double the antibiotic and antimycotic doses and to also add this supplement to the collection media.
5. The lysing solution is intended for lysing the red blood cells that can interfere following direct immunofluorescence staining with antibodies, prior to flow cytometry analysis.
6. Using 96-well plates is particularly helpful when dealing with several samples simultaneously. However, if you are only processing one sample, a FACS tube or a 1.5-mL tube is the best option.

7. The viability dye is used to differentiate between live and dead cells, even after fixing.
8. Hypoxia has been shown to increase the growth of the tissue-derived cells [13].
9. A colony is defined as at least five population doublings of the same initial individual cell, meaning one cell produces 32 descendants. Some samples show very high ability to form colonies. If the colonies overgrow, it is difficult to quantify them.
10. The CFU-F is quantified as the number of colonies per number of cells. As not all of the cells are MSCs and have the ability to attach to plastic and form colonies, counting of the freshly isolated cells is not representative. Hence, replicates are used for exact quantification, by counting the trypsinised cells. It is imperative to perform both tests at the same time, i.e. methyl violet staining and trypsinisation.

Acknowledgements

Janja Zupan was funded by UK Arthritis Research in 2016–2018 and is currently part of the P3-0298 Research Programme 'Genes, hormones and personality changes in metabolic disorders', funded by the Slovenian Research Agency.

References

1. Sakaguchi Y, Sekiya I, Yagishita K et al (2005) Comparison of human stem cells derived from various mesenchymal tissues: superiority of synovium as a cell source. Arthritis Rheum 52:2521–2529
2. De BC, Dell'Accio F, Tylzanowski P et al (2001) Multipotent mesenchymal stem cells from adult human synovial membrane. Arthritis Rheum 44:1928–1942
3. Kurth TB, Dell'Accio F, Crouch V et al (2011) Functional mesenchymal stem cell niches in adult mouse knee joint synovium *in vivo*. Arthritis Rheum 63:1289–1300. https://doi.org/10.1002/art.30234
4. Roelofs AJ, Zupan J, Riemen AHK et al (2017) Joint morphogenetic cells in the adult mammalian synovium. Nat Commun 8:15040. https://doi.org/10.1038/ncomms15040
5. De Bari C, Roelofs AJ (2018) Stem cell-based therapeutic strategies for cartilage defects and osteoarthritis. Curr Opin Pharmacol 40:74–80. https://doi.org/10.1016/j.coph.2018.03.009
6. Murata Y, Uchida S, Utsunomiya H et al (2018) Synovial mesenchymal stem cells derived from the cotyloid fossa synovium have higher self-renewal and differentiation potential than those from the paralabral synovium in the hip joint. Am J Sports Med 14:1–2. https://doi.org/10.1177/0363546518794664
7. Dominici M, Le BK, Mueller I et al (2006) Minimal criteria for defining multipotent mesenchymal stromal cells. The International Society for Cellular Therapy position statement. Cytotherapy 8:315–317
8. Sacchetti B, Funari A, Remoli C et al (2016) No identical 'mesenchymal stem cells' at different times and sites: human committed progenitors of distinct origin and differentiation potential are incorporated as adventitial cells in microvessels. Stem Cell Reports 6:897–913. https://doi.org/10.1016/j.stemcr.2016.05.011
9. de SE, Casado P, Neto V et al (2014) Synovial fluid and synovial membrane mesenchymal stem cells: latest discoveries and therapeutic

perspectives. Stem Cell Res Ther 5:112. https://doi.org/10.1186/scrt501

10. Hermida-Gómez T, Fuentes-Boquete I, Gimeno-Longas MJ et al (2011) Quantification of cells expressing mesenchymal stem cell markers in healthy and osteoarthritic synovial membranes. J Rheumatol 38:339–349. https://doi.org/10.3899/jrheum.100614
11. De Bari C, Dell'Accio F, Karystinou A et al (2008) A biomarker-based mathematical model to predict bone-forming potency of human synovial and periosteal mesenchymal stem cells. Arthritis Rheum 58:240–250. https://doi.org/10.1002/art.23143
12. Čamernik K, Barlič A, Drobnič M et al (2018) Mesenchymal stem cells in the musculoskeletal system: from animal models to human tissue regeneration? Stem Cell Rev 14 (3):346–369. https://doi.org/10.1007/s12015-018-9800-6
13. Tsai C-C, Yew T-L, Yang D-C et al (2012) Benefits of hypoxic culture on bone marrow multipotent stromal cells. Am J Blood Res 2:148–159

Methods in Molecular Biology (2019) 2045: 155–165
DOI 10.1007/7651_2019_208

Published online: 08 February 2019

3D-Embedded Cell Cultures to Study Tendon Biology

Renate Gehwolf, Gabriel Spitzer, Andrea Wagner, Christine Lehner, Nadja Weissenbacher, Herbert Tempfer, and Andreas Traweger

Abstract

Tendons harbor various cell populations, including cells displaying classical adult mesenchymal stromal cell criteria. Previous studies have shown that a tenogenic phenotype is more effectively maintained in a 3D cell culture model under mechanical load. This chapter describes a method to isolate tendon-derived cells from rat Achilles tendons and the subsequent formation of 3D-embedded cell cultures. These tendon-like constructs can then be analyzed by various means, including histology, immunohistochemistry, qPCR, or standard protein analysis techniques.

Keywords Tendon stem and progenitor cells, 3D-embedded culture, Tenogenesis, Achilles tendon

1 Introduction

Tendons resemble connective tissues rich in highly organized collagen fibers, displaying a remarkably high tensile strength, enabling musculoskeletal forces to be transmitted and redirected across skeletal joints, and thereby facilitating joint motion and locomotor movement [1]. Due to their remarkable biomechanical properties, tendons not only allow the safe transmission of muscle forces over long lengths but partially also enable the storage and release of elastic energy, reducing energy costs and minimizing the risk of injury. Tendon and ligament disorders are among the most frequent musculoskeletal conditions for which patients seek medical advice, comprising approximately 40% of all musculoskeletal disorders (United States Bone and Joint Initiative: The Burden of Musculoskeletal Diseases in the United States (BMUS), Third Edition, 2014. Rosemont, IL. Available at http://www.boneandjointburden.org; accessed on 24.10.2018). Consequently, there is a growing socioeconomic need for effective and reproducible strategies to repair tendon and ligament injuries and to treat chronic tendinopathies.

Tendinopathies often are the consequence of repetitive (over-) loading; however, the underlying causes involve a spectrum of different factors, including several intrinsic (e.g., age, body habitus, nutrition, metabolic diseases, or genetics) and extrinsic factors

(e.g., certain drugs, smoking) resulting in acute or chronic changes to the tendon structure itself [2, 3]. However, we need to better understand the underlying pathologic pathways contributing to the onset and progression of tendinopathies in order to effectively address tendon disorders in the clinic.

Mature tendons harbor various cell types; however, mainly due to the lack of reliable tendon-specific markers, our knowledge about their identity remains fragmentary. Tenocytes comprise approximately 90% of the tendon cellular compartment [4]. Synovial cells of the endo-/epitenon, entheseal chondrocytes, and vascular endothelial cells form the remaining 10%. Finally, a small population of multipotent tendon stem and progenitor cells (TSPCs) has been identified in tendons, which exhibit classical adult mesenchymal stromal cell (MSC) criteria [5–7]. However, we still know very little about this cell population and how it contributes to tendon disease, damage, and repair. Therefore, next to in vivo studies, suitable in vitro models are required to better characterize TSPCs and to make use of this cell source for treating injured tendons.

Standard 2D cell cultures often do not allow for the analysis of morphological aspects and limit the assessment of functional cellular features. Engineered, three-dimensional (3D) cultures based on cells embedded in an extracellular matrix (ECM) are useful in vitro models to simulate more mature tissues. Early examples of such models include Matrigel™-based 3D organoids for mammary acini [8] or lung tissue [9]. These 3D-organoid culture models are valuable tools to study normal tissue development and disease processes as they are amenable to experimental manipulation and optical observation [10, 11]. Previous studies have shown that 3D culture is a potent driver of tenogenesis and maintains the tenogenic lineage [12, 13]. TSPCs embedded in a hydrogel contract the matrix to form a tendon-like construct, demonstrating collagen fibrillogenesis and structural similarities to tendon tissue under intrinsic load [14, 15].

In this chapter, we describe the isolation and cultivation of TSPCs from rat Achilles tendons and detail the formation of tendon-like constructs as a 3D platform resembling the in vivo environment to investigate tendon biology and pathology.

2 Materials

All steps involving cell culture medium must be performed in a laminar flow cabinet. Unless otherwise specified, the standard medium used is *Minimum Essential Medium Eagle Alpha Modification* (Sigma-Aldrich-Aldrich; #M4526) supplemented with 10% FBS, 100 units/ml penicillin, and 0.1 mg/ml streptomycin (Sigma-Aldrich-Aldrich, #P4333). The complete cell culture medium further

contains 0.05 mM L-proline (1000× stock solution; Sigma-Aldrich-Aldrich, #P0380), 0.2 mM ascorbic acid (100× stock solution; Sigma-Aldrich-Aldrich, #A8960), and 10 μg/ml aprotinin (100× stock solution; Sigma-Aldrich, #A6106). The stocks are prepared in sterile H_2O, filtered through a 0.45 μm syringe filter, and aliquots are stored at −20 °C until further use.

2.1 Tendon Cell Isolation and Culture

Minimum Essential Medium Eagle, Alpha Modification, Sigma-Aldrich, #M4526

Fetal Bovine Serum

Glutamax (100 × stock solution), Gibco by Life Technologies, #35050-038

Collagenase type II, Gibco by Life Technologies, #17101015

Trypsin-EDTA solution, Sigma-Aldrich, #T4049

2.2 Tendon-Like Constructs

Cell culture dishes, various sizes, depending on number of constructs used

1.5 ml Eppendorf tubes

Pipettes and sterile tips (with and without filter)

Fine forceps (e.g., Dumont Forceps; Fine Science Tools)

10 ml syringe, Luer-Lock tip, BD, #300912

Syringe filter, pore size 0.45 μm (e.g., Rotilabo®-syringe filters; Carl Roth)

184 Silicone Elastomer Kit, SYLGARD (Dow Corning)

Insect Pins, Austerlitz, stainless steel, diameter 0.1 mm (Fine Science Tools, #26002-10)

Silk braided black sutures, USP 0, metric EP 3.5 (SMI AG, #8350025)

PureCol EZ Gel solution, Sigma-Aldrich, #5074

Penicillin (10,000 units/ml) and streptomycin (10 mg/ml), 100× stock, Sigma-Aldrich, #P4333

Aprotinin, Sigma-Aldrich, #A6106

L-Ascorbic acid 2-phosphate sesquimagnesium salt hydrate, Sigma-Aldrich, #A8960

L-proline, Sigma-Aldrich, #P0380

Minimum Essential Medium Eagle, Alpha Modification, Sigma-Aldrich, #M4526

Fetal Bovine Serum (e.g. Gibco by Life Technologies)

Collagenase type II, Gibco, #17101015

Trypsin-EDTA solution, Sigma-Aldrich #T4049

2.3 RNA Isolation

TRIzol Reagent, Ambion, Thermo Fisher Scientific, #15596026

Chloroform, MERCK, #1.02445

1-Bromo-3-Chloropropane (BCP), Sigma-Aldrich, #B9673

EtOH p.A., MERCK, #1.11727

2-Propanol, p.A., Sigma-Aldrich, #59304-1L-F

RNaseZap, Invitrogen, Thermo Fisher Scientific, #AM9780

Ultra TURRAX, T10 basic and Dispersing Element, S10N-5G, IKA, #3304000

GlycoBlue co-precipitant, 15 mg/μl, Invitrogen, Thermo Fisher Scientific, #AM9515

PCR grade water, Jena Bioscience, #PCR 258

SUPERase-In RNase Inhibitor, 20 units/μl, Invitrogen Thermo Fisher Scientific, #AM2696

NanoDrop 2000c spectrometer, Thermo Scientific

Experion automated electrophoresis system and Experion RNA StdSens Analysis Kit, Biorad, #700-7103

2.4 Histology

Paraformaldehyde, Fisher Chemical, #30525-89-4

1× Phosphate buffered saline without Calcium chloride and Magnesium chloride

15% (w/v) and 30% (w/v) sucrose in PBS

O.C.T. compound, Tissue-Tek, #4583

DAPI (4′,6-Diamidine-2′-phenylindole dihydrochloride), Sigma-Aldrich # 10236276001

Cryostat, e.g. LEICA CM 1950

2.5 Lysates for Western Blot

RIPA-Buffer, Sigma-Aldrich, #R0278

Phosphatase Inhibitor Cocktail 3, Sigma-Aldrich, #P0044

Protease Inhibitor Cocktail, Sigma-Aldrich, #P8340

Potter homogenisator suitable for 1.5 ml reaction tubes

3 Methods

3.1 Preparation of the Culture Dishes

1. Add 5 ml Sylgard 184 Silicone Elastomer Curing Agent to 45 ml Sylgard 184 Silicone Elastomer Base in a 50 ml tube. Slowly tilt the tube until the viscous solution is homogenously mixed. This can take up to 10 min (*see* **Note 1**).
2. Fill the cell culture dishes up to 5 mm with the Silicone Elastomer. There can be small air bubbles in the silicone gel.

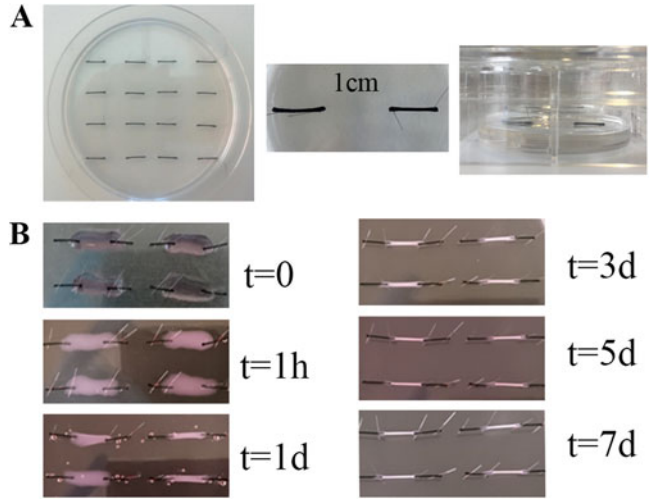

Fig. 1 Time course of tendon-like construct formation. (**a**) Silk sutures mounted on silicone by minutien insect pins. (**b**) Time course of collagen gel contraction by tendon cells and formation of tendon-like constructs over a time span of 7 days

Wait several minutes for them to disappear, and carefully remove the remaining bubbles with a pipette tip. Let the silicone cure overnight at 48 °C.

3. Pairs of 8 mm long silk sutures are pinned with insect pins in rows on the silicone plated dishes (*see* **Note 2**). The tendon-like construct will form between the ends of a pair of sutures. The gap should measure exactly 10 mm. The distance between the rows should be at least 10 mm to prevent the constructs from coming in contact with each other (Fig. 1).
4. The dishes are then placed in 70% ethanol for 30 min and dried under a laminar flow over night.
5. The next day the dishes are treated with UV light for 30 min and then stored in sterile plastic bags until further use.

3.2 Primary Tendon Cell Isolation

1. Rats are anesthetized with isoflurane and euthanized with an intracardiac injection of pentobarbital.
2. The Achilles tendons are dissected in a laminar flow hood, cut into small pieces, and digested at 37 °C o/n in complete medium containing 3 mg/ml collagenase type II.
3. The next day most of collagen matrix should be digested. If there are some tissue fragments remaining, gently dissociate them with a sterile 1 ml pipette to assist in the release of the tendon cells.
4. Pipette the solution into a 15 ml conical tube, and fill it up with standard medium. Centrifuge at 150 × *g* for 5 min at RT, and

carefully discard the supernatant. Resuspend the cell pellet in 4 ml standard medium, and transfer it to a 25 cm^2 cell culture flask. After 1 day of incubation at 37 °C, the tendon cells should have settled and start proliferating.

5. After several days, the cells will be sub-confluent (approx. 70%) and must be passaged. The medium is removed, and the cells are washed with sterile PBS and trypsinized until most cells are detached (approximately 2 min). The reaction is stopped by adding excess standard medium. The solution is then transferred to a 15 ml conical tube and centrifuged at 150 × *g* for 5 min. Discard the supernatant, and carefully resuspend the cell pellet in standard medium. The cells can now be split to several 75 cm^2 culture flasks, depending on the amount of cells needed for the planned tendon like constructs. An almost confluent 75 cm^2 flask contains approximately 1 million tendon-derived cells. See the next chapter how to determine the amount of cells required for each construct.

3.3 Tendon-Like Constructs

1. Calculate the volume for every component before starting the experiment. Every tendon construct requires a total volume of 130 μl (hydrogel with cells). Calculate the total volume of all constructs required, and add up to 50% to compensate for loss. The solution is very viscous, and some of it will adhere to the surface of the tubes and pipette tips.
2. The gel solution for the constructs should contain 2.5×10^5 cells/ml. Calculate the total number of tendon cells required, and prepare them as outlined above.
3. Perform the preparation of the collagen solution on ice to prevent gelation. Mix 40% PureCol (5 mg/ml collagen, Sigma-Aldrich) with 60% alphaMEM (without FBS), and add 100 units/ml penicillin, 0.1 mg/ml streptomycin, and aprotinin to a 1× final concentration (*see* **Note 3**). The collagen concentration of the PureCol can vary between different batches. The final gel solution must contain 2 mg/ml collagen. If necessary, adjust the added volume accordingly, and add sterile 1 M NaOH to adjust the pH to 7.2–7.6. Gently swirl the tube (avoid bubbles) until the components are homogenously mixed, and store on ice until further use (*see* **Notes 4** and **5**).
4. Remove the medium from the culture flasks, and wash the cells with sterile PBS. Trypsinize the cells, stop the reaction by adding excess standard medium, transfer the solution to a 15 ml conical tube, and centrifuge at 150 × *g* for 5 min at RT. Carefully discard the supernatant, and resuspend the cell pellet in 5 ml standard medium. Determine the cell number, and transfer the required amount of cells to a new 15 ml conical tube.

Centrifuge as above, discard supernatant, and carefully resuspend the cell pellet in the prepared chilled collagen gel solution. Maintain the tube on ice to keep the solution liquid.

5. Pipette 130 μl of the cell collagen solution between and around the pins (*see* Fig. 1). Start by placing a drop on the pin and around the end of the silk suture. Then connect the ends by pipetting the rest between them. Carefully place the culture dishes in an incubator at 37 °C, 5% CO_2 and 95% humidity, and wait for 1 h for the constructs to set (*see* **Note 6**). Then slowly add complete cell culture medium until the constructs are fully submerged.
6. The medium should be exchanged every other day. The cells reorganize the collagen gel, and after 7 days of contraction, the tendon-like constructs are ready for further experiments (Fig. 1) (*see* **Note 7**).

3.4 RNA Isolation

1. Place one tendon-like construct into 1 ml TRIzol reagent. Several constructs (up to 8) can be pooled to increase the final amount of RNA. The samples can be stored at −80 °C for at least 1 month.
2. Samples are briefly homogenized with an Ultra Turrax. Before and after use, the Ultra Turrax is cleaned with RNase Zap (1/10 in autoclaved H_2O) and autoclaved H_2O and pure EtOH. In between sample homogenization, the Ultra Turrax is rinsed with sterile 0.1 M NaOH washed with autoclaved H_2O and pure EtOH. Homogenize the sample only for a few seconds at a time, and keep them on ice.
3. Add 100 μl BCP for every 1 ml TRIzol reagent, and shake it vigorously for 15 s, but do not vortex. Incubate the sample for 5 min at room temperature on a shaker.
4. Centrifuge the tube at 12,000 × *g* for 15 min at 4 °C. The sample will be separated into three phases. Clear aqueous upper phase containing the RNA, interphase, and red organic lower phase. The interface contains proteins and can be white, but usually it is very thin. Transfer the upper phase to a new 1.5 ml tube without disrupting the other phases.
5. Add 1 volume of chloroform and shake the sample by hand for 15 s. Centrifuge the tube at 12,000 × *g* for 15 min at 4 °C. Transfer the upper phase to a new tube. Perform this step two times.
6. To increase visibility and precipitation of the RNA, 0.5 μl GlycoBlue as co-precipitant can be added to the sample. Add 1 volume of 2-propanol and shake by hand for 15 s. Incubate the sample at −20 °C for 30 min to precipitate the RNA.

7. Centrifuge at max speed in a tabletop centrifuge for 30 min at 4 °C. The RNA pellet will be white or, if GlycoBlue was added, blue. Carefully discard the supernatant, and shortly centrifuge the tube again, and remove the rest of the supernatant.
8. Wash the pellet by adding 1 ml 70% EtOH, and invert the tube several times. Centrifuge at 12,000 × *g* for 10 min at 4 °C, and discard the supernatant. Repeat this step with 100% EtOH.
9. Air-dry the pellet until it starts to become slightly translucent, but do not over dry the pellet as it then can be difficult to bring the RNA into solution. Resuspend the pellet in 15 μl RNase free H_2O, and add 0.5 μl RNase inhibitor.
10. The RNA concentration is determined with a NanoDrop 2000c spectrometer (or equivalent instrument); use RNase free water as blank. The RNA can now be transcribed to cDNA to perform qPCR or stored at −80 °C for up to 1 year.

3.5 Histology

1. Remove the medium from the culture dishes and wash it with PBS at RT. Fix the constructs for 30 min at RT by submerging them in 4% PFA. Wash 2× 15 min in PBS, and incubate constructs in 15% (w/v) and 30% (w/v) sucrose in PBS at 4 °C for 24 h each.
2. During sample fixation with paraformaldehyde, the entire constructs can be stained with DAPI by adding DAPI (4′,6-Diamidine-2′-phenylindole dihydrochloride) 1/10,000 to PBS during one of 15 min washing steps.
3. Carefully remove the construct from the insect pins and sutures, and place it in O.C.T. compound, and snap freeze on dry ice.
4. Section the construct into 12–20 μm thin sections, and mount them on microscope slides. Let the sections air dry at room temperature for approximately 1 h, and then store them at −20 °C for further use.
5. The sections can be used, e.g., for polarization microscopy, immunocytochemical, and immunohistological stainings (Fig. 2).

3.6 Protein Lysates for Western Blot

1. Remove the medium from the culture dishes, and wash constructs 1× with PBS.
2. Remove the constructs from the insect pins, and place them into chilled RIPA buffer containing 1% phosphatase inhibitor and 1% protease inhibitor cocktail. To increase the protein concentration, several constructs can be pooled in one tube. We generally achieved good results by pooling three constructs in 100 μl RIPA buffer. Keep the tube on ice.

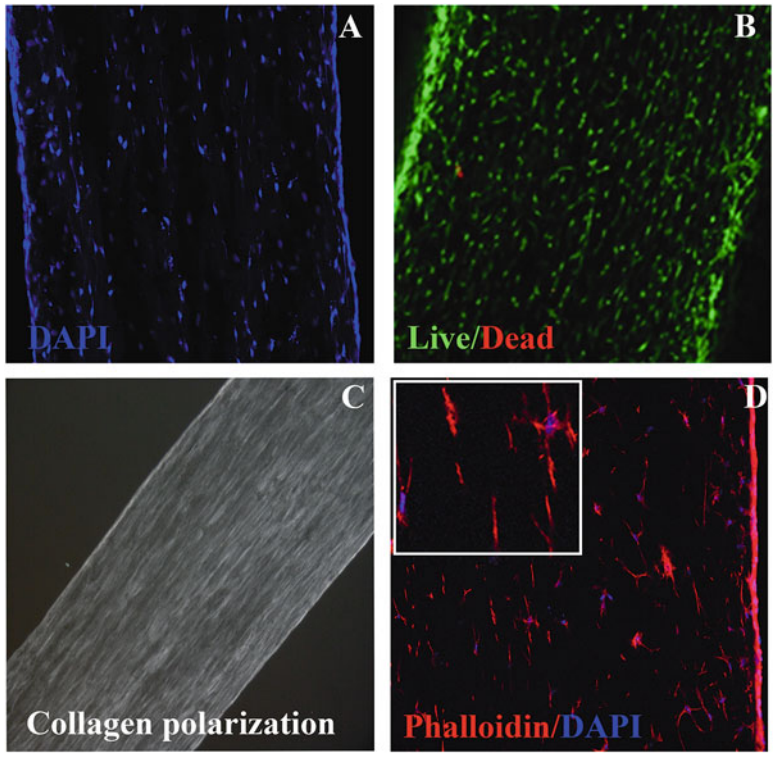

Fig. 2 Histological analysis of tendon-like constructs after 7 days of contraction. Cryosections of tendon-like constructs were analyzed for (**a**) cell distribution by DAPI-staining, (**b**) cell viability by Live/Dead Assay, (**c**) collagen structure by polarization microscopy, and (**d**) actin cytoskeletal organization by staining with phalloidin

3. Grind the constructs with a small tissue grinder (glass/PTFE Potter-Elvehjem) on ice.
4. Centrifuge the lysate at 12,000 × *g* for 10 min at 4 °C. Transfer the supernatant to new tube and discard the pellet.
5. The lysate can be used for standard SDS-PAGE and Western Blot analysis or stored at −20 °C.

4 Notes

1. Placing the tube with the Silicone Elastomer on an orbital shaker generally does not result in a homogenous solution. Preferentially, this step should be performed by hand.
2. The insect pins are very thin and can only be handled with fine tweezers. Wearing safety goggles is advised.
3. Aprotinin inhibits proteases and is therefore necessary for proper gelation.

4. Keep PureCol solution on ice during the entire procedure as this avoids gelation of the collagen solution.
5. We have tested various collagen solutions and have only achieved consistent results with PureCol solution. Further, it is generally not necessary to adjust the pH of final collagen/cell solution as the pH of PureCol EZ Gel solution is already adjusted to a neutral pH.
6. If the constructs do not remain attached to the sutures as you submerge them in complete cell culture medium for the first time, wait for another 30 min to allow further gelation of the construct.
7. Parts of the collagen gel can stick to the silicone surface and hinder proper formation of the tendon-like construct. Carefully detach the construct with a pipette tip to allow further contraction.

References

1. Tempfer H, Lehner C, Grütz M, Gehwolf R, Traweger A (2017) Biological augmentation for tendon repair: lessons to be learned from development, disease, and tendon stem cell research. In: Gimble JM, Marolt D, Oreffo R, Redl H, Wolbank S (eds) Cell engineering and regeneration. Springer, Cham, pp 1–31. https://doi.org/10.1007/978-3-319-37076-7_54-1
2. Millar NL, Murrell GA, McInnes IB (2017) Inflammatory mechanisms in tendinopathy—towards translation. Nat Rev Rheumatol 13 (2):110–122. https://doi.org/10.1038/nrrheum.2016.213
3. Murrell GA (2002) Understanding tendinopathies. Br J Sports Med 36(6):392–393
4. Kannus P (2000) Structure of the tendon connective tissue. Scand J Med Sci Sports 10 (6):312–320
5. Bi Y, Ehirchiou D, Kilts TM, Inkson CA, Embree MC, Sonoyama W, Li L, Leet AI, Seo BM, Zhang L, Shi S, Young MF (2007) Identification of tendon stem/progenitor cells and the role of the extracellular matrix in their niche. Nat Med 13(10):1219–1227. https://doi.org/10.1038/nm1630
6. Salingcarnboriboon R, Yoshitake H, Tsuji K, Obinata M, Amagasa T, Nifuji A, Noda M (2003) Establishment of tendon-derived cell lines exhibiting pluripotent mesenchymal stem cell-like property. Exp Cell Res 287 (2):289–300
7. Tempfer H, Wagner A, Gehwolf R, Lehner C, Tauber M, Resch H, Bauer HC (2009) Perivascular cells of the supraspinatus tendon express both tendon- and stem cell-related markers. Histochem Cell Biol 131 (6):733–741. https://doi.org/10.1007/s00418-009-0581-5
8. Barcellos-Hoff MH, Aggeler J, Ram TG, Bissell MJ (1989) Functional differentiation and alveolar morphogenesis of primary mammary cultures on reconstituted basement membrane. Development 105(2):223–235
9. Schuger L, O'Shea KS, Nelson BB, Varani J (1990) Organotypic arrangement of mouse embryonic lung cells on a basement membrane extract: involvement of laminin. Development 110(4):1091–1099
10. Matsusaki M, Case CP, Akashi M (2014) Three-dimensional cell culture technique and pathophysiology. Adv Drug Deliv Rev 74:95–103. https://doi.org/10.1016/j.addr.2014.01.003
11. Shamir ER, Ewald AJ (2014) Three-dimensional organotypic culture: experimental models of mammalian biology and disease. Nat Rev Mol Cell Biol 15(10):647–664. https://doi.org/10.1038/nrm3873
12. Barsby T, Bavin EP, Guest DJ (2014) Three-dimensional culture and transforming growth factor beta3 synergistically promote tenogenic differentiation of equine embryo-derived stem cells. Tissue Eng Part A 20 (19-20):2604–2613. https://doi.org/10.1089/ten.TEA.2013.0457
13. Kapacee Z, Richardson SH, Lu Y, Starborg T, Holmes DF, Baar K, Kadler KE (2008) Tension is required for fibripositor formation.

Matrix Biol 27(4):371–375. https://doi.org/10.1016/j.matbio.2007.11.006

14. Bayer ML, Yeung CY, Kadler KE, Qvortrup K, Baar K, Svensson RB, Magnusson SP, Krogsgaard M, Koch M, Kjaer M (2010) The initiation of embryonic-like collagen fibrillogenesis by adult human tendon fibroblasts when cultured under tension. Biomaterials 31 (18):4889–4897. https://doi.org/10.1016/j.biomaterials.2010.02.062
15. Gehwolf R, Wagner A, Lehner C, Bradshaw AD, Scharler C, Niestrawska JA, Holzapfel GA, Bauer HC, Tempfer H, Traweger A (2016) Pleiotropic roles of the matricellular protein Sparc in tendon maturation and ageing. Sci Rep 6:32635. https://doi.org/10.1038/srep32635

Methods in Molecular Biology (2019) 2045: 167–180
DOI 10.1007/7651_2019_216

Published online: 03 April 2019

Targeted, Amplicon-Based, Next-Generation Sequencing to Detect Age-Related Clonal Hematopoiesis

Brooke Snetsinger, Christina K. Ferrone, and Michael J. Rauh

Abstract

Aging hematopoietic stem cells acquire mutations that sometimes impart a selective advantage. Next-generation DNA sequencing (NGS) can be used to detect expanded peripheral blood progeny of a mutant clone, usually carrying just one cancer-driver mutation, most often in the epigenetic regulator genes, *DNMT3A* or *TET2*. This phenomenon is known as clonal hematopoiesis (CH), age-related CH (ARCH) when considering its association with age, and CH of indeterminate potential (CHIP) when the variant allele fraction (VAF) is at least 2% in peripheral leukocytes. CHIP is present in at least 10–15% of adults older than 65 years and is a risk factor for hematological neoplasms and diseases exacerbated by mutant, hyper-inflammatory, monocytes/macrophages, such as atherosclerotic cardiovascular disease. Therefore, the detection of CHIP has important clinical consequences. Herein, we present a protocol for the generation of targeted, amplicon-based, NGS libraries for ion semiconductor sequencing and CHIP detection, using Ion Torrent platforms.

Keywords Clonal hematopoiesis (CH), Age-related clonal hematopoiesis (ARCH), Clonal hematopoiesis of indeterminate potential (CHIP), Next-generation DNA sequencing (NGS), Amplicon, Library, Ion semiconductor, Ion Torrent, Peripheral blood, *DNMT3A*, *TET2*

1 Introduction

The normal polyclonal composition of peripheral blood cells can be disrupted when acquired mutations in hematopoietic stem cells (HSC) impart a selective advantage, leading to clonal hematopoiesis (CH). Age-related clonal hematopoiesis (ARCH) or CH of indeterminate potential (CHIP), the latter defined when the variant allele fraction (VAF) reaches at least 0.02 in peripheral blood cells, is found in at least 10–15% of adults greater than 65 years of age [1–5]. CHIP is marked by mutations (median VAF approx. 0.1) in myeloid cancer-associated genes, most often in epigenetic regulators, *DNMT3A* or *TET2*. CHIP places an individual at increased risk of acquiring an overt hematological neoplasm, at an overall rate of 0.5% to 1.0% per year [1, 2], although more recent studies are pinpointing those at greater risk of acute myeloid leukemia (AML) transformation [6, 7]. Although initially unexpected, CHIP is also associated with increased risk of mortality

from non-hematological cancers and other diseases, like cardiovascular disease [1, 8, 9]. As demonstrated by our group and others, this is related, at least in part, to increased inflammatory properties of monocytes and macrophages derived from the mutant CHIP clone [10–13]. Thus, CHIP is a common consequence of aging HSC, contributing to morbidity and mortality, and is an emerging public health issue.

Next-generation DNA sequencing (NGS) has been essential for identifying and defining CHIP [1, 2, 4]. The minimal VAF (at least 0.02) for CHIP was arbitrarily defined, conveniently near the lower detection threshold of conventional NGS [4]. In actuality, error-corrected NGS has revealed CH to be nearly ubiquitous in healthy adults, albeit with median VAF (0.0024) at least tenfold less than the standard definition of CHIP [14]. Not very much is known of the clinical significance, if any, of CH at ultralow VAF, and these clones appear to be relatively stable [14]. Therefore, this chapter will focus on the identification of CHIP (VAF $\geq$0.02) with its well-described clinical consequences.

Semiconductor technology permits nonoptical nucleic acid sequencing by massively parallel detection of ions produced during template-directed synthesis [15]. We, and others, have applied Ion Torrent™ semiconductor sequencing in the identification of myeloid neoplasms and CHIP [16–19]. Herein, we present a protocol to extract genomic DNA (gDNA) from peripheral blood collection tubes, determine the resultant quality and quantity of gDNA, prepare and sequence amplicon-based libraries that amplify recurrently mutated regions in 48 myeloid cancer-associated genes (using AmpliSeq™ technology), and analyze the sequence data for variants compatible with CHIP.

2 Materials

Prepare all solutions using ultrapure water (prepared by purifying deionized water, to attain a resistivity of 15 MΩ cm at 25 °C) and analytical grade reagents. Prepare and store all reagents at room temperature (unless indicated otherwise).

1. PAXgene Blood DNA tubes (Qiagen, 761115).
2. PAXgene Blood DNA kit (Qiagen, 761133).
3. Eppendorf DNA LoBind Tubes 1.5 mL (Fisher, 13-698-791).
4. Low TE Buffer (Thermo, 12090015).
5. Axygen™ AxyPrep Mag™ FragmentSelect Kits (Fisher, 14-223-162).
6. MicroAmp™ Optical 8-Tube Strip, 0.2 mL (Thermo, 4316567).

7. MicroAmp™ Optical 8-Tube Strip, Cap (Thermo, 4323032).
8. MicroAmp™ Optical Adhesive Film (Thermo, 4311971).
9. MicroAmp™ Fast Optical 96-Well Reaction Plate, 0.1 mL (Thermo, 4346907).
10. MicroAmp™ Fast Optical 96-Well Reaction Plate, 0.2 mL (Thermo, N8010560).
11. Loading buffer: In 5 mL of dH_2O dissolve 4 g sucrose, 25 mg bromophenol blue, 25 mg xylene cyanol, and 4 mL 0.5 M EDTA (pH 8.0). Top up to 10 mL with H_2O and aliquot 500 μL into fresh microcentrifuge tubes. Store at 4 °C.
12. 5× TBE running buffer: In 800 mL of dH_2O dissolve 54 g tris, 27.5 g boric acid, 20 mL 0.5 M EDTA (pH 8.0), top up to 1 L with H_2O. Store at room temperature. Dilute to 1× for a working solution.
13. 1% agarose gel: Melt 1 g of agarose in 100 mL 1× TBE buffer. Allow mixture to cool until flask doesn't burn to the touch. Add 3.5 μL RedSafe, swirl to combine, then quickly cast gel, add combs, and allow to set for 15 min.
14. TaqMan™ RNase P Detection Reagents Kit (Thermo, 4316831).
15. TaqMan™ Universal PCR Master Mix (Thermo, 4304437).
16. Ion AmpliSeq™ Library Kit 2.0 (Thermo, 4480441).
17. NGS Panel (i.e., custom amplicon, 48 myeloid cancer-associated genes, AmpliSeq™ panel described in ref. [16], or other Ion Torrent compatible product). Our "pan-myeloid" panel targets all coding exons or hotspots for *ASXL1*, *BCOR*, *BCORL1*, *BOD1L*, *BRAF*, *BRCC3*, *CALR*, *CBL*, *CEBPA*, *CSF3R*, *CUX1*, *DNMT3A*, *ETV6*, *EZH2*, *FLT3*, *GATA1*, *GATA2*, *GNAS*, *GNB1*, *IDH1*, *IDH2*, *JAK2*, *KDM6A*, *KIT*, *KRAS*, *MPL*, *NF1*, *NF-E2*, *NPM1*, *NRAS*, *PHF6*, *PTPN11*, *RAD21*, *RIT1*, *RUNX1*, *SETBP1*, *SF3B1*, *SH2B3*, *SMC1A*, *SMC3*, *SRSF2*, *STAG2*, *TET2*, *TLR2*, *TP53*, *U2AF1*, *WT1*, and *ZRSR2*.
18. Ion Xpress™ Barcode Adapters 1–16 Kit (Thermo, 4471250).
19. Ion Xpress™ Barcode Adapters 17–32 Kit (Thermo, 4474009).
20. Agencourt AMPure XP, 60 mL (Beckman-Coulter, A63881).
21. Ion Library TaqMan™ Quantitation Kit (Thermo, 4468802).

3 Methods

This protocol begins with gDNA extraction from blood collected in PAXgene DNA tubes. However, other collection methods are acceptable. The protocol is geared to manual NGS library

preparation using AmpliSeq™ technology and sequencing on the Ion Proton platform. However, readers may wish instead to utilize automated workflows (i.e., Ion Torrent Chef) and sequencing platforms (i.e., Ion PGM or S5 series) with necessary adjustments.

3.1 gDNA Extraction from PAXgeneDNA Blood Tubes (See Note 3)

1. Transfer blood into a 50 mL processing tube, and invert to mix five times (*see* **Note 1**).
2. Centrifuge at 2,500 × *g* for 5 min.
3. Carefully remove and discard supernatant and add 5 mL BG2, vortex pellet until dissolved.
4. Centrifuge at 2,500 × *g* for 3 min.
5. Discard supernatant and resuspend each sample with freshly prepped 5 mL BG3 + 50 μL PreAnalytiX protease (*see* **Note 2**).
6. Vortex pellet for 20 s.
7. Incubate tubes in the water bath at 65 °C for 10 min, and then vortex on high for 5 s.
8. Add 5 mL isopropanol, and mix by inverting at least 20× (DNA clump should be visible).
9. Transfer DNA clump to 1.5 mL centrifuge tube with as little solution as possible. Discard 50 mL tube and its contents.
10. Centrifuge 1.5 mL tube with DNA clump at 2,500 × *g* for 3 min.
11. Discard supernatant and leave tube inverted on absorbent paper for 1 min.
12. Add 1 mL 70% ethanol and vortex.
13. Centrifuge at 2,500 × *g* for 3 min.
14. Discard supernatant and leave tube inverted on absorbent paper for 5 min.
15. Wipe outside mouth of tube and leave tube inverted for an additional 5 min.
16. Add 1 mL low TE buffer and incubate at 65 °C in the water bath for 1 h.
17. Transfer contents to a fresh, fully labeled 1.5 mL centrifuge tube.
18. Incubate overnight at room temperature before freezing sample at −20 °C, or proceed to purification.

3.2 Purification of gDNA

1. Transfer 10 μL of gDNA to fresh 0.2 μL strip tube.
2. Add 90 μL of low TE buffer to sample and mix (*see* **Note 4**).
3. Add 100 μL of Axygen AxyPrepMag beads to sample (*see* **Note 5**).
4. Incubate at room temperature for 5 min (*see* **Note 6**).

5. Place strip tube onto magnet for 5 min.
6. Remove and discard supernatant while still on the magnet.
7. Add 200 μL of fresh 70% ethanol and rotate tubes on magnet to rotate beads.
8. Remove and discard supernatant while still on the magnet.
9. Repeat ethanol rinse.
10. Spin down tubes briefly and place back on magnet.
11. Air dry for maximum of 5 min; take special care not to over dry.
12. Remove tubes from magnet and resuspend in 20 μL of low TE buffer.
13. Incubate at room temperature for 5 min.
14. Place tubes back on magnet for 5 min.
15. Carefully collect supernatant in fresh labeled 1.5 mL tube.

3.3 Determine gDNA Quality (Optional)

1. Determine the approximate quantity of the gDNA from extractions on a spectrophotometer.
2. If the quantity is 20 ng/μL or more, proceed to 3.4 Quantify gDNA with qPCR kit.
3. If the quantity is less than 20 ng/μL, load 10 μL gDNA, mixed with 2 μL loading dye onto a 1% agarose gel.
4. Run gel for at least 30 min at 120 V.
5. If the gDNA is of good quality, it should visualize as a bright solid single (sometimes two) band(s) at the top of the gel. Proceed to 3.4 Quantify gDNA with qPCR kit.
6. If the band is of poor quality, it is not advisable to proceed to library creation; consider starting gDNA extractions over if possible (*see* **Note 7**).

3.4 Quantify gDNA with qPCR Kit

1. Utilizing TaqMan™ RNase P Detection Reagents and Master Mix, prepare the following standards fresh as follows:

Standard #	Concentration (ng/μL)	Control volume	NFH_2O (μL)
1	5	7.5 μL of Stock	7.5
2	2.5	7.5 μL of Std 1	7.5
3	1.25	7.5 μL of Std 2	7.5
4	0.625	7.5 μL of Std 3	7.5
5	0.3125	7.5 μL of Std 4	7.5
6	0.15625	7.5 μL of Std 5	7.5
7	0.078125	77.5 μL of Std 6	7.5

2. Using the following equation to determine the Master Mix (MM) #:

$$\text{MM\#} = [(7\ \text{Standards} + 1\ \text{negative}) \times 2\ \text{duplicates}] + (\#\text{Samples} \times 2\ \text{dilutions} \times 2\ \text{duplicates})$$

3. For each gDNA sample, prepare 1/10 and 1/50 dilutions.
4. Add 1.25 μL of these diluted samples to designated well on a 96-well plate.
5. To prepare MM, combine the following reagents in a 1.5 mL centrifuge tube:

Component	Volume
TaqMan Universal Master Mix	5 μL × 1.2_{error} × $MM_{\#}$
RNAse P Primer Probe Mix	0.5 μL × 1.2_{error} × $MM_{\#}$
Nuclease-free H_2O (NFH_2O)	3.25 μL × 1.2_{error} × $MM_{\#}$

6. Aliquot 8.75 μL of MM into all the wells containing sample. For a negative control, add 8.75 μL of MM to two wells with 1.25 μL of nano-filtered (NF)-H_2O.
7. Seal plate with adhesive film and spin down.
8. Place the plate into the qPCR machine, and set up the standards and samples to the following settings:
   - Passive reference = ROX
   - Reporter/quencher = TAMRA

   Standard mode:

Stage	Temp (°C)	Time
Hold	50	2 min
Hold	95	10 min
Cycle (40 cycles)	95 60	15 s 1 min

9. To determine the ng/μL concentration, multiply the qPCR C_t value by the dilution factor.

3.5 Ion Torrent AmpliSeq Library Preparation (See Note 8)

1. In 0.1 μL 96-microwell PCR plate, make the following MMs per sample.
   - 4.5 μL 5× Ion AmpliSeq HIFI Master Mix
   - 2 μL gDNA (~20 ng)
   - 11.5 μL NFH_2O

2. In new wells on the PCR plate, add 8 μL of MM per pool for each sample, and then add:
   - 2 μL 2× Ion AmpliSeq primer pool 1 or 2 (i.e., for two-pool panel)
3. Run on PCR machine at (*see* **Note 9**):

Hold	99 °C	2 min
16 cycles	99 °C 60 °C	15 s 4 min
Hold	10 °C	∞

4. After cycling, combine same 10 μL reaction samples into a single well (totaling 20 μL).
5. Add 2 μL FuPa and mix.
6. Run on PCR machine at (*see* **Note 10**):

1 Cycle	50 °C 55 °C 60 °C	10 min 10 min 20 min
Hold	10 °C	1 h (MAX)

7. In a new row of 0.2 mL strip tubes, make the diluted barcode solution mix:
   - 1 μL Ion P1 adaptor
   - 1 μL Ion Xpress Barcode X
   - 2 μL NFH_2O
8. Remove seal and add the following to each well:
   - 4 μL Switch solution
   - 2 μL Diluted barcode solution
9. Add 2 μL DNA ligase to each well. Mix well by pipetting up and down.
10. Run on PCR machine:

1 Cycle	22 °C 68 °C 72 °C 10 °C	30 min 5 min 5 min 24 h

11. Add 45 μL of Agencourt AMPure beads to each well, mix by pipette (*see* **Note 11**).
12. Incubate for 5 min at room temperature.
13. Incubate plate on magnetic rack for 2 min and discard supernatants.

14. While plate is on the magnet, carefully add 150 μL of 70% ethanol to each well.
15. Rock plate and magnet side to side.
16. Remove supernatant.
17. Repeat ethanol rinse again.
18. Air dry pellet for 5 min.
19. Remove plate from magnet.
20. Resuspend the pellet with 50 μL low TE.
21. Incubate plate on magnet for 2 min and transfer supernatant to a new, labeled (sample name and barcode) 1.5 mL centrifuge tube.

3.6 Quantify Libraries with Ion Torrent Library Quantification Kit

1. Prepare the following standards fresh as follows:

Standard #	Concentration (pM)	Control volume	NFH_2O (μL)
1	6.8	2.5 μL of Stock	22.5
2	0.68	2.5 μL of Std 1	22.5
3	0.068	2.5 μL of Std 2	22.5
4	0.0068	2.5 μL of Std 3	22.5
5	0.00068	2.5 μL of Std 4	22.5

2. Using the following equation to determine the Master Mix (MM) #:

$$MM_{\#} = [(5\ \text{Standards} + 1\ \text{negative}) \times 2\ \text{duplicates}] + (\#\text{Samples} \times 2\ \text{dilutions} \times 2\ \text{duplicates})$$

3. For each sample library, prepare dilutions of 1/100 and 1/500.
4. Pipette 4.5 μL into designated well of a 0.1 mL 96-microwell plate or tube.
5. To prepare MM mix the following reagents in a 1.5 mL centrifuge tube (*see* **Note 12**):

Component	Volume
Ion Library TaqMan qPCR Mix 2×	$5\ \mu L \times 1.2_{error} \times MM_{\#}$
Ion Library TaqMan Quantification Assay 20×	$0.5\ \mu L \times 1.2_{error} \times MM_{\#}$
NFH_2O	$2.0\ \mu L \times 1.2_{error} \times MM_{\#}$

6. Aliquot 5.5 μL of MM into all the wells containing sample. For a negative control, add 5.5 μL of MM to 2 wells with 4.5 μL of NFH_2O.
7. Seal plate with adhesive film, and spin down.
8. Place the plate into the qPCR machine, and set up the standards and samples to the following settings:
   - Passive reference = ROX
   - Reporter/quencher = FAM/MGB
   - Fast mode:

Stage	Temp (°C)	Time
Hold	50	2 min
Hold	95	20 s
Cycle (40 cycles)	95 60	1 s 20 s

9. To determine the pM concentration, multiply the qPCR C_t value by the dilution factor.

3.7 Template Preparation

1. Usually, libraries with a concentration of at least 60 pM are suitable for further processing and sequencing.
2. Each library must be diluted to 100 pM or to the concentration of the library with the weakest (i.e., lowest) concentration.
3. Pool barcoded libraries by equal portions, 5 μL of each barcoded library to a single labeled tube (*see* **Note 13**).

3.8 Templating and Sequencing

Libraries are templated using the Ion OneTouch 2 system and Ion PI™ Template OT2 200 Kit v3 (Thermo, 4488318) and then sequenced using the Ion Proton™ System and Ion PI™ Sequencing 200 Kit v3 (Thermo, 4488315). As an example, barcoded libraries, in a batch of 12 to 30 libraries, can be run together on a single Ion PI™ v3 chip (Thermo, 4488315). However, the choice of how many barcoded libraries to pool is influenced by the NGS panel size and desired depth of coverage per sample. Sequences are aligned to the human genome (i.e., version hg19) and variants called in Ion Torrent Suite software.

3.9 Analysis

The analysis described is particular to the custom AmpliSeq™ panel utilized in our laboratory (see refs. [16] and [19]). Users may wish to apply their own analysis, in consultation with local experts and/or the published literature. As an overview, files are uploaded into Ion Reporter and each sample independently filtered through a workflow of optimized and strict variant calling geared to the particular AmpliSeq™ panel. Variants are filtered to exclude common single nucleotide polymorphisms (SNPs) and

synonymous substitutions, variants with low *P*-values or low coverage. Annotation with cancer mutation databases, such as COSMIC (https://cancer.sanger.ac.uk/cosmic), may be helpful, along with assessing the functional impact of variants on the resultant proteins. As mentioned, CHIP variants by definition may present with VAF as low as 0.02, near the limit of detection of conventional NGS, so variant calling in Ion Reporter should be complemented by visual inspection (such as in the Integrated Genomics Viewer, IGV: http://software.broadinstitute.org/software/igv/) to exclude false positives (artifacts). Users may wish to apply other software, besides Ion Reporter and IGV. Finally, validation of variants using orthogonal technology (i.e., ddPCR, other NGS platform, or Sanger sequencing where possible) may also be helpful, particularly when obtaining results from a new NGS panel.

3.9.1 Uploading .vcf File to Ion Reporter

1. Download files to computer hard drive.
2. Log into Ion Reporter.
3. Click on "Define Samples," "Manual."
4. Click on "Upload VCF" found on the left side of the screen.
5. Files must be uploaded one by one. To do this click "Upload VCF" (left-side menu), "Select file" navigating to the .vcf.gz file on your hard drive.
6. Once file is selected, click on the "Upload VCF."
7. Close window.
8. Continue to upload all the .vcf files.
9. In the left-side menu, click the appropriate Data subfile, select the VCF tab, and this should bring up a list of all of the .vcf files uploaded to this account; check the box of the first file you uploaded today.
10. Once the ONE file is selected, click the "Add a Sample" tab to the right side which becomes highlighted in blue.
11. In the box, type in the Sample Name.
12. Once filled in click the "Add to Sample List" button that becomes highlighted in blue.
13. Continue to add .vcf files and their Sample Names until all samples have been properly labeled; click "Next →" at the bottom of the screen.
14. The screen will ask to confirm sex but should auto-fill to Unknown; click "Next →" at the bottom of the screen.
15. "Save" the uploads, and wait for them to load. May take a few minutes.
16. Once they have been successfully uploaded, you will be taken back to the Samples screen.

3.9.2 Analyzing Samples in Ion Reporter

1. At the top of the screen, click on "Analyses" tab.
2. On the right side of the screen, click the blue "Launch Analysis," "Manual."
3. Select "Annotate Variants," scroll down, and click "Next →."
4. Select all of the files to be analyzed; click "Next →."
5. Click "Next →."
6. Each analysis will generate a new name with a "_c###" extension code; consider manually deleting the code, leaving only the sample name as you entered it, for sample naming simplicity.
7. Click "Launch Analysis"; wait for confirmation.
8. Once they have been successfully submitted for analysis, you will be taken back to the Analyses screen; you may notice that the analyses you just submitted are on the list; they are pending and not accessible yet. They may take several minutes to a few hours to be approved.
9. Once the analyses are complete, click on the analysis title to access the variant calls.
10. A list of all the variants will appear; there may be as many as 300 calls.
11. To filter the results, create/select a "Strict" filter on the right-side menu with the following parameters:
    - Include variants as low as VAF=0.02.
    - Filter out synonymous variants.
    - Filter out *P*-value of higher than desired stringency.
    - Filter out all common SNP.
    - Filter out false positives (can annotate/flag, if experienced with NGS panel).
12. Usually, the list of variants will be reduced (i.e., to less than 15 calls).
13. These calls can be copy and pasted into a spreadsheet for analysis or exported.
14. Save Excel file, and use tabs to perform analyses.

3.9.3 Visual Inspection (in IGV)

1. On rare occasion filters fail in eliminating all of the false positive variants. It is recommended to double check suspicious results against the raw .bam file using the Integrated Genomics Viewer (http://software.broadinstitute.org/software/igv/).
2. Download raw Ion Torrent runs (.bam and .bai files) and save files.
    - .bam and .bai files must be in the same folder and have the exact same name to open properly.

3. Open IGV and select the desired genome reference (e.g., hg19).
4. Drag .bam files into IGV or open by file directory in IGV.
5. Copy and paste the chromosome position number of the suspicious variant into the search bar of the IGV program.
6. Scroll down and inspect to determine if features suspicious for false positives:
   - Is the variant found exclusively near the edge of an amplicon?
   - Are mutations only found in one direction (i.e., strand bias)?
   - Is there poor mapping/coverage?
   - Is the variant found in most other samples?
7. Continue this process for all variant calls, and consider orthogonal validation and literature or variant database review as indicated.

3.9.4 Limitations

The detection of CHIP is limited by the choice of targeted genes and coding regions and their amenability to amplicon-based sequencing. The lack of variant detection after applying the recommended filters does not exclude the presence of CHIP. For example, our 48-gene panel does not cover *PPM1D*, a rare CHIP driver in unselected individuals, but more commonly found mutated in patients exposed to cancer chemotherapy [2, 20]. Users may wish to include this gene in their original CHIP panel design or "spike-in" coverage for an existing panel. Moreover, the arbitrarily defined lower bound of CHIP variant frequency (VAF 0.02) is near the limit of detection of conventional NGS, such as described in this protocol. Related to this, a proportion of subjects with CHIP do not have mutations in detectable cancer-driver genes (perhaps related to drifting/contraction of HSC populations with age) [21]. Finally, deep, error-corrected NGS reveals more ubiquitous clonal hematopoiesis in adults at a median VAF at least an order of magnitude lower than CHIP [14], but the protocol as described here is not sensitive enough to detect these mutant clones.

4 Notes

1. Samples should be kept at room temperature for 2 h prior to extraction procedure.
2. After the addition of BG3, samples can be stored for up to 7 days at 4 °C. Add 1.4 mL BG4 to lyophilized PreAnalytiX protease, and store at 4 °C for up to 2 weeks or −20 °C for possible longer storage.

3. Once PaxGeneDNA blood tubes are collected, they may be stored for up to 14 days at room temperature, 28 days at 4 °C, and 3 months at −20 °C.
4. For gDNA extracted from dried cellular smears or FFPE tissue, add 20–50 μL of sample to 100 μL AMPure beads.
5. Axygen Fragment Select beads must be at room temperature for at least 30 min before using. Vortex Fragment Select beads for 30 s prior to use.
6. If bead clumping occurs, start again with a more diluted sample.
7. If the gDNA is of poor quality, it will visualize as the following:
   (a) Multiple bands
   (b) Smear throughout well
   (c) Faint bands/no band(s)
8. When running a multi-pool panel (which has previously been successful) with similar numbers of primer pairs, the target amplification reaction of 20 μL can be split into multiple equal reactions. For example, if working with two primer pools, one can run two 10 μL reactions, and pool them in **step 2**, rather than 20 μL reactions of each pool. This may save on HIFI mix. However, this is not recommended when running an NGS panel for the first time.
9. After initial PCR step, products can stay at 10 °C overnight or −20 °C long term.
10. After second PCR step, products can be stored at −20 °C overnight.
11. Agencourt AMPure XP beads must be at room temperature for at least 30 min before using. Vortex AMPure beads for 30 s prior to use.
12. Do not vortex the Ion Library TaqMan qPCR Mix 2×.
13. Pooled libraries are stable at 4 °C, or months at −20 °C.

Acknowledgments

The authors thank Dr. Harriet Feilloter, Dr. Xudong Liu, Dr. Amy McNaughton, Dr. Xiao Zhang, and Dr. Paul Park for initial assistance with Ion Torrent Sequencing. Funding was provided by the Southeastern Ontario Academic Medical Organization (SEAMO) Innovation Fund, the University Hospitals Kingston Fund (UHKF)/Women's Giving Circle, and the Ontario Institute for Cancer Research (OICR)/Ontario Molecular Pathology Research Network (OMPRN).

References

1. Jaiswal S, Fontanillas P, Flannick J et al (2014) Age-related clonal hematopoiesis associated with adverse outcomes. N Engl J Med 371:2488–2498
2. Genovese G, Kähler AK, Handsaker RE et al (2014) Clonal hematopoiesis and blood-cancer risk inferred from blood DNA sequence. N Engl J Med 371:2477–2487
3. McKerrell T, Park N, Moreno T et al (2015) Leukemia-associated somatic mutations drive distinct patterns of age-related clonal hemopoiesis. Cell Rep 10:1239–1245
4. Steensma DP, Bejar R, Jaiswal S et al (2015) Clonal hematopoiesis of indeterminate potential and its distinction from myelodysplastic syndromes. Blood 126:9–16
5. Shlush LI (2018) Age-related clonal hematopoiesis. Blood 131:496–504
6. Abelson S, Collord G, Ng SWK et al (2018) Prediction of acute myeloid leukaemia risk in healthy individuals. Nature 559:400–404
7. Desai P, Mencia-Trinchant N, Savenkov O et al (2018) Somatic mutations precede acute myeloid leukemia years before diagnosis. Nat Med 24:1015–1023
8. Bowman RL, Busque L, Levine RL (2018) Clonal hematopoiesis and evolution to hematopoietic malignancies. Cell Stem Cell 22:157–170
9. Steensma DP (2018) Clinical consequences of clonal hematopoiesis of indeterminate potential. Blood Adv 2:3404–3410
10. Zhang Q, Zhao K, Shen Q et al (2015) Tet2 is required to resolve inflammation by recruiting Hdac2 to specifically repress IL-6. Nature 525:389–393
11. Fuster JJ, MacLauchlan S, Zuriaga MA et al (2017) Clonal hematopoiesis associated with TET2 deficiency accelerates atherosclerosis development in mice. Science 355:842–847
12. Jaiswal S, Natarajan P, Silver AJ et al (2017) Clonal hematopoiesis and risk of atherosclerotic cardiovascular disease. N Engl J Med 377:111–121
13. Cull AH, Snetsinger B, Buckstein R et al (2017) Tet2 restrains inflammatory gene expression in macrophages. Exp Hematol 55:56–70.e13
14. Young AL, Challen GA, Birmann BM et al (2016) Clonal haematopoiesis harbouring AML-associated mutations is ubiquitous in healthy adults. Nat Commun 7:12484
15. Rothberg JM, Hinz W, Rearick TM et al (2011) An integrated semiconductor device enabling non-optical genome sequencing. Nature 475:348–352
16. Sekeres MA, Othus M, List AF et al (2017) Randomized Phase II Study of azacitidine alone or in combination with lenalidomide or with vorinostat in higher-risk myelodysplastic syndromes and chronic myelomonocytic leukemia: North American Intergroup Study SWOG S1117. J Clin Oncol 35:2745–2753
17. Buscarlet M, Provost S, Zada YF et al (2017) DNMT3A and TET2 dominate clonal hematopoiesis and demonstrate benign phenotypes and different genetic predispositions. Blood 130:753–762
18. Buscarlet M, Provost S, Zada YF et al (2018) Lineage restriction analyses in CHIP indicate myeloid bias for TET2 and multipotent stem cell origin for DNMT3A. Blood 132:277–280
19. Cook E, Izukawa T, Young S et al (2018) Feeding the fire: the comorbid and inflammatory backdrop of clonal hematopoiesis of indeterminate potential (CHIP) by mutation subtype. Blood 130:426
20. Coombs CC, Zehir A, Devlin SM et al (2017) Therapy-related clonal hematopoiesis in patients with non-hematologic cancers is common and associated with adverse clinical outcomes. Cell Stem Cell 21:374–382
21. Zink F, Stacey SN, Norddahl GL et al (2017) Clonal hematopoiesis, with and without candidate driver mutations, is common in the elderly. Blood 130:742–752

Methods in Molecular Biology (2019) 2045: 181–186
DOI 10.1007/7651_2019_207

Published online: 06 March 2019

Column-Free Method for Isolation and Culture of C-Kit Positive Stem Cells from Atrial Explants

Sherin Saheera and Renuka R. Nair

Abstract

Ever since the discovery of stem cells, their isolation from tissues and expansion in culture has been extensively studied due to its potential for therapeutic application. The magnetic-assisted cell sorting (MACS) method is the most widely used technique for the sorting of cells based on their cell surface markers. Though effective, the major drawbacks are high cost and the requirement for the frequent replacement of the columns. In the column-free method, the cells are sorted using the same principle of immune-magnetic isolation but does not require magnetic columns, making it cost-effective. The isolation of c-kit$^+$ stem cells from atrial explants using column-free magnet is found to be efficient and yields homogenous population of stem cells. This method saves time and labor and is economical when working with large sample sizes.

Keywords Cardiac stem cells, C-Kit$^+$, Immuno-magnetic separation, Column-free method

1 Introduction

The field of bench to bedside research gained momentum after the discovery of stem cells. From embryonic to tissue-resident stem cells, a variety of techniques have been employed to isolate the specific cell of interest. Stem cell isolation and culture have been carried out manually by using commercially available kits as well as high-end techniques. However, the purity and the homogeneity of the cultured cells have been a major concern. Here, we describe a cost-effective and efficient column-free method for the isolation of cardiac-specific stem cells from atrial explants. Atrial tissue harbors the majority of cardiac stem cells [1]. Current protocols for isolating c-kit$^+$ cells use magnetic-assisted cell sorting (MACS) from cardiospheres, tissue digests, and atrial explant cultures. High cost and replacement of magnetic columns after every isolation make it incompatible for use for large-sized samples. The use of column-free magnet for sorting cells is a novel improvisation and is now widely used for various other cell types. The procedure for isolation of c-kit$^+$ cells from cultured atrial explants using column-free method based on the principles of immuno-magnetic isolation is described. The cells so sorted were a pure population

of c-kit$^+$ cells without contamination from hematopoietic or endothelial stem cells.

2 Materials

1. Atrial explant culture medium: Iscove's Modified Eagles Medium (IMDM, with L-Glutamine and 25 mM HEPES Buffer) with 10% Fetal Bovine Serum and antibiotics (100 U/mL penicillin G and 100 μg/mL gentamicin).
2. Trypsinizing solution: PBS containing 0.05% trypsin and 0.02% EDTA.
3. Sorting of c-kit$^+$ cells: EasySep^{TM} FITC positive selection kit, EasySep^{TM} magnet (Stemcell Technologies), anti-rat c-kit antibody, anti-rat FITC conjugated secondary antibody.
4. Sorting medium: PBS containing 2% FBS.
5. c-kit$^+$ cell culture medium: Iscove's Modified Eagles Medium (IMDM), 10% fetal bovine serum, 10 ng/ml basic fibroblast growth factor (bFGF), 1 mL/100 mL B27 serum supplement, 500 μL/100 mL Insulin Selenium Transferrite and antibiotics (penicillin and gentamicin).

3 Methods

All procedures to be performed in sterile cabinet.

3.1 Pre-coating of Culture Plates with Gelatin

1. Sterilize 2% gelatin in distilled water.
2. Add 5 mL of gelatin solution to 100 mm dishes, and leave it in the clean air cabinet for 20 min.
3. Remove the gelatin and allow the dishes to dry for 1 h in the hood. If the culture plates are not for immediate use, they should be sealed and stored at 4 °C.

3.2 Rat Atrial Explants Are the Source of C-Kit$^+$ Cells

1. For the isolation of c-kit$^+$ stem cells from atrial explants, the animals should be sacrificed and the heart excised immediately in sterile conditions.
2. Sterilize all surgical instruments; autoclave phosphate-buffered saline (PBS), and filter sterilize the medium before starting the experiment.
3. Pre-coat the culture dishes with gelatin.

3.3 Sacrifice of Animal and Isolation of Atrial Tissue

1. Rats are anesthetized by injection of xylazine (5 mg/kg) and ketamine (70 mg/kg).

2. After clamping to the surgical board, wipe with 70% alcohol and betadine. With surgical blades, cut the skin and remove the outer layer.
3. Wipe with betadine and cut open the chest.
4. Without disturbing the other blood vessels, cut a few mm above the aorta and excise the heart.
5. Immerse in cold Ca^{2+}/Mg^{2+}-free PBS, and wash it thoroughly to get rid of all the blood. Place the heart in a petri dish with PBS, remove all the adherent fat and other tissues, and separate the atria from the ventricles.
6. Atria should be washed in PBS 2–3 times before using it for the atrial explant culture.

3.4 Atrial Explant Culture

1. Using surgical blades mince the atrial tissue into small pieces of about 2 mm^3.
2. Wash extensively in fresh cold PBS, and carefully seed onto the surface of gelatin-coated dishes, and supplement with 1.5 mL of explant culture medium.
3. Ensure that the explants settle on the culture surface, and do not float in the medium. On the following day, gently supplement 3 mL of the same medium without disturbing the explants.
4. Carefully replace 2 ml medium from the top once in 3 days.
5. Fibroblast-like cells migrate from the explants in 5–6 days and become confluent within 2 weeks (Fig. 1i–iv). Then, round phase-bright cells start migrating from the explant and are seen loosely attached to the fibroblast layer. Once there are enough number of phase-bright cells, subject the explant culture to mild trypsinization.

3.5 Trypsinization for Isolation of the Migrated Cells

1. Remove the medium in the culture plate, and wash the cells carefully with PBS.
2. Incubate the cells with the trypsinizing solution for about 2 min at 37 °C.
3. Neutralize the reaction by adding double the volume of serum containing medium. Collect the medium and centrifuge at $112 \times g$ for 5 min.
4. Wash the cells with PBS to remove any trace of trypsin, and resuspend in PBS containing 2% FBS for sorting c-kit^+ cells.

Sorting of c-kit^+ cells: C-kit^+ cells are sorted using the EasySep™ magnet and EasySep FITC positive selection kit. The EasySep™ magnet is designed for cell separation procedures using EasySep™ reagents.

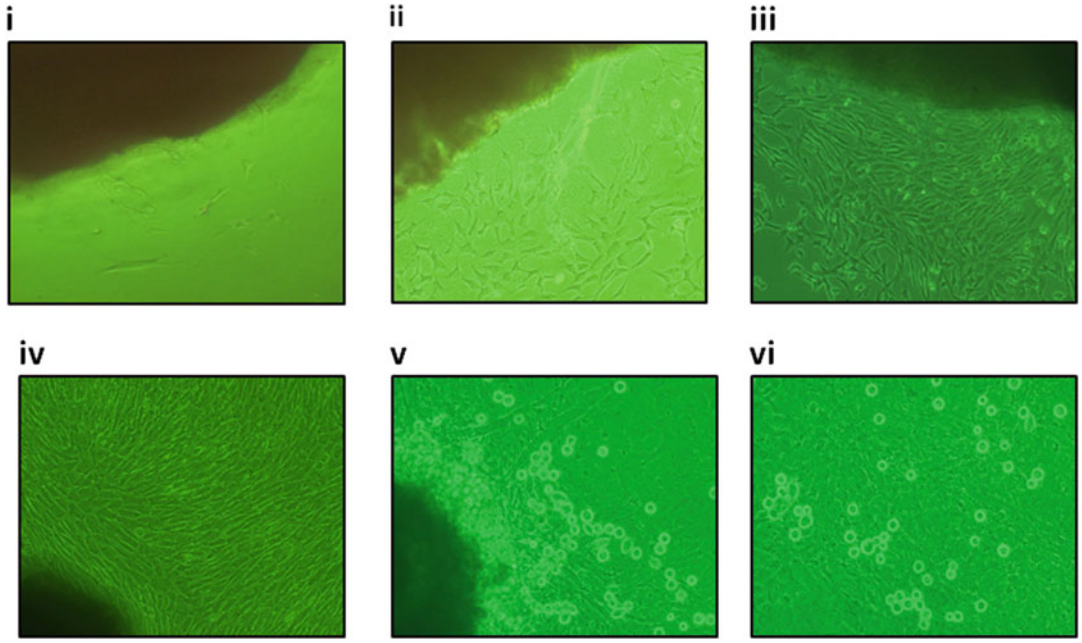

Fig. 1 Representative phase-contrast images of atrial explant culture. Atrial explants were placed on gelatin-coated dishes and supplemented with IMDM containing 10% FBS and antibiotics. (i–iii) 3rd, 5th, and 7th Day—Atrial explants attached to the culture surface and cells started migrating from the explant. (iv) 9th Day—Monolayer of fibroblast-like cells is seen around explants. (v–vi) 12th Day—Small, round, phase-bright cells are seen migrating from the explant

3.6 EasySep™ Reagents (See Note 1)

The EasySep™ Magnet generates a high gradient magnetic field in the interior cavity which is strong enough to separate cells labeled with magnetic EasySep™ particles without the use of columns. This magnet is designed to hold a standard 5 mL (12 × 75 mm) polystyrene round-bottom tube.

1. Suspend a total of two million cells in the sorting medium, and incubate with the primary rat anti-c-kit antibody for 30 min (*see* **Note 2**).
2. Wash and incubate the cells with secondary anti-rat FITC for 15 min.
3. After washing, add 10 μL FITC selection cocktail, and incubate for 15 min.
4. Add 5 μL of magnetic nanoparticles and allow it to stand for 10 min.
5. Bring the volume of sorting medium to 2.5 mL, and let it stand in the magnet for 5 min.
6. Pour out the medium without removing the tube from the magnet.

7. Repeat the washing **steps 2** to **3** times to ensure maximum purity.
8. Remove the tube, and wash with the c-kit growth medium, and plate it onto pre-coated 35 mm dish (*see* **Note 3**).
9. The total time for sorting is 30 min after binding with the appropriate antibody.
10. The c-kit positive cells are expanded in culture (*see* **Note 4**).

4 Notes

1. While using the isolation kit, properly mix the reagents with the cell suspension. Properly mix magnetic nanoparticles before and after addition.
2. The efficiency of sorting will depend on the initial cell count. So exercise caution in maintaining the appropriate cell density, and do not add more than what is recommended.
3. Since the initial cell yield after sorting is very low, it is recommended to seed in plates with smaller surface area to enhance plating efficiency and proliferation. On seeding in larger plates, the cultures have to be kept for about a week or two to see the small cell clones. Change the medium only after the colonies have formed.
4. By the third day after plating the immune-magnetically sorted, cells can be seen attaching to the culture surface (Fig. 2i). Initially, cell numbers will be very low. However, by virtue of the self-renewal capacity of stem cells, they proliferate rapidly and form clusters by the sixth day (Fig. 2ii). The cultures become confluent in less than 2 weeks (Fig. 2iii).

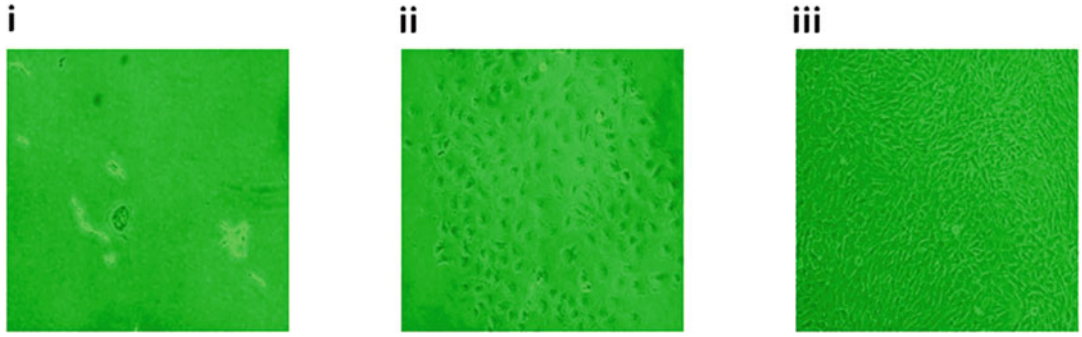

Fig. 2 Culture of c-kit^{+} cardiac stem cells isolated by immuno-magnetic isolation. Cells that migrated from atrial explants were trypsinized and subjected to immuno-magnetic isolation using anti c-kit FITC antibody. (i) 3rd Day—Isolated round cells attached to the culture surface. (ii) 6th Day—Attached cells formed clusters. (iii) 12th Day—Confluent culture of CSCs

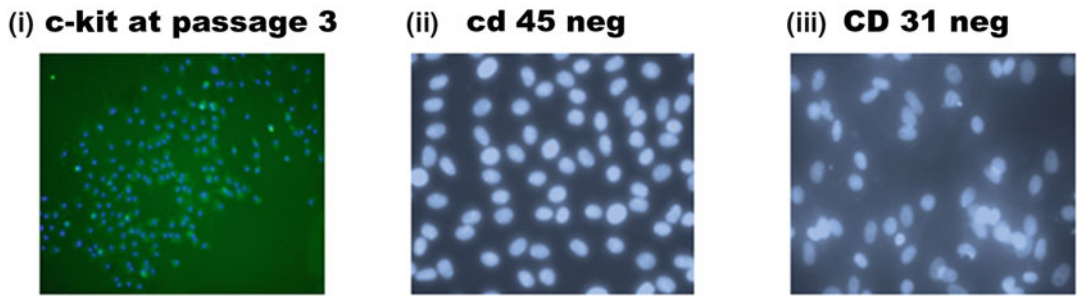

Fig. 3 Representative images of immunocytochemistry for the expression of cell surface markers. (i) Merged image of CSCs expressing c-kit shown as green where nuclei is stained blue. (ii) Merged image of CSCs expressing CD45 where nuclei is seen as blue. (iii) Merged image of CSCs expressing CD31 where nuclei is stained blue. Figures are adapted with modification from an earlier publication (Ref. No. 2)

Change the medium every 3rd day. Once confluent, passage them, and characterize the cells at passage 3 using cell-specific markers by FACS and immunocytochemistry. On the average more than 90% of the cells are positive for c-kit and negative for hematopoietic and endothelial markers (Fig. 3) as reported earlier [2]. The sorting of cells using column-free magnet is advantageous in terms of cost, labor, and time. Shorter isolation time and lower mechanical damage are expected to enhance cell viability.

References

1. He J-Q, Vu DM, Hunt G et al (2011) Human cardiac stem cells isolated from atrial appendages stably express c-kit. PLoS One 6:e27719
2. Saheera S, Nair RR (2017) Accelerated decline in cardiac stem cell efficiency in spontaneously hypertensive rat compared to normotensive Wistar rat. PLoS One 12:e0189129

Methods in Molecular Biology (2019) 2045: 187–199
DOI 10.1007/7651_2019_214

Published online: 20 March 2019

Histological Assessment of Cre-loxP Genetic Recombination in the Aging Subventricular Zone of Nestin-CreER^{T2}/Rosa26YFP Mice

Saad Omais, Nour N. Halaby, Karl John Habashy, Carine Jaafar, Anthony T. Bejjani, and Noël Ghanem

Abstract

The use of inducible transgenic Nestin-CreER^{T2} mice has proved to be an essential research tool for gene targeting and studying the molecular pathways implicated in adult neurogenesis, namely, inside the adult subgranular zone (SGZ) of the dentate gyrus and the adult subventricular zone (SVZ) lining the lateral ventricles. Several lines of Nestin-CreER-expressing mice were generated and used in adult neurogenesis research in the past two decades; however, their suitability for studying neurogenesis in aged mice remains elusive. Here, we assessed the efficiency of Cre-loxP genetic recombination in the aging SVZ using the Nestin-CreER^{T2}/Rosa26YFP line designed by Lagace et al. (J Neurosci 27(46):12623–12629, 2007). This analysis was performed in 12-month-old (middle-aged) mice and 20-month-old (old) mice compared to 2-month-old (young adult) mice. To evaluate successful recombination, our approach relies on the histological assessment of Cre mRNA level of expression and the YFP reporter gene's expression inside the aging SVZ by combining in situ hybridization and immunohistochemistry. Using co-immunolabeling, this approach also provides the advantage of estimating the percentage of recombined progeny [(GFP+Nestin+)/Nestin+] and the rate of cell proliferation [(GFP+Ki67+)/GFP+] inside the aging SVZ niche.

Keywords Adult neurogenesis, Subventricular zone, Neural stem and progenitor cells, Aging, Nestin-CreER^{T2}/Rosa26YFP mice, Immunohistochemistry, In situ hybridization

1 Introduction

Research in the field of adult neurogenesis has grown rapidly over the past five decades [1]. Such success could not have been possible if not for the development of various genetic tools, particularly viral and transgenic reporter mouse models [2]. A remarkable example is the inducible and conditional Nestin-CreER^{T2} model system, whereby the expression of the Cre recombinase enzyme (fused with a mutated estrogen receptor) is regionally controlled by the Nestin promoter in combination with various genetic elements (e.g., exon(s) 1–3 and/or second intron of the Nestin gene). Nestin is an intermediate filament protein and well-characterized marker of neural stem and progenitor cells, also known to be highly

expressed in the canonical neurogenic sites of the adult mammalian brain: the subventricular zone (SVZ) lining the lateral ventricles (LV) and the subgranular zone (SGZ) of the hippocampal dentate gyrus. Upon tamoxifen (TAM) administration, the Cre enzyme undergoes nuclear translocation and excises sequence(s) of interest that are flanked by loxP sites (e.g., specific exon(s), a stop cassette) in order to induce gene deletion(s) and/or reporter gene expression [3, 4]. The genetic manipulation of adult neurogenesis using Cre-expressing reporter mice including Nestin-Cre lines has been previously reviewed [5, 6].

Several discrepancies with respect to specificity and efficiency of reporter gene's expression have been described in distinct Nestin-CreER^{T2} mouse lines (reviewed in [7]). Such differences could be attributed to three main factors: (1) a strain-specific effect (genetic background), (2) regional differences in reporter gene's expression due to various transgene insertion sites and/or distinct reporter lines used such as different levels of expression in the SVZ versus the SGZ in the same line and ectopic expression in non-neurogenic sites such as the hypothalamus and the cerebellum, and (3) the survival period following tamoxifen administration, namely, the interval associated with peak in reporter expression which can be variable among distinct lines and/or neurogenic sites [5]. For instance, the Nestin-CreER^{T2} designed by Lagace et al. was consistently more region-specific but less efficient in terms of recombination efficiency in the adult brain compared to similar lines created by Dranovsky et al., Imayoshi et al., and Suzanne J. Baker's laboratory which showed higher recombination efficiency but with substantial ectopic expression [3, 4, 7–9].

In addition to the above, recent attention has shifted to the study of adult neurogenesis during aging [10], and studies have also used Nestin-CreER^{T2} lines for this purpose. For instance, one study established the long-term/continuous requirement of adult neurogenesis in the structural integrity of the mouse olfactory bulb [11], while another study characterized the role of the cell cycle inhibitor – Btg1 – in age-dependent maintenance of neural stem cell self-renewal and expansion capacity [12]. However, such studies relied on initial tamoxifen treatments that were performed in young adult mice, e.g., 2-month-old followed by long survival periods (e.g., 12–18 months) which could not only result in suboptimal targeting of the Nestin-positive cell population in the neurogenic sites over time but would also confound potentially distinct roles of the target genes or molecular processes in young adult mice versus old mice. To our knowledge, no study has thus far addressed the specificity or efficiency of the Nestin-CreER^{T2} transgenic model system inside the aging neurogenic sites following acute treatment, e.g., 30-day survival period.

In this chapter, we assessed the efficiency of Cre-loxP genetic recombination in the aging SVZ using the Nestin-CreER^{T2}/Rosa26YFP line designed by Lagace et al. in combination with Rb$^{floxed/floxed}$ line [13], both of which we have previously used to study the role of the Retinoblastoma protein, Rb, during adult neurogenesis in young adult mice [4, 14]. In this Nestin-Cre line, the reporter cassette is comprised of a stop codon that is flanked by two loxP sites and located ahead of the YFP gene [15]. We performed tamoxifen treatments (or vehicle-only treatment) in 12-month-old (12 m; middle-aged) mice and 20-month-old (20 m; old) mice compared to 2-month-old (2 m; young adult) mice, all carrying the Nestin-CreER^{T2}/Rosa26YFP genotype/Rb$^{flox/+}$ (phenotypically similar to Rb$^{+/+}$ or wild-type mice). Mice were sacrificed 30 days later. Successful Cre recombination was examined by histological assessment of Cre mRNA level of expression and YFP gene expression inside the aging SVZ by combining in situ hybridization and immunohistochemistry on adjacent brain sections (Fig. 1). Using double immunohistochemistry, we further show that this model system provides the advantage of estimating the percentage of recombined progeny [(GFP+Nestin+)/Nestin+] (Fig. 2) and the rate of cell proliferation [(GFP+Ki67+)/GFP+] (Fig. 3) inside the aging SVZ niche. Our preliminary analyses indicate that the efficiency of recombination remains largely consistent across all age groups despite age (70% in 12 m, 79% in 20 m versus 75–85% in 2 m; [14]), whereas the rate of cell proliferation steadily decreases with age (23% in 12 m, 13% in 20 m versus 30% in 2 m; [14]).

This study highlights the efficiency of the Nestin-CreER^{T2}/Rosa26YFP mouse line (and potentially other Nestin-Cre lines) for studying the age-specific alterations inside the brain neurogenic niches, in hopes of better understanding their contribution to neuronal plasticity [16] as well as their potential involvement in neurodegenerative diseases [17, 18].

2 Materials

2.1 Solvents, Solutions, and Buffers

1. Phosphate Buffer Saline (PBS): To prepare 1 L of 10× PBS, dissolve 80 g of NaCl, 14.4 g of Na_2HPO_4, 2 g of KCl, and 2.4 g of KH_2PO_4 in 1 L of deionized distilled water (ddH_2O). Autoclave solution and adjust the pH to 7.4 with 1 N HCl. To prepare 1 L of 1× PBS, dilute 100 mL of 10× PBS in 900 mL of ddH_2O, and then readjust the pH to 7.4.
2. Riboprobe Synthesis Mix: Add 5 μL of 5× transcription buffer (Thermo, Lot# 00462634), 2 μL of T7 RNA polymerase (Thermo, Lot# 00463555), 2 μL of 100 mM of 1,4-dithiothreitol (DDT), 1 μL of RiboLock RNase inhibitor

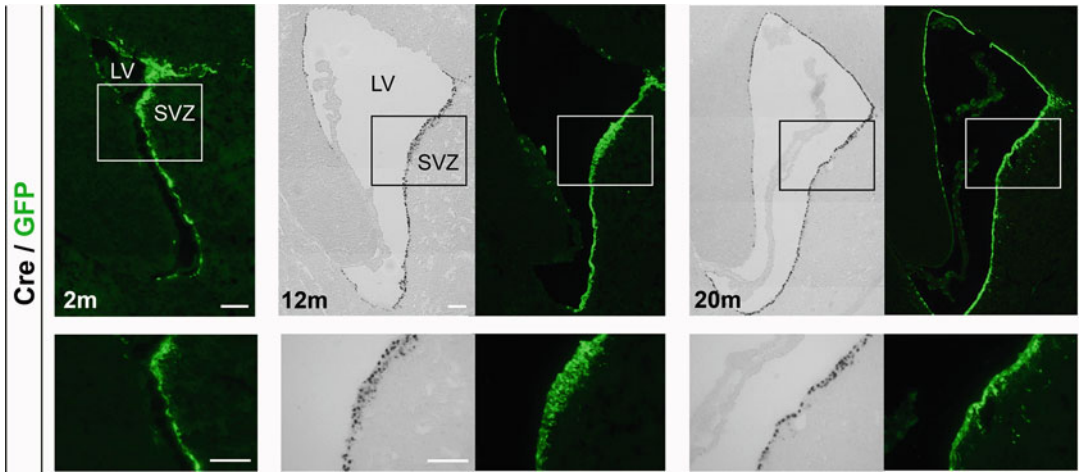

Fig. 1 Comparison of Cre and YFP expressions in the adult subventricular zone of Nestin-CreER^{T2}-YFP young adult, middle-aged, and old mice. Top panels showing immunofluorescent staining against GFP (in green) and in situ hybridization with an antisense Cre riboprobe (in black; bright field) performed on adjacent sections in 2-month-old mice (2 m), 12-month-old mice (12 m), and 20-month-old mice (20 m). In each age group, mice were treated with tamoxifen for 5 consecutive days and sacrificed 28 days later. Bottom panels are higher magnification images of the boxes shown in top panels, respectively. Scale bar = 100 μm. *LV* lateral ventricle, *SVZ* adult subventricular zone

(Thermo, Lot# 00095453), and 2.5 μL of 10× Dig RNA Labeling Mix (Roche, 11277073910) to 0.5–1 μg of Cre cDNA (pooled and purified from PCR product) diluted in 12.5 μL.

3. 10× Salt: To prepare 1 L, dissolve 114 g of NaCl, 14.04 g of Tris–HCl (pH=7.5), 1.34 g of Tris base, 7.8 g of $NaH_2PO_4 \cdot 2H_2O$, and 7.1 g of Na_2HPO_4 in 1 L of DEPC distilled water, and then add 100 mL of 0.5 M EDTA.
4. 50% Formamide: To prepare 50 mL, dilute 25 mL of formamide in 25 mL ddH_2O, and then add 2.5 mL of 10× salt.
5. Denhardt's solution: to prepare 50 mL of 100× Denhardt's solution, dissolve in DEPC H2O 2% or 1 g (weight/volume) of each of the following chemicals: bovine serum albumin (BSA), Ficoll and polyvinyl pyrolidone. Make aliquots and store at −20 °C.
6. rRNA: dissolve yeast ribosomal RNA (rRNA) in DEPC water at 10 mg/mL. Heat to 65 °C to help dissolve better. It is fine if not all rRNA enters solution. Make aliquots and store at −20 °C.
7. Hybridization Buffer: To prepare 50 mL, mix 5 mL of 10× salt, 25 mL of deionized formamide, 10 mL of 10% dextran sulfate, 5 mL of 10 mg/mL rRNA, 500 μL of 100×

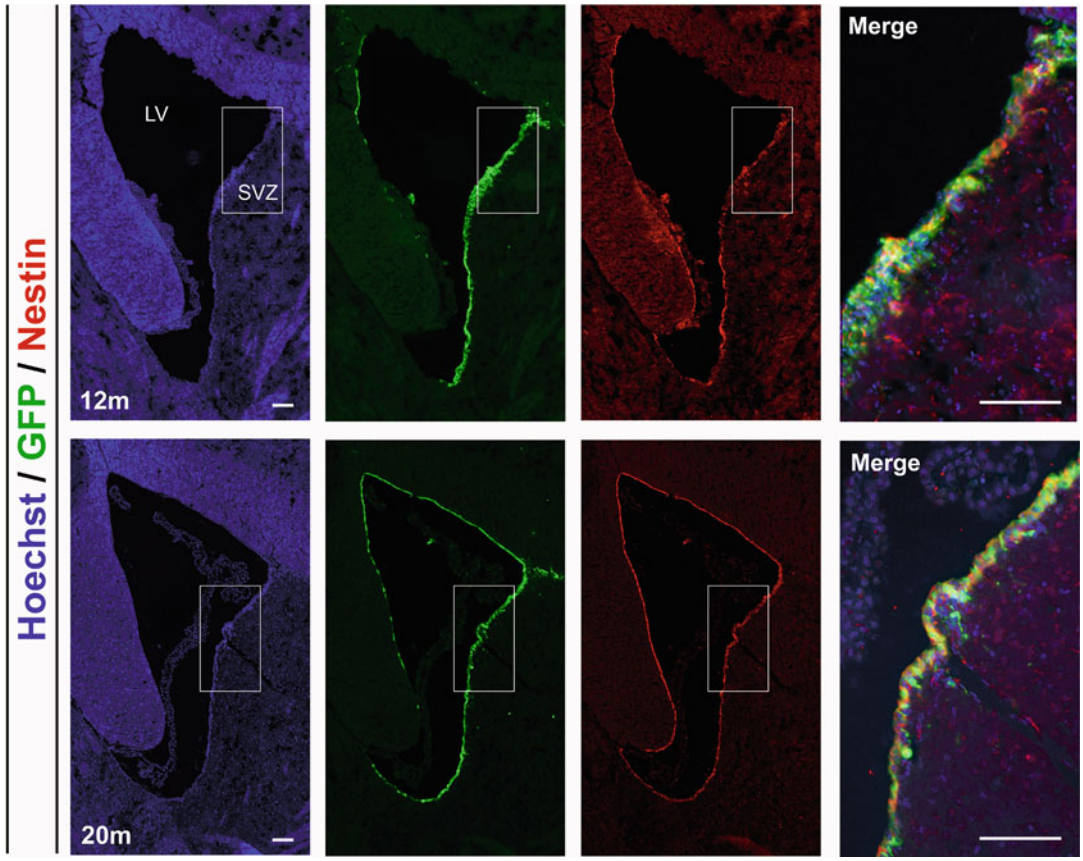

Fig. 2 Histological assessment of Cre recombination efficiency in the adult subventricular zone of Nestin-CreER^{T2}-YFP middle-aged and old mice. Panels showing immunofluorescent staining for Hoechst (in blue), anti-GFP (in green), and anti-Nestin (in red): top panels, 12-month-old mice; lower panels, 20-month-old mice. The merged panels correspond to higher magnification images of the regions shown in boxes in each age group. Experimental diagram and legend as in Fig. 1, scale bar = 100 μm

Denhardt's reagent, and 4.5 mL of Baxter H_2O. Mix well to dissolve and store at −20 °C.

8. Saline Sodium Citrate (20× SSC): To prepare 250 mL, dissolve 43.8 g of NaCl and 22.05 g of sodium citrate in 250 mL ddH_2O. Autoclave solution and adjust pH to 7.
9. Wash Buffer: To prepare 90 mL, mix 45 mL of deionized formamide with 4.5 mL of 20× SSC and 900 μL of 10% Tween-20, and then complement with ddH_2O. This solution is prepared fresh and directly pre-warmed at 65 °C before use (*see* **Note 1**).
10. Maleic Acid Buffer-Tween (MABT): To prepare 1 L of 5× MABT, dissolve 58.05 g of maleic acid in ~850 mL ddH_2O, and then add an initial mass of 34 g of NaOH pellets, and keep adding while monitoring the solution's pH to reach a reading

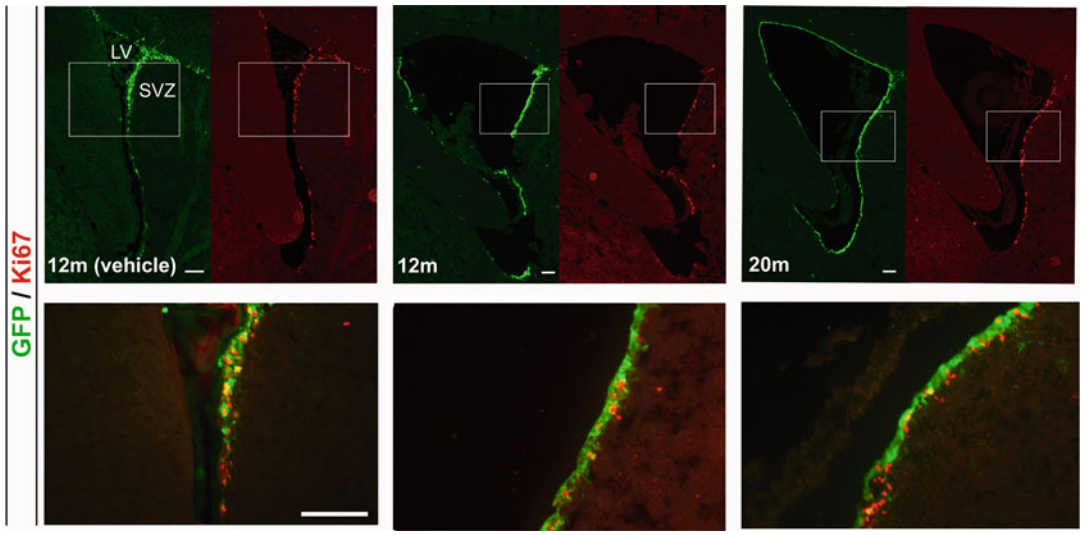

Fig. 3 Histological assessment of neural stem/progenitor cells' proliferation in the adult subventricular zone of Nestin-CreER^{T2}-YFP middle-aged and old mice. Top panels showing immunofluorescent staining with anti-GFP (in green) and anti-Ki67 (proliferation marker; in red) in 12-month-old vehicle-treated mice, 12-month-old and 20-month-old tamoxifen-treated mice, respectively. Lower panels are merged and higher magnification images of the regions shown in boxes in each age group. Experimental diagram and legend as in Fig. 1, scale bar = 100 μm

of 7.5. Last, add 43.8 g of NaCl and 5 mL of Tween-20. Finally, complement volume with ddH_2O to reach 1 L. To prepare 1 L of 1× MABT, dilute 200 mL in 800 mL of ddH_2O.

11. Blocking Reagent (10%): To prepare 50 mL, dissolve 5 g of blocking reagent in 10 mL of 5× MABT, and complement with ddH_2O to reach final volume. Heat might be needed to dissolve the reagent. Store in aliquots at −20 °C.
12. In Situ Hybridization Blocking Solution: To prepare 5 mL, add 1 mL of 100% sheep serum, 1 mL of 10% blocking reagent, and 1 mL of 5× MABT to 2 mL of RNase-/DNase-free H_2O.
13. Pre-stain Buffer: To prepare 90 mL, mix 1.8 mL of 5 N NaCl, 9 mL of 1 M Tris (pH=9), 900 μL of 10% Tween-20, and 4.5 mL of 1 M $MgCl_2$ in 73.8 mL of ddH_2O.
14. Stain Buffer: To prepare 40 mL, mix 0.8 mL of 5 N NaCl and 4 mL of 1 M Tris (pH = 9) in 32.8 mL of ddH_2O. Weigh 4 g of polyvinyl alcohol (PVA), and add to buffer while stirring gently. Heat to help dissolve but do not exceed 80 °C. Once dissolved, allow to cool down, and then add 0.4 mL of 10% Tween-20 and 2 mL of 1 M $MgCl_2$. Just before use, add 180 μL of 4-nitro blue tetrazolium chloride (NBT, prepared at 100 mg/mL in 70% dimethylformamide (DMF)), and allow to stain the solution, followed by 140 μL of 5-bromo-4-chloro-3-indolyl-phosphate (BCIP, prepared at 50 mg/mL in 100% DMF) (*see* **Note 2**).

15. Immunohistochemistry Blocking Solution: To prepare 1 mL, dissolve 0.01 g of bovine serum albumin (BSA), 50 μL of donkey serum (final concentration, 5%), and 30 μL of 10% Triton-X (final concentration, 0.3%) in ~920 mL of 1× PBS (*see* **Note 3**).

2.2 Riboprobe Primers and Antibodies

1. Cre Riboprobe Primers: we designed and used the following primers to make a Cre riboprobe – (5′ to 3′) forward primer GCAGAACGAAAACGCTGGTT and reverse primer TTGCCCCCGTTTCACTATCC. A T7 promoter (TAATACGACTCACTATAGGG) was added ahead of the reverse primer to create the antisense riboprobe. The amplified product is a 411-bp fragment with Cre recombinase sequence (NCBI, GenBank reference sequence: X03453.1), which was amplified by PCR using cDNA extracted from GFP-positive neurospheres (derived from cultured Nestin-CreER^{T2}/YFP SVZ tissue). Fragment size was confirmed by gel electrophoresis following PCR amplification and, later on, after riboprobe synthesis.
2. Primary Antibodies: double immunohistochemistry was done by combining chicken anti-GFP (1:1000, Abcam ab13970) with rabbit anti-Ki67 (1:500, Cell Marque) and chicken anti-Nestin (1:100, Abcam ab134017) with rabbit anti-GFP (1:300, EnCor RPCA-GFP). All sections were counterstained with Hoechst (1:50,000, Invitrogen H21486). For in situ hybridization, sheep anti-digoxigenin-alkaline phosphatase (α-Dig) (Roche, 11093274910) was used at 1:1500.
3. Secondary Antibodies: we used Alexa Donkey anti-chicken 488, Alexa Donkey anti-rabbit 488, Donkey anti-rabbit Cy3, and Donkey anti-chicken Cy3 at 1:400.

3 Methods

3.1 Animals and Tissue Preparation

Mice of three different age groups (2 m, 12 m, and 20 m) carrying the Nestin-CreER^{T2}/Rosa26^{YFP}/Rb$^{+/-}$ genotype were generated as described earlier [14]. All animal experiments were performed in accordance with the approved guidelines of the institutional animal care and use committee (IACUC) of the American University of Beirut, which abides by the guidelines of the Canadian Council on Animal Care. Mice received TAM treatment (Sigma T5648-5G, prepared at 30 mg/mL in 90% sunflower oil and 10% ethanol absolute) made daily before each injection. 180 mg/kg of tamoxifen solution was administered to animals by intraperitoneal (ip) injection (*see* **Note 4**) for 5 consecutive days according to body weight, and animals were sacrificed 30 days later. Mice received a combination of xylazine/ketamine anesthetic followed

by pericardial perfusion to efficiently fix the brains in 4% paraformaldehyde (PFA). Following dissection, brains were further bathed in 4% PFA overnight and then subjected to a sucrose gradient from 20% to 30% over 3–5 days to ensure tissue dehydration. Finally, tissues were snap-frozen in cold isopentane (−35 °C to −38 °C) and stored at −80 °C. When ready for use, brains were embedded in OCT medium (Tissue-Tek, Surgipath) and sectioned using a cryostat at a thickness of 10 μm on superfrost slides and then stored in −80 °C pending histological treatment. For in-depth description of this step, please refer to [19].

3.2 In Situ Hybridization

3.2.1 Riboprobe Synthesis

1. Run multiple PCR reactions with the Cre riboprobe primers using cDNA extracted from any Cre-expressing tissue, e.g., GFP-positive neurospheres as described above.
2. After verification of the right PCR product on DNA gel electrophoresis (run 2 μL of each PCR reaction), pool the amplified Cre cDNA product from all PCR reactions, and purify using GFX™ PCR DNA and Gel Band Purification Kit (GE Healthcare). Quantify the purified Cre cDNA fragment (eluted in a final volume of ~25–30 μL) using a nanodrop, and then prepare the desired volume for riboprobe synthesis mix in RNase-free water (i.e., 12.5 μL) assuming ~0.5–1 μg of starting cDNA is needed.
3. Incubate the mix at 37 °C for 2–3 h. Afterward, add 2.5 μL of 4 M lithium chloride to the resulting solution/product, and mix well by pipetting, and then add 75 μL of pre-chilled 100% RNase-free ethanol. Mix well and store at −80 °C for at least 30 min (or at −20 °C overnight).

3.2.2 Riboprobe Purification

1. Centrifuge the riboprobe mix at maximum speed in 4 °C for 15–20 min.
2. Remove carefully the supernatant; add 100 μL of 70% cold ethanol to wash the pellet, and then centrifuge at maximum speed for 8–10 min.
3. Decant the supernatant and allow the pellet to air-dry. Add 50 μL of RNase-/DNase-free water with 1 μL of RNase inhibitor. Mix by pipetting carefully to help dissolve the RNA. Keep solution on ice.
4. Take 2–3 μL of riboprobe, and mix with appropriate volumes of water and gel loading dye to a final concentration of 1×: incubate in a heat block at 75 °C for 10 min, and then put immediately on ice for 5–10 min (this step will resolve the secondary structure(s) of RNA).

5. Run the sample on a DNA gel for 20–25 min at 180 V. Verify the size of riboprobe product (*see* **Note 5**).
6. Make several aliquots of the riboprobe (e.g., 5 μL each) and store at −80 °C.

3.2.3 Riboprobe Hybridization

1. Pre-warm the hybridization oven at 65 °C. Meanwhile, warm the slides at room temperature (RT) for at least 30 min (*see* **Note 6**).
2. Pre-warm a sealable plexiglass box or humidifying chamber (containing two sheets of Whatman paper wet with 50% formamide) in the oven at 65 °C. Also, pre-warm the hybridization buffer (stored at −20 °C) in the oven at 65 °C for at least 30 min (volume of buffer depends on the number of slides; prepare 200–250 μL/slide).
3. Add the riboprobe to the hybridization buffer at the desired dilution, e.g., 1:500 (ranging from 1:250 to 1:1000; this depends on the intensity and specificity of the probe).
4. Vortex well for 1–2 min and then incubate at 65 °C for 5–10 min. Repeat this step twice.
5. Place the slides in the plexiglass/humidified chamber. Vortex quickly the riboprobe solution, and then add immediately to the slides. Place coverslips gently to ensure proper buffer distribution.
6. Incubate the slides overnight at 65 °C.

3.2.4 Post Hybridization Washes

1. Prepare fresh wash buffer, and pre-warm it at 65 °C for at least 30 min (*see* **Note 7**).
2. Remove all slides from the hybridization chamber/oven, and hold vertically for the coverslips to fall off gently; do not exert excessive force as this may distort the tissues (*see* **Note 8**).
3. Transfer the slides into a Coplin jar containing the pre-warmed wash buffer. Incubate in the oven at 65 °C for 30 min with gentle shaking. Repeat this washing step twice.
4. Transfer the slides into a Coplin jar containing 1× MABT. Wash three times, 20 min each, at RT on rotating shaker.

3.2.5 Blocking and Anti-digoxigenin Staining

1. Remove the slides from the Coplin jar, remove the excess liquid, and then outline the sections with a hydrophobic pen, and place in humidified chamber.
2. Add the in situ hybridization blocking solution to the slides (~200 μL/slide). Incubate at RT for 1.5–2 h.
3. Remove the blocking solution from the slides, and then add the α-Dig, prepared at 1:1500 in the same blocking solution (~200 μL/slide).

4. Incubate the slides with α-Dig in the humidified chamber overnight at RT.

3.2.6 Post-antibody Washes and Substrate Reaction

1. Wash the slides 4–5 times, 20 min each, with 1× MABT at RT on a rotating shaker.
2. Meanwhile, prepare the pre-stain and stain buffers as detailed above.
3. Incubate the slides twice with the pre-stain solution, for 10 min each, in a Coplin jar on the rotating shaker.
4. Transfer the slides into a new covered Coplin jar containing the staining buffer (*see* **Note 9**).
5. Incubate the staining reaction in the dark at RT. mRNA Cre staining takes around 3 h to develop (Fig. 1). If left overnight, the staining intensifies, but no background is formed (*see* **Note 10**).
6. Stop the staining reaction, and remove the staining buffer by washing several times in 1× PBS (*see* **Note 11**).
7. Mount slides with coverslips using (1:1) glycerol/PBS solution. Store slides at 4 °C.

3.3 Immunohistochemistry

1. Slides with matching SVZ levels are taken out from −80 °C and left to dry out at RT for 30–60 min inside a slide box or by using a slide warmer.
2. Wash slides once with 1× PBS in a Coplin jar on a rotating shaker to remove embedding medium.
3. Remove excess liquid, and mark slides with a hydrophobic pen around the sections. Add immunohistochemistry blocking solution to slides for 1–2 h in a humidified chamber.
4. The following two combinations of antibodies is added (~200 μL/slide): chicken anti-nestin (1:100) with rabbit anti-GFP (1:300) (Fig. 2) and chicken anti-GFP (1:1000) with rabbit anti-Ki67 (1:500) (Fig. 3) (*see* **Note 12**). Primary antibodies' dilutions are made in the same blocking solution. Incubate slides in primary antibodies overnight in a humidified chamber.
5. The next day, wash 2–3 times in 1× PBS, 5–10 min each, to remove non-specific binding of primary antibody.
6. Add secondary fluorescent antibodies diluted in blocking solution at 1:400 (~200 μL/slide). Two combinations of Donkey-based antibodies were used: anti-chicken 488 with anti-rabbit Cy3 and anti-rabbit 488 with anti-chicken Cy3. Slides are then left in secondary antibodies for 1–2 h.
7. Wash 2–3 times in 1× PBS, 5–10 min each, to remove non-specific binding of secondary antibodies.

8. Mount slides in (1:3) glycerol/PBS solution with coverslips.
9. Staining can be observed with fluorescent microscopy using the proper filters (e.g., upright Leica microscope (DM6B)), and counts were made using ImageJ software.

4 Notes

1. Deionized formamide takes some time to thaw. It is recommended to remove it from −20 °C to 4 °C 1 day earlier, that is, 1 day prior to in situ hybridization day 1 (Subheading 3.2.3).
2. Just before adding the slides to the staining jar, make sure that no bubbles are formed in the staining buffer. This can be avoided by stirring gently with a magnetic stirrer for a couple of minutes.
3. A final concentration of 0.1% Triton-X also works with GFP, Nestin, and Ki67 immunohistochemistry. Higher concentration of Triton-X helps permeabilize better the tissues but may cause higher background.
4. Oral gavage can also be used to deliver tamoxifen and is more systematic in terms of treatment in order to avoid fluctuations in dose among animals. The maximum daily dose of Tamoxifen administered to aged animals should not exceed 5.4 mg (corresponding to 30 g of mouse body weight) because this may increase the rate of lethality.
5. This step is to ensure specific band formation; few μLs of the PCR product (Subheading 3.2.1, **step 1**) as well as the riboprobe product (Subheading 3.2.2, **step 3**) can be run side by side on DNA gel.
6. Temperature settings set by the oven might be off the desired temperature by 2–3 °C. Check if this is the case by placing a thermometer within the incubator and comparing the two readings. Hybridization temperature should not drop below 63 °C or exceed 68 °C.
7. For washes in one Coplin jar (fits up to 8 slides), 40–45 mL of washing buffer is needed. In case more slides are used, more Coplin jars and higher volumes should be set accordingly.
8. In case some coverslips would not fall off, immerse slides in the washing buffer for 5 min, and then try removing them again.
9. NBT and BCIP solutions can be used up to 2–3 weeks. Fresh preparations are preferred.
10. The appropriate staining time largely depends on the intensity and specificity of each probe. Unless necessary, avoid excessive

staining as this may lead to high background formation. The Cre probe generated here did not show staining on tissues derived from vehicle-treated brains, thus confirming its specificity. As a negative control, a Cre sense riboprobe can be synthesized by adding the T3 promoter sequence (AATTAACCCTCACTAAAGGG) ahead of the Cre forward primer and using the T3 RNA polymerase (instead of the T7 RNA polymerase) in the riboprobe synthesis mix (Subheading 2.1, **step 2**).

11. After longer staining incubation and to ensure proper stopping of reaction, it is highly recommended that slides are washed with TE buffer (Tris 10 mM/EDTA 1 mM, pH = 8) for 15 min followed by rinsing in ddH_2O for 15 min and then washing with 1× PBS.
12. The rabbit anti-Ki67 antibody was used in this study without antigen retrieval. Other Ki67 antibodies (and antibodies targeting nuclear proteins in general) may require this step: incubate tissues in 10 mM sodium citrate (pH = 6) for 20 min at 95 °C before proceeding with Subheading 3.3, **step 3** (do not boil the tissues). Note that the GFP signal may be weakened by this procedure and could be amplified by using the TSA kit (tyramide signal amplification from PerkinElmer, ABC kit Fluorescein).

Acknowledgments

N.G. laboratory is supported by the University Research Board (URB) at the American University of Beirut, Kamal A. Shair CRSL Research Fund (KAS), Farouk Jabre Biomedical Research Grant (FJ), and the Lebanese National Council for Scientific Research (LNCSR). Part of this study was performed using common equipment and material available at the Kamal A. Shair Central Research Science Laboratory (KAS-CRSL) at AUB. The in situ hybridization protocol described in this study is adopted and modified from Wallace and Raff, Development 1999;126:2901–2909.

References

1. Bond AM, Ming GL, Song H (2015) Adult mammalian neural stem cells and neurogenesis: five decades later. Cell Stem Cell 17 (4):385–395. https://doi.org/10.1016/j.stem.2015.09.003
2. Enikolopov G, Overstreet-Wadiche L, Ge S (2015) Viral and transgenic reporters and genetic analysis of adult neurogenesis. Cold Spring Harb Perspect Biol 7(8):a018804. https://doi.org/10.1101/cshperspect.a018804
3. Imayoshi I, Ohtsuka T, Metzger D, Chambon P, Kageyama R (2006) Temporal regulation of Cre recombinase activity in neural stem cells. Genesis 44(5):233–238. https://doi.org/10.1002/dvg.20212
4. Lagace DC, Whitman MC, Noonan MA, Ables JL, DeCarolis NA, Arguello AA, Donovan MH, Fischer SJ, Farnbauch LA, Beech RD, DiLeone RJ, Greer CA, Mandyam CD, Eisch AJ (2007) Dynamic contribution of nestin-expressing stem cells to adult neurogenesis. J Neurosci 27(46):12623–12629. https://

doi.org/10.1523/JNEUROSCI.3812-07.2007

5. Dhaliwal J, Lagace DC (2011) Visualization and genetic manipulation of adult neurogenesis using transgenic mice. Eur J Neurosci 33 (6):1025–1036. https://doi.org/10.1111/j.1460-9568.2011.07600.x
6. Imayoshi I, Sakamoto M, Kageyama R (2011) Genetic methods to identify and manipulate newly born neurons in the adult brain. Front Neurosci 5:64. https://doi.org/10.3389/fnins.2011.00064
7. Sun MY, Yetman MJ, Lee TC, Chen Y, Jankowsky JL (2014) Specificity and efficiency of reporter expression in adult neural progenitors vary substantially among nestin-CreER(T2) lines. J Comp Neurol 522(5):1191–1208. https://doi.org/10.1002/cne.23497
8. Dranovsky A, Picchini AM, Moadel T, Sisti AC, Yamada A, Kimura S, Leonardo ED, Hen R (2011) Experience dictates stem cell fate in the adult hippocampus. Neuron 70 (5):908–923. https://doi.org/10.1016/j.neuron.2011.05.022
9. Vandenbosch R, Clark A, Fong BC, Omais S, Jaafar C, Dugal-Tessier D, Dhaliwal J, Lagace DC, Park DS, Ghanem N, Slack RS (2016) RB regulates the production and the survival of newborn neurons in the embryonic and adult dentate gyrus. Hippocampus 26 (11):1379–1392. https://doi.org/10.1002/hipo.22613
10. Conover JC, Todd KL (2017) Neuronal stem cell niches of the brain. In: Biology and engineering of stem cell niches. Elsevier Inc., Amsterdam, pp 75–91. https://doi.org/10.1016/B978-0-12-802734-9.00006-8
11. Imayoshi I, Sakamoto M, Ohtsuka T, Takao K, Miyakawa T, Yamaguchi M, Mori K, Ikeda T, Itohara S, Kageyama R (2008) Roles of continuous neurogenesis in the structural and functional integrity of the adult forebrain. Nat Neurosci 11(10):1153–1161. https://doi.org/10.1038/nn.2185
12. Farioli-Vecchioli S, Micheli L, Saraulli D, Ceccarelli M, Cannas S, Scardigli R, Leonardi L, Cina I, Costanzi M, Ciotti MT, Moreira P, Rouault JP, Cestari V, Tirone F (2012) Btg1 is required to maintain the pool of stem and progenitor cells of the dentate gyrus and subventricular zone. Front Neurosci 6:124. https://doi.org/10.3389/fnins.2012.00124
13. Marino S, Vooijs M, van Der Gulden H, Jonkers J, Berns A (2000) Induction of medulloblastomas in p53-null mutant mice by somatic inactivation of Rb in the external granular layer cells of the cerebellum. Genes Dev 14 (8):994–1004
14. Naser R, Vandenbosch R, Omais S, Hayek D, Jaafar C, Al Lafi S, Saliba A, Baghdadi M, Skaf L, Ghanem N (2016) Role of the retinoblastoma protein, Rb, during adult neurogenesis in the olfactory bulb. Sci Rep 6:20230. https://doi.org/10.1038/srep20230
15. Srinivas S, Watanabe T, Lin CS, William CM, Tanabe Y, Jessell TM, Costantini F (2001) Cre reporter strains produced by targeted insertion of EYFP and ECFP into the ROSA26 locus. BMC Dev Biol 1:4
16. Katsimpardi L, Lledo PM (2018) Regulation of neurogenesis in the adult and aging brain. Curr Opin Neurobiol 53:131–138. https://doi.org/10.1016/j.conb.2018.07.006
17. Omais S, Jaafar C, Ghanem N (2018) "Till Death Do Us Part": a potential irreversible link between aberrant cell cycle control and neurodegeneration in the adult olfactory bulb. Front Neurosci 12:144. https://doi.org/10.3389/fnins.2018.00144
18. Hollands C, Bartolotti N, Lazarov O (2016) Alzheimer's disease and hippocampal adult neurogenesis; exploring shared mechanisms. Front Neurosci 10:178. https://doi.org/10.3389/fnins.2016.00178
19. Gazalah H, Mantash S, Ramadan N, Al Lafi S, El Sitt S, Darwish H, Azari H, Fawaz L, Ghanem N, Zibara K, Boustany RM, Kobeissy F, Soueid J (2016) Postnatal neural stem cells in treating traumatic brain injury. Methods Mol Biol 1462:689–710. https://doi.org/10.1007/978-1-4939-3816-2_38

Methods in Molecular Biology (2019) 2045: 201–215
DOI 10.1007/7651_2018_119

Published online: 21 February 2018

Infrared Spectroscopy and Imaging in Stem Cells and Aging Research

Ceren Aksoy and Feride Severcan

Abstract

The effect of aging process on stem cell function is crucial because of their critical role in tissue regeneration and repair. The impact of aging on stem cells needs to be understood clearly for the success of clinical application and obtaining desired therapeutic outcome throughout the novel stem cell based therapies. The existing methods used to monitor and characterize the stem cells have some unwanted effects on the properties of stem cells and these methods also do not provide real-time information about cellular conditions. These challenges enforce the usage of nondestructive, rapid, sensitive, high-quality, label-free, cheep, and innovative chemical monitoring methods. In this context, vibrational spectroscopy provides promising alternative to get new information into the field of stem cell biology for chemical analysis, quantification, and imaging of stem cells. Infrared spectroscopy and imaging coupled with chemometric methods can be used as novel and complimentary methods to obtain new insight into stem cell studies for future therapeutic and regenerative medicine.

Keywords Aging, ATR-FTIR spectroscopy, FTIR imaging, Infrared Spectroscopy, Mesenchymal stem cell, Stem cell aging

1 Introduction

The studies performed to understand the mechanisms of aging have gained increased attraction, since aging is an unavoidable consequence of all tissues and organs of the mammalian organisms. There is a strong evidence that the aging process has an adverse effect on stem cells and/or their niche functions, which means increased senescence cell numbers and increased deterioration of the self-renewal, proliferation, and differentiation capacities of stem cells [1–3]. Recent studies showed that stem cells of elderly donors had decreased proliferation capacity and increased senescence compared with stem cells obtained from younger donors [4]. Reduction in stem cell functions with age is caused by intrinsic molecular alterations like oxidative damage of DNA, decreased mitochondrial function, epigenetic alterations, or extrinsic changes in the stem cell microenvironment (niche) [5, 6]. For the success of any therapeutic application of stem cells in regenerative medicine, it is important to understand the interconnected roles of such intrinsic and extrinsic

factors. These factors are crucial to clarify the reciprocal interactions between stem cell aging on tissue homeostasis and aged cellular microenvironment of elderly donor on stem cells [7–9]. In this scope, investigation of markers of cellular aging is important to deeply understand the underlying mechanisms of intrinsic and extrinsic changes that cause aging process [10]. Additionally, the control and regulation of stem cells and interactions with their niche are important in terms of cell therapy and regenerative medicine for gaining basic knowledge of stem cell applications into clinic [11].

In the bone marrow microenvironment, there is a mutual interaction between hematopoietic stem cells (HSCs), mesenchymal stem cells (MSCs), non-stem cells, and extra cellular matrix components and molecular signals to control stimuli for differentiation and self-renewal [11, 12]. The factors contributing the maintenance of HSCs in their niches have been recently investigated and the existing studies showed that MSCs facilitate HSCs maintenance through the secretion of soluble factors and cell–cell contact in bone marrow [13]. That is why understanding of interactions between HSCs with MSCs will provide valuable information through the design of stem cell based cellular therapies [14]. In this context, we studied the effect of aged bone marrow microenvironment on MSCs by using MSCs of different aged healthy donors via infrared (IR) spectroscopy and imaging which may be useful through donor selection in allogenic stem cell transplantation as well as in other stem cell therapies [15].

Fourier transform infrared (FTIR) spectroscopy and microspectroscopy can be used as a novel, nondestructive, operator independent research method in stem cell research that enables real-time chemical monitoring, high-quality data collection with less experimental complexity to identify novel molecular marker (s) [16]. Attenuated total reflection (ATR) mode of FTIR spectroscopy is a powerful tool to study biomedical samples. In this technique, sample preparation procedure is reduced, because the samples can directly be placed on an ATR crystal before spectral measurements have been performed [17].

FTIR microspectroscopy (FTIRM) is an imaging technique in which a microscope is coupled with an infrared spectrometer. It provides spatially resolved information on unstained thin tissue samples or cell monolayers by allowing the generation of infrared (IR) images with high image contrast [18]. Unlike staining techniques, IR microscopy with its label-free, noninvasive, and nondestructive properties generates information about relative concentrations and structure of macromolecules by considering alterations in the infrared spectra and the specific heterogeneities [19, 20]. FTIRM of biological systems is a developing area to investigate cells in different stages such as their growth cycles

[21], cancerous states [22], and contaminated states with pathogens [23].

With these advantages, FTIR spectroscopy and microspectroscopy can successfully be used to characterize the biochemical makeup of intact live stem cells. Optical signals are generated intrinsically from the sample and they are used to obtain information about relative concentrations and structure of biomolecules such as protein, lipids, carbohydrates, and nucleic acids. This information help us to understand similarities and differences between stem cell populations, stem cell lineages, the level of maturation, and differentiation of stem cells under healthy and disease states [24–29].

2 Materials

2.1 Cell Lines

The number and the variety of cells in the sampling groups in FTIR spectroscopy and FTIR imaging studies are very important parameters to be able to obtain statistically meaningful results (*see* **Note 1**).

2.2 Cell Culture Media and Supplements

2.2.1 Cell Culture Media Used for Isolation and Cultivation of Bone Marrow Mesenchymal Stem Cells

- Ficoll (1.077 g/l; Biochrom AG, Berlin, Germany). Stored at 4 °C (*see* **Note 2**)
- 0.9% Phosphate buffer solution (PBS) (Sigma, USA). Stored at 4 °C (*see* **Note 3**)
- Cultivation medium: Dulbecco's modified Eagle's medium-low glucose (DMEM-LG; Biochrom AG, Berlin, Germany), 10% (vol/vol) fetal bovine serum (FBS; Biochrom AG, Berlin, Germany), 1% (vol/vol) L-glutamine (0.584 g/l; Biochrom AG, Berlin, Germany), 1% (vol/vol) penicillin (100 units/ml) and streptomycin (100 g/ml) (Biochrom AG, Berlin, Germany), and 0.1% (vol/vol) leukemia inhibitory factor (LIF) (0.5 μg/ml in 1% BSA solution; Invitrogen) (*see* **Note 4**)
- 0.25% Trypsin and 1 mM EDTA (Sigma, USA)
- 10% FBS (Biochrom AG)
- Centrifuge (Eppendorf International 5810)
- Trypan blue dye (Sigma, USA)
- Thoma cell counter
- Light microscope (Leica)

2.2.2 Freezing and Storage of Bone Marrow Mesenchymal Stem Cells

- Cryo.s vials (Greiner Bio-One) (*see* **Note 5**)
- Freezing medium containing 10% (vol/vol) DiMethylSulfoxide (DMSO; AppliChem, Germany) supplemented with 20% (vol/vol) FBS and 70% (vol/vol) DMEM-LG

- Mr. Frosty Freezing Container (Nalgene Labware, Rochester, NY, http://www.nalgenunc.com) (*see* **Note 6**)
- 196 °C liquid nitrogen and nitrogen carrying tank

2.2.3 Differentiation Media and Stains used for Characterization of Bone Marrow Mesenchymal Stem Cells

- Adipogenic induction medium: DMEM-LG (Biological Industries, Israel), 10% of FBS (Gibco, USA), 1 μM dexamethasone (Sigma, USA), 60 μM indomethacin (Sigma, USA), 500 μM IBMX (Sigma, USA), and 5 μg/ml insulin (Sigma, USA)
- Oil Red O (Sigma, USA) stain is used to visualize adipogenic differentiation of bone marrow mesenchymal stem cells (BM-MSCs)
- Osteogenic induction medium: DMEM-LG (Biological Industries, Israel), 10% of FBS (Gibco, USA), 100 nM dexamethasone (Sigma, USA), 10 mM beta glycerophosphate (Sigma, USA), and 0.2 mM ascorbic acid (Sigma, USA)
- Alizarin Red (Sigma, USA) stain is used to visualize osteogenic differentiation
- 10% Buffered formalin

2.3 Flow Cytometer and Flow Cytometer Markers

- FACS Aria Flow Cytometer (Becton, Dickinson Biosciences, USA)
- CD34 (BD Biosciences, USA), CD45 (BD Biosciences, USA), CD73 (BD Biosciences, USA), CD90 (BD Biosciences, USA), CD105 (E-Bioscience, USA), and CD133 (E-Bioscience) (*see* **Note 7**)
- Fluorescent isothiocyanate (FITC) or phycoerythrin (PE)

2.4 Attenuated Total Reflectance Fourier Transform Infrared Spectrometer and Fourier Transform Infrared Microspectroscope

- PerkinElmer Spectrum 100 FTIR spectrometer with ZnSe Diamond ATR attachment
- Nitrogen (N_2) gas
- PerkinElmer Spectrum Spotlight 400 imaging FTIR microscope
- MirrIR low-e microscope slides (Kevley Technologies)

2.5 Software

- BD FACSDiva Software v6.1.2 (Becton, Dickinson Biosciences, USA) to analyze flow cytometry results
- Spectrum One Software Program (PerkinElmer) to analyze attenuated total reflectance Fourier transform infrared (ATR-FTIR) results
- OPUS 5.5 software (Bruker Optics, GmbH) to analyze ATR-FTIR results via cluster analysis

- ISys software (Spectral Dimensions, Olney, MD, USA) to analyze FTIR microscopy results
- Graph Pad Prism 5 to perform statistical analysis (One Way ANOVA and Tukey's Multiple Comparison Test for this study)

3 Methods

3.1 Isolation and Cultivation of Mesenchymal Stem Cells from Bone Marrow Aspirates

1. Bone marrow aspirates are centrifuged at 2300 rpm for 15 min and then supernatant is removed.
2. Cell pellet is diluted with an equal volume of PBS and this cell suspension is subjected with an equal volume of Ficoll solution very gently and slowly by pipetting to prevent cell burst. Finally, cell suspension with Ficoll is centrifuged at 2000 rpm for 15 min.
3. After centrifugation, white layer of mononuclear cells (MNCs) is collected by pipetting and transferred into the 15 ml conical falcon tube.
4. MNCs are washed twice with 5 ml PBS solution and centrifuged at 1500 rpm for 5 min to remove excessive Ficoll.
5. Finally, MNCs are seeded on T25 culture flask in the presence of DMEM-LG medium at 37 °C in a 5% CO_2 environment to obtain primary BM-MSCs.
6. After 3 days nonadherent MNCs are discarded from T25 flask. The attached primary BM-MSCs (*see* **Note 7**) are expanded by replacing culture medium twice.
7. BM-MSCs are detached by 10 min exposure to 0.25% Trypsin + 1 mM EDTA in PBS and 3×10^5 viable passage 0 (P0) - BM-MSCs cells are seeded into the T75 culture flask and continue passaging until obtaining passage 3 (P3) BM-MSCs (*see* **Note 8**).

3.1.1 Freezing and Storage of Bone Marrow Mesenchymal Stem Cells

BM-MSCs in different passages are stored by freezing in medium containing 10% (vol/vol) DMSO (AppliChem, Germany) with 20% (vol/vol) FBS and 70% (vol/vol) DMEM-LG for long-term preservation at −196 °C.

1. Trypsinized BM-MSCs are suspended in freezing medium on ice and then cell suspension is aliquoted into cryovials as 1×10^6 MSCs/1 ml/tube on ice. Cryovials are placed in a Mr. Frosty Freezing Container (Nalgene Labware, Rochester, NY, http://www.nalgenunc.com) for 24 h at −80 °C.
2. Finally, cryovials are transferred to −196 °C liquid nitrogen tank for long-term preservation.

3.2 Characterization of Bone Marrow Mesenchymal Stem Cells by Differentiation Experiments and Flow Cytometry Analysis

BM-MSCs from healthy donors are induced for differentiation by cultivating them into the special differentiation media for 21 days.

3.2.1 Adipogenic and Osteogenic Differentiation Experiments

1. *For adipogenic differentiation*, confluent (90%) cells from P3 of BM-MSCs cultures in six-well plates are treated with adipogenic differentiation medium given in Sect. 2.2.3 by replacing the fresh medium for every 3 days during 21-day period.
   (a) Meanwhile, the cells in the control wells are cultured for 21 days in DMEM-LG with 10% FBS.
   (b) At the end of differentiation period, cells are fixed with 10% buffered formalin for 20 min at room temperature (RT) and stained with Oil Red O for 10 min at RT to visualize adipogenic differentiation under the light microscope.
2. *For osteogenic differentiation*, confluent (70–80%) BM-MSCs from P3 in six-well plates are subjected to osteogenic differentiation medium defined in Sect. 2.2.3 by replacing the fresh medium for every 3 days during 21-day period.
   (a) Meanwhile, the cells in control wells are cultured for 21 days in DMEM-LG with 10% FBS.
   (b) For the visualization of calcium deposits under the light microscope, differentiated cells are fixed with 10% buffered formalin for 20 min at RT and stained with Alizarin Red solution (pH 4.2) for 10 min at RT.

3.2.2 Flow Cytometry Analysis

1. Trypsinized passage 3 BM-MSCs are separated into different tubes in 2 ml PBS buffer at a density of 2×10^5 cells/tube for specific cell surface marker staining.
2. After centrifugation at 1500 rpm for 5 min, supernatant is removed and cell pellet is distributed by finger tapping.
3. 100 μl PBS-BSA-Na azide and CD34, CD45, CD73, CD90, CD105, and CD133 flow cytometry markers, FITC, or phycoerythrin (PE) antibodies are added into homogenized cell pellet and then tubes are incubated at +4 °C for 30 min after covering with thnfoil.
4. At the end of 30 min incubation in dark, cells are washed twice with 2 ml PBS-BSA-Na azide and centrifuged at 1500 rpm for 10 min.
5. Finally, cells are resuspended in 200 μl PBS-BSA-Na azide in FACS tubes and analyzed in FACS Aria.
6. The analysis of acquired data is carried out using BD FACSDiva Software v6.1.2 (Beckon Dickinson Biosciences, USA).

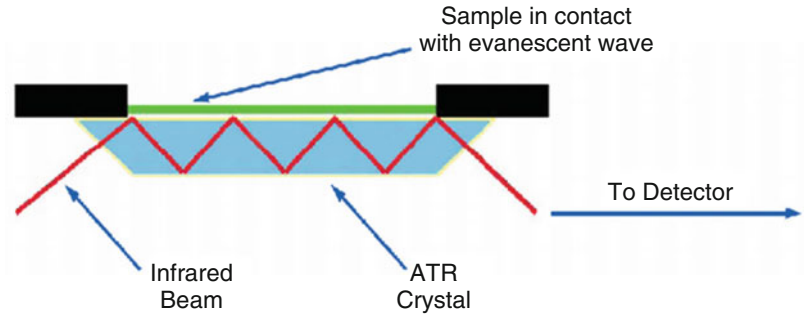

Fig. 1 Schematic representation of attenuated total reflection (ATR) top plate (PerkinElmer TCH material)

3.3 Attenuated Total Reflectance Fourier Transform Infrared Spectrometry

3.3.1 Sample Preparation

1. 2×10^6 BM-MSCs are harvested by 5-min centrifugation at 1500 rpm, after 10 min trypsin (0.25% trypsin+1 Mm EDTA) treatment at 37 °C in a 5% CO_2 environment.
2. Then, cell pellet is washed twice with 1 ml 0.9% PBS solution to remove all growing media. The cell pellet is resuspended in 10 μl 0.9% PBS buffer and then cell suspension is deposited on Diamond/ZnSe (Di/ZnSe) crystal plate of the Universal ATR unit of the FTIR spectrometer (Fig. 1) by pipetting.
3. Finally, PBS buffer is rapidly evaporated using mild N_2 flux for 30 min to obtain a homogenous thin film of entire cells on ATR crystal.

3.3.2 Data Acquisition and Spectral Measurements

Infrared spectra of BM-MSCs are obtained in the 4000–650 cm^{-1} region at room temperature by scanning the homogenous cell film on ATR-Di/ZnSe crystal with Spectrum 100 FTIR spectrometer in the one-bounce ATR mode (*see* **Note 9**).

1. A total of 100 scans are taken for each interferogram at 4 cm^{-1} resolution.
2. The spectrum of atmospheric water vapor and carbon dioxide interference are recorded in background and then subtracted automatically using the Spectrum One software program.
3. Figure 2 shows the general representative FTIR spectra of healthy human BM-MSCs from different age donors in the 3800–800 cm^{-1} spectral region.
4. Recording and analysis of the spectral data are performed using the Spectrum One software from PerkinElmer.

3.3.3 Analysis of Spectral Measurements

Spectral and Statistical Analyses

The results of the spectral measurements are expressed as "mean ± standard error" values. The baseline-corrected and non-normalized average spectra are used to perform accurate measurements of the mean values of the band positions, band areas, and band widths. These spectral measurements have to be applied for

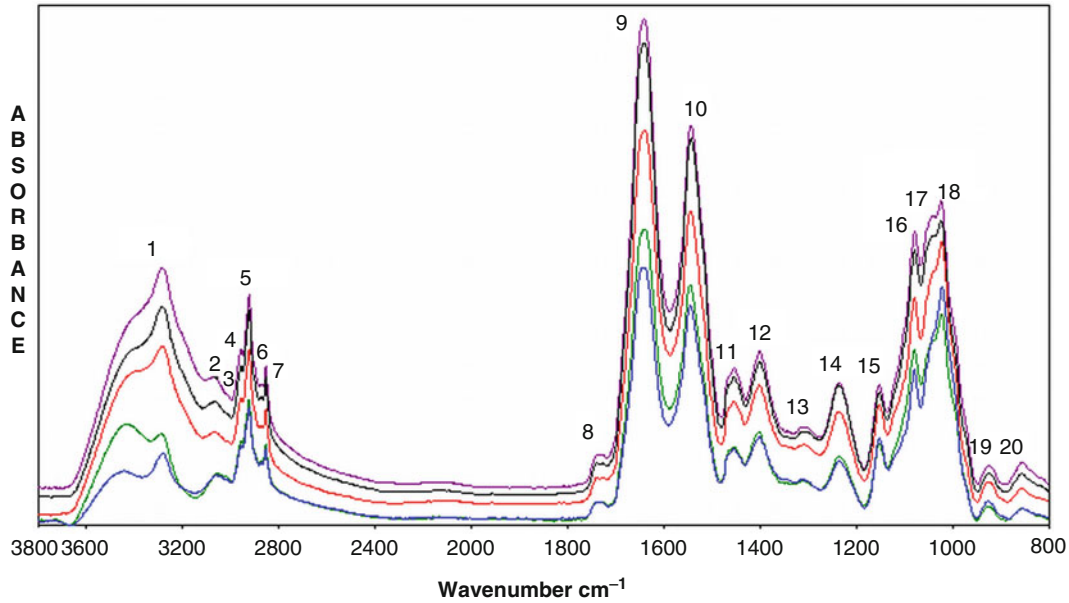

Fig. 2 The general representative infrared spectra of healthy bone marrow mesenchymal stem cells (BM-MSCs) from different age donors. Red line represents infants' BM-MSCs, black line represents children's BM-MSCs, purple line represents adolescents' BM-MSCs, green line represents early adults' BM-MSCs, and blue line represents mid-adults' BM-MSCs in the 3800–800 cm^{-1} region (The spectra were normalized with respect to the amide A band)

the spectrum of each individual in the sampling groups. In order to remove the noise, the spectra are first smoothed with nine-point Savitzky–Golay smooth function. The band positions are measured using the wavenumber value corresponding to the center of weight of each band. The bandwidths of specific bands are calculated as the width at 0.80× height of the signal in terms of cm^{-1}. Band areas are calculated using Spectrum software. The spectrum contains several bands representing many different functional groups of lipids, proteins, carbohydrates, and nucleic acids. The band assignments of major absorptions in infrared spectrum of human bone marrow mesenchymal stem cells in 3800–800 cm^{-1} region based on the literature are given in Table 1.

After the spectral measurements are performed, the data should be evaluated by normality test in order to decide which statistical test will be used.

Cluster Analysis

Cluster analysis is performed by OPUS 5.5 Software and is used to find out spectral relationships among sampling groups by considering the spectral measurements (*see* **Note 10**).

Table 1
General band assignment of bone marrow mesenchymal stem cells (BM-MSCs)

Peak no.	Wavenumber (cm^{-1})	Definition of the spectral assignments
1	3330	*Amide A:* N–H and O–H stretching vibrations of polysaccharides, proteins
2	3065	*Amide B:* N–H vibrations of proteins
3	3015	*Olefinic = CH stretching:* unsaturated lipids, cholesterol esters
4	2957	*CH_3 antisymmetric stretching:* lipids, protein side chains, with some contribution from carbohydrates and nucleic acids
5	2924	*CH_2 antisymmetric stretching:* mainly lipids, with the little contribution from proteins, carbohydrates, and nucleic acids
6	2873	*CH_3 symmetric stretching:* protein side chains, lipids, with some contribution from carbohydrates and nucleic acids
7	2852	*CH_2 symmetric stretching:* mainly lipids, with the little contribution from proteins, carbohydrates, and nucleic acids
8	1740	*C=O stretching vibrations* of triglycerides, cholesterol esters
9	1639	*Amide I:* C=O stretching vibrations of proteins
10	1545	*Amide II:* N–H bending and C–N stretching vibrations of proteins
11	1453	*CH_2 bending vibrations* of lipids
12	1402	*COO^- symmetric stretching:* fatty acid side chains
13	1310	*Peptide side chain vibrations*
14	1234	*$PO^-{}_2$ antisymmetric stretching:* fully hydrogen bonded, mainly nucleic acids with the little contribution from phospholipids
15	1152	*CO–O–C antisymmetric stretching vibrations* of glycogen and nucleic acid ribose
16	1080	*$PO^-{}_2$ symmetric stretching:* nucleic acids and phospholipids; C–O stretching: glycogen, polysaccharides, and glycolipids
17	1045	*CO stretching vibrations* of carbohydrates, glycogen; deoxyribose/ribose of nucleic acids
18	1025	*Mainly from glycogen*
19	925	*Sugar vibrations* in backbone of DNA-Z form
20	855	Vibrations in N-type sugars in nucleic acid backbone

3.3.4 Fourier Transform Infrared Microspectroscopy Experiments

Slide Preparation

1. Passage 3 BM-MSCs are trypsinized and then trypsin is blocked with 10% FBS. Cells are collected with centrifugation at 1500 rpm for 5 min and are washed with PBS once. Then, two final washings have to be performed with normal serum physiologic solution to remove salt crystals.

2. The cell pellet is dissolved in 1 ml of culture medium and cells are counted with Thoma counter by using trypan blue. 25,000 MSCs are placed on silver (Ag/SnO_2) coated low-e microscope slides (*see* **Note 11**) and they are incubated on slide at 37 °C in a 5% CO_2 environment overnight for their attachment.
3. At the end of cultivation time, MSCs on low-e microscope slide are fixed with 10% formalin for 10 min (*see* **Note 12**).
4. After fixation, excess formalin is removed by washing gently the slides with serum physiologic solution (0.9% NaCl) [34, 35] (*see* **Note 13**) and then they have to be dried very quickly under a stream of dry and compressed air at room temperature for at least 1 h to evaporate excess water in solution.

Collection of Spectral Images and Preprocessing of Spectral Data

PerkinElmer FTIR microscope coupled with PerkinElmer Spotlight 400 software is used to map MSC samples on low e-microscope slides. The microscope is equipped with a liquid nitrogen cooled MCT detector and a CCD camera to provide an optical image of the area under interrogation.

1. An aperture size of 6.25 μm × 6.25 μm is used to obtain spectra from confluent cell monolayers.
2. IR image maps are collected in the reflection mode through the spectral range between 4000 and 700 cm^{-1} with a 4-cm^{-1} resolution and 32 scan numbers. At least 3 spectra have to be acquired from each sample.
3. Background spectra are collected from a separate piece of blank MirrIR low-e slide.
4. Whole baseline correction is performed between 3800 and 800 cm^{-1} region.
5. Then, spectral masking is applied for the analysis by using ISys software to get rid of the contributions from the surface around the cellular regions by marking the cells.
6. The chemical maps are constructed for each group by taking area of specifically selected spectral bands arisen from lipids, proteins, and nucleic acids (*see* **Note 14** and Fig. 3) [15, 29].

4 Notes

1. In our study, human BM-MSCs that were obtained from five different age group donors classified as infants (0–3 years of age, $n = 5$), children (aged >3–12, $n = 5$), adolescents (aged >12–19, $n = 5$), early adults (aged >19–35, $n = 5$), and mid-adults (aged >35–50, $n = 5$) were used. Human bone marrow aspirates (3–5 ml), which were obtained from posterior iliac crest of healthy bone marrow transplantation donors, were

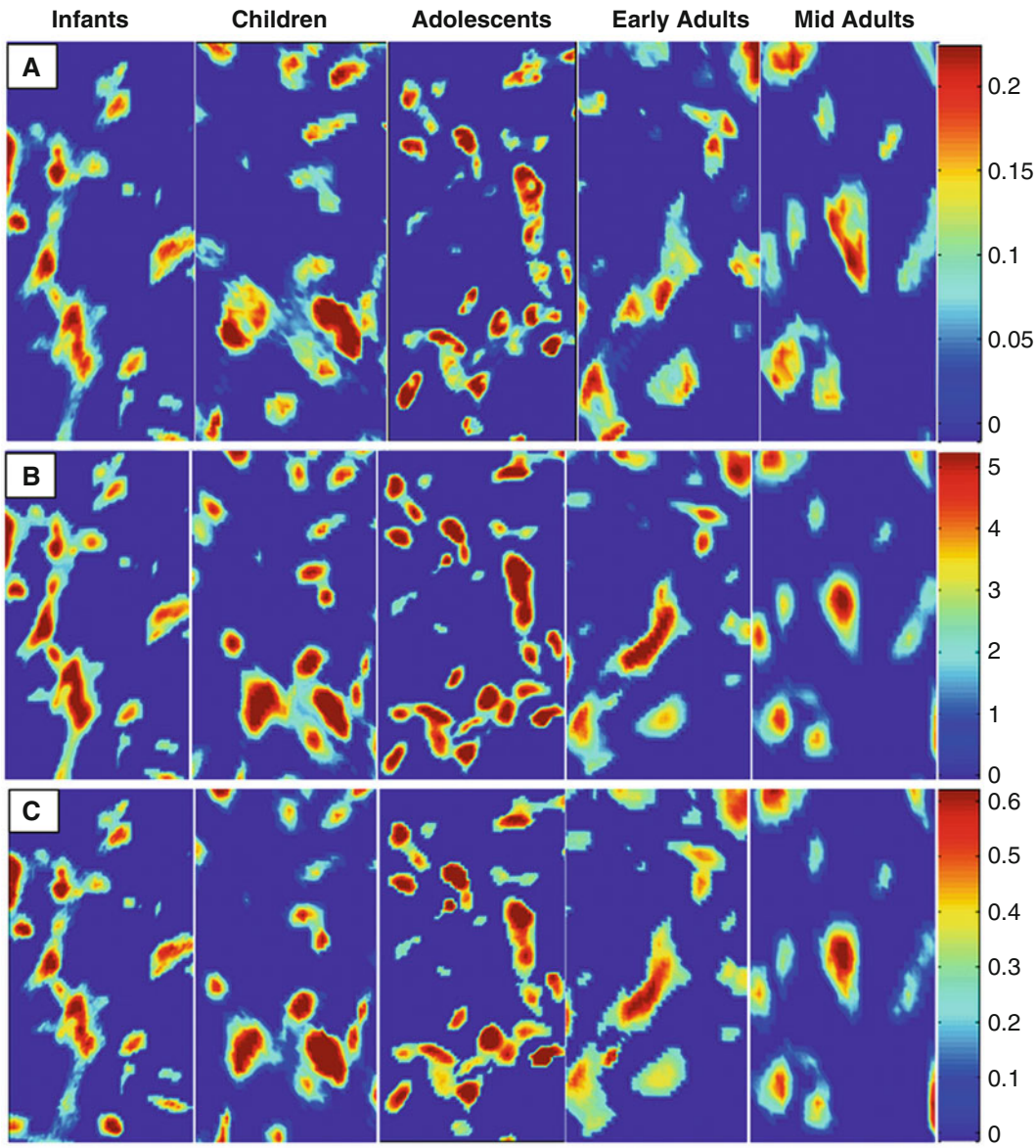

Fig. 3 Spectral image maps that reflect distribution of lipids, proteins, and nucleic acids in the BM-MSCs from five different age groups. These maps were derived, respectively, by taking the peak integrated areas of: (**a**) CH_2 symmetric stretching bands of lipids, (**b**) amide II band of proteins, and (**c**) PO_2^- symmetric stretching bands of nucleic acids

used as a source of BM-MSCs. Marrow samples were obtained during the marrow harvest procedure after signing of informed consent prepared by the ethics committee of the Hacettepe University Children's Hospital, Bone Marrow Transplantation Unit Ankara, Turkey [15].

2. Ficoll density gradient solution is used to extract MNCs from bone marrow.

3. PBS solution is used for cell washing.
4. LIF is not required to cultivate human stem cells, and it is especially used for the cultivation of mouse embryonic stem cells. Although we observed that there was no effect of absence of LIF on the growth of human BM-MSCs, we had to use it since we had started our study by using LIF.
5. Cryogenic vials are designed for storing biological material, human or animal cells, at temperatures as low as −196 °C but should be used only in the gas phase of liquid nitrogen.
6. The Mr. Frosty Freezing Container System provides the critical, repeatable, 1 °C/min cooling rate required for successful cryopreservation of cells. Easy to use in any mechanical freezer.
7. According to International Society for Cellular Therapy (ISCT) recommendations, MSCs have to be adherent to plastic surfaces when cultivated in appropriate complete media, they must express CD73, CD90, and CD105 surface antigens while they lack expression of CD34 and CD45, and finally they have to have the capacity to differentiate osteoblast, adipocytes, and chondroblasts using specific in vitro inducing media [30, 31].
8. Count the cells by using Thoma cell counter and trypan blue dye. Since passage 3 BM-MSCs are more active, they show high proliferation and multilineage capacity and should be preferred to eliminate late passage dependent aging of cells independently from donor age.
9. ATR mode of FTIR spectroscopy is a powerful tool to study biomedical samples. In this technique, the samples can be directly placed on an ATR crystal and investigated, so that the sample preparation procedure is reduced before spectral measurements. It is based on the total reflection phenomenon. When the radiation beam passes through an ATR crystal, it is internally reflected, which causes creation of an evanescent wave protruding only a few micrometers beyond the surface of ATR crystal (Fig. 1) [28].
10. Hierarchical cluster analysis calculates the similarities between the spectra of samples by using distance calculation and classification algorithms. The results are presented in the form of a *dendrogram* which shows clustering in two dimensions by graphical means. The measure of similarity is heterogeneity, where increasing heterogeneity corresponds to increasing dissimilarity. The heterogeneity calculations were made by using the OPUS 5.5 software program with Euclidian distance and Ward's algorithm [32]. Ward's algorithm clusters as much homogeneous objects as possible by combining the spectra that form a within-cluster variance with the smallest distance [33].

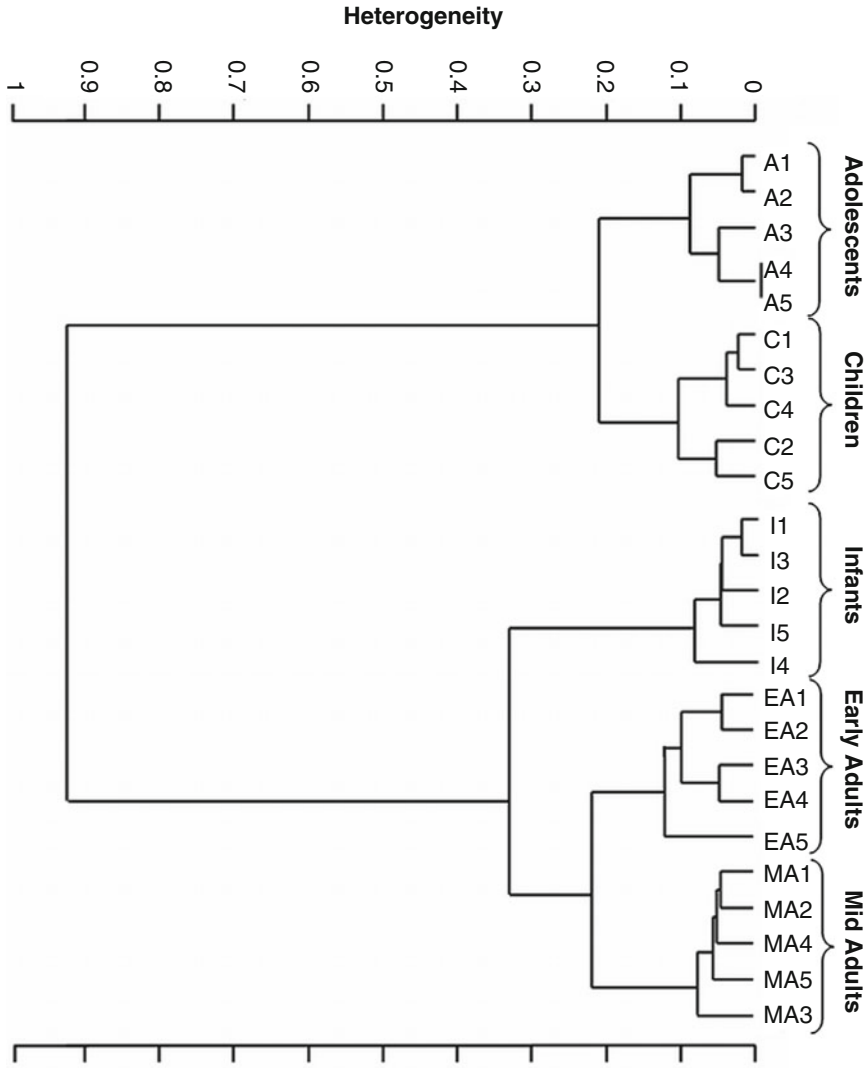

Fig. 4 Hierarchical cluster analysis performed on the vector-normalized spectra of BM-MSCs of infants, children, adolescents, early adults, and mid-adults and resulting from Ward's algorithm. The study was conducted in the 3000–2800 cm^{-1} spectral regions

In the presented study, the analysis was applied to the first-derivative and vector-normalized spectra of 25 independent spectra of five sampling groups in two different regions, namely 3000–2800 cm^{-1}. The result of cluster analysis was demonstrated with an example in Fig. 4. As seen from the dendrogram, all samples were successfully distinguished.

11. The low-e MirrIR slides are coated with Ag/SnO_2 layer which provides the reflectance property of slides. Infrared beam is reflected by Ag/SnO_2 layer through a thin sample. Since the low-e slides are transparent in the visible region, before IR imaging of cells samples can be examined by light microscope.

12. Fixation is a major issue after cells are deposited onto microscope slides. Air drying is a mild form of fixation and for further fixation some chemicals such as ethanol, methanol, acetone, and formalin are used. Ethanol and methanol cause minor spectral changes because of removal of phospholipids and minor changes are observed in the main protein bands amide I and amide II. Acetone fixation decreases cell volume, breaks hydrogen bonds, and causes coagulation of water-soluble proteins and the destruction of cellular organelles. Therefore, 10% buffered solution of formaldehyde, called as formalin, is used to fix cells on microscope slides. Formalin preserves lipids, protein secondary structure of cells, and it has little impact on carbohydrates which means that it does not harm the spectra of cells [34, 35].
13. After fixation, cells have to be washed with deionized water or physiological saline solution (0.9% NaCl) in order to prevent hemolysis [34, 35].
14. The specific integrated spectral regions for the infrared bands are used to determine distribution of functional groups in the FTIR spectral images. In our presented study, the average chemical maps are colored according to the peak integrated areas of CH_2 symmetric stretching, amide II, and PO_2^- symmetric stretching bands in order to observe distribution of lipids, proteins, and nucleic acids in BM-MSCs, respectively. Red color corresponds to the highest ratio and blue color corresponds to the lowest ratio in the color bars that are stated in the chemical maps.

References

1. Ahmed AS, Sheng MH, Wasnik S et al (2017) Effect of aging on stem cells. World J Exp Med 7(1):1–10
2. Buom-Yong R, Kyle EO, Jon MO et al (2006) Effects of aging and niche microenvironment on spermatogonial stem cell self-renewal. Stem Cells 24(6):1505–1511
3. Sethe S, Scutt A, Stolzing A (2006) Aging of mesenchymal stem cells. Ageing Res Rev 5 (1):91–116
4. Stenderup K, Justesen J, Claudsen C (2003) Aging is associated with decreased maximal life span and accelerated senescence of bone marrow stromal cells. Bone 33:919–926
5. Molofsky AV, Slutsky SG, Joseph NM et al (2006) Increasing p16INK4a expression decreases forebrain progenitors and neurogenesis during ageing. Nature 443:448–452
6. Wagers AJ, Conboy IM (2005) Cellular and molecular signatures of muscle regeneration: current concepts and controversies in adult myogenesis. Cell 122:659–667
7. Rando TA (2006) Stem cells, ageing and the quest for immortality. Nature 441:1080–1086
8. Greco SJ, Rameshwar P (2008) Microenvironmental considerations in the application of human mesenchymal stem cells in regenerative therapies. Biologics 2:699–705
9. Drummond-Barbosa D (2008) Stem cells, their niches and the systemic environment: an aging network. Genetics 180:1787–1797
10. Stolzing A, Jones E, McGonagle D et al (2008) Age-related changes in human bone marrow-derived mesenchymal stem cells: consequences for cell therapies. Mech Ageing Dev 129 (3):163–173
11. Becerra J, Santos-Ruiz L, Andrades JA et al (2011) The stem cell niche should be a key issue for cell therapy in regenerative medicine. Stem Cell Rev 7:248–255

12. Mitsiadis TA, Barran O, Rochat A et al (2007) Stem cell niches in mammals. Exp Cell Res 313:3377–3385
13. Wagner W, Roderburg C, Wein F et al (2007) Molecular and secretory profiles of human mesenchymal stromal cells and their abilities to maintain primitive hematopoietic progenitors. Stem Cells 25:2638–2647
14. Purton LE, Scadden DT (2008) The hematopoietic stem cell niche. In: Silberstein L (ed) Stem Book, The Stem Cell Research Community, Massachusetts
15. Aksoy C, Aerts-Kaya F, Kuşkonmaz BB et al (2014) Structural investigation of donor age effect on human bone marrow mesenchymal stem cells: FTIR spectroscopy and imaging. Age 36:9691
16. Aksoy C, Severcan F (2012) Role of vibrational spectroscopy in stem cell research. Spectrosc Intern J 27(3):167–184
17. Kazarian SG, Chan KLA (2006) Applications of ATR-FTIR spectroscopic imaging to biomedical samples. Biochim Biophys Acta 1758:858–867
18. Cakmak G, Miller LM, Severcan F et al (2012) Amifostine, a radioprotectant agent, protects rat brain tissue lipids against ionizing radiation induced damage: an FTIR microspectroscopic imaging study. Arch Biochem Biophys 520 (2):67–73
19. Bechtel HA, Martin MC, May TE, Lerch P (2009) Improved spatial resolution for reflection mode infrared microscopy. Rev Sci Instrum 80:126106
20. Cakmak G, Zorlu F, Severcan F et al (2011) Screening of protective effect of amifostine on radiation-induced structural and functional variations in rat liver microsomal membranes by FT-IR spectroscopy. Anal Chem 83:2438–2444
21. Matthaus C, Boydston-White S, Miljkovic M et al (2006) Raman and infrared microspectral imaging of mitotic cells. Appl Spectrosc 60:1–8
22. Dukor R (2002) Handbook of vibrational spectroscopy. Wiley, New York
23. Erukhimovitch V, Talyshinsky M, Souprun Y et al (2005) FTIR microscopy detection of cells infected with viruses. Methods Mol Biol 292:161–172
24. Krafft C, Salzer R, Seitz S et al (2007) Differentiation of individual human mesenchymal stem cells probed by FTIR microscopic imaging. Analyst 132:647–653
25. Diem M, Boydston-White S, Chiriboga L (1999) Infrared spectroscopy of cells and tissues: shining light onto a novel subject. Appl Spectrosc 53:148–161
26. Chan JW, Lieu DK (2009) Label-free biochemical characterization of stem cells using vibrational spectroscopy. J Biophotonics 2:656–668
27. Rojewski MT, Weber BM, Schrezenmeier H (2008) Phenotypic characterization of mesenchymal stem cells from various tissues. Transfus Med Hemother 35(3):168–184
28. Aksoy C, Guliyev A, Kilic E et al (2012) Bone marrow mesenchymal stem cells in patients with beta thalassemia major: molecular analyses with attenuated total reflection-Fourier transform infrared (ATR-FTIR) spectroscopy study as a novel method. Stem Cells Dev 21 (11):2000–2011
29. Aksoy C, Uckan D, Severcan F (2012) FTIR spectroscopic imaging of mesenchymal stem cells in beta thalassemia disease state. Biomed Spectr Imaging 1:67–78
30. Horwitz EM, Le Blanc K, Mr D et al (2005) Clarification of the nomenclature for MSC: the international society for cellular therapy position statement. Cytotherapy 7:393–395
31. Dominici M, Le Blanc K, Mueller I et al (2006) Minimal criteria for defining multipotent mesenchymal stromal cells. The International Society for Cellular Therapy position statement. Cytotherapy 8:315–317
32. Ward JJH (1963) Hierarchical grouping to optimize an objective function. J Am Stat Assoc 58(301):236–244
33. Severcan F, Bozkurt O, Gurbanov R, Gorgulu G (2010) FT-IR spectroscopy in diagnosis of diabetes in rat animal model. J Biophotonics 3:621–631
34. Aksoy C (2012) Characterization of stem cells by vibrational spectroscopy. In: Severcan F, Haris PI (eds) Application of vibrational spectroscopy in diagnosis and screening, vol 6. IOS Press, Amsterdam
35. Romeo MJ, Mohlenhoff B, Diem M (2006) Infrared micro-spectroscopy of human cells: causes for the spectral variance of oral mucosa (buccal) cells. Vib Spectr 42:9–14

Methods in Molecular Biology (2019) 2045: 217–224
DOI 10.1007/7651_2018_120

Published online: 15 March 2018

Use of U-STELA for Accurate Measurement of Extremely Short Telomeres

Nedime Serakinci, Huseyin Cagsin, and Merdiye Mavis

Abstract

Telomeres are repetitive genetic materials that protect the chromosomes by capping the ends of chromosomes. Each time a cell divides, telomeres get shorter. Telomere length is mainly maintained by telomerase. This enzyme is present in the embryonic stem cells in high concentrations and declines with age. It is still unclear to what extend there is telomerase in adult stem cells, but considering these are the founder cells to the cells of the all tissues in a body, understanding the telomere dynamics and expression of telomerase in adult stem cells is very important.

Telomere length has been implicated as one of the markers for neoplastic transformation in both in vivo and in vitro studies. During cancerogenesis, telomeres shorten due to high cell turnover and repeats are added by active telomerase or alternative lengthening of telomeres (ALT). This gradual shortening is replication driven and does not necessarily explain the presence of ultrashort telomeres. Ultrashort telomeres are observed when there is a sudden shortening in telomeres not related with cell division and may arise from breaks in telomeres due to oxidative damage and replication slippage.

Universal STELA is an accurate method for evaluation of ultrashort telomeres in hMSC-telo1 cells. Compared to TRF assay, U-STELA is developed to overcome several problems in detecting abrupt telomere shortening in a single chromosome.

Keywords Mesenchymal stem cells, Telomerase, Telomere homeostasis, Telomere length, U-STELA

1 Introduction

Telomeres are specialized structures localized at the ends of each chromosome and are composed of a special DNA-sequence, tandem repetitions of TTAGGG together with telomere specific proteins. At the very end of the DNA strand, there is a short overhang due to the 3′-strand being a little longer than the 5′-strand. This complex protects the chromosome ends very effectively and if the ends of the chromosomes were not protected, the cellular DNA quality control system detects the ends as double stranded DNA breaks and forces the cell to go into replicative arrest.

Different mechanisms can lead into telomere shortening. Major mechanism is the one that is based on the end-replication problem during cell division which is incomplete replication of the telomeres and these results in telomere shortening at which in each

cell division telomeres shorten 30 ± 50 bp [1]. In order for DNA polymerase to start to replicate the DNA, RNA primer is needed. RNA primer binds to the 3′ end of the DNA and polymerase binds to the DNA–RNA double strand and starts to replicate DNA. As the DNA polymerase moves along the template DNA, RNA primer gets separated from the template DNA resulting in region at the end of template DNA which is not replicated. This leads into newly synthesized DNA which is shorter than the template DNA [2].

In addition to the end-replication problem, there are other factors such as suppressed telomerase expression, telomere repair problem, and reactive oxygen species that play role in telomere shortening [3, 4].

Short telomeres can enhance the initiation of tumorigenesis as they trigger chromosomal instability and genetic changes that result in cellular transformation [2].

The presence of ultrashort telomeres in human cancers has been observed and it is believed that mean telomere length shortening does not have a role in the generation of chromosomal instability but the ultrashort telomeres have [5, 6]. It is also suggested that ultrashort telomeres are generated as a consequence of abrupt shortening of telomeres [7].

All these suggest that telomere length might be used as a marker which indicates the replicative potential of the cell and the residual capacity of the cell to divide more [8].

Difference in the telomere lengths among different adult tissues is probably arising due to different replicative histories of cells, differences in regulatory pathways that are specific to cell type and microenvironment of the cells [9].

There have been several methods quantifying the telomere length in a tissue; however, evaluating cell type-specific telomere length provides more relevant information regarding the particular cell type and pathologies. Universal STELA is an accurate method for evaluation of ultrashort telomeres in hMSC-telo1 cells [10]. Compared to TRF assay, U-STELA is developed to overcome several problems in detecting abrupt telomere shortening in a single chromosome [11].

2 Materials

2.1 Cell Culture of Mesenchymal Stem Cells

1. Dulbecco's Modified Eagle's Medium (DMEM; 1×, Gibco™): 4.5 g/l D-glucose, L-glutamine, and pyruvate (*see* **Note 1**)
2. Fetal bovine serum (FBS; BI Biological Sciences): heat inactivated European grade (*see* **Note 2**)
3. L-glutamine solution (BI Biological Sciences): 200 mM (29.2 mg/ml) (*see* **Note 2**)

4. Trypsin–EDTA solution B (BI Biological Sciences): 0.25% trypsin and 0.005% EDTA in Pucks's Saline A with phenol red (*see* **Note 2**)
5. Phosphate buffered saline (PBS; 1×): dissolve 8 g of NaCl (136.9 mM), 0.2 g KCl (2.7 mM), 1.15 g Na_2HPO_4 (8.33 mM), 0.2 g KH_2PO_4 (1.47 mM) in 1 l distilled water, and pH 7.4 (*see* **Note 3**)
6. Pen-Strep Solution (Biological Industries) (*see* **Note 2**)

2.2 DNA Isolation

1. Eppendorf
2. Falcon tubes
3. Pipette tips (0.1–1 μl, 1–10 μl, 10–100 μl, and 100–1000 μl)
4. Cell lysis buffer: 10 mM Tris, 1 mM EDTA, 150 mM NaCl, 0.5% SDS, sterile water, and 10.5 pH
5. Proteinase K
6. Isopropanol
7. 70% ethanol
8. 100% ethanol
9. TE buffer
10. Nanodrop (Thermo Fischer)

2.3 Universal STELA

1. MseI and NdeI (NEB, Medinova, Denmark)
2. Double stranded oligo corresponding to sticky ends generated by MseI and NdeI (11 + 2-mer and 42-mer oligo + adapter sequence for PCR)
3. 11 + 2-mer-panhandle 5′-TAC CCG CGT CCG C-3′
4. 42-mer-panhandle 5′-TGT AGC GTG AAG ACG ACA GAA AGG GCG TGG TGC GGA CGC GGG-3′
5. Telorette (sequence TTAGGG-20n noncomplementary sequence to 3′ overhang) Telorette 1 5′-TGC TCC GTG CAT CTG GCA TCC CCT AAC-3′
6. Telorette 2 5′-TGC TCC GTG CAT CTG GCA TCT AAC CCT-3′
7. Telorette 3 5′-TGC TCC GTG CAT CTG GCA TCC CTA ACC-3′
8. Telorette 4 5′-TGC TCC GTG CAT CTG GCA TCC TAA CCC-3′
9. Telorette 5 5′-TGC TCC GTG CAT CTG GCA TCA ACC CTA-3′
10. Telorette 6 5′-TGC TCC GTG CAT CTG GCA TCA CCC TAA-3′
11. Fill in sequence for PCR

12. Adapter primer (5′-TGT AGC GTG AAG ACG ACA GAA-3′)
13. Teltail primer (5′-TGC TCC GTG CAT CTG GCA TC-3′-DIG)
14. Failsafe enzyme (Epicentre)
15. T4 ligase (NEB)
16. NEBuffer
17. ATP (NEB)
18. Failsafe PCR PreMix H (Epicentre)
19. PCR tubes or plates

2.4 Gel Electrophoresis

1. Agarose (Amersham)
2. TBE buffer 1*
3. DIG-labeled DNA Molecular Weight Marker (Roche)
4. EtBr 10 mg/ml (Sigma)
5. Loading dye (Roche)

2.5 Southern Blot

1. Telomere probe (TTAGGG)7-DIG
2. Blotting paper (Bio-Rad)
3. Nylon membrane filter or nitrocellulose (Amersham)
4. Anti-digoxigenin-AP, Fab fragments (Roche)
5. Membrane washing and blocking buffers (Roche)
6. NBT/BCIP (Roche)
7. DIG Easy Hyb (Roche)

3 Methods

3.1 Cell Culture

3.1.1 Changing Media and Maintaining hMSC-telo1 Cells in Culture

1. Remove and discard the spent media from the culture flask.
2. Wash the cells with 10 ml of 1× PBS (*see* **Note 4**).
3. Remove and discard PBS from the culture flask.
4. Pipette 10 ml of DMEM supplemented with 10% FBS, 1% penicillin and streptomycin, and 1% L-glutamine into the culture flask (*see* **Note 5**).
5. Keep the cells at 5% CO_2 and 37 °C in incubator.

3.1.2 Passaging hMS Cells

1. When hMSC-telo1 cells reached to a desired confluency, cells are subcultured.
2. Remove and discard the spent media from the culture flask.
3. Wash the cells with 10 ml of 1× PBS (*see* **Note 4**).
4. Remove and discard PBS from the flask.
5. Add 5 ml of trypsin–EDTA solution B to the cell culture flask.

6. Incubate the culture flask at room temperature and after observing the dissociation of cells from the bottom of culture flask under the microscope, cells were resuspended in 25 ml of DMEM supplemented with 10% FBS, 1% penicillin and streptomycin, and 1% L-glutamine.
7. Cell suspension was transferred into 50 ml conical tube and centrifuged at 1400 rpm for 3 min at room temperature.
8. Discard the supernatant and resuspend the cells in 1 ml of DMEM supplemented with 10% FBS, 1% penicillin and streptomycin, and 1% L-glutamine.
9. Determine total cell count by utilizing hemacytometer.
10. Add desired volume of cell suspension and 10 ml of DMEM supplemented with 10% FBS, 1% penicillin and streptomycin, and 1% L-glutamine into new culture flask (*see* **Note 5**).
11. Keep the cells at 5% CO_2 and 37 °C in incubator.

3.1.3 Calculating the Population Doubling Level

1. PD = ln[(Nfinish)/(Nstart)]/ln2.
2. The initial seeding number (Nstart) and the 80% confluence harvested cell number (Nfinish). Thus, the cumulative population doubling level (PDL) is the sum of PDs.

3.1.4 Pelleting Cells for DNA and/or RNA Isolation

1. Trypsinize cells as above.
2. Spin down cells and discard the medium.
3. Resuspend the cells in 1 ml of 1× PBS.
4. Following this, transfer cells to the Eppendorf tube and spin down at 13–14,000 rpm for 2 min.
5. Discard medium and resuspend cells in 1× PBS.
6. Remove as much PBS as possible with a pipette.
7. Wash the 50 ml tube with 1 ml PBS, transfer to the Eppendorf, and spin again.
8. Keep the cells at −20 °C.

3.2 DNA Isolation

1. Start with the heat block.
2. Cells thrown down—2000 rpm (3 min).
3. The cells are transferred to a 1.5-ml Eppendorf tube and spun down again—7000–8000 rpm.
4. Discard the supernatant and then add 0.5 ml of lysis buffer.
5. In this step, one can set the cells at −20 °C.
6. Add 100 μg of 5 μl proteinase K and incubate at 55 °C 2 h (you may want adding proteinase K more after 1 h if one considers the need).

7. If lysis does not seem to be complete, one can put the suspension further adding 100 μg proteinase K and incubate at 37 °C overnight.
8. Set the centrifuge to cool down at 4 °C.
9. After lysis, add 165 μl of 6 M NaCl.
10. Shake vigorously for 15 s (do not use vortex!).
11. Centrifuge 5 min—13,000 rpm, Biofuge at 4 °C.
12. Transfer the supernatant into a new Eppendorf tube, and spin at 13,000 rpm, for 5 min, at 4 °C.
13. Transfer the supernatant into a new Eppendorf tube and add twice sample volume of ice-cold absolute alcohol.
14. Invert the tube to precipitate the DNA until DNA is visible. If you cannot see, place the tube at −80 °C for 20 min.
15. Spin down the DNA, 5 min 13,000 rpm.
16. Pour the supernatant from and wash the DNA in 70% alcohol.
17. Dissolve DNA in 50–100 μl of TE buffer depending on the pellet.
18. Measure up the day after.

3.3 Universal STELA

1. Digest 1 μg of DNA with 1 μl of MseI and 0.5 μl of NdeI in 50 μl of volume containing 5 μl CutSmart buffer. Incubate it at 37 °C for 1 h followed by 20 min of inactivation at 65 °C.
2. 0.5 μl of digested DNA is mixed with 3 μl of 12-mer and 42-mer panhandles and 0.5 μl of dH_2O to make 7 μl of volume.
3. Use centrifuge to decrease the temperature from 65 to 16 in 49 min.
4. Add 0.5 μl (20 units) of T4 DNA ligase quickly with 1.5 μl (1*)T4 DNA ligase reaction buffer and 6 μl dH_2O to make it 15 μl of volume and incubate the sample overnight at 16 °C (*see* **Note 6**).
5. Add 0.5 μl (20 units) of T4 DNA ligase with 2.5 μl telorette working solution, 1 μl (1*)T4 DNA ligase reaction buffer, and 6 μl of water to make it 25 μl volume and incubate at 35 °C overnight (*see* **Note 6**) followed by 20 min of inactivation at 65 °C.
6. Prepare a diluent of the reaction at 1:20 using 5 μl from the stock.
7. Prepare the PCR reaction with 1.2 μl of adapter and teltail (0.1 μM), 2 μl ligated DNA (40 pg), 6 μl of failsafe master mix, 0.5 μl of failsafe enzyme, and 1.1 μl of dH_2O.

8. The PCR conditions are as follows:
   (a) 1 cycle at 68 °C for 5 min
   (b) 1 cycle at 95 °C for 2 min
   (c) 26 cycles at 95 °C for 15 s
   (d) 26 cycles at 58 °C for 30 s
   (e) 26 cycles at 72 °C for 12 min
   (f) 1 cycle at 72 °C for 15 min
   (g) 1 cycle at 4 °C for ∞
9. Prepare 0.8% agarose gel.
10. Load marker and the samples to gel.
11. Run the PCR products at 70 V for 3 h.
12. Visualize the spread under UV light.
13. Transfer DNA to a positively charged membrane overnight using blotting papers, weight, and blotting buffer (*see* **Note 7**).
14. Incubate the blot at 60 °C for 2 h with DIG labeled telomere probe.
15. Wash the blot with washing and blocking buffers to stop and remove unspecific hybridization.
16. Visualize blot using either autoradiograph or chemiluminescence with NBT/BCIP (*see* **Note 8**).

4 Notes

1. Never directly pipette or pour from stock media, take an aliquot into 50 ml falcon tubes and use from the aliquot.
2. Keep additives (sera, pen/strep aso.) aliquoted in the freezer.
3. PBS needs to be added 60 μl 0.5 M EDTA per 100 ml PBS before use.
4. In order to prevent the disturbance of the attached cell layer by the each step, PBS should be gently added to the side of the flask that is opposite to the attachment surface of the cells.
5. If media get in the lid of the culture flask, wipe the lid and the outside of the flask carefully with a tissue with a 70% ethanol. If necessary, change the lid.
6. During U-STELA, overnight incubations must be carried out in termocyclers rather than water bath, this helps to ensure the efficient ligation.
7. Remember to wear unpowdered gloves and hold the membrane out on the edges with a forceps.
8. If weak signals are seen, increase the amount of DNA in the gel or check the viability of the probe.

References

1. Martens UM, Chavez EA, Poon SSS, Schmoor C, Lansdorp PM (2000) Accumulation of short telomeres in human fibroblasts prior to replicative senescence. Exp Cell Res 256:291–299
2. Serakinci N, Hoare SF, Kassem M, Atkinson SP, Keith WN (2006) Telomerase promoter reprogramming and interaction with general transcription factors in the human mesenchymal stem cell. Regen Med 1(1):125–131
3. Jiang H, Ju Z, Rudolph KL (2007) Telomere shortening and ageing. Z Gerontol Geriatr 40:314–324
4. Grach A (2013) Telomere shortening mechanisms. In: Stuart D (ed) The mechanisms of DNA replication. InTech, Rijeca
5. Hemann MT, Strong MA, Hao LY, Greider CW (2001) The shortest telomere, not average telomere length, is critical for cell viability and chromosome stability. Cell 107(1):67–77
6. Capper R, Britt-Compton B, Tankimanova M, Rowson J, Letsolo B, Man S, Haughton M, Baird DM (2007) The nature of telomere fusion and a definition of the critical telomere length in human cells. Genes Dev 21 (19):2495–2508
7. Friis-Ottossen M, Bendix L, Kølvraa S, Norheim-Andersen S, De Angelis PM, Clausen OPF (2014) Telomere shortening correlates to dysplasia but not to DNA aneuploidy in long-standing ulcerative colitis. BMC Gastroenterol 14:8
8. Cherif H, Tarry JL, Ozanne SE, Hales CN (2003) Ageing and telomeres: a study into organ- and gender-specific telomere shortening. Nucleic Acids Res 31 (5):1576–1583
9. Friedrich U, Griese EU, Schwab M, Fritz P, Thon KP, Klotz U (2000) Telomere length in different tissues of elderly patients. Mech Ageing Dev 119(3):89–99
10. Bendix L, Horn PB, Jensen UB, Rubelj I, Kolvraa S (2010) The load of short telomeres, estimated by a new method, Universal STELA, correlates with number of senescent cells. Aging Cell 9:383–397
11. Montpetit AJ, Alhareeri AA, Montpetit M, Starkweather AR, Elmore LW, Filler K, Mohanraj L, Burton CW, Menzies VS, Lyon DE, Collins JB, Teefet JM, Jackson-Cook CK (2014) Telomere length: a review of methods for measurement. Nurs Res 63(4):289–299

Methods in Molecular Biology (2019) 2045: 225–233
DOI 10.1007/7651_2018_198

Published online: 30 November 2018

Surface Antigen-Based Identification of In Vitro Expanded Skeletal Muscle-Derived Mesenchymal Stromal/Stem Cells Using Flow Cytometry

Klemen Čamernik and Janja Zupan

Abstract

Mesenchymal stem/stromal cells (MSCs) can be isolated from several connective tissues in the adult organism by harnessing their propensity for plastic adherence in vitro. Upon culture expansion, the resulting cell cultures are composed of many different cell types at different stages of differentiation. Hence, their identity must be confirmed. Flow cytometry is an indispensable method for accurate quantification of MSC surface antigens. Here, we present a protocol that uses flow cytometry for the identification of MSCs based on the set of surface antigens required by the International Society for Cellular Therapy.

Keywords Flow cytometry, Identification, Mesenchymal stem/stromal cells, Skeletal muscle, Surface markers

1 Introduction

Mesenchymal stem/stromal cells (MSCs) are multipotent progenitor cells that can differentiate into cells of the mesoderm lineage. In our bodies, these cells provide a reservoir for tissue formation and repair and are present in most connective tissues [1]. MSC isolation from skeletal muscle involves enzymatic digestion and mechanical degradation of the tissue, which releases the cells into the surrounding medium. The cellular suspension obtained in this way contains many different types of cells, ranging from terminally differentiated myotubes to different multipotent progenitor cells. These progenitor cells share common characteristics, such as plastic adhesion and self-renewal, but can differ in their ability for multilineage differentiation. Some, like paired box 7 (Pax7)-positive satellite cells, favour myogenic differentiation and contribute to muscle regeneration [2], while others, such as fibro/adipogenic progenitor cells, have a tendency for differentiation to adipose and fibrous tissues and are thought to contribute to myosteatosis [3].

To successfully study specific cell populations, these must first be identified. Different progenitor cells express specific antigens on their surfaces. Using fluorophore-conjugated antibodies directed

against these surface antigens, flow cytometry can then distinguish between the different cells based on their immunophenotype. Identification of these progenitors is far from easy, as there is no single surface marker that will identify a specific population.

In 2006, the International Society for Cellular Therapy created a set of minimal criteria to help standardisation of the reliable identification of MSCs in vitro. These include their propensity for plastic adherence; their ability to differentiate into osteoblasts, adipocytes, and chondrocytes; and the presence and absence of specific surface antigens. Culture-expanded MSCs must be >95% positive for the three markers CD90, CD73 and CD105 and <2% positive for the markers CD45, CD14, CD19, CD34 and HLA-DR [4]. Here, we present a detailed protocol using immunophenotyping with flow cytometry for surface antigen analysis of culture-expanded skeletal muscle-derived MSCs.

2 Materials

The majority of reagents used are hazardous. Materials safety and data sheets for all chemicals should be consulted before use and the chemicals handled appropriately. Diligently follow all waste disposal regulations when disposing of biological waste materials. Before starting with the surface antigen analysis using flow cytometry, you should consult with the manager of your flow cytometer or core facility. You will need to know what kind of machine is available, and in particular, what lasers are available to select the optimal fluorophore-conjugated antibodies for your analysis. Those not familiar with the method of flow cytometry should get a basic knowledge first [5].

2.1 General Equipment

1. Laminar air flow (LAF) cabinet to carry out all of the sterile procedures involving primary cells. Good laboratory practice indicates that a single LAF cabinet should be dedicated to primary cells only. Simultaneous use of the LAF cabinet for working with other cell types is strongly ill-advised and in particular with immortalised cell lines.
2. Cell culture incubator with normoxic conditions: 37 °C; 5% CO_2; relative humidity, 85% to 95%.
3. Inverted phase contrast or bright-field microscope for monitoring cell cultures and the rate of trypsinization.
4. Benchtop swing-out bucket centrifuge with a rotor for 96-well plates.
5. Flow cytometer.

2.2 Plastic and Glassware

1. Serological pipettes (5 mL, 10 mL).
2. Micropipettes (10 μL, 200 μL 1,000 μL).
3. Tubes (1.5 mL).
4. Six-well plates.
5. Ninety-six-well plates.
6. FACS tubes: 5 mL, round-bottomed, polystyrene tubes.

2.3 Cell Preparation

1. 0.25% trypsin/ethylenediaminetetraacetic acid (EDTA).
2. Phosphate-buffered saline (PBS; 10×): Weigh out 80.0 g NaCl, 2.0 g KCl, 14.4 g Na_2HPO_4 and 2.4 g KH_2PO_4 and dissolve in 1.0 L distilled water. Measure the pH of the solution and adjust it to pH 7.4 using 1.0 M NaOH. Autoclave or filter sterilise.
3. PBS (1×): In the LAF cabinet, take 20 mL PBS (10×) and add it to 180 mL distilled water. Mix wells. Autoclave or filter sterilise.
4. Growth medium: Low glucose Dulbecco's modified Eagle's medium (LG-DMEM), 20% foetal bovine serum, 10% horse serum, 2 mM L-glutamine, 2% antibiotic/antimycotic (100× stock; 8.5 g/L sodium chloride, amphotericin B 0.025 g/L, 6.028 g/L penicillin G sodium salt, 10 g/L streptomycin sulfate). Add 1 mL 100× antibiotic/antimycotic stock solution, 0.5 mL 200 mM (100×) L-glutamine stock solution, 5 mL horse serum and 10 mL foetal bovine serum to a 50 mL conical tube. Make up to 50 mL with LG-DMEM.

2.4 Cell Staining

1. Cell staining buffer: 2 mM EDTA in PBS (1×) with 0.5% foetal bovine serum. Dissolve 0.0584 g EDTA (molecular weight, 292.24) in 100 mL PBS (1×) and add 500 μL foetal bovine serum. Filter sterilise.
2. Viability dye: Prepare the working solution by diluting 1:10 in PBS (1×). Keep protected from light.
3. Fluorophore-conjugated antibodies against selected surface antigens.

3 Methods

3.1 Cell Preparation

Both culture expanded and cryopreserved cells can be used. Freshly isolated cells can also be used (*see* **Note 1**). In this case, extra steps are required to remove the red blood cells (*see* **Note 2**). All of the procedures carried out with cell cultures are performed in a LAF cabinet under sterile conditions.

Important! The quality of the flow cytometry data depends greatly on cell viability and yield. To increase the accuracy of the

data, make sure you have enough cells. Take care to avoid any procedures that can cause excessive cell death, as dead cells can cause a high degree of autofluorescence. Dead cells also release DNA into the surrounding medium, which sticks to the cells and can cause cell clumping. Cell clumps not only cause doublets to appear on dot plots, which distorts the data, but can also block the nozzle of the flow cytometer. There are some recommendations on how to avoid cell clumping in **Note 3**.

1. Seed at least 10,000 to 20,000 cells in a six-well plate and incubate them under normoxic conditions until the cells reach at least 70% to 80% confluence. The number of the cells can be scaled up or down depending on availability. Use appropriate culture growth vessels.
2. Transfer the cells from the incubator to the LAF cabinet.
3. Remove the growth medium from the six-well plate.
4. Wash cells with PBS (1×) once.
5. Add enough of the trypsin to cover the bottom of the cell culture plate. For one well in a six-well plate, you will need approximately 200 μL. Make sure the trypsin is distributed evenly over the bottom of the well, to cover the cell layer entirely.
6. Incubate the cells at 37 °C in a cell culture incubator until all of them have detached, meaning that they will have a round morphology and are floating in the medium (*see* **Note 4**).
7. Wash the well with 1 mL growth medium by pipetting up and down several times and then transfer the trypsinised cells to a 1.5 mL tube.
8. Centrifuge at 300 × *g* for 5 min. Carefully remove the supernatant (aspirate).
9. Wash the cells by gently resuspending them in 1 mL cell staining buffer and centrifuge again at 300 × *g* for 5 min (*see* **Note 5**). The goal is to completely remove the growth medium as it contains high amounts of serum, which can cause high backgrounds in flow cytometry analysis.
10. Gently resuspend the cells in 200 μm cell staining buffer and keep the tubes on ice to prevent dying of the cells.

3.2 Cell Staining

1. Transfer the 200 μm cell suspension in cell staining buffer to 96-well plates. Prepare as many replicates as needed based on the number of the surface markers to be analysed. Adjust the volume of the transferred cells accordingly. Transfer at least 20 μL cell suspension to a special FACS tube labelled as 'unstained' and prefilled with 500 μL PBS (1×). Keep both the 96-well plate and the FACS tube with the unstained cells on ice (*see* **Note 6**).

2. Centrifuge the cells in the 96-well plates at 300 × *g* for 3 min and decant the supernatant by quickly inverting the plate.
3. Add the viability dye and the fluorophore-conjugated antibodies into the appropriate wells, diluting all of the reagents as per the manufacturer instructions (*see* **Note 7**).
4. Add as much PBS (1×) to each well, as needed to achieve the final concentration of the antibody as suggested by the manufacturer. For example, if the recommended antibody dilution for labelling of cells and subsequent analysis by flow cytometry is 1:11 for up to 10^7 cells in 100 μL buffer, you should add 10 μL of the antibody and top this up with 100 μL PBS (1×). Mix gently by pipetting.
5. Incubate the plates at 4 °C for at least 30 min, protected from light.
6. Add an additional 100 μL PBS (1×) to top up the wells. Repeat **step 2**.
7. Prepare the appropriate number of FACS tubes (one per well) and prefill them with 300 μL PBS (1×). Keep the tubes on ice.
8. Add 200 μL PBS (1×) to each well of the 96-well plates, resuspend the cells, and transfer the contents of each well to their respective FACS tube, for a total volume of cell suspension of about 500 μL.
9. Analyse the cells using the flow cytometer.

3.3 Analysis

The sample analysis will depend on your flow cytometer and the software provided. Therefore, this section will only focus on the basic steps of the cell analysis using flow cytometry.

1. Switch on the power button on your flow cytometer. Usually it takes several minutes for the system to be ready for use and for the lasers to adjust to their working temperature.
2. Open your flow cytometer software and set up a new experiment.
3. Select the channels according to the fluorochrome your antibodies are conjugated to.
4. Create at least four dot plots as shown on Fig. 1: specifically forward scatter area (FSC-A) versus side scatter area (SSC-A) (Fig. 1a left), FSC height (FSC-H) versus FSC-A (Fig. 1a middle) (*see* **Note 8**), FCS-A versus viability dye (Fig. 1a right) and FSC-A versus fluorophore-conjugated antibody (Fig. 1b). If analysing more than one surface antigen conjugated to different fluorophores (e.g. APC, FITC), set a dot plot for each one, as shown in Fig. 1b.
5. Set the voltages for each photomultiplier tube (PMT) using the unstained sample.

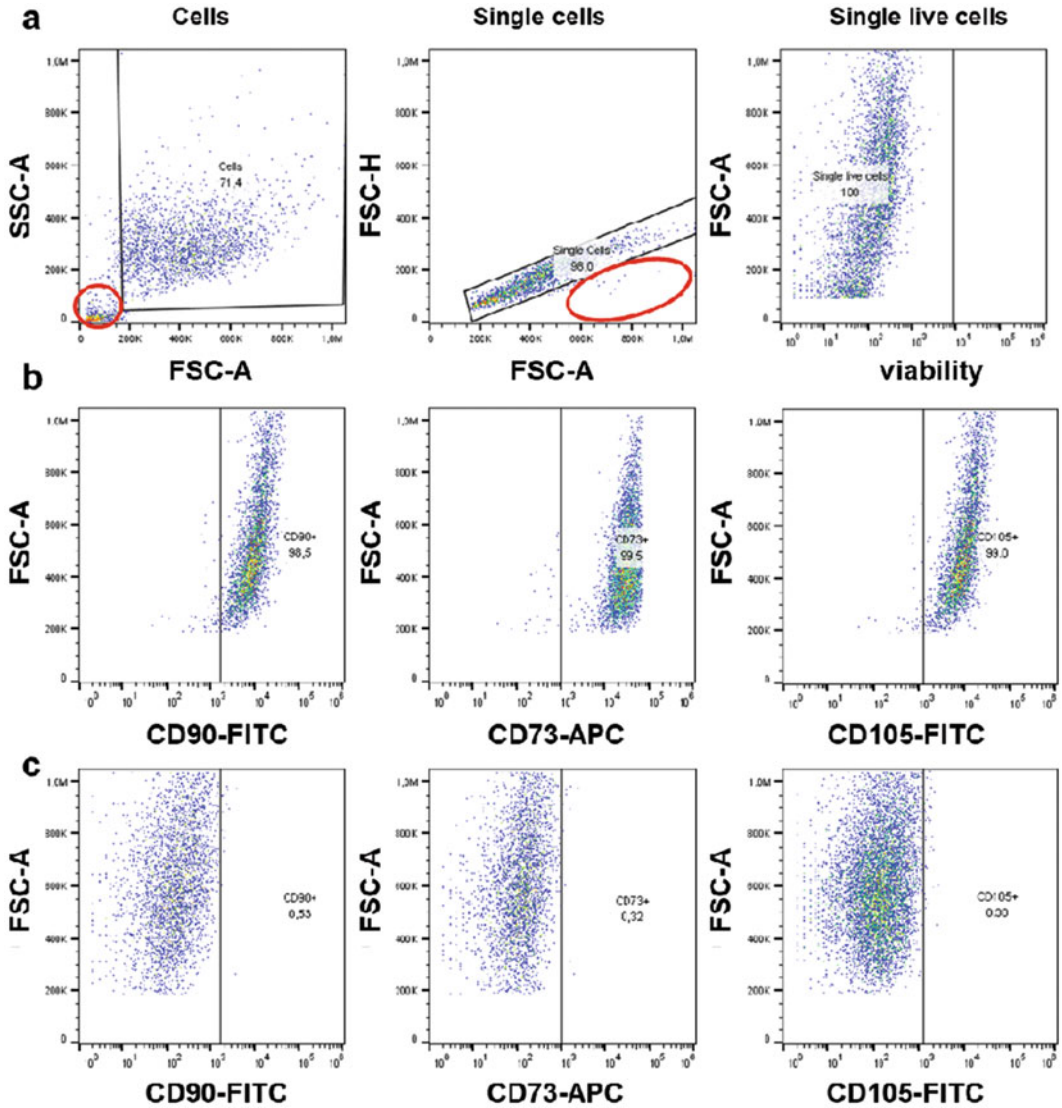

Fig. 1 Flow cytometry dot plots to identify in vitro expanded skeletal muscle-derived MSCs. (**a**) Gating strategy for the analysis of single live cells. Each dot on the dot plot represents a single event. The gate is placed in such a way as to encompass the entire population of the cells of interest on the FSC-A versus SSC-A dot plot (left). Note that the events marked with a red circle are not located within the gate. This represents cellular debris, which can be left out. FSC-H versus FSC-A dot plot encompassing cells that represent single cells (middle). The area marked with the red ellipse represents the location where doublets and multiplets appear. On FSC-A versus viability dye channel dot plots, the gate presents live cells as the viability dye labels dead cells only (right). (**b**) Dot plots of cells stained for CD90, CD73 and CD105. More than 95% of all of the live cells express these markers, therefore confirming the MSC phenotype. (**c**) Dot plots of unstained cells used to set up the gate for CD90, CD73 and CD105. *FSC-A* forward scatter area, *FSC-H* forward scatter height, *SSC-A* side scatter area

6. Double check that the voltages are correct for each PMT by briefly running the sample stained with specific antibody to be recorded in this channel.
7. Once you can detect a positive signal with your stained sample and a negative one with your unstained control, you can start recording all of your samples, including the unstained sample. Once recorded, it is no longer possible to change the voltages.
8. When you have recorded all of your samples, you can proceed with the cleaning of the flow cytometer, according to the manufacturer or core-facility instructions, and then you can shut it down. Make sure you export the files from the software.
9. You can then proceed with the analysis of the flow cytometry data. You will need to draw the gate for your population of cells on the FSC-A versus SSC-A dot plot (Fig. 1a). Within this population, you can gate single cells based on FSC-H and FSC-A. Within the population of single cells, you can then gate single live cells based on FSC-A versus viability dye fluorophore dot plot. For viability dye and the rest of the fluorophores, you will need to set up the gates based on the unstained sample for each individual channel, as shown on Fig. 1c. This will enable you to identify the specific population of cells and provide the data on the percentages of the cells expressing specific marker(s) (Fig. 1b) (*see* **Note 9**).

4 Notes

1. The quality of the data depends on the yield of the cells, among other factors. As MSCs are extremely rare, in particular when isolated from fresh tissue, make sure you have enough starting cells to ensure statistically significant data—at least a few hundred thousand events.
2. Red blood cells represent a significant proportion of blood cells and can make the surface antigen analysis difficult. To facilitate the analysis, red blood cells are usually lysed. This can be achieved using water, ammonium chloride or commercially available erythrocyte lysis buffers.
3. To avoid cell clumping, EDTA is added to the cell staining buffer. Alternatively, you can wash the cells thoroughly with Ca^{2+}/Mg^{2+} free PBS and add DNase I, which degrades any DNA released into the medium by dead cells. If you have enough cells available, you can also filter the cells through a 0.70 μm filter.
4. Prolonged exposure to trypsin can kill cells or damage the cell surface antigens. This can make surface antigen-based identification of cell populations difficult [6]. It is therefore important

to limit the exposure time of trypsin to a minimum. There are some alternatives to trypsin available. Scraping the cells gently using a cell scraper also works.

5. Avoid vortexing and excessive or aggressive centrifugation, as this can kill cells. As mentioned before, high numbers of dead cells cause high autofluorescence and can cause cell clumping.
6. It is strongly advisable to perform the staining step on ice. This can prevent cell death. Bear in mind though that some antibodies will not bind at low temperatures, so check the antibody datasheets before performing the experiment. It is also important to note that as for other chemical reactions, antibody binding is temperature dependent, and therefore longer antigen incubation times may be required when staining cells on ice.
7. Antibodies used in flow cytometry are fluorophore conjugated, meaning that they are subject to photobleaching when exposed to direct light. To increase the quality of the data, always stain cells in the dark, or at least in a semi-dark room and out of direct light, or use suitable covering for the samples, such as aluminium foil.
8. When two or more cells clump together, the flow cytometer records this as one event. If cells with two different surface antigens are clumped together, the flow cytometer will only record one surface antigen. These are the so-called doublets or multiplets that need to be excluded from the analysis. One way of doing this is by setting the correct gate on the FSC-H versus FSC-A dot plot, as shown in Fig. 1a. The doublets will have the same height as the singlets but a larger area.
9. The X axis on the dot plot is a logarithmic scale. The PMT voltages should be adjusted so all of the events above 10^3 are positively stained cells. Bear in mind, though, that on the viability dot plot, the positively stained cells represent a population of dead cells, and therefore single live cells are located below 10^3, as shown in Fig. 1a.

Acknowledgements

This work was supported by the Slovenian Research Agency, J3-7245 Research Project and P3-0298 Research Programme.

References

1. Čamernik K, Barlič A, Drobnič M et al (2018) Mesenchymal stem cells in the musculoskeletal system: from animal models to human tissue regeneration. Stem Cell Rev 14(3):346–369. https://doi.org/10.1007/s12015-018-9800-6
2. Relaix F, Zammit PS (2012) Satellite cells are essential for skeletal muscle regeneration: the

cell on the edge returns centre stage. Development 139:2845–2856. https://doi.org/10.1242/dev.069088

3. Hamrick MW, McGee-Lawrence ME, Frechette DM (2016) Fatty infiltration of skeletal muscle: mechanisms and comparisons with bone marrow adiposity. Front Endocrinol (Lausanne) 7:1–7. https://doi.org/10.3389/fendo.2016.00069
4. Dominici M, Le BK, Mueller I et al (2006) Minimal criteria for defining multipotent mesenchymal stromal cells. The International Society for Cellular Therapy position statement. Cytotherapy 8:315–317
5. Hawley TS, Hawley RG (eds) (2018) Flow cytometry protocols. Springer, New York, NY
6. Autengruber A, Gereke M, Hansen G et al (2012) Impact of enzymatic tissue disintegration on the level of surface molecule expression and immune cell function. Eur J Microbiol Immunol 2:112–120

Methods in Molecular Biology (2019) 2045: 235–244
DOI 10.1007/7651_2019_215

Published online: 16 April 2019

Analysis of Stem Cells and Their Activity in Human Skeletal Muscles by Immunohistochemistry

Rasmus Jentoft Boutrup

Abstract

Immunohistochemistry (IHC) is a frequently used technique in life science and in clinic diagnostic. IHC is a high precision method to localize different cell types or their expression in tissue. Over the years, different approaches of IHC have emerged, and the technique has become more and more sophisticated. However, the principles still remains: the inherent and spontaneous non-covalent interaction between an antibody and (hypothetical) any target of interest. That means, using this technique allows you to analyze a wide range of histological tissues (muscles, organs, neurons, etc.) from humans or animals under the microscope. Literally, IHC makes the invisible to the human eye clearly visible. In this chapter, we present an approach how to analyze human skeletal muscle tissue for content and activity of muscle stem cells, termed satellite cells.

Keywords MeSH terms, Immunohistochemistry, Antibodies, Antigens, Stem cells, Muscles

Abbreviations

BSA	Bovine serum albumin
DAPI	4′,6-Diamidino-2-phenylindole
FBS	Fetal bovine serum
GS	Goat serum
Pax7	Paired box protein-7
SC	Satellite cell
PBS	Phosphate buffered saline
MHC-I	Myosin heavy chain I
nMHC	Neonatal myosin heavy chain

1 Introduction

Immunohistochemistry (IHC) is a widely used method for clinical diagnostics in pathology (i.e., detecting abnormal cells) [1] and in research when localizing biomarkers or expressed proteins in cells (e.g., distinguish between cell types) [2]. IHC was invented for nearly a century ago [1], and since the first study was reported,

the approach has improved with new techniques. However, the fundamentals in IHC remain, i.e., the spontaneous non-covalent interaction between a paratope on an antibody (AB) and an epitope on an antigen (AG) [3]. Under normal circumstances ABs (or the AB-AG interaction) are colorless and not visible in a microscope. By conjugating a fluorophore or a color-generating tag (i.e., an enzyme generating a detectable dye) to the AB, it becomes visible when exposed to light with a certain wavelength [3]. Using an appropriated approach and validated ABs, IHC is a technique with high specificity and sensitivity.

Different approaches of IHC exist, and an exhaustive survey is outside the scope of this chapter. Here, we present the two-layer, or indirect, method on human skeletal muscle tissue, an approach using primary and secondary ABs. Using the two-layer (a fluorophore conjugated to the secondary AB) instead of the one-layer method (a fluorophore conjugated to the primary AB), more conjugated AB is attached per AG which amplifies the signal [3, 4]. Furthermore, conjugating a tag to the primary AB may impair the specificity and thus reduce the binding efficiency. In turn, some risk of increased background noise exists when using the two-layer method due to increased risk of non-specific binding by the secondary AB [3].

Samples are incubated with an AB determined the specific epitope to the AG of interest (e.g., Pax7, a transcription factor expressed in muscle stem cells). Then, a second AB conjugated with a fluorescent molecule determined the first AB (now serving as AG) is added. When exposed to light with a specific wavelength in a light microscope, cell membranes, structures, organelles, DNA, etc. appear in a colorful and fascinating way.

In this chapter, we present a step-by-step protocol to detect skeletal muscle stem cells; satellite cells (SCs), in different states of the cell cycle (quiescent, proliferation, or differentiating); and content of myonuclei in muscle fibers. SCs are instrumental in muscle regeneration and as a myonuclear donor during muscle hypertrophy. In normal conditions SCs are quiescent (expressing $Pax7^+$), but after a mechanical or chemical stimuli, the SC enters the cell cycle and proliferates (expressing $Pax7^+/myoD^+$) and either reenters the quiescent state or differentiates (expressing $myogenin^+$) [2]. Furthermore, in this chapter, we present a method to analyze and determine myofiber-specific content of SCs and nuclei and content of regenerating myofibers. All staining is done on human skeletal muscle tissue obtained from m. quadriceps femoris using the two-layer IHC counterstaining approach based on our previous study [2].

2 Materials

2.1 Reagents

- HistoFix (or another fixation media)
- 1× phosphate buffered saline (1× PBS) (*see* **Note 1**)
- Fetal bovine serum (FBS)
- Bovine serum albumin (BSA)
- Goat serum (GS)
- Triton X-100
- Sodium azide
- Mounting media containing DAPI (Invitrogen A/S)

2.2 Primary Antibodies

- IgG Pax7 from mouse (Neuromics)
- IgG myoD from rabbit (Abcam)
- IgG myogenin from mouse (Developmental Studies Hybridoma Bank)
- IgG MHC-I from mouse (Developmental Studies Hybridoma Bank)
- IgG nMHC from mouse (Novocastra)
- IgG laminin from rabbit (Dako)

2.3 Secondary Antibodies Conjugated with a Fluorophore

- IgG anti-mouse with Alexa Fluor 488 from goat (Invitrogen A/S)
- IgG anti-rabbit with Alexa Fluor 488 from goat (Invitrogen A/S)
- IgG anti-mouse with Alexa Fluor 568 from goat (Invitrogen A/S)
- IgG anti-rabbit with Alexa Fluor 568 from goat (Invitrogen A/S)

2.4 Other Materials

- ImmunoPen
- Vertical staining jar/Coplin staining jar
- Incubation tray for microscope slides
- Ultrapure water
- Demineralized water
- A fluorescence microscope and appropriated light filters and software

2.5 Preparations

Free the obtained muscle biopsy from visible fat and connective tissue, mount in Tissue-Tek, and snap freeze in isopentane cooled by liquid nitrogen. Store the biopsy at −80 °C until cutting into cryosections at −18 °C. Transfer the cryosections to microscope slides (*see* **Note 2**), and store at −80 °C until further analyses.

All reagents (antibodies, washing buffer, etc.) are dissolved in ultrapure water, if nothing else is mentioned. Always make sure to store all reagents according to the manufactures descriptions (in most cases at +5 °C). All procedures are carried out at room temperature if nothing else is mentioned. Use gloves to minimize contamination.

Before starting to incubate with ABs, prepare a washing buffer and blocking buffer.

2.6 Washing Buffer

Prepare a phosphate buffered saline 1× (PBS) (*see* **Note 1**).

2.7 Blocking Buffer

1. In another bottle make a 0.2% Triton X-100 dilution in 1× PBS. For example, dilute 80 μL Triton X-100 in 40 mL 1× PBS.
2. For 16 mL final solution of blocking buffer: take 14.72 mL of the 0.2% Triton X-100-1× PBS solution, and add 0.32 g BSA + 800 μL FBS + 320 μL GS + 160 μL 10% sodium azide. The exact amount depends on the number of samples. Use approximately 500 μL per slide.

3 Methods

3.1 Staining A: Staining for Myofiber-Type-Specific Satellite Cells (Pax7/MHC-I/Laminin/DAPI Co-staining)

1. Allow sections to thaw and dry at room temperature (RT), and encircle each cryosection with an ImmunoPen (*see* **Note 3**).
2. Fix the sections in HistoFix (*see* **Note 4**) for 4 min (max 8 min) in a vertical staining jar or similar. Make sure that the slides are fully covered.
3. Wash slides in 1× PBS three times × 5 min (*see* **Note 5**).
4. Place all slides in an incubation tray (*see* **Note 6**).
5. Block sections in blocking buffer for 1.5 h at RT (*see* **Notes 7** and **8**). Use approx. 500 μL per slide.
6. Tilt the blocking buffer, and let the slides stay in the incubation tray.
7. Incubate sections with the primary antibody against Pax7 from mouse (to detect SCs) dissolved in 1× PBS in a 1:500 solution with 1% BSA overnight at 4 °C. Use approx. 200 μL per slide.

8. Wash slides in 1× PBS 3 × 5 min in a vertical staining jar. After washing place the slides back in the incubation tray.
9. Incubate sections with a secondary anti-mouse antibody from goat conjugated with Alexa Fluor 568 (to visualize the primary antibody) in 1× PBS in a 1:200 solution with 1% BSA for 1.5–2 h at RT in dark (*see* **Note 9**). Use approx. 250 μL per slide.
10. Wash slides in PBS 3 × 5 min as above (remember **Note 9**).
11. Incubate sections with primary antibodies against myosin heavy chain type I (MHC-I) from mouse and laminin from rabbit (to detect muscle fiber type I and basal lamina, respectively), both dissolved in a 1× PBS 1:500 solution with 1% BSA in dark at RT for 2 h. Use approx. 250 μL per slide.
12. Wash slides in 1× PBS 3 × 5 min as above.
13. Incubate sections with secondary antibodies conjugated with Alexa Fluor 488 (goat anti-mouse) and Alexa Fluor 488 (goat anti-rabbit) (to detect MHC-I and lamina, respectively) both dissolved in 1× PBS in 1:500 solution with 1% BSA for 1 h at RT in dark. Use approx. 250 μL per slide.
14. Wash slides in 1× PBS 3 × 5 min as above.
15. Tilt the slides, and wipe off excess PBS carefully without touching the sections (*see* **Note 10**).
16. Add a mounting media containing DAPI (to visualize nucleus), and gently put on a coverslip. Dry flat overnight in dark, and store afterward at −20 °C (*see* **Note 11**).

3.2 Staining B: Staining for Active and Proliferating Satellite Cells (Pax7/MyoD/DAPI Co-staining)

1. Perform **steps 1–6** as in staining A.
2. Incubate sections with primary antibodies against Pax7 from mouse (to detect SCs) and MyoD from rabbit (to detect active SCs) in 1× PBS in a 1:500 and 1:750 solution, respectively, with 1% BSA overnight at 4 °C (*see* **Notes 6–8**).
3. Wash slides in PBS 3 × 5 min (*see* **Note 5**).
4. Incubate sections with secondary antibodies conjugated with Alexa Fluor 568 (goat anti-mouse) (to visualize SCs) and Alexa Fluor 488 (goat anti-rabbit) (to visualize active SCs) both in a 1:200 PBS solution with 1% BSA for 2 h at RT in dark (*see* **Note 9**).
5. Wash slides in PBS 3 × 5 min.
6. Tilt the slides, and wipe off excess PBS carefully without touching the sections (*see* **Note 10**).

7. Add a mounting media containing DAPI (to visualize nucleus), and gently put on a coverslip. Dry flat overnight in dark, and store afterward at −20 °C (*see* **Note 11**).

3.3 Staining C: Staining for Differentiating Satellite Cells (Myogenin/Laminin/DAPI)

1. Perform **steps 1–6** as in staining A.
2. Incubate sections with primary antibodies against myogenin from mouse (to detect differentiating SCs) and laminin from rabbit (to detect basal lamina) in a 1:50 and 1:500 1× PBS solution, respectively, with 1% BSA overnight at 4 °C (*see* **Notes 6–8**). Use approx. 200 μL per slide.
3. Wash slides in 1× PBS 3 × 5 min (*see* **Note 5**).
4. Incubate sections with secondary antibodies conjugated with Alexa Fluor 568 (goat-antimouse) (to visualize differentiating SCs) and Alexa Fluor 488 (goat-antirabbit) (to visualize basal lamina) in a 1:200 and 1:500 1× PBS solution, respectively, with 1% BSA for 2 h at RT in dark (*see* **Note 9**). Use approx. 250 μL per slide.
5. Wash slides in 1× PBS 3 × 5 min.
6. Tilt the slides, and wipe off excess PBS carefully without touching the sections (*see* **Note 10**).
7. Add a mounting media containing DAPI (to visualize nucleus), and gently put on a coverslip. Dry flat overnight in dark, and store afterward at −20 °C (*see* **Note 11**).

3.4 Staining D: Staining for Regenerating Myofibers (nMHC/Laminin/DAPI)

1. Allow sections to thaw and dry at RT, and encircle each section with an ImmunoPen (*see* **Note 3**).
2. Wash and hydrate slides in PBS 3 × 5 min (*see* **Notes 5** and **12**).
3. Block sections in blocking buffer for 1.5 h at RT (*see* **Notes 7** and **8**). Use approx. 500 μL per slide.
4. Incubate sections with primary antibodies against neonatal myosin heavy chain (nMHC) from mouse (to detect regenerating fibers) and laminin from rabbit (to detect basal lamina) in a 1:100 and 1:500 1× PBS solution, respectively, with 1% BSA for 2 h at RT. Use approx. 200 μL per slide.
5. Wash slides in 1× PBS 3 × 5 min.
6. Incubate sections with secondary antibodies conjugated with Alexa Fluor 488 (goat anti-mouse) and Alexa Fluor 568 (goat anti-rabbit) both in a 1:500 1× PBS solution with 1% BSA for 1.5 h at RT in dark (*see* **Note 9**). Use approx. 250 μL per slide.
7. Wash slides in 1× PBS 3 × 5 min.

8. Fix the sections in HistoFix for 4 min (max 8 min) in a vertical staining jar (*see* **Note 4**). Make sure that the slides are fully covered.
9. Wash slides in 1× PBS 2 × 5 min.
10. Tilt the slides, and wipe off excess PBS carefully without touching the sections (*see* **Note 10**).
11. Add a mounting media containing DAPI (to visualize nucleus), and gently put on a coverslip. Dry flat overnight in dark, and store afterward at −20 °C (*see* **Note 11**).

3.5 Controls

Controls are a critical part of doing IHC. To check if the procedure is working and to check primary antibody specificity, do a staining on tissue that is known to express the antigen (positive control) or on tissue that is known to lack the antigen (negative controls).

However, an easy and fast way to check for sufficient blocking and non-specific binding of the secondary antibodies and to check that any detection is done by the primary antibody only is to do a "no primary antibody control." Do the following:

1. Perform staining A, B, C, or D as listed above on one or two control samples side by side when doing the primary staining. However, on control samples, incubation with primary antibodies are omitted (just incubate sections with the dilution agent; that means 1× PBS and 1% BSA only).
2. If done appropriately, the secondary antibodies should not interact with the tissue, and no fluorescence should be detected in the microscope.

3.6 Analysis of the Samples

Use your appropriated fluorescence microscope and software (e.g., ImageJ) to capture, analyze, and count the content of SCs, myonuclei, etc. in the samples. Furthermore, measuring fiber size is also possible (using software, e.g., Leica QWin Lite).

Satellite cells are identified if they are co-stained with DAPI and $Pax7^+$ or $myogenin^+$ and located just beneath the basal lamina (*see* Fig. 1 as an example of a Pax7/DAPI staining). Furthermore, it is possible by this approach to determine the fiber-specific content of satellite cells and myonuclei and fiber size. To determine the content of newly regenerating fibers, identify muscle fibers expressing nMHC, as shown in Fig. 2.

4 Notes

1. First, we made 500 mL 10× PBS. To do this, dissolve 40 g NaCl, 1 g KCl, 7.2 g Na_2HPO_4, and 1.2 g KH_2PO_4 in 500 mL ultrapure water (pH = 7.4). Then, take 100 mL of the 10× PBS, and dilute it with 900 mL ultrapure water to make

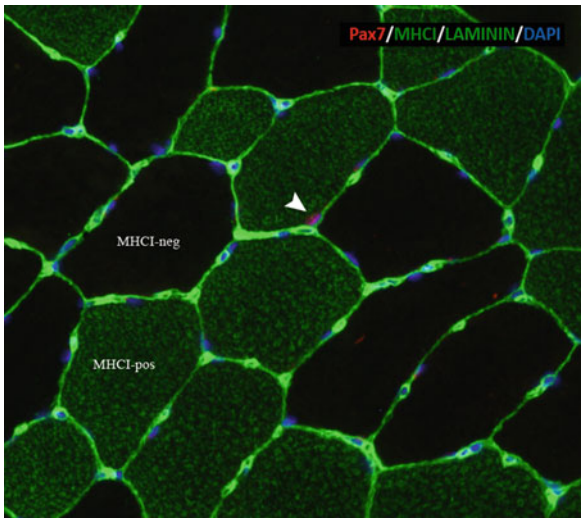

Fig. 1 An illustration of the staining with antibody against Pax7 (satellite sells, red), MHCI (muscle fiber type I, green), laminin (cell membrane, green), and DAPI (myonucleus, blue). White arrow denotes a satellite cell. Note that the illustration is a merge of different images using different light filters

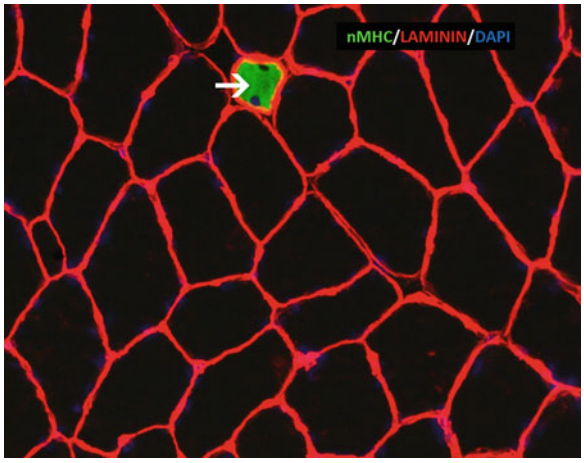

Fig. 2 An illustration of the staining with antibodies against nMHC (neonatal myosin heavy chain, green), laminin (cell membrane, red), and DAPI (myonucleus, blue). White arrow points out nMHC-positive fibers

1000 mL of 1× PBS solution. It is also possible to buy fabricated PBS mixtures or tablets and then just dissolve them into ultrapure water.

2. Add two or three cryosections from each muscle sample to the same slide to do a duplicate or triplicate analysis.
3. When encircling cryosections with an ImmunoPen, the procedure is more cost-efficient because less reagents are needed.
4. We used HistoFix (Histolab, Gothenburg, Sweden) with 6% formaldehyde. However, other fixation media might be applicable.
5. Always do the wash in a vertical staining jar. Place two slides back to back to minimize the amount of buffer used. To save time, keep the slides in the jar while pouring the washing buffer down to the sink. Just place a finger across the top of the slides.
6. To prevent the sections to dry out or dehydrate, it is important to store all slides at a humid environment (surrounded with demineralized water) in a tray designed for microscope slides when they are stored at room temperature or in a fridge. Use a cover to prevent contamination and to keep the sections hydrated.
7. At each step, be aware not to introduce air bubbles. Use the point of an unattached pipette tip to puncture any air bubbles.
8. When adding solutions to the sections, be aware that the pipette tip does not touch the cryosections. Even small contacts can destroy the samples and make them unusable. Use one hand to support the pipette and avoid any sudden movements.
9. Fluorophores exposed to light will fade over time and lose its ability to produce a visible fluorescence. Whenever it is possible, store the slides in dark after secondary antibodies with a fluorophore are added.
10. If excess PBS is still attracted to the cryosections, try to wave the slides gently.
11. It's very critical to avoid any air bubbles in the mounting media since air bubbles will blur the sample in the microscope.
12. No fixing before incubating with ABs. The AB against nMHC is only effective on unfixed tissue.

Acknowledgments

I would like to thank Jean Farup for introducing me to the amazing world of immunohistochemistry and for sharing all his great knowledge about muscle and satellite cells. I would also thank my colleague on VIA University College, Malene Munk Jørgensen, for her critical review of this manuscript.

References

1. Duraiyan J, Govindarajan R, Kaliyappan K, Palanisamy M (2012) Applications of immunohistochemistry. J Pharm Bioallied Sci 4(Suppl 2): S307–S309. https://doi.org/10.4103/0975-7406.100281
2. Boutrup RJ, Farup J, Vissing K, Kjaer M, Mikkelsen UR (2018) Skeletal muscle stem cell characteristics and myonuclei content in patients with rheumatoid arthritis: a cross-sectional study. Rheumatol Int 38(6):1031–1041. https://doi.org/10.1007/s00296-018-4028-y
3. Kalyuzhny AE (2016) Immunohistochemistry. Essential elements and beyond, vol 36(6), Springer International, Cham, p 3226. doi: https://doi.org/10.1007/978-3-319-30893-7
4. Ramos-Vara JA, Miller MA (2014) When tissue antigens and antibodies get along: revisiting the technical aspects of immunohistochemistry—the red, brown, and blue technique. Vet Pathol 51(1):42–87. https://doi.org/10.1177/0300985813505879

Methods in Molecular Biology (2019) 2045: 245–258
DOI 10.1007/7651_2018_190

Published online: 22 September 2018

Methods for Detection of Autophagy in Mammalian Cells

Bindu Singh and Sangeeta Bhaskar

Abstract

Autophagy is a conserved catabolic process that degrades cytoplasmic constituents in the lysosome and thus contributes to the maintenance of intracellular homeostasis. The process of autophagy has been involved in many physiological and pathological processes. Therefore, there is a developing need to identify, quantify, and manipulate the autophagic process accurately in the cells. As autophagy involves dynamic and complex processes, therefore various approaches are needed to study this process precisely. In this chapter, we have tried to elaborate the approaches and methods to monitor autophagy, with a primary focus on mammalian macroautophagy. Autophagy induction can be detected using Western blotting of LC3 (marker protein for autophagosomes) in which LC3-II levels represent the quantity of autophagosomes formed on induction to a particular stimulus. This can also be confirmed by puncta formation assay using confocal microscopy. Further, the autophagic flux can be examined using bafilomycin A1 as inhibitor of autophagosome–lysosome fusion and acidification of lysosomal compartments, thereby leading to accumulation of autophagosomes which is represented by high LC3-II levels. The autophagolysosomal degradation or proteolysis which is the last step of autophagy can be analyzed by DQ-BSA assay.

Keywords Autophagy, DQ-BSA, LC3, Puncta formation, Western blotting

1 Introduction

Autophagy is a lysosomal degradation pathway responsible for degradation of damaged/surplus organelles or cell components into basic biomolecules, which are again recycled into the cytosol [1]. It is a catabolic process, which is known to occur in response to a diverse number of stimuli. Autophagy, being a vital cellular housekeeping system, contributes in maintaining intracellular homeostasis by driving the flow of biomolecules in a continuous cycle of degradation and regeneration [2]. Furthermore, autophagy has been shown to play crucial roles in antigen presentation, pathogenic infections, and cell death. It is also involved in development and differentiation, aging, and innate and adaptive immunity [3, 4]. It also helps the cell in adaptation to cellular stress. The autophagic process consists of the following steps (Fig. 1):

(a) *Autophagosome formation:* This step includes induction, nucleation of vesicles, cargo sequestration, expansion of

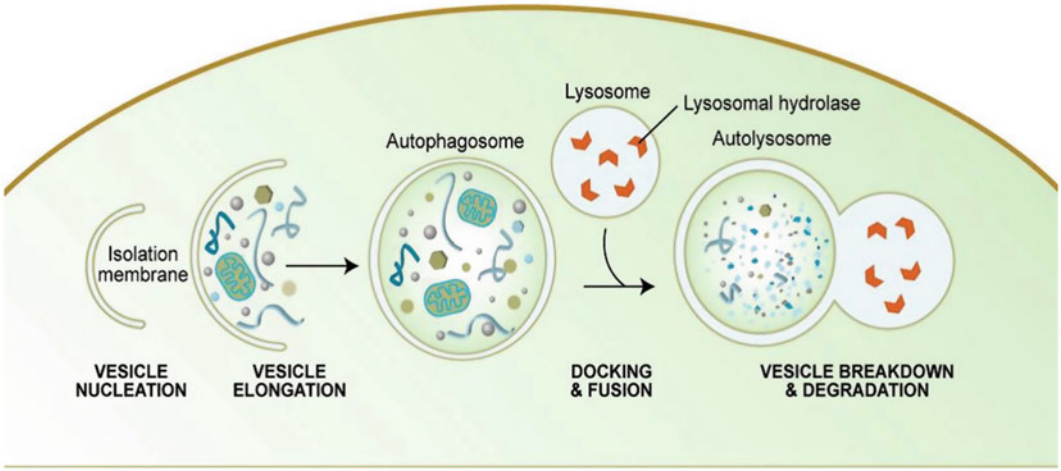

Fig. 1 Schematic diagram depicting the steps of autophagic pathway. Autophagy initiates with the formation of the phagosome membrane (nucleation) which undergoes expansion to form an autophagosome (elongation). The fully formed autophagosome then fuses with an endosome/lysosome (docking and fusion steps), resulting in the formation of an autophagolysosome. Finally, the segregated material is degraded within the autophagolysosome (breakdown and degradation) and recycled back to the cytosol (Meléndez, A. and Levine B.; WormBook, doi: https:/doi.org/10.1895/wormbook.1.147)

autophagosomal membrane, and finally the completion of autophagosome formation.

(b) *Autophagosome–lysosome fusion:* When autophagosome formation is complete, the outer membrane of the autophagosome fuses with the lysosome, thus releasing the autophagic contents into the lumen of lysosomes.

(c) *Lysosomal degradation/proteolysis, and nutrient recycling:* The autophagic cargo is degraded along with the inner autophagosomal membrane and the resulting biomolecules such as free fatty acids, amino acids, etc., are discharged back into the cytosol.

Each step of this process exerts distinct functions in a range of cellular frameworks. These step-dependent functions allow autophagy to be multifunctional [5].

1.1 Microtubule-Associated Protein 1 Light Chain 3 (LC3)

The protein LC3 (or MAP 1LC3) is the mammalian ortholog of yeast ATG8. It is a peculiar constituent of the autophagosome membrane and is presently the extremely specific marker of the autophagosomes [6]. It exists in two forms: LC3-I (the 14 kDa cytosolic form) and LC3-II (formed upon conjugation of PE to LC3-I and has molecular weight of 16 kDa). LC3-II is recruited to the inner as well as outer autophagosomal membranes [1]. In mammals, LC3-I (free form) to LC3-II (PE-conjugated form) conversion step is an important regulatory step in the process of autophagosome formation. Quantification of LC3-II corelates with

the quantity of autophagosomes formed or in a way it determines the extent of autophagy induced in response to a particular stimulus. The PE posttranslational modification which takes place at the C-terminal of glycine residue in LC3-I is needed for association of LC3 with the autophagosomal membranes. Lipidation of LC3-I is a hallmark of the induction of autophagy. The two forms can be differentiated in their electrophoretic mobility shift; non-lipidated LC3-I form migrates slowly, while the lipidated form (LC3-II) moves faster [7].

1.2 Measurement of Autophagy

Autophagosomes being the intermediate structures in dynamic autophagic pathway, the number of autophagosomes seen at a particular time point is a function of the balance between their rate of formation and the rate of their conversion into autolysosomes. Thus, increase/accumulation in the numbers of autophagosomes in cells does not always correlate to enhanced autophagic activity in the cells. This can represent either induction of autophagy or suppression of later steps in the autophagic pathway downstream of autophagosome formation. If there is a blockage at any step following formation of autophagosomes, it results in the rise of autophagosome numbers.

Thus, for the overall estimation of autophagic activity, the assessment of quantity of autophagosomes formed is inadequate. For this reason, various methods are often needed to be used in combination in order to differentiate between basal levels and induction of autophagy as well as suppression of downstream steps of the autophagic process.

Usually, "autophagic flux" is monitored for estimation of autophagic activity. The term "autophagic flux" is used to denote the dynamic process of autophagosomes formation, fusion of autophagosomes with lysosomes, and the degradation of autophagic substrates within the lysosome. "Autophagic flux" is a more decent indicator of autophagic activity rather than measuring the autophagosome numbers alone. In the following sections, we will discuss various methods for monitoring the number of autophagosomes as well as the autophagic flux.

2 Materials

2.1 SDS Polyacrylamide Gel Components

1. *Resolving gel buffer:* 1.5 M Tris–HCl, pH 8.8. Weigh 181.70 g Tris and transfer to a glass beaker. Add 900 mL of dH_2O. Mix with the help of a magnetic stirrer and adjust pH with HCl. After mixing, make up the volume to 1 L with dH_2O. Store at 4 °C.
2. *Stacking gel buffer:* 0.5 M Tris–HCl, pH 6.8. Weigh 60.60 g Tris and prepare 1 L solution as in previous step. Store at 4 °C.

3. *30% Acrylamide solution* (*29.2:0.8 acrylamide:bis-acrylamide*): Weigh 29.20 g of acrylamide and 0.8 g bis-acrylamide (cross-linker) and transfer to a beaker. Add 40 mL of dH_2O to the acrylamide mixture and mix it using magnetic stirrer till the solution becomes clear. Make up the volume to 100 mL with dH_2O and filter through a 0.45-μm filter (*see* **Note 1**). Store at 4 °C, in amber color bottle.
4. *10% Ammonium persulfate* (Merck, Germany): 10% w/v solution in dH_2O. It is best to prepare this fresh each time.
5. *N,N,N,N′*-tetramethyl-ethylenediamine (TEMED) (Merck, Germany). Store at 4 °C (*see* **Note 2**).
6. *SDS PAGE running buffer (10×):* Weigh 30.30 g Tris–HCl (0.25 M), pH 8.3, 144 g glycine (1.92 M), and 10 g SDS (0.1%). Add 900 mL of dH_2O and mix well. Make up the volume to 1 L. Dilute 100 mL of 10× SDS buffer to 1 L with dH_2O. (Concentrations given in brackets are the final molarity/percentage of that particular component in final 10× solution.)
7. *M-2 lysis buffer:* Take 5 mL of 1 M Tris pH 7.4 (50 mM), 3 mL of 5 M NaCl (150 mM), 10 mL of 100% glycerol (10%), 1 mL Triton-X-100 (1%), 100 μL of 0.5 M EDTA (0.5 mM), 100 μL of 0.5 M EGTA (0.5 mM), and 100 μL of 100× protease inhibitor cocktail (1×) in a reagent bottle and add dH_2O to make up the volume to 100 mL and mix it well. Store at 4 °C.

2.2 Immunoblotting Components

1. *PVDF membrane* (Millipore)
2. *Transfer buffer (10×):* Weigh 30.3 g Tris (0.25 M) and 14.4 glycine (1.92 M) and mix by adding 500 mL of dH_2O and make up the volume to 1 L with dH_2O. Store at 4 °C. Whenever needed, dilute 100 mL of 10× transfer buffer to 800 mL with dH_2O and then add 200 mL of absolute methanol (20% v/v) (*see* **Note 3**)
3. *Tris-buffered saline (10×):* Weigh 24.2 g Tris (0.2 M) and 80 g NaCl (1.5 M) and mix with dH_2O. Adjust the pH to 7.4 and make up the volume to 1 L
4. *Wash buffer, TBST:* TBS with 0.1% Tween-20. Store at 4 °C. Take 100 mL of 10× TBS and dilute it with 800 mL dH_2O. Add 1 mL of Tween-20 (use a cut end 1 mL tip to aspirate Tween-20 easily) and mix using a magnetic stirrer. Use this as wash buffer as well as diluent for antibodies and for preparation of blocking buffer
5. *Blocking solution:* 5% skimmed milk in TBST. Store at 4 °C. Weigh 5 g of skimmed milk powder and dissolve it in 100 mL TBST using magnetic stirrer

6. *Antibody diluent solution:* 5% BSA in TBST. Store at 4 °C. Weigh 5 g of BSA and dissolve it in 100 mL TBST using magnetic stirrer. Use this as a diluent for primary antibody
7. Absolute Methanol: To be used for activation of PVDF membrane as well as for preparation of transfer buffer

2.3 Antibodies

1. LC3A/B (D3U4C) XP® Rabbit mAb (Cell Signalling Technology, #12741)
2. β-Actin (D6A8) Rabbit mAb (Cell Signalling Technology, #8457)
3. Anti-rabbit IgG, HRP-linked antibody (Cell Signalling Technology, #7074)

2.4 Reagents for LC3 Puncta Formation Assay

1. *Cell line:* RAW 264.7 macrophage (murine macrophage cell line) available from ATCC
2. *Plasmid:* eGFP-LC3 available from Addgene
3. *Selection antibiotic:* G418 or Geneticin (Gibco, Thermo Fisher Scientific)

2.5 Reagents for DQ-BSA Assay

1. *DQ-BSA Red* (Invitrogen, Thermo Fisher Scientific)
2. *DAPI* (Invitrogen, Thermo Fisher Scientific)

3 Methods

Level of LC3-II can be quantified using biochemical assays to determine autophagosome numbers. The conversion of cytosolic LC3-I to LC3-II can be detected by Western blotting with antibodies against LC3. The molecular weight of LC3-II (a PE-conjugated form) is higher than that of LC3-I, but in SDS-PAGE, apparently LC3-II migrates faster than LC3-I because of increased hydrophobicity of LC3-II. The amount of LC3-II quantified from Western blotting usually corresponds to the number of autophagosomes [7]. However, not all LC3-II is present on the membranes of autophagosomes, as it has been observed that some LC3-II population can be generated ectopically in an autophagy-independent manner. In such cases, other approaches including GFP-LC3 labelling methods and autophagic flux assays are needed to assess autophagic activity.

3.1 Macrophage Culture and Infection with Mycobacterium

1. Culture RAW 264.7 (murine macrophage cell line) in RPMI 1640 medium, containing 10% FBS and 1× antibiotic mixture and maintain in a humidified CO_2 incubator at 37 °C.
2. For harvesting RAW 264.7 macrophages, scrape the cells gently and pellet down by centrifugation at 300 × *g* for 10 min.

3. Count the cells using hemocytometer and seed 1.5×10^6 cells in each well of a 6-well culture plate. Let the plate be kept in CO_2 incubator at 37 °C for overnight for optimal adherence of the cells.
4. Prior to infection, harvest the mycobacterial culture (OD_{600} 0.6–0.8) by centrifuging at a speed of 3000 × *g* for 10 min followed by washing with PBS for 10 min (*see* **Note 4**).
5. Infect the adhered macrophages with mycobacteria at MOI of 10 and incubate in CO_2 incubator to allow active infection for required time periods.

3.2 Macrophage Lysate Preparation

1. After the incubation, gently wash the cells thrice with PBS (*see* **Note 5**) and harvest them by pipetting.
2. Pellet down the cells at a speed of 300 × *g* for 10 min.
3. Discard the supernatant and resuspend the pellet in ice-cold M-2 lysis buffer containing 1× protease inhibitor cocktail (*see* **Note 6**). For the lysis to occur, let the tubes stand on ice for 30 min with vortexing in between.
4. Again centrifuge the lysate at 4 °C at 3000 × *g* for 15 min to pellet down the cellular debris.
5. Collect the supernatant (containing the total cell proteins) and quantify the protein content of cell lysate by standard bicinchoninic acid assay (BCA) method.

3.3 Western Blotting

3.3.1 15% SDS Polyacrylamide Gel Electrophoresis

1. *Resolving gel (10 mL):* Add 2.6 mL of 1.5 M Tris–HCl (pH −8.8), 5 mL of 30% acrylamide, 100 μL of 10% SDS, 100 μL of 10% APS, and 20 μL TEMED in a 50-mL tube and make up the volume to 10 mL with dH_2O (*see* **Note 7**). Cast the gel by pouring the resolving gel components within the gel cassette. Leave the space for stacking gel and layer the resolving gel by isobutanol (*see* **Note 8**).
2. *Stacking gel (6 mL):* Prepare the stacking gel 0.75 mL of 1 M Tris–HCl (pH −6.8), 1 mL of 30% acrylamide, 60 μL of 10% SDS, 60 μL of 10% APS, and 10 μL TEMED in a 50-mL tube and make up the volume to 6 mL with dH_2O.
3. *Sample preparation:* Take 20 μg of protein from each protein sample in 1.5 mL tubes and add 5× dye. Heat the protein samples at 95 °C at 5 min and cool on ice. Centrifuge the samples at 13,000 × *g* for 30 s to bring down the condensate. Load the protein samples on SDS-PAGE gel along with prestained protein ladder. Electrophorese at 80 V till the proteins get stacked at the bottom of the stacking gel and then continue to run at 100 V till the dye reaches the bottom of the gel.

3.3.2 Electrophoretic Transfer

1. Immediately after the electrophoresis is done, separate the gel plates with the help of a spatula. The gel remains on one of the glass plates. Remove the stacking gel.
2. Rinse the gel with deionized water to remove traces of SDS running buffer. Excise the gel with the help of spatula in such a way that protein part remains and extra gel is removed. Transfer carefully to a container with Western blot transfer buffer and gently put it above the layer of 3–4 pieces of Whatman filter paper placed in the tray.
3. Cut a PVDF membrane to the size of the gel and activate it by immersing in methanol for 5 min. Rinse it with distilled water.
4. Put the membrane on the gel in such a way that no air bubble is present in between the membrane and the gel. Again put 3–4 pieces of Whatman filter paper above the gel–membrane sandwich. Place the whole setup within the transfer cassette (*see* **Note 9**).
5. Place the cassette within the transfer apparatus and run the transfer at 60 V for 2.5 h at 4 °C.

3.3.3 Blocking

Immediately after the transfer is complete, remove the filter papers and gently take out the membrane containing proteins from the transfer assembly with the help of a clean forceps. Put this membrane in a box containing 20 mL of blocking buffer and keep it on a shaker for 1 h at RT.

3.3.4 Primary and Secondary Antibody Incubation

1. Wash the membrane thrice using 1× TBST each for 5 min.
2. Incubate the membrane with anti-LC3 primary antibody (1:1000) diluted in 5% w/v BSA in TBST for overnight at 4 °C with gentle shaking.
3. Following the antibody incubation, again wash the membrane three times with TBST, 5 min each.
4. Add anti-rabbit IgG, HRP-linked antibody diluted in TBST (1:5000) and incubate for 1 h at RT.
5. Wash again with TBST for three times.

3.3.5 Detection

1. Prepare the ECL substrate by mixing solution A and B (provided in the kit) in the ratio 1:1 and incubate for 5 min (as per manufacturer instructions). Then, incubate the membrane for 5 min with ECL substrate (Clarity Western ECL substrate from Bio-Rad Laboratories).
2. Place the membrane incubated with ECL in the chemiluminescent detector and detect at exposure time of 20 s to 1 min. Figure 2 shows the Western blot for LC3.

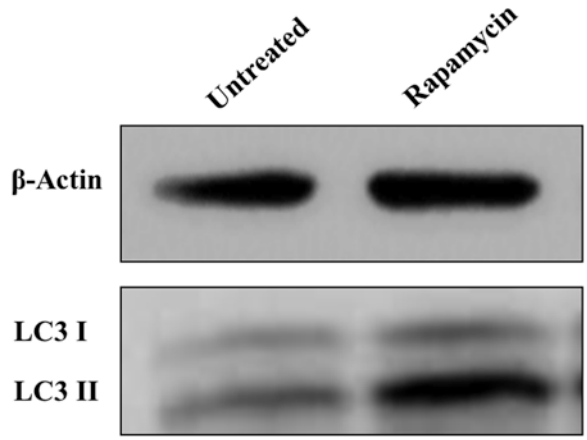

Fig. 2 Shown is the representative blot depicting the level of lipidated LC3-II in untreated and rapamycin-treated RAW 264.7 macrophages

3.4 Visualization of LC3 Puncta by Confocal Microscopy

GFP-LC3 or LC3 present endogenously can be visualized either as punctate structures or a diffuse cytoplasmic pool that mainly represent autophagosomes using fluorescence microscopy. The number of LC3 puncta formed per cell is usually an explicit measure of autophagosome numbers. The number of punctate structures can be counted visually or automatically determined using various image analysis software/programs. Although the number of puncta is notably increased after induction of autophagy, few punctae are also seen even under normal conditions. Usually, it is preferred to count the "average number of GFP-LC3 punctae per cell" in cell population under evaluation.

3.4.1 Preparation of RAW 264.7 Expressing GFP-LC3

1. Harvest RAW 264.7 macrophages and seed them at a density of 0.5×10^6 per well in a 6-well plate and incubate for 24 h in a 5% CO_2 incubator for optimal adherence.
2. On the day of transfection, dilute eGFP-LC3 plasmid DNA in incomplete RPMI media and add Lipofectamine-2000.
3. Incubate the mixture for 5 min at RT.
4. Dropwise add the DNA–Lipofectamine mixture to the cells.
5. After 6 h, replace the transfection media by complete RPMI medium and again incubate the cells for 48 h.
6. Keep the transfected cells in the selection media containing G418 antibiotic (1000 μg/mL) for 15 days to select the positive population (*see* **Note 10**).
7. Keep changing the media whenever it gets exhausted for the positive cells to survive well.

8. Observe for the GFP-LC3 fluorescence in fluorescence microscope.
9. Preserve the cells in FBS containing 10% DMSO under liquid nitrogen and revive when experiment is to be done.

3.4.2 Puncta Formation Assay

1. Prior to experiment, thaw RAW 264.7 cells expressing GFP-LC3 and culture them.
2. When the confluence of cells becomes about 80%, harvest the cells and seed on sterile coverslips (18 × 18 cm^2) placed in 12-well plate and keep overnight at 37 °C in CO_2 incubator for adherence (*see* **Note 11**).
3. Next day, harvest the mycobacterium culture by the previously mentioned procedure and infect the macrophages at an MOI of 1:10. Take rapamycin (1 μM) as positive control for autophagy induction. Also, starvation can be used as positive control. This can be done by incubating the cells in the presence of HBSS for 2 h. Keep the plates at 37 °C in 5% CO_2 incubator.
4. After specified time-points, take the plates out and gently wash the cells thrice with 1× PBS (*see* **Note 5**).
5. Fix the cells with 4% paraformaldehyde for 10 min. Again wash with PBS.
6. Prepare DAPI solution (1 μg/mL) and add 500 μL of this solution in each well containing the coverslips in the plate. Incubate for 10 min in dark.
7. Wash the cells twice with PBS and take out cover slips and let them dry (*see* **Note 12**).
8. Put a drop of mounting media (Prolong Gold Antifade Mountant, Thermo Fisher Scientific) on a clean slide. Pick the cover slips using a clean forceps and mount it by inverting it on the slide where mounting media is kept and seal the coverslips using a transparent nail-paint (*see* **Note 13**).
9. Visualize the slides using Zeiss LSM 510 Meta Confocal Microscope at 63× objective. Quantify punctate structures using ImageJ software. Figure 3 shows the puncta formation in untreated and rapamycin-treated RAW 264.7 macrophages.

3.4.3 Monitoring Autophagic Flux

The above described methods are suitable to assess the number of autophagosomes formed in the cell, which generally—but not always—indicates the level of autophagic activity in the cell. As discussed above, the accumulation of autophagosomes does not always denote autophagy induction; in fact, it may symbolize either the increased generation of autophagosomes and/or a block in autophagosome–lysosome fusion. Similar thing is true for the evaluation of LC3-II by Western blotting. When the cells are cultured with chloroquine or ammonium chloride (agents known to impair

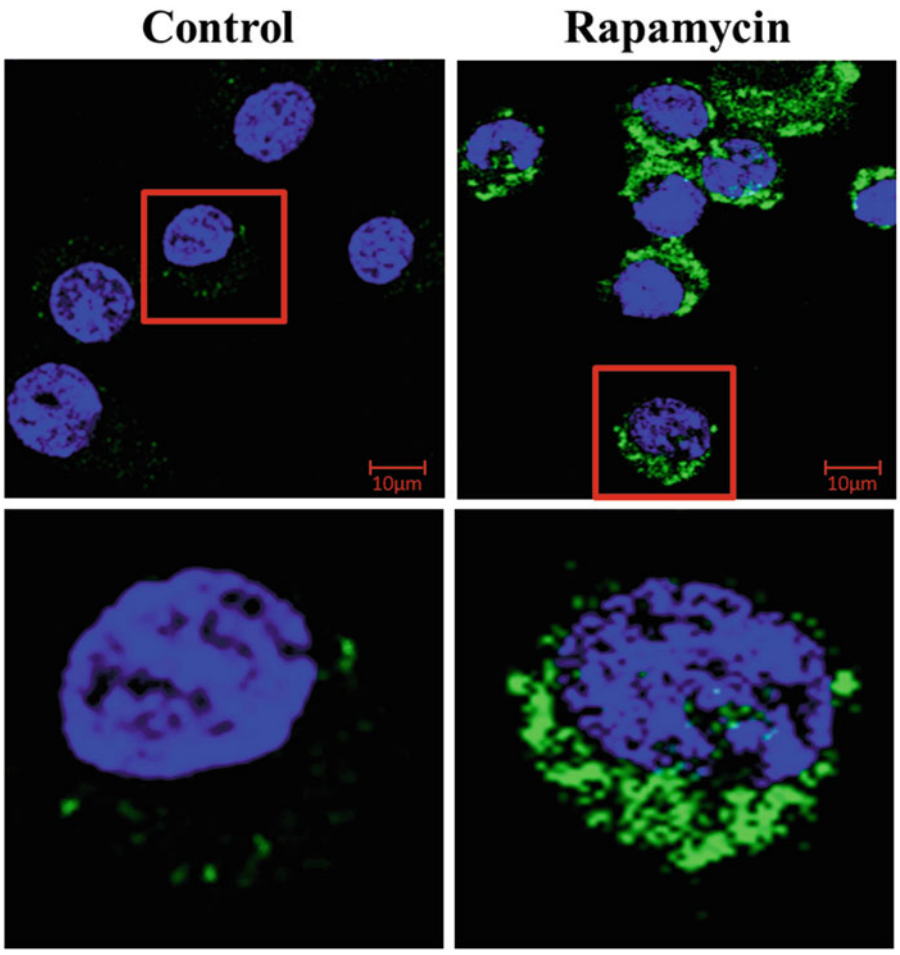

Fig. 3 Images depicting LC3 puncta formation in RAW 264.7 cells expressing GFP-LC3 (taken at 63× magnification). Shown are the merged images of GFP-LC3 (green) and DAPI (blue)

lysosomal acidification), leading to accumulation of LC3-II even under normal conditions also because LC3-II turnover by basal autophagy is also blocked in this situation. Thus, it becomes difficult to differentiate between authentic induction of autophagy (for example, in response to external stimulus or starvation), and impairment of autophagolysosomal fusion by simply quantitating autophagosome numbers (e.g., by electron microscopy or by detection of GFP-LC3 puncta using confocal microscopy) or by quantitating LC3-II levels (by Western blot analysis). It is possible to differentiate whether the increased number of autophagosomes is due to induction of autophagy or as a result of blockage of any downstream steps, by performing "autophagic flux" assays.

3.4.4 LC3 Turnover Assay

One of the prominent methods generally used to determine autophagic flux is the analysis of LC3 turnover. It is based on the observation that LC3-II present on autophagosomal membranes is degraded in autolysosomes. As detailed above, treatment of cells with chloroquine or bafilomycin A1 (lysosomal acidification inhibitors) or with lysosomal protease inhibitor impairs autophagosome–lysosome fusion, causing accumulation of LC3-II by blocking its degradation [8]. Therefore, the differences in the amount of LC3-II between samples with or without lysosomal inhibitors could be the amount of LC3 which is delivered to lysosomes for degradation [9–12].

3.5 Quantification of Lysosomal Degradation

3.5.1 Quantification of Lysosomal Degradation by DQ-BSA Assay by Confocal Microscopy

To quantify the lysosomal activity, the self-quenched reporter substrate, DQ-BSA-Red, which upon proteolytic cleavage produces brightly fluorescent products, was used. This provides a measure of the overall proteolytic/lysosomal activity within the cell. Following is the protocol for this assay:

1. Harvest RAW 264.7 macrophages and seed them at a density of 0.5×10^6 in 1 mL complete RPMI on the sterile coverslips placed in each well of a 12-well plate and keep overnight in a CO_2 incubator for adherence (*see* **Note 11**).
2. Next day, wash the cells three times with incomplete RPMI (*see* **Note 5**).
3. Dilute DQ-BSA-Red in complete RPMI medium to a final concentration of 10 μg/mL (Stock 1 mg/mL). Put 100 μL drop on parafilms (cut as glass slide shaped and keep on a solid support like 12-well plate cover).
4. Put the coverslips inverted on DQ BSA drop (cells facing the DQ BSA) on the parafilm (*see* **Note 12**).
5. Put the parafilms (aluminum foil covered) 5% CO_2 incubator for 1 h at 37 °C.
6. After incubation, remove the coverslips gently from parafilms and put again in the same 12-well plates (*see* **Note 14**) and wash three times with 1 mL of incomplete RPMI.
7. Subsequently, incubate the cells in incomplete RPMI for 2 h in a 5% CO_2 incubator at 37 °C.
8. After incubation, again put the coverslips in the 12-well plates as earlier and wash three times with incomplete RPMI as earlier.
9. Infect the macrophages with mycobacteria (MOI—1:10) for 1 h (*see* **Note 4**).
10. After incubation of 1 h, wash the coverslips placed in wells of the plate thrice with PBS to remove extracellular bacteria.
11. Then, chase the bacteria in the same plate for 2 h in 1 mL of incomplete RPMI at 37 °C in a CO_2 incubator.

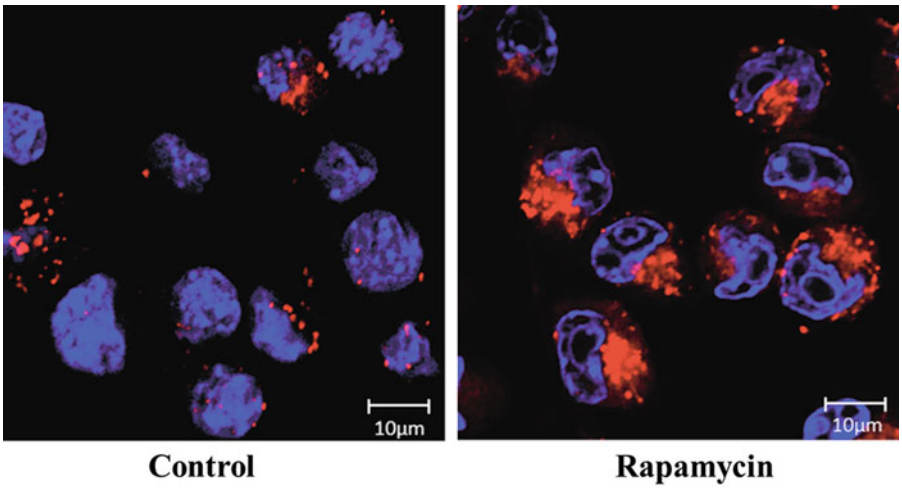

Fig. 4 Shown here are the merged images of DQ-BSA Red (red) and DAPI (blue), depicting the proteolysis of DQ-BSA in untreated and rapamycin-treated macrophages

12. After incubation, wash again three times with 1 mL of PBS.
13. Fix the cells with 4% paraformaldehyde (freshly prepared) for 10 min at RT.
14. Wash again three times with PBS as earlier and stain with DAPI by following the procedure mentioned in Sect. 3.4.2.
15. Give two washes (5 min each) with 1 mL PBS and take out the coverslips and let them dry (*see* **Note 14**).
16. Mount the coverslips on clean glass slides with Prolong Antifade Gold (Thermo Fisher Scientific) and seal the coverslips using a transparent nail-paint (*see* **Note 13**).
17. Visualize by confocal microscopy to analyze the DQ-BSA fluorescence in the experimental groups. Figure 4 shows the images depicting DQ-BSA fluorescence in untreated and rapamycin-treated RAW 264.7 cells.

3.5.2 Flow Cytometry for Detection of DQ-BSA$^+$ Cells

Apart from fluorescence detection, flow cytometry can also be used for measuring percentage of DQ-BSA$^+$ cells. For this, the following protocol can be used.

1. Harvest and seed the macrophages in a 24-well plate at a density of 0.5×10^6 per well and keep overnight in a CO_2 incubator for adherence.
2. Next day, wash the cells three times with incomplete RPMI.
3. Dilute DQ-BSA-Red in complete RPMI medium to a final concentration of 10 μg/mL (stock concentration—1 mg/mL). Add 500 μL of it to the cells and incubate for 1 h at 37 °C.
4. After incubation, wash 3 times with 500 μL of incomplete RPMI.

5. Subsequently, incubate the cells in incomplete RPMI for 2 h in a 5% CO_2 incubator at 37 °C.
6. Again wash thrice with incomplete RPMI as earlier.
7. Infect the macrophages with mycobacteria (MOI—1:10) for 1 h (*see* **Note 4**).
8. After infection, wash the cells thrice with PBS to remove extracellular bacteria.
9. Then, chase the bacteria in the same plate for 2 h in of incomplete RPMI at 37 °C in a CO_2 incubator.
10. Wash 3 times with 500 μL of PBS.
11. Fix the cells with 4% paraformaldehyde (freshly prepared) for 10 min at RT and then wash the cells thrice with PBS.
12. Harvest the cells by gentle scraping in 1.5 mL tubes.
13. Pellet down the cells at 300 × *g* for 10 min and give a wash with PBS.
14. Finally, resuspend the cells in 500 μL PBS.
15. Analyze the samples using BD FACS Verse™.

4 Notes

1. Extreme care should be taken to avoid skin contact while preparing acrylamide solution as unpolymerized acrylamide is a neurotoxin.
2. TEMED should be stored in brown bottle to protect from light. Storing at 4 °C reduces its pungent smell.
3. Do not add methanol directly to the 10× buffer, since it precipitates the ingredients of the buffer.
4. For infection of macrophages with mycobacteria, first single cell suspension of the mycobacteria should be made by passing the aliquot of the washed mycobacterial culture 10–15 times through 26G needle and then determine OD_{600}.
5. Washing should be done gently by adding PBS to the wells by the side walls as RAW macrophages are semi-adherent and get detached easily by little force.
6. Protease inhibitor cocktail should be added to the lysis buffer (kept on ice) immediately before lysis in order to prevent its degradation.
7. TEMED should be added immediately before pouring the gel into the gel assembly. Care should be taken that there is minimum time lag, in order to prevent the polymerization before adding to the gel assembly.

8. Overlay with isobutanol prevents the contact with atmospheric oxygen (which inhibits polymerization of acrylamide) and also helps in levelling of the resolving gel solution.
9. Hold one of the top corners of the membrane with a clean forceps. First, lower the opposite corner at the bottom of the membrane on the lower corner of the gel and gently release the membrane little by little to lay the complete membrane on the gel. This will prevent trapping of bubbles in between the gel and the membrane. Roll out the air bubbles from the gel–-membrane sandwich by using a 10-mL pipette prior to placing in transfer cassette.
10. The concentration of selection antibiotic should be optimized with particular cell types.
11. Sterilize the coverslips by dipping them in 75% ethanol for 30 min. Take out the coverslips and air dry them. This step should be performed in BSL 2 hood. Keep the dried coverslips in UV light for 30 min for further sterilization.
12. While taking out the coverslips, be cautious that the coverslips do not get broken as they are very fragile.
13. Coverslips should be kept on the glass slide in such a way that the front side of the coverslip where the cells are adhered should be kept inverted facing the glass slide.
14. Care should be taken that the cells remain on the upper side of the coverslip while putting the coverslips back to the wells of the plates.

References

1. Tanida I, Ueno T, Kominami E (2008) LC3 and autophagy. Methods Mol Biol 445:77–88
2. Wirawan E, Vanden Berghe T, Lippens S, Agostinis P, Vandenabeele P (2012) Autophagy: for better or for worse. Cell Res 22(1):43–61
3. Xu Y et al (2007) Toll-like receptor 4 is a sensor for autophagy associated with innate immunity. Immunity 27(1):135–144
4. Levine B, Deretic V (2007) Unveiling the roles of autophagy in innate and adaptive immunity. Nat Rev Immunol 7(10):767–777
5. Mizushima N (2007) Autophagy: process and function. Genes Dev 21(22):2861–2873
6. Kabeya Y et al (2004) LC3, GABARAP and GATE16 localize to autophagosomal membrane depending on form-II formation. J Cell Sci 117(Pt 13):2805–2812
7. Kabeya Y et al (2000) LC3, a mammalian homologue of yeast Apg8p, is localized in autophagosome membranes after processing. EMBO J 19(21):5720–5728
8. Tanida I, Minematsu-Ikeguchi N, Ueno T, Kominami E (2005) Lysosomal turnover, but not a cellular level, of endogenous LC3 is a marker for autophagy. Autophagy 1(2):84–91
9. Klionsky DJ et al (2012) Guidelines for the use and interpretation of assays for monitoring autophagy. Autophagy 8(4):445–544
10. Mizushima N, Levine B, Cuervo AM, Klionsky DJ (2008) Autophagy fights disease through cellular self-digestion. Nature 451 (7182):1069–1075
11. Mizushima N, Yoshimori T (2007) How to interpret LC3 immunoblotting. Autophagy 3 (6):542–545
12. Rubinsztein DC (2010) Autophagy: where next? EMBO Rep 11(1):3

Methods in Molecular Biology (2019) 2045: 259–269
DOI 10.1007/7651_2018_164

Published online: 23 May 2018

Metabolomic and Proteomic Analyses of Mouse Primordial Germ Cells

Yohei Hayashi and Yasuhisa Matsui

Abstract

Primordial germ cells (PGCs), the precursors of gametes, are the only cells capable of acquiring totipotency upon fertilization, but the molecular mechanisms regulating germ cell characteristics have not been fully elucidated. Although intracellular metabolic status and regulation are responsible for the control of cell function and differentiation, little is known about the metabolic features of PGCs. Here, we describe use of an integrated metabolomic, proteomic, and energy metabolic analysis method to comprehensively elucidate the metabolic characteristics of PGCs using mass spectrometry.

Keywords Glycolysis, Metabolome, Oxidative phosphorylation, Primordial germ cells, Proteome

1 Introduction

In mouse embryos, germ cells first develop as primordial germ cells (PGCs) from a subset of cells in the post-implantation epiblast (a population of pluripotent stem cells) on embryonic day (E)7.25 [1]. Following their initial appearance, PGCs actively proliferate to increase in number and concomitantly migrate and colonize the genital ridges, undifferentiated embryonic gonads, on E10.5. Male and female PGCs then enter into mitotic arrest and prophase I of meiotic division, respectively, on E14.5. When PGCs first appear on E7.25, they form a cluster consisting of only about 40 cells, but after active proliferation, their number reaches approximately 25,000 cells per fetus by E13.5 [1, 2]. After their initial development, PGCs undergo characteristic epigenetic reprogramming, including the global reduction of histone H3 lysine 9 di-methylation (H3K9me2) and DNA methylation [3–5]. As a result of dynamic changes in epigenetic state, PGCs have developmental potential to generate gametes and acquire totipotency upon fertilization. However, the characteristics of PGCs at the metabolite level, which may be closely linked to their developmental potential, have not been fully examined.

Regarding the metabolic status of germ cells in mouse embryos, Brinster and Harstad reported that mouse E15 germ cells exhibit 70% lower oxidative activity for glucose and 60% higher oxidative

activity for pyruvate compared with unfertilized ova [6]. In that report, the authors identified germ cells using three visual criteria: large nuclei, motility (characteristic blebbing and pseudopodia extension), and alkaline phosphatase staining of representative cells. They used 300 and 100 germ cells to investigate glucose and pyruvate oxidation, respectively. Because they identified germ cells based on visual characteristics, it was impossible to collect a sufficient number of cells to perform comprehensive metabolic analyses.

The recent development of Oct4-deltaPE-GFP transgenic mice has enabled acquisition of large numbers of GFP-labeled PGCs using flow cytometry, thus greatly expanding PGC availability [7]. In addition, high-throughput and comprehensive analysis of intracellular metabolites and proteins is now possible thanks to recent developments in mass spectrometry technology [8, 9].

Here, we demonstrate the methods for metabolomic, proteomic, and metabolic activity analyses of mouse PGCs. In our recent study [10], we purified PGCs, gonadal somatic cells (Somas), and embryonic stem cells (ESCs) using cell sorting. Metabolites were extracted from sorted E13.5 male PGCs, Somas, and ESCs using methanol:chloroform:water extraction and measured using capillary electrophoresis time-of-flight mass spectrometry (CE-TOFMS). For proteomic analysis, proteins in whole-cell extracts were digested to peptides in solution and then analyzed by nano-liquid chromatography–tandem mass spectrometry (nanoLC-MS/MS). To estimate energy metabolic activity, a Seahorse XF24 analyzer was used to measure the oxygen consumption rate (OCR) as oxidative phosphorylation (OXPHOS) activity and the extracellular acidification rate (ECAR) as glycolytic activity. Combining the results of these analyses, we provide a detailed description of the metabolic characteristics of PGCs compared with Somas and ESCs.

2 Materials

All solutions are prepared using ultrapure water (distilled water processed by Milli-Q to attain a sensitivity of 18.2 MΩ-cm at 25 °C) and analytical-grade reagents. All reagents are prepared and stored at room temperature unless indicated otherwise.

2.1 Primordial Germ Cell, Soma, and Embryonic Stem Cell Preparation for Flow Cytometry

1. Animals: MCH mice are purchased from Japan SLC. Oct4-deltaPE-GFP transgenic mice [7] are maintained in a C57BL/6J genetic background. The mice are kept and bred in an environmentally controlled and specific pathogen-free facility.
2. Collagenase: 1.2 mg/mL collagenase (Sigma-Aldrich), 10% fetal bovine serum (FBS) in desterilized Dulbecco's phosphate-buffered saline (DPBS; Gibco) prepared at the time of use.

3. ES medium for VR15: KnockOut Dulbecco's modified Eagle medium (DMEM; Gibco) supplemented with 15% FBS, 4 mM L-glutamine (Gibco), 0.01 mM nonessential amino acids (Gibco), 0.1 mM β-mercaptoethanol (Sigma-Aldrich), and 1000 U/mL leukemia inhibitory factor (Millipore).
4. 10× Trypsin–ethylenediaminetetraacetic acid (EDTA) solution (Sigma-Aldrich) diluted with DPBS to 1×.
5. Sorting medium: 10% FBS in DMEM (Gibco). Store at 4 °C.
6. D2F medium: 2% FBS in DMEM. Store at 4 °C.

2.2 Metabolite Extraction for Metabolomics

1. 5% Mannitol in water. Prepare at time of use.
2. Methanol containing 2.5 μM each of three internal standard (IS)1s: L-methionine sulfone (MetSul, Wako 502-76641), 2-(N-morpholino)ethanesulfonic acid (MES; Dojindo 349-01623), and D-camphor-10-sulfonic acid (CSA; Wako 037-01032). Prepare at time of use (*see* **Note 1**).
3. HMT 5-kDa ultrafiltration tube: UltrafreeMC-PLHCC 250/pk for metabolome analysis (UFC3LCCNB-HMT).
4. Water containing 200 μM each of two IS2s: 3-aminopyrrolidine (3-AP; Sigma-Aldrich 404624) and trimesate (Wako 206-03641). Prepare at time of use (*see* **Note 2**).

2.3 Protein Preparation for Shotgun Proteomics

1. Cell lysis buffer for whole-cell extract: 20 mM HEPES (pH = 7.9), 10% glycerol, 400 mM KCl, 1 mM EDTA, 1 mM $MgCl_2$, 0.1% NP-40, 0.5 mM dithiothreitol (DTT), and 1× protease inhibitor cocktail (Roche 04693132001). Prepare at time of use (*see* **Note 3**).
2. 50 mM NH_4HCO_3.
3. 100 mM DTT. Store at 4 °C.
4. 200 mM iodoacetamide.
5. Trypsin (lyophilized powder, Promega). Store at −20 °C.
6. C18 Spin Columns (Thermo Fisher Scientific).
7. Loading solution: 5% acetonitrile containing 0.5% trifluoroacetic acid (TFA).

2.4 Extracellular Flux Analysis

1. DMEM containing 10% FBS and 1 mM sodium pyruvate. Store at 4 °C.
2. XF running medium: XF Base Medium (Seahorse Bioscience 102353-100), 25 mM glucose, 2 mM L-glutamine, and 1 mM sodium pyruvate. Prepare at time of use.
3. XF24 Cell Culture Microplates (Seahorse Bioscience 100777-004).

4. FluxPak Mini-XF24 assay pack (Seahorse Bioscience 100867-100).
5. Working solution of drugs for the perturbation of OXPHOS: 0.5 μM oligomycin (an ATP synthase inhibitor, Alomone Labs O-500), 1 μM FCCP (an OXPHOS uncoupler, Sigma C2920), 1 μM rotenone (Sigma R8875), and 1 μM antimycin (Sigma A8764) (known inhibitors of the electron transport chain) in XF running medium (75 μL/well). Prepare at time of use (*see* **Note 4**).

3 Methods

All procedures are carried out at room temperature unless otherwise specified.

3.1 Primordial Germ Cell, Soma, Embryonic Stem Cell Preparation and Flow Cytometry

1. Embryos are obtained from female MCH mice mated with male Oct4-deltaPE-GFP transgenic mice [7]. Noon on the day of the plug is defined as E0.5. E11.5–E13.5 embryos are collected and dissected in DMEM containing 10% FBS. The genital ridges of embryos are dissected.
2. Genital ridges containing PGCs from Oct4-deltaPE-GFP transgenic mice are washed once and incubated with 1 mL of 1.2 mg/mL collagenase in DPBS containing 10% FBS for 1 h at 37 °C. Cultured ESCs are detached from the plate by incubation for 5–10 min at 37 °C with 1× trypsin–EDTA solution (*see* **Note 5**). To prepare single-cell suspensions for flow cytometry, cells within the samples are dissociated by pipetting. Next, 9 mL of sorting medium is added, and the samples are filtered through a 40-μm pore size nylon mesh (BD Falcon 352340).
3. Samples are centrifuged at 1000 rpm for 5 min at 4 °C, and the supernatant is removed. Cells are resuspended with D2F medium (~1×10^6 cells/mL) and transferred to a polypropylene standard test tube (Beckman Coulter). A fluorescence activated cell sorter (*see* **Note 6**) is used to sort and collect viable PGCs exhibiting intense Oct4-deltaPE-GFP expression and Somas lacking Oct4-deltaPE-GFP expression (Fig. 1). For the metabolomic analysis, sorted cells are immediately treated for metabolite extraction as described below. For proteomic analysis, sorted cells are washed with 1 mL of DPBS, and the supernatant is removed and stored at −80 °C.

3.2 Metabolite Extraction for Metabolomics

1. The sorted PGCs, Somas, and ESCs are transferred to new 15-mL tubes and washed twice with 10 mL of 5% mannitol. Add 1 mL of MeOH containing 2.5 μM each of three IS1s. Leave at rest for 10 min, vortex, and transfer 400 μL each to two new 1.5-mL tubes.

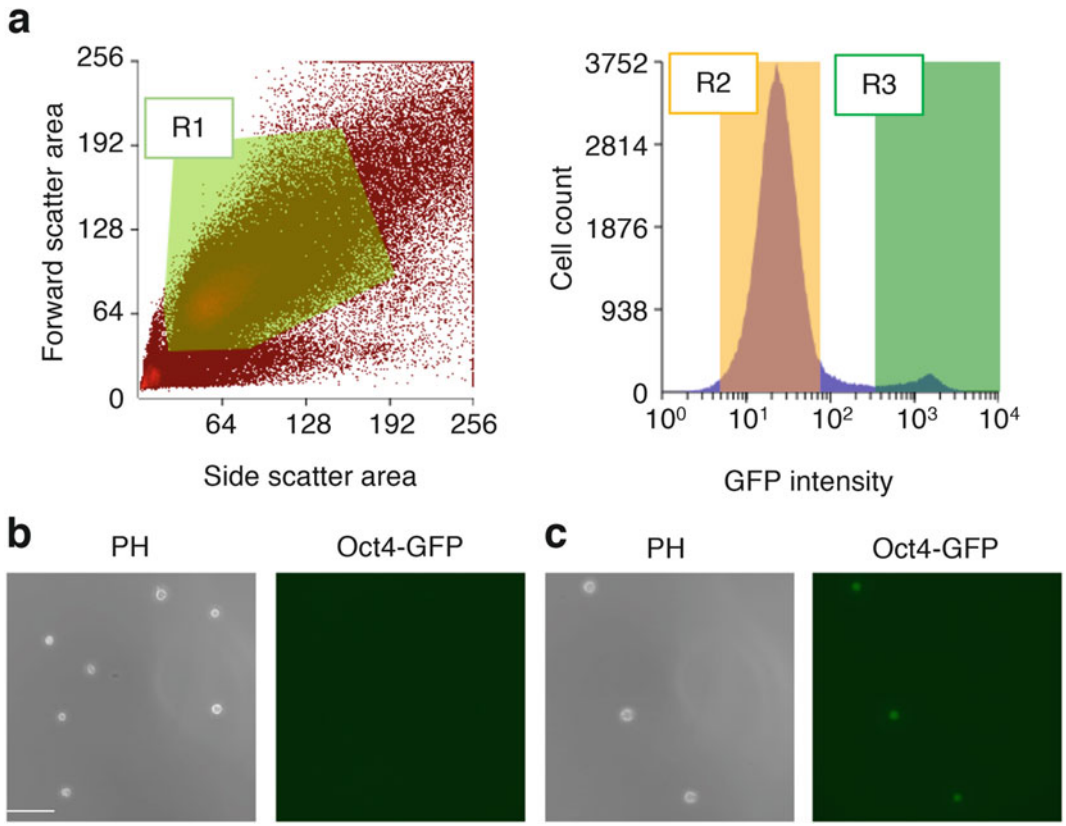

Fig. 1 FACS of cells isolated from genital ridges of E13.5 Oct4-deltaPE-GFP transgenic embryos. (**a**) Representative forward vs. side scatter plot (left panel) and histogram (right panel) of flow cytometry results (Bio-Rad S3e cell sorter). Viable cells were first sorted with gate R1 (left panel), and Oct4-deltaPE-GFP-negative (R2) and Oct4-deltaPE-GFP-positive (R3) cells were sorted as gonadal somatic cells (Somas) and primordial germ cells (PGCs), respectively (right panel). (**b**, **c**) Representative images of sorted Somas (**b**) and PGCs (**c**). PH: phase contrast. Scale bar: 50 μm

2. Add 400 μL of $CHCl_3$ and 200 μL of Milli-Q water and mix well. Centrifuge at 10,000 × *g* for 3 min at 4 °C, and transfer 400 μL of the aqueous layer to an HMT 5-kDa ultrafiltration tube. Centrifuge at 9100 × *g* for 2 h at 20 °C, collect the filtrate, and store at −80 °C.
3. Combine the filtered cell extract from approximately 5×10^5 cells (sorting ~5 times) for one specimen of each cell type and dry using an evacuated centrifuge for 2 h at 40 °C. Add 25 μL of Milli-Q water containing 200 μM each of two IS2s for CE-MS analysis. Three specimens of each cell type are then analyzed as three biological replicates.
4. Concentrations of all charged metabolites in samples are measured by CE-TOFMS. In our study [10], we used previously established methods [8, 11, 12]. If the cell volume differs by cell

a

	Features (positive)	Missing/Zero	Features (processed)
PGC-1	145	366	123
PGC-2	141	370	123
PGC-3	139	372	123
Soma-1	138	373	123
Soma-2	124	387	123
Soma-3	121	390	123
ESC-1	123	388	123
ESC-2	119	392	123
ESC-3	114	397	123

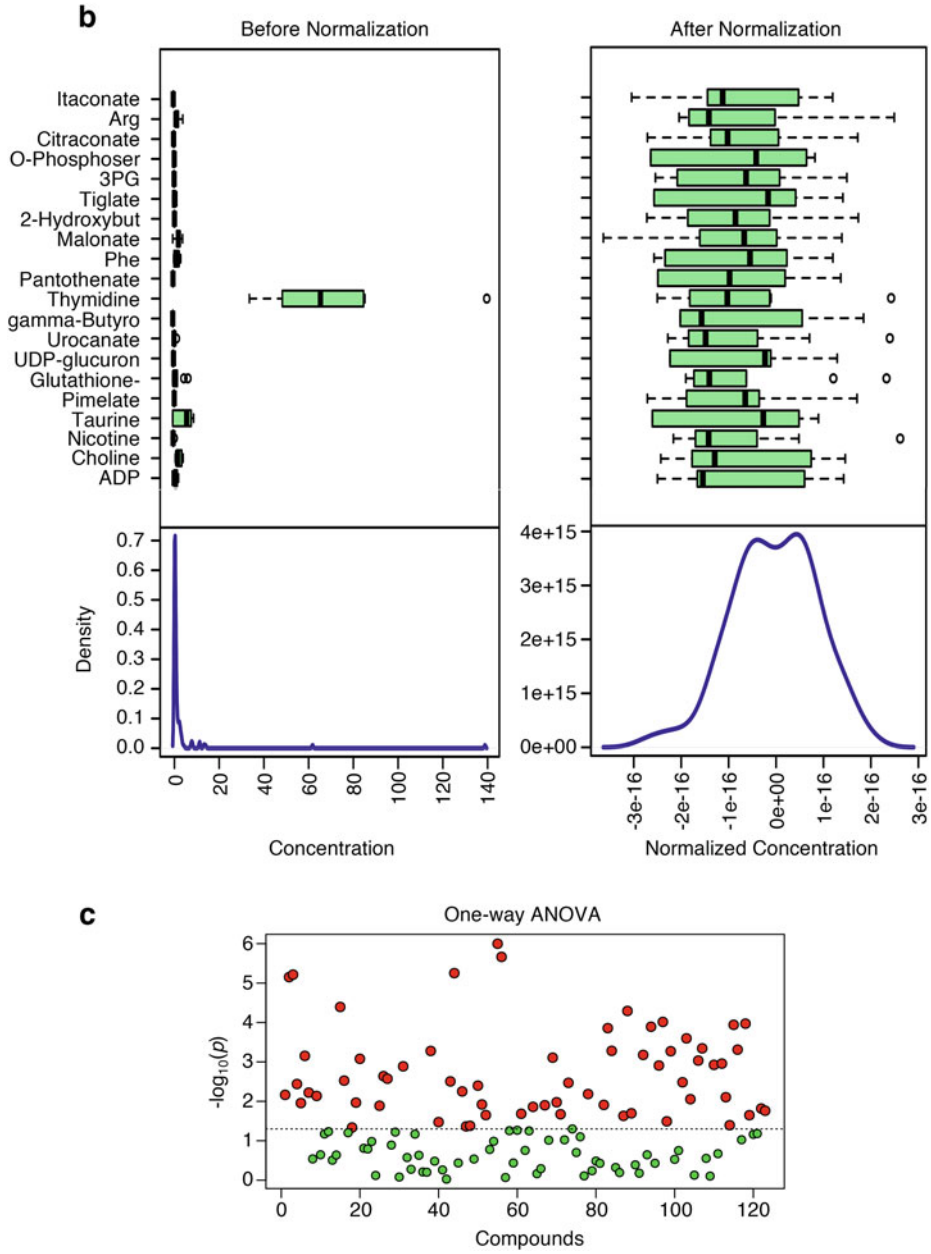

Fig. 2 Summaries of data analysis using MetaboAnalyst 3.0 in our study [10]. (**a**) Data filtering of entered metabolites. "Features" and "Missing/Zero" columns show the number of entered metabolites with concentration values and missing values, respectively, in each sample. Metabolites with missing values for more than

type, standardize the resulting concentrations by volume for each cell type.

5. The resulting concentrations of metabolites per cell or volume are then processed, normalized, and statistically analyzed using MetaboAnalyst 3.0 to identify differentially abundant metabolites among PGCs, Somas, and ESCs (http://www.metaboanalyst.ca/MetaboAnalyst/faces/home.xhtml) (*see* **Note 7**) (Fig. 2) [13]. Statistical differences are assessed using the Student's *t*-test or one-way analysis of variance (Fig. 2).

3.3 Preparation for Shotgun Proteomics

1. PGCs, Somas, and ESCs from ~5 cell sortings (~5 × 10^5 cells) are suspended in cell lysis buffer for preparing whole-cell extracts. Protein concentration of samples is determined using the Lowry method (*see* **Note 8**).
2. Whole-cell extracts (5 μg, three biological replicates) are diluted at least tenfold with 50 mM NH_4HCO_3 to a final volume of 90 μL. Subsequently, 15 μL of 100 mM DTT (in water) is added, followed by incubation for 30 min at 56 °C. Reduced cysteine residues are alkylated by adding 15 μL of 200 mM iodoacetamide (in water) and incubating for 30 min at room temperature in the dark.
3. For in-solution digestion, 1 μg of trypsin is added, and samples are incubated overnight at 37 °C. The digest reaction is stopped by adding 3 μL of TFA. Digested peptides are purified using C18 spin columns, dried via vacuum centrifugation, and dissolved in 50 μL of loading solution.
4. Tryptic peptides (10 μL) are subjected to nanoLC-MS/MS analysis to quantify each peptide peak. In our study [10], the peptides were loaded onto and analyzed using an Easy-nLC 1000 system (Thermo Fisher Scientific) equipped with reversed-phase C18 columns (trap column: Acclaim PepMap 100, 75 μm × 20 mm; separation column: PepMap RSLC, 75 μm × 250 mm; Thermo

Fig. 2 (continued) half of the tested samples were omitted, and 123 processed data were obtained. (**b**) The 123 processed data were then normalized to make the concentration values comparable to each other. Box plots and kernel density plots show concentration values of metabolites and their distribution in PGCs, Somas, and embryonic stem cells (ESCs) before and after normalization, respectively, using an auto-scaling method (mean-centered and divided by the standard deviation of each variable). The box plots show 20 representative metabolites among the 123 processed data. The bands inside the boxes indicate the median value, and right and left whiskers indicate maximum and minimum values excluding outliers, respectively. Circles indicate outliers. The density plots are based on all metabolites. Selected methods: row-wise normalization: N/A; data transformation: N/A; data scaling: auto-scaling. (**c**) Statistical differences in the normalized concentration of each metabolite among PGCs, Somas, and ESCs. The vertical and horizontal axes indicate −log10 (*p* value) calculated using one-way analysis of variance (ANOVA) and numbers assigned to the 123 processed metabolites, respectively. Each circle shows a metabolite. Metabolites exhibiting statistical significance (*p* value threshold of 0.05) are indicated as red circles

Fisher Scientific). The resulting full-scan MS/MS spectra (from mass-to-charge ratio [*m/z*] 350 to 2000) were used for quantification of each peptide peak using Proteome Discoverer 1.4 (Mascot and Sequest HT) according to the manufacturer's instructions, and the data were searched against the mouse UniProt protein database (a comprehensive resource of protein sequences and functions, http://www.uniprot.org/proteomes/UP000000589) for protein identification (*see* **Note 9**). For semi-quantification of each protein, the node "Precursor Ions Area Detector" was used.

5. Peak area values for each protein calculated in the previous section are processed, normalized, and statistically analyzed using MetaboAnalyst 3.0 in the same way as the metabolomic data. The differentially expressed proteins identified among PGCs, Somas, and ESCs are functionally annotated using the Database for Annotation, Visualization, and Integrated Discovery (DAVID; https://david.ncifcrf.gov/, Classification stringency: medium) [14].

3.4 Extracellular Flux Analysis

1. A Seahorse extracellular flux analyzer is used to measure the OCR and ECAR of PGCs and Somas in culture (*see* **Note 10**). Sorted cells are resuspended with 500 μL of DMEM containing 10% FBS and 1 mM sodium pyruvate and then incubated in 1.5-mL tubes for about 1 h at 37 °C and 5% CO_2. Centrifuge at 1000 rpm for 5 min at 4 °C and remove the supernatant.
2. Resuspend the cells with 100 μL of XF running medium. Cells are plated in XF24 Cell Culture Microplates at a density of 4–24 × 10^4 cells per well (*see* **Note 11**). Gently add 575 μL of XF running medium to each well and incubate for at least 30 min at 37 °C (but not in 5% CO_2) (*see* **Note 12**).
3. Add 75 μL of drug working solution to the A (oligomycin, an ATP synthase inhibitor), B (FCCP, an OXPHOS uncoupler), and C (rotenone/antimycin, electron transport chain inhibitors) ports of a FluxPak sensor cartridge (*see* **Note 13**). Place the plate into the Seahorse XF24 Analyzer and start the measurement protocol (Fig. 3). Cells are sequentially treated with 75 μL of 5 μM oligomycin (final 0.5 μM), 11 μM FCCP (final 1 μM), and 12 μM rotenone + 12 μM antimycin (final 1 μM each) at defined time points, and OCR and ECAR are measured following the manufacturer's instructions (Fig. 3).
4. OXPHOS activity is determined by subtracting the OCR after the addition of antimycin and rotenone (Fig. 3b, black arrow) from the basal OCR (Fig. 3b, red arrow) to eliminate oxygen consumption other than mitochondrial OXPHOS. Glycolytic activity is determined as basal ECAR (Fig. 3c, red arrow).

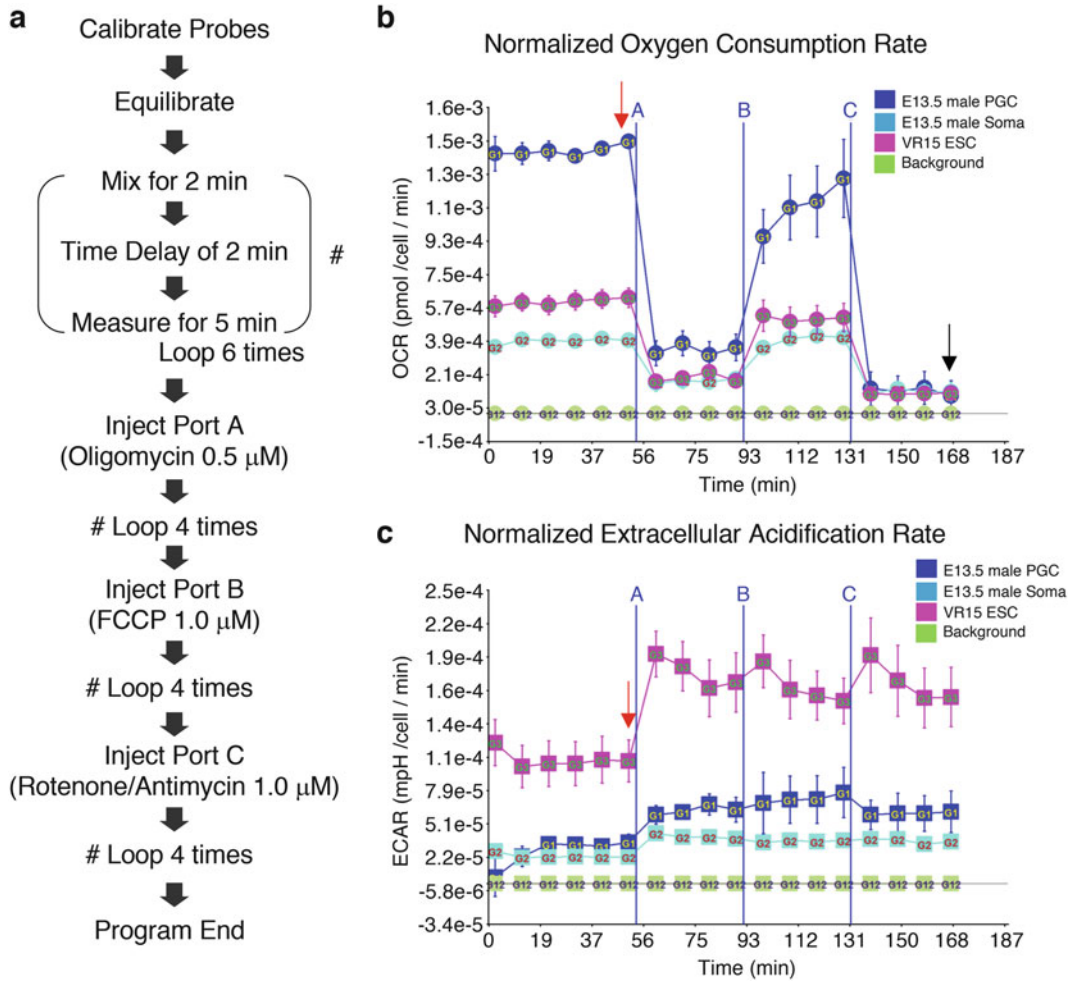

Fig. 3 Extracellular flux analysis of E13.5 PGCs, Somas, and ESCs. (**a**) Protocol for the XF24 Analyzer used in our study [10]. (**b**, **c**) Representative charts of oxygen consumption rate (OCR) (**b**) and extracellular acidification rate (ECAR) (**c**). Red arrows indicate basal OCR or ECAR. Basal respiration was determined by subtracting the OCR after the addition of antimycin and rotenone (black arrow) from the basal OCR

4 Notes

1. IS1 stock solutions: L-methionine sulfone (10 mM), MES (100 mM), and CSA (100 mM). Store at 4 °C in the dark.
2. IS2 stock solutions: 3-AP (100 mM) and trimesate (10 mM in 0.1 N NaOH). Store at 4 °C in the dark.
3. A simple method for preparing cell lysis buffer (1 mL): mix 644 μL of Milli-Q water, 40 μL of 0.5 M HEPES (pH 7.9), 125 μL of 80% glycerol, 133 μL of 3 M KCl, 2 μL of 0.5 M EDTA, 1 μL of 1 M $MgCl_2$, 10 μL of 10% NP-40, 5 μL of 0.1 M DTT, and 40 μL of 25× protease inhibitor cocktail.

4. Stock solutions of drugs: oligomycin (5 mM in DMSO), FCCP (11 mM in DMSO), and rotenone/antimycin (12 mM in DMSO). Store at −30 °C.
5. In our study [10], Vasa-RFP (VR15) ESCs [15, 16] were cultured in ES medium on mouse embryonic fibroblasts inactivated with mitomycin C (Sigma-Aldrich). Viable VR15 ESCs were sorted using a Bio-Rad S3e cell sorter after 3 days in culture.
6. In our study [10], a Bio-Rad S3e cell sorter (sorting mode: Purity) was used to sort and collect viable PGCs (~1×10^5 cells/~30–50 embryos [~6–8 pregnant mice]/sorting) and Somas. Sorting requires approximately 30 min, and we confirmed that the survival rate is high (>93%) for each cell type immediately after sorting.
7. In our study [10], metabolites with missing values for more than half of tested samples were omitted, and remaining missing values were replaced with one-half of the minimum positive value in the original data (default configuration). The processed data were normalized using an auto-scaling method (mean-centered and divided by the standard deviation of each variable). $p < 0.05$ was considered indicative of a statistically significant difference (Fig. 2).
8. Whole-cell extract from ~5×10^5 cells typically contains ~30–100 μg of protein.
9. In our study [10], up to two missed cleavages were allowed. Precursor and fragment mass tolerances were set to 10 ppm and 0.4 Da, respectively. Variable modifications were oxidation of methionine and deamination of asparagine or glutamine; static modification was carbamidomethylation of cysteine. The resulting sequences were filtered and validated, taking into account a false discovery rate of <5%.
10. As a Seahorse XF24 Analyzer was used in our study [10], our protocol is optimized for this analyzer. Several conditions, including cell number and culture volume, should be changed when using other analyzers, such as the XF96.
11. Appropriate cell number needed to obtain energy metabolic activity above the detection limit depends on cell type: ~8×10^4 cells for E13.5 PGCs; ~2×10^5 cells for E13.5 Somas and ESCs for the XF24 Analyzer.
12. As PGCs do not adhere to the plate, PGCs would move to one side if medium is vigorously added. For the XF24 Analyzer, an equal distribution of cells within each well is important to obtain reliable results.
13. Oligomycin is added to verify ATP production-coupled respiration to eliminate the contribution of ATP production-uncoupled

proton leakage from basal respiration, and FCCP is added to verify the maximum respiration capacity of cells to eliminate the possibility of respiratory suppression brought about by differences in medium conditions. For details, refer to the Seahorse XF Cell Mito stress test kit site (https://www.agilent.com/en/products/cell-analysis/seahorse-xf-consumables/kits-reagents-media/seahorse-xf-cell-mito-stress-test-kit).

Acknowledgments

Y.M. was supported by a Grant-in-Aid for Scientific Research (KAKENHI) in the Innovative Areas, "Mechanisms regulating gamete formation in animals" (grant #25114003) from the Ministry of Education, Culture, Sports, Science and Technology of Japan, and by AMED-CREST (grant #JP17gm0510017h) from the Japan Agency for Medical Research and Development.

References

1. Ginsburg M, Snow MH, McLaren A (1990) Primordial germ cells in the mouse embryo during gastrulation. Development 110:521–528
2. Saitou M, Yamaji M (2012) Primordial germ cells in mice. Cold Spring Harb Perspect Biol 4: pii: a008375
3. Seki Y, Hayashi K, Itoh K et al (2005) Extensive and orderly reprogramming of genome-wide chromatin modifications associated with specification and early development of germ cells in mice. Dev Biol 278:440–458
4. Seisenberger S, Andrews S, Krueger F et al (2012) The dynamics of genome-wide DNA methylation reprogramming in mouse primordial germ cells. Mol Cell 48:849–862
5. Ng JH, Kumar V, Muratani M et al (2013) In vivo epigenomic profiling of germ cells reveals germ cell molecular signatures. Dev Cell 24:324–333
6. Brinster RL, Harstad H (1977) Energy metabolism in primordial germ cells of the mouse. Exp Cell Res 109:111–117
7. Yoshimizu T, Sugiyama N, De Felice M et al (1999) Germline-specific expression of the Oct-4/green fluorescent protein (GFP) transgene in mice. Develop Growth Differ 41:675–684
8. Soga T, Ohashi Y, Ueno Y et al (2003) Quantitative metabolome analysis using capillary electrophoresis mass spectrometry. J Proteome Res 2:488–494
9. Aebersold R, Mann M (2003) Mass spectrometry-based proteomics. Nature 422:198–207
10. Hayashi Y, Otsuka K, Ebina M et al (2017) Distinct requirements for energy metabolism in mouse primordial germ cells and their reprogramming to embryonic germ cells. Proc Natl Acad Sci U S A 114:8289–8294
11. Soga T, Baran R, Suematsu M et al (2006) Differential metabolomics reveals ophthalmic acid as an oxidative stress biomarker indicating hepatic glutathione consumption. J Biol Chem 281:16768–16776
12. Soga T, Igarashi K, Ito C et al (2009) Metabolomic profiling of anionic metabolites by capillary electrophoresis mass spectrometry. Anal Chem 81:6165–6174
13. Xia J, Sinelnikov IV, Han B et al (2015) MetaboAnalyst 3.0—making metabolomics more meaningful. Nucleic Acids Res 43: W251–W257
14. Huang da W, Sherman BT, Lempicki RA (2009) Systematic and integrative analysis of large gene lists using DAVID bioinformatics resources. Nat Protoc 4:44–57
15. Imamura M, Aoi T, Tokumasu A et al (2010) Induction of primordial germ cells from mouse induced pluripotent stem cells derived from adult hepatocytes. Mol Reprod Dev 77:802–811
16. Maeda I, Okamura D, Tokitake Y et al (2013) Max is a repressor of germ cell-related gene expression in mouse embryonic stem cells. Nat Commun 4:1754

Methods in Molecular Biology (2019) 2045: 271–281
DOI 10.1007/7651_2018_118

Published online: 07 March 2018

Reprogramming of Aged Cells into Pluripotent Stem Cells by Nuclear Transfer

Dan-Ya Wu, Xia Zhang, and Yi-Liang Miao

Abstract

Stem cells have the potential to differentiate into specialized cell types under specific conditions in vivo or in vitro, which are used to cure many diseases related to aging. Somatic cell nuclear transfer (SCNT) can reprogram differential somatic cells into cloned embryos and embryonic stem cells can be derived from these cloned embryos. Recipient oocytes have healthier mitochondria and can improve the metabolism competence, lessen the ROS damage, and rejuvenate mitochondrial function of aged cells during reprogramming. Here, we describe a protocol to isolate aged somatic cells and reprogram them into embryonic stem cells by SCNT. These stem cells can be used to differentiate into regenerative somatic cells and replace the aged cells.

Keywords Aged cells, Embryonic stem cell, Nuclear transfer, Reprogramming

1 Introduction

In recent years, more and more stem cell technologies are used to cure many diseases that are currently limited to traditional clinical, especially aging related degenerative diseases. As we know, the birth of cloned sheep "Dolly" provides a chance to create patient-specific pluripotent embryonic cells from the differentiated somatic cells [1]. There are two methods to reprogram differentiated somatic cells into pluripotent stem cells. One method is somatic cell nuclear transfer (SCNT). SCNT can reprogram differential somatic cells into cloned embryos and nuclear transfer-embryonic stem cells (NT-ESCs) can be derived from these cloned blastocysts. Another method is iPS (induced pluripotent stem) technology that can reprogram differential somatic cells into pluripotent stem cells by defined four transcription factors in 2006 [2]. However, iPS technology can suffer the somatic genome mutations no more than six generations and cannot rejuvenate telomeres and mitochondrial function in somatic cells [3, 4]. It was reported that genes related to the stress response and DNA damage were expressed at a much lower level in the cells differentiated from iPS cells which were derived from cells in aged mice [5].

Mouse is widely used in life and medical sciences since the late eighteenth century and it is compact, cost-effective, and easily available, conserving almost 99% of human genes and physiologically resembling humans. And, it has been proved that one human year was almost equivalent to 9 mice days according to their entire lifespan [6]. Thus, we introduce a protocol to isolate aged somatic cells from 18-month-old mouse and reprogram them into embryonic stem cells by SCNT.

2 Materials

2.1 Medium

2.1.1 Somatic Cell Culture Medium

DMEM (Gibco, Cat#. 11965-092) supplemented with 10% Fetal Bovine Serum (FBS) (Hyclone, Cat#. SH30070.03), penicillin, and streptomycin.

2.1.2 SCNT Embryos Construction and Culture Medium

1. Basic CZB stock medium: 2380 mg NaCl (Sigma, Cat#. S05886), 180 mg KCl (Sigma, Cat#. P-5405), 145 mg $MgSO_4 \cdot 7H_2O$ (Sigma, Cat#. M-1880), 20 mg EDTA.2Na (Sigma, Cat#. E-6635), 2.65 ml Na-Lactate (Sigma, Cat#. L-7900), 500 mg D-glucose (Sigma, Cat#. G-6152), 80 mg KH_2PO_4 (Sigma, Cat#. P-5655), and 495 ml of Specialty Media ultra-pure water (TMS-006-B, 500 ml). The stock medium should be filtered by 0.22 μm filter and can be stored at 4 °C for several months
2. CZB medium: 198 ml basic CZB stock medium adding 422 mg $NaHCO_3$ (Sigma, Cat#. S-5761), 2 ml $CaCl_2 \cdot 2H_2O$ (100× stock) (Sigma, Cat#. C-7902), 6 mg pyruvate (Sigma, Cat#. P-4562), glutamine (200×, Gibco, Cat#. 21051-024), and 1000 mg BSA (Sigma, Cat#. A3311). The pH of medium should be adjusted to 7.4 and filtered by 0.22 μm filter, stored at 4 °C for up to 2 weeks
3. Hepes-CZB medium (H-CZB): 198 ml basic CZB stock media adding 1040 mg Hepes·2Na (Sigma, Cat#. H8651), 84 mg $NaHCO_3$, 2 ml $CaCl_2 \cdot 2H_2O$ (100× stock), 6 ml pyruvate, 30 mg glutamine, and 14 mg PVA (Sigma, Cat#. P-8136). The pH of medium should be adjusted to 7.4 and filtered by 0.22 μm filter, stored at 4 °C for up to 2 weeks
4. Ca^{2+}-free CZB: 100 ml basic CZB stock media adding 211 mg $NaHCO_3$, 3 mg pyruvate, glutamine (use 200× stock), and 500 mg BSA. The pH of medium should be adjusted to 7.4 and filtered by 0.22 μm filter, stored at 4 °C for up to 2 weeks
5. Activation solution: Ca^{2+}-free CZB adding 10 mM $SrCl_2$ (Sigma, Cat#. 255521) and 5 μg/ml cytochalasin B (Sigma, Cat#. C-6762)

6. Embryo culture medium: G-1TM PLUS medium (Vitrolife, Cat#. 10132) or EmbryoMax KSOM+AA with D-glucose medium (Millipore, Cat#. MR-106-D)

2.1.3 ESC-Derivation Medium

2i Medium: KO-DMEM (Gibco, Cat#. 10829018) supplemented with 15% Knockout Serum Replacement for ESCs/iPSCs (Gibco, Cat#. 10828028), MEM Non-Essential Amino Acids Solution (Gibco, Cat#. 111040050), GlutaMAX™ Supplement (Gibco, Cat#. 35050061), 2-mercaptoethanol (Specialty Media, Cat#. ES-007-E), EmbryoMax 100× nucleosides (Millipore, Cat#. ES-008-D), leukemia inhibitory factor (LIF) (Millipore, Cat#. ESG1107), 1 μM PD0325901 (Sigma, Cat#. PZ0162-5MG), and 3 μM CHIR99021 (Sigma, Cat#. SML1046-5MG).

2.1.4 ESC Culture Medium

KO-DMEM (Gibco, Cat#. 10829018) supplemented with 15% FBS, MEM Non-Essential Amino Acids Solution, GlutaMAX™ Supplement, 2-mercaptoethanol, EmbryoMax 100× nucleosides, and LIF.

2.2 Animals

All mice should be handled in accordance with the rules stipulated by the Animal Care and Use Committee. They are housed in the experiment animal center under a 14-h light, 10-h dark schedule and provided with food and water ad libitum.

2.2.1 Aged Mice

As stated in the introduction, one human year is almost equivalent to 9 mice days according to their entire lifespan [6]. So, 18-month-old mice are used in this protocol.

2.2.2 Oocytes Donor Mice

BDF1 mice are used as oocyte donors, which are F1 hybrids of C57BL/6 female and DBA/2 male mice.

2.3 Micromanipulation Equipment

2.3.1 Holding Pipette

In general, holding pipette for mouse oocyte has an outside diameter of about 80 μm, an inner diameter of about 10 μm, and an angle of about 30 °C at the tip. It can be made using pipette puller and microforge, or purchased from commercial company (Humagen Fertility Diagnostics).

2.3.2 Injection Pipette

There are two kinds of injection pipettes (one for enucleation and the other for nuclear injection). The pipette for enucleation has an inner diameter of about 7–8 μm, while the pipette for nuclear injection has an inner diameter of about 4–7 μm (depending on the cell source). It can be made using pipette puller and microforge, or purchased from commercial company. To prevent stickiness, the injection pipette could be washed by aspirating and releasing small volumes of hydrofluoric acid (10%) first, water next, and 100% ethanol last. The injection pipettes should be backfilled with mercury (toxic) about 1 mm using a 1-ml syringe (*see* **Note 1**).

2.3.3 Workstation for Micromanipulation

A piezo workstation is used during nuclear transfer because the mouse oocyte plasma membranes are soft and exquisitely sensitive. Firstly, the holding and injection pipettes are installed to the pipette holders and the holders are put on the manipulators. Next, the injection pipette is washed by immersing into a 10% PVP drop and releasing a small volume of mercury and aspirating a small volume of 10% PVP medium while applying piezo pulses of high power and frequency continuously. This process should be repeated until mercury moves smoothly up and down the inner surface of the injection pipette. Finally, the holding and injection pipettes are dropped into the same H-CZB drop and the manipulation system is ready to use for removal of chromosomes and nuclear injection.

3 Methods

Carry out all procedures at room temperature unless otherwise specified.

3.1 Preparation of Somatic Cells from Aged Animals

The 18-month-old mouse tail tip fibroblast (TTF) [7] cells are used as donor nucleus in this experiment. Besides, the sertoli cells of male testis [8] or the cumulus cells around oocytes [9] are also fine choices. The steps of the preparation of TTF are as follows:

1. Using 75% alcohol in mice tail for disinfection, shearing mice tail around 4 cm long, removing the skin carefully, and putting it into a 60-mm-diameter culture dish with Ca^{2+} and Mg^{2+}-free PBS to wash off the blood and adipose tissue.
2. Using the dissection forceps and scissors that have been autoclaved to cut off the tail tip tissue about 2 mm long and placing on the bottom of culture dishes, sucking the liquid around the tissue.
3. Cell medium is gently added after 1 h, do not disturb the tissue, so that the liquid slowly covered it. And cultured in a humidified atmosphere of 5% CO_2 at 37 °C for a week (do not move the dish) and the TTFs become confluent on the bottom, and then cell medium should be changed every 2 days until TTFs grow to ~90% confluence. TTFs can be frozen or passaged at this stage (*see* **Note 2**).
4. Digest the cells with trypsin and then wash cells with PBS; finally, put it in the 3% PVP medium at 4 °C [9] (*see* **Notes 3** and **4**).

3.2 Reconstruction of Cloned Blastocyst by Somatic Cell Nuclear Transfer

The methods of nuclear removal from MII oocytes include chemical enucleation [10] and mechanical removal of the chromosome–spindle complex [9]. In this protocol, we use mechanical removal of the chromosome–spindle complex (*see* **Notes 5** and **6**).

3.2.1 Nuclear Removal

1. Usually, to reduce the impact of prolonged culture at room temperature on oocyte quality and nuclear position, we place a small group of 20–25 oocytes into a drop of H-CZB medium with 7.5 μg/ml cytochalasin B (CB). CB has a reversible effect on the cytoskeleton and can decrease the death of oocyte (*see* **Note 7**).
2. The holding pipette and injection pipette are used to find the nucleus and the nucleus is positioned at 3 (or 9) o'clock.
3. A hole is punched through the zona pellucida (ZP) by injection pipette applying piezo pulses, and then the oocyte nuclear is sucked out by injection pipette. The less cytoplasm is sucked out, the better the embryo develops. In general, we place the oocyte upward side of pipettes and move the enucleated oocytes to the downward of pipettes.
4. After oocytes are enucleated in each group, they are washed 3–4 times by CZB medium (overnight balance) to remove CB completely and cultured in CZB medium at least 30 min before nuclear injection in the incubator. We usually spend 1.5–2 h on this step (*see* **Note 8**).

3.2.2 Nuclear Injection

The single somatic cells are prepared before nuclear injection and placed in the 3% PVP medium at 4 °C for up to 2 h.

1. 20–30 enucleated oocytes are placed in the drop of H-CZB medium with 3.5 μg/ml CB and cell suspension is added into the 3% PVP medium drop.
2. A couple of slight piezo pulses are used to break cytoplasm membrane of TTFs along with repeated suction by injection pipette (*see* **Notes 9** and **10**).
3. After 3–5 nuclei aspirated, enucleated oocyte is punched a hole in the ZP by applying piezo pulses and a nucleus is injected into the cytoplasm of enucleated oocyte. The injection pipette is immediately withdrawn gently and a small amount of cytoplasm is absorbed to seal the plasma membrane and minimize oocyte death after injection.
4. After a group of injection finished, the injected oocytes should be stayed in the drop about 15–30 min to recover, and after that, CZB medium (overnight balance) is used to wash the oocyte 3–4 times to remove CB completely and cultured in CZB medium approximately 1 h in the incubator before activation.

3.2.3 Oocyte Activation

During fertilization, the sperm enters the oocyte and evokes a series of repetitive calcium oscillations to activate oocytes [11–13]. It was found that strontium chloride ($SrCl_2$) could lead to oocyte activation efficiently and was widely used for SCNT in mouse [14, 15].

1. After nuclear injection, oocytes are incubated in the pre-equilibrated Ca^{2+}-free CZB medium containing 10 mM $SrCl_2$ and 5 μg/ml CB for 4–6 h, and most of the oocytes would have pronucleus.
2. Ca^{2+}-free CZB is used to wash reconstructed embryos at least five times to remove $SrCl_2$ completely after activation, and then they are washed using pre-equilibrated G-1TM PLUS medium for 3–4 times and cultured in G-1TM PLUS medium until they develop into the blastocyst in the incubator (*see* **Note 11**).

3.3 Derivation of Pluripotent Stem Cells from Cloned Blastocysts

3.3.1 Preparation of Mouse Embryonic Fibroblasts

Mouse embryonic fibroblasts (MEFs) secrete LIF and other factors, which not only support ESCs growth and multiplication but also inhibit ESCs differentiation. So, our laboratory derives the NT-ESCs using 2i medium with MEFs and the efficiency can reach 80%. The steps of MEF preparation are as follows:

1. The embryos of 12.5–13.5 days are obtained from the pregnant female mouse, and washed 3–4 times in PBS and put in 60 mm dish in the clean bench. Must be sure to wash out blood. Penicillin and streptomycin can be added into PBS properly to avoid contamination. Both the ICR and C57BL/6J can be used to prepare MEFs.
2. Use dissection forceps and scissors to dissect out the uterine and release the embryos, wash 3–4 times in PBS. And then, successively remove the fetal membrane and cut off the placenta, wash with PBS every time.
3. Remove the heads, the viscerals, the limbs, and the tails, then transfer the embryos into 1.5 ml centrifuge tube and cut into small pieces. Trypsinize the tissues 10–15 min with 0.5 ml 0.25% trypsin/EDTA in the 37 °C incubator, shake them every 5 min.
4. Suspend the trypsinization by adding cell culture medium 1:1–2, centrifugation (10 min at 1500–2000 rpm), and abandon supernatant. Then, 5 ml cell culture medium suspension is cultured in the 100 mm Petri dish in the 37 °C, 5% CO_2 incubator. Cell suspension can be cultured after cell strainers to remove superfluous tissue. In general, 1–2 of 100 mm Petri dish could be used for one embryo.
5. Change culture medium next day and let the MEFs grow till ~90% confluence (commonly 2 days); MEFs are considered to be at passage 0 at this stage and can be frozen or expanded cultured (*see* **Note 12**).

6. As a feeder layer, completely confluence MEFs should be mitotically inactivated by treated with mitomycin C (10 mg/ml for 2 h or 1 mg/ml overnight) at least one day before the culture of ESCs. Afterwards, wash MEFs with PBS at least 3 times and trypsinize, seed onto the 96-well plate which has been covered with 0.1% gelatin for 30 min at 37 °C and discard it. MEFs should be covered the entire well, and the density of MEFs are 20,000–25,000 cells per cm^2. The proper passages of MEFs are no more than 3, and the use of the prepared feeder layer should not exceed a week.

3.3.2 Derivation of Nuclear Transfer-Embryonic Stem Cells from Cloned Blastocysts

1. The medium of feeder layer should be changed to 2i medium at least 2 h before derivation.
2. Collect the blastocysts from SCNT at E3.5-E4 and seed individually to a well of 96 well plate and be cultured in 37 °C, 5% CO_2 incubator. 1% protease is used to remove the ZP of clone blastocysts, which can improve the success rate of the NT-ESCs derivation (*see* **Notes 13** and **14**).
3. It usually takes 3 days to allow blastocysts attach to the MEFs feeder layer, do not move it during this time.
4. Hereafter, change fresh 2i medium every 2 days. About the seventh day after plating, we can look at an inner cell mass outgrowth and then it can be digested. Trypsinize all cells in a well with 0.05% trypsin/EDTA, suspend with 2i medium, and transfer into a 12-well plate with prepared MEFs feeder layer 1 day advance (*see* **Note 15**).
5. The NT-ESCs are considered to be at passage 1 at this stage. 2i medium should be half changed every day till the typical colony morphology appeared which approximately needs 3–4 days.
6. We can passage the NT-ESCs normally with 2i medium that can be changed into ESCs culture medium (*see* **Note 16**).

3.4 Evaluation of Pluripotency in Nuclear Transfer-Embryonic Stem Cells

To evaluate the pluripotency of NT-ESCs, the following experiments should be done as follows:

3.4.1 Karyotype Analysis

1. The NT-ESCs are incubated in ESCs culture medium with 0.4 μg/ml colcemid (Invitrogen, Thermo Fisher Scientific) for 4 h and harvested from MEFs with 0.05% trypsin/EDTA.
2. After incubation in hypotonic solution with 0.075 M KCl at 37 °C for 15–20 min and centrifugation, the cells are fixed with a methanol/acetic acid mixture (3:1, v/v) and centrifuged, repeat twice.

3. The fixed cells are mounted on glass slides (precooling in advance at 4 °C) and stained with Giemsa for 10–15 min after drying.
4. The numbers of metaphase chromosomes are counted.

3.4.2 Alkaline Phosphatase (AP) Staining

An Alkaline Phosphatase Detection Kit (Millipore, SCR004) was used.

1. According to the manufacturer's instructions, NT-ESCs are fixed with 4% paraformaldehyde for 1–2 min followed by rinsing with 1× TBS-T buffer (20 mM Tris–HCl, pH 7.4, 150 mM NaCl, and 0.05% Tween-20).
2. Stain solution (a mixture of 2:1:1 ratio of Fast Red Violet (FRV), Naphthol AS-BI phosphate solution, and water) is applied to cover the cells at room temperature in dark for 15 min.
3. After rinsing the cells with 1× TBS-T buffer, cell images are taken.

3.4.3 Quantitative Reverse-Transcription PCR

1. Total RNA is extracted using TRIzol (Invitrogen, Thermo Fisher Scientific) and reverse transcription is performed using FastQuant RT Kit (Tiangen, KR106-02).
2. Quantitative real-time PCR is performed using SYBR Premix Ex Taq (Takara, Kusatsu, Japan). The reactions are performed in triplicate on a 1/10 dilution of the cDNA obtained from above.
3. Gene expression in each sample is normalized to GAPDH, and the relative quantification of expression is estimated using the comparative CT method.

3.4.4 Western Blots

1. Proteins isolated from NT-ESCs are resolved by 10% SDS-PAGE (120 V for 1.5–2 h) and transferred to polyvinylidenedifluoride membranes.
2. Membranes are blocked for 1 h, and then membranes are incubated overnight at 4 °C, respectively, with Oct4 (1:500, Abcam, Cat#. AB181557), Sox2 (1:500, Abcam, Cat#. ab79351), Nanog (1:500, Abcam, Cat#. ab80892), SSEA-1 (1:500, Abcam, Cat#. ab16285), and actin antibodies.
3. Primary antibody binding is visualized by HRP-conjugated secondary antibody for 1 h and detected by enhanced chemiluminescence (LumiGLO, Cell Signaling).

3.4.5 Immunofluorescence Staining

1. NT-ESCs are seeded on gelatin-coated cover slips and fixed with 4% paraformaldehyde for 20 min.
2. After permeabilized with 0.5% Triton-X solution and blocked with 1–3% bovine serum albumin (BSA) solution, the cells are incubated with primary antibodies against Oct4 (1:500,

Abcam, Cat#. AB181557), Sox2 (1:500, Abcam, Cat#. ab79351), Nanog (1:500, Abcam, Cat#. ab80892), and SSEA-1 (1:500, Abcam, Cat#. ab16285).

3. Then, the cells are incubated with the appropriate secondary antibodies after washing three times. DNA was labeled with DAPI (Merck, Millipore).
4. Stained cells are mounted on cover slips and observed using an LSM 800 microscope (Zeiss, Germany).

3.4.6 Teratoma

1. Approximately, 1× 107 NT-ESCs cells are injected subcutaneously into the hind limbs of 6-week-old male severe-combined immunodeficiency beige mice.
2. After approximately 4 weeks, fully formed teratoma is dissected.
3. Teratoma is fixed with PBS containing 4% paraformaldehyde, embedded in paraffin, sectioned and stained with hematoxylin and eosin for histological analysis. Teratoma should contain three germ layers (endoderm, mesoderm, and ectoderm tissues).

3.4.7 Chimera Assay

1. ICR or CD1 embryos at the blastocyst stage are collected and 10–15 single NT-ESCs cells are injected into the blastocysts.
2. These injected blastocysts are transplanted into the uteri of pseudopregnant mice.
3. Caesarean sections are performed on day 19.5, and pups are fostered by lactating ICR mothers.

3.4.8 Tetraploid Complementation

1. Tetraploid embryos are first produced by the electrofusion of 2-cell stage embryos collected from mated female ICR mice.
2. 10–15 single NT-ESCs cells are subsequently injected into the cavity of tetraploid blastocysts.
3. The tetraploid complemented embryos were cultured in G-1TM PLUS medium for 2–3 h and then transplanted into the uteri of pseudopregnant mice.
4. Caesarean sections are carried out on day 19.5 and pups are fostered by lactating ICR mothers.

4 Notes

1. Pipettes can be purchased from commercial company (Humagen Fertility Diagnostics) or made in the laboratory. Their quality contributes greatly to the success of SCNT.
2. When cell medium is gently added into the dish, the tail tip tissue must be dry and should not be disturbed, otherwise the tissue will not easily adhere to the bottom of dish.

3. When used as donor nuclear, TTFs should be taken from passages 1 to 3 and 100% confluence to make sure the cells at G0 or G1 phases.
4. The TTFs can be used for about 2 h.
5. The medium of SCNT embryos construction and culture (CZB, HCZB, Ca^{2+}-free CZB, and G1-plus) should be overnight balanced in CO_2 incubator.
6. The fresh MII oocytes should be obtained 13–14 h post-hCG.
7. The oocytes should be treated with cytochalasin B in HCZB medium for 5 min at room temperature before enucleation and injection.
8. The enucleated oocytes should be cultured in CZB medium at least 30 min before nuclear injection in the incubator. Otherwise, it is fragile likely to die.
9. The cells with small, round, and normal form are chosen for injection.
10. Ensure that the cytoplasm membrane of TTFs is broken during nuclear injection.
11. It is necessary to pre-equilibrate Ca^{2+}-free CZB medium completely; otherwise, there will be black precipitations in the medium when adding $SrCl_2$ stock solution, which do harm to the development of cloned embryos. The role of CB in this step is to prevent the emission of the second polar body. To improve the rate of blastocyst, the drugs which are associated with epigenetics are used to treat reconstructed oocytes, such as a histone deacetylase inhibitor—Trichostatin A (TSA) or Scriptaid (SCR), which can increase histone acetylation and DNA demethylation of somatic cell genomics [16–18]. Moreover, the recent studies showed that overexpression of *kdm4b* and *kdm5b*, which were associated with histone demethylation, could significantly improve the blastocyst rate of cloned embryos (even up to 95%) [19].
12. When MEF cells are used as feeder, the passage number is recommended no more than three. Cellular activity from highly passaged cells may be compromised.
13. It is necessary to use well-expanded blastocysts. Morula or overexpanded blastocysts would be more difficult to derive ESCs.
14. Removing the ZP of clone blastocysts with 1% protease or acid Tyrode's solution can improve the success rate of the NT-ESCs derivation.

15. Do not centrifuge when ICM outgrowth is digested at the first time and just transfer cell suspension into the new wells.
16. NT-ESCs can be passaged normally with ESCs culture medium (Sect. 2.1.4), but 2i medium is more suitable for maintaining pluripotency.

Acknowledgement

This work was supported by the National Key Research and Development Program of China, Stem Cell and Translational Research (Grant No.2016YFA0100203).

References

1. Campbell KH, Mcwhir J, Ritchie WA et al (1996) Sheep cloned by nuclear transfer from a cultured cell line. Nature 380:64–66
2. Takahashi K, Yamanaka S (2006) Induction of pluripotent stem cells from mouse embryonic and adult fibroblast cultures by defined factors. Cell 126:663–676
3. Gao S, Zheng C, Chang G et al (2015) Unique features of mutations revealed by sequentially reprogrammed induced pluripotent stem cells. Nat Commun 6:6318
4. Le R, Kou Z, Jiang Y et al (2014) Enhanced telomere rejuvenation in pluripotent cells reprogrammed via nuclear transfer relative to induced pluripotent stem cells. Cell Stem Cell 14:27–39
5. Yang Y, Jiao J, Gao R et al (2015) Enhanced rejuvenation in induced pluripotent stem cell-derived neurons compared with directly converted neurons from an aged mouse. Stem Cells Dev 24:2767–2777
6. Dutta S, Sengupta P (2016) Men and mice: relating their ages. Life Sci 152:244–248
7. Ogura A, Inoue K, Takano K et al (2000) Birth of mice after nuclear transfer by electrofusion using tail tip cells. Mol Reprod Dev 57:55–59
8. Ogura A, Inoue K, Ogonuki N et al (2000) Production of male cloned mice from fresh, cultured, and cryopreserved immature Sertoli cells. Biol Reprod 62:1579–1584
9. Wakayama T, Perry AC, Zuccotti M et al (1998) Full-term development of mice from enucleated oocytes injected with cumulus cell nuclei. Nature 394:369–374
10. Gasparrini B, Gao S, Ainslie A et al (2003) Cloned mice derived from embryonic stem cell karyoplasts and activated cytoplasts prepared by induced enucleation. Biol Reprod 68:1259–1266
11. Knott JG, Kurokawa M, Fissore RA et al (2005) Transgenic RNA interference reveals role for mouse sperm phospholipase Czeta in triggering Ca^{2+} oscillations during fertilization. Biol Reprod 72:992–996
12. Saunders CM, Larman MG, Parrington J et al (2002) PLC zeta: a sperm-specific trigger of Ca (2+) oscillations in eggs and embryo development. Development 129:3533–3544
13. Ducibella T, Fissore R (2008) The roles of Ca^{2+}, downstream protein kinases, and oscillatory signaling in regulating fertilization and the activation of development. Dev Biol 315:257–279
14. Kline D, Kline JT (1992) Repetitive calcium transients and the role of calcium in exocytosis and cell cycle activation in the mouse egg. Dev Biol 149:80–89
15. Bos-Mikich A, Whittingham DG, Jones KT (1997) Meiotic and mitotic Ca^{2+} oscillations affect cell composition in resulting blastocysts. Dev Biol 182:172–179
16. Kishigami S, Mizutani E, Ohta H et al (2006) Significant improvement of mouse cloning technique by treatment with trichostatin A after somatic nuclear transfer. Biochem Biophys Res Commun 340:183–189
17. Wang F, Kou Z, Zhang Y et al (2007) Dynamic reprogramming of histone acetylation and methylation in the first cell cycle of cloned mouse embryos. Biol Reprod 77:1007–1016
18. Ogura A, Inoue K, Wakayama T (2003) Recent advancements in cloning by somatic cell nuclear transfer. Philos Trans R Soc Lond B Biol Sci 368:20110329
19. Liu W, Liu X, Wang C et al (2016) Identification of key factors conquering developmental arrest of somatic cell cloned embryos by combining embryo biopsy and single-cell sequencing. Cell Discov 2:16010

Methods in Molecular Biology (2019) 2045: 283–298
DOI 10.1007/7651_2018_140

Published online: 13 June 2018

Generation of Transplantable Retinal Pigmented Epithelial (RPE) Cells for Treatment of Age-Related Macular Degeneration (AMD)

Harshini Surendran, Reena J. Rathod, and Rajarshi Pal

Abstract

Age-related macular degeneration (AMD) is the foremost cause of blindness in people over the age of 60 worldwide. Clinically, this disease starts with distortion in central vision eventually leading to legal blindness. Vision loss has a significant impact on quality of life and incurs a substantial cost to the economy. Furthermore, AMD is a complex and progressive neurodegenerative disorder that triggers visual impairment due to the loss of retinal pigmented epithelium (RPE) and the light-sensitive photoreceptors that they support, protect and provide nutrition. Currently, there is no curative treatment for the most common form of this disease, i.e., dry AMD. A novel approach to treat AMD involves the transplantation of RPE cells derived from human induced pluripotent stem cells (iPSCs) in the outer retina. These iPSC-derived RPE cells not only show characteristics similar to native RPE but also could replace as well as regenerate damaged pathologic RPE and produce supportive growth factors and cytokines. Several clinical trials are being conducted taking advantage of a variety of cell- and tissue engineering-based approaches. Here, we present a simple, cost effective, and scalable cell-culture model for generation of purified RPE thus providing the foundation for developing an allogeneic cell therapy for AMD.

Keywords Age-related macular degeneration, Eye, Induced pluripotent stem cells, Retina, Retinal pigment epithelial cells

1 Introduction

Human eyes are one of the most complex organs in the human system. The eye does not grow like other organs and the size generally remains the same from birth. It originates from the neuroepithelium, surface ectoderm, and extracellular mesenchyme. Human eyes are made of three layers constituting of different tissue types: (a) outer layer—cornea and sclera, (b) middle layer—choroid, ciliary body, and iris, and (c) innermost layer—retina. The critical event in eye development is the separation of bilayered optic neuroepithelium, which gives rise to the optic cup made of retinal cells (Fig. 1a) [1, 2]. The retina lining the back of the eye and lying on the choroid layer receives the light and converts it into chemical energy utilizing most of the nourishments provided from the vessels [3]. Retina is an outgrowth of the forebrain with complex

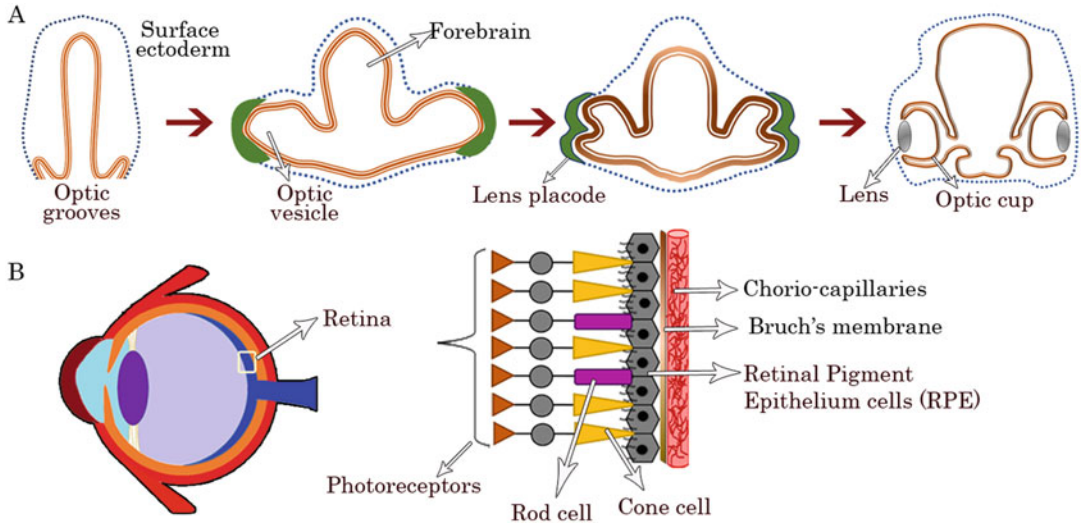

Fig. 1 (**a**) Eye organogenesis—formation of optic groove from neural tube surrounded by surface ectoderm followed by eye field specification leading to evolution of optic vesicle. Invagination of optic vesicles to from bilateral optic cups with defined lens. (**b**) Retinal layer of human eye—diagrammatic representation showing anatomical arrangement of photoreceptor cells—rods and cones onto retinal pigment epithelium (RPE), Bruch's membrane, and choriocapillaris

nervous structure constituting four major cell types: (a) retinal pigment epithelium next to choroid layer, (b) light-sensitive layer of rods and cones, (c) bipolar nerve cells, and (d) the ganglion cells that connect with optic nerve fibers.

Retinal pigment epithelium (RPE) is a layer of tissue beneath the photosensitive cells. RPE cells absorb excess light and circulate nutrients to the photoreceptors while removing waste from them. The light absorbed by the eyes hits the photoreceptors—rods process poor light vision whereas cones process colored and detailed vision (Fig. 1b). The absorbed light is transmitted to nerve and ganglion cells that communicate with optic nerve fibers and convert this light into electrochemical signals. The electrical signals are then translated into image by the brain.

Abnormal eye conditions have emerged as a potential threat to the sight of a person especially in the old age. Major eye diseases include age-related macular degeneration (AMD), glaucoma, diabetic retinopathy, cataract, and many others that result in huge societal and financial burden. In this chapter, we are going to focus on AMD because it does not have a cure and thus poses a huge challenge.

AMD is the major cause of irreversible blindness in the elderly people worldwide and happens due to loss of RPE layer of the retina. Studies have shown the involvement of genetic as well as

environmental factors in the early onset of AMD, but the disease pathogenesis still remains unclear. AMD is of two forms—dry AMD or wet AMD, classified based on the lack or presence of choroidal neovascularization, respectively. Dry AMD accounts for 90% of AMD cases and is characterized by deposition of lipid and protein aggregates between the RPE layer and its basal Bruch's membrane. This in turn leads to thickening of Bruch's membrane thereby inhibiting the nutrient diffusion through RPE. Severe forms of dry AMD would lead to progressive wet AMD. Wet AMD happens due to invasion of choroidal blood vessels in the retina resulting in central vision loss [2].

NIH-NEI statistics in 2014 estimated $139 billion as annual economic burden due to vision loss and eye disorders in the USA. Moreover, 2.1 million Americans have advanced AMD and an estimated 3.7 million will have advanced AMD by 2030. India is home for ten million patients suffering from degenerative diseases of the eye (APEDS 2001), majority of them below 40 years of age with estimated cost of $10 billion annually (ILO 1998).

Unfortunately, there exist no curative therapies for all these chronic degenerative diseases of the eye. Currently, gene therapy and stem cell therapy are amid various fascinating breakthrough discoveries thus creating unparallel expectations and opening up unique possibilities for unmet medical needs. These findings are most advanced in the eye since the eye is "immune-privileged" and the blood ocular barrier allows for a closed system. Over the last decade, researchers have successfully studied many parts of the complex eye employing various model systems like zebrafish, rodents, and humans aiding in better understanding the disease etiology, thus creating a scope in treating the problem instead of delaying the cause [4–8].

The advent of induced pluripotent stem cell (iPSC) technology [9] has offered unprecedented opportunity to generate cells of therapeutic importance that are immunologically compatible. During the last 10 years, stem cell research has achieved a thorough understanding of basic biology—molecular mechanisms governing self-renewal and lineage-specific differentiation, largely due to focus on humanized in vitro culture systems. Pluripotent stem cell-derived retinal cell transplantation in the eye is one idiosyncratic therapy being explored for retinal degenerative disorders such as retinitis pigmentosa (RP) and AMD [10–12]. Therefore, stem cell replacement therapy raises a genuine hope potential to transform the premises and promises of medical practice in the years to come.

In this chapter, we describe a highly efficient and robust method to generate pure RPE cells from iPSCs using specific combination and appropriate concentration of growth factors and small molecules. Our protocol is a tightly controlled one that

efficiently recapitulates the key signalling events associated with retinogenesis within a dynamic, complex, microenvironment of cells. The authenticity of differentiated cells was confirmed by spatiotemporal expression of key markers at gene and protein levels.

2 Materials

2.1 Cell Culture

2.1.1 Equipment

Biosafety cabinet, CO_2 incubator, inverted microscope connected with camera for imaging, liquid nitrogen LN_2 cryotank, Mr. Frosty freezing container, pipette gun, and water bath.

2.1.2 Plasticware

Four-well dishes, 6-well ultralow attachment plates, and cell lifter. Centrifuge and microfuge tubes, cell-culture plates, cryovials, measuring cylinders, racks, stands, spray bottles, Kimwipes, serological pipettes 5 ml, 10 ml, and Stericup funnel with bottle.

2.1.3 Chemicals and Reagents

70% Ethanol, Accutase, trypsin–EDTA, Matrigel (stem cell grade), Vitronectin Cryosolution (commercially available—stem cell grade), Dulbecco's phosphate-buffered saline (DPBS), and neural rosette selection reagent.

2.2 Media Composition

2.2.1 mTeSR

100 ml of mTeSR™1 supplement (5×) was added with 400 ml of mTeSR™1 basal media (*see* **Note 1**).

2.2.2 Differentiation Media (See **Note 2**)

Differentiation Induction Media

	For 500 ml	Final concentration
DMEM/F12	425 ml	
Knock Out Serum	50 ml	10%
Sodium pyruvate	5 ml	1%
Sodium bicarbonate	5 ml	1%
HEPES buffer	5 ml	1%
Nonessential amino acids	5 ml	1%
N1 media supplement (100×)	5 ml	1×
IWRI (2 mM)	500 μl	2 μM
SB431542 (10 mM)	500 μl	10 μM
LDN 193189 (1 mM)	50 μl	100 nM
IGF1 (100 ng/ml)	50 μl	10 ng/ml

Differentiation Propagation Media

	For 500 ml	Final concentration
DMEM/F12	470 ml	
Knock Out Serum	5 ml	1%
Sodium pyruvate	5 ml	1%
Sodium bicarbonate	5 ml	1%
HEPES buffer	5 ml	1%
Nonessential amino acids	5 ml	1%
N1 media supplement (100×)	5 ml	1×

Retinal Pigment Epithelium Maturation Media

	For 500 ml	Final concentration
MEMα modified	465–440 ml	
Knock Out Serum	25–50 ml	5–10%
GlutaMAX	5 ml	1%
Taurine (50 mg/ml)	2.5 ml	0.25 mg/ml
Hydrocortisone (20 mg/ml)	250 μl	10 μg/ml
Tri-iodo-thyronine (2 mg/ml)	10 μl	0.0065 μg/ml
N1 media supplement (100×)	5 ml	1×

2.2.3 Cryosolution

10% DMSO added with 90% KOSR and filtered through 0.22 μm filters.

2.3 Real-Time PCR

Microfuge (1.5 ml, 0.5 ml), TRIzol, real-time PCR (RT-PCR) machine, NanoDrop spectrophotometer, RNA isolation kit, reverse transcription kit, and SYBR green master mix.

2.4 Immunofluorescence and Flow Cytometry

Fluorescence-activated cell sorter (FACS), microscope with monochromator laser, 4′,6-diamidino-2-phenylindole (DAPI), fetal bovine serum (FBS), paraformaldehyde, and Triton X-100.

3 Methods

3.1 Schematic Flow Through

The procedure for iPSC maintenance, RPE differentiation and characterization in a step-wise manner has been depicted in form of a schematic in Fig. 2.

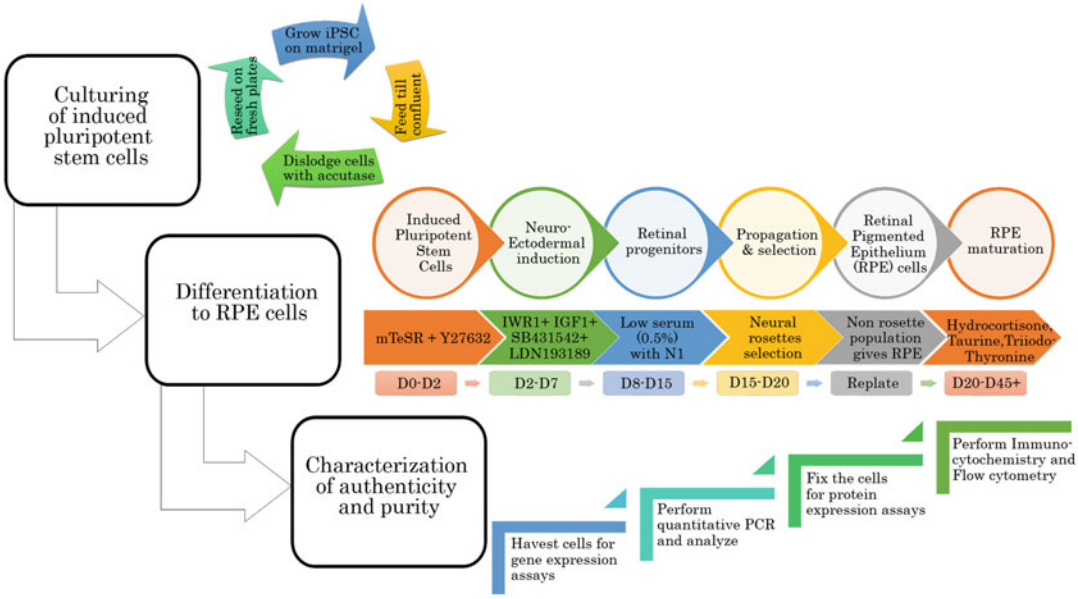

Fig. 2 Flow through of RPE differentiation and characterization. Detailed schematic diagram showing steps towards de novo generation of RPE from induced pluripotent stem cells (iPSCs). (1) Maintenance and culture of iPSC; (2) differentiation to RPE with a snapshot of protocol followed along with time points; and (3) characterization of authenticity and purity of the differentiated cells

3.2 Preparation of Matrigel-Coated Plates

1. Thaw a Matrigel aliquot on ice at 4 °C for an hour (*see* **Note 3**) and dilute to 0.5–1% in ice cold DMEM media.
2. Add 1 ml/10 cm^2 of the Matrigel solution to the tissue culture plate, spread it uniformly all over the plate, and store it inside an incubator overnight at standard culture conditions (*see* **Note 4**).
3. After taking out the plate, wash once with DMEM to remove the Matrigel completely and use it for further experiments.

3.3 Maintenance of Induced Pluripotent Stem Cells

1. Grow iPSCs cultures in mTeSR with everyday media change and passage them using Accutase at 85–90% confluency.
2. Upon reaching desired confluency, aspirate out the media and wash the culture with 1× DPBS thrice.
3. Add 1 ml/10 cm^2 of pre-warmed Accutase and incubate for 3 min inside the incubator.
4. Neutralize the enzyme immediately three times (v:v) with 10% serum containing media and transfer the cells to 15 ml falcon tube after mild trituration using 2 ml serological pipette (*see* **Note 5**).
5. Centrifuge the cells at 800 × *g* for 2 min and aspirate out spent media.
6. Mildly dislodge the cell pellet and seed them at the ratio of 1:5 to 1:6 on freshly coated Matrigel plates with 10 μM Y27632 and place it inside the CO_2 incubator (*see* **Notes 2** and **6**).

7. Next day, remove the media completely and add fresh mTeSR media and maintain the cultures in the same way until it reaches desired confluency.
8. Freeze the cells (whenever required) at 1×10^6 cells/ml of freezing media in one cryovial for up to 96 h at −80 °C in Mr. Frosty and then transfer to LN_2 tank.
9. Check freeze thaw viability (>80%). At every 5–6 passages, standard quality control assays like karyotyping (cytogenetic stability), gene expression and immunophenotyping (pluripotency), and sterility testing are to be carried out for every iPSC line.

3.4 Differentiation of Induced Pluripotent Stem Cells to Retinal Pigment Epithelium Cells

Targeted generation of RPE from iPSCs is described below in a day-wise fashion encompassing eye field specification, optic cup formation, and retinal differentiation (steps).

3.4.1 Day 0–2

1. Once the iPSCs are 80–90% confluent, dissociate the cells enzymatically as described previously in Subheading 3.3, **steps 2–5**.
2. Seed the cells onto non adherent or ultra low attachment petridish (*see* **Note 7**) with 10 μM Y27632 in mTeSR media allowing cells to form forced aggregates called embryoid bodies (EB).
3. Grow the cells in mTeSR for 48 h with media change at 24 h interval.

3.4.2 Day 2–4

1. Gradually shift the medium of the suspension cultures with EBs from mTeSR to differentiation induction media (DIM) (*see* **Note 8**).
2. Feed the EBs in suspension every day for 2 more days.

3.4.3 Day 5–7

1. Attach 4-day old EBs onto 1% Matrigel-coated tissue culture plates in DIM (*see* **Note 9**).
2. Culture the cells in DIM for 2 more days with media change every day.
3. Keep the cells in DIM for a total of 6–7 days.

3.4.4 Day 8–20

1. Switch the cells to differentiation propagation media (DPM) and culture them for 8–10 more days with media change every alternate day (Fig. 3a–c).
2. Whenever confluent between 7–10 days in DPM, selection of neural rosettes is to be carried out (*see* **Note 10**).
3. Aspirate out the medium from the well containing neural rosettes and wash the culture with DMEM/F12.

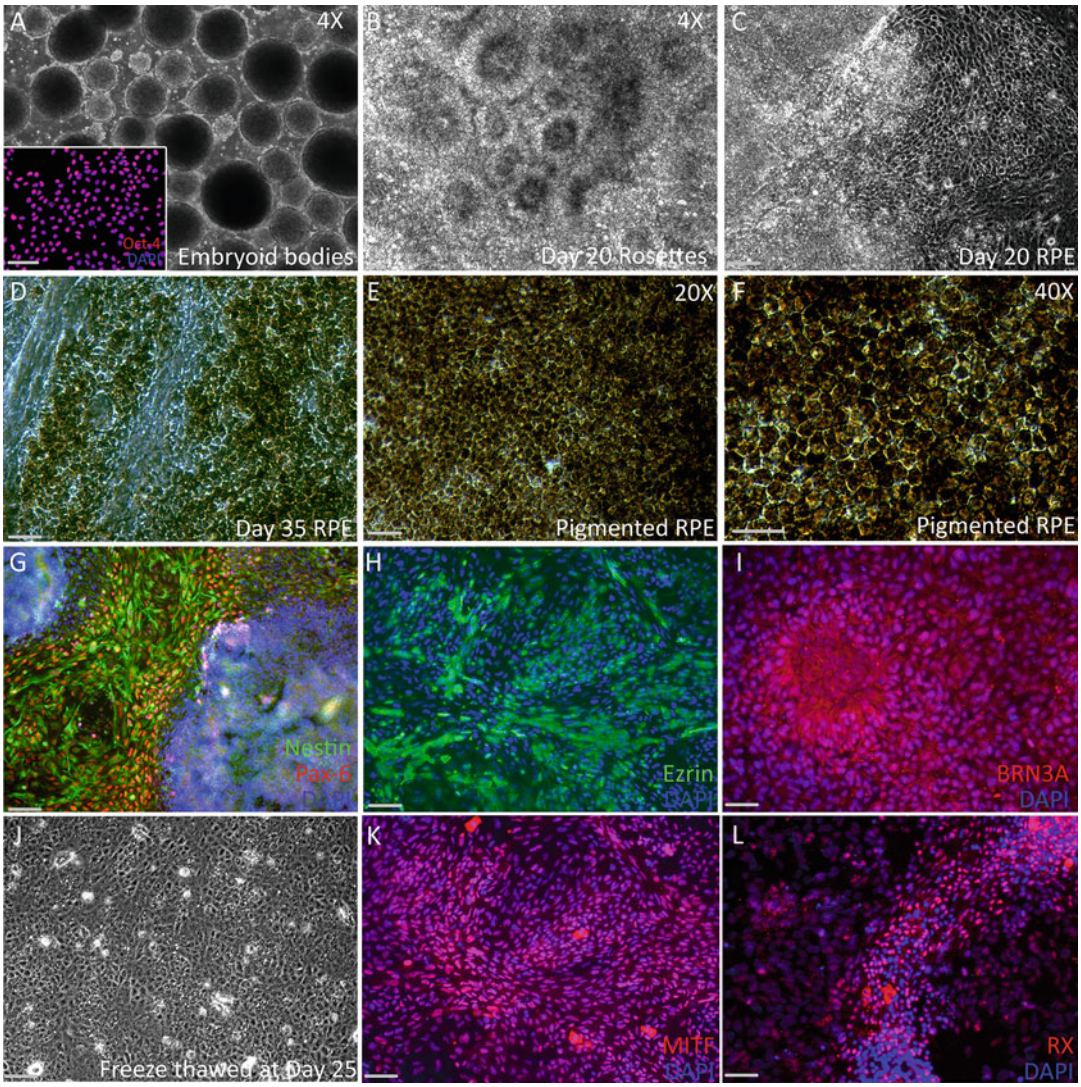

Fig. 3 Differentiation of retinal progenitor cells from iPSC cells. (**a**) Day 2 embryoid bodies, (**a** inset) Oct-4 staining in NcGMP1 iPSC; (**b**, **c**), day 20 rosette and non-rosette populations; (**d**) RPE-like cells after rosette selection; (**e**, **f**) pigmented RPE progenitors cells; and (**g–i**) immunostaining of RPE progenitors against Pax-6, Nestin, Ezrin, and BRN3A. (**j**) Freeze thaw viability of RPE progenitors; (**k**, **l**) immunostaining against MITF and RX on freeze thawed cells. Scale bars represent 100 μm. Images unless mentioned are at 10× magnification

4. Add 1 ml of Neural Rosette Selection Reagent per 10 cm^2 and incubate at 37 °C for 15–30 min, keep checking it intermittently.
5. Once the rosette(s) layer lifts off (first), remove the Selection Reagent carefully and discard the solution.
6. Dislodge the neural rosettes from the well by adding DMEM/F12 specifically on the rosette clusters and gently flush only the clusters.

7. Collect the cell suspension containing the selected neural rosettes in 15 ml conical tube, seed them on 1% Matrigel-coated plates and continue growing them at high density in DPM for another 30–40 days to differentiate into non-RPE cells such as photoreceptors (rod and cone cells). Split them when they become confluent.

3.4.5 Day 17–20

1. After rosettes are selected out, dissociate the cells in the parent plate (*see* **Note 11**) with Accutase and seed back the cells at 1.5×10^6 cells/10 cm^2 in freshly coated (1% Matrigel) plates.
2. Continue growing the cells for 3 more days in DPM.
3. The cells at this stage should be tested for expression of key markers (Fig. 3g–i).

3.4.6 Cryopreservation of Retinal Pigment Epithelium Progenitors

1. Split the cells whenever they reach confluency between day 20–25, retinal pigment epithelium progenitors (RPE-P) could also be freeze thawed (Fig. 3j–l).
2. Splitting of these cells can be done as described in Subheading 3.3, **steps 2–5**.
3. Pellet the cells and freeze at 1.5×10^6 cells per ml of cryosolution in Mr. Frosty at −80 °C.
4. Within next 96 h, transfer the cells to LN_2 tanks.
5. Revive the cells (whenever desired after 72 h in LN_2) by quick exposing the vial to 37 °C water bath for a minute.
6. Add 4 ml of RPE maturation media to the vial and transfer the contents to 15 ml falcon.
7. Centrifuge the cells at $800 \times g$ for 2 min and aspirate out the spent media.
8. Distribute the cells at 1.5×10^6 cells/10 cm^2 with 10 μM Y27632.

3.4.7 Day 20–45+

1. Gradually switch the non-rosette population to retinal pigment epithelium maturation media (RMM) (*see* **Note 12**) and one can grow them for up to 90–120 days (*see* **Note 13**).
2. Pigmentation patches start showing up after 20–25 days in RMM. Initially, brown pigmentation appears in pockets of cells that gradually becomes black in color and slowly spreads all over the plate. Intensity of pigmentation could be categorized into light, medium, and heavy and can be correlated with the number of days the cells are grown in RMM (Fig. 3d, f).
3. Split the cultures whenever they reach confluency and maintain in RMM for long-term experiments (functional studies like differential electrical responses by electrophysiology, polarized cytokine secretion profiling, vectorial fluid transport measurement, and phagocytosis assay).

4. Wash the cells thrice with 1× DPBS.
5. Add 0.05% trypsin–EDTA (*see* **Note 14**) and incubate at 37 °C for 5 min.
6. The cells lifting off are the non-RPE (undesired) population and hence discarded.
7. Wash the cells once again with 1× DPBS and incubate with 1:1 Accutase:0.25% trypsin–EDTA again at 37 °C for 5 min (*see* **Note 15**).
8. Scrape off RPE-like colonies/clusters using a cell lifter and then dissociate the clumps carefully in 10% serum media.
9. Centrifuge the cells at 800 × *g* for 2 min and replate onto freshly coated Matrigel plates and continue growing for few more passages.
10. Harvest and characterize the mature RPE cells for late stage RPE-specific transcription factors, structural proteins, and secretory factors (Fig. 4).

3.5 Confirmation of Authenticity and Purity of Retinal Pigment Epithelium Cells

3.5.1 Indirect Immunofluorescence

1. Fix the cells with 2–4% paraformaldehyde in DPBS (pH 7.4) for 15–20 min at room temperature. Wash the cells in DPBS thrice, 2 min each wash.
2. Permeabilize the samples for 10 min with DPBS containing either 0.1–0.25% Triton X-100 (*see* **Note 16**) and wash again in DPBS thrice, 2 min each wash.
3. Incubate the cells with 3–5% FBS for at least 30 min to block unspecific binding of the antibodies.
4. Add primary antibody solution (optimized concentration) in DPBS to the cells and incubate overnight at 4 °C.
5. Next day, decant the antibody solution and wash the cells thrice in DPBS, 2 min each wash.
6. Incubate the cells with appropriate secondary antibody for 1–2 h at room temperature in the dark.
7. Decant the antibody solution and wash the cells thrice in DPBS, 2 min each wash.
8. Counterstain with 1 μg/ml DAPI for 7–10 min at room temperature and visualize under fluorescent microscope.

3.5.2 Flow Cytometry

1. Fix the cells with 1–2% paraformaldehyde in DPBS (pH 7.4) for 10 min at 4 °C and wash once with DPBS (*see* **Note 17**).
2. Permeabilize the cells for 5–7 min with DPBS containing 0.1–0.25% Triton X-100 4 °C (*see* **Note 16**) and wash once in DPBS.
3. Incubate the cells with 3–5% FBS for at least 30 min at 4 °C.
4. Add diluted primary antibody in DPBS, incubate for 30–45 min at 4 °C.

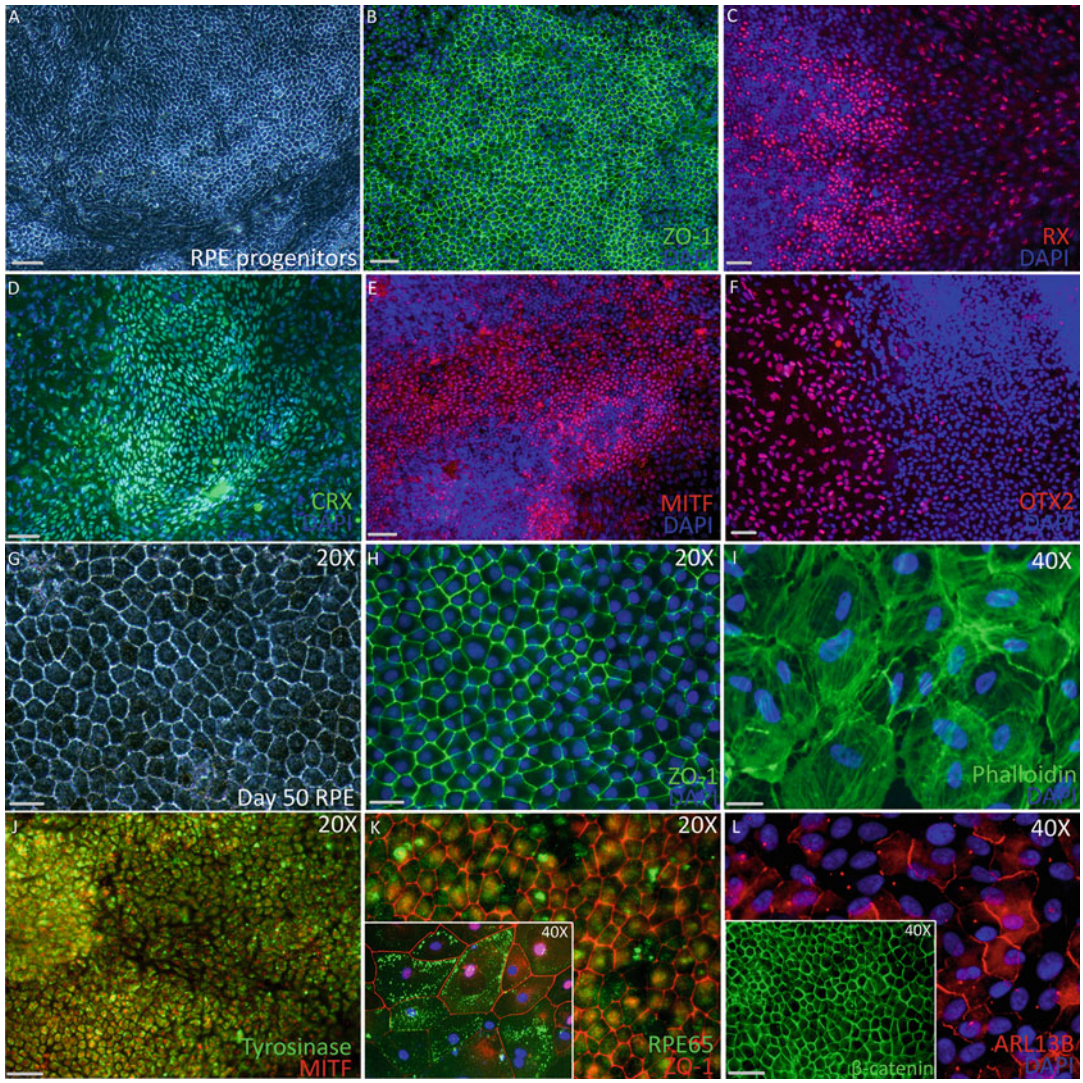

Fig. 4 RPE characterization by immunocytochemistry. (**a**, **g**) Purified mature RPE cells (**b**, **h**), immunostaining of RPE for ZO-1. (**c**–**f**) Immunofluorescence images of transcription factors RX, CRX, MITF, OTX2, and (**i**) phalloidin. (**j**–**l**) Immunostaining of mature RPE-specific markers like tyrosinase, RPE-65, ARL13B, β-catenin (inset) in pigmented cells. Scale bars represent 100 μm. Images unless mentioned are at 10× magnification

5. Wash the cells and incubate with appropriate secondary antibody for 30 min at 4 °C in the dark.
6. Wash the cells and dissociate them with sheath solution. Run the cells on the flow cytometer and analyze with respective secondary antibody controls (Fig. 5a–c).
7. For each experiment carried out in triplicates (biological), a minimum of 10,000 events would be acquired and stored.

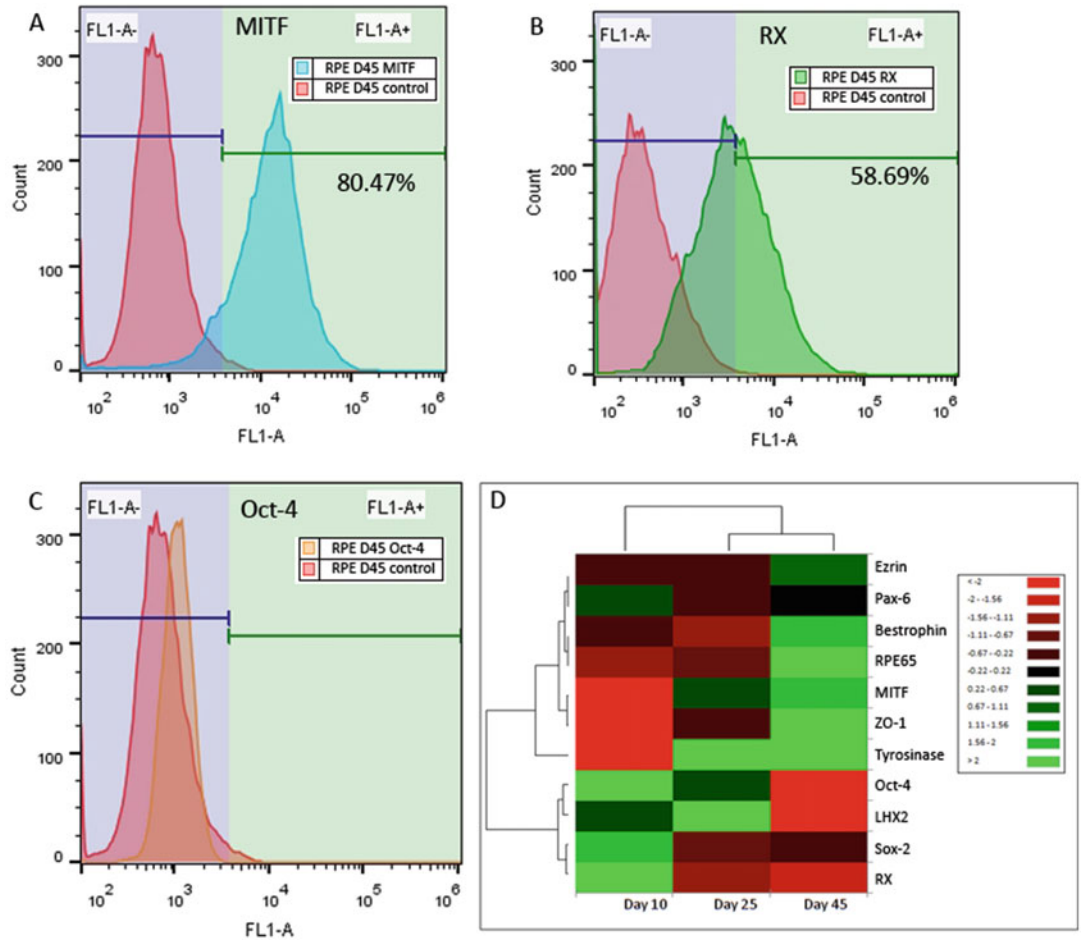

Fig. 5 RPE characterization by flow cytometry and quantitative real-time PCR (RT-PCR). (**a**, **b**) Flow cytometry analysis of RX, MITF in committed RPE cells and (**c**) Oct-4. (**d**) RT-PCR-based quantification of key gene expression represented as heat map

3.6 RNA Isolation, Complementary DNA Synthesis, and Real-Time PCR

1. RNA isolation is based on spin column chromatography kit (*see* **Note 18**) using a proprietary resin as the separation matrix.
2. Lyse the cells in lysis solution, add equal volumes of ethanol, and transfer the content to the column.
3. Wash the cells thrice with wash solution and treat with DNase for 20 min at room temperature.
4. Elute RNA with preheated (65 °C) elution buffer (RNase-free water) and quantify with NanoDrop Spectrophotometer.
5. 500 ng of RNA would be Reverse transcribed to complementary DNA (cDNA) using a commercially available kit.
6. Add 2.5 μg of OligodT and 0.5 mM dNTP mix to RNA and denature at 65 °C for 5 min and then added with 1× buffer,

0.05 M DTT, 40 U of RNase out, and 200 U of reverse transcriptase.

7. Incubate the reaction mix (*see* **Note 19**) at 42 °C for 60 min followed by 70 °C for 10 min for enzyme inactivation.
8. Add 20 ng of cDNA with 1× SYBR green master mix and 0.5 μM of primer pair(s) for RT-PCR reaction.
9. Run samples with dissociation stage in triplicate with housekeeping gene as control for every reaction.
10. Perform normalization based on the average expression of constitutive gene β-actin using ΔΔCt method (*see* **Note 20**).
11. Represent the fold change or relative expression for selected genes in the form of a heatmap (Fig. 5d).

3.7 Study Results

3.7.1 Induction of Human Induced Pluripotent Stem Cell to Retinal Progenitors

All experiments were conducted after obtaining required approval from the Institutional Committee for Stem Cell Research (IC-SCR) registered with the National Apex Committee for Stem Cell Research and Therapy, Indian Council of Medical Research (ICMR), New Delhi, India. Healthy cultures of NcGMP1 iPSC line (procured from XCell Sciences, Novato, CA, USA) was characterized morphologically by the presence of tightly packed cells with high nuclear to cytoplasmic ratio with abundance of key transcription factor Oct-4 shown in the inset in Fig. 3a. NcGMP1 iPSC was differentiated via formation of forced aggregates called embryoid bodies (Fig. 3a). Cells were cajoled towards retinal progenitors through dual SMAD inhibition via neuroectodermal specification as marked by distinct rosette formation with plenty of Pax-6 and Nestin protein expression (Fig. 3b, g). Further propagation and removal of neural rosettes promotes RPE enrichment followed by the appearance of pigmentation patches (Fig. 3c–f). RPE progenitors are characterized by markers of epithelial polarization Ezrin and ganglion marker BRN3A (Fig. 3h, i). At this stage, RPE progenitors were successfully frozen and stored in LN2. Cryopreserved cells were revived and viability was found to be greater than 80% (Fig. 3j); besides, they retained positivity for key transcription factors like MITF, and RX (Fig. 3k, l).

3.7.2 Differentiation and Characterization of Retinal Pigment Epithelium Cells by Immunocytochemistry

RPE cells are characterized by tightly packed cuboidal pigmented epithelial cells (Fig. 4a, g) with apical/basal polarity as indicated by tight junction protein ZO-1 (Fig. 4b, h) and retinal transcription factors RX, CRX with RPE-specific transcription factor MITF (Fig. 4c–e). Cells expressed high levels of filamentous actin as shown by phalloidin staining (Fig. 4I) and mature RPE markers like RPE-65 and tyrosinase (Fig. 4j, k). Mature ciliated RPE cells displayed positivity against ARL13B protein in the absence of WNT pathway as represented by inactivated β-catenin (inset) in the cell membrane (Fig. 4l). These mature RPE cultures showed less

positivity against the photoreceptor transcription factor OTX2 indicating the purity of RPE population generated de novo (Fig. 4f).

3.7.3 Quantifying Efficacy of the Differentiation Protocol by Flow Cytometry and Real Time PCR Analysis

Early retinal and RPE-specific transcription factors RX and MITF were quantified by flow cytometry in RPE committed cells (Fig. 5a, b). Concurrently, pluripotent marker Oct-4 (Fig. 5c) was found to be negative by flow cytometry and further reconfirmed by RT-PCR as <0.01. Figure 5d shows the heat map representing fold change of key genes that are regulated in a spatiotemporal fashion thus recapitulating in vivo retinogenesis leading to generation of pure and functional RPE cells.

3.8 Significance of the Study

RPE cells were differentiated from undifferentiated stem cells, grown till maturation, freeze-thawed, and well characterized. Ongoing studies in the laboratory include the transplantation of RPE cells in rodent model of inherited retinal degenerative (RCS rats) in collaboration with Dr. Trevor McGill, Casey Eye Institute, Oregon Health and Science University, USA. These studies would help us understand the functional efficacy of RPE cells in vivo. These data along with Safety studies in cGMP laboratory would help us move towards Phase I clinical trials. In the near future, we aim to establish stem cell-based therapy employing iPSC-derived retinal progenitors for the treatment of AMD patients globally.

4 Notes

1. Culture media mTeSR™1 should be aliquoted and stored at −20 °C for prolonged storage until the date of expiry.
2. Differentiation media was prepared in sterile conditions, filtered through 0.22 μm Stericups and stored in 4 °C to be used within 10 days from the time it is made.
3. Matrigel solidifies above 4 °C and loses its property. So, it is critical to keep Matrigel on ice throughout the work. Diluted/resuspended Matrigel should be used within 7 days.
4. Culture conditions indicate temperature at 37 °C with 5% CO_2 and 5% O_2.
5. Trituration should be very gentle avoiding complete dissociation of the iPSC colonies. Small groups of 5–10 cells in the form of a colony while seeding is mostly preferable.
6. Regular maintenance does not include Y27632; media supplemented with 10 μM Y27632 is recommended only during freeze thaw and splitting.

7. Cells from 10 cm^2 tissue culture dish was seeded back onto 10 cm^2 suspension non-coated dish leading to formation of forced aggregates called embryoid bodies (EB).
8. On day 2, 2:1 mTeSR:DIM was added, on day 3, 1:1 mTeSR: DIM was added, and on day 4 cells shifted to complete DIM.
9. EBs from 10 cm^2 suspension dish was attached on 15 cm^2 tissue culture-coated dish. This allows the EBs more space thus promoting rapid proliferation.
10. This protocol uses STEMdiff neural rosette selection reagent, which is commercially available (from Stem Cell Technologies and works effectively for this protocol); however, other standard methods for selecting neural rosette population can also be used.
11. Post-selection of rosettes, the cells remaining in the plate (designated as parent plate) would be retinal cells other than photoreceptors which can be purified and expanded to mature RPE using RMM.
12. On day 19, 2:1 DPM:RMM was added, on day 20, 1:1 DPM: RMM was added, and on day 21 cells shifted completely to RMM.
13. RPE cells were grown for 90–120 days with alternate day media change and selection by passaging whenever they reach confluency.
14. In less concentrated trypsin–EDTA, non-pigmented and non-RPE cell population (largely photoreceptor- and mesenchymal-like cells) would lift off and the plate left with undesired cell population was flushed and discarded.
15. Pigmented RPE cells are very sticky and form clumps even in trypsin. If pipetted too hard, a large proportion of cells would die. Moreover, Accutase is too mild for these cells and at the same time use of trypsin could damage the cells. Therefore, 1:1 of Accutase and trypsin was used.
16. The optimal percentage of Triton X-100 should be determined for each protein of interest.
17. The cells were topped up with 1 ml of DPBS and centrifuged at 800 rpm for 2 min and pelleted down.
18. RNA was isolated using Qiagen RNeasy kit and manufacturer's instructions were followed as is.
19. The reaction volume was made up to 20 μl with nuclease-free water as per manufacturer's instructions in SuperScript III reverse transcriptase kit.
20. Real-time raw data cycle threshold value was double normalized—first with housekeeping control followed by undifferentiated iPSC control and plotted as $2^{-\Delta\Delta Ct}$.

Acknowledgements

Eyestem Research Private Limited, Bangalore is acknowledged for funding and other facilities. The authors thank Centre for Cellular and Molecular Platforms (CCAMP), NCBS-TIFR Campus, Bangalore for incubation support in the form of infrastructure. We gratefully thank Drs. Dhruv Sareen, Cedars Sinai Medical Centre, CA, USA; Mahendra Rao, InStem, Bangalore; Kapil Bharti, NEI-NIH, MD, USA, and Deepak Lamba, Buck Institute, CA, USA for their crucial suggestions to develop this protocol.

References

1. Bharti K, Gasper M, Ou J et al (2012) A regulatory loop involving PAX6, MITF, and WNT signaling controls retinal pigment epithelium development. PLoS Genet 8(7):e1002757
2. Zhao C, Wang Q, Temple S (2017) Stem cell therapies for retinal diseases: recapitulating development to replace degenerated cells. Development 144(8):1368–1381
3. Centanin L, Wittbrodt J (2014) Retinal neurogenesis. Development 141(2):241–244
4. Assawachananont J, Mandai M, Okamoto S et al (2014) Transplantation of embryonic and induced pluripotent stem cell-derived 3D retinal sheets into retinal degenerative mice. Stem Cell Reports 2(5):662–674
5. Lamba DA, Gust J, Reh TA (2009) Transplantation of human embryonic stem cell-derived photoreceptors restores some visual function in Crx-deficient mice. Cell Stem Cell 4(1):73–79
6. Lund RD, Kwan AS, Keegan DJ et al (2001) Cell transplantation as a treatment for retinal disease. Prog Retin Eye Res 20(4):415–449
7. Mandai M, Fujii M, Hashiguchi T et al (2017) iPSC-derived retina transplants improve vision in rd1 end-stage retinal-degeneration mice. Stem Cell Reports 8(1):69–83
8. Tucker BA, Park IH, Qi SD et al (2011) Transplantation of adult mouse iPS cell-derived photoreceptor precursors restores retinal structure and function in degenerative mice. PLoS One 6 (4):e18992
9. Takahashi K, Yamanaka S (2006) Induction of pluripotent stem cells from mouse embryonic and adult fibroblast cultures by defined factors. Cell 126(4):663–676
10. Wiley LA, Burnight ER, DeLuca AP et al (2016) cGMP production of patient-specific iPSCs and photoreceptor precursor cells to treat retinal degenerative blindness. Sci Rep 6:30742
11. Cramer AO, Wang W, Lu S-J et al (2016) Function of human pluripotent stem cell-derived photoreceptor progenitors in blind mice. Sci Rep 6(1):29784
12. Song WK, Park KM, Kim HJ et al (2015) Treatment of macular degeneration using embryonic stem cell-derived retinal pigment epithelium: preliminary results in Asian patients. Stem Cell Reports 4(5):860–872

Methods in Molecular Biology (2019) 2045: 299–310
DOI 10.1007/7651_2018_121

Published online: 15 February 2018

Histopathological and Behavioral Assessments of Aging Effects on Stem Cell Transplants in an Experimental Traumatic Brain Injury

Jea-Young Lee, Roger Lin, Hung Nguyen, M. Grant Liska, Trenton Lippert, Yuji Kaneko, and Cesar V. Borlongan

Abstract

Traumatic brain injury (TBI) displays cognitive and motor symptoms following the initial injury which can be exacerbated by secondary cell death. Aging contributes significantly to the morbidity of TBI, with higher rates of negative neurological and behaviors outcomes. In the recent study, young and aged animals were injected intravenously with human adipose-derived mesenchymal stem cells (hADSCs) (Tx), conditioned media (CM), or vehicle (unconditioned media) following TBI. The beneficial effects of hADSCs were analyzed using various molecular and behavioral techniques. More specially, DiR-labeled hADSCs were used to observe the biodistribution of the transplanted cells. In addition, a battery of behavior tests was conducted to evaluate the neuromotor function for each treatment group and various regions of the brain were analyzed utilizing Nissl, hematoxylin and eosin (H&E), and human nuclei (HuNu) staining. Finally, flow cytometry was also performed to determine the levels of various proteins in the spleen. Here, we discuss the protocols for characterizing the histopathological and behavioral effects of transplanted stem cells in an animal model of TBI, with an emphasis on the role of aging in the therapeutic outcomes.

Keywords Aged, Animal model, Neurodegeneration, Neurogenesis, Regenerative medicine

1 Introduction

Traumatic brain injury (TBI) is extremely prevalent in the American population, accounting for approximately 30% of all injury-related fatalities and affecting an estimated two million people from all age demographics [1]. Aging is regarded as a significant comorbidity of TBI, with elderly patients experiencing higher rates of negative health outcomes following injury. Indeed, a dramatic increase in mortality and morbidity is observed in TBI patients of increasing age [2].

Regenerative therapies, such as stem cell transplantation, have been demonstrated to effectively confer neuroprotection, neuror-

egeneration, and amelioration of functional deficits in animal models of neurological disorders including Alzheimer's disease, Parkinson's disease, stroke, and TBI [3–13]. Certain classes of stem cells—such as human adipose-derived mesenchymal stem cells (hADSCs)—and their secreted molecules (referred to as their secretome) have been distinguished as especially promising for the treatment of neurological diseases and disorders. hADSCs have demonstrated therapeutic potential in TBI, owed largely to their potent secretory profile of cytokines, chemokines, trophic factors, microRNAs, and long noncoding RNA (lncRNA), in addition to their proliferative capacity and flexibility in lineage differentiation [14, 15]. Two lncRNAs have received particular attention, metastasis associated lung adenocarcinoma transcript 1 (MALAT1) and nuclear enriched abundant transcript 1 (NEAT1), because of their importance in cellular differentiation via their role in alternative splicing of various pre-mRNAs [16–18]. Being in a proliferative but non-differentiating state, stem cells secrete many lncRNAs, including MALAT1 and NEAT1, apparently unloading these molecules which are not needed by the stem cells prior to receiving differentiation cues. These secreted lncRNAs can, however, be absorbed by adjacent cells, potentially serving as survival/proliferation signals through incompletely understood mechanisms such as gene expression modulation, mRNA splicing, and migration [19–21].

Despite accumulating evidence demonstrating that aging affects endogenous neurogenic processes and that the aged brain is less receptive to stem cell graft survival, the vast majority of cell transplantation investigations are performed in young animals [22, 23]. Additionally, the complex mechanisms utilized by stem cells to confer their therapeutic effects and the homing patterns of transplanted cells are not entirely understood. The present protocol allows for the evaluation and analysis of the effects which intravenous hADSCs exert on cognitive and motor functions following TBI, as well as their biodistribution patterns in the acute and subacute pathological phases of young and aged rats. Further, emphasis is placed on the spleen as a site of stem cell homing due to its centrality in systemic inflammation [24] and support of the neuroprotective mechanisms of stem cell transplantation after TBI [25–27]. In hopes of further detailing these mechanisms of action, conditioned media (CM) from hADSCs with silenced NEAT1 and MALAT1 was also used. The present chapter, based on our previous report [28], details the protocols necessary to reveal the histopathological and behavioral effects of transplanted stem cells in an animal model of TBI, incorporating the age of the transplant recipients as a key factor influencing the therapeutic outcomes.

2 Materials

2.1 Fluorescent Labeling of Cultured Human Adipose-Derived Mesenchymal Stem Cell Grafts and CM Preparation

1. Noncoated T-75 flasks
2. Supplemented growth medium (PM-1; ZenBio)
3. Osteoblast differentiation medium (DM; ZenBio)
4. Alizarin Red (1% Alizarin Red; CM-0058; Lifeline Technology)
5. 0.1 M PBS–10% formalin
6. Light microscope
7. DM2 adipocyte differentiation medium
8. Oil red stain
9. Molecular biology grade isopropanol
10. 1,1-dioctadecyl-3,3,3,3-tetramethylindotricbocyanine iodide (DiR)
11. 0.45-mm pore sized filter
12. Microcentrifuge

2.2 Preparation of Human Adipose-Derived Mesenchymal Stem Cell-Derived CM with Knockdown of Nuclear Enriched Abundant Transcript 1 and Metastasis Associated Lung Adenocarcinoma Transcript 1

1. Antisense RNA (NEAT1 and MALAT1 or Scramble Control Obtained from ISIS Pharmaceuticals)

2.3 Measurement of Human Vascular Endothelial Growth Factor, Stem Cell Factor, and Tissue Inhibitor of Metalloproteinase 3 Concentration

1. Human VEGF Quantikine ELISA Kit (DVE00; R&D Systems)
2. Human SCF Quantikine ELISA Kit (DCK00; R&D Systems)
3. Human TIMP-3 DuoSet (DY973; R&D Systems)
4. Synergy HT plate reader (Bio-Tex)

2.4 Surgical Procedures

1. Controlled cortical impact instrument (Pittsburgh Precision Instruments)

2. Electrical bone drill
3. Scalpel and hemostats
4. Thermal blanket pad
5. Anesthetic machine with 1–2% isoflurane
6. Small-animal stereotaxic frame (David Kopf Instruments)
7. Linear variable displacement transducer (Macrosensors)
8. Rectal thermometer
9. Ketoprofen analgesic

2.5 Intravenous Administration of Human Adipose-Derived Mesenchymal Stem Cells, CM, and Vehicle

1. Anesthetic machine with 1–2% isoflurane
2. Sterile unconditioned media
3. Conditioned media
4. 4×10^6 viable hADSCs/injection
5. Syringe and 21½ gauge needle

2.6 XenoLight DiR for In Vivo and Ex Vivo Biodistribution Imaging Procedures

1. DiR-labeled 4×10^6 hADSCs (Tx group)
2. Anesthetic machine with 3% isoflurane
3. IVIS Spectrum 200 Imaging System
4. Living Image software 4.0

2.7 Radial Arm Water Maze

1. Water tank of ~150 cm diameter and 40 cm height
2. 10-cm diameter platform
3. Six metal arm dividers

2.8 Brain and Organ Harvesting, Fixation, and Sectioning

1. Cold PBS
2. Cold 4% paraformaldehyde
3. Peristaltic pump
4. 30% sucrose
5. OCT embedding compound
6. Cryostat

2.9 Measurement of Impact Area, Peri-Impact Area, and Hippocampal Cell Loss

1. Cresyl violet nissl stain
2. Light microscope
3. Hematoxylin and eosin (H&E) stain
4. Nikon Eclipse 600 microscope
5. Computer-assisted image analysis system (NIH Image)

2.10 Measurement of Cell Survival: Human Nuclei Staining Analysis

1. Human nuclei (HuNu) antibody (1:50; MAB1281; Millipore)
2. PBS containing 0.1% Tween 20
3. 5% normal goat serum
4. Goat anti-mouse IgG Alexa Fluor 488 antibody (green; 1:500; Invitrogen)
5. Hoechst 33258 stain
6. Fluoromount medium
7. Confocal microscope

2.11 Flow Cytometry

1. FITC-, phycoerythrin-, or adenomatous polyposis coli-conjugated monoclonal antibodies against CD31, CD34, CD44, CD45, CD73, CD90, CD105, CD106, and CD117 antibody
2. TrypLE Select (Invitrogen)
3. PBS with 10% FBS
4. Centrifuge
5. Binding buffer (PBS/2% FBS/0.01% sodium azide)
6. BD Accuri C6 flow cytometer (BD Biosciences)

3 Methods

3.1 Fluorescent Labeling of Cultured Human Adipose-Derived Mesenchymal Stem Cell Grafts and CM Preparation

1. Suspend hADSCs (6.7×10^5 cells/T-75 flask, ZenBio Catalog #ASC-S) in 10 mL of supplemented growth medium (PM-1; ZenBio) and culture in noncoated T-75 flasks at 37 °C in humidified atmosphere containing 5% carbon dioxide to 90% confluency then subculture.
2. Routinely assess and verify the multipotency of hADSCs by flow cytometry of stem cell markers, $CD31^-$, $CD34^-$, $CD45^-$, $CD106^-$, $CD117^-$ and $CD44^+$, $CD73^+$, $CD105^+$, $CD90^+$, and by differentiation protocol of osteoblast (DM; ZenBio) and adipocytes (ZenBio) as published previously (*see* **Note 1**).
3. For graft preparation, incubate 4×10^6 hADSCs with Xeno-Light 1,1′-dioctadecyl-3,3,3′,3′-tetramethylindotricbocyanine iodide (DiR) (catalog#125964; Caliper Life Sciences) for 30 min to label and evaluate cell migration after transplantation. Rinse with PBS and centrifuge twice of the labeled cells then resuspend in 500 mL of PBS before the transplantation.
4. For CM preparation, collect and percolate hADSC culture media at passages 2–4 with 0.45-mm pore sized filter to avoid contamination then cryopreserve for additional experiments.

3.2 Preparation of Human Adipose-Derived Mesenchymal Stem Cell-Derived CM with Knockdown of Nuclear Enriched Abundant Transcript 1 and Metastasis Associated Lung Adenocarcinoma Transcript 1 and ELISA Measurement

1. Culture hADSCs to 80% confluency.
2. Treat with antisense RNA of NEAT1 and MALAT1 or scramble control (ISIS Pharmaceuticals) for 48 h.
3. Collect CM for 24 h then store at −80 °C until need.
4. Verify CM without NEAT1, MALAT1, and scramble control in the appropriate conditions.
5. Measure CM by Human VEGF Quantikine ELISA Kit (DVE00; R&D Systems), Human SCF Quantikine ELISA Kit (DCK00; R&D Systems), and Human TIMP-3 DuoSet (DY973; R&D Systems), according to the instructions of the manufacturer.
6. Use Synergy HT plate reader (Bio-Tex) at 450 nm to measure the absorbance from each sample.

3.3 Surgical Procedures

1. Randomly assign the animals to appropriate experimental groups and control groups.
2. Maintain the animals under anesthesia through the surgical procedure with 1–2% isoflurane in nitrous oxide/oxygen (69%/30%) mixture using a face mask.
3. Maintain the animals' body temperature within the normal range using a computer-operated thermal blanket and a rectal thermometer.
4. Prepare the rats by shaving the head region to expose the skin, followed by appropriate aseptic cleaning steps.
5. Fix the animals head in a stereotaxic frame to ensure the consistency of the impact area.
6. Make a longitudinal incision to expose the skull.
7. Craniotomy was performed using an electrical drill of approximately 4-mm radius centered from bregma +0.2 mm anterior and +0.2 mm lateral right. Avoid breaking the dura matter during the craniotomy (*see* **Note 2**).
8. Impact the brain using the control cortical apparatus with a velocity of 6.0 m/s, reaching a depth of 0.5 mm (mild) below the dura matter and remain in the brain for 150 ms. Angle impactor rod at 15° vertically to maintain a perpendicular position in reference to the tangential plane of the brain curvature at the impact surface. A linear variable displacement transducer was connected to the impactor to verify the consistency.
9. Ensure there is no excessive bleeding and close the incision with staples or sutures (*see* **Note 3**).
10. Administer analgesic compound such as ketoprofen after the surgery and as needed thereafter (*see* **Note 4**).
11. Monitor the animals closely with weight and health surveillance recording as per IACUC guidelines (*see* **Note 5**).

3.4 Intravenous Administration of Human Adipose-Derived Mesenchymal Stem Cells, CM, and Vehicle

1. Three hours after mild CCI TBI surgery, re-anesthetize rats as described above.
2. Expose the jugular vein using aseptic techniques.
3. Administer 500 μL of vehicle, CM, or hADSCs (4×10^6 cells in saline) in 15–20 s via the jugular vein (*see* **Note 6**).
4. Close the incision and monitor the animals' health closely as per IACUC guidelines.

3.5 XenoLight DiR for In Vivo and Ex Vivo Biodistribution Imaging Procedures

1. Transplant DiR-labeled 4×10^6 hADSCs (Tx group) into the jugular vein three hours following TBI surgery. Shave the animals to minimize light scattering of the DiR fluorescence emitted from the transplanted hADSCs.
2. Anesthetize animals with 3% isoflurane, then transfer animals into the IVIS Spectrum 200 Imaging System (Xenogen), setting the isoflurane level 1–2% until imaging is complete.
3. Evaluate the bio-distribution of DiR-labeled hADSC grafts at 1, 4, 12, 24, 48, and 72 h from a ventral position. Additional images of the head region may be captured with a greater magnification.
4. Maintain consistent illumination settings for each image [exposure time Auto; lamp voltage high; f/stop 2; field of view B (for head) and C (for whole body); binning 8; emission filter 800 nm; and excitation filter 745 nm].
5. Analyze all images with Living Image software 4.0 (Xenogen). To investigate the variable DiR fluorescence intensity, particular regions of interest (ROIs) can be positioned on the head and abdomen of the animals.

3.6 Neurological Testing

1. Subject each animal to a battery of behavioral tests to examine cognitive, motor, and neurological performance of the animals before and after TBI and following transplantation on days 0, 1, 3, and 7. The radial arm water maze (RAWM) test may be conducted on day 7 following TBI.
2. Perform elevated body swing test (EBST) by holding animals 1 in. from the base of the tail and raising 1 in. off of the surface. The number and direction of the swings are logged for 20 trials. A swing is counted when the head of the animal deviated 10° from the vertical axis to the left or right.
3. Accumulate a total number of swings to the biased direction for the group and divide by n of that group, resulting in the average number of biased swings per group.
4. Conduct forelimb akinesia on all animals prior to and following TBI surgery to analyze neuromotor function.
5. Ipsilateral and contralateral forepaw strength and mobility should be determined by two experimentally blind parties

using the subsequent scale: a scale of 1 to 3, where 1 is normal, 2 is impaired, and 3 is severely impaired.

6. Determine scores for each animal and a mean score for each treatment group for analysis.
7. Conduct paw grasp test prior to and following TBI surgery to analyze neuromuscular function.
8. Hold animals upright by their bodies, touching a smooth, rounded pole.
9. Ipsilateral and contralateral paw grip strength should be determined by two experimentally blind parties using the subsequent scale. On a scale of 1 to 3, 1 is normal, 2 is impaired, and 3 is severely impaired.
10. Determine scores for each animal and a mean score for each treatment group for analysis.

3.7 Radial Arm Water Maze

1. The RAWM test analyzes place and spatial learning, requiring the animal to learn how to utilize distal cues to navigate through the arm and locate the hidden platform.
2. Position a six-arm RAWM in a water tank of 150-cm diameter and a 40-cm height, with a 10-cm diameter platform 1 cm below the surface of the water. Randomly change the starting positions of the animals every trial.
3. Perform two sets of four trials with a 30-min rest period in-between for 3 days. Allot a 60-s maximum per trial and allow the animal to remain on the platform for 30 s after the trial. If the rats do not reach the platform, guide them to the platform and allow them to rest for 30 s.
4. On day 4 of RAWM, give animals four trials to train for a new platform position (reversal training). Perform RAWM analysis by averaging the trials per training set and then a total of two sets per day. Quantify reversal training by counting the number of errors in a trial.

3.8 Brain and Organ Harvesting, Fixation, and Sectioning

1. Under deep anesthesia, euthanize animals on day 11 after TBI for immunohistochemical investigations.
2. Perfuse animals through the ascending aorta with 200 mL of cold PBS, followed by 200 mL of 4% paraformaldehyde in phosphate buffer (PB).
3. Collect brains, spleen, lungs, and liver and postfix in the same fixative for 24 h, followed by 30% sucrose in PB daily until completely sunk.
4. Cut all tissues at a thickness of 30 μm with a cryostat and store at 20 °C.

3.9 Nissl Staining for Calculation of Impact and Peri-Impact Area

1. Stain serial sections corresponding to the same group of animals with Nissl for impact- and peri-impact calculations.
2. Collect every sixth coronal tissue section, beginning at anteroposterior (AP) 2.28 mm and ending at AP 0 mm posterior from bregma and process for Nissl staining from each brain perfused at day 11 after TBI.
3. Examine using a light microscope (Olympus) and Keyence microscope.
4. Measure impact area of brain damage in each slice and quantify by a computer-assisted image analysis system (NIH Image) and calculate by the following formula: [(area of the damaged region in each section) × 0.030] (cubic millimeters).
5. Count cell death for peri-impact area of brain damage using a computer-assisted image analysis system (NIH ImageJ).
6. Express impact and peri-impact area as a percentage of the ipsilateral hemisphere compared with the contralateral hemisphere.

3.10 Hematoxylin and Eosin Staining of the Hippocampus

1. Perform routine H&E within the hippocampal area, starting at coordinates AP 1.7 mm and ending AP 3.9 mm from bregma, coronal brain sections (30 μm) covering the whole dorsal hippocampus.
2. Examine a total of six sections per animal with Nikon Eclipse 600 microscope at 20.
3. Count cells presenting with nuclear and cytoplasmic staining (H&E) in the CA3 neurons, ensuring that CA3 cell counting spans the whole CA3 area, starting from the endohilar neurons to the beginning of curvature of the CA2 region in both the ipsilateral and contralateral sides.
4. Express neuron degeneration as a percentage of the ipsilateral CA3 compared with the contralateral CA3.

3.11 Human Nuclei Staining for Quantification of Transplanted Cell

1. For HuNu stain, select every sixth 30-μm thick coronal tissue section of brain and spleen, spanning the area of injury in the case of the brain and the entire red pulp in the case of spleen.
2. Wash free-floating sections three times for 5 min in PBS.
3. Block sections for 60 min at room temperature with 5% normal goat serum (Invitrogen) in PBS containing 0.1% Tween 20 (PBST; Sigma).
4. Incubate overnight at 4 °C with mouse monoclonal anti-HuNu (1:50; MAB1281; Millipore) with 5% normal goat serum.
5. Wash five times for 10 min in PBST and then soak in 5% normal goat serum in PBST containing corresponding secondary

antibodies, goat anti-mouse IgG Alexa Fluor 488 (green; 1:500; Invitrogen), for 90 min at room temperature.

6. Wash five times for 10 min in PBST and three times for 5 min in PBS.
7. Process for Hoechst 33258 (bisBenzimide H33258 trihydrochloride; Sigma) for 30 min, wash 3 times in PBS, mount on slides, and coverslip with Fluoromount (Sigma) (*see* **Note7**).
8. Examine using a confocal microscope (Olympus). Control studies should include exclusion of primary antibody substituted with 5% normal goat serum in PBS. No immunoreactivity should be observed in these controls.

3.12 Flow Cytometry

1. Perform immunophenotypical analysis of cultured cells using FITC-, phycoerythrin-, or adenomatous polyposis coli-conjugated monoclonal antibodies against CD31, CD34, CD44, CD45, CD73, CD90, CD105, CD106, and CD117 and appropriate isotype controls.
2. Use TrypLE Select (Invitrogen), wash, and resuspend cells at a concentration of 10^6 cells/ml.
3. Incubate at 4 °C for 10 min in PBS with 10% FBS.
4. Centrifuge cells for 5 min at 1200 rpm.
5. Resuspend cell pellet in binding buffer (PBS/2% FBS/0.01% sodium azide), followed by incubation with optimized concentrations of specific mAbs at 4 °C for 30 min.
6. Wash with the binding buffer, resuspend in 0.5 mL of the same buffer, and analyze within 1 h using the BD Accuri C6 flow cytometer (BD Biosciences).

4 Notes

1. For cell transplantation, it is recommended to use low passages of hADSCs between 2 and 9.
2. Intact dura matter prevents excessive bleeding and facilitates recovery postsurgery.
3. Slight bleeding is normal; use sterile gauze and saline to quickly rinse before closure of the incision aids in the wound healing process.
4. Consult with your institution's IACUC and veterinarian for appropriate dosage of anesthesia and analgesia.
5. Animals can be fed with regular diet postoperatively. If the animal loses more than 20% of its weight, special diet (i.e., peanut butter) is recommended.

6. During cell transplantation, it is important to slowly administer the cells to avoid embolism. The entry site should be underneath a muscle to minimize bleeding from withdrawing the needle.
7. Alternative nuclear immunostaining, such as DAPI can be used as substitute.

References

1. Taylor CA, Bell JM, Breiding MJ, Xu L (2017) Traumatic brain injury-related emergency department visits, hospitalizations, and deaths—United States, 2007 and 2013. MMWR Surveill Summ 66(9):1–16. https://doi.org/10.15585/mmwr.ss6609a1. PubMed: 28301451
2. Hawkins BE, Cowart JC, Parsley MA, Capra BA, Eidson KA, Hellmich HL, Dewitt DS, Prough DS (2013) Effects of trauma, hemorrhage and resuscitation in aged rats. Brain Res 1496:28–35. https://doi.org/10.1016/j.brainres.2012.12.027. PubMed: 23274538
3. Bjorklund LM, Sanchez-Pernaute R, Chung S, Andersson T, Chen IY, McNaught KS, Brownell AL, Jenkins BG, Wahlestedt C, Kim KS, Isacson O (2002) Embryonic stem cells develop into functional dopaminergic neurons after transplantation in a Parkinson rat model. Proc Natl Acad Sci U S A 99(4):2344–2349. https://doi.org/10.1073/pnas.022438099. PubMed: 11782534
4. Bjugstad KB, Teng YD, Redmond DE Jr, Elsworth JD, Roth RH, Cornelius SK, Snyder EY, Sladek JR Jr (2008) Human neural stem cells migrate along the nigrostriatal pathway in a primate model of Parkinson's disease. Exp Neurol 211(2):362–369. https://doi.org/10.1016/j.expneurol.2008.01.025. PubMed: 18394605
5. Clarkson ED (2001) Fetal tissue transplantation for patients with Parkinson's disease: a database of published clinical results. Drugs Aging 18(10):773–785. PubMed: 11735624
6. Fraser JK, Wulur I, Alfonso Z, Hedrick MH (2006) Fat tissue: an underappreciated source of stem cells for biotechnology. Trends Biotechnol 24(4):150–154. https://doi.org/10.1016/j.tibtech.2006.01.010. PubMed: 16488036
7. Harting MT, Sloan LE, Jimenez F, Baumgartner J, Cox CS Jr (2009) Subacute neural stem cell therapy for traumatic brain injury. J Surg Res 153(2):188–194. https://doi.org/10.1016/j.jss.2008.03.037. PubMed: 18694578
8. Isacson O, Costantini L, Schumacher JM, Cicchetti F, Chung S, Kim K (2001) Cell implantation therapies for Parkinson's disease using neural stem, transgenic or xenogeneic donor cells. Parkinsonism Relat Disord 7(3):205–212. PubMed: 11331188
9. Lindvall O, Brundin P, Widner H, Rehncrona S, Gustavii B, Frackowiak R, Leenders KL, Sawle G, Rothwell JC, Marsden CD et al (1990) Grafts of fetal dopamine neurons survive and improve motor function in Parkinson's disease. Science 247(4942):574–577. PubMed: 2105529
10. Liu YP, Lang BT, Baskaya MK, Dempsey RJ, Vemuganti R (2009) The potential of neural stem cells to repair stroke-induced brain damage. Acta Neuropathol 117(5):469–480. https://doi.org/10.1007/s00401-009-0516-1. PubMed: 19283395
11. Mahmood A, Lu D, Lu M, Chopp M (2003) Treatment of traumatic brain injury in adult rats with intravenous administration of human bone marrow stromal cells. Neurosurgery 53(3):697–702. discussion 702–693 [PubMed: 12943585]
12. Muraoka K, Shingo T, Yasuhara T, Kameda M, Yuen WJ, Uozumi T, Matsui T, Miyoshi Y, Date I (2008) Comparison of the therapeutic potential of adult and embryonic neural precursor cells in a rat model of Parkinson disease. J Neurosurg 108(1):149–159. https://doi.org/10.3171/JNS/2008/108/01/0149. PubMed: 18173325
13. Yang M, Donaldson AE, Jiang Y, Iacovitti L (2003) Factors influencing the differentiation of dopaminergic traits in transplanted neural stem cells. Cell Mol Neurobiol 23(4–5):851–864. PubMed: 14514036
14. Lendeckel S, Jodicke A, Christophis P, Heidinger K, Wolff J, Fraser JK, Hedrick MH, Berthold L, Howaldt HP (2004) Autologous stem cells (adipose) and fibrin glue used to treat widespread traumatic calvarial defects: case report. J Craniomaxillofac Surg 32(6):370–373. https://doi.org/10.1016/j.jcms.2004.06.002. PubMed: 15555520

15. Xue S, Zhang HT, Zhang P, Luo J, Chen ZZ, Jang XD, Xu RX (2010) Functional endothelial progenitor cells derived from adipose tissue show beneficial effect on cell therapy of traumatic brain injury. Neurosci Lett 473 (3):186–191. https://doi.org/10.1016/j.neulet.2010.02.035. PubMed: 20178832
16. Derrien T, Johnson R, Bussotti G, Tanzer A, Djebali S, Tilgner H, Guernec G, Martin D, Merkel A, Knowles DG, Lagarde J, Veeravalli L, Ruan X, Ruan Y, Lassmann T, Carninci P, Brown JB, Lipovich L, Gonzalez JM, Thomas M, Davis CA, Shiekhattar R, Gingeras TR, Hubbard TJ, Notredame C, Harrow J, Guigo R (2012) The GENCODE v7 catalog of human long noncoding RNAs: analysis of their gene structure, evolution, and expression. Genome Res 22(9):1775–1789. https://doi.org/10.1101/gr.132159.111. PubMed: 22955988
17. Wapinski O, Chang HY (2011) Long noncoding RNAs and human disease. Trends Cell Biol 21(6):354–361. https://doi.org/10.1016/j.tcb.2011.04.001. PubMed: 21550244
18. Zhang B, Arun G, Mao YS, Lazar Z, Hung G, Bhattacharjee G, Xiao X, Booth CJ, Wu J, Zhang C, Spector DL (2012) The lncRNA Malat1 is dispensable for mouse development but its transcription plays a cis-regulatory role in the adult. Cell Rep 2(1):111–123. https://doi.org/10.1016/j.celrep.2012.06.003. PubMed: 22840402
19. Ikegame Y, Yamashita K, Hayashi S, Mizuno H, Tawada M, You F, Yamada K, Tanaka Y, Egashira Y, Nakashima S, Yoshimura S, Iwama T (2011) Comparison of mesenchymal stem cells from adipose tissue and bone marrow for ischemic stroke therapy. Cytotherapy 13(6):675–685. https://doi.org/10.3109/14653249.2010.549122. PubMed: 21231804
20. Kim WS, Park BS, Sung JH, Yang JM, Park SB, Kwak SJ, Park JS (2007) Wound healing effect of adipose-derived stem cells: a critical role of secretory factors on human dermal fibroblasts. J Dermatol Sci 48(1):15–24. https://doi.org/10.1016/j.jdermsci.2007.05.018. PubMed: 17643966
21. Sun J, Zhou H, Deng Y, Zhang Y, Gu P, Ge S, Fan X (2012) Conditioned medium from bone marrow mesenchymal stem cells transiently retards osteoblast differentiation by downregulating runx2. Cells Tissues Organs 196 (6):510–522. https://doi.org/10.1159/000339245. PubMed: 22906827
22. Carlson ME, Conboy IM (2007) Loss of stem cell regenerative capacity within aged niches. Aging Cell 6(3):371–382. https://doi.org/10.1111/j.1474-9726.2007.00286.x. PubMed: 17381551
23. Conboy IM, Conboy MJ, Wagers AJ, Girma ER, Weissman IL, Rando TA (2005) Rejuvenation of aged progenitor cells by exposure to a young systemic environment. Nature 433 (7027):760–764. https://doi.org/10.1038/nature03260. PubMed: 15716955
24. Borlongan CV, Hadman M, Sanberg CD, Sanberg PR (2004) Central nervous system entry of peripherally injected umbilical cord blood cells is not required for neuroprotection in stroke. Stroke 35(10):2385–2389. https://doi.org/10.1161/01.STR.0000141680.49960.d7. PubMed: 15345799
25. Acosta SA, Tajiri N, Shinozuka K, Ishikawa H, Sanberg PR, Sanchez-Ramos J, Song S, Kaneko Y, Borlongan CV (2014) Combination therapy of human umbilical cord blood cells and granulocyte colony stimulating factor reduces histopathological and motor impairments in an experimental model of chronic traumatic brain injury. PLoS One 9(3): e90953. https://doi.org/10.1371/journal.pone.0090953. PubMed: 24621603
26. Tajiri N, Acosta S, Portillo-Gonzales GS, Aguirre D, Reyes S, Lozano D, Pabon M, Dela Pena I, Ji X, Yasuhara T, Date I, Solomita MA, Antonucci I, Stuppia L, Kaneko Y, Borlongan CV (2014) Therapeutic outcomes of transplantation of amniotic fluid-derived stem cells in experimental ischemic stroke. Front Cell Neurosci 8:227. https://doi.org/10.3389/fncel.2014.00227. PubMed: 25165432
27. Tajiri N, Kaneko Y, Shinozuka K, Ishikawa H, Yankee E, McGrogan M, Case C, Borlongan CV (2013) Stem cell recruitment of newly formed host cells via a successful seduction? Filling the gap between neurogenic niche and injured brain site. PLoS One 8(9):e74857. https://doi.org/10.1371/journal.pone.0074857. PubMed: 24023965
28. Tajiri N, Acosta SA, Shahaduzzaman M, Ishikawa H, Shinozuka K, Pabon M, Hernandez-Ontiveros D, Kim DW, Metcalf C, Staples M, Dailey T, Vasconcellos J, Franyuti G, Gould L, Patel N, Cooper D, Kaneko Y, Borlongan CV, Bickford PC (2014) Intravenous transplants of human adipose-derived stem cell protect the brain from traumatic brain injury-induced neurodegeneration and motor and cognitive impairments: cell graft biodistribution and soluble factors in young and aged rats. J Neurosci 34 (1):313–326. https://doi.org/10.1523/JNEUROSCI.2425-13.2014. PubMed: 24381292

Methods in Molecular Biology (2019) 2045: 311–321
DOI 10.1007/7651_2018_189

Published online: 30 August 2018

3D Age-Specific Mortality Trajectory: A Survival Analysis Protocol

Yuhui Lin

Abstract

Three-dimensional age-specific mortality trajectory features the rate of aging and risk for mortality of a population with respect to time (t) and age (x). Demographic and clinical records of patients are key elements to the assessment of interventional outcomes during survival analysis. Herein, a step-by-step protocol shows the retrieval of parametric estimations from both conventional and modified maximum likelihood estimation (MLE) to determine mortality trajectory of hematopoietic stem cells transplant (HSCT) patients characterized by their treatment type.

Keywords 3D trajectory, Age-specific mortality trajectory, Heterogeneity, Maximum likelihood estimation, Parametric model, Survival analysis, Transplant

1 Introduction

Organ transplant is a lifesaving opportunity. Patients who have received a transplant would have a "program reset" in their presumed mortality schedule. In comparison to pretransplant patients who are receiving novel drug therapy or cocktail of interventions, posttransplant patients are likely to experience a variety of hazard shapes at each posttransplant time-lapse interval, e.g., first 6 weeks, first 100 days, and <12 months. In this protocol study, the analytical approach to address survival analysis of allogeneic HSCTs is discussed.

The major drawback in conventional survival analysis is the lack of clarity to estimate and interpret obtained survival and hazard estimates when two entities related to time are involved, age (x) and calendar time (y). Previous scientific and medical studies have shown that survival probabilities of transplant patients and graft survival have been improving over the course of calendar time, and most analytical approaches could not disentangle the collinearity effects of the two time-related entities x, y without penalizing the likelihood estimation.

An improvement in survival probability illustrates an increase in life expectancy and a lower risk for mortality. Most clinicians would

agree that among transplant patients, a non-intended selective group of patients would outperform in recovery to their usual observations. Biologists would also recognize that in laboratory cell culture, some cells expire quicker than the rest despite being in the same flask and preset environmental conditions. This is known as heterogeneous mixing in selection for survival. In transplants, some patients are more likely to develop graft versus host disease (GvHD), and such occurrence could be due to a specific genetic mutation that encourages the onset of host-immune cells to rapidly decline graft survival and to trigger graft rejection. From an individual's survival and disease prognosis to the overview of a group or population of interest, heterogeneous mixing describes the changes in the proportion of robust to frail posttransplant patients over time-lapse intervals. This collective mixing is highly vulnerable to lifesaving effects made in novel and translational medicine that occurs over calendar time and the beneficial effects might be selective towards different age groups.

Due to the complexity and the stringency in selection for survival among transplant patients, a modified survival analysis has to be called for whereby the two entities related to time can be described in conjunction with mortality risk, age-specific mortality rate, and rate of aging $d(log(\mu(x)))/dx$, *N.B. derivative*. If an intervention is truly lifesaving, we would then expect that mortality rate would be lower and the mathematical pace for patients to age from, e.g., 40 to 70 would decelerate from the usual intervention.

2 Materials

2.1 Determining the Rate of Aging, d(log (μ(x)))/dx

In mathematics, rate is referred as the change in each unit with relation to a time entity. In statistics, time is most often referred as calendar time or duration time. However, in recent clinical studies, age has shown to be a significant factor in disease prognosis. Instead of producing the usual graphs in $S(t)$ or $\mu(t)$, the rate of change in mortality $\mu(x)$ in relation to age (x) is presented, $d(\mu(x))/dx$ *or demographic rate of aging*, $d(log(\mu(x)))/dx$. If an exposure accelerates aging, the risk for mortality represented by the magnitude of $log\ \mu(x)$ will be elevated *and* the rate of change in $log\ \mu(x)$ will be faster than the control group, $d(log(\mu(x)))/dx$, a steeper slope in Figs. 1 and 2.

2.2 Basic Structure of Survival Analysis

The following information of each individual must be available: vital status θ (dead==1 or alive==0), date of death or date of last follow-up, date of birth, and intervention or transplant age, Table 1. Subsidiary numeric information such as transplant year can be obtained from demographic calendar dates, or vice versa.

The longitudinal data has to be restructured to a long-format, specifically for transplant patients who have survived long enough

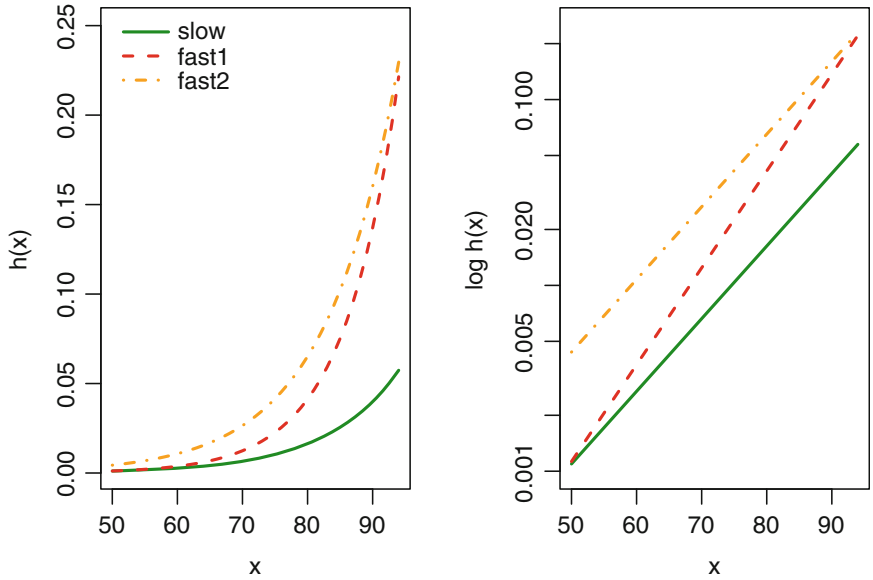

Fig. 1 Two fast lanes. Prior to disease onset, an individual's hazard *h(x)* from age 50 to 90 can be illustrated using a Gompertz hazard function, green solid line. On the absolute scale, *h(x)* has the exponential characteristic and the hazard shape appears to be flat until age 65, left diagram. If a disease were to trigger an increase in mortality risk, there are two possible trajectories with the assumption that the hazard shape retains itself, red and orange *h(x)*. *h(x)* would have to change leading to an increase in the magnitude for mortality. The only informative approach to illustrate the trajectories is to transform the *y-axis* to a semilogarithmic scale, right diagram. Fast 1: Red *log h(x)* shows the same initial mortality rate at 0.001 and its magnitude risk and rate then depart from the green *log h(x)* with every *x*-increment. Fast 2: Orange *log h(x)* shows a different risk and mortality rate to the green *log h(x)* but the pace remains the same, parallel to green *log h(x)*—an identity of proportional hazard models

to benefit from interventions that prolong their remaining life expectancy, Table 2. Such interventions would influence the risk for mortality through calendar effects; for example, Table 1 shows posttransplant patient A (id. 1: year 2005–2007) and posttransplant patient B (id. 2) with similar probability of graft survival and transplant age but the novel drug was only introduced and released for treatment in year 2010. Patient A would have benefited from the therapy if the novel treatment was introduced in 2005 or 2006, and would have likely to survive beyond 2007. This scenario is better known as calendar effects from medical progress, and the negligence to restructure the data to a long-format will lead to misleading estimates [1, 2]. This data treatment can be achieved using the embedded function in R *Survival* or *EHA* package.

2.3 Identifying Covariates from the Literature

Covariates which have a significant effect on risk estimates such as demographic, geographic, pretransplant regimen, donor source, and the occurrence of GvHD should be first identified prior to multivariate analysis, forward or backward selection using

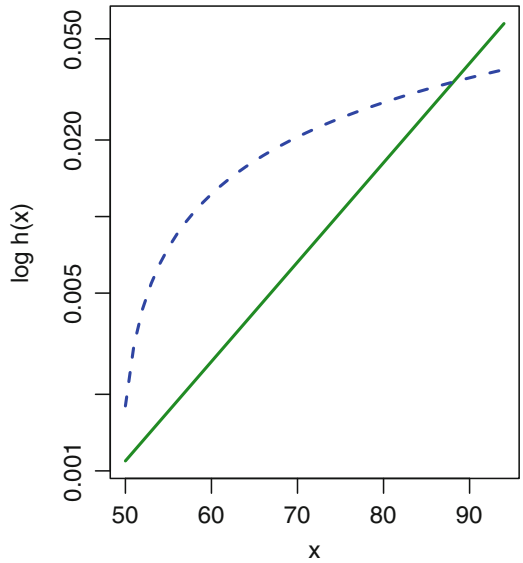

Fig. 2 From human mortality shape to machine-like hazard shape. Once an organ shows to deteriorate in its function and causes malfunction in its intended physiological processes, the hazard shape is likely to change to an accelerated failure time (AFT) hazard, blue *log h(x)*. The usual mortality hazard which is increasing exponentially, though it shows to be a linear line on a semilogarithmic scale, is the hazard shape of human mortality from age 50 to 90. If an organ transplant does not revert the malfunction process to norm, the individual will have to follow AFT *log h(x)* trajectory until a successful intervention occurs

Table 1
A general sample of an anonymized transplant data in short format

id	DOB	DOD	Transplant year	Gender	Dead	agvhd
1	23/02/1955	14/09/2007	2005	F	1	N
2	19/12/1955	31/12/2010	2010	F	0	N
3	04/03/1940	19/07/2004	2004	M	1	Y
4	05/10/1980	03/01/2006	2003	F	1	N
.	.	.	.	.	.	
.	.	.	.	.	.	
n						

S.Time represents the number of days to last follow-up or observed event, death. Last survival follow-up is fixated on 31st December 2010. DOB as Date of Birth and DOD as Date of Death presented in the format DD/MM/YYYY. The variable "dead" as the event indicator

likelihood ratio test or Aikake's information criterion (AIC) [3]. These recorded covariates are known as observed heterogeneity. In the event whereby heterogeneous effects were not observed

Table 2
Long-format data sample featuring a long-term survival patient, e.g., Table 1 patient id. 4

id	DOB	DOD	Transplant Year	Gender	Calendar (y)	Dead
4	05/10/1980	03/01/2006	2003	F	2003	0
4	05/10/1980	03/01/2006	2003	F	2004	0
4	05/10/1980	03/01/2006	2003	F	2005	0
4	05/10/1980	03/01/2006	2003	F	2006	1

N.B. The inclusion of a new dummy variable column—calendar (y) to track the vital status of patient #4 across calendar time. The event indicator "dead" is then updated according to calendar time

Table 3
Design matrix δ represents the variable of interest for age-specific mortality trajectory

id	DOB	DOD	Transplant year	Gender	Calendar (y)	Dead	$\delta 1$	$\delta 2$
1	23/02/1955	14/09/2007	2005	F	2005	0	1	0
1	23/02/1955	14/09/2007	2005	F	2006	0	1	0
1	23/02/1955	14/09/2007	2005	F	2007	1	1	0
2	19/12/1955	31/12/2010	2010	F	2010	0	1	0
3	04/03/1940	19/07/2004	2004	M	2004	1	1	0
4	05/10/1980	03/01/2006	2003	F	2003	0	0	1
4	05/10/1980	03/01/2006	2003	F	2004	0	0	1
4	05/10/1980	03/01/2006	2003	F	2005	0	0	1
4	05/10/1980	03/01/2006	2003	F	2006	1	0	1

or made available for data analysis, a frailty survival model is highly encouraged to obtain the parameter estimates and age-specific mortality trajectory.

2.4 Design Matrix for 3D Survival Analysis

On the contrary to calendar effects from medical progress which can be resolved by restructuring the data format, the design matrix δ is catered to posttransplant time-lapse intervals and exposure of interest, e.g., donor source type, treatment type, and biomarkers, Table 3. Therefore, the binary design matrix permits the presentation of the hazard shapes and mortality trajectories by exposure or treatment-type specific to its respective posttransplant time interval (t), i.e., autologous vs. allogeneic; graft-type; related vs. unrelated donor source in first 100 days; >100 days; >12 months, etc. Such approach also permits the inclusion of all individuals' profiles to enter the analysis without separation by groups during MLE, Table 3.

Once the design matrix is introduced, the preparation for three-dimensional analysis: calendar time (y), posttransplant time-lapse (t), and vital status (θ) shall then be ready for optimization.

3 Methods

Herein, the statistical procedures were illustrated using R-software, an open source statistical program which can be downloaded on the Internet [3]. There are a few ready-made software packages that can assist in the decision-making of applied conventional MLE and optimization process. As much as of its convenience in analytical work, analysts and readers should be aware of the analytical limitations while trying out the "semi-autopilot" mode written in the packages.

3.1 Missing Exposure of Interest and Vital Status

Missing variables are often treated as list-wise deletion in most statistical software and packages. A list-wise deletion in prospective study can be well-managed, but it is not advisable in case-control and other longitudinal data studies. In the event whereby missing information occurs in the exposure of interest, e.g., donor source type, smoking status, and duration of waiting time to transplant, the first approach is to consider a random sampling with replacement. The random sampling process draws information from patients in the same study and replaces the missing values. There are more tedious and sophisticated ways to test drive the quality of the data, but as a guideline variable with missing information of 10–15% should not be considered as a suitable candidate for the measured outcome.

Prior to an in-depth statistical analysis, a histogram or density plot of the patients by ages at death in accordance to gender and exposure of interest should be presented as a supplementary material for better interpretation of the analytical outcomes.

Missing information in vital status should be considered as loss to follow-up, and has to be removed prior to analysis.

3.2 Determining the Hazard Shape

The mortality schedule of humans in adulthood is mostly, if not, best described using the Gompertz and Gompertz–Makeham functions with a frailty distribution. However, there are rare scenarios whereby the Gompertz-based functions do not fit. The safest approach is to first test the parametric fit using the classic Gompertz framework, and to check if the optimized parameters reach a convergence during conventional MLE, Program Script 1. Optimized parameters must attain convergence in MLE; else refer to Sect. 4.

If none of the Gompertz-based functions fits the data or a divergence of the hazard lines on the semilog scale were to occur, it is then an open question for an accelerated failure time (AFT) hazard model, a model containing the mathematical function for

flexibility to create different curves with increasing time or age. In considering the occurrence of graft rejection and graft failure among transplant patients, an AFT model such as Weibull is a more suitable analytical choice to the Gompertz function, Program Script 2.

Program Script 1:

```
Gompertz<- function(pars, x){
a<- pars[1]
b<-pars[2]
out<- a*exp(b*x)
return(out)
}
```

Program Script 2:

```
Weibull<- function(pars,x){
lambda<- pars[1]
k<-pars[2]
out<- lambda*k*x^(k-1)
return(out)
}
```

1. Once the hazard function is determined, the survival function for the respective hazard function has to be determined.
2. Left or right truncation may require a separate function to be called for in the likelihood function.
3. Age at death (x) and age at exposure (j, also known as entry age) have to be prepared in the data.

3.3 Fundamentals of MLE

When a survival dataset is made available and a mathematical function has to be fitted to the information provided in the data, a set of probabilities for the mathematical parameters is created to describe the data. A surface of the log-likelihoods is hence generated and the purpose of maximum likelihood estimation (MLE) is to find the best of the best peak among all the inclines on the specified surface. MLE has shown to be very useful in studies whereby selection process for the event of interest is not stringent at the beginning of survival time and a huge uncertainty in the fitted residuals using regression models [4].

However, in computer programming of the summation of log-likelihoods from all individuals, a negative term has to be introduced, i.e., negative log-likelihood to achieve a maximization, not minimization.

There are two ways to set the maximization process during optimization: to introduce the return values of log-likelihood function as negative or to use the package *optim* and follow the instruction with the inclusion of *fnscale=-1*. Either one of the approaches instructs the log-likelihood to be maximized.

Since MLE is dependent on the mortality surface, the initial values of the parameters would require some wise guesses to kick start the optimization process. The better the initial values for MLE, the less amount of effort for the computer to spot the best peak on the mortality surface. For surface plots, use *lattice* R-package. *Plotly* R-package is encouraged to define the contours of the parameters using heatmaps which run in accordance to the log-likelihoods.

Maximum likelihood estimation (MLE): ω represents the parameters of the parametric function to be optimized, e.g., Weibull function would be λ and κ. Age at recruitment or entry as j and age at death as x.

$$\log L(\omega; x, j) = \Sigma \log\left(\overline{\mu}(x)\bar{S}(x)tr.\bar{S}(j)\right)$$

3.4 Returning to Conventional Approach

The modified MLE was constructed in a format to permit the return of conventional MLE analysis given the condition that all individuals share the same characteristic for the exposure of interest, e.g., all individuals experienced an event within the first 100 days and had received grafts from related donors only, Program Script 3. The absence of δ returns the modified MLE to conventional terms.

3.5 Optimization Process

Once the likelihood estimation function is written as an R-script, *optim* would then assist in defining the optimized parameter estimates, Program Script 3 and 4a, 4b. For selection of optimization process, refer to the general-purpose optimization *optim* R-manual guide [5].

When the parametric hazard $\mu(x)$ and survival $S(x)$ functions are set, the likelihood function can be written in this format to call for the respective functions, Program Script 3. θ is the event indicator for vital status also known as right censoring, dead or alive. δ is the binary design matrix. *Betas* are the beta coefficients for categorical and continuous covariates, in the format of matrices. *N.B.* for left truncation (*tr.surv.out, S(j)*), it is the inverse of *S(x)* replacing x as j for entry age, i.e., *exposure age*.

Hessian matrix for standard errors and subsequent calculations for 95% confidence intervals has to be set as *hessian = True* for the *optim* function to return the matrix, Program Script 4a and 4b.

Program Script 3:

```
likelihood.cure<- function(pars, x, entry, delta, theta, mu,
surv, covs=F){
   betas <- ncol(covs)
  if(typeof(betas)!="NULL") {
    beta <- pars[(length(pars)+1-betas):(length(pars))]
  }  else {
    beta <- F
  }
  mu.out<- ((mu(pars, x)*exp(covs%*%beta))^theta)^delta
  surv.out<- ((surv(pars,x))^exp(covs%*%beta))^delta
  tr.surv.out<-(1/(surv(pars,x=entry))^exp(covs%*%beta))^delta
  loglike<-sum(log(mu.out*surv.out*tr.surv.out))
  return(-loglike)
}
```

Program Script 4a (Univariate):

```
initial.v<- c(0.02,0.15)
model.base<- with(dat, optim(initial.v , fn= likelihood.cure ,
x= aged, entry=entry, mu=Weibull, surv= s.Weibull, theta= dead,
delta= delta1, method='Nelder-Mead', control=list(maxit=5000),
hessian=T, covs=F))
```

Program Script 4b (Multivariate):

```
dat$met.agvhd<- as.matrix(dat$agvhd)
initial.v<- c(0.02, 0.15, 1)
model.base<- with(dat, optim(initial.v , fn= likelihood.cure ,
x= aged, entry=entry, mu=Weibull, surv= s.Weibull,, theta=
dead, delta= delta1, method='Nelder-Mead', control=list(max-
it=5000), hessian=T, covs=met.agvhd))
```

3.5.1 MLE as Building Blocks: Aikake's Information Criteria (AIC)

For multivariate analysis, AIC or likelihood ratio test can be used as a tool to determine the goodness of fit when a covariate is included or excluded from the survival regression model. It is also useful to highlight that likelihood ratio test is strictly for nested model selection, i.e., models that share the same parametric distribution but with different covariates. For the assessment of goodness of fit among different range of parametric distributions, AIC is the appropriate statistical choice. Program Script 5 shows the model selection process of two models using their respective AIC values and to attain the p-values for goodness of fit.

Program Script 5 (Model Selection):

```
aic0<- 2*length(model.base$par)-2*(model.base$value)
aic1<- 2*length(model1$par)-2*(model1$value)
D0 <- -2*(model.base$value-model1$value)
p0<- 1-pchisq(D0,df=1)
p0
```

For troubleshoot, please refer to Notes.

4 Notes

The following may result in non-convergence of the parameter estimates during MLE optimization:

1. A flat surface: Human mortality tends to have one or multiple distinct inclines. A flat surface often indicates bad data. An MLE attempt would be to reduce the number of parameter estimates to be optimized and to set different sets of initial values for optimization.
2. Negative parameter values: A situation which is often described in the constant term of the Gompertz–Makeham function. The solution is to exponentiate the parameters in the likelihood function and include *log* in the initial values for MLE. This approach restricts all parameters to never go below zero.
3. Time-out: Increase the number of iterations. By default in *optim*, the number of runs is at *control=list(maxit=500)*.
4. Ties: Two individuals share the same exit time, i.e., age at death. A common situation in twins and not common among non-related individuals. The option is to break ties by including a minute difference from an assumed distribution to the ages at death.
5. Missing values: As a rule of thumb, variables containing 10–15% missing information should not be considered as a suitable candidate.
6. Correlations in the parameters: Most often simulated datasets assist in the understanding of the correlations in a mathematical function. If an exposure for death is nonselective to age and gender, and the selection for mortality among exposed individuals is completed within a short duration (e.g., less than a week), it is likely that a more sophisticated model has to be called for. However, it is not guaranteed that the correlation of parameters can be disentangled. Such exposure may include, but not limited to, infectious diseases.
7. Hessian matrix: MLE convergence occurs when *hessian* = *F*, but error messages or *NA* in the Hessian matrix output when

hessian = *T* while retrieving the standard errors and 95% confidence intervals of each optimized parameters. When parameter estimates are less than six decimal places (e.g., 0.000001 or 1e−6), the inverse of its Hessian matrix will become problematic as the values are read as zero and the inverse of zero leads to infinity, 0/1. The solution is to check whether the parameter (s) is essential or makes any significant difference to the model; AIC selection procedure would be useful in this case.

N.B. The delta method for standard errors has to be applied when logarithm is introduced to the initial values during MLE; refer to Sect. 4, **step 2**.

Acknowledgments

The author would like to thank her advisors, fellow colleagues, and postdoctorates at the Max Planck Institute for Demographic Research, Germany (2011–2014) for their discussions in statistics and mathematics as the general procedures were a collective knowledge of various human datasets that she was granted permission to work and publish. Special thanks to the editors for the chapter arrangement and delivering mathematical programming at a comprehensive level to the general audience.

References

1. Lin Y (2018) AFT survival model to capture the rate of aging and age-specific mortality trajectories among first-allogeneic hematopoietic stem cells transplant patients. PLoS One 13. https://doi.org/10.1371/journal.pone.0193287
2. Lin Y, Gajewski A, Poznańska A (2016) Examining mortality risk and rate of ageing among Polish Olympic athletes: a survival follow-up from 1924 to 2012. BMJ Open 6:e010965. https://doi.org/10.1136/bmjopen-2015-010965
3. R Core Team (2015) R: a language and environment for statistical computing. R Foundation for Statistical Computing
4. Promislow T, Pletcher C (1999) Below-threshold mortality: implications for studies in evolution, ecology and demography. J Evol Biol 12:314–328
5. R-core R-core@R-project.org. Optim—general-purpose optimization. R-Man

Methods in Molecular Biology (2019) 2045: 323–335
DOI 10.1007/7651_2019_242

Published online: 15 June 2019

Isolation, Expansion, and Characterization of Wharton's Jelly-Derived Mesenchymal Stromal Cell: Method to Identify Functional Passages for Experiments

Shuh-Wen Aung, Noor Hayaty Abu Kasim, and Thamil Selvee Ramasamy

Abstract

The therapeutic potential of human mesenchymal stromal stem cells (hMSCs) for cell-based therapeutic is greatly influenced by the in vitro culture condition including the culture conditions. Nevertheless, there are many technical challenges needed to be overcome prior to the clinical use including the quantity, quality, and heterogeneity of the cells. Therefore, it is necessary to develop a stem cell culture procedure or protocol for cell expansion in order to generate reproducible and high-quality cells in accordance with good manufacturing practice for clinical and therapeutic purposes. Here we assessed the MSCs characteristic of human Wharton's jelly mesenchymal stromal cells in in vitro culture according to the criteria established by the International Society for Cellular Therapy. Besides, the viability of the WJMSCs was determined in order to increase the confidence that the cells are employed to meet the therapeutic efficacy.

Keywords Wharton's jelly, Mesenchymal stromal cells, In vitro passaging, Replication senescence, Stemness

1 Introduction

The ability to self-renew, differentiate into other cells, and secrete therapeutic molecules make hMSCs valuable cellular resources for research and development of therapeutics aiding repair or restore function of damaged organ or tissue [1–3]. Wharton's jelly-derived MSCs (WJMSCs) have drawn great attention in recent years owing to the stemness properties and accessibility from donor via procedures with minimal invasion [4, 5]. However the therapeutic effects of WJMSCs are still controversial as clinical trials using hMSCs, in general, not showing consistent and significant therapeutic outcomes [6, 7]. This phenomenon is, in large part, due to MSCs that are prone to undergo replicative stress and morphologically heterogeneous during in vitro expansion, which hampers their therapeutic actions [8–14]. To address this issue, here we demonstrate the method to isolate, expand, and characterize WJMSCs culture to produce WJMSCs which achieve the quality and quantity acceptable for clinical and therapeutic applications.

2 Materials

This protocol is use to isolate MSCs derived from human Wharton's jelly samples received from donors who have given their consent (medical ethics approval: DFRD1503/0013 [L]). All cell culture activities should be executed inside the biological safely cabinet aseptically. Sterile the forceps, scalpel handles, scissors, stainless steel basin, and ultrapure water by autoclaving. Prepare and store all reagents at 4 °C prior to the procedure. Thaw the culture media in the water bath at 37 °C prior to use.

2.1 Isolation of MSCs from Human Wharton's Jelly of an Umbilical Cord

1. Washing buffer: Mix Dulbecco's phosphate-buffered saline without calcium and magnesium (DPBS (−)(−)), Antibiotic-Antimycotic (anti-anti) 1% freshly in sterile 50 mL Falcon tubes.
2. Collagenase digestion solution (0.1%): Dissolved 30 mg of collagenase type1 in 30 mL of Dulbecco's Modified Eagle's Medium Knock-Out (DMEM-KO). Filter the mixture using 0.2 μm syringe filter into the sterile 50 mL Falcon tubes.
3. Complete culture media (CCM): Mix 10% fetal bovine serum (FBS), 1% Glutamax, and 0.5% anti-anti followed by make up to 250 mL with DMEM-KO. Add about 2 ng/mL basic fibroblast growth factor (bFGF) to complete culture media prior to use.
4. Growth kinetic analysis: trypan blue exclusion assay
5. TrypLE Express.
6. Cell counting chamber slide.
7. Trypan blue dye.

2.2 Immunophenotyping Using Flow Cytometry

1. Sample buffer: 1× phosphate-buffered saline (PBS), 0.5% bovine serum albumin (BSA), and 2 mM ethylenediaminetetraacetic acid (EDTA).
2. Human MSC phenotyping kit (Miltenyi Biotec, Germany).

2.3 Multi-lineage Differentiation

1. Multi-lineage culture medium including StemPro adipogenesis, chondrogenesis, and osteogenesis differentiation kits (Gibco, USA).
2. 1× PBS solution.
3. 10% formalin.
4. Absolute isopropanol (IPA).
5. 60% IPA.
6. Double distilled water (ddH_2O).
7. 1 M hydrochloric acid (HCl).

8. 0.3% Oil Red O stock solution: Dissolve 0.35 g Oil Red O in 100 mL absolute IPA and then filter with 0.45 μm syringe filter.
9. Oil Red O working solution: Prepare fresh when needed. Mix 6 mL of 0.3% Oil Red O in isopropanol and 4 mL ddH_2O.
10. 0.1% Safranin O working solution: Dissolve 0.1 g of Safranin O in 100 mL ddH_2O.
11. 2% Alizarin Red working solution: Dissolve 2 g of Alizarin Red in 90 mL ddH_2O, mix, and adjust the pH to 4.1 to 4.3 with 1 M of HCl. Then, bring up to 100 mL with ddH_2O and filter the solution with filter paper.

2.4 Senescence Examination

1. Senescence β-Galactosidase Staining Kit (Cell Signaling Technology, USA).
2. Fixation solution: Dilute the 10× fixation solution to a 1× with distilled water.
3. Staining solution: Dilute the 10× staining solution (redissolve by heating to 37 °C with agitation) to a 1× with ddH_2O.
4. X-gal: Dissolve 20 mg of X-gal in 1 mL dimethylformamide to prepare a 20 mg/mL stock solution (*see* **Note 1**).

2.5 Cell Cycle Analysis: Propidium Iodide (PI) Staining and Flow Cytometry Analysis

1. Sample buffer: Dissolve 0.1 g of glucose in 100 mL DPBS (−)(−).
2. Fixative: 70% ethanol (ice-cold).
3. Staining solution: Propidium iodide (2 μg/mL), RNase A (10 μg/mL) in sample buffer. Prepare solution directly before use (*see* **Note 2**).

3 Methods

3.1 Isolation of hWJMSCs

Wharton's jelly is the gelatinous substance located within the umbilical cord, and it protects the vessels and prevents the cord from kinking. Wharton's jelly is rich with mesenchymal stem cells and can be isolated and expanded in vitro. The isolation protocol as below:

1. Rinse the umbilical cord with 1× PBS to remove blood contaminates.
2. Cut the cord to 3 cm fragment using a sterile scissor.
3. Remove the blood vessels from the cord by incising the cord lengthwise using sterile scissors and forceps.
4. Rinse the processed cord with washing buffer for three times in 50 mL tubes.
5. Immerse the processed cord into the 70% ethanol for 30 s and followed by an immediate rinse with 1× DPBS(−)(−).

6. Incubate the fragmented cord in the washing buffer at 37 °C for 1 h.
7. Shred or mince the fragmented cord into smaller size by using sterile scissor.
8. Transfer the shredded tissue into a fresh 50 mL tube, and add collagenase digestion solution, until the cord tissues are submerged completely in the collagenase digestion solution.
9. Incubate 9 h or overnight in the CO_2 incubator at 37 °C.
10. Add equal volume of culture media to dilute the collagenase-Wharton's jelly mixture.
11. Strain the digested cord mixture using 100 μm nylon filters.
12. Centrifuge at 300 × *g* for 6 min at room temperature.
13. Gently remove top (70%) of the collagenase-culture media mixture using serological pipette.
14. Resuspend the remaining mixture (30%) with double volume of complete culture media.
15. Seed the culture into T75 culture flask, and incubate in the CO_2 incubator at 37 °C.
16. Examine the culture the following days for any contamination or abnormal culture.
17. Complete media change after 2 to 3 days of incubation or after cell growth was observed.
18. Change the media every 3 days to remove waste accumulated in the media.

3.2 Cell Expansion and Cryopreservation

Upon reaching confluency of 80% to 90%, discard culture media from the culture flask, and rinse the adherent cells with 1× DPBS—twice to remove excess culture medium.

Dissociate the adherent cells by adding 2 mL of TrypLE Express into the culture flask, and incubate for 3 min at room temperature.

1. Dilute the TrypLE Express solution by adding double volume of culture media to the volume of TrypLE Express that was previously added.
2. Collect the cell suspension into a fresh 50 mL tube, and harvest the cell by centrifugation at 300 × *g* for 6 min at room temperature.
3. Remove the supernatant, and resuspend the cell pellet with 1 mL of complete culture media.
4. Take 10 μL of cell culture suspension, and mix with 10 μL of trypan blue dye.
5. Conduct cell count using cell counter.

6. Seed the cells into a fresh culture flask with cell seeding density of 5000 cell/cm^2.
7. Cryopreserve 1 million cells in 1 mL freezing medium containing 45% (vol/vol) of culture medium, 45% (vol/vol) of FBS, and 10% (vol/vol) of dimethyl sulfoxide (DMSO) in cryogenic vial, and keep in liquid nitrogen container at the vapor phase for long-term storage to ensure maximum viability of the preserved cells.

3.3 MSCs Basic Characterization

3.3.1 Growth Kinetic Analysis: Trypan Blue Dye Exclusion Assay

The proliferation rate of culture is determined by plating cells with density of 5000 cells/cm^2 into a 6-well culture dish for several passages and measurement of viable cells at indicated day post-seeding or upon 90% confluency. Three replicates are prepared for each passage. Protocol as below:

1. Wash cell culture with DPBS (−)(−) twice to remove floaters (those floating cells in medium are death cells).
2. Add 2 mL of TrypLE Express, and incubate at room temperature for 3 min to dissociate cells from culture flask.
3. Add double volume of DPBS (−)(−), and collect the cell mixture to collection tube.
4. Harvest the cells by centrifugation at 1250 × *g* for 6 min at room temperature.
5. Remove the supernatant, and resuspend the cell pellet with 1 mL complete culture media.
6. Take 10 μL of cell culture suspension, and mix with 10 μL of trypan blue dye.
7. Conduct cell count using cell counter.
8. Reseed the cells into a fresh culture dish according to the area of the culture dish 5000 cell/cm^2.
9. Incubate the culture in CO_2 incubator at 37 °C.
10. Conduct cell count after 72 to 96 h for six consecutive passages.
11. Add 0.5 mL of TrypLE Express, and incubate at room temperature for 3 min to dissociate cells from culture well.
12. Follow **steps 3** to 7.
13. Determine the growth kinetics of isolated MSCs including the number of live and dead cells for six consecutive passages (*see* Fig. 1). Cell count and population doubling time (PDT) are determined at each passages using the following equations:

$$\mathrm{PDT} = D\log(2)/(\log(\mathrm{NH}) - \log(\mathrm{NI}))$$

where NI is the inoculum cell number, NH is the cell harvest number, and D is the duration of the culture in hours.

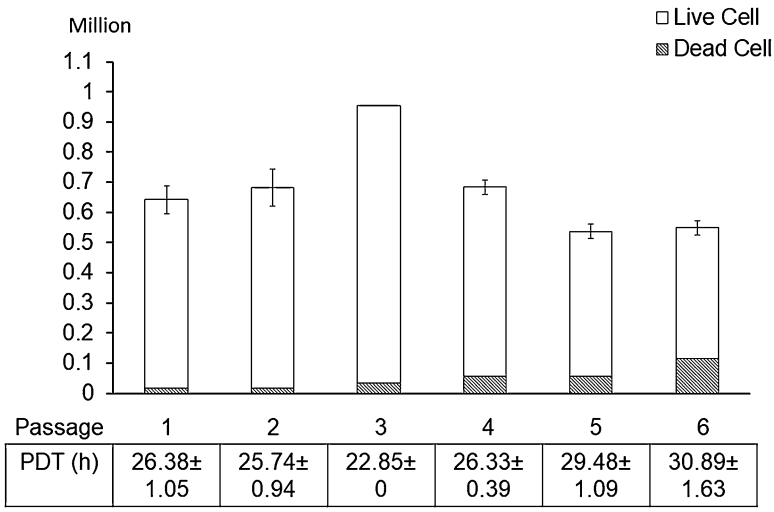

Fig. 1 Growth kinetics of WJMSCs during in vitro culture for six passages. Total cell number (live and dead cell), PDT for each of six passages in WJMSCs after 96 h of cultivation to assess their in vitro proliferation capability

3.3.2 Tri-lineage Differentiation

An in vitro tri-lineage differentiation study is performed to determine the multi-lineage capacity of the MSCs. Culture at 80% confluency is cultured differentiation into adipocytes, chondrocytes, and osteoblasts lineages in vitro using StemPro® adipogenesis, chondrogenesis, and osteogenesis differentiation kits (Gibco, USA), respectively. Protocol as below:

Adipocytes, Chondrocytes, and Osteocytes Differentiation

1. Grow cell until 80% of confluency in 6-well culture plate.
2. Remove medium and rinse the culture once with DPBS (−) (−).
3. Replace the growth media with adipocytes, chondrocytes, and osteoblasts differentiation induction media, respectively.
4. Incubate the culture at 37 °C in the CO_2 incubator, and change at 3-day intervals.

Adipocytes, Chondrocytes, and Osteocytes Staining

Assess the differentiation state by staining after 21 days of differentiation culture (*see* Fig. 2). Fix the cell culture with 10% formalin solution, and rinse with 2 mL 1× PBS for three times. Prepare the staining solution just prior to use (prepare as in Subheading 2.4, **items 9–11**).

Oil Red O Staining for Adipocytes

1. After fixation, add 2 mL of Oil Red O working solution into the adipocytes differentiated culture well, and incubate for 10 min at room temperature in dark.
2. Wash the cells with 60% isopropanol.

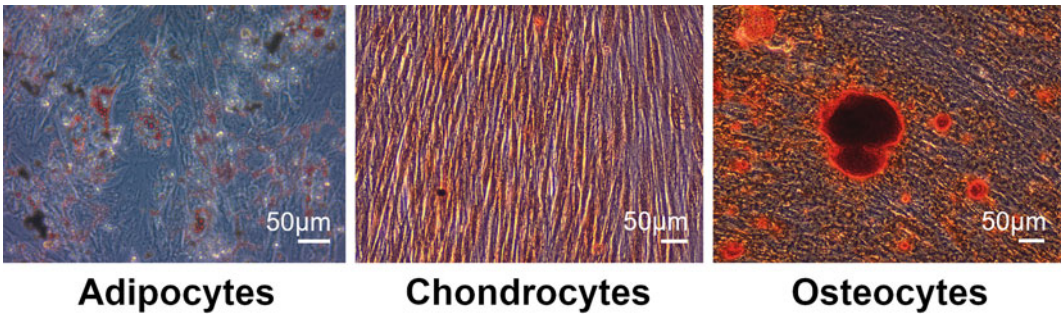

Fig. 2 Tri-lineage differentiation capacity of WJMSCS at P3. Phase contrast images of adipogenic (total magnification of 100; 10 ocular, 10 objective), chondrogenic (total magnification of 100; 10 ocular, 10 objective), and osteogenic (total magnification of 100; 10 ocular, 10 objective) differentiation potential of WJMSCs at P3 after 21 days of induction. Oil Red O solution is used to stain intracellular oil droplet in red confirmed adipogenesis; Safranin O solution is used to stain the extracellular deposition of glycosaminoglycan in orange confirmed chondrogenesis; Alizarin Red solution is used to stain the calcium deposits in bright-orange confirmed osteogenesis

3. Wash with 2 mL of ddH_2O four times.
4. Aspirate the ddH_2O and add 1 mL of 1× PBS and then observe under light microscope.

Safranin O Staining for Chondrocytes

1. After fixation add 2 mL of 0.1% Safranin O solution into the chondrocytes differentiated culture well, and incubate for 15 min at room temperature in dark.
2. Wash with 2 mL of ddH_2O three times.
3. Aspirate the ddH_2O, add 1 mL of 1× PBS, and then observe under light microscope.

Alizarin Red Staining for Osteocytes

1. After fixation, add 2 mL of 2% Alizarin Red solution in the osteocytes differentiated culture well, and incubate for 45 min at room temperature in dark.
2. Wash with 2 mL of ddH_2O three times.
3. Aspirate the ddH_2O, and add 1 mL of 1× PBS then observe under light microscope.

3.3.3 MSC Immunophenotyping

Based on the minimal criteria for defining human multipotent mesenchymal stromal cells standard set by International Society for Cellular Therapy [15], sample cells are characterized with regard to MSC status by assessing their cell surface antigen profile by immunophenotyping using flow cytometry technique. A number of cells in population expressing cluster of differentiation (CD)105, CD90, and CD73 antigen (markers of human MSCs) and negative markers CD45, CD34, CD20 as well as CD14 (hematopoietic markers) were determined by flow cytometry. Protocol as below.

Compensation of Flow Cytometer

1. Conduct compensation analysis to all five sets of fluorochrome-conjugated aliquot before flow cytometry acquisition and analysis.
2. Prepare five aliquots (PerCP, PE, APC, FITC, blank), each with up to 0.5×10^6 MSCs.
3. Centrifuge cell suspension at $300 \times g$ for 10 min.
4. Remove supernatant and resuspend aliquots PerCP, PE, APC, and FITC in 100 μL of sample buffer and aliquot blank in 500 μL of sample buffer.
5. Add 10 μL of CD73-Biotin in aliquot PerCP, CD105-PE in aliquot PE, 10 μL of CD73-APC in aliquot APC, and 10 μL of CD90-FITC in aliquot FITC.
6. Mix each aliquot well, and incubate for 10 min in the dark in the refrigerator (4 °C).
7. Add 1 mL of sample buffer and centrifuge at $300 \times g$ for 10 min.
8. Remove supernatant completely.
9. Resuspend each cell pellet separately in 500 μL sample buffer in aliquot PE, APC, and FITC.
10. Add 10 μL of Anti-Biotin-PerCP to aliquot PerCP, mix well, and incubate for 10 min in the dark in the refrigerator (4 °C).
11. Wash cells following **steps 7** to **9**.
12. Compensate instrument by following the instructions in the instrument user manual.

MSC Immunophenotyping Staining

1. Harvest cells from culture using TrypLE Express dissociation technique, and determine its total cell number following Subheading 3.2, **steps 1–7**.
2. Prepare four sets of 0.5×10^6 h WJMSCs suspension aliquots and two sets of 1×10^6 h WJMSCs suspension aliquots in 100 μL of sample buffer and one set of blank aliquot in 500 μL, respectively, for one sample.
3. Add 10 μL of fluorochrome-conjugated antibodies CD73-Biotin, CD105-PE, CD73-APC, and CD90-FITC to each 100 μL cell suspension, respectively, and mix by pipetting up and down.
4. Incubate for 10 min in the dark at 4 °C (*see* **Note 3**).
5. Add 1 to 2 mL of sample buffer to the aliquots and followed by centrifugation at $300 \times g$ for 10 min (except for the aliquot CD-73-Biotin).
6. Remove the supernatant and resuspend the cell pellet with 500 μL sample buffer.

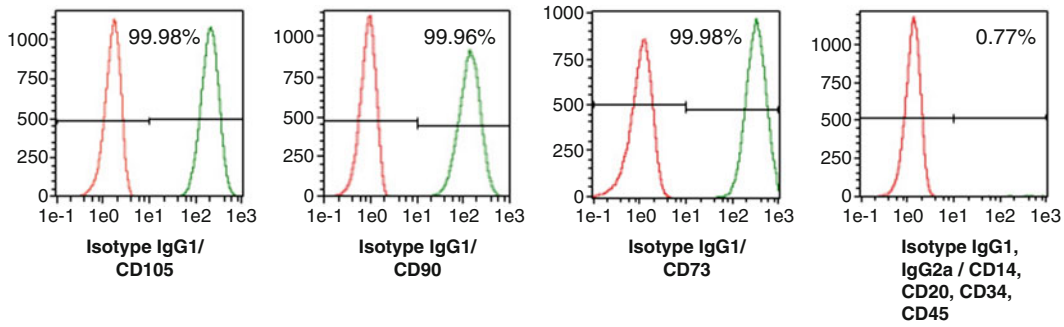

Fig. 3 MSCs immunophenotyping of WJMSCs at P3. Flow cytometry analysis histograms demonstrating percentage of WJMSCs at P3 stained for hMSCs surface markers (CD105, CD90, and CD73 and hematopoietic markers CD45, CD34, CD20, and CD14). Red-colored histograms are for control immunoglobulins, and green-colored histograms are for specific markers

7. Add 10 μL of Anti-Biotin-PerCP to the CD-73-Biotin aliquot and incubate for another 10 min the dark, and then continue with **steps 5** and **6**.
8. Conduct flow cytometric analysis where at least 10,000 events were collected for each cocktail to determine percentage of cells expressing the respective markers (*see* Fig. 3).

3.4 Assessment of Senescence Using β-Galactosidase (SA-β-Gal) Assay and PI Staining Analysis

Senescent cells showed increase level of lysosomal β-galactosidase [16]. SA-β-gal assay is one of the analytical approaches to determine cell senescence in vitro. The SA-β-gal positive cells stain blue-green, which can be observed under bright-field microscopy. Protocol as below:

3.4.1 Senescence β-Galactosidase (SA-β-gal) Assay

1. Remove culture medium from cell culture and rinse once with 1× PBS.
2. Add 1 mL of fixative solution to allow cells to fix for 10 to15 min at room temperature.
3. Remove fixation solution and wash two times with 1× PBS.
4. Add 1 mL of SA-β-gal staining solution (prepare as in Subheading 2.5, **item 3**), and incubate at 37 °C at least overnight, no CO_2 (*see* **Note 4**).
5. Observe the developed blue-colored stains under microscope indicated the senescence cells (*see* Fig. 4).

3.4.2 Cell Cycle Analysis

Propidium iodide (PI) is a fluorescent dye that intercalates into double-stranded nucleic acid. It can penetrate cell membranes of dead or dying cells, and it is widely used for evaluation of cell death, apoptosis, or DNA content in cell cycle analysis. The protocol as below:

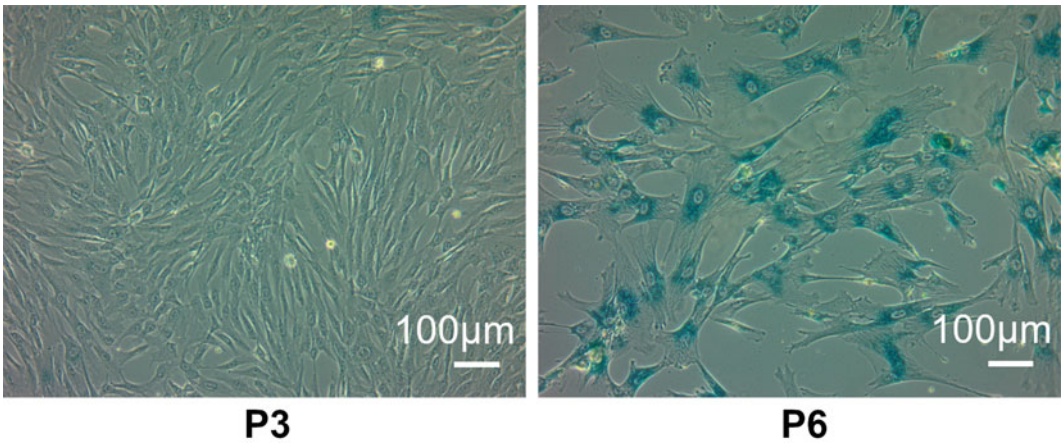

Fig. 4 SA-β-gal activity of WJMSCs at P3 and P6. Representative positive SA-β-gal staining of senescent WJMSCs at P6 showing larger cell size in comparison to P3

Cell Preparation

1. Upon reaching sub-confluency of 70% to 80%, discard culture media from the culture flask, and rinse the adherent cells with 1× DPBS—twice to remove excess culture medium.
2. Dissociate the adherent cells by adding 2 mL of TrypLE Express into the culture flask, and incubate for 3 min at room temperature.
3. Dilute the TrypLE Express solution by adding double volume of culture media to the volume of TrypLE Express that was previously added.
4. Collect the cell suspension into a fresh 50 mL tube, and harvest the cell by centrifugation at 300 × *g* for 10 min at 4 °C.
5. Remove the supernatant, and add 1 mL of sample buffer to resuspend the cell pellet.
6. Take 10 μL of cell suspension and mix with 10 μL of trypan blue dye.
7. Determine total cell number using cell counter.
8. Adjust the cell concentration to 1.0×10^6 cells/mL in sample buffer.
9. Centrifuge the cell suspension at 300 × *g* for 10 min at 4 °C.
10. Decant all the supernatant.
11. Vigorously vortex the pellet in the remaining buffer for 10 s. Continue to vortex the cells, and slowly add 1 mL of ice-cold 70% ethanol drop by drop to the pellet.
12. Seal the tubes, and allow samples to fix in ethanol overnight at −20 °C (>18 h) for maximum resolution of cellular DNA.

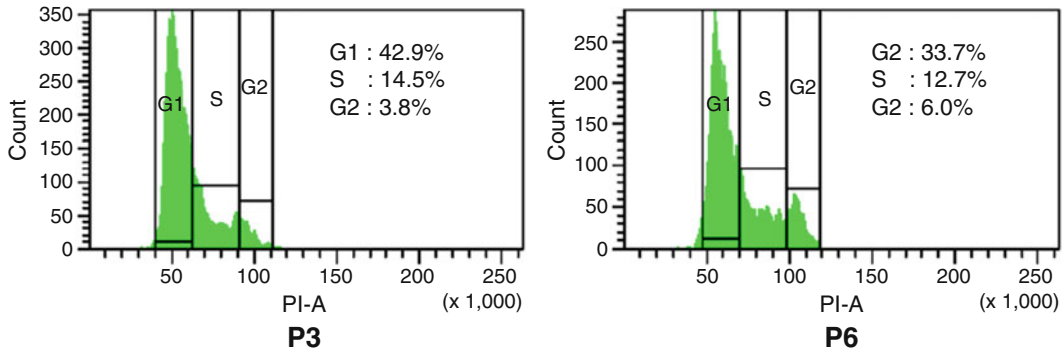

Fig. 5 Flow cytometry analysis of cell cycle progression of WJMSCs at P3 and P6. Cells at P3 and P6 were harvested after incubated for 96 h. Cell population in G2/M phase was increased at P6 compared to P3

Staining

1. Prepare the staining solution just prior to use (prepare as in Subheading 2.5, **item 3**).
2. Briefly vortex the sample tubes from **step 12**, and add 10 mL sample buffer.
3. Centrifuge at a higher speed at 500 × *g* for 10 min at 4 °C (*see* **Note 5**).
4. Aspirate the supernatant without disturbing the cell pellet.
5. Gently vortex the tube to resuspend cells in residual buffer.
6. Add 1 mL of staining solution and vortex carefully.
7. Incubate for 30 to 40 min at room temperature.
8. Filter the sample through 35 μm cell strainer cap into 12 × 75 mm tube before analyzing with flow cytometer (*see* **Note 6**).
9. Analyze the samples within 3 h from the preparation time (*see* Fig. 5).

4 Notes

1. Always use polypropylene plastic or glass to make and store X-gal. Do not use polystyrene.
2. Propidium iodide is a suspected carcinogen; always wear proper protective clothing and gloves when handling the solution. Contact with eyes, skin, and mucous membranes should be avoided.
3. Higher temperatures or longer incubation times may lead to non-specific cell labeling.
4. The presence of CO_2 can cause changes to the pH which may affect staining results.

5. Check to see that there is a visible cell pellet. If no pellet is visible, recentrifuge at a higher speed until cell pellet is seen. After ethanol fixation, cells require higher g-force to form pellet.
6. Minimize cell clumps by passing the sample through 35 μm cell strainer cap into 12 × 75 mm tube before analyze is recommended as cells in suspension may attach to one another and form clumps for a variety of reasons. The most common cause of cell clumping is that dead cells release nucleic acids that cause intact cells to clump. These aggregates may plug the instrument.

Acknowledgments

This research was supported by High Impact Research MOHE Grant UM.C/625/1/HIR/MOHE/DENT/01 from Ministry of Higher Education Malaysia, Fundamental Research Grant Scheme (FRGS FP044-2014B) from Ministry of Education, Malaysia, and University of Malaya Research Grant (RP019C-13HTM) from University of Malaya.

References

1. Heathman TR, Nienow AW, McCall MJ, Coopman K, Kara B, Hewitt CJ (2015) The translation of cell-based therapies: clinical landscape and manufacturing challenges. Regen Med 10:49–64
2. Buzhor E, Leshansky L, Blumenthal J, Barash H, Warshawsky D, Mazor Y, Shtrichman R (2014) Cell-based therapy approaches: the hope for incurable diseases. Regen Med 9:649–672
3. Wei X, Yang X, Han ZP, Qu FF, Shao L, Shi YF (2013) Mesenchymal stem cells: a new trend for cell therapy. Acta Pharmacol Sin 34:747–754
4. Kalaszczynska I, Ferdyn K (2015) Wharton's jelly derived mesenchymal stem cells: future of regenerative medicine? Recent findings and clinical significance. Biomed Res Int 2015:430847
5. Batsali AK, Kastrinaki MC, Papadaki HA, Pontikoglou C (2013) Mesenchymal stem cells derived from Wharton's Jelly of the umbilical cord: biological properties and emerging clinical applications. Curr Stem Cell Res Ther 8:144–155
6. Galipeau J, Sensebe L (2018) Mesenchymal stromal cells: clinical challenges and therapeutic opportunities. Cell Stem Cell 22:824–833
7. Trounson A, McDonald C (2015) Stem cell therapies in clinical trials: progress and challenges. Cell Stem Cell 17:11–22
8. Sepulveda JC, Tome M, Fernandez ME, Delgado M, Campisi J, Bernad A, Gonzalez MA (2014) Cell senescence abrogates the therapeutic potential of human mesenchymal stem cells in the lethal endotoxemia model. Stem Cells 32:1865–1877
9. Wagner W, Horn P, Castoldi M, Diehlmann A, Bork S, Saffrich R, Benes V, Blake J, Pfister S, Eckstein V et al (2008) Replicative senescence of mesenchymal stem cells: a continuous and organized process. PLoS One 3:e2213
10. Wagner W, Ho AD, Zenke M (2010) Different facets of aging in human mesenchymal stem cells. Tissue Eng Part B Rev 16:445–453
11. Wagner W, Bork S, Lepperdinger G, Joussen S, Ma N, Strunk D, Koch C (2010) How to track cellular aging of mesenchymal stromal cells? Aging 2:224–230
12. Hayflick L (1965) The limited in vitro lifetime of human diploid cell strains. Exp Cell Res 37:614–636
13. Wagner W, Bork S, Horn P, Krunic D, Walenda T, Diehlmann A, Benes V, Blake J, Huber FX, Eckstein V et al (2009) Aging and replicative senescence have related effects on

human stem and progenitor cells. PLoS One 4: e5846

14. Turinetto V, Vitale E, Giachino C (2016) Senescence in human mesenchymal stem cells: functional changes and implications in stem cell-based therapy. Int J Mol Sci 17(7)
15. Dominici M, Le Blanc K, Mueller I, Slaper-Cortenbach I, Marini F, Krause D, Deans R, Keating A, Prockop D, Horwitz E (2006) Minimal criteria for defining multipotent mesenchymal stromal cells. The International Society for Cellular Therapy position statement. Cytotherapy 8:315–317
16. Kurz DJ, Decary S, Hong Y, Erusalimsky JD (2000) Senescence-associated (beta)-galactosidase reflects an increase in lysosomal mass during replicative ageing of human endothelial cells. J Cell Sci 113:3613–3622

Methods in Molecular Biology (2019) 2045: 337–346
DOI 10.1007/7651_2019_243

Published online: 28 June 2019

CRISPR Base Editing in Induced Pluripotent Stem Cells

Ya-Ju Chang, Christine L. Xu, Xuan Cui, Alexander G. Bassuk, Vinit B. Mahajan, Yi-Ting Tsai, and Stephen H. Tsang

Abstract

Induced pluripotent stem cells (iPSCs) have demonstrated tremendous potential in numerous disease modeling and regenerative medicine-based therapies. The development of innovative gene transduction and editing technologies has further augmented the potential of iPSCs. Cas9-cytidine deaminases, for example, have developed as an alternative strategy to integrate single-base mutations (C → T or G → A transitions) at specific genomic loci. In this chapter, we specifically describe CRISPR (clustered regularly interspaced short palindromic repeats) base editing in iPSCs for editing precise locations in the genome. This state-of-the-art approach enables highly efficient and accurate modifications in genes. Thus, this technique not only has the potential to have biotechnology and therapeutic applications but also the ability to reveal underlying mechanisms regarding pathologies caused by specific mutations.

Keywords Base editing, iPS cells, Target-AID, Cas9, Precise gene editing

1 Introduction

Genome engineering through the CRISPR (clustered regularly interspaced short palindromic repeats)/Cas9 system has revolutionized technology in many fields [1, 2]. CRISPR/Cas9 harnesses the innate machinery of the adaptive immune system in bacteria and archaeal species [3, 4]. These species protect themselves against invaders (foreign DNA and phages) by storing pieces of their DNA into their molecular memories as "spacer" sequences in between palindromic "repeat sequences." Together, these fragments are transcribed as the CRISPR RNA (crRNA) in the CRISPR/Cas9 system. The crRNA and *trans*-activating crRNA (tracrRNA)—a sequence that forms a "handle" for the Cas9 protein—join together and complex into a single-guide RNA (sgRNA) with the Cas9 endonuclease and guide Cas9 to the complementary site in the endogenous DNA. The activity of Cas9 depends on the presence of a protospacer adjacent motif (PAM) sequence in the target DNA, thus enabling the CRISPR/Cas9 complex to

Ya-Ju Chang and Christine L. Xu contributed equally to this work and are co-first authors.

recognize its nonself DNA sequence, target a specific genomic locus, and generate a double-strand break (DSB) [5].

The DSBs can be subsequently repaired by two DNA repair mechanisms: nonhomologous end joining (NHEJ) or homology-directed repair (HDR). NHEJ involves the error-prone process of joining the broken DNA strands back together, and insertions and deletions (indels) can form as a result. Precision gene editing using HDR requires the presence of a homologous template to guide the specific DNA repair process. The simultaneous delivery of the desired template into target cells during DSBs has its restrictions [6, 7]. NHEJ occurs at a much higher rate than HDR in eukaryotic cells, especially in nondividing cells. This is a challenge and limitation especially in precise gene editing, which would be necessary to correct mutations in the genomes of postmitotic cells for specific treatments or therapies.

CRISPR base editing is a new method of genome editing (developed in 2016), and it allows for the conversion of a specific DNA base into another at a targeted genomic locus. The advanced base editing technique enables a single-base correction without the DNA DSBs which are necessary for traditional CRISPR [8–10]. Because many genetic diseases are associated with single-point mutations, CRISPR base editing has advantages in research and in therapeutic applications. There are many research groups developing base editing using modified CRISPR-Cas9 systems. Cas9-cytidine deaminase fusion enzymes allow for the targeted conversion of genomic deoxycytidine to deoxythymidine (C:G → T:A) without the induction of DSBs [11]. This reduces the incidence of insertions and deletion (indels) and possibilities of off-target effects. CRISPR base editors (BEs) depend on site-specific modification of the DNA base guided by the Cas9-guide RNA (gRNA) complex to induce the conversion of deoxycytidine to deoxyuridine (C → U) (Fig. 1). In contrast to HDR-mediated genome editing, base editing's precise DNA modification avoids large-scale base deletions. The first edition BEs (discussed in more detail below) are linked to cytidine deaminase or adenosine deaminase, and they substitute C → T with G → A in DNA [12]. Because BEs are highly specific, they will likely be useful for numerous gene correction therapies.

Base editors were developed to overcome problems in the traditional CRISPR/Cas9 system such as inefficient gene editing, random insertion deletion (indel) creation, and off-targeting effects due to the reliance on DSBs to induce the DNA repair pathway [13]. In order to create precise base editors, Komor et al. reprogrammed deaminases to induce specific point mutations in the genome. Specifically, the apolipoprotein B mRNA editing enzyme, catalytic polypeptide-like (APOBEC) family of cytidine deaminases were repurposed for their properties of converting cytidine (C) to uracil (U).

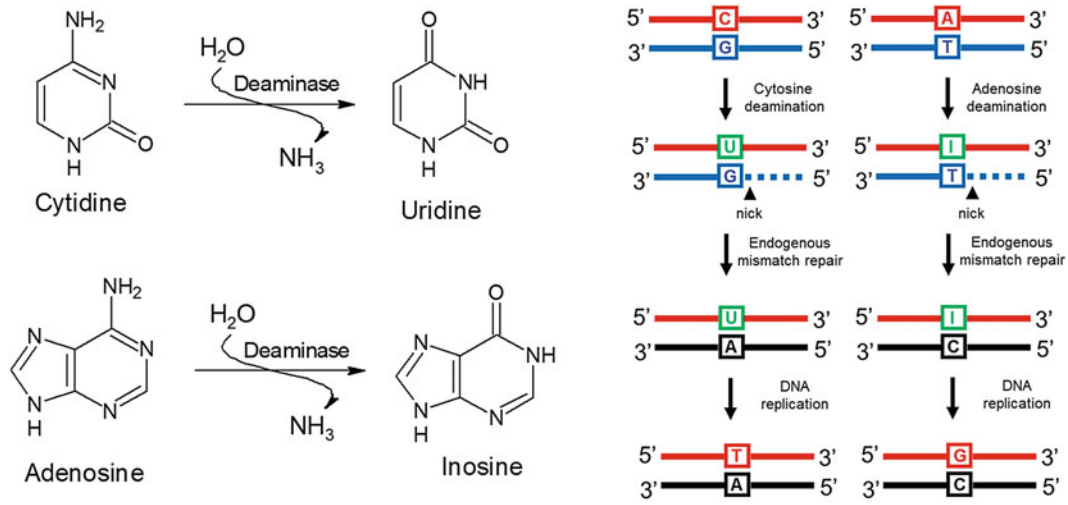

Fig. 1 Hydrolytic deamination in cytidine to uridine (C → U) and adenosine to inosine (A → I) conversion. Cytidine/adenosine deaminase catalyzes hydrolytic deamination at the C6 position, inducing uridine/inosine to pair with adenosine/cytidine and thus change to thymine/guanosine

After cytidine deaminases create a lesion in the DNA, there are three possible repair mechanisms that can occur [10]: (1) During DNA replication, the uracil can be replaced by a tyrosine (T). (2) Through base excision repair (BER) mediated by uracil N-glycosylase (UNG), the uracil can be excised and replace by a different nucleotide. This method, however, is typically error-free, which doesn't suit the purposes of base editors. (3) Mismatch repair, a process where an error-prone polymerase repairs the DNA lesion, increases the chance of creating mutations nearby. Usually, this process also involves the incorporation of uracil as well (Fig. 2).

Thus far, Dr. David Liu's lab has developed many different base editors [13]. The first edition base editor, BE1, is a rat deaminase rAPOBEC1 fused to a deactivated Cas9 (dCas9), which is a Cas9 with inactivated nuclease domains. Transfecting BE1 and sgRNA has been shown to convert C → T. The BE2 has an additional unit, a uracil DNA glycosylase inhibitor (UGI) derived from the *Bacillus subtilis* bacteriophage PBS1. As the name suggests, UGI inhibits the uracil DNA glycosylase, blocking the excision of uridine and therefore the BER pathway. Consequently, the UGI disfavors error-free repair caused by UNG's excision of U and BE2s increase efficiency of C → T conversion by threefold. The BE3 (Fig. 3) involves an rAPOBEC1 fused to a nickase Cas9 D10A and a UGI. A nickase Cas9 creates single-stranded DNA breaks rather than DSBs, because only one out of two nuclease domains is functional. The efficiency of BE3 editing is sixfold higher than BE2. Finally, the BE4 has optimized longer linkers, and two fused

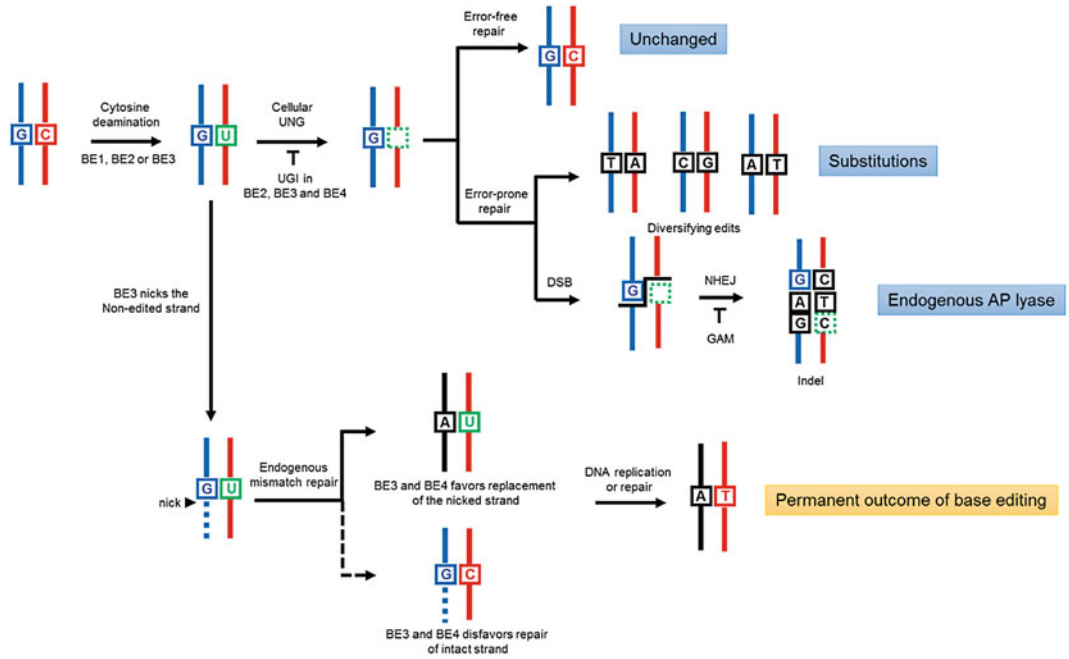

Fig. 2 Schematic of cytosine base editing in cells. The conversion of C into U could cause the onset of base excision repair, where U is excised by uracil DNA N-glycosylase (UNG). C can be inserted through error-free repair. Error-prone repair results in base substitutions or indels through formation of abasic site removed by AP lyase and leaving a DSB. However, uracil N-glycosylase (UNG)-mediated excision of the uracil can be inhibited by BE2, BE3, and BE4. Thus, BE3/BE4 can make a nick on the non-edited strand (containing the G of original C·G targeting base pair), inducing endogenous mismatch repair on the nicked strand that replaces the G with an A. BE3/BE4 converts the original C·G base pair to A·U, and DNA replication or repair concludes the process by converting the strand to a T·A

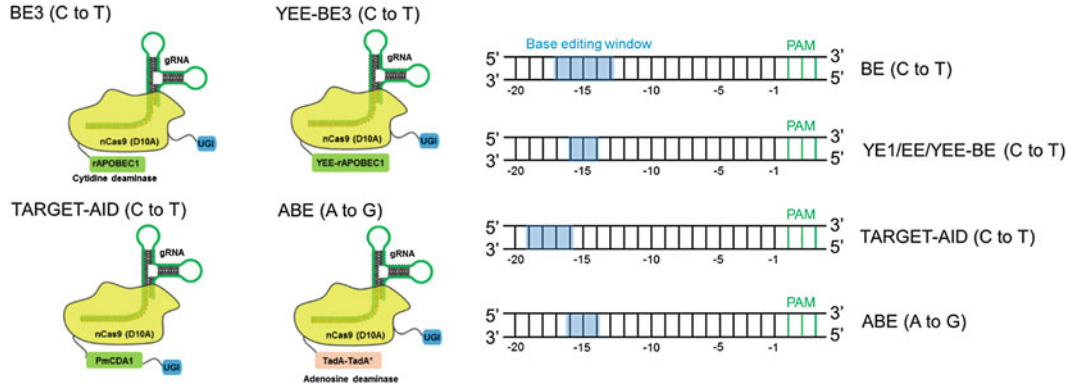

Fig. 3 Structural representation of base editors and their activity window corresponding to PAM sites [13, 15–17]

copies of UGI attached to the cytidine deaminase. The purpose of these additional units is to reduce UNG-mediated BER, which they have been shown to do.

Although BE3 has gained popularity for its highly efficient site-specific conversion of C → T, two drawbacks limit its utility: (1) The BE3 requires the target cytidine to be within a range of 13 to 17 bp away from the PAM (Fig. 3); (2) Due to the high activity of BE3, all of the cytidines within the editing window (which is usually 4–6 bases long) will be converted into tyrosines, leading to potential undesired changes at the target sites [10, 14]. These "off-target" mutations can be circumvented by more tightly restricting the window of nucleotides that BE3 can access. Kim et al. created a triple mutant rAPOBEC1, (YEE-BE3), which has a restricted targetable window of 1–2 bases [15]. This comes at a cost, however, because the YEE-BE3 also produces edits at a rate that is 2.9-fold lower than BE3.

Another base editor developed by Nishida et al. in 2016 [16], Target-AID (Fig. 3), uses the activation-induced cytidine deaminase (AID). AID carries out somatic hypermutation, the immunologically relevant process that allows antibodies to have genetic variation and diversification. Specifically, AID targets the human Ig locus and generates diverse mutations affecting the production of antibodies. The subsequent antigen binding selection process ensures that the antibodies have high affinity and specificity. Nishida et al. fused a dCas9 from *Streptococcus pyogenes* together with PmCDA1, an AID orthologue from the sea lamprey to create Target-AID. This complex was shown to carry out efficient site-specific mutagenesis. Adding PmCAD1 to a Cas9 D10A nickase generated higher rates of gene editing in yeast, but it also induced point mutations and deletions in mammalian cells. Alternatively, adding UGI to PmCDA1 suppressed collateral deletions, and it increased site-specific gene editing efficiency.

A different class of base editors using adenine deaminase-based (ABE) base editors has been generated by Gaudelli et al. [17, 18] (Fig. 3). ABEs do not exist in nature, so *Escherichia coli* TadA, a tRNA adenine deaminase, has been studied and tested with directed evolution methods to create ABEs. Deaminating adenosine creates inosine, which can base pair with cytidine. The cytidine is corrected to guanine, so ultimately, the ABE will convert an adenosine into a guanine. Gaudelli et al. replaced the rAPOBEC1 from BE3 with TadA from *E. coli*. Variations of these ABEs have been developed with antibiotic resistance complementation and antibiotic selective pressures in bacteria. This has led to the generation of ABEs with different targeting activity windows. For example, the ABE5.3 has a window of 3–6 bp from the protospacer, and ABE7.8, ABE7.9, and ABE7.10 have windows of 4–9 bp from the protospacer.

iPS cells are a valuable platform for disease modeling and regenerative medicine discovery, because of their ability to be programmed and differentiated into virtually any other cell type. For many genetic diseases, correcting the gene mutation via deleting or inserting desired sequences at a specific locus of the genome would

ameliorate the disease [19]. Therefore, CRISPR-based genome editing of patient-derived iPS cells shows great promise for future autologous replacement therapies. The challenge of correcting the individual gene mutation occurs in the reprogramming of iPS cells. Bypassing the limitations provides a valuable way to model the progression of disease in a dish, as well as a method for developing therapies that can move toward clinical trials [20–22]. iPS cells are difficult to transfect, and thus, to achieve successful gene editing in iPS cells, one needs to strike a balance between cell tolerance and delivery efficiency. Delivery efficiency is dependent on the delivery method and reagents. In general, increasing transfection efficiency relies on the proper dissociation of iPS cells into single cells, because cell clumps reduce the chance that reagents are delivered into cells. The delivery efficiency is also restricted by cell cycle coordination of the donor nucleus and recipient cytoplast. Although the optimal coordination period of cells is still being heavily debated, the G0/G1 phase is considered to be the best stage for the maintenance of normal ploidy [23, 24]. Thus, optimizing the experimental cell conditions for efficient CRISPR-based base editing on patient-derived iPS cells would be a crucial step before developing gene therapy protocols for clinical trials.

2 Materials

1. 4D-Nucleofector™ System (Lonza).
2. P3 Primary Cell 4D-Nucleofector Kit S (Lonza, #V4XP-3032).
3. mTeSR™ media (StemCell, #85850).
4. Y-27632 2HCl (Selleckchem, #129830-38-2).
5. ReLeSR™ (StemCell, #05873).
6. Dulbecco's phosphate-buffered saline (Thermo Fisher Scientific, #14040216).
7. pSI-Target-AID-NG (Addgene,# 119861).
8. pSpCas9(BB)-2A-GFP (PX458) (Addgene, #48138).
9. Corning Matrigel Matrix (Corning, #354248).
10. Opti-MEM I medium (Thermo Fisher Scientific, #31985062).
11. Daidzein (Sigma-aldrich, #D7802).

3 Methods

BE-Designer is a sgRNA designing tool for CRISPR base editors. It provides a list of potential target sgRNA sequences for base editors based on possible editable sequences in a target window,

3.1 Construct Design: Design sgRNA with Web Tool—BE-Designer [25]

relative target positions, GC content, and potential off-target sites. Furthermore, BE-Designer provides analysis for CRISPR base editors with different endonucleases and recognizes a variety of PAM sites. The application supports many reference genomes from a variety of species, including vertebrates, plant, and bacteria. BE-Designer and BE-Analyzer can be freely accessed at http://www.rgenome.net/be-designer/and http://www.rgenome.net/be-analyzer/.

Clone sgRNA Expression Plasmid

1. Prepare transfection-quality plasmids for experiment, gRNA-Cas9:pSpCas9(BB)-2A-GFP (PX458), and base editor, pSI-Target-AID-NG plasmid.
2. Transfect pSpCas9(BB)-2A-GFP (PX458) and pSI-Target-AID-NG plasmid in iPS cells; in general use 1:1 ratio of sgRNA-Cas9 plasmid:pSI-Target-AID-NG plasmid.
3. Harvest transfected iPS cells, and quantify base editing efficiency using high-throughput sequencing.

3.2 Preparation of iPS Cells for Nucleofection in Lonza System

The following protocol describes the optimized condition for using the Lonza/4D-Nucleofector System reagent transfection system for CRISPR-based genome editing of iPS cells cultured under mTeSR media with ROCK inhibitor (Y-27632). These steps can be employed to efficiently deliver the CRISPR-Cas9 plasmid and avoid the NHEJ or HDR pathway, allowing base editing to occur.

3.2.1 Pre-nucleofection

1. Culture iPS cells in Matrigel-coated plates until they are semi-confluent.
2. Pre-treat iPS cells with Daidzein for cell cycle synchronization: Replace the media to mTeSR media with 100 μM Daidzein 24 h before the nucleofection (*see* **Note 1**).
3. Pre-treat iPS cells with ROCK inhibitor (Y-27632): Replace the media to mTeSR media with 10 μM ROCK inhibitor (Y-27632) 1 h before nucleofection (*see* **Note 2**).
4. Each electroporation reaction will need 5.0×10^5 cells, and we typically include a reaction without plasmid as a control.

3.2.2 Plate and Buffer Preparation

1. Coat a new 12-well plate with matrigel/DMEM, and incubate at 37 °C for 2 h before use (*see* **Note 3**).
2. Replace coated matrigel/DMEM to 1 mL mTeSR media with 10 μM ROCK inhibitor (Y-27632) each well. Incubate the plate at 37 °C for cell seeding after the nucleofection reaction.
3. Prepare 70 μL additional pre-warmed mTeSR with 10 μM ROCK inhibitor (Y-27632) per reaction for cell recovery after nucleofection.

3.2.3 Cell Preparation

1. Aliquot sufficient ReLeSR™ to passage the iPS cells. Warm reagents at room temperature (*see* **Note 4**).
2. After 1 h ROCK inhibitor (Y-27632) pre-treatment, inspect the plate to visualize the morphology under a dissection microscope.
3. Aspirate and replace ReLeSR™ per well and incubate at 37 °C for 5 min.
4. Quench the ReLeSR™ reaction by adding 1 mL mTeSR for each well. Gently detach cells using a sterile pipette tip.
5. Dissociate the cells into a single cell suspension by pipetting the suspension carefully up and down 3–4 times.

3.2.4 Count Cells

1. Count an aliquot of the detached cells and determine cell density.
2. Transfer the required number of cells (5.0×10^5 cells per reaction) to a new tube.
3. Centrifuge cells $100 \times g$ for 3 min at room temperature, and discard the supernatant.
4. Wash cells using PBS and gently pipette up and down, centrifuge cells $100 \times g$ for 3 min at room temperature, and discard the supernatant.
5. Resuspend cell in Lonza P3 Nucleofector solution at 20 μL/reaction. Work quickly but carefully, and avoid leaving cells in Nucleofector solution for longer than 15 min. Avoid bubble formation.

3.2.5 Nucleofection

1. Transfer iPS cell suspension to the Nucleocuvette strip (P3 Primary Cell 4D-Nucleofector Kit).
2. Transfer each cell with nucleofection buffer to each well of Nucleocuvette strip, and click the lid into place (*see* **Note 5**).
3. Place the Nucleocuvette strip with closed lid into the retainer of the 4D-X core unit. Check for proper orientation of the strip.
4. Use the electroporation protocol "DS150," and press start on the display of the core unit. After run completion, the screen should display a green "+" over the wells which means that successful transfection has occurred (*see* **Note 6**).
5. Aspirate recovery media (mTeSR with ROCK inhibitor Y-27632) 70 μL for each well.

3.2.6 Post-nucleofection

1. Transfer iPS cells from each well to the pre-incubated 12-well plate, and incubate overnight in 37 °C/5% CO_2 incubator (*see* **Note 7**).
2. Change media daily with fresh mTeSR without ROCK inhibitor (Y-27632) after nucleofection.
3. Incubate the cells for 4 days, and then pick up the single clone iPS cells to further experiments.

3.3 Analysis of NGS Data of CRISPR Base Edited Cells

1. Compare the edited cell with control group by using free web tool. BE-Analyzer can be freely accessed at http://www.rgenome.net/be-analyzer/.
2. BE-Analyzer requires some basic information to analyze: full reference sequence (5′-NGG-3′), the type of base editor, target DNA sequence (5′ to 3′ without PAM), additional flanking windows for CRISPR base editing, and minimum frequency.

4 Notes

1. Daidzein can be used for synchronizing iPS cells at G0/G1 stage and has no deleterious effect in sustaining cell survival and pluripotency.
2. ROCK inhibitor (Y-27632) may result in a spindle-shaped cell morphology. This change will not affect the pluripotency of iPS cells, and it will reverse after ROCK inhibitor is removed.
3. The plates can be sealed and stored overnight at 4 °C or incubated for 2 h at 37 °C. To avoid a potential sample swap, we maintain distinct lines on separate plates.
4. One hour before the cell passage, add ROCK inhibitor (Y-27632) to each plate at a final concentration of 10 μM.
5. Make sure there are no bubbles in the wells, because it might affect the nucleofection efficiency.
6. For different cells, one might have to use a different program. DS150 is a suitable program for iPS cell lines in this experiment.
7. Because plasmid-based transfections require time for nuclear incorporation end expression, we typically wait 24 h before further operation.

Acknowledgments

The Jonas Children's Vision Care and Bernard & Shirlee Brown Glaucoma Laboratory are supported by the National Institutes of Health [P30EY019007, R01EY018213, §R01EY024698, R01EY026682, R21AG050437], National Cancer Institute Core [5P30CA013696], Foundation Fighting Blindness [TA-NMT-0116-0692-COLU], the Research to Prevent Blindness (RPB) Physician-Scientist Award, and unrestricted funds from RPB, New York, NY, USA. S.H.T. is a member of the RD-CURE Consortium and is supported by Kobi and Nancy Karp, the Crowley Family Fund, the Rosenbaum Family Foundation, the Tistou and Charlotte Kerstan Foundation, the Schneeweiss Stem Cell Fund, New York State [C029572], and the Gebroe Family

Foundation. YJC and CLX contributed equally to this work. YJC and CLX wrote and edited the manuscript. XC and YTT were responsible for developing and finalizing the protocol. AGB, VBM, and SHT oversaw the writing process.

Conflict of Interest: The authors declare that the research was conducted in the absence of any commercial or financial relationships that could be construed as a potential conflict of interest.

References

1. Tong Y, Weber T, Lee SY (2018) CRISPR/Cas-based genome engineering in natural product discovery. Nat Prod Rep. https://doi.org/10.1039/c8np00089a
2. Wang H, La Russa M, Qi LS (2016) CRISPR/Cas9 in genome editing and beyond. Annu Rev Biochem 85:227–264
3. Dy RL et al (2014) Remarkable mechanisms in microbes to resist phage infections. Annu Rev Virol 1(1):307–331
4. Chibani-Chennoufi S et al (2004) Phage-host interaction: an ecological perspective. J Bacteriol 186(12):3677–3686
5. Jiang F, Doudna JA (2017) CRISPR-Cas9 structures and mechanisms. Annu Rev Biophys 46:505–529
6. Hsu PD, Lander ES, Zhang F (2014) Development and applications of CRISPR-Cas9 for genome engineering. Cell 157(6):1262–1278
7. de la Fuente-Nunez C, Lu TK (2017) CRISPR-Cas9 technology: applications in genome engineering, development of sequence-specific antimicrobials, and future prospects. Integr Biol (Camb) 9(2):109–122
8. Rees HA, Liu DR (2018) Base editing: precision chemistry on the genome and transcriptome of living cells. Nat Rev Genet 19(12):770–788
9. Rees HA, Liu DR (2018) Publisher correction: base editing: precision chemistry on the genome and transcriptome of living cells. Nat Rev Genet 19(12):801
10. Hess GT et al (2017) Methods and applications of CRISPR-mediated base editing in eukaryotic genomes. Mol Cell 68(1):26–43
11. Kim D et al (2017) Genome-wide target specificities of CRISPR RNA-guided programmable deaminases. Nat Biotechnol 35(5):475–480
12. Eid A, Alshareef S, Mahfouz MM (2018) CRISPR base editors: genome editing without double-stranded breaks. Biochem J 475(11):1955–1964
13. Komor AC et al (2016) Programmable editing of a target base in genomic DNA without double-stranded DNA cleavage. Nature 533(7603):420–424
14. Zuo E et al (2019) Cytosine base editor generates substantial off-target single-nucleotide variants in mouse embryos. Science 364(6437):289–292
15. Kim YB et al (2017) Increasing the genome-targeting scope and precision of base editing with engineered Cas9-cytidine deaminase fusions. Nat Biotechnol 35(4):371–376
16. Nishida K et al (2016) Targeted nucleotide editing using hybrid prokaryotic and vertebrate adaptive immune systems. Science 353(6305)
17. Gaudelli NM et al (2017) Programmable base editing of A*T to G*C in genomic DNA without DNA cleavage. Nature 551(7681):464–471
18. Komor AC, Badran AH, Liu DR (2018) Editing the genome without double-stranded DNA breaks. ACS Chem Biol 13(2):383–388
19. Ebert AD, Liang P, Wu JC (2012) Induced pluripotent stem cells as a disease modeling and drug screening platform. J Cardiovasc Pharmacol 60(4):408–416
20. Masip M et al (2010) Reprogramming with defined factors: from induced pluripotency to induced transdifferentiation. Mol Hum Reprod 16(11):856–868
21. Malik N, Rao MS (2013) A review of the methods for human iPSC derivation. Methods Mol Biol 997:23–33
22. Kelaini S, Cochrane A, Margariti A (2014) Direct reprogramming of adult cells: avoiding the pluripotent state. Stem Cells Cloning 7:19–29
23. Ghule PN et al (2011) Reprogramming the pluripotent cell cycle: restoration of an abbreviated G1 phase in human induced pluripotent stem (iPS) cells. J Cell Physiol 226(5):1149–1156
24. Kwon DJ et al (2017) Effects of cell cycle regulators on the cell cycle synchronization of porcine induced pluripotent stem cells. Dev Reprod 21(1):47–54
25. Hwang GH et al (2018) Web-based design and analysis tools for CRISPR base editing. BMC Bioinformatics 19(1):542

INDEX

A

Kursad Turksen (ed.), *Stem Cells and Aging: Methods and Protocols*, Methods in Molecular Biology, vol. 2045, https://doi.org/10.1007/978-1-4939-9713-8,

B

C

D

E

F

G

H

I

L

M

N

O

P

Q

R

S

T

U

W